

**An excursion into the chemistry of more
nucleophilic saturated N-heterocyclic carbenes**

by

Gargi Kundu

10CC17A26014

A thesis submitted to the
Academy of Scientific & Innovative Research
For the Award of the Degree of
DOCTOR OF PHILOSOPHY
in
SCIENCE

Under the supervision of

Dr. Sakya Singha Sen



CSIR-National Chemical Laboratory, Pune

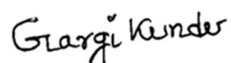


Academy of Scientific and Innovative Research
AcSIR Headquarters, CSIR-HRDC campus
Sector 19, Kamla Nehru Nagar,
Ghaziabad, U.P.–201 002, India

August-2022

Certificate

This is to certify that the work incorporated in this Ph.D. thesis entitled, “*An excursion into the chemistry of more nucleophilic saturated N-heterocyclic carbenes*”, submitted by *Gargi Kundu* to the Academy of Scientific and Innovative Research (AcSIR), in partial fulfillment of the requirements for the award of the Degree of *Doctor of Philosophy in Science*, embodies original research work carried-out by the student. We, further certify that this work has not been submitted to any other University or Institution in part or full for the award of any degree or diploma. Research material(s) obtained from other source(s) and used in this research work has/have been duly acknowledged in the thesis. Image(s), illustration(s), figure(s), table(s) etc., used in the thesis from other source(s), have also been duly cited and acknowledged.



(Signature of Student)

Gargi Kundu

Date: 18-08-2022



(Signature of Supervisor)

Dr. Sakya Singha Sen

Date: 18-08-2022

STATEMENTS OF ACADEMIC INTEGRITY

I, Gargi Kundu, a Ph.D. student of the Academy of Scientific and Innovative Research (AcSIR) with Registration No. 10CC17A26014 hereby undertake that, the thesis entitled “An excursion into the chemistry of more nucleophilic saturated N-heterocyclic carbenes” has been prepared by me and that the document reports original work carried out by me and is free of any plagiarism in compliance with the UGC Regulations on “*Promotion of Academic Integrity and Prevention of Plagiarism in Higher Educational Institutions (2018)*” and the CSIR Guidelines for “*Ethics in Research and in Governance (2020)*”.

Gargi Kundu

Signature of the Student

Date : 18-08-2022

Place : CSIR-NCL, Pune

It is hereby certified that the work done by the student, under my supervision, is plagiarism-free in accordance with the UGC Regulations on “*Promotion of Academic Integrity and Prevention of Plagiarism in Higher Educational Institutions (2018)*” and the CSIR Guidelines for “*Ethics in Research and in Governance (2020)*”.

NA

Signature of the Co-supervisor (if any)

Name :

Date :

Place :

Sakya Singha Sen

Signature of the Supervisor

Name : Dr. Sakya Singha Sen

Date : 18-08-2022

Place: CSIR-NCL, Pune

*This dissertation is dedicated to
Maa, Baba, Didi, Tinku and Bunu*

Acknowledgement

The process of earning a doctorate and writing a dissertation is long and arduous, and it is certainly would not have been possible without close association with many people. I take this opportunity to express my deepest gratitude to the people whose immense support made my academic journey successful. However, mentioning is not sufficient to thank them in the right way.

*It gives me immense pleasure and pride to express my sincere gratitude and respect to my supervisor, **Dr. Sakya Singha Sen**, for constant assistance, inspiring guidance, tremendous support, and constructive criticism throughout my Ph.D. journey. His encouragement and belief in me showed a new hope, made me realize that doing research is an amazing feeling. I feel incredibly fortunate for the freedom rendered by him in the laboratory to fulfill my dream with proper planning and the research's execution. I got inspiration a lot from his own stories, not only in the research field but also about how to balance a busy life in an exciting way. I'll miss our long conversations, biryani treats after betting and taunting in silly reasons more than anything. And I will always remain a prodigious fan of his natural story telling style, knowledge in diverse suspects, and being cool in difficult situations. I am a big follower of his believe in three words — “Work, Finish, Publish”. I am thankful to him for making me a better person and helping me to identify my true potential. I appreciate his encouragement to cherish every achievement in professnal and personal carrier. I wish him to remain such easy approachable and down to earth nature in the coming days as well. I have seen many feathers being added to his crown and wish to see many more to come in future days. Lastly, I am very much grateful and lucky to get the opportunity to work under his supervision.*

*This journey (Ph.D.) cannot be successful without the suggestions given by my Doctoral Advisory Committee (DAC) members during the DAC meetings. I express my sincere thanks to the Doctoral Advisory Committee members, **Dr. E. Balaraman**, **Dr. Kumar Vanka**, **Dr. Subashchandrabose Chinnathambi**, and **Dr. T. Raja**, for their contribution in stimulating suggestions and encouragement during my Ph.D.*

*I am grateful to **Prof. Ashish Lele** (Director, CSIR-NCL), **Prof. A. K. Nangia** (Former Director, CSIR-NCL), **Dr. Shubhangi B. Umbarkar** (Head, Catalysis and Inorganic Chemistry Division), **Dr. D. Srinivas** and **Dr. C. S. Gopinath** (Former Head, Catalysis and Inorganic Chemistry Division), for giving me this opportunity and providing all necessary infrastructure and facilities to carry out my research work. I would like to acknowledge all the support from Catalysis and Inorganic Chemistry Division office staff. I am also highly thankful to the **Council of Scientific & Industrial Research (CSIR)**, New Delhi, and the **Academy of Scientific and Innovative Research (AcSIR)**, Ghaziabad, for the financial assistance and coursework facilities, respectively.*

*My sincere thanks to **Dr. Sayan Bagchi**, **Dr. Samir Chikkali**, **Dr. E Balaraman**, **Dr. C. V. Ramana**, **Dr. B. L. V. Prasad**, **Dr. Paresh Dhepe**, **Dr. Santosh Babu**, **Dr. Pradip Maity**, **Dr. Utpal Das**, **Dr. Arup Kumar Rath**, **Dr. Janardan Kundu**, **Dr. Ramesh Samanta**, **Mrs. Kohle**, **Mr. Iyer**, **Mr. Purushothaman**, **Library staff**, **Student academic office staff**, and all other scientists of NCL for their motivation, constant encouragement, and support.*

*I am highly grateful to our collaborators **Dr. Kumar Vanka** (CSIR-NCL, Pune) and his doctoral students, **Dr. Shailja Jain**, **Soumya Ranjan Dash**, **Vipin Raj K**, **Dr. Ruchi Dixit**, **Dr. Tamal Das** and **Dr. Debasis Koley** (IISER, Kolkata) and his doctoral students, **Dr. Sriman De** for their essential support in DFT calculations, **Dr. Rajesh Gonnade** (CSIR-NCL, Pune) and his group members, **Dr. Ekta**, **Dr. Samir**, **Dr. Veer**, **Christy**, **Tabrez**, **Debjani** and **Bhupender**, for single-crystal X-ray diffraction measurements, and for valuable suggestions and help at different parts of my research journey, **Dr. B. Shantakumari** and her students for the help in HRMS analysis, and **Mrs. Ansanas** for elemental analysis. I would also like to thank **Dr. Sapna Ravindranathan**, **Dr. Udaya Kiran Mareli**, **Dr. T. G. Ajithkumar**, and their team **Dinesh**, **Satish**, **Meenakshi**, **Deepali**, **Sherminaj**, and **Nita** for the NMR facilities. My sincere thanks to **Dr. Srinu** for helping me in single-crystal X-ray diffraction studies. I am also grateful to our collaborator for helping me EPR measurement, **Dr. Tapan Kumar paine** and **Abhisek das** (IACS, Kolkata).*

*I consider myself highly privileged to work and spend most of my day with the Sen Lab's wonderful and motivated young research team of colleagues. My experience studying through our group lectures has been fantastic. It is my pleasure to thank my labmates, **Dr. Sanjukta Pahar**, **Rohit Kumar**, **Kritika Gour**, **VS Ajith Kumar**, **Vishal Sharma**, **Biplab Mahata**, **Kajal Balayan**, **Debjit Pramanik**, **Prateeksha**. I would like to express my deepest gratitude to my former labmates, **Dr.***

Sandeep Yadav, Dr. V. S. V. S. N. Swamy, and Dr. Milan Bisai, for instructing me the sensitive chemistry; especially Dr. Moumita Pait, for giving me the initial glimpses of carbene chemistry and her love and support throughout my PhD journey.

I am highly grateful to Dr. Shabana Khan (from IISER-Pune) and her research group Dr. Shiv Pal, Dr. Neha, Dr. Nasrina, Nilanjana, Javed, Moushaki, and Ruksana for their kind support and help during the different fragments of my research journey.

Beyond the group, many well-wishers from CSIR-NCL made my journey more comfortable. I feel that this journey is incomplete without hostel life. I am thankful to Dr. Ayesha, Dr. Debu da, Dr. Ashish, Dr. Rangrajan, Neha, Chandan, Arindam, Dr. Abhijit Da, Dr. Pranab da, Dr. Suwendu, Dr. Argya da, Samadhan, Srijan, Pooja, Naru Da, Dr. Rahul, Dipesh, Manish, Pawan, Dr. Subhrashis da, Dr. Arun Dadwal, Priyanka Walko, Priyanka Halder, Ravi Ranjan, Himanshu, Akash, Sairam, Viksit, Dr. Goudappagouda, Dr. Vivek, Sangram, Rajni, Kranti, Jyoti, Chandni, Indrajeet, Dr. Suman Devi, Priyanka Katariya, Lakshmi, Gitanjali, Amrita, from NCL for their kind help and support. I wish to thank Mr. Mane, Mr. Koli, Ms. Nita, Mrs. Uma, Mr. Pathan, Mr. Deshmukh, Mr. Date, and all support staff whose names are not mentioned here, but had always been ready to understand my problem and helped me in all possible manners.

I am immensely grateful to Prof. Sundargopal Ghosh from IIT Madras for the opportunity to join his team as an M.Sc. intern, for access to the laboratory and research facilities. I would also like to acknowledge the teachers I learned from since childhood; I would not have been here without their guidance, blessings, and support. I also highly grateful to my M.Sc. labelmates, Dr. Koushik, Dr. Anangsha Di, Dr. Rini Di, Dr. Aric anna, Dr. Rosmita Di, Dr. Ranjit Da, Dr. Jafar Da, Dr. Benson da, Dr. Rosmita Di for their guidance and support. I would like to express my deepest gratitude to my M.Sc co-guide Dr. Barik da for his continuous mental support and inspiration during my MSc project and invaluable lessons on handling of sensitive chemicals.

I am immensely thankful to my all the teachers in school especially Suvra Di, Gouri Di, Champa Di, Hiramoni Di, Koushik Sir, Rampada Sir, Chinmoy Sir, Mohitosh Sir for encouraging me to look beyond the horizon. I am also thankful to Dr. Samaresh Sir for giving me a chance to work in his laboratory which inspired me to become a researcher during my B. Sc.

*I would like to give special thanks to my friends since childhood **Aritri, Susmita, Sukanya saha, Krishna, Shreya, Parinita, Rimjhim, Rahla, Late Arunava, Nishith, Sadhu, Dipannita Di, Umi, Sukanya Bera, Sanchita, Sourav kaur, Arijit** for their kind support and love.*

*My family is always a source of inspiration and great moral support for me in pursuing my education. I owe a lot to my beloved parents, who encouraged and helped me at every stage of my personal and academic life and longed to see this achievement come true. My sincere thanks to my beloved family members, my father '**Dinabandhu**' and mother '**Asima**'. It would be incomplete without mentioning about my dear mother. I am fortunate to have my mother, who always lived for us and made countless sacrifices to improve our lives. I am glad to announce that today whatever I am, it is only because of my mother. There are not enough words to describe how blessed I am to have both of them. My sincere thanks my sisters **Manisha (Didi), Mousumi (Tinku) and Durba (bunu)**, for their endless love, support, and sacrifice. I owe to thank my little sister **Durba**, my best friend, critic, best gossip partner for her inspiration, understanding, support, love and for being with me in all the good and bad times of my life. I am also highly grateful to **Debojit da and Swapan Da** for providing me the strength and support in every possible way. I am very much indebted to my whole family, who supported me in every possible way to see the completion of this research work.*

*At last, I give my humble obeisance to **Lord Krishna, Lord Shiva, Maa Durga, Ma Saraswati, Ma Lakshmi and Lord Ganesha** for bestowing me with powers to complete this task up to my satisfaction. I offer my respectful obeisance to my family Guru Sri **Adwaitywa Maharaj** for blessing me throughout my life.*

Many others have helped me directly or indirectly throughout my research. I also offer my humble thanks to them.

Gargi Kundu

CONTENT OF THE THESIS

Content	Page No.
Abbreviations	iv
General remarks	vi
Synopsis	vii
Chapter 1:	
Introduction to Saturated N-heterocyclic Carbene Chemistry	1-38
1.1 Introduction	2
1.1.1 A brief history of N-heterocyclic carbenes	2
1.1.2 Structure and general properties of NHCs	3
1.1.3. Electronic structure of carbenes	4
1.1.4 Different types of N-heterocyclic carbenes	5
1.1.5 Different types carbenes except NHCs	6
1.1.5.1 Cyclic (alkyl)- (amino)carbenes, CAAC	6
1.1.5.2 N, N'-Diamidocarbenes, DAC	7
1.2 Carbenes as an alternative to the transition metal complexes	8
1.2.1 Carbenes in small molecule activations	9
1.2.2 Carbenes in C-F activations	13
1.2.3 Carbenes in B-H, Si-H, P-H activations	16
1.3 Carbenes in the stabilization of Kekulé diradicals	19
1.4. Aim and outline of the thesis	22
1.5 References	25
Chapter 2:	
Carbenes in C-F Bond Activation and Their Subsequent Reactivities	39-66
2.1 Introduction	40
2.2 C-F activation of hexafluorobenzene	41
2.3 Mechanism for the C-F bond activation of C ₆ F ₆	45

2.4 Reactivity of the mesoionic compound with $B(C_6F_5)_3$	46
2.5 C-F activation of octafluorotoluene	48
2.6 C-F activation of pentafluoropyridine	51
2.7 Mechanism study for triple C-F activation	53
2.8 C-F activation of tetrafluoropyridine	57
2.9 Conclusion	58
2.10 References	59

Chapter 3:

Saturated N-heterocyclic Carbene based Kekulé Di-radicaloids via Double C-F Activation	67-104
3.1 Introduction	69
3.2 5-SIDipp based Thiele's hydrocarbon with a tetrafluorophenylene linker	72
3.3 Enhancing diradical character of Chichibabin's Hydrocarbon through fluoride substitution	79
3.4 Closed-Shell Kekulé Diradicaloids Spanned by Naphthalene and its Perfluoro Spacer	86
3.5 Conclusion	94
3.6 References	95

Chapter 4:

Stepwise Nucleophilic Substitution to Access Saturated N-heterocyclic Carbene-haloboranes with Boron–methyl Bonds	105-130
4.1 Introduction	106
4.2 Preparation of 5-SIDipp-boranes and haloborane adducts	108
4.3 Nucleophilic substitution at the tetracoordinate 5-SIDipp-haloborane centre	112
4.4 Preparation of first carbene·MeBCl ₂ adduct and its stepwise nucleophilic substitution	118
4.5 Lewis pair mediated tetrahydrofuran and diethyl ether activation	122
4.6 Conclusion	125
4.7 References	125

Chapter 5:	
The Chemistry of Six-membered N-heterocyclic Carbene Boranes	131-176
5.1: Introduction	133
5.2 Selective electrophilic mono- and di-iodination at 6-SIDipp·BH ₃ Center	134
5.3 Mono- and di-bromination at 6-SIDipp·BH ₃ center	142
5.4 Reactivity of 6-SIDipp with 9-BBN and ring expansion of 6-NHC	145
5.5 6-SIDipp mediated B-H activation of HBpin, HBcat and B ₂ neop ₂	148
5.6 6-SIDipp stabilized borenium cations; isolation of a cationic analogue of borinic Acid and its reactivity	153
5.7 6-SIDipp stabilized dihydroxyborenium cations	161
5.8. Nucleophilic substitution at 6-SIDipp·PhBCl ₂ center	166
5.9 Conclusion	168
5.10 References	170
Appendix: Experimental details, NMR and crystal data	177-223

Abbreviations

Units and standard terms

BDE	Bond Dissociation Energy
°C	Degree Centigrade
DFT	Density Functional Theory
mg	Milligram
h	Hour
mL	Milliliter
Hz	Hertz
min	Minute
mmol	Millimole
NPA	Natural Population Analysis
ppm	Parts per million
%	Percentage
MP	Melting Point
Calcd.	Calculated
CCDC	Cambridge Crystallographic Data Centre
CIF	Crystallographic Information file

Chemical Notations

Ar	Aryl
Me	Methyl
Et	Ethyl
Ph	Phenyl
Ad	Adamentyl
Dipp	Diisopropylaniline
<i>i</i> Pr	Isopropyl
<i>t</i> Bu	Tertiary butyl
MeOH	Methanol

MeCN	Acetonitrile
THF	Tetrahydrofuran
DCM	Dichloromethane
CDCl ₃	Deuterated chloroform
C ₆ D ₆	Deuterated benzene
DMSO-d ₆	Deuterated dimethyl sulfoxide
HBpin	Pinacolborane
TMSCN	Trimethylsilyl cyanide
TMSCl	Trimethylsilylchloride
<i>n</i> -BuLi	<i>n</i> -butyllithium
NHC	<i>N</i> -Heterocyclic carbene
NHSi	<i>N</i> -Heterocyclic silylene


Other Notations

δ	Chemical shift
J	Coupling constant in NMR
HRMS	High Resolution Mass Spectrometry
NMR	Nuclear Magnetic Resonance
rt	Room temperature
XRD	X-Ray Diffraction
equiv.	Equivalents
VT	Variable temperature

General remarks

- ❖ All chemicals were purchased from commercial sources and used without further purification.
- ❖ All reactions were carried out under inert atmosphere following standard procedures using Schlenk techniques and glovebox.
- ❖ The solvent used were purified by an MBRAUN solvent purification system MBSPS-800 and further dried by activated molecular sieves prior to use.
- ❖ Column chromatography was performed on silica gel (100-200 mesh size).
- ❖ Deuterated solvents for NMR spectroscopic analyses were used as received. All ^1H , ^{13}C , ^{19}F , ^{29}Si and ^{11}B NMR analysis were obtained using a Bruker or JEOL 200 MHz, 400 MHz or 500 MHz spectrometers. Coupling constants were measured in Hertz. All chemical shifts are quoted in ppm, relative to TMS, using the residual solvent peak as a reference standard.
- ❖ HRMS spectra were recorded at UHPLC-MS (Q-exactive-Orbitrap Mass Spectrometer) using electron spray ionization [(ESI+, +/- 5 kV), solvent medium: acetonitrile and methanol] technique and mass values are expressed as m/z. GC-HRMS (EI) was recorded in Agilent 7200 Accurate-mass-Q-TOF.
- ❖ All the reported melting points are uncorrected and were recorded using Stuart SMP-30 melting point apparatus.
- ❖ Chemical nomenclature (IUPAC) and structures were generated using ChemDraw Professional 15.1.

Synopsis

 Synopsis of the Thesis to be submitted to the Academy of Scientific and Innovative Research for Award of the Degree of Doctor of Philosophy in Chemistry	
Name of the Candidate	Ms. Gargi Kundu
Degree Enrolment No. & Date	PhD in Chemical Sciences (10CC17A26014); August 2017
Title of the Thesis	An excursion into the chemistry of more nucleophilic saturated N-heterocyclic carbenes
Research Supervisor	Dr. Sakya Singha Sen (CSIR-NCL, Pune)

Keywords: *N-heterocyclic carbene, C-F activation, Kekule di-radicaloids, NHC-Boranes, Borenium cations.*

This thesis deals with the more nucleophilic saturated N-heterocyclic carbenes reactivity with the main group elements. It is divided into six chapters. The first chapter is the introduction of saturated N-heterocyclic carbenes and its various applications in small molecules activation. The second to fifth chapters narrate our approach to the synthesis and reactivity of novel SNHC based strong bond activations and their further derivatizations. A detailed theoretical study is done to understand the mechanism for NHC based *mono* and *triple* C-F activations. The second chapter describes carbenes in C-F bond activation and their subsequent reactivities towards Lewis acids like BF_3 and $\text{B}(\text{C}_6\text{F}_5)_3$. The third chapter contains the synthesis of SNHC based Kekule di-radicaloids via double C-F activations of perfluoro-arenes. DFT calculations have investigated the singlet-triplet energy gap for these systems. The synthesis of first NHC-haloboranes with a boron-

methyl bond is included in fourth chapter. In the fifth chapter, we have introduced a more nucleophilic six saturated NHC and utilized it for the B-H bond activation, substitution, the stabilization of the borenium cations. The final chapter of the thesis describes the summary of Ph.D. work with the future outline.

Chapter I: Introduction to saturated N-heterocyclic chemistry

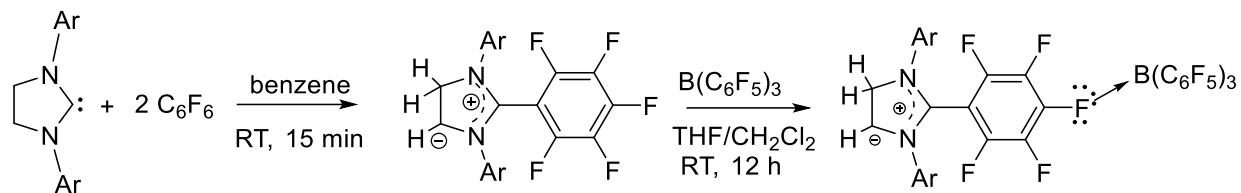
Carbenes are known as neutral compounds containing a divalent carbon atom with a six-electron valence shell. The incomplete electron octet and coordinative unsaturation, make the free carbenes highly reactive transient intermediates in organic transformations and unstable such as cyclopropanation. The first N-heterocyclic carbene (NHC) 1,3-di(adamantyl)imidazol-2-ylidene was synthesized by Arduengo in 1991.¹ Two bulky adamantyl groups bound to the nitrogen atoms help in the kinetic stabilization of the lone pair of the electrons at the carbene carbon atom and disfavors dimerization to the corresponding olefin (the Wanzlick equilibrium).² The electronic stabilization provided by the nitrogen atoms, however, is a much more important factor. NHCs show a singlet ground-state electronic configuration with the highest occupied molecular orbital (HOMO) and the lowest unoccupied molecular orbital (LUMO) best described as a formally sp^2 -hybridized lone pair and an unoccupied p-orbital at the C^2 carbon, respectively.³ The adjacent electron-withdrawing and p-electron-donating nitrogen atoms stabilize this structure both inductively by lowering the energy of the occupied s-orbital and mesomerically by donating electron density into the empty p-orbital. In my thesis work we have mainly used the saturated five and six membered N-heterocyclic carbenes due to its higher nucleophilic nature. The chemistry of SNHCs is rarely reported due to its difficulties in the synthesis and low yield. In our laboratory, we have modified the synthetic procedures of the SNHCs to get better yield. We have mainly

studied the SNHCs for the strong bond activations (C-F and B-H)⁴ and further stabilized SNHC based low valent main group elements like carbon based di-radicaloids, borenium cations.

Chapter II: Carbenes in C-F bond activation and their subsequent reactivities

The activation of C-F bonds of fluorinated hydrocarbons is of fundamental interest from the standpoint of the potential application of organofluorine compounds in synthetic organic chemistry, pharmacy, and agrochemistry as well as the ever-increasing environmental concerns related to the fluorinated compounds. Fluorinated hydrocarbons are not only contributing to the global warming but causing depletion to the ozone layer. Generally, transition metals are involved in the C-F bond activation, which has issues with terrestrial abundance and toxicity. As a result, there is a need to develop new synthetic strategies for the activation of C-F bonds.

Due to our recent interest in C-F bond activation by compounds with low valent main group elements, we intended to explore saturated NHC for the C-F bond activation. While both cyclic alkyl amino carbenes (*cAACs*) and IPr have been explored for the C-F bond activation recently, their different electronic properties are reflected in their mode of C-F bond activation. We have observed herein that the reaction of SIPr with C₆F₆ has led to the activation of one of the C-F bonds with concomitant deprotonation from the backbone, resulting in the formation of an unprecedented mesoionic compound along with HF elimination. The HF elimination is confirmed by adding one more equivalent of SIPr, which forms an imidazolium salt with HF₂⁻ as the counter anion. Subsequent to the isolation of the mesoionic compound, we intended to derivatize this it by reacting with B(C₆F₅)₃, but it forms a rare donor-acceptor adduct, where the fluoride atom of the C₆F₅ moiety coordinates to boron leaving the carbanion moiety intact. Such epitomization of Lewis basicity of a fluoride atom of C₆F₅ ligand in a metal free system is unprecedented.



Scheme 1. C-F bond activation of C_6F_6 by **SIPr** and subsequent reactivity (Ar=2,6-*i*Pr₂C₆H₃).

In order to understand the mechanism for the C-F bond activation of C_6F_6 , quantum chemical calculations have been done with density functional theory (DFT) at the PBE/TZVP level of theory (Figure 3). The approach of C_6F_6 to the carbene leads to the formation of **Int_1** via **Ts_1**, which is a very stable intermediate ($\Delta G = -16.6$ kcal/mol). The barrier for this step is 22.4 kcal/mol. Subsequent to this, calculations suggest that a molecule of the C_6F_6 acts as a “fluoride shuttle”, transferring a fluoride to the backbone carbon (see **Ts_2** in Figure 1) to yield the experimentally observed product. This mediating role of C_6F_6 was seen to be important, for it was seen that without the fluoride transferring assistance of C_6F_6 molecule, it was difficult to break the C-H bond to eliminate HF from the intermediate **Int_1**. This is in line with our observation why the reaction takes place at room temperature in presence of an excess C_6F_6 . Note that, Kuhn and coworkers also used a huge excess of C_6F_6 in presence of BF_3 for carbene mediated C-F bond activation.

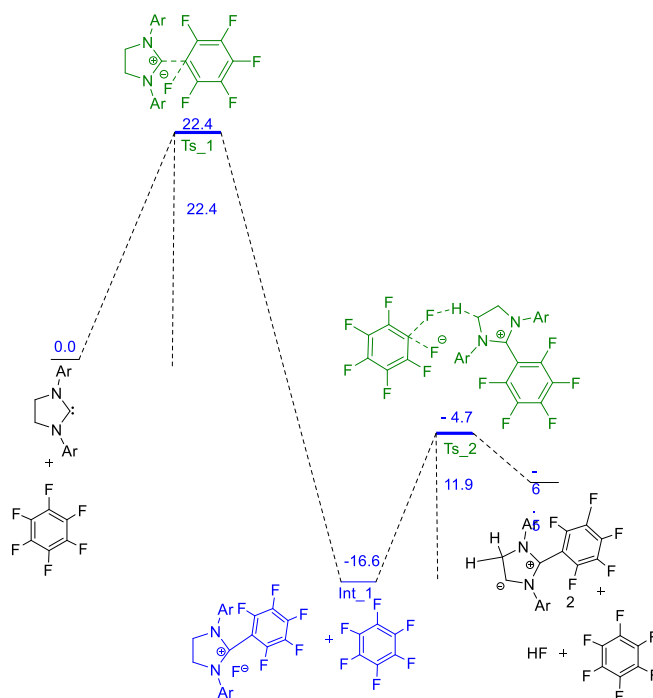
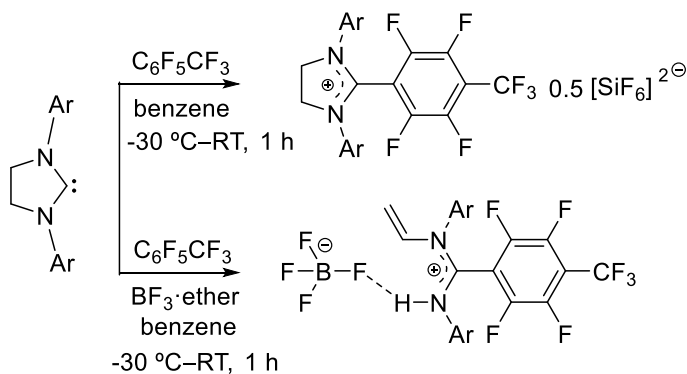


Figure 1. The reaction energy profile diagram for the C–F bond activation of C₆F₆ by SIPr. The values (in kcal/mol) have been calculated at the PBE/TZVP level of theory with DFT

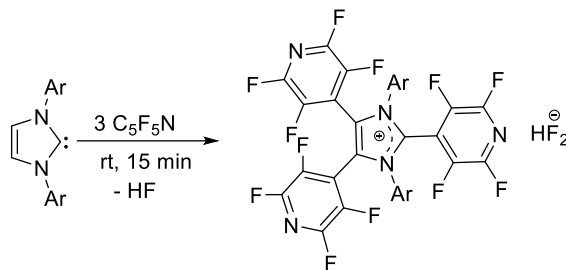


Scheme 2. C-F bond activation of C₆F₅CF₃ by SIPr

The elimination of HF during the C–F bond activation was further manifested in the reaction of SIPr with C₆F₅CF₃. The reaction led to the activation of the *para*-C–F bond relative to the CF₃ group, resulting in the formation of a imidazolium salt along with [SiF₆]²⁻ as the counter anion

(Scheme 2). The source of $[\text{SiF}_6]^{2-}$ can be attributed to the glass surface, which can react with the *in situ* liberated HF from the system. We could not stop the reaction of HF with the glass vessel even when performing the reaction at $-30\text{ }^\circ\text{C}$.

Triple C-F activation :



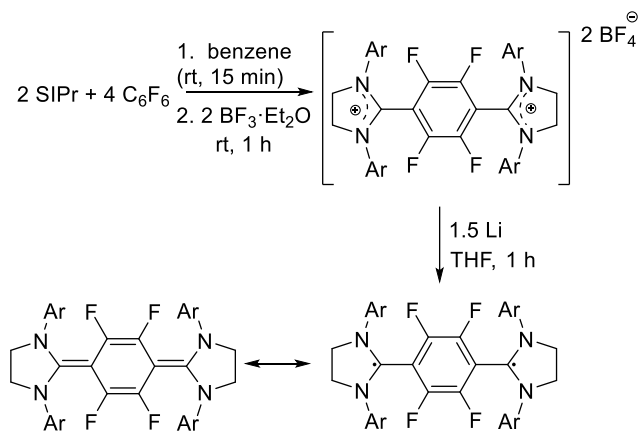
Scheme 3. Previous examples of single and double C-F activation of perfluoroarenes by NHCs. This work describes the triple C-F bond activation and synthesis of **1** (Ar=2,6-*i*Pr₂-C₆H₃)

The reaction of IDipp (IDipp=1,3-bis(2,6-diisopropylphenyl)-imidazole-2-ylidene) with $\text{C}_5\text{F}_5\text{N}$ in toluene led to the ‘*penta*-substituted’ imidazolium bifluoride salt, along with the liberation of one molecule HF (Scheme 3).

Chapter III: Saturated N-Heterocyclic carbene based Kekulé di-radicaloids via double C-F activation

Due to lower HOMO-LUMO energy gap of saturated NHCs than their unsaturated counterparts, the capability of saturated NHCs to stabilize organic radicals should be better. Recently, we have studied the reactivity of C_6F_6 and $\text{C}_6\text{F}_5\text{CF}_3$ with SIPr. In this chapter, we have shown the utilization of C–F bond activation of C_6F_6 chemistry to realize a SIPr based Thiele's hydrocarbon spanned by a C_6F_4 linker. The question remain whether the four substituted fluorine atoms at the central phenylene ring of **3** would destabilize the quinoid state and stabilize the biradical state. A further

impetus comes from the works of Abe and coworkers who showed the increase in the biradical character in 1,4-Bis-(4,5-diphenylimidazol-2-ylidene) tetrafluoro cyclohexa-2,5-diene (tf-BDPI-2Y) from parent BDPI-2Y. Although tf-BDPI-2Y was not structurally characterized, they were able to obtain the single crystal structure of the dimerized product (tF-BDPI-2YD).



Scheme 4. Stepwise access to fluorine-based Thiele's hydrocarbon.

We have performed the reaction of SIPr and C_6F_6 , but have added BF_3 -ether to the reaction mixture after 15 minutes for the isolation of the orange colored dicationic salt with two BF_4^- molecules as the counter anions (Scheme 4). Surprisingly, in situ addition of Mg powder at $0^\circ C$ in the reaction mixture of SIPr and C_6F_6 in THF led to the formation of the fluorine version of Thiele's hydrocarbon in one step. The Mg is oxidized to Mg(II) by capturing two fluoride anions and is precipitated out as MgF_2 from the system. The generation of MgF_2 also inhibits the HF elimination. In order to get the electronic structure and to understand the bonding scenario in Thiele's hydrocarbon, DFT calculations were performed at B3LYP/def2-SVP level of theory (see Computational Details). Computed electronic states of it reveal that close-shell singlet remains the electronic ground state with singlet-triplet energy difference ($\Delta E_{S \rightarrow T}$) of $-23.7 \text{ kcal mol}^{-1}$. The

computed bond lengths and angles of singlet state, than the triplet state structure, are in good agreement with the experimentally obtained X-ray crystal structure, as can be seen from the alignments and superposition plot of the conformers. It is of note here that the replacement of H by F led to decrease of S→T gap by 5.4 kcal mol⁻¹. No diradical character was found for this compound indicating the quinoidal bond nature. Ongoing studies are focused on extending the C-F bond activation to other NHC derived diradicaloids.

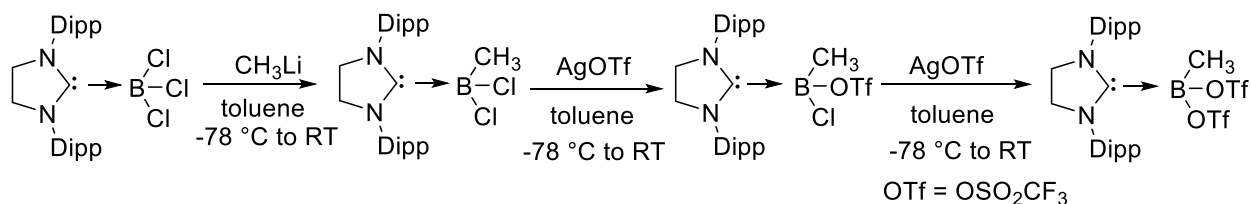
Chapter IV: Stepwise nucleophilic substitution to access saturated N-heterocyclic carbene haloboranes with boron–methyl bonds

The combination of an N-heterocyclic carbene (NHC) with a borane usually results in a complex called a NHC·borane. The synthesis of more than two dozen NHC·borane complexes of composition NHC·BX₃, NHC·BHX₂, NHC·BH₂X, etc. have been reported, mainly from the groups of Curran, Braunschweig, Robinson, Tamm, and others. Interestingly, a survey of known NHC·RBX₂ with different R groups reveal that common functional groups in carbon chemistry like methyl groups are rarely found bound to boron atoms in NHC·borane adducts. For example, NHC·BCl₂Ph is known,ⁱ but NHC·BCl₂Me is unknown. One reason could be the needed borane (MeBCl₂) is not widely available. It is prepared from the reaction of Me₃SnCl with excess BCl₃ that gives rise to a mixture of products (eqn. 1). MeBCl₂ has a boiling point of 11 °C, ignites in contact with air, and should be stored in a Schlenk tube equipped with a grease-free stopcock at a temperature below –30 °C.ⁱⁱ So, *handling of MeBCl₂ under laboratory condition is non-trivial.* The other reason is that in carbon chemistry the methyl group behaves as electron donor (+I effect), while in boron chemistry that the methyl groups, contrary to the common conviction, are electron-withdrawing (–I effect) due to the difference in electronegativity between carbon (2.5) and boron

(2.0). So, we were interested to make NHC·haloborane adducts, where one of the substituents of the boron atom is a methyl group. It is of note here that MeBCl₂ was detected as an intermediate in the chemical vapor deposition synthesis of boron carbide,ⁱⁱⁱ and studying the chemistry of MeBCl₂ might provide a deeper understanding of its chemical reactivity.



Herein we demonstrate a detailed study of nucleophilic substitution reactions of SIDipp·BCl₃ compound, which led to SIDipp·BMeCl₂ adduct. This is the first carbene·BMeCl₂ adduct and it does not require the use of hazardous MeBCl₂. Removal of another chlorine from this with the trifluoromethanesulfonate (OTf) group resulted in an unusual NHC·borane, SIDipp·B(Me)(Cl)(OTf), where the three groups attached to the boron center are different. Subsequent removal of another chloride by OTf moiety led to SIDipp·B(Me)(OTf)₂.

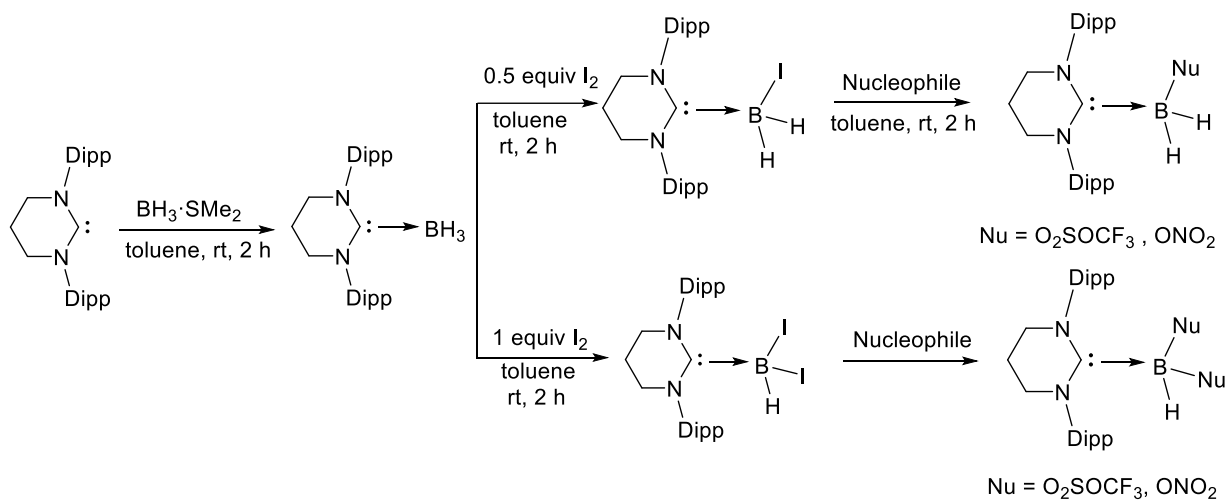


Scheme 5. Synthesis of NHC-Boranes with the boron methyl bond.

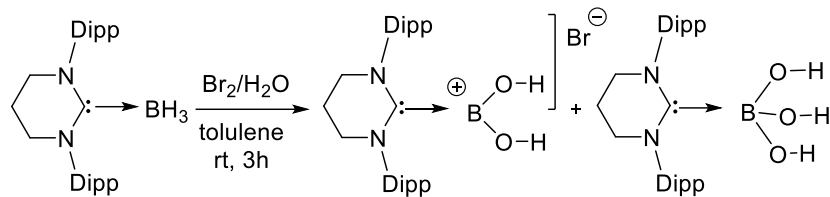
NHC·boranes are typically readily accessible, but we have mentioned in the introduction that no NHC adduct of MeBCl₂ has been known. The hesitance of the chemistry community probably stems from the synthetic routes, which are tedious and require special techniques. Here we have prepared saturated N-Heterocyclic carbene boranes bearing methyl groups by simple salt metathesis reaction starting from SIDipp·BCl₃.

Chapter V: The chemistry of six-membered N-heterocyclic carbene boranes

The reports of six-membered carbenes are limited in literature partly due to their less thermal stability and structural rigidity though they feature higher HOMO and Lower HOMO-LUMO gap compared to typical five-membered NHCs. Due to our current interest in boron chemistry, we have studied the synthesis and reactivity of saturated six-membered N-heterocyclic carbene (6-SIDipp) borane adduct. 6-NHC-BH₃ is amenable to further functionalization via iodination, providing access to NHC mono and diboryl iodides, selectively, which undergo nucleophilic substitution reactions with AgOTf and AgNO₃ to give boron compounds with OTf and ONO₂ functionalities (Scheme 6). Dihydroxyborenium cations, the cationic analogues of phenylboronic acid, are difficult to prepare due to the lacking of any R group. Herein, we have prepared a dihydroxyborenium cation conveniently by reacting **1** with bromine-water.



Scheme 6. Synthesis and halogenation of 6NHC-BH₃ and subsequent nucleophilic substitution reactions.



Scheme 7. Preparation of a dihydroxy borenium cation in a single step from 6NHC-BH₃.

The reaction of **1** with bromine water led to an immediate color change from colorless to yellow and afforded a 6-SIDipp stabilized dihydroxyborenium cation at room temperature in 3 h (Scheme 7). Both the compounds are separated by fractional crystallization. There is no report of the formation of NHC·B(OH)₃ type Lewis adducts so far.

While the body of work on carbene-borane chemistry is growing, the carbene component is mainly restricted to two classes of carbenes: (a) Arduengo type five-membered NHC and (b) CAAC. Here, we have introduced a new NHC, 6-SIDipp for NHC·borane chemistry, and described a detailed study of substitution reactions of 6-SIDipp·BH₃. These results have uncovered the facile substitution to the coordinatively saturated *sp*³ boron atom in 6-SIDipp·BH₃ with a range of functional groups such as iodide, triflate, ONO₂.

Details of Publications:

1. **G. Kundu**, S. Tothadi, S. S. Sen, Six membered saturated N-Heterocyclic carbene reactivity with boranes: B-H activation vs adduct formation. (*Manuscript under preparation*)
2. **G. Kundu**, S. R. Das, S. Tothadi, K. Vanka, S. S. Sen, Saturated N-Heterocyclic carbene based Kekule bi-radicaloids with a naphthalene linker. (*Manuscript under preparation*)
3. **G. Kundu**, K. Balayan, S. Tothadi, Six-membered saturated NHC Stabilized borenium cations: isolation of a cationic analogue of borinic Acid (*Manuscript under revision*).

4. **G. Kundu**, V. S. Ajithkumar, S. Tothadi, S. S. Sen, *Chem. Comm.* **2022**, 58, 3783-3786.
5. **G. Kundu**, V. S. Ajithkumar, M. K. Bisai, S. Tothadi, T. Das, K. Vanka, S. S. Sen, *Chem. Commun.* **2021**, 57, 4428–4431.
6. **G. Kundu**, S. Pahar, S. Tothadi, S. S. Sen, *Organometallics* **2020**, 39, 4696 – 4703.
7. **G. Kundu**, S. De, S. Tothadi, A. Das, D. Koley, S. S. Sen, *Chem. Eur. J.* **2019**, 25, 16533 – 16537. (*Hot paper*)
8. M. Pait ^{||}, **G. Kundu** ^{||}, S. Tothadi, S. Karak, S. Jain, K. Vanka, S. S. Sen. *Angew. Chem. Int. Ed.* **2019**, 58, 2804 – 2808. (^{||}: *Equal contribution*)

References:

1. Arduengo, A. J.; Harlow; R. L.; Kline, M. *J. Am. Chem. Soc.* **1991**, 113, 361–363.
2. Wanzlick, H.-W.; Schönher, H.-J. *Angew. Chem. Int. Ed.* **1968**, 7, 141–142.
3. Hopkinson, M. N.; Richter, C.; Schedler M.; Glorius, F. *Nature*, **2014**, 510, 485-496.
4. (a) Paul, U. S. D.; Radius, U. *Chem. Eur. J.* **2017**, 23, 3993–4009. (b) Styra, S.; Melaimi, M.; Moore, C. E.; Rheingold, A. L.; Augenstein, T.; Breher, F.; Bertrand, G. *Chem. Eur. J.* **2015**, 21, 8441–8446. (c) Kim, Y.; Lee, E. *Chem. Commun.* **2016**, 52, 10922–10925. (d) Leclercq, M. C.; Gorelsky, S. I.; Gabidullin, B. M.; Korobkov, I.; Baker, R. T. *Chem. Eur. J.* **2016**, 22, 8063–8067. (e) Sen, S. S.; Roesky, H. W. *Chem. Commun.* **2018**, 54, 5046–5057.

Gargi Kundu

Gargi Kundu
(Student)

Sakya Singha Sen

(Dr. Sakya Singha Sen)
(Supervisor)

Chapter-1

Introduction to Saturated N-heterocyclic Carbene Chemistry

Abstract: This chapter presents an overview of the formidable synthetic challenges in the development of the chemistry of N-heterocyclic carbenes and the use of the compounds with main group elements in small molecule activation and other plentiful applications in commercially important developments. A general introduction delineating the summary of important compounds in this research area is given with the literature reports. The aims of the thesis and the results are subsequently outlined.

1.1. Introduction:

1.1.1 A brief history of N-heterocyclic carbenes:

Carbenes are a fascinating class of organic molecules with a divalent carbon atom having six electrons in its valence shell.¹ The incomplete octet and coordinative unsaturation make carbenes inherently unstable and highly reactive, which can be generated as transient intermediates in many organic transformations such as cyclopropanation. Despite the attempted syntheses as early as 1835, the isolation and unambiguous characterization of a free, uncoordinated carbene remained elusive until pioneering studies in the late 1980s and early 1990s.^{2,3} In 1988, Bertrand and co-workers reported the first preparation of an isolable carbene stabilized by the adjacent phosphorus and silicon substituents via photolysis of the diazo compounds and diazo- η^5 -phosphorus derivatives.⁴

Based on the type of the carbon framework involved, carbene molecules are classified as classical carbene or N-heterocyclic carbenes (NHCs). In 1991, Arduengo et al. reported the first N-heterocyclic carbene (NHC) [1,3-di(adamantyl)imidazol-2-ylidene (IAd)] with structural features (Figure 1.1.1) inspired by previous understandings.⁵ NHCs are excellent ligands for transition metals, and have been used in multiple applications like catalytic transformations. Lately, studying their reactivity after coordination with main group elements and application as organocatalysts have unlocked new vistas, which are constantly evolving since last decades.

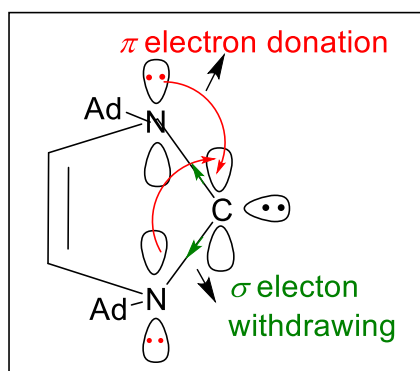


Figure 1.1.1. Ground-state electronic structure of imidazol-2-ylidenes (Ad = adamantane).

1.1.2. Structure and general properties of NHCs:

The stability of an NHC is determined by the stability of the lone pair of electrons on the carbon centre (C2). The lone pair of the electron is stabilized through i) electronic and steric effects of the substituents, ii) ring sizes and degree of heteroatom stabilization.⁶ For the IAd carbene, the wingtip nitrogen atoms provide electronic stabilizations through σ -electron-withdrawing and π -electron-donating nature, thereby stabilizing the structure both a) inductively through lowering the energy of the occupied s-orbital and b) mesomerically by donating electron density into the empty p-orbital (Figure 1.1.2). The bulky adamantyl groups on nitrogen atoms of the NHC sterically protect (Figure 1.1.2) the lone pair of electrons at C2 position. This also facilitates to stabilize the species kinetically by inhibiting any possible dimerization via Wanzlick equilibrium to form the corresponding olefin. The unsaturated backbone further provides electronic stabilization due to aromaticity. The cyclic structure favours bent singlet ground state, and the ring geometry influences sterics and electronics.

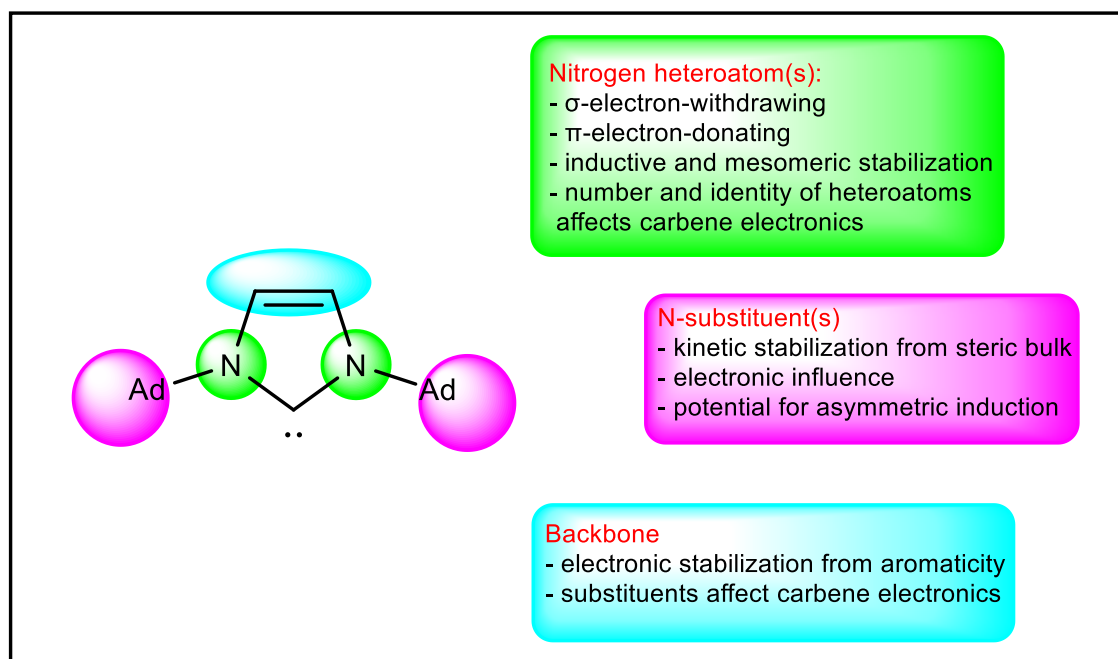


Figure 1.1.2. General structural features of IAd, detailing the effects of the ring size, nitrogen heteroatoms, and the ring backbone and nitrogen-substituents on the stability and reactivity of the NHC.

1.1.3. Electronic structure of carbene:

Based on the location of the non-bonding electrons in different orbitals and their spin states, carbenes can exist in two different forms:

- **Singlet carbene**, where the non-bonding electrons stay in the same orbital, and both of them have opposite spins
- **Triplet carbene**, where the non-bonding electrons exist in different orbitals, and they have parallel spins

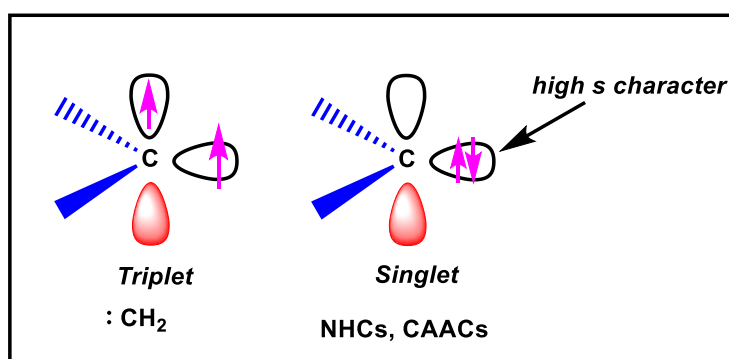


Figure 1.1.3. Electronic states of different NHCs.

In contrast to classical carbenes, NHCs such as IAd display a singlet ground-state electronic configuration, where the sp^2 hybridized lone pair is the highest occupied molecular orbital (HOMO) and an unoccupied p -orbital at the C2 carbon is the lowest unoccupied molecular orbital (LUMO) (Figure 1.1.3).

1.1.4. Different types of N-heterocyclic carbenes:

Based on the hybridization of the C3 and C4 atoms of 5-membered NHCs, they are classified into two types; (i) unsaturated NHCs and (ii) Saturated NHCs. In this thesis, we have established their relative advantages for various reactions.

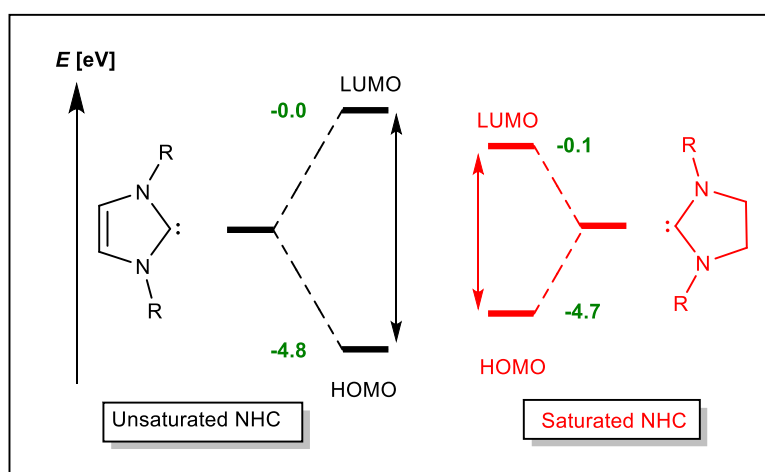


Figure 1.1.4: HOMO-LUMO gap between typical unsaturated NHCs and saturated NHCs.

The calculated values are taken from Munz et al. *Organometallics* 2018, 37, 275–289.⁷

Why saturated N-heterocyclic carbene?

- *Sigma donation increases*
- *π -acidity increases*
- *HOMO-LUMO gap decreases*
- *Higher nucleophilic character can be useful for the activation of C-F, C-N, C-H sigma bonds as well as small molecules*

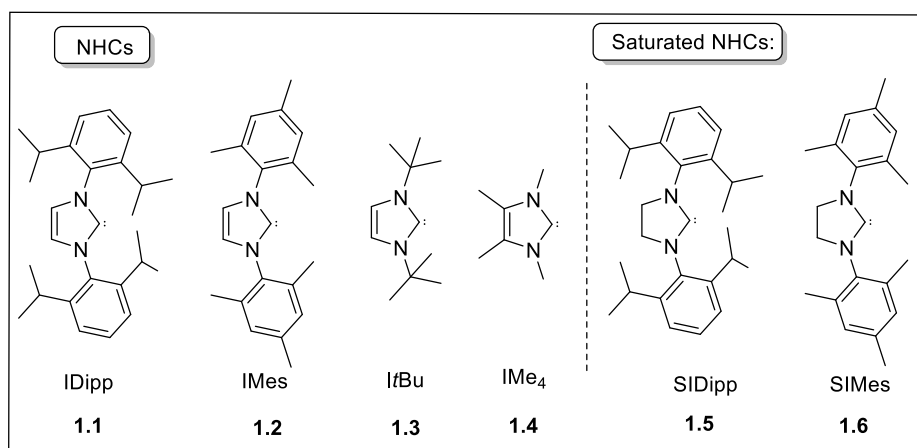


Figure 1.1.5. Structures of some of the commonly applied NHCs. Dipp, diisopropyl; Mes, mesityl; *t*Bu, tert-butyl

1.1.5. Different types carbenes except NHCs:**1.1.5.1. Cyclic (alkyl)- (amino)carbenes, CAAC:**

cyclic(alkyl)(amino)carbenes (CAACs) are a novel class of stable singlet carbene ligands developed by Bertrand and co-workers in 2005. The replacement of one of the electronegative nitrogen atoms of NHCs by a strong σ -donor sp^3 (alkyl) carbon atom makes CAAC ligands even more electron-rich, surpassing most NHCs and phosphines (Figure 1.1.1.1).⁸⁻¹⁰ Furthermore, owing to the presence of a quaternary carbon atom in a position at the adjacent

to the carbene center, CAACs feature a steric environment that differentiate them melodramatically from both NHCs and phosphines.

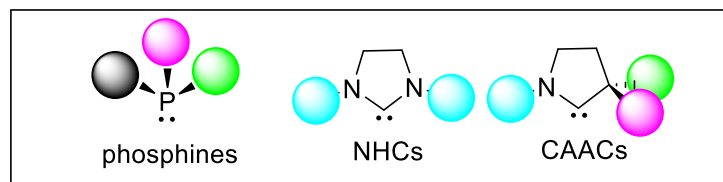


Figure 1.1.5.1: General structural features of CAACs.

1.1.5.2. *N,N'*-Diamidocarbenes, DAC:

A *N,N'*-diamidocarbene (DAC) (Figure 1.1.5.2) is constituted when carbonyl groups are incorporated into an N-heterocyclic carbene scaffold. Through quick and high-yielding procedures, DACs were found to activate a broad range of primary as well as secondary aliphatic and aromatic amines.^{8, 11-13} The nonbonding electron pairs of the nitrogen atoms undergo resonance with the vacant $\pi^*(C=O)$ orbitals, which results in the decrease of the electron density at the carbene carbon atom. While DAC carbene has a singlet ground state with a calculated singlet–triplet gap of ~ 45 kcal/mol, which is very lower than the typical NHCs (81 kcal/mol).⁸ This substantially lower HOMO-LUMO energy for DACs leads to an enhanced electrophilicity and an exceptional reactivity. The relative rates measured for the insertion of the DAC into the primary amines were consistent with an electrophilic activation mechanism. Collectively, these results constituted the first ambiphilic process for an isolable carbene. Similar to transient, electrophilic carbenes and unlike NHCs, DACs underwent a variety of transformations with a broad range of small molecules including the metal-free transfer hydrogenations,¹⁴ insertion into pnictogen-H bond, and the unprecedented reversible coupling of carbon monoxide.^{8, 11-13, 15} Along with this, formal [2+1] cycloadditions were seen between

DACs and a range of alkenes, aldehydes, alkynes, and nitriles including the first examples between an isolable carbene and alkynes or electron-rich alkenes.

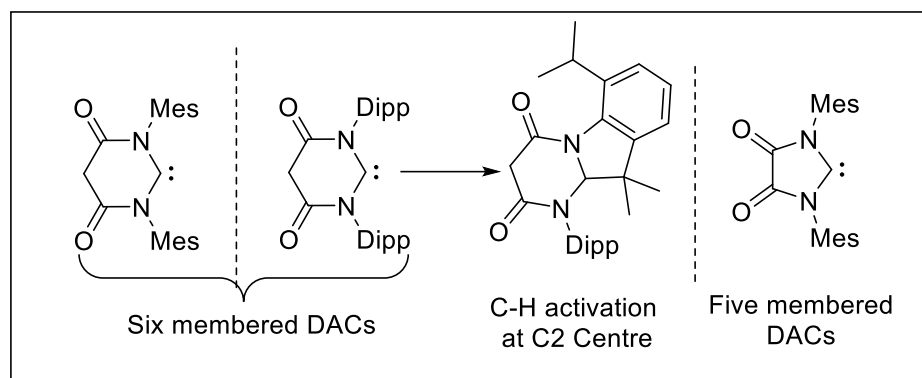


Figure 1.1.5.1: General structural features of DACs.

1.2 Carbenes as an alternative to the transition metal complexes

The quest for "metal-free" catalysis is on the horizon. Increasing pressures for catalytic processes with reduced environmental impact spur the search for improved synthetic transformations with minimal waste production, less energy consumption, and avoid the generation of toxic substances. One approach to accomplishing this target is to use more benign main group compounds as catalyst. Striking headways in the field of low valent main-group compounds have been accomplished such as B(I),^{16, 17} Al(I),^{18, 19} Si(0),^{20, 21} and Ge(0)²²⁻²⁴ in the form of multiple bonded species, carbenoids, and donor stabilized (e.g. imine, phosphine) atoms.²⁵⁻²⁹ These highly reactive species have similar features with those of transition-metal complexes in the form of small energy separated frontier orbitals (Figure 1.2.1).³⁰

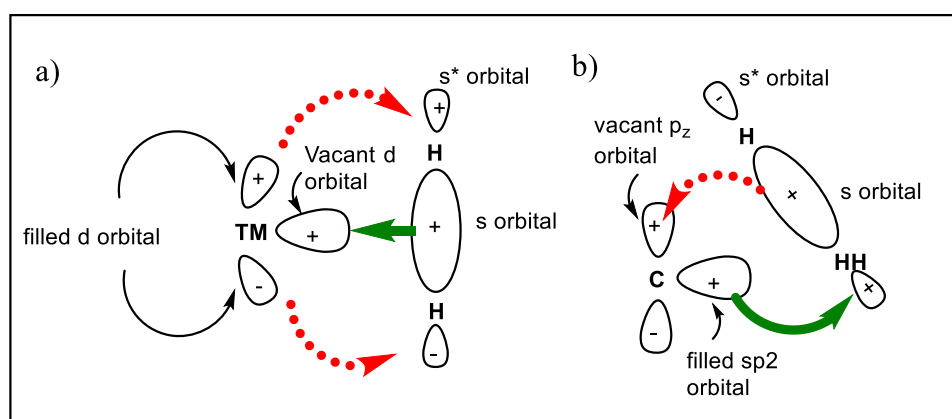


Figure 1.2.1. Frontier orbital interaction of dihydrogen with (a) transition metals, (b) singlet main group species e.g. carbenes, tetrylene

1.2.1. Carbenes in small molecule activations:

The importance of small molecules like H_2 , CO , CO_2 , NH_3 is that they are ubiquitous, relatively inexpensive, synthons for constructing more complex molecules, and produced in large scales in industrial processes. Moreover, the most of the homogeneous catalytic cycles involve such small molecules, like hydrogen, olefins, carbon monoxide, ammonia. Therefore, it is deemed desirable to use them into syntheses of value-added chemical products.³¹ However, at the same time they are thermodynamically very stable. The activation of such relatively inert bonds usually requires a catalyst. The typical catalysts feature late transition metals. It is the amenability of a transition metal to be in a variety of oxidation states, to coordinate to a substrate, and to be a good source/sink for electrons depending on the nature of the transition state. As a result, the most active transition metal catalysts are based on Pt, Pd, Rh, Ru, Ir, Os etc. However, the current trend in catalysis is to move to cheaper and greener alternatives because late transition metal based catalysts are expensive as well as there are some concerns on the incorporation of such heavy metals into products. Main group elements, on the other hand, are cheap, more abundant, and have lesser issues with respect to toxicity. The small

molecule activation by compounds with main group element has been summarized by Nikonov and co-workers (ref 32).^{31, 32}

Singlet carbenes have a filled nonbonding orbital and a vacant orbital, which resembles to the transition metal centers.^{33,34} Even though the orbitals of carbenes do not as exactly match for interaction with hydrogen like transition metal, the group of Bertrand and co-workers in 2007 reported the activation of dihydrogen demonstrating sufficient overlap between them.^{6, 35, 36} In that work, they have shown that suitably designed CAAC (**1.7**) can undergo an oxidative addition with H₂ at the carbene carbon centre (Figure 1.2.1.1.).^{35,36} Computational studies reveal that the carbene's lone pair of electrons interact with the antibonding orbital of H₂ at first with subsequent attack from the hydride to the carbocation.. This nucleophilic activation process was also observed in the reaction of **1.7** with NH₃ (Figure 1.2.1.1.).³⁵

Activation of ammonia is a challenging reaction, as the N–H bond dissociation energy is high (107.6 kcal/mol).³⁷ The high π acceptor properties of five and six membered DACs resulted in facile cleavage of the N-H bond of NH₃.^{13, 38} Initially, it was hypothesized that nucleophilic NHCs were inert toward NH₃ activation, although examples of ammonia splitting by NHCs have been recently documented in literature.³⁹

The mechanism for ammonia activation by DACs was investigated by reacting **1.11** with various para-substituted anilines.⁴⁰ The Hammett plot featured a negative slope, consistent with the build-up of positive charge at the amine nitrogen atom, and hence it has proved that the electrophilic nature of DACs actually helps in the ammonia activation.⁴¹

On the basis of experimental studies and due to more basicity and nucleophilicity of ammonia compared to aniline, the insertion of DACs into the N-H bond of ammonia is likely initiated by overlap of NH₃ lone pair with the empty orbital of carbene.⁴⁰ However, the activation of N-

H bonds of diarylamines with **1.11** underwent fastest when the diarylamines are electron deficient in nature. All these results suggest that **1.11** can cleave the N–H bonds of acidic or basic amines through both nucleophilic or electrophilic pathways, respectively.⁴¹ Notably, **1.11** represents the first isolable carbene to mechanistically exhibit ambiphilicity, a property usually reserved for more transient species such as the halocarbenes and 2-adamantylidene.^{42, 43}

While the NHCs and CAACs are less reactive towards carbon monoxide, DACs **1.10** and **1.11** can smoothly forms ketenes **1.15** and **1.16** from the reaction with carbon monoxide at ambient temperature in a reversible way (Figure 1.2.1.1.).^{4, 44, 45} Similarly, DACs can react with isonitriles, which are isoelectronic with CO, to give the respective ketenimines.⁴⁶

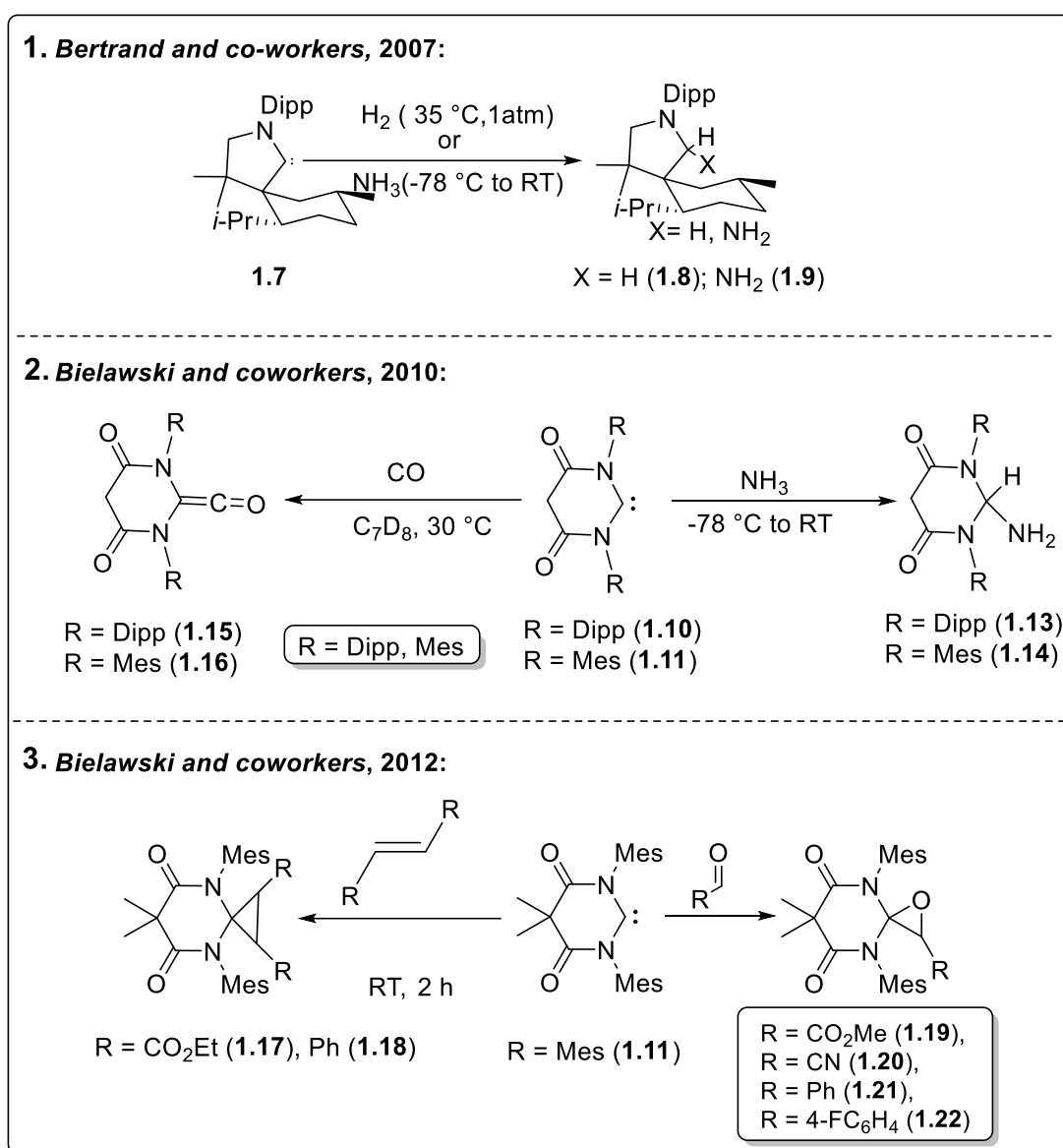


Figure 1.2.1.1. Carbene mediated small molecules activations; (1) CAAC mediated ammonia and hydrogen activations; (2) DAC mediated carbonyl and ammonia activations; (3) DAC mediated [2+1] cycloaddition reactions.

The chemistry of **1.10** and **1.11** mainly reflects that of the seven membered DAC, which also shows similar reactivities with isonitriles and carbon monoxide (Figure 1.2.1.1). Analogous reactions with CAACs and bicyclic NHCs have also been reported, while only DACs react reversibly with carbon monoxide.^{12, 13}

The [2+1] cycloaddition reaction, which is known as a cyclopropanation, with stable diamidocarbene derivatives, is a hallmark of carbene chemistry. Though this reactivity was witnessed only with transient species (e.g., triplet carbenes derived from diazo compounds), it is rarely seen for isolable stable carbenes. For example, the known NHCs and CAACs are not reactive towards olefins, and they can't convert them to exocyclic olefins or polymers.^{47, 48} DAC **1.7** enables the cyclopropanation reaction of electron-deficient as well as electron-rich alkenes including the vinyl ethers and the alkyl derivatives (Figure 1.2.1.1.).⁴⁹⁻⁵¹ The reaction of **1.11** with the *cis*-olefins (for example *cis*-stilbene) and diethyl maleate resulted in the *cis*-cyclopropanes, **1.17** and **1.18**, respectively via a stepwise process involving bond rotation prior to ring closure.⁴⁷ The treatment of the five-membered DAC with the same methyl acrylate produced an exocyclic olefin in place of a cyclopropane. DACs undergo similar [2+1] cycloadditions with aryl or alkyl aldehydes also to give epoxides like **1.19-1.22**.⁴⁷

1.2.2. Carbenes in C-F activations:

The activation of C-F bonds in fluorinated hydrocarbons is of fundamental interest from the standpoint of potential application in synthetic organic chemistry, pharmaceutical and agrochemistry as well as the ever-increasing environmental concerns related to the fluorinated compounds. Fluorinated hydrocarbons are major source for the alarming depletion to the ozone layer. Generally, transition metals are involved in the C-F bond activation, which has issues with terrestrial abundance and toxicity. Therefore, a huge effort is underway to develop new synthetic strategies for the activation of the C–F bonds.

Characteristics of the C-F bond

- Strongest covalent single bond
- Notoriously robust
- Toxicity of perfluorinated compounds

The activation of thermodynamically robust C–F bond usually requires an electron rich transition metal fragment.⁴⁸ There is an increasing recognition that the chemistry of the compounds with low-valent main-group elements resembles that of transition-metal complexes.⁴⁹⁻⁵¹ In fact, the groups of Timms and Margrave reported in early 1970s that one of the C–F bonds of C₆F₆ underwent oxidative addition with SiF₂ (generated *in situ*) to give C₆F₅SiF₃.³⁰ Surprisingly, even after their report, the research interest on the C–F bond activation by compounds with main group elements was remarkably low for the next three decades. It was only recently that N-heterocyclic carbene (NHCs) and cyclic alkyl amino carbenes (CAACs) have been explored for the C–F bond activation of perfluoroarenes.⁵²⁻⁵⁷ Alongside carbenes, the use of low-valent aluminum and silicon compounds has also emerged as powerful candidates to selectively activate the C–F bond of perfluoroarenes.^{30, 58-71}

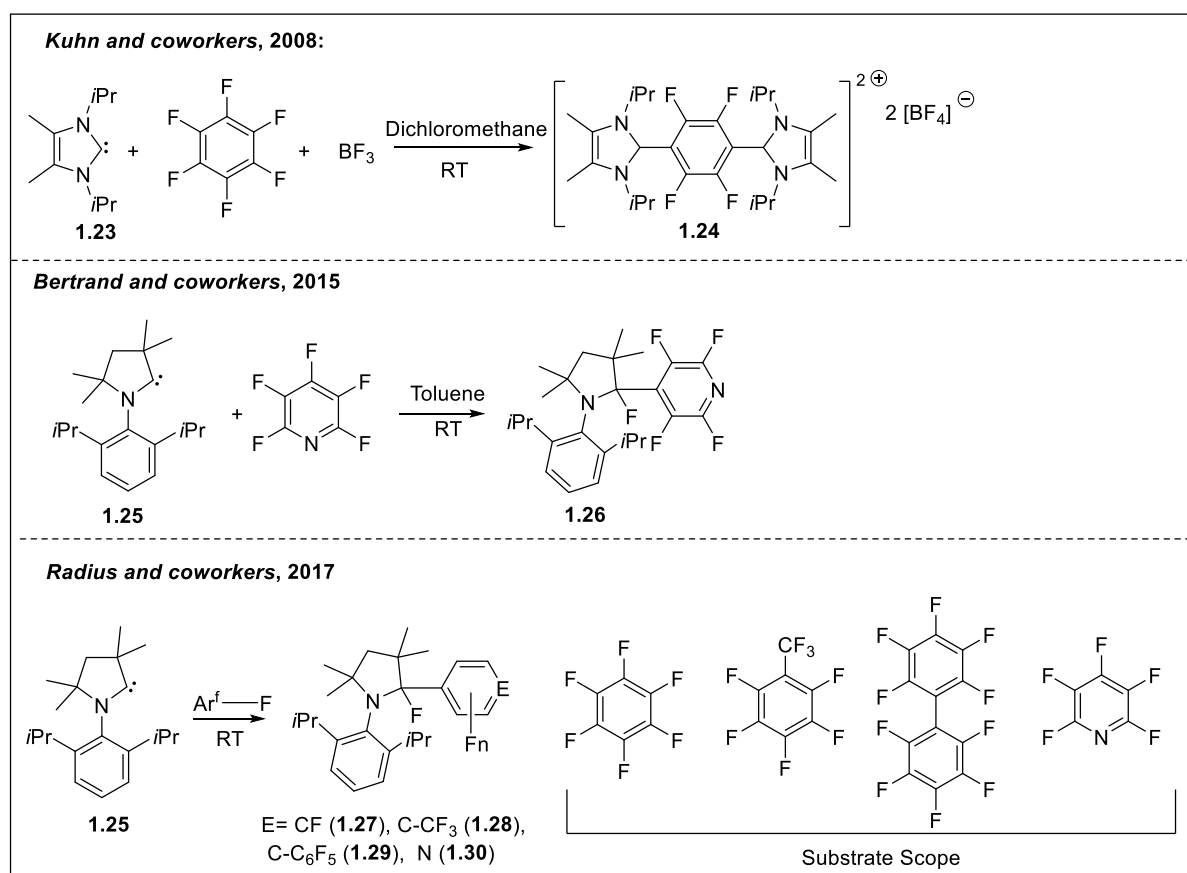


Figure 1.2.2.1. Carbenes in C-F activations of perfluoroarenes.

The very different electronic properties of various carbenes are reflected in their mode of the C–F bond activation. In 2015, Bertrand and co-workers showed the oxidative addition of the *para* C–F bond of pentafluoropyridine into the CAAC carbene centre which resulted **1.26** (Figure 1.2.2.1). Afterwards, the fluoride abstraction from this generated an iminium-pyridyl adduct, which was further treated with excess magnesium to produce a CAAC stabilized mono-radical compound. Later in 2017, the group of Radius has shown the 1,1-activation of the C–F bonds of different class of perfluoroarenes at the carbene center for CAAC^{methyl} (Figure 1.2.2.1).⁷² While CAAC has shown the oxidative addition at the carbene carbon centre, NHCs have a propensity to form octafluorotolyl imidazolium salt with HF₂⁻ as counter anion.^{73,74} The treatment of two equivalents of octafluorotoluene leads to an unexpected sequential substitution of fluorides in two separate perfluoro arene rings.⁵⁵ The utility for an excess C₆F₆ has also been noted by Kuhn and coworkers, who used C₆F₆ and *i*Pr₂Im^{Me2} in ~ 7:1 ratio in presence of BF₃·ether to activate the C–F bond.⁷² In this context, the saturated NHCs are predicted to be a stronger σ -donor and π -acceptor than their unsaturated analogues, but weaker than CAACs in both these aspects. A further impetus comes from the reactions of 5-SNHC with fluoroalkenes **1.31-1.33** by the group of Baker et al. in 2016 (Figure 1.2.2.2).⁶²

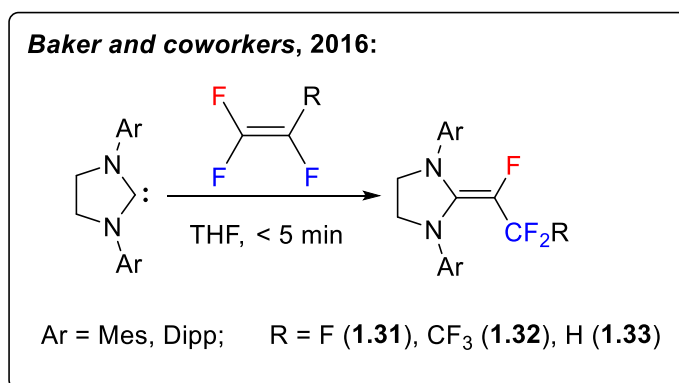


Figure 1.2.2.2: 5-SIDipp mediated C–F activations of perfluoro alkenes.

1.2.3. Carbenes in B-H, Si-H, P-H activations:

For the past years, it was thought that only the transition-metal centers can cleave the enthalpically strong bonds like B-H, Si-H and P-H etc. due to presence of their incompletely filled *d*-orbitals. In recent years, it has proved that many non-metallic systems are also capable of breaking these strong bonds.^{30, 58-61, 63-66, 69-71} As an example, singlet carbenes can easily activate small molecules like NH₃, CO,⁷⁵ H₂,³⁵ and P₄,⁷⁶⁻⁷⁸ which we have discussed above. Interestingly, carbenes can easily activate ammonia; which is a challenging target even for transition metals.^{11, 79-90} Similarly, the cleavage of bonds like Si-H, B-H and P-H and the oxidative addition of hydrosilanes, hydro-boranes, and hydrophosphines at vacant coordination sites of transition metals are well-established and are well-thought-out as key steps for the transition-metal-catalyzed hydrosilylation, hydroboration, and hydrophosphination of multiple bonds. In 2010, Bertrand and co-workers shows the E-H (E = Si, B, P) bond activations at the different NHC and CAAC centres (Figure 1.2.2.3.).⁹¹ The BH₃ forms an adduct with NHCs as well as CAAC carbenes, but HBpin are shown to undergo 1,1 B-H activation (Figure 1.2.2.4) at the carbene carbon center of CAACs (**1.39a**, **1.39b**, **1.40a**, **1.40b**). On the other hand, the 5-SIDipp underwent in to the C-N bond rupture of the SNHC and an unexpected dimer, **1.34** formation (Figure 1.2.2.3.).⁹¹ The reaction of phenylsilane with CAACs and 5-SIDipp led to the Si-H bond activation at the carbene carbon atom and furnish **1.36** (Figure 1.2.2.3) and **1.41a**, **1.41b**, **1.42a**, **1.42b** (1.2.2.4) at mild condition.⁹¹

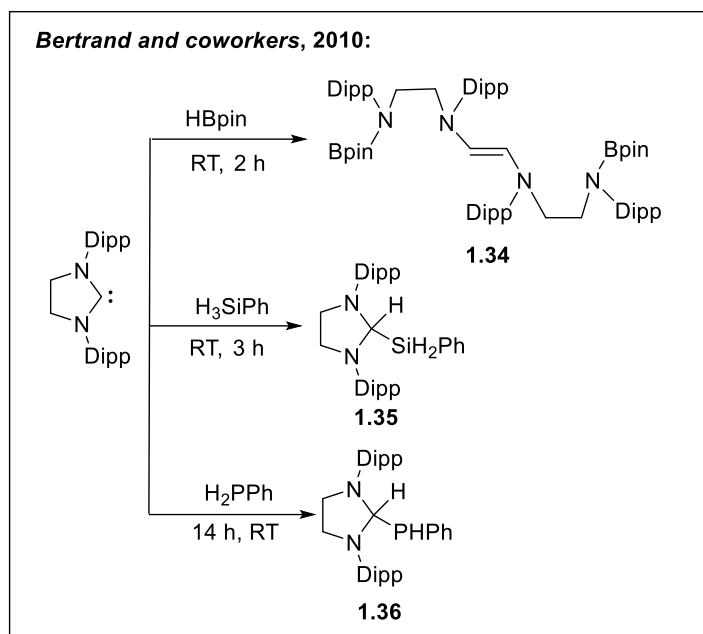


Figure 1.2.2.3. 5-SIDipp mediated C-F, B-H, P-H bond activation.

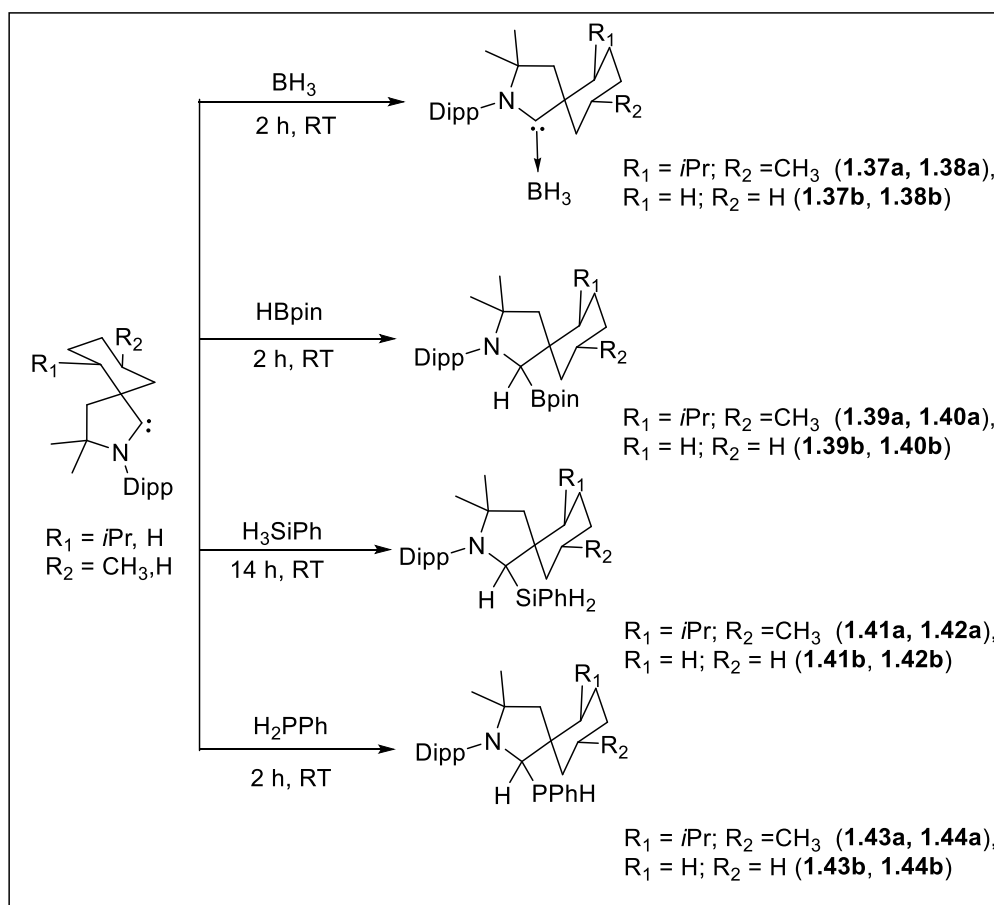


Figure 1.2.2.4. 5-SIDipp and CAAC mediated B-H, Si-H and P-H activations.

Carbenes are known to form Lewis acid–base adducts^{34, 92} with compounds of other main-group elements. In 2010, the group of Bertrand and co-workers have studied their reactivity with primary and secondary phosphanes.⁹¹ CAAC carbenes react with phenylphosphane at room temperature, which resulted in the oxidative-addition products **1.43a** and **1.44a** as mixtures of diastereomers.⁹¹ While the CAACs were inert towards the sterically more demanding diphenylphosphane, the smaller CAAC underwent a slow but clean reaction at room temperature to give the oxidative addition products, **1.43b** and **1.44b** (Figure 1.2.2.4). Further, they have also extended the similar reactivity with 5-SIDipp, which did not react with diphenylphosphane, but underwent insertion into the P-H bond of phenylphosphane (Figure 1.2.2.3) to form the adduct **1.36**.⁹¹

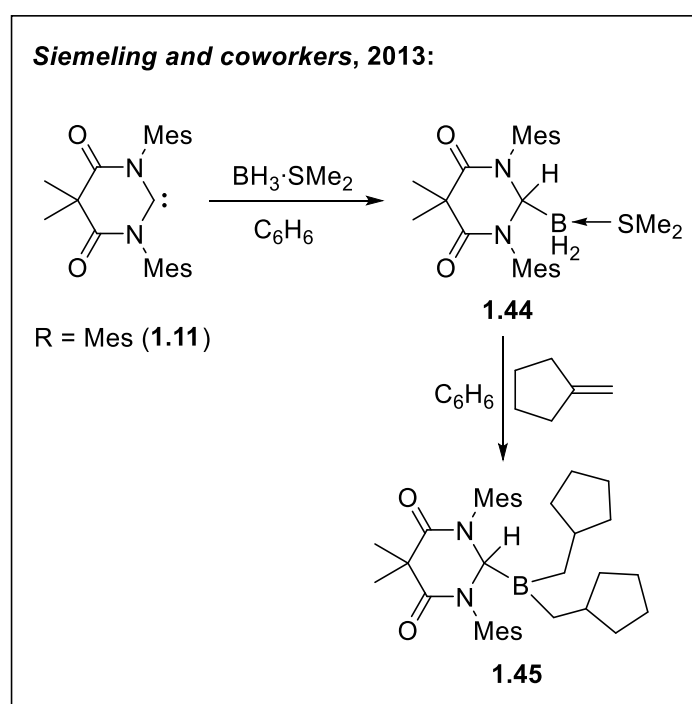


Figure 1.2.2.5. DAC mediated B-H activations of BH_3 .

Though the NHCs and CAACs forms a stable Lewis acid-base adduct with BH_3 , in 2013, the group of Siemeling and coworkers has reported that DAC **1.7** inserts into a diverse array of the B–H (Figure 1.2.2.5.) and B–B bonds, but forms Lewis adducts with boron trihalides.^{34, 92}

While the latter reflects the nucleophilic character of DAC, its insertions into BH_3 and other B–H fragments are consistent with an ambiphilic description given that the (formerly carbenic) carbon center abstracts a hydride following ligation to the borane. The insertion product, **1.44** derived from the reaction of **1.7** and $\text{BH}_3\cdot\text{SMe}_2$ was found to enable hydroborations through a polar mechanism involving hydride transfer. The chemistry of the tetra-coordinate $\text{DAC}\cdot\text{BH}_3$ adducts is different compared to the analogous $\text{NHC}\cdot\text{BH}_3$ species, whose reactions often occur through the radical pathways, and need initiators, although addition to arynes via a polar mechanism has been described.^{93, 94}

1.3 Carbenes in the stabilization of Kekulé diradicals:

Molecular species bearing two unpaired electrons in two energetically equivalent molecular orbitals are termed as diradical species.⁹⁵ Based on electron delocalization and frontier molecular orbitals, diradicals can be divided into three classes: (a) Kekulé, (b) non-Kekulé, and (c) antiaromatic. Based on the spin state of individual electrons in Kekulé and non-Kekulé diradicals, they can exist in singlet state (where the individual electron spins are opposite) or triplet state (where the individual electron spins are same).⁹⁶ Molecules having partial singlet diradical nature in their ground state are often called as diradicaloids,⁹⁷⁻⁹⁹ where the interaction between the two oppositely spinning electrons leads to their further classification as open shell and closed shell diradicaloids. Because of the presence of two unpaired electrons, diradicaloids possess very high reactivity. Stabilization of diradicaloids is typically achieved through delocalization over π -conjugated moieties, and their development are of great interests to chemists owing to their discrete chemical properties and potential applications in molecular electronics, nonlinear optics, and organic spintronics.¹⁰⁰⁻¹⁰³

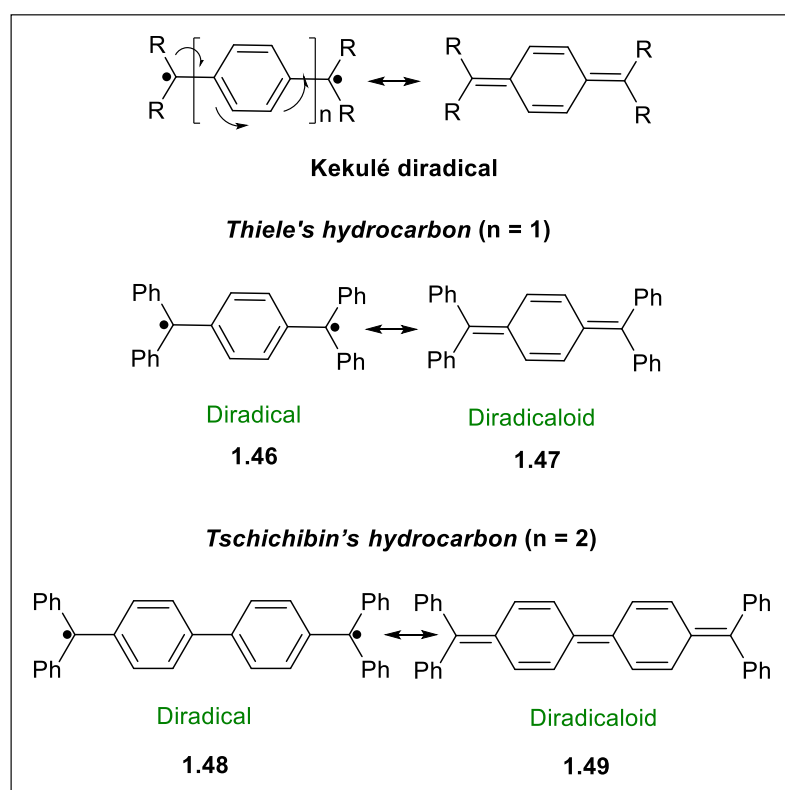


Figure 1.3.1. Electronic distribution in different conformations of Kekulé diradicals.

Kekulé diradicaloids have received remarkable attention primarily due to their unique electronic properties, which is originated from the intermediate bonding of the frontier π -electrons. Based on the number of aryl moieties involved in the formation of the diradicaloid, they are named as Thiele's hydrocarbon ($n = 1$), Chichibabin hydrocarbon ($n = 2$) or Muller's hydrocarbon ($n = 3$).¹⁰⁴⁻¹¹⁰ While studies on linker length variation in Kekulé diradicaloids are often cited in literatures, instances on functionality variation on them is very scarce.

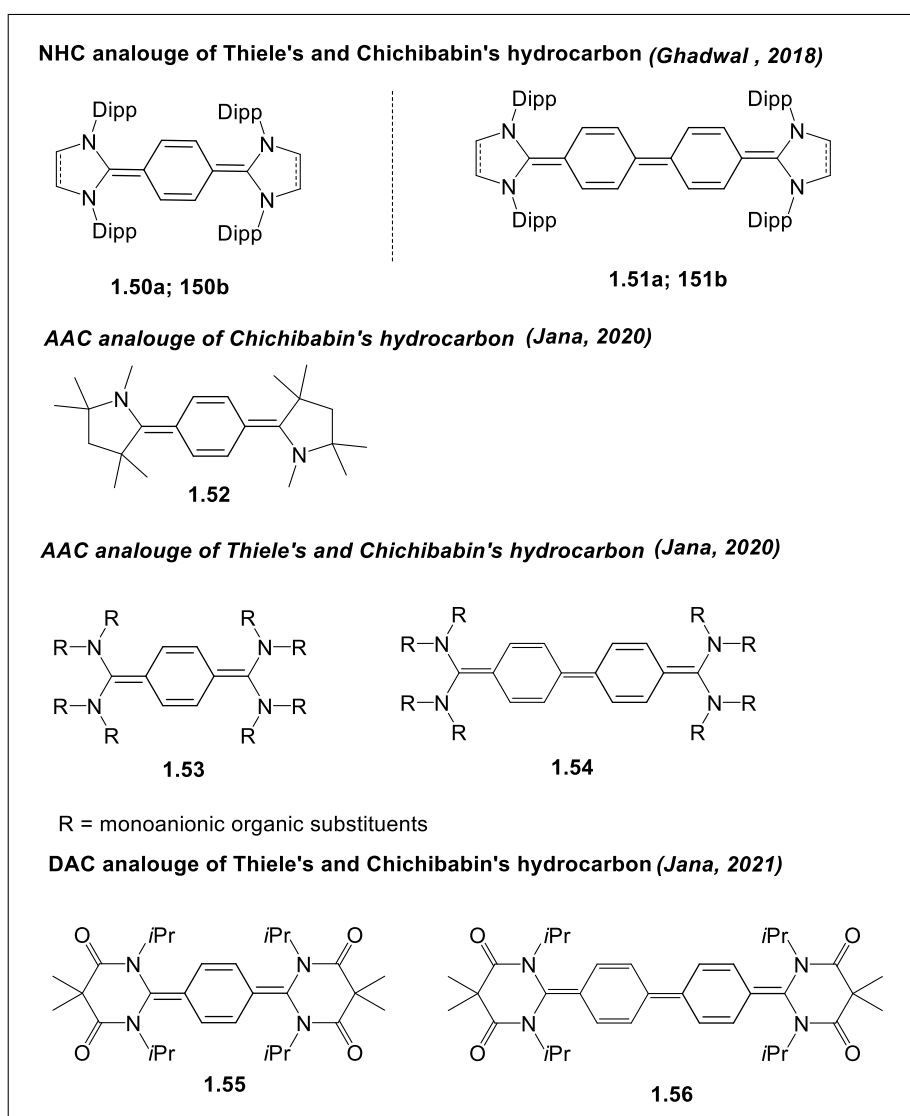


Figure 1.3.2. Selected carbene analogues of Thiele's and Chichibabin's hydrocarbon.

Radicals derived from NHCs are astoundingly small,^{53, 54, 104, 105, 107, 110-112} although very recently NHC derivatives of Kekulé diradicaloids have been realized by Ghadwal and co-workers.^{110, 113, 114}

Of the various Kekulé hydrocarbons, Thiele's and Chichibabin's hydrocarbons are interesting because of their existence in intermediate form between an open-shell biradical and a closed-shell quinonoid form.¹¹⁵ The inherent reactivity from the existence of two unpaired electrons creates a high synthetic challenge for Chichibabin hydrocarbon. In 2018, the group of Ghadwal and co-workers accessed the first NHC analogues of Thiele's and Chichibabin's (Figure 1.3.2.)

hydrocarbons with a singlet-triplet gap of -25.6 (**1.50a**) and -10.7 kcal mol⁻¹ (**1.51a**) (B3LYP).^{114, 116} Later on, the same group prepared the first SNHC analogues of Thiele's and Chichibabin's hydrocarbons with a singlet and triplet energy gap -29.1 (**1.50b**) and -10.7 (**1.51b**) kcal mol⁻¹, (Figure 1.3.2.) respectively. Motivated by this work, the group of Jana and co-workers reported the Thiele's and Chichibabin's hydrocarbon based on diamido carbene (**1.55** and **1.56**) and acyclic diaminocarbenes (**1.53** and **1.54**) (Figure 1.3.2.).¹¹⁷⁻¹¹⁹

1.4 Aim and outline of the thesis:

From the aforementioned section of the thesis it is apparent that the proper kinetic and/or thermodynamic support of the ligands permitted the synthetic chemists to overcome the challenges associated with the stabilization of compounds with low valent main group elements with NHCs. A fair number of bottleable stable NHCs have been reported and made the chemistry rich with their novel and unprecedented bonding and reactivity studies. In this regard, saturated NHCs represent a special class due to their more nucleophilic character compared to their unsaturated analogues. Higher HOMOs of the SNHCs results in the lower HOMO-LUMO gap compared to the unsaturated NHCs. In the same vein, the six-membered saturated NHC possesses more nucleophilicity than 5-membered NHCs and CAACs. A detailed literature survey revealed while unsaturated NHCs are well explored, the chemistry of saturated NHCs has a modicum of precedence due to the difficulty in the synthesis and low yield. Furthermore, the NHC stabilized radicals are still at early days due to the lower sigma donation of NHCs than CAACs. The main aim of the thesis is to further extend our knowledge on the synthesis, and reactivity of a more nucleophilic saturated NHCs towards the small molecule activations and in the stabilization of the low valent main group elements. The work covers the development of unusual main-group compounds, which challenge previously held views on structure, bonding and stability. In addition, such exotic molecules were employed for

important reactions, such as small molecule activation. All the compounds prepared were characterized by multinuclear NMR spectroscopy, single crystal X-ray diffraction, and HRMS spectrometry. The following chapters will cover all these aspects of the thesis.

Chapter 2 accounts the deprotonation of 5-SIDipp by the C-F bond of C₆F₆ and it affords a mesoionic compound with concomitant elimination of HF. Neither, NHCs nor CAACs are known to generate such mesoionic compounds by such a single-step C-F bond activation. The formation of HF during the reaction is supported by the addition of another molecule of 5-SIDipp in the reaction medium, and leads to the imidazolium bifluoride. The reaction of the mesoionic compound with B(C₆F₅)₃ results in the donor–acceptor adduct, where the Lewis basicity of the fluoride atom of the C₆F₅ moiety is illustrated by its coordination to B(C₆F₅)₃. Such a donor–acceptor interaction from the fluoride atom of a metal-free system to borane is unprecedented. Further, we have extended the C-F bond activations of *n*-pentafluoropyridine with IDipp carbene and prepared a fully functionalized imidazolium scaffold via sequential para-C-F bond activations of C₅F₅N. We have also shown the activation of *ortho* and *meta* -C-F bonds over the C-H bond when the IDipp was treated with the tetrafluoropyridine.

Chapter 3 illustrates a new synthetic pathway to prepare the NHC based Kekulé di-radicaloids. To prepare the NHC analogue of Thiele’s hydrocarbon we have exploited the C-F activation of C₆F₆ and the replacement of the hydrogens with fluorines reduce the $\Delta E_{S \rightarrow T}$ by 5.4 kcalmol⁻¹. Further, we have prepared the NHC analogue of the Chichibabin’s hydrocarbon from the reduction of the dicationic imidazolium salt. The extension of fluorine based phenylene spacer to the biphenylene spacer reduces the $\Delta E_{S \rightarrow T}$ to -3.7 kcalmol⁻¹ with a higher diradical character ($\gamma = 0.61$). We have also explored the naphthalene based Kekulé hydrocarbons for the first time. In this case, we have noticed that the increase of one more

fused ring in the spacer decreases the $\Delta E_{S \rightarrow T}$ significantly ($\Delta E_{S \rightarrow T}$ for **3.6**: $-15.8 \text{ kcal mol}^{-1}$ and $\Delta E_{S \rightarrow T}$ of **3.9**: $-17.1 \text{ Kcal mol}^{-1}$).

Chapter 4 described the NHC·borane chemistry with 5-SIDipp. NHC·boranes are typically readily accessible, but no NHC adduct of MeBCl_2 has been known. The hesitancy of the chemistry community probably stems from the synthetic routes, which are tedious and require special techniques. Herein, we have prepared saturated N-Heterocyclic carbene boranes bearing methyl groups by simple salt metathesis reaction starting from 5-SIDipp· BCl_3 . 5-SIDipp· BMeCl_2 is the first carbene· MeBCl_2 adduct and its preparation does not require the hazardous MeBCl_2 . Further, we have shown the selective nucleophilic substitution at the tetra-coordinated boron center to obtain several boranes with rare functional groups such as $-\text{ONO}_2$, $-\text{OTf}$, $-\text{OH}$ etc. The combination of 5-SIDipp and $\text{B}(\text{C}_6\text{F}_5)_3$ were shown to affect the C–O bond cleavage differently for THF and diethyl ether.

Chapter 5 represents the reactivity of 6-SNHC in boron chemistry. While the body of work on carbene-borane chemistry is growing, the carbene component is mainly restricted to two classes of carbenes: (a) Arduengo type five-membered NHC and (b) CAAC. Here, we have introduced a new NHC, 6-SIDipp for NHC·borane chemistry, and described a detailed study of substitution reactions of 6-SIDipp· BH_3 . These results have uncovered the facile substitution at the coordinatively saturated sp^3 boron atom in 6-SIDipp· BH_3 with a range of functional groups such as bromide, iodide, triflate, ONO_2 , chloride etc. We have further stabilized the cationic analogue of phenylboronic acid (dihydroxyborenium cation) and diphenylborinic acid (monohydroxyborenium cation). While 6-NHC forms a stable adduct with BH_3 and BRCl_2 ($\text{R}=\text{H}, \text{Ph}$), the reaction with 9-BBN first forms an adduct with 6-SIDipp, which subsequently undergoes ring expansion to a seven membered ring at room temperature within 6 h. Finally, for the first time, we have realized the stronger nucleophilic properties of six-membered NHC

(6-SIDipp) than those of typical five-membered NHCs toward the 1,1-activation of the B-H bond of HBpin at the carbene carbon. We have also shown the theoretical studies to investigate the mechanism of the B-H activation of HBpin at the carbene carbon atom of 6-SIDipp.

1.5 References:

1. Hopkinson, M. N.; Richter, C.; Schedler, M.; Glorius, F., An overview of N-heterocyclic carbenes. *Nature* **2014**, *510*, 485-496.
2. Arduengo III, A. J.; Krafczyk, R., Auf der Suche nach Stabilen Carbenen. *Chemie in unserer Zeit* **1998**, *32*, 6-14.
3. Dumas, J. B.; Peligot, E., Mémoire sur l'esprit-de-bois et les divers composés éthers qui en proviennent. *Ann. Chim. Phys.* **1835**, *58*, 5-74.
4. Igau, A.; Grutzmacher, H.; Baceiredo, A.; Bertrand, G., Analogous .alpha.,.alpha.'-bis-carbenoid, triply bonded species: synthesis of a stable .lambda.3-phosphino carbene-.lambda.5-phosphaacetylene. *J. Am. Chem. Soc.* **1988**, *110*, 6463-6466.
5. Arduengo, A. J.; Harlow, R. L.; Kline, M., A Stable Crystalline Carbene. *J. Am. Chem. Soc.* **1991**, *113*, 361-363.
6. Lavallo, V.; Canac, Y.; Präsang, C.; Donnadiou, B.; Bertrand, G., Stable Cyclic (Alkyl)(Amino)Carbenes as Rigid or Flexible, Bulky, Electron-Rich Ligands for Transition-Metal Catalysts: A Quaternary Carbon Atom Makes the Difference. *Angew. Chem. Int. Ed.* **2005**, *44*, 5705-5709.
7. Munz, D. Pushing Electrons-Which Carbene Ligand for Which Application? *Organometallics* **2018**, *37*, 275-289
8. Hudnall, T. W.; Moorhead, E. J.; Gusev, D. G.; Bielawski, C. W., N,N'-Diamidoketenimines via Coupling of Isocyanides to an N-Heterocyclic Carbene. *J. Org. Chem.* **2010**, *75*, 2763-2766.

9. Miura, M., Rational Ligand Design in Constructing Efficient Catalyst Systems for Suzuki–Miyaura Coupling. *Angew. Chem. Int. Ed.* **2004**, *43*, 2201-2203.
10. Zapf, A.; Beller, M., The development of efficient catalysts for palladium-catalyzed coupling reactions of aryl halides. *Chem. Commun.* **2005**, 431-440.
11. César, V.; Lugan, N.; Lavigne, G., Reprogramming of a Malonic N-Heterocyclic Carbene: A Simple Backbone Modification with Dramatic Consequences on the Ligand's Donor Properties. *Eur. J. Inorg. Chem.* **2010**, *2010*, 361-365.
12. Hudnall, T. W.; Bielawski, C. W., An N,N'-Diamidocarbene: Studies in C–H Insertion, Reversible Carbonylation, and Transition-Metal Coordination Chemistry. *J. Am. Chem. Soc.* **2009**, *131*, 16039-16041.
13. Hudnall, T. W.; Moerdyk, J. P.; Bielawski, C. W., Ammonia N–H Activation by a N,N'-diamidocarbene. *Chem. Commun.* **2010**, *46*, 4288-4290.
14. Moerdyk, J. P.; Bielawski, C. W., N,N'-Diamidocarbenes Facilitate Selective C-H Insertions and Transfer Hydrogenations. *Chem. Eur. J.* **2013**, *19*, 14773-14776.
15. Hudnall, T. W.; Tennyson, A. G.; Bielawski, C. W., A Seven-Membered N,N'-Diamidocarbene. *Organometallics* **2010**, *29*, 4569-4578.
16. Gehrhus, B.; Hitchcock, P. B.; Lappert, M. F.; Heinicke, J.; Boese, R.; Bläser, D., Synthesis, Structures and Oxidative Addition Reactions of New Thermally Stable Silylenes; Crystal Structures of [Si{N(CH₂tBu)}₂C₆H₄-1,2] and [(Si{N(CH₂tBu)}₂C₆H₄-1,2)(μ-E)]₂ (E = Se or Te). *J. Organomet. Chem.* **1996**, *521*, 211-220.
17. Gehrhus, B.; Lappert, M. F.; Heinicke, J.; Boese, R.; Bläser, D., Synthesis, Structures and Reactions of New Thermally Stable Silylenes. *J. Chem. Soc., Chem. Commun.* **1995**, 1931-1932.
18. Denk, M.; Green, J. C.; Metzler, N.; Wagner, M., Electronic Structure of a Stable Silylene: Photoelectron Spectra and Theoretical Calculations of Si(NRCHCHNR),

Si(NRCH₂CH₂NR) and SiH₂(NRCHCHNR). *Journal of the Chemical Society, Dalton Transactions* **1994**, 2405-2410.

19. Gehrhus, B.; Hitchcock, P. B.; Lappert, M. F., Synthesis of a Stable Biphenyl-Bis(carbene) and -Bis(silylene) [M{(NCH₂But)₂C₆H₃-3,4}]₂ (M = C or Si). *Z. Anorg. Allg. Chem.* **2005**, *631*, 1383-1386.
20. Driess, M.; Yao, S.; Brym, M.; van Wüllen, C.; Lentz, D., A New Type of N-Heterocyclic Silylene with Ambivalent Reactivity. *J. Am. Chem. Soc.* **2006**, *128*, 9628-9629.
21. Kira, M.; Ishida, S.; Iwamoto, T.; Kabuto, C., The First Isolable Dialkylsilylene. *J. Am. Chem. Soc.* **1999**, *121*, 9722-9723.
22. Abe, T.; Tanaka, R.; Ishida, S.; Kira, M.; Iwamoto, T., New Isolable Dialkylsilylene and Its Isolable Dimer That Equilibrate in Solution. *J. Am. Chem. Soc.* **2012**, *134*, 20029-20032.
23. Asay, M.; Inoue, S.; Driess, M., Aromatic Ylide-Stabilized Carbocyclic Silylene. *Angew. Chem. Int. Ed.* **2011**, *50*, 9589-9592.
24. Ishida, S.; Abe, T.; Hirakawa, F.; Kosai, T.; Sato, K.; Kira, M.; Iwamoto, T., Persistent Dialkylsilanone Generated by Dehydrobromination of Dialkylbromosilanol. *Chem. Eur. J.* **2015**, *21*, 15100-15103.
25. Driess, M.; Grützmacher, H., Main Group Element Analogues of Carbenes, Olefins, and Small Rings. *Angew. Chem. Int. Ed. Engl.* **1996**, *35*, 828-856.
26. Fischer, R. C.; Power, P. P., π -Bonding and the Lone Pair Effect in Multiple Bonds Involving Heavier Main Group Elements: Developments in the New Millennium. *Chem. Rev.* **2010**, *110*, 3877-3923.
27. Martin, D.; Soleilhavoup, M.; Bertrand, G., Stable Singlet Carbenes as Mimics for Transition Metal Centers. *Chem. Sci.* **2011**, *2*, 389-399.

28. Power, P. P., Interaction of Multiple Bonded and Unsaturated Heavier Main Group Compounds with Hydrogen, Ammonia, Olefins, and Related Molecules. *Acc. Chem. Res.* **2011**, *44*, 627-637.
29. Sen, S. S.; Roesky, H. W.; Stern, D.; Henn, J.; Stalke, D., High Yield Access to Silylene RSiCl (R = PhC(NtBu)₂) and Its Reactivity toward Alkyne: Synthesis of Stable Disilacyclobutene. *J. Am. Chem. Soc.* **2010**, *132*, 1123-1126.
30. Power, P. P., Main-Group Elements as Transition Metals. *Nature* **2010**, *463*, 171-177.
31. Chu, T.; Nikonov, G. I., Oxidative Addition and Reductive Elimination at Main-Group Element Centers. *Chem. Rev.* **2018**, *118*, 3608-3680.
32. Wiberg, N., De Gruyter: 2008.
33. Berson, J. A., Non-Kekulé Molecules as Reactive Intermediates. In *Reactive Intermediate Chemistry*, 2003; pp 165-203.
34. Bourissou, D.; Guerret, O.; Gabbai, F. P.; Bertrand, G., Stable Carbenes. *Chem. Rev.* **2000**, *100*, 39-92.
35. Frey, G. D.; Lavallo, V.; Donnadieu, B.; Schoeller, W. W.; Bertrand, G., Facile Splitting of Hydrogen and Ammonia by Nucleophilic Activation at a Single Carbon Center. *Science* **2007**, *316*, 439-441.
36. Lavallo, V.; Mafhouz, J.; Canac, Y.; Donnadieu, B.; Schoeller, W. W.; Bertrand, G., Synthesis, Reactivity, and Ligand Properties of a Stable Alkyl Carbene. *J. Am. Chem. Soc.* **2004**, *126*, 8670-8671.
37. Moerdyk, J. P.; Bielawski, C. W., Reductive generation of stable, five-membered N,N'-diamidocarbenes. *Chem. Commun.* **2014**, *50*, 4551-4553.
38. Blanksby, S. J.; Ellison, G. B., Bond Dissociation Energies of Organic Molecules. *Accounts Chem. Res.* **2003**, *36*, 255-263.

39. Teator, A. J.; Tian, Y.; Chen, M.; Lee, J. K.; Bielawski, C. W., An Isolable, Photoswitchable N-Heterocyclic Carbene: On-Demand Reversible Ammonia Activation. *Angew. Chem. Int. Ed.* **2015**, *54*, 11559-11563.
40. Moerdyk, J. P.; Blake, G. A.; Chase, D. T.; Bielawski, C. W., Elucidation of Carbene Ambiphilicity Leading to the Discovery of Reversible Ammonia Activation. *J. Am. Chem. Soc.* **2013**, *135*, 18798-18801.
41. Moss, R. A.; Ge, C.-S.; Włostowska, J.; Jang, E. G.; Jefferson, E. A.; Fan, H., Derived absolute rate constants for additions of ambiphilic carbenes to alkenes. *Tetrahedron Letters* **1995**, *36*, 3083-3086.
42. Moss, R. A.; Wang, L.; Krogh-Jespersen, K., The Nucleophilicity of a Dialkylcarbene: Unusual Activation Parameters for Additions of Adamantanylidene to Simple Alkenes. *J. Am. Chem. Soc.* **2014**, *136*, 4885-4888.
43. Rojisha, V. C.; Nijesh, K.; De, S.; Parameswaran, P., Singlet 2-adamantylidene – An Ambiphilic Foiled Carbene Stabilized by Hyperconjugation. *Chem. Commun.* **2013**, *49*, 8465-8467.
44. Martin, D.; Lassauque, N.; Donnadieu, B.; Bertrand, G., A Cyclic Diaminocarbene with a Pyramidalized Nitrogen Atom: A Stable N-Heterocyclic Carbene with Enhanced Electrophilicity. *Angew. Chem. Int. Ed.* **2012**, *51*, 6172-6175.
45. Siemeling, U.; Färber, C.; Bruhn, C.; Leibold, M.; Selent, D.; Baumann, W.; von Hopffgarten, M.; Goedecke, C.; Frenking, G., N-Heterocyclic Carbenes Which Readily add Ammonia, Carbon Monoxide and Other Small Molecules. *Chem. Sci.* **2010**, *1*, 697-704.
46. Moerdyk, J. P.; Bielawski, C. W., Stable Carbenes. In *Contemporary Carbene Chemistry*, 2013; pp 40-74.

47. Martin, D.; Canac, Y.; Lavallo, V.; Bertrand, G., Comparative Reactivity of Different Types of Stable Cyclic and Acyclic Mono- and Diamino Carbenes with Simple Organic Substrates. *J. Am. Chem. Soc.* **2014**, *136*, 5023-5030.
48. Moerdyk, J. P.; Bielawski, C. W., Diamidocarbenes as versatile and reversible [2 + 1] cycloaddition reagents. *Nature Chemistry* **2012**, *4*, 275-280.
49. Ahrens, T.; Kohlmann, J.; Ahrens, M.; Braun, T., Functionalization of Fluorinated Molecules by Transition-Metal-Mediated C–F Bond Activation To Access Fluorinated Building Blocks. *Chem. Rev.* **2015**, *115*, 931-972.
50. Amii, H.; Uneyama, K., C–F Bond Activation in Organic Synthesis. *Chem. Rev.* **2009**, *109*, 2119-2183.
51. Kuehnle, M. F.; Lentz, D.; Braun, T., Synthesis of Fluorinated Building Blocks by Transition-Metal-Mediated Hydrodefluorination Reactions. *Angew. Chem. Int. Ed.* **2013**, *52*, 3328-3348.
52. Azhakar, R.; Roesky, H. W.; Wolf, H.; Stalke, D., Metal free and selective activation of one C–F bond in a bound CF₃ group. *Chem. Commun.* **2013**, *49*, 1841-1843.
53. Chu, T.; Boyko, Y.; Korobkov, I.; Nikonov, G. I., Transition Metal-like Oxidative Addition of C–F and C–O Bonds to an Aluminum(I) Center. *Organometallics* **2015**, *34*, 5363-5365.
54. Jana, A.; Samuel, P. P.; Tavčar, G.; Roesky, H. W.; Schulzke, C., Selective Aromatic C–F and C–H Bond Activation with Silylenes of Different Coordinate Silicon. *J. Am. Chem. Soc.* **2010**, *132*, 10164-10170.
55. Kim, Y.; Lee, E., Activation of C–F Bonds in Fluoroarenes by N-Heterocyclic Carbenes as an Effective Route to Synthesize Abnormal NHC Complexes. *Chem. Commun.* **2016**, *52*, 10922-10925.

56. Paul, U. S. D.; Radius, U., Ligand versus Complex: C–F and C–H Bond Activation of Polyfluoroaromatics at a Cyclic (Alkyl)(Amino)Carbene. *Chem. Eur. J.* **2017**, *23*, 3993-4009.
57. Swamy, V. S. V. S. N.; Parvin, N.; Vipin Raj, K.; Vanka, K.; Sen, S. S., C(sp³)–F, C(sp²)–F and C(sp³)–H bond activation at silicon(ii) centers. *Chem. Commun.* **2017**, *53*, 9850-9853.
58. Ashley, A. E.; Thompson, A. L.; O'Hare, D., Non-Metal-Mediated Homogeneous Hydrogenation of CO₂ to CH₃OH. *Angew. Chem. Int. Ed.* **2009**, *48*, 9839-9843.
59. Geier, S. J.; Chase, P. A.; Stephan, D. W., Metal-Free Reductions of N-Heterocycles via Lewis Acid Catalyzed Hydrogenation. *Chem. Commun.* **2010**, *46*, 4884-4886.
60. Geier, S. J.; Stephan, D. W., Lewis Acid Mediated P–P Bond Hydrogenation and Hydrosilylation. *Chem. Commun.* **2010**, *46*, 1026-1028.
61. Grimme, S.; Kruse, H.; Goerigk, L.; Erker, G., The Mechanism of Dihydrogen Activation by Frustrated Lewis Pairs Revisited. *Angew. Chem. Int. Ed.* **2010**, *49*, 1402-1405.
62. Leclerc, M. C.; Gorelsky, S. I.; Gabidullin, B. M.; Korobkov, I.; Baker, R. T., Selective Activation of Fluoroalkenes with N-Heterocyclic Carbenes: Synthesis of N-Heterocyclic Fluoroalkenes and Polyfluoroalkenyl Imidazolium Salts. *Chem. Eur. J.* **2016**, *22*, 8063-8067.
63. Neu, R. C.; Ouyang, E. Y.; Geier, S. J.; Zhao, X.; Ramos, A.; Stephan, D. W., Probing Substituent Effects on the Activation of H₂ by Phosphorus and Boron Frustrated Lewis pairs. *Dalton Trans.* **2010**, *39*, 4285-4294.
64. Niemeyer, J.; Erker, G., Fullerene-Mediated Activation of Dihydrogen: A New Method of Metal-Free Catalytic Hydrogenation. *ChemCatChem* **2010**, *2*, 499-500.
65. Peng, Y.; Guo, J.-D.; Ellis, B. D.; Zhu, Z.; Fettingner, J. C.; Nagase, S.; Power, P. P., Reaction of Hydrogen or Ammonia with Unsaturated Germanium or Tin Molecules under

Ambient Conditions: Oxidative Addition versus Arene Elimination. *J. Am. Chem. Soc.* **2009**, *131*, 16272-16282.

66. Schwendemann, S.; Tumay, T. A.; Axenov, K. V.; Peuser, I.; Kehr, G.; Fröhlich, R.; Erker, G., Metal-Free Frustrated Lewis Pair Catalyzed 1,4-Hydrogenation of Conjugated Metallocene Dienamines. *Organometallics* **2010**, *29*, 1067-1069.

67. Sen, S. S.; Roesky, H. W., Silicon-Fluorine Chemistry: From the Preparation of SiF₂ to C–F Bond Activation using Silylenes and its Heavier Congeners. *Chem. Commun.* **2018**, *54*, 5046-5057.

68. Stahl, T.; Klare, H. F. T.; Oestreich, M., Main-Group Lewis Acids for C–F Bond Activation. *ACS Catal.* **2013**, *3*, 1578-1587.

69. Stephan, D. W., Frustrated Lewis Pairs: A New Strategy to Small Molecule Activation and Hydrogenation Catalysis. *Dalton Trans.* **2009**, 3129-3136.

70. Stephan, D. W.; Erker, G., Frustrated Lewis Pairs: Metal-free Hydrogen Activation and More. *Angew. Chem. Int. Ed.* **2010**, *49*, 46-76.

71. Ullrich, M.; Lough, A. J.; Stephan, D. W., Dihydrogen Activation by B(*p*-C₆F₄H)₃ and Phosphines. *Organometallics* **2010**, *29*, 3647-3654.

72. Styra, S.; Melaimi, M.; Moore, C. E.; Rheingold, A. L.; Augenstein, T.; Breher, F.; Bertrand, G., Crystalline Cyclic (Alkyl)(amino)Carbene-Tetrafluoropyridyl Radical. *Chem. Eur. J.* **2015**, *21*, 8441-8446.

73. Kuhn, N.; Fahl, J.; Boese, R.; Henkel, G., Zur Reaktion von 2,3-Dihydroimidazol-2-ylidenen mit Pentafluorpyridin: Carbene als Reaktionspartner in der nucleophilen aromatischen Substitution/. *Zeitschrift für Naturforschung B* **1998**, *53*, 881-886.

74. Mallah, E.; Kuhn, N.; Maichle-Mößner, C.; Steimann, M.; Ströbele, M.; Zeller, K.-P., Nucleophilic Aromatic Substitution with 2,3-Dihydro-1,3-diisopropyl- 4,5-dimethylimidazol-2-ylidene. *Zeitschrift für Naturforschung B* **2009**, *64*, 1176-1182.

75. Lavallo, V.; Canac, Y.; Donnadieu, B.; Schoeller, W. W.; Bertrand, G., CO Fixation to Stable Acyclic and Cyclic Alkyl Amino Carbenes: Stable Amino Ketenes with a Small HOMO–LUMO Gap. *Angew. Chem. Int. Ed.* **2006**, *45*, 3488-3491.
76. Back, O.; Kuchenbeiser, G.; Donnadieu, B.; Bertrand, G., Nonmetal-Mediated Fragmentation of P₄: Isolation of P₁ and P₂ Bis(carbene) Adducts. *Angew. Chem. Int. Ed.* **2009**, *48*, 5530-5533.
77. Masuda, J. D.; Schoeller, W. W.; Donnadieu, B.; Bertrand, G., NHC-Mediated Aggregation of P₄: Isolation of a P₁₂ Cluster. *J. Am. Chem. Soc.* **2007**, *129*, 14180-14181.
78. Masuda, J. D.; Schoeller, W. W.; Donnadieu, B.; Bertrand, G., Carbene Activation of P₄ and Subsequent Derivatization. *Angew. Chem. Int. Ed.* **2007**, *46*, 7052-7055.
79. Cossairt, B. M.; Piro, N. A.; Cummins, C. C., Early-Transition-Metal-Mediated Activation and Transformation of White Phosphorus. *Chem. Rev.* **2010**, *110*, 4164-4177.
80. Cummins, C. C., Terminal, Anionic Carbide, Nitride, and Phosphide Transition-Metal Complexes as Synthetic Entries to Low-Coordinate Phosphorus Derivatives. *Angew. Chem. Int. Ed.* **2006**, *45*, 862-870.
81. Kubas, G. J., HETEROLYTIC SPLITTING OF H-H, Si-H, AND OTHER σ BONDS ON ELECTROPHILIC METAL CENTERS. In *Advances in Inorganic Chemistry*, Academic Press: 2004; Vol. 56, pp 127-177.
82. Lavallo, V.; Frey, G. D.; Donnadieu, B.; Soleilhavoup, M.; Bertrand, G., Homogeneous Catalytic Hydroamination of Alkynes and Allenes with Ammonia. *Angew. Chem. Int. Ed.* **2008**, *47*, 5224-5228.
83. Nakajima, Y.; Kameo, H.; Suzuki, H., Cleavage of Nitrogen–Hydrogen Bonds of Ammonia Induced by Triruthenium Polyhydrido Clusters. *Angew. Chem. Int. Ed.* **2006**, *45*, 950-952.

84. Peruzzini, M.; Gonsalvi, L.; Romerosa, A., Coordination Chemistry and Functionalization of White Phosphorus via Transition Metal Complexes. *Chem. Soc. Rev.* **2005**, *34*, 1038-1047.
85. Scheer, M.; Balázs, G.; Seitz, A., P₄ Activation by Main Group Elements and Compounds. *Chem. Rev.* **2010**, *110*, 4236-4256.
86. Shen, Q.; Hartwig, J. F., Palladium-Catalyzed Coupling of Ammonia and Lithium Amide with Aryl Halides. *J. Am. Chem. Soc.* **2006**, *128*, 10028-10029.
87. Surry, D. S.; Buchwald, S. L., Selective Palladium-Catalyzed Arylation of Ammonia: Synthesis of Anilines as Well as Symmetrical and Unsymmetrical Di- and Triarylamines. *J. Am. Chem. Soc.* **2007**, *129*, 10354-10355.
88. van der Vlugt, J. I., Advances in Selective Activation and Application of Ammonia in Homogeneous Catalysis. *Chem. Soc. Rev.* **2010**, *39*, 2302-2322.
89. Zhao, J.; Goldman, A. S.; Hartwig, J. F., Oxidative Addition of Ammonia to Form a Stable Monomeric Amido Hydride Complex. *Science* **2005**, *307*, 1080-1082.
90. Crabtree, R. H., *The Organometallic Chemistry of the Transition Metals*. 7 ed.; Wiley: 2019; p 464.
91. Frey, G. D.; Masuda, J. D.; Donnadieu, B.; Bertrand, G., Activation of Si-H, B-H, and P-H Bonds at a Single Nonmetal Center. *Angew. Chem. Int. Ed.* **2010**, *49*, 9444-9447.
92. Kuhn, N.; Al-Sheikh, A., 2,3-Dihydroimidazol-2-ylidenes and Their Main-Group Element Chemistry. *Coord. Chem. Rev.* **2005**, *249*, 829-857.
93. Li, X.; Curran, D. P., Insertion of Reactive Rhodium Carbenes into Boron-Hydrogen Bonds of Stable N-Heterocyclic Carbene Boranes. *J. Am. Chem. Soc.* **2013**, *135*, 12076-12081.

94. Pan, X.; Lacôte, E.; Lalevée, J.; Curran, D. P., Polarity Reversal Catalysis in Radical Reductions of Halides by N-Heterocyclic Carbene Boranes. *J. Am. Chem. Soc.* **2012**, *134*, 5669-5674.
95. Abe, M., Diradicals. *Chem. Rev.* **2013**, *113*, 7011-7088.
96. Salem, L.; Rowland, C., The Electronic Properties of Diradicals. *Angew. Chem. Int. Ed. Engl.* **1972**, *11*, 92-111.
97. Breher, F., Stretching Bonds in Main Group Element Compounds—Borderlines between Biradicals and Closed-Shell Species. *Coord. Chem. Rev.* **2007**, *251*, 1007-1043.
98. Grützmacher, H.; Breher, F., Odd-Electron Bonds and Biradicals in Main Group Element Chemistry. *Angew. Chem. Int. Ed.* **2002**, *41*, 4006-4011.
99. Jung, Y.; Head-Gordon, M., How Diradicaloid Is a Stable Diradical? *ChemPhysChem* **2003**, *4*, 522-525.
100. Kamada, K.; Ohta, K.; Kubo, T.; Shimizu, A.; Morita, Y.; Nakasuji, K.; Kishi, R.; Ohta, S.; Furukawa, S.-i.; Takahashi, H.; Nakano, M., Strong Two-Photon Absorption of Singlet Diradical Hydrocarbons. *Angew. Chem. Int. Ed.* **2007**, *46*, 3544-3546.
101. Morita, Y.; Suzuki, S.; Sato, K.; Takui, T., Synthetic organic spin chemistry for structurally well-defined open-shell graphene fragments. *Nature Chemistry* **2011**, *3*, 197-204.
102. Nakano, M.; Champagne, B., Theoretical Design of Open-Shell Singlet Molecular Systems for Nonlinear Optics. *The Journal of Physical Chemistry Letters* **2015**, *6*, 3236-3256.
103. Sun, Z.; Ye, Q.; Chi, C.; Wu, J., Low Band Gap Polycyclic Hydrocarbons: from Closed-Shell near Infrared Dyes and Semiconductors to Open-Shell Radicals. *Chem. Soc. Rev.* **2012**, *41*, 7857-7889.
104. Arnold, P. L.; Liddle, S. T., Deprotonation of N-Heterocyclic Carbenes to Afford Heterobimetallic Organolanthanide Complexes. *Organometallics* **2006**, *25*, 1485-1491.

105. Barry, B. M.; Soper, R. G.; Hurmalainen, J.; Mansikkamäki, A.; Robertson, K. N.; McClellan, W. L.; Veinot, A. J.; Roemmele, T. L.; Werner-Zwanziger, U.; Boéré, R. T.; Tuononen, H. M.; Clyburne, J. A. C.; Masuda, J. D., Mono- and Bis(imidazolidinium ethynyl) Cations and Reduction of the Latter To Give an Extended Bis-1,4-([3]Cumulene)-p-carboquinoid System. *Angew. Chem. Int. Ed.* **2018**, *57*, 749-754.
106. Jiang, C.; Bang, Y.; Wang, X.; Lu, X.; Lim, Z.; Wei, H.; El-Hankari, S.; Wu, J.; Zeng, Z., Tetrabenzochichibabin's hydrocarbons: substituent effects and unusual thermochromic and thermomagnetic behaviours. *Chem. Commun.* **2018**, *54*, 2389-2392.
107. Kikuchi, A.; Iwahori, F.; Abe, J., Definitive Evidence for the Contribution of Biradical Character in a Closed-Shell Molecule, Derivative of 1,4-Bis-(4,5-diphenylimidazol-2-ylidene)cyclohexa-2,5-diene. *J. Am. Chem. Soc.* **2004**, *126*, 6526-6527.
108. Maiti, A.; Zhang, F.; Krummenacher, I.; Bhattacharyya, M.; Mehta, S.; Moos, M.; Lambert, C.; Engels, B.; Mondal, A.; Braunschweig, H.; Ravat, P.; Jana, A., Anionic Boron- and Carbon-Based Hetero-Diradicaloids Spanned by a p-Phenylene Bridge. *J. Am. Chem. Soc.* **2021**, *143*, 3687-3692.
109. Ni, Y.; Gordillo-Gómez, F.; Peña Alvarez, M.; Nan, Z.; Li, Z.; Wu, S.; Han, Y.; Casado, J.; Wu, J., A Chichibabin's Hydrocarbon-Based Molecular Cage: The Impact of Structural Rigidity on Dynamics, Stability, and Electronic Properties. *J. Am. Chem. Soc.* **2020**, *142*, 12730-12742.
110. Rottschäfer, D.; Busch, J.; Neumann, B.; Stämmler, H.-G.; van Gastel, M.; Kishi, R.; Nakano, M.; Ghadwal, R. S., Diradical Character Enhancement by Spacing: N-Heterocyclic Carbene Analogues of Müller's Hydrocarbon. *Chem. Eur. J.* **2018**, *24*, 16537-16542.
111. Chitnis, S. S.; Krischer, F.; Stephan, D. W., Catalytic Hydrodefluorination of C-F Bonds by an Air-Stable P^{III} Lewis Acid. *Chem. Eur. J.* **2018**, *24*, 6543-6546.

112. Mallov, I.; Johnstone, T. C.; Burns, D. C.; Stephan, D. W., A model for C–F activation by electrophilic phosphonium cations. *Chem. Commun.* **2017**, *53*, 7529-7532.
113. Rottschäfer, D.; Ho, N. K. T.; Neumann, B.; Stammler, H.-G.; van Gastel, M.; Andrada, D. M.; Ghadwal, R. S., N-Heterocyclic Carbene Analogues of Thiele and Chichibabin Hydrocarbons. *Angew. Chem. Int. Ed.* **2018**, *57*, 5838-5842.
114. Rottschäfer, D.; Neumann, B.; Stammler, H.-G.; Andrada, D. M.; Ghadwal, R. S., Kekulé Diradicaloids Derived from a Classical N-Heterocyclic Carbene. *Chem. Sci.* **2018**, *9*, 4970-4976.
115. Tschitschibabin, A. E., Über das Triphenylmethyl. *Ber. Dtsch. Chem. Ges.* **1907**, *40*, 3056-3058.
116. Rottschäfer, D.; Neumann, B.; Stammler, H.-G.; van Gastel, M.; Andrada, D. M.; Ghadwal, R. S., Crystalline Radicals Derived from Classical N-Heterocyclic Carbenes. *Angew. Chem. Int. Ed.* **2018**, *57*, 4765-4768.
117. Maiti, A.; Chandra, S.; Sarkar, B.; Jana, A., Acyclic Diaminocarbene-Based Thiele, Chichibabin, and Müller Hydrocarbons. *Chem. Sci.* **2020**, *11*, 11827-11833.
118. Maiti, A.; Sobottka, S.; Chandra, S.; Jana, D.; Ravat, P.; Sarkar, B.; Jana, A., Diamidocarbene-Based Thiele and Tschitschibabin Hydrocarbons: Carbonyl Functionalized Kekulé Diradicaloids. *J. Org. Chem.* **2021**, *86*, 16464-16472.
119. Maiti, A.; Stubbe, J.; Neuman, N. I.; Kalita, P.; Duari, P.; Schulzke, C.; Chandrasekhar, V.; Sarkar, B.; Jana, A., CAAC-Based Thiele and Schlenk Hydrocarbons. *Angew. Chem. Int. Ed.* **2020**, *59*, 6729-6734.

CONTENT OF THE THESIS

Content	Page No.
Abbreviations	iv
General remarks	vi
Synopsis	vii
Chapter 1:	
Introduction to Saturated N-heterocyclic Carbene Chemistry	1-38
1.1 Introduction	2
1.1.1 A brief history of N-heterocyclic carbenes	2
1.1.2 Structure and general properties of NHCs	3
1.1.3. Electronic structure of carbenes	4
1.1.4 Different types of N-heterocyclic carbenes	5
1.1.5 Different types carbenes except NHCs	6
1.1.5.1 Cyclic (alkyl)- (amino)carbenes, CAAC	6
1.1.5.2 N, N'-Diamidocarbenes, DAC	7
1.2 Carbenes as an alternative to the transition metal complexes	8
1.2.1 Carbenes in small molecule activations	9
1.2.2 Carbenes in C-F activations	13
1.2.3 Carbenes in B-H, Si-H, P-H activations	16
1.3 Carbenes in the stabilization of Kekulé diradicals	19
1.4. Aim and outline of the thesis	22
1.5 References	25
Chapter 2:	
Carbenes in C-F Bond Activation and Their Subsequent Reactivities	39-66
2.1 Introduction	40
2.2 C-F activation of hexafluorobenzene	41
2.3 Mechanism for the C-F bond activation of C ₆ F ₆	45

2.4 Reactivity of the mesoionic compound with $B(C_6F_5)_3$	46
2.5 C-F activation of octafluorotoluene	48
2.6 C-F activation of pentafluoropyridine	51
2.7 Mechanism study for triple C-F activation	53
2.8 C-F activation of tetrafluoropyridine	57
2.9 Conclusion	58
2.10 References	59

Chapter 3:

Saturated N-heterocyclic Carbene based Kekulé Di-radicaloids via Double C-F Activation **67-104**

3.1 Introduction	69
3.2 5-SIDipp based Thiele's hydrocarbon with a tetrafluorophenylene linker	72
3.3 Enhancing diradical character of Chichibabin's Hydrocarbon through fluoride substitution	79
3.4 Closed-Shell Kekulé Diradicaloids Spanned by Naphthalene and its Perfluoro Spacer	86
3.5 Conclusion	94
3.6 References	95

Chapter 4:

Stepwise Nucleophilic Substitution to Access Saturated N-heterocyclic Carbene-haloboranes with Boron–methyl Bonds **105-130**

4.1 Introduction	106
4.2 Preparation of 5-SIDipp-boranes and haloborane adducts	108
4.3 Nucleophilic substitution at the tetracoordinate 5-SIDipp-haloborane centre	112
4.4 Preparation of first carbene·MeBCl ₂ adduct and its stepwise nucleophilic substitution	118
4.5 Lewis pair mediated tetrahydrofuran and diethyl ether activation	122
4.6 Conclusion	125
4.7 References	125

Chapter 5:	
The Chemistry of Six-membered N-heterocyclic Carbene Boranes	131-176
5.1: Introduction	133
5.2 Selective electrophilic mono- and di-iodination at 6-SIDipp·BH ₃ Center	134
5.3 Mono- and di-bromination at 6-SIDipp·BH ₃ center	142
5.4 Reactivity of 6-SIDipp with 9-BBN and ring expansion of 6-NHC	145
5.5 6-SIDipp mediated B-H activation of HBpin, HBcat and B ₂ neop ₂	148
5.6 6-SIDipp stabilized borenium cations; isolation of a cationic analogue of borinic Acid and its reactivity	153
5.7 6-SIDipp stabilized dihydroxyborenium cations	161
5.8. Nucleophilic substitution at 6-SIDipp·PhBCl ₂ center	166
5.9 Conclusion	168
5.10 References	170
Appendix: Experimental details, NMR and crystal data	177-263

Abbreviations

Units and standard terms

BDE	Bond Dissociation Energy
°C	Degree Centigrade
DFT	Density Functional Theory
mg	Milligram
h	Hour
mL	Milliliter
Hz	Hertz
min	Minute
mmol	Millimole
NPA	Natural Population Analysis
ppm	Parts per million
%	Percentage
MP	Melting Point
Calcd.	Calculated
CCDC	Cambridge Crystallographic Data Centre
CIF	Crystallographic Information file

Chemical Notations

Ar	Aryl
Me	Methyl
Et	Ethyl
Ph	Phenyl
Ad	Adamentyl
Dipp	Diisopropylaniline
<i>i</i> Pr	Isopropyl
<i>t</i> Bu	Tertiary butyl
MeOH	Methanol

MeCN	Acetonitrile
THF	Tetrahydrofuran
DCM	Dichloromethane
CDCl ₃	Deuterated chloroform
C ₆ D ₆	Deuterated benzene
DMSO-d ₆	Deuterated dimethyl sulfoxide
HBpin	Pinacolborane
TMSCN	Trimethylsilyl cyanide
TMSCl	Trimethylsilylchloride
<i>n</i> -BuLi	<i>n</i> -butyllithium
NHC	<i>N</i> -Heterocyclic carbene
NHSi	<i>N</i> -Heterocyclic silylene


Other Notations

δ	Chemical shift
J	Coupling constant in NMR
HRMS	High Resolution Mass Spectrometry
NMR	Nuclear Magnetic Resonance
rt	Room temperature
XRD	X-Ray Diffraction
equiv.	Equivalents
VT	Variable temperature

General remarks

- ❖ All chemicals were purchased from commercial sources and used without further purification.
- ❖ All reactions were carried out under inert atmosphere following standard procedures using Schlenk techniques and glovebox.
- ❖ The solvent used were purified by an MBRAUN solvent purification system MBSPS-800 and further dried by activated molecular sieves prior to use.
- ❖ Column chromatography was performed on silica gel (100-200 mesh size).
- ❖ Deuterated solvents for NMR spectroscopic analyses were used as received. All ^1H , ^{13}C , ^{19}F , ^{29}Si and ^{11}B NMR analysis were obtained using a Bruker or JEOL 200 MHz, 400 MHz or 500 MHz spectrometers. Coupling constants were measured in Hertz. All chemical shifts are quoted in ppm, relative to TMS, using the residual solvent peak as a reference standard.
- ❖ HRMS spectra were recorded at UHPLC-MS (Q-exactive-Orbitrap Mass Spectrometer) using electron spray ionization [(ESI+, +/- 5 kV), solvent medium: acetonitrile and methanol] technique and mass values are expressed as m/z. GC-HRMS (EI) was recorded in Agilent 7200 Accurate-mass-Q-TOF.
- ❖ All the reported melting points are uncorrected and were recorded using Stuart SMP-30 melting point apparatus.
- ❖ Chemical nomenclature (IUPAC) and structures were generated using ChemDraw Professional 15.1.

Synopsis

 Synopsis of the Thesis to be submitted to the Academy of Scientific and Innovative Research for Award of the Degree of Doctor of Philosophy in Chemistry	
Name of the Candidate	Ms. Gargi Kundu
Degree Enrolment No. & Date	PhD in Chemical Sciences (10CC17A26014); August 2017
Title of the Thesis	An excursion into the chemistry of more nucleophilic saturated N-heterocyclic carbenes
Research Supervisor	Dr. Sakya Singha Sen (CSIR-NCL, Pune)

Keywords: *N-heterocyclic carbene, C-F activation, Kekule di-radicaloids, NHC-Boranes, Borenium cations.*

This thesis deals with the more nucleophilic saturated N-heterocyclic carbenes reactivity with the main group elements. It is divided into six chapters. The first chapter is the introduction of saturated N-heterocyclic carbenes and its various applications in small molecules activation. The second to fifth chapters narrate our approach to the synthesis and reactivity of novel SNHC based strong bond activations and their further derivatizations. A detailed theoretical study is done to understand the mechanism for NHC based *mono* and *triple* C-F activations. The second chapter describes carbenes in C-F bond activation and their subsequent reactivities towards Lewis acids like BF_3 and $\text{B}(\text{C}_6\text{F}_5)_3$. The third chapter contains the synthesis of SNHC based Kekule di-radicaloids via double C-F activations of perfluoro-arenes. DFT calculations have investigated the singlet-triplet energy gap for these systems. The synthesis of first NHC-haloboranes with a boron-

methyl bond is included in fourth chapter. In the fifth chapter, we have introduced a more nucleophilic six saturated NHC and utilized it for the B-H bond activation, substitution, the stabilization of the borenium cations. The final chapter of the thesis describes the summary of Ph.D. work with the future outline.

Chapter I: Introduction to saturated N-heterocyclic chemistry

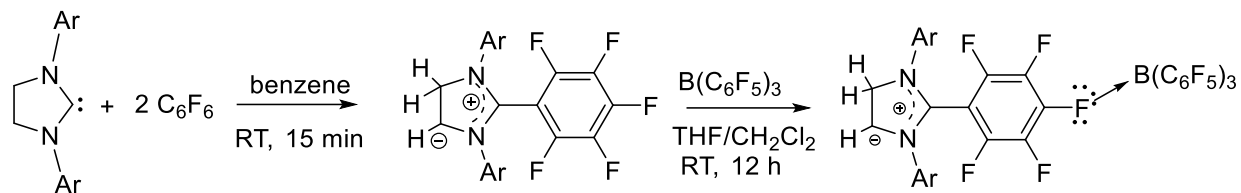
Carbenes are known as neutral compounds containing a divalent carbon atom with a six-electron valence shell. The incomplete electron octet and coordinative unsaturation, make the free carbenes highly reactive transient intermediates in organic transformations and unstable such as cyclopropanation. The first N-heterocyclic carbene (NHC) 1,3-di(adamantyl)imidazol-2-ylidene was synthesized by Arduengo in 1991.¹ Two bulky adamantyl groups bound to the nitrogen atoms help in the kinetic stabilization of the lone pair of the electrons at the carbene carbon atom and disfavors dimerization to the corresponding olefin (the Wanzlick equilibrium).² The electronic stabilization provided by the nitrogen atoms, however, is a much more important factor. NHCs show a singlet ground-state electronic configuration with the highest occupied molecular orbital (HOMO) and the lowest unoccupied molecular orbital (LUMO) best described as a formally sp^2 -hybridized lone pair and an unoccupied p-orbital at the C^2 carbon, respectively.³ The adjacent electron-withdrawing and p-electron-donating nitrogen atoms stabilize this structure both inductively by lowering the energy of the occupied s-orbital and mesomerically by donating electron density into the empty p-orbital. In my thesis work we have mainly used the saturated five and six membered N-heterocyclic carbenes due to its higher nucleophilic nature. The chemistry of SNHCs is rarely reported due to its difficulties in the synthesis and low yield. In our laboratory, we have modified the synthetic procedures of the SNHCs to get better yield. We have mainly

studied the SNHCs for the strong bond activations (C-F and B-H)⁴ and further stabilized SNHC based low valent main group elements like carbon based di-radicaloids, borenium cations.

Chapter II: Carbenes in C-F bond activation and their subsequent reactivities

The activation of C-F bonds of fluorinated hydrocarbons is of fundamental interest from the standpoint of the potential application of organofluorine compounds in synthetic organic chemistry, pharmacy, and agrochemistry as well as the ever-increasing environmental concerns related to the fluorinated compounds. Fluorinated hydrocarbons are not only contributing to the global warming but causing depletion to the ozone layer. Generally, transition metals are involved in the C-F bond activation, which has issues with terrestrial abundance and toxicity. As a result, there is a need to develop new synthetic strategies for the activation of C-F bonds.

Due to our recent interest in C-F bond activation by compounds with low valent main group elements, we intended to explore saturated NHC for the C-F bond activation. While both cyclic alkyl amino carbenes (*cAACs*) and IPr have been explored for the C-F bond activation recently, their different electronic properties are reflected in their mode of C-F bond activation. We have observed herein that the reaction of SIPr with C₆F₆ has led to the activation of one of the C-F bonds with concomitant deprotonation from the backbone, resulting in the formation of an unprecedented mesoionic compound along with HF elimination. The HF elimination is confirmed by adding one more equivalent of SIPr, which forms an imidazolium salt with HF₂⁻ as the counter anion. Subsequent to the isolation of the mesoionic compound, we intended to derivatize this it by reacting with B(C₆F₅)₃, but it forms a rare donor-acceptor adduct, where the fluoride atom of the C₆F₅ moiety coordinates to boron leaving the carbanion moiety intact. Such epitomization of Lewis basicity of a fluoride atom of C₆F₅ ligand in a metal free system is unprecedented.



Scheme 1. C-F bond activation of C_6F_6 by **SIPr** and subsequent reactivity (Ar=2,6-*i*Pr $_2$ C $_6$ H $_3$).

In order to understand the mechanism for the C-F bond activation of C_6F_6 , quantum chemical calculations have been done with density functional theory (DFT) at the PBE/TZVP level of theory (Figure 3). The approach of C_6F_6 to the carbene leads to the formation of **Int_1** via **Ts_1**, which is a very stable intermediate ($\Delta G = -16.6$ kcal/mol). The barrier for this step is 22.4 kcal/mol. Subsequent to this, calculations suggest that a molecule of the C_6F_6 acts as a “fluoride shuttle”, transferring a fluoride to the backbone carbon (see **Ts_2** in Figure 1) to yield the experimentally observed product. This mediating role of C_6F_6 was seen to be important, for it was seen that without the fluoride transferring assistance of C_6F_6 molecule, it was difficult to break the C–H bond to eliminate HF from the intermediate **Int_1**. This is in line with our observation why the reaction takes place at room temperature in presence of an excess C_6F_6 . Note that, Kuhn and coworkers also used a huge excess of C_6F_6 in presence of BF_3 for carbene mediated C–F bond activation.

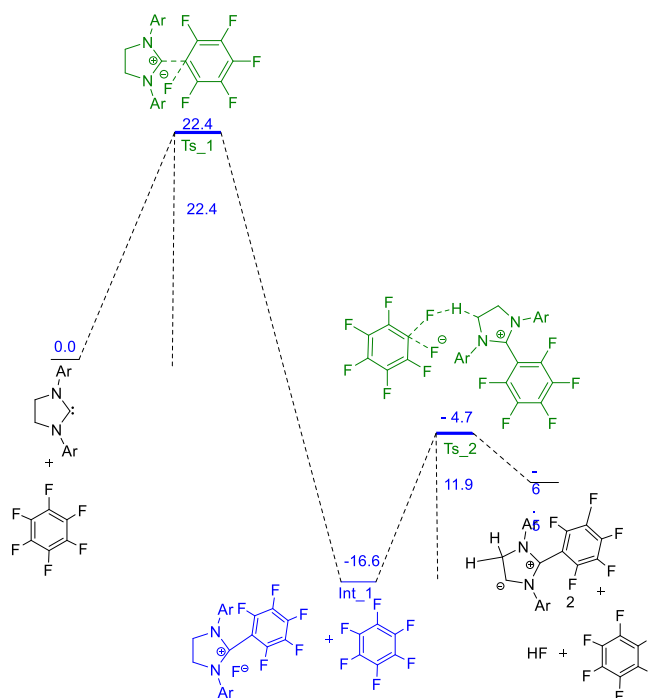
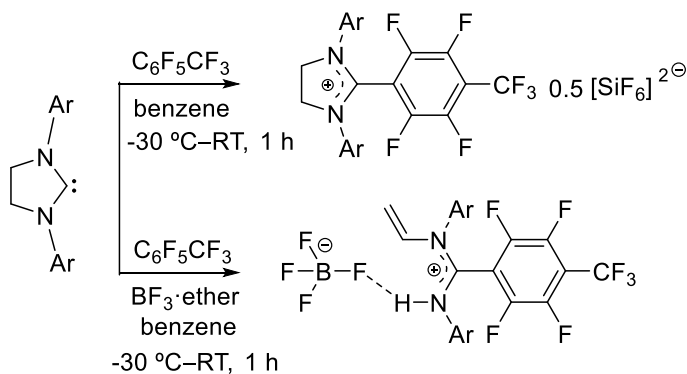


Figure 1. The reaction energy profile diagram for the C–F bond activation of C₆F₆ by SIPr. The values (in kcal/mol) have been calculated at the PBE/TZVP level of theory with DFT

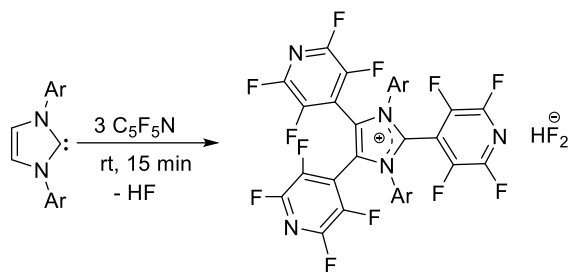


Scheme 2. C-F bond activation of C₆F₅CF₃ by SIPr

The elimination of HF during the C–F bond activation was further manifested in the reaction of SIPr with C₆F₅CF₃. The reaction led to the activation of the *para*-C–F bond relative to the CF₃ group, resulting in the formation of a imidazolium salt along with [SiF₆]²⁻ as the counter anion

(Scheme 2). The source of $[\text{SiF}_6]^{2-}$ can be attributed to the glass surface, which can react with the *in situ* liberated HF from the system. We could not stop the reaction of HF with the glass vessel even when performing the reaction at $-30\text{ }^\circ\text{C}$.

Triple C-F activation :



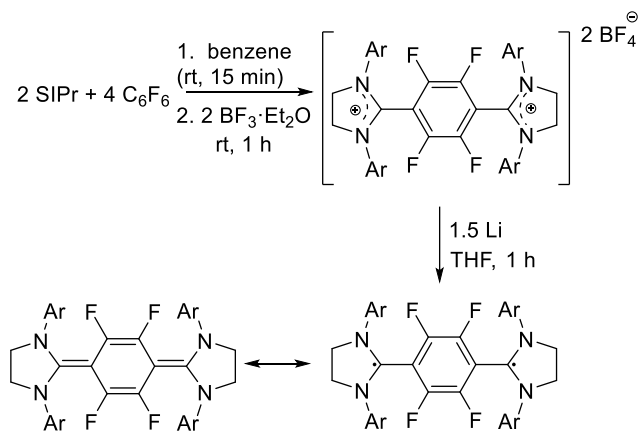
Scheme 3. Previous examples of single and double C-F activation of perfluoroarenes by NHCs. This work describes the triple C-F bond activation and synthesis of **1** (Ar=2,6-*i*Pr₂-C₆H₃)

The reaction of IDipp (IDipp=1,3-bis(2,6-diisopropylphenyl)-imidazole-2-ylidene) with $\text{C}_5\text{F}_5\text{N}$ in toluene led to the ‘*penta*-substituted’ imidazolium bifluoride salt, along with the liberation of one molecule HF (Scheme 3).

Chapter III: Saturated N-Heterocyclic carbene based Kekulé di-radicaloids via double C-F activation

Due to lower HOMO-LUMO energy gap of saturated NHCs than their unsaturated counterparts, the capability of saturated NHCs to stabilize organic radicals should be better. Recently, we have studied the reactivity of C_6F_6 and $\text{C}_6\text{F}_5\text{CF}_3$ with SIPr. In this chapter, we have shown the utilization of C–F bond activation of C_6F_6 chemistry to realize a SIPr based Thiele's hydrocarbon spanned by a C_6F_4 linker. The question remain whether the four substituted fluorine atoms at the central phenylene ring of **3** would destabilize the quinoid state and stabilize the biradical state. A further

impetus comes from the works of Abe and coworkers who showed the increase in the biradical character in 1,4-Bis-(4,5-diphenylimidazol-2-ylidene) tetrafluoro cyclohexa-2,5-diene (tf-BDPI-2Y) from parent BDPI-2Y. Although tf-BDPI-2Y was not structurally characterized, they were able to obtain the single crystal structure of the dimerized product (tF-BDPI-2YD).



Scheme 4. Stepwise access to fluorine-based Thiele's hydrocarbon.

We have performed the reaction of SIPr and C_6F_6 , but have added BF_3 -ether to the reaction mixture after 15 minutes for the isolation of the orange colored dicationic salt with two BF_4^- molecules as the counter anions (Scheme 4). Surprisingly, in situ addition of Mg powder at $0^\circ C$ in the reaction mixture of SIPr and C_6F_6 in THF led to the formation of the fluorine version of Thiele's hydrocarbon in one step. The Mg is oxidized to Mg(II) by capturing two fluoride anions and is precipitated out as MgF_2 from the system. The generation of MgF_2 also inhibits the HF elimination. In order to get the electronic structure and to understand the bonding scenario in Thiele's hydrocarbon, DFT calculations were performed at B3LYP/def2-SVP level of theory (see Computational Details). Computed electronic states of it reveal that close-shell singlet remains the electronic ground state with singlet-triplet energy difference ($\Delta E_{S \rightarrow T}$) of $-23.7 \text{ kcal mol}^{-1}$. The

computed bond lengths and angles of singlet state, than the triplet state structure, are in good agreement with the experimentally obtained X-ray crystal structure, as can be seen from the alignments and superposition plot of the conformers. It is of note here that the replacement of H by F led to decrease of S→T gap by 5.4 kcal mol⁻¹. No diradical character was found for this compound indicating the quinoidal bond nature. Ongoing studies are focused on extending the C-F bond activation to other NHC derived diradicaloids.

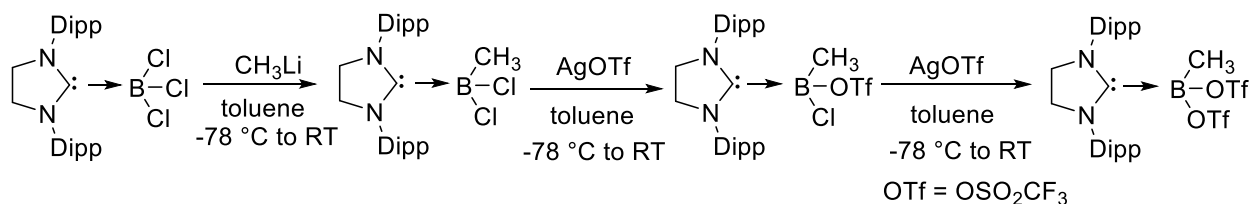
Chapter IV: Stepwise nucleophilic substitution to access saturated N-heterocyclic carbene haloboranes with boron–methyl bonds

The combination of an N-heterocyclic carbene (NHC) with a borane usually results in a complex called a NHC·borane. The synthesis of more than two dozen NHC·borane complexes of composition NHC·BX₃, NHC·BHX₂, NHC·BH₂X, etc. have been reported, mainly from the groups of Curran, Braunschweig, Robinson, Tamm, and others. Interestingly, a survey of known NHC·RBX₂ with different R groups reveal that common functional groups in carbon chemistry like methyl groups are rarely found bound to boron atoms in NHC·borane adducts. For example, NHC·BCl₂Ph is known,ⁱ but NHC·BCl₂Me is unknown. One reason could be the needed borane (MeBCl₂) is not widely available. It is prepared from the reaction of Me₃SnCl with excess BCl₃ that gives rise to a mixture of products (eqn. 1). MeBCl₂ has a boiling point of 11 °C, ignites in contact with air, and should be stored in a Schlenk tube equipped with a grease-free stopcock at a temperature below –30 °C.ⁱⁱ So, *handling of MeBCl₂ under laboratory condition is non-trivial.* The other reason is that in carbon chemistry the methyl group behaves as electron donor (+I effect), while in boron chemistry that the methyl groups, contrary to the common conviction, are electron-withdrawing (–I effect) due to the difference in electronegativity between carbon (2.5) and boron

(2.0). So, we were interested to make NHC·haloborane adducts, where one of the substituents of the boron atom is a methyl group. It is of note here that MeBCl₂ was detected as an intermediate in the chemical vapor deposition synthesis of boron carbide,ⁱⁱⁱ and studying the chemistry of MeBCl₂ might provide a deeper understanding of its chemical reactivity.



Herein we demonstrate a detailed study of nucleophilic substitution reactions of SIDipp·BCl₃ compound, which led to SIDipp·BMeCl₂ adduct. This is the first carbene·BMeCl₂ adduct and it does not require the use of hazardous MeBCl₂. Removal of another chlorine from this with the trifluoromethanesulfonate (OTf) group resulted in an unusual NHC·borane, SIDipp·B(Me)(Cl)(OTf), where the three groups attached to the boron center are different. Subsequent removal of another chloride by OTf moiety led to SIDipp·B(Me)(OTf)₂.

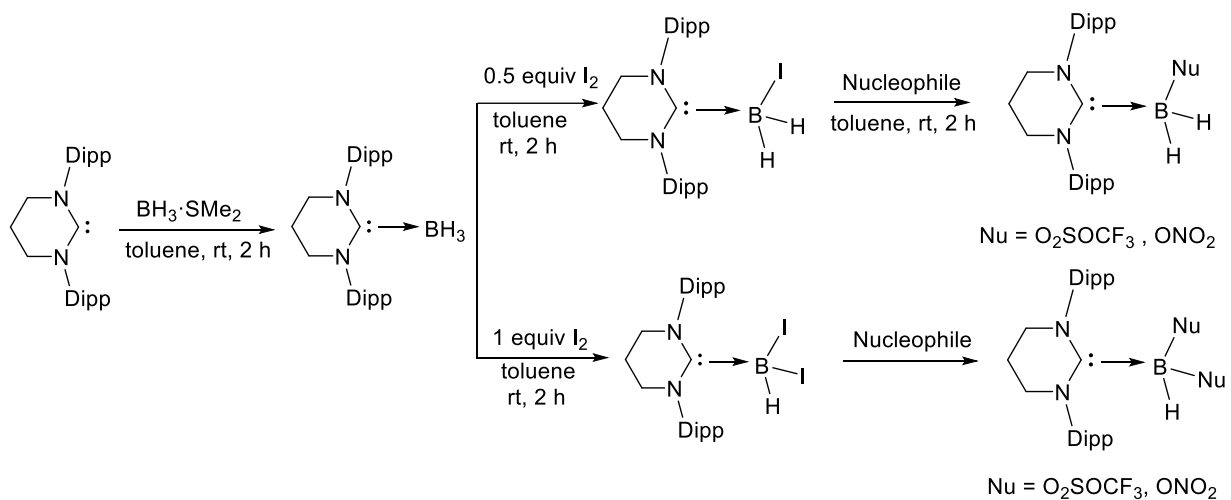


Scheme 5. Synthesis of NHC-Boranes with the boron methyl bond.

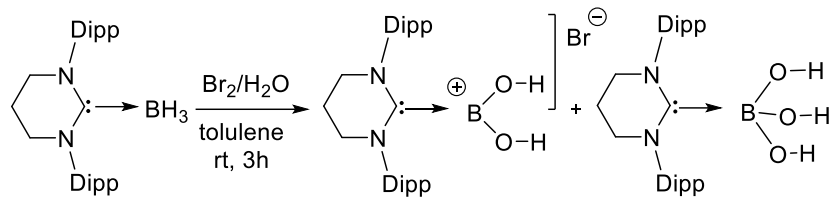
NHC·boranes are typically readily accessible, but we have mentioned in the introduction that no NHC adduct of MeBCl₂ has been known. The hesitance of the chemistry community probably stems from the synthetic routes, which are tedious and require special techniques. Here we have prepared saturated N-Heterocyclic carbene boranes bearing methyl groups by simple salt metathesis reaction starting from SIDipp·BCl₃.

Chapter V: The chemistry of six-membered N-heterocyclic carbene boranes

The reports of six-membered carbenes are limited in literature partly due to their less thermal stability and structural rigidity though they feature higher HOMO and Lower HOMO-LUMO gap compared to typical five-membered NHCs. Due to our current interest in boron chemistry, we have studied the synthesis and reactivity of saturated six-membered N-heterocyclic carbene (6-SIDipp) borane adduct. 6-NHC-BH₃ is amenable to further functionalization via iodination, providing access to NHC mono and diboryl iodides, selectively, which undergo nucleophilic substitution reactions with AgOTf and AgNO₃ to give boron compounds with OTf and ONO₂ functionalities (Scheme 6). Dihydroxyborenium cations, the cationic analogues of phenylboronic acid, are difficult to prepare due to the lacking of any R group. Herein, we have prepared a dihydroxyborenium cation conveniently by reacting **1** with bromine-water.



Scheme 6. Synthesis and halogenation of 6NHC-BH₃ and subsequent nucleophilic substitution reactions.



Scheme 7. Preparation of a dihydroxy borenium cation in a single step from 6NHC-BH₃.

The reaction of **1** with bromine water led to an immediate color change from colorless to yellow and afforded a 6-SIDipp stabilized dihydroxyborenyl cation at room temperature in 3 h (Scheme 7). Both the compounds are separated by fractional crystallization. There is no report of the formation of NHC·B(OH)₃ type Lewis adducts so far.

While the body of work on carbene-borane chemistry is growing, the carbene component is mainly restricted to two classes of carbenes: (a) Arduengo type five-membered NHC and (b) CAAC. Here, we have introduced a new NHC, 6-SIDipp for NHC·borane chemistry, and described a detailed study of substitution reactions of 6-SIDipp·BH₃. These results have uncovered the facile substitution to the coordinatively saturated *sp*³ boron atom in 6-SIDipp·BH₃ with a range of functional groups such as iodide, triflate, ONO₂.

Details of Publications:

1. **G. Kundu**, S. Tothadi, S. S. Sen, Six membered saturated N-Heterocyclic carbene reactivity with boranes: B-H activation vs adduct formation. (*Manuscript under preparation*)
2. **G. Kundu**, S. R. Das, S. Tothadi, K. Vanka, S. S. Sen, Saturated N-Heterocyclic carbene based Kekule bi-radicaloids with a naphthalene linker. (*Manuscript under preparation*)
3. **G. Kundu**, K. Balayan, S. Tothadi, Six-membered saturated NHC Stabilized borenium cations: isolation of a cationic analogue of borinic Acid (*Manuscript under revision*).

4. **G. Kundu**, V. S. Ajithkumar, S. Tothadi, S. S. Sen, *Chem. Comm.* **2022**, 58, 3783-3786.
5. **G. Kundu**, V. S. Ajithkumar, M. K. Bisai, S. Tothadi, T. Das, K. Vanka, S. S. Sen, *Chem. Commun.* **2021**, 57, 4428–4431.
6. **G. Kundu**, S. Pahar, S. Tothadi, S. S. Sen, *Organometallics* **2020**, 39, 4696 – 4703.
7. **G. Kundu**, S. De, S. Tothadi, A. Das, D. Koley, S. S. Sen, *Chem. Eur. J.* **2019**, 25, 16533 – 16537. (*Hot paper*)
8. M. Pait ^{||}, **G. Kundu** ^{||}, S. Tothadi, S. Karak, S. Jain, K. Vanka, S. S. Sen. *Angew. Chem. Int. Ed.* **2019**, 58, 2804 – 2808. (^{||}: *Equal contribution*)

References:

1. Arduengo, A. J.; Harlow; R. L.; Kline, M. *J. Am. Chem. Soc.* **1991**, 113, 361–363.
2. Wanzlick, H.-W.; Schönher, H.-J. *Angew. Chem. Int. Ed.* **1968**, 7, 141–142.
3. Hopkinson, M. N.; Richter, C.; Schedler M.; Glorius, F. *Nature*, **2014**, 510, 485-496.
4. (a) Paul, U. S. D.; Radius, U. *Chem. Eur. J.* **2017**, 23, 3993–4009. (b) Styra, S.; Melaimi, M.; Moore, C. E.; Rheingold, A. L.; Augenstein, T.; Breher, F.; Bertrand, G. *Chem. Eur. J.* **2015**, 21, 8441–8446. (c) Kim, Y.; Lee, E. *Chem. Commun.* **2016**, 52, 10922–10925. (d) Leclerc, M. C.; Gorelsky, S. I.; Gabidullin, B. M.; Korobkov, I.; Baker, R. T. *Chem. Eur. J.* **2016**, 22, 8063–8067. (e) Sen, S. S.; Roesky, H. W. *Chem. Commun.* **2018**, 54, 5046–5057.

Gargi Kundu

Gargi Kundu
(Student)

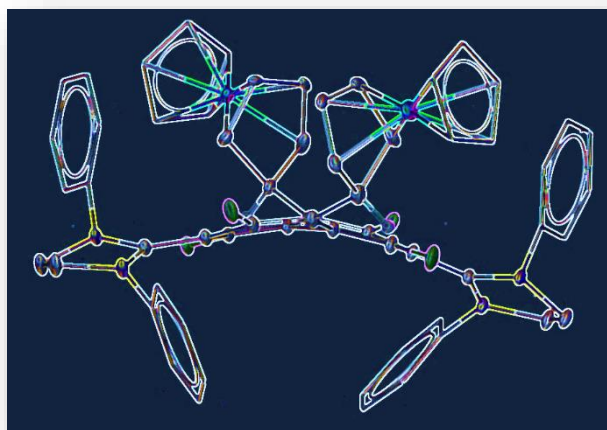
Sakya Singha Sen

(Dr. Sakya Singha Sen)
(Supervisor)

Chapter-3

Saturated N-heterocyclic Carbene based Kekulé Di-radicaloids via Double C-F Activation

Abstract: The synthesis of 5-SIDipp derived Kekulé diradicaloids with perfluoro substituted spacers have been described, in an attempt to tune their diradical character. Two synthetic routes have been described to access Thiele's hydrocarbon analogue, **3.2**. The cleavage of C-F bond of C_6F_6 by 5-SIDipp in the presence of BF_3 led to double C-F activated compound with tetrafluoro borate as the counter anion (**3.1**), which upon reduction by lithium metal afforded **3.2**. Alternatively, **3.2** can be directly accessed in one step by reacting 5-SIDipp with C_6F_6 in presence of Mg metal. Experimental and computational studies support the cumulenec closed-shell singlet state of **3.2** with a singlet-triplet energy gap (ΔE_{S-T}) of $-23.7 \text{ kcal mol}^{-1}$. Further, we have prepared the 5-SIDipp derived Chichibabin's Hydrocarbon with an octafluorobiphenylene spacer (**3.4**). The addition of two equivalents of 5-SIDipp with decafluorobiphenyl gives the double C-F activated imidazolium salt with two fluoride anions, **3.3**. Further reduction of **3.3** with two equivalents cobaltocene gives the fluorine substituted SNHC based Chichibabin's Hydrocarbon, **3.4**. Quantum chemical calculations suggested a singlet state of **3.4** with a singlet-triplet energy gap (ΔE_{S-T}) of $-3.7 \text{ kcal mol}^{-1}$, which is significantly lower compared to the hydrogen substituted NHC-based Chichibabin's hydrocarbons ($-10.7 \text{ kcal mol}^{-1}$, B3LYP). Interestingly, the diradical character (y) of **3.4** is also noticeably higher ($y = 0.61$) compared to



the related CHs ($y = 0.41-0.43$; B3LYP). Furthermore, we have extended this procedure to prepare a closed-shell Kekulé diradicaloid (**3.6**) separated by a naphthalene moiety and stabilized by two capping 5-SIDipp from the reduction of the corresponding dication (**3.5**). Quantum chemical calculations suggested a singlet state of **3.6** with a singlet–triplet energy gap (ΔE_{S-T}) of $-15.8 \text{ kcal mol}^{-1}$. In order to prepare the *perfluoro* analogue of **3.6**, we exploited the C–F bond activation approach by SIDipp, which allows access to the dicationic salt with two fluoride as counter-anions (**3.7**). The reduction of **3.7** with cobaltocene resulted in an over-reduction and formation of **3.9**, where the two out of six C–F bonds in the perfluoronaphthalene linker are unprecedentedly replaced by Cp*Co moiety. Quantum chemical calculations suggested a singlet state of **3.9** with a singlet–triplet energy gap (ΔE_{S-T}) of $-17.1 \text{ kcal mol}^{-1}$. All the complexes are well characterized by single crystal X-ray and mass spectrometry.

3.1. Introduction:

Molecular species bearing two unpaired electrons in two energetically equivalent molecular orbitals are termed as diradical species.¹ Based on electron delocalization and frontier molecular orbitals, diradicals can be divided into three classes (Figure 3.1): (a) Kekulé, (b) non-Kekulé, and (c) antiaromatic. Based on the spin state of individual electrons in Kekulé and non-Kekulé diradicals, they can exist in singlet state (where the individual electron spins are opposite) or triplet state (where the individual electron spins are same).² Molecules having partial singlet diradical nature in their ground state are often called as diradicaloids,³⁻⁵ where the interaction between the two oppositely spinning electrons leads to their further classification as open shell and closed shell diradicaloids. Because of the presence of two unpaired electrons, diradicaloids possess very high reactivity. Stabilization of diradicaloids is typically achieved through delocalization over π -conjugated moieties and their development are of great interests to chemists, owing to their discrete chemical properties and potential applications in molecular electronics, nonlinear optics, and organic spintronics.⁶⁻⁹

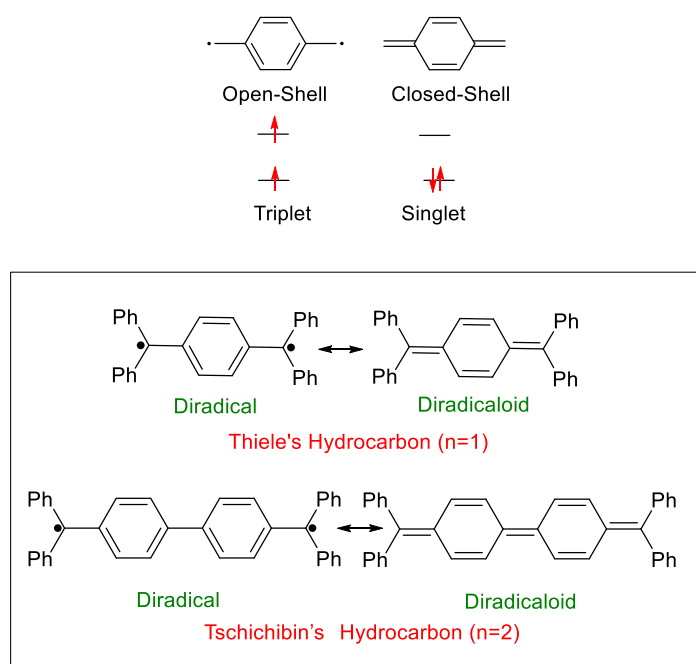


Figure 3.1. Electronic distribution in different conformations of Kekulé diradicals.

Kekulé diradicaloids have received remarkable attention primarily due to their unique electronic properties, which is originated from the intermediate bonding of the frontier π -electrons. Based on the number of aryl moieties involved in the formation of the diradicaloid, they are named as Thiele's hydrocarbon ($n = 1$), Chichibabin hydrocarbon ($n = 2$) or Muller's hydrocarbon ($n = 3$).¹⁰⁻¹⁶ While studies on linker length variation in Kekulé diradicaloids are often cited in literatures, instances on functionality variation on them is very scarce. To understand the role of substitution on the arene core, we chose Thiele's hydrocarbon as our first system and studied its chemistry by substituting the four H atoms with F atoms. To accomplish the synthesis, we choose N-heterocyclic carbene (NHC) based C-F activation as the preferred reaction. This novel reaction yielded NHC stabilized diradicaloids quantitatively in a single step reaction along with simultaneous insertion of F atoms onto their arene cores. The activation of the C-F bonds of perfluoroarenes by compounds with Si(II), P(III), Al(I) atoms has become an increasingly popular topic of research over the last few years thanks to pioneering works by Stephan, Roesky, Nikonov and many others.¹⁷⁻²⁴ The group of Kuhn, and later the groups of Lee and Radius investigated the C-F bond activation using N-heterocyclic carbenes (NHCs).²⁵⁻²⁹ In 2015, Bertrand and co-workers reported the activation of the C-F bond of C_5F_5N by a cyclic (alkyl)(amino)carbene (*cAAC*) and subsequently isolated a (*cAAC*)-tetrafluoropyridyl radical by reducing the C-F bond activated product.³⁰ In fact, the *cAAC* moieties are excellent for stabilizing a variety of organic, main-group and transition-metal radical species, as demonstrated from the extensive studies by the groups of Bertrand, Roesky, Braunschweig, and others.³¹⁻⁵⁰ In contrast, radicals derived from NHCs are astoundingly small,^{10, 11, 13, 16, 51-54} although very recently NHC derivatives of Kekulé diradicaloids have been realized by Ghadwal and co-workers.^{16, 52, 53}

Due to higher HOMO of saturated NHCs than their unsaturated counterparts,⁵⁵ it won't be erroneous to think the capability of saturated NHCs to stabilize organic radicals should be

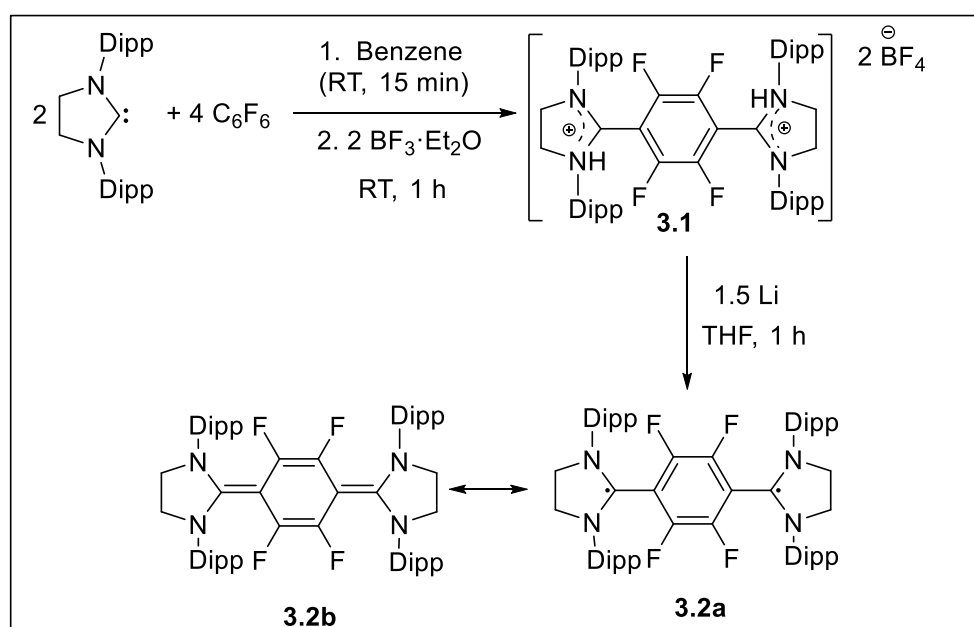
better.⁵¹ Recently, we have studied the reactivity of C_6F_6 and $C_6F_5CF_3$ with 5-SIDipp. In this chapter, we have shown the utilization of the C-F bond activation chemistry of C_6F_6 to realize a 5-SIDipp based Thiele's hydrocarbon spanned by a C_6F_4 linker. The question remain whether the four substituted fluorine atoms at the central phenylene ring of the Thiele's hydrocarbon would destabilize the quinoid state and stabilize the biradical state. A further impetus comes from the works of Abe and co-workers, who showed the increase in the biradical character in 1,4-Bis-(4,5-diphenylimidazol-2-ylidene) tetrafluoro cyclohexa-2,5-diene (tf-BDPI-2Y) from parent BDPI-2Y.¹³ Although tf-BDPI-2Y was not structurally characterized, they were able to obtain the single crystal structure of the dimerized product (tF-BDPI-2YD).¹³

Of the various Kekulé hydrocarbons, Chichibabin hydrocarbons are interesting because of their existence in intermediate form between an open-shell biradical and a closed-shell quinonoid form.⁵⁶ The inherent reactivity from the existence of two unpaired electrons creates a high synthetic challenge for Chichibabin hydrocarbon. By substituting diphenyl carbene scaffold with an isoelectronic NHC, Ghadwal and co-workers accessed a stable Chichibabin's hydrocarbon with a singlet-triplet gap of $-10.7 \text{ kcal mol}^{-1}$ (B3LYP).^{53, 54} Motivated by this work, Jana and co-workers reported Chichibabin's hydrocarbon based on diamido carbene, CAAC as well as acyclic diaminocarbenes.⁵⁷⁻⁵⁹ To continue investigating the role of arene substituents on the diradical character of the resulting Chichibabin hydrocarbon, we have developed a system based on our saturated 5-membered NHC (5-SIDipp) and altered the substituents between H and F atoms.

It is explicit from the aforementioned discussion that the diverse library of carbenes allows for the generation of a range of diradicaloids with varying terminus, but the spacer in these molecules has been restricted to either phenylene or biphenylene group. Notable exceptions came from the groups of Bertrand and Masuda, who independently reported the

synthesis of organic Kekulé diradicaloids with 1,4-diethynylphenyl spacer with CAACs or imidazoline-2-ylidene, respectively.^{11, 36} Recently, Aldridge and co-workers reported an organoboron analogues of Thiele's hydrocarbon using a pyridine spacer.⁶⁰ We wondered if a naphthalene spacer would permit for the preparation of diradicals based on 5-SIDipp, and here we report our findings. We also wished to analyze the impact of the substituton of the hydrogen atoms of the naphthelene spacer by fluorine atoms on its diradical character.

3.2. 5-SIDipp based Thiele's hydrocarbon with a tetrafluorophenylene linker:



Scheme 3.1. Stepwise access to **3.2**. C_6F_6 was used in 1: 2 ratio with 5-SIDipp to perform the reaction at room temperature. The excess amount of C_6F_6 acts as a "fluoride shuttle".⁶¹

We have performed the reaction of 5-SIDipp and C_6F_6 in benzene, but have added BF_3 ·ether to the reaction mixture after 15 minutes for the isolation of the orange coloured dicationic salt (**3.1**) with two BF_4^- molecules as the counter anions (Scheme 3.1).^{28, 62} Interestingly, the addition of BF_3 led to the double C-F bond activation from C_6F_6 . The activation of another C-F bond is reflected in the ^{19}F NMR spectrum, which shows signals at $\delta -142.22$ ppm for the

four fluorine atoms on the phenyl core and at -148.37 ppm for the eight fluorine atoms of two BF_4 moieties. The ^{11}B NMR exhibits a signal at $\delta -1.11$ ppm, corresponding to the BF_4^- anions. In the HRMS, the molecular ion peak was found at m/z 464.3034 with the highest relative intensity, which supports the formation of **3.1**. The cyclic voltamogram of **3.1** (Figure 3.2) exhibits two reversible redox waves at $E_{p,red} = -0.95$ V, -1.91 V and oxidation at $E_{p,oxd} = -0.57$ V, -1.79 V, respectively. The reduction potential of **3.1** is significantly lower compared to the related C2-protonated imidazolium salts (ca. -2.3 V)⁶³ of NHCs, presumably due to the electron withdrawing effect of the fluoride atoms.

The molecular structure of **3.1** (Figure 3.2) reveals that the C2-C3 bond distance in the imidazolium rings is $1.530(6)$ Å, a value similar to that in 5-SIDipp [$1.5144(19)$ Å],⁶⁴ and other reported imidazolium salts. The average C-C bond length in the C_6F_4 linker is 1.38 Å, which is in agreement with that expected for the aryl ring. The C1/C10 carbene carbon adopts a trigonal planar geometry with an average angle of 114° (N1-C1-N2/N3-C10-N4). The C1-C4 bond length is $1.486(5)$ Å, indicating a C-C single bond. The bridging tetrafluorophenylene ring of **3.1** are planar and twisted by 65.6° (av) from the plane of the imidazole rings.

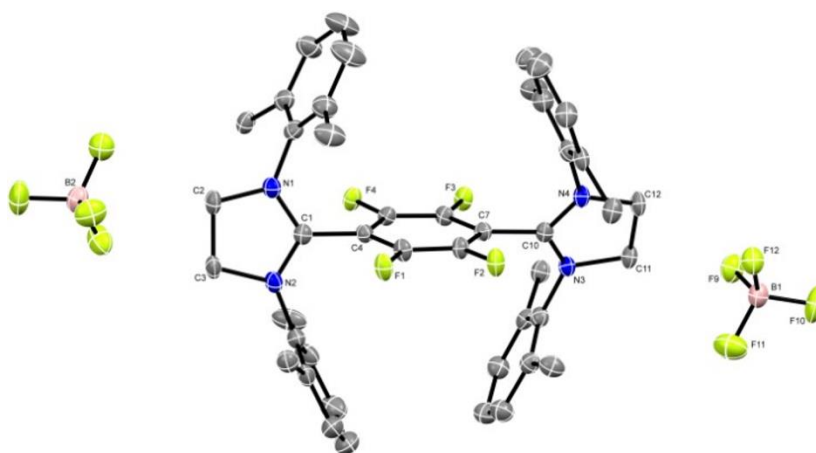


Figure 3.2. The molecular structure (ORTEP) of **3.1** with anisotropic displacement parameters drawn at 50 % probability level. The methyl groups of Dipp units and the hydrogen atoms are not shown for clarity. Selected bond lengths (Å) and angles ($^\circ$): C1-N1 $1.313(5)$, C1-N2

1.324(5), C2-N1 1.488(5), C2-C3 1.530(6), C1-C4 1.486(5); N1-C1-N2 114.6(4), C3-C2-N1 102.9(3), N1-C1-C4 122.0(4), N2-C1-C4 123.2(4).

After observing a strong visible luminescence under UV lamp, we have studied the photo-physical phenomenon of **3.1**, which shows a very intense absorption band at 356 nm along with weaker, broad bands at higher energy region (Figure 3.3). Upon exciting at $\lambda_{\max} = 356$ nm and 450 nm, **3.1** gives a strong emissive band at 636 nm with a huge Stokes shift ca. 12079 cm^{-1} and at $\lambda_{\max} = 510$ nm excitation it shows small Stokes shift ca. 2056 cm^{-1} . The lifetime measurement of **3.1** shows very short lifetimes 2.72 ns (B1 = 30.12 %) and 10.87 ns (B2 = 69.86 %) with bi-exponential in character; which is indicative of fluorescence.

Based on the cyclic voltammetry data, we wonder whether the reduction of **3.1** can serve as a precursor to access the 5-SIDipp mediated carbon diradical or tetrafluoro substituted quinoid hydrocarbon. Gratifyingly, the addition of lithium metal to the THF solution of **3.1** resulted in a colour change from yellowish orange to black immediately, and compound **3.2** was obtained as black solid in 62% yield along with the formation of an imine, $\text{CH}_2=\text{CH}-\text{N}(\text{Dipp})-\text{CH}=\text{N}(\text{Dipp})$.

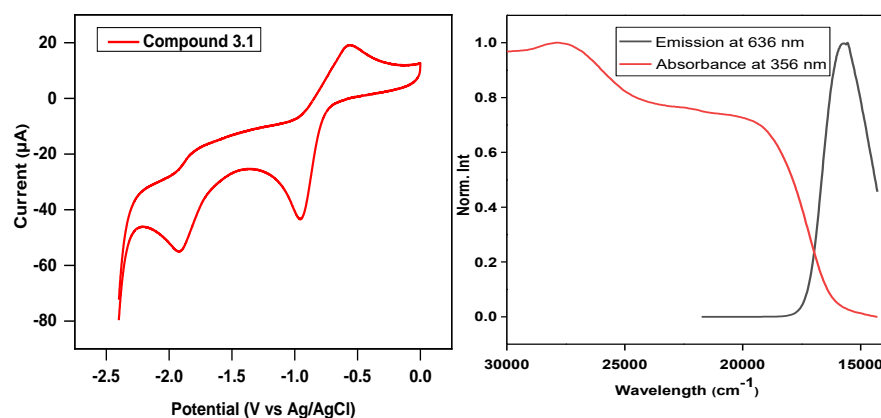
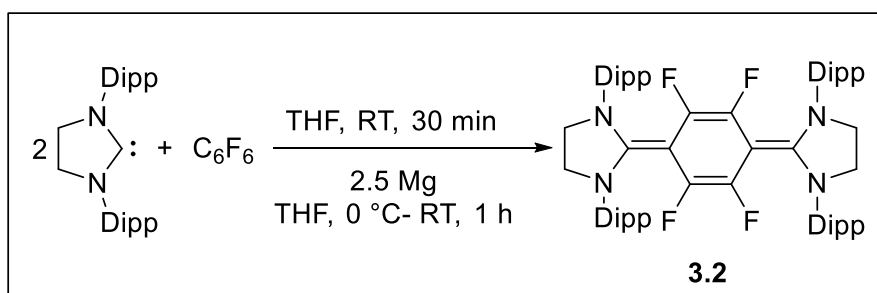


Figure 3.3. The cyclic voltammogram of **3.1** recorded at 0.7 V s^{-1} (left). Absorption (red lines) and emission (black lines) spectra of **3.1** at room temperature in the solid state (right).

Surprisingly, in situ addition of Mg powder at $0 \text{ }^\circ\text{C}$ in the reaction mixture of 5-SIDipp and C_6F_6 in THF led to the formation of **3.2** (Scheme 3.2) in one step. Mg is oxidized to Mg(II) by capturing two fluoride anions and is precipitated out from the system as MgF_2 . The generation of MgF_2 also inhibits the HF elimination. The molecular ion peak was observed at m/z 928.6006 with the highest relative intensity. To the best of our knowledge, there is no report so far on such single step access to any NHC based diradicaloid. **3.2** is stable in the solid state under inert atmosphere. However, in the solution state, we have observed gradual formation of the aforementioned imine after 2-3 days.



Scheme 3.2. One step methodology to access **3.2**.

Single crystals of **3.2** were grown by keeping the THF solution of **3.2** at 4 °C for 2-3 days. The molecular structure of **3.2** (Figure 3.4) reveals the trigonal planar geometry at the C5/C10 carbon atom with a N1-C5-N4/N3-C10-N2 angle of 108.3(2)^o/108.6(2)^o, which is in between of 5-SIDipp and its imidazolium salt (**3.1**). The C5-N4/N1 [1.397(av) Å] and C10-N2/N3 [1.40 (av) Å] bond lengths are significantly longer compared to those in **3.1** (C1-N1/N2 1.318 (av) Å and C10-N3/N4 1.326 (av) Å). The mean bond lengths of C5-C6/C9-C10 is 1.385Å, which is shorter compared to those in the dicationic salt, **3.1** (1.482 Å). There are some bond alternations in the C₆F₄ linker across C_{ortho}-C_{ipso} bond, which suggests that the unpaired electrons are delocalized into the aryl ring. (av. C_{ortho} 1.450 Å and av. C_{ipso} 1.346 Å). The imidazole rings of **3.2** are twisted by 23.6° (av) from the plane of the bridging phenylene ring, which is substantially lesser than those in **3.1**, indicating a significant contribution of the quinoid resonance form in the former. These geometric parameters suggest a close-shell singlet state as the ground state for **3.2**. Further conformation for the quinoidal character of **3.2** comes from the slight pyramidalization of one of the nitrogen atoms in the NHC units (the sum of the angles at the nitrogen atom {ΣN = 350.7^o}).⁶⁵

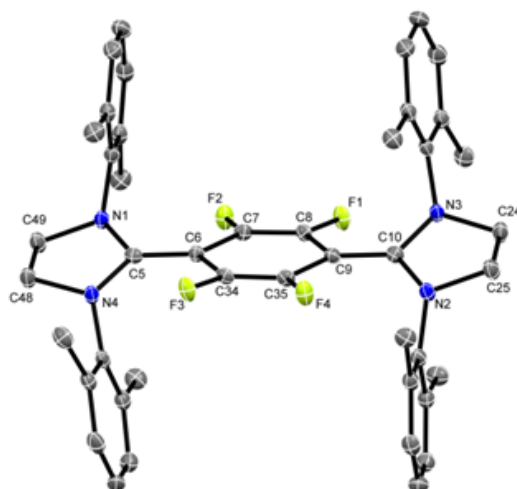


Figure 3.4. Molecular structure (ORTEP) of **3.2** with anisotropic displacement parameters drawn at 50 % probability level. The methyl groups of Dipp moieties and the hydrogen atoms are not shown for clarity. Selected bond lengths (Å) and angles (°): C5-N1 1.390(4), C5-N4 1.404(3), N2-C10 1.398(4), N3-C10 1.402(3), C5-C6 1.385(4), C10-C9 1.384(4), C9-C35 1.449(3), C35-C34 1.344(4), C34-C6 1.451(4), C7-F2 1.356(3); N1-C5-N4 108.3(2), N2-C10-N3 108.6(2), C9-C10-N2 126.60(17), C8-C9-C35 110.3(2).

In order to get the electronic structure and to understand the bonding scenario in compound **3.2**, DFT calculations were performed at B3LYP/def2-SVP level of theory (see Computational Details). Computed electronic states of **3.2** reveal that close-shell singlet remains the electronic ground state with singlet-triplet energy difference ($\Delta E_{S \rightarrow T}$) of $-23.7 \text{ kcal mol}^{-1}$. The computed bond lengths and angles of singlet state are in good agreement with the experimentally obtained X-ray crystal structure of those of the triplet state, which can be seen from the alignment and super position plot of the conformers. It is of note here that the replacement of H by F led to decrease of S \rightarrow T gap by $5.4 \text{ kcal mol}^{-1}$.⁵³

To gain insight into the bonding nature in **3.2**, we have also performed natural bond orbital (NBO) analysis at the B3LYP/def2-TZVPP//B3LYP/def2-SVP level of theory. NBO

population analysis entails that C5-C6/C9-C10 bonds in **3.2** shows a double bond character with σ and π occupancies of 1.973/1.973 e and 1.776/1.784 e , respectively. The σ -bond is formed mainly from the overlap of sp^2 -hybridized orbital of C5/C9 and sp^2 -hybridized orbital of C6/C10 atoms, while the π -bond is originated by the sideways overlap of pure p orbital of both the bonding partners. Calculated Wiberg bond indices (WBI) of C5-C6/C9-C10 bonds are 1.394 and 1.403 respectively, indicating significant double bond characters for both the cases. Thus, from the NBO results, we can predict the quinoidal bond nature in compound **3.2**. Additionally, we have measured the diradical character of **3.2** as described by Nakano et al,⁶⁶ but our calculated results reveal absence of any diradical character.

Room temperature UV-Vis spectra of a THF solution of **3.2** features two intense absorption bands at $\lambda_{\max} = 384$ and 476 nm with a shoulder at 769 nm ($\log \epsilon = 4.13$ -4.63 $M^{-1} \text{cm}^{-1}$). Subsequently, we have carried out time-dependent density functional theory calculations (TDDFT) to analyze the UV-Vis spectral signatures of **3.2**. The compound **3.2** in the close-shell configuration gives two main absorption bands at 446 and 332 nm, respectively. The higher-lying signal corresponds to the HOMO \rightarrow LUMO excitation with an oscillator strength of 1.1079, whereas the lower-lying signal designates the HOMO \rightarrow LUMO+2 transition ($f = 0.0635$). The HOMO represents the π orbital of C5-C6/C9-C10 bonds delocalized over benzene moiety, whereas the LUMO and LUMO+2 designate the lone pair of the carbene carbon and the π^* orbital of the -Dipp groups bonded to the nitrogen atoms, respectively. The selected KS-MOs of **3.2** are depicted in figure 3.5.

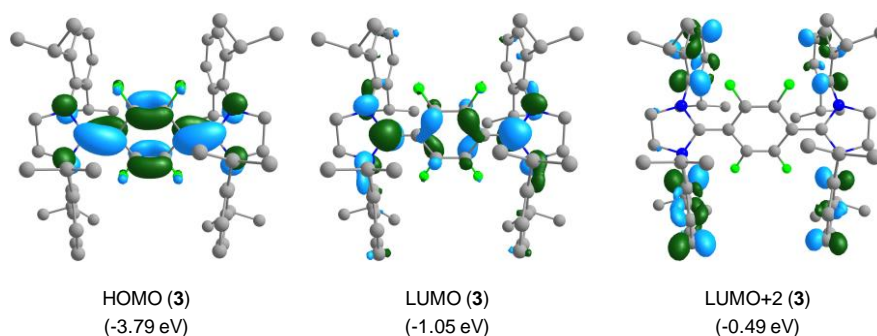


Figure 3.5. Selected KS-MOs of **3.2** (isosurface = 0.045 a.u.) at B3LYP/def2-TZVPP//B3LYP-def2-SVP level of theory. Hydrogen atoms are omitted for clarity.

Though our single crystal data and calculated result indicate a close-shell ground state for **3.2**, but the latter displays a doublet EPR signal characteristics of a monoradical impurity,⁶⁷⁻⁷³ which could not be isolated. Due to the presence of this paramagnetic impurity, we were unable to obtain well resolved ¹H and ¹³C NMR resonances.

3.3. Enhancing diradical character of Chichibabin's Hydrocarbon through fluoride substitution:

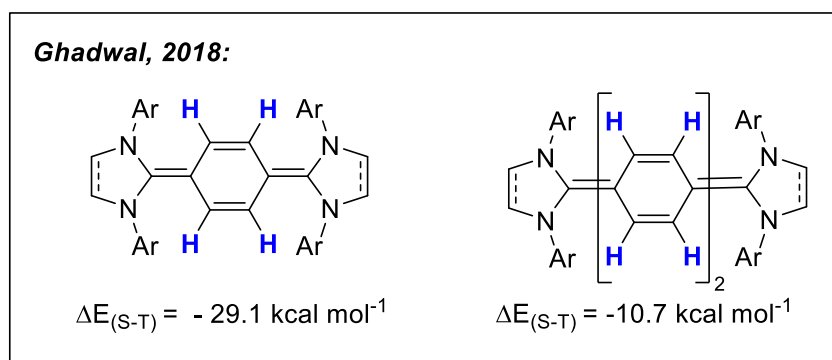
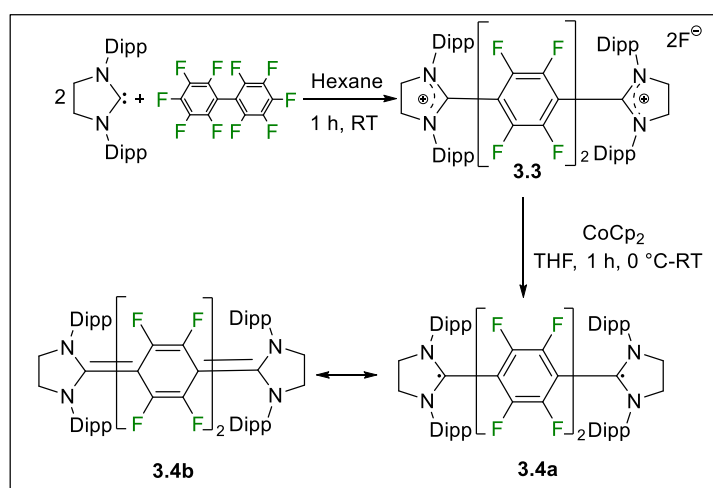


Figure 3.6. Decrease of singlet-triplet energy gap from the NHC based Thiele's to Chichibabin's hydrocarbon.^{52, 53}

In order to prepare the NHC based Chichibabin's hydrocarbon, we resort to the NHC mediated C-F activation strategy. We have treated decafluorobiphenyl with two equivalents of 5-SIDipp in *n*-hexane, which led to the formation of a yellow precipitation of the doubly C-F activated fluoride salt (**3.3**) at room temperature within 1 hour (Scheme 3.3). The solid precipitate was further dissolved in dichloromethane and kept at -36 °C to give yellow crystals of **3.3** within two days. **3.3** was characterized through NMR spectroscopy, mass spectrometry, and single crystal X-ray diffraction studies. The activation of another C-F bond is reflected in the ^{19}F NMR spectrum, which shows signals at δ -134 ppm for four *ortho* fluorine atoms and -144 ppm for the four *meta* fluorine atoms of the octafluoro-biphenyl rings.



Scheme 3.3. Preparation of NHC based Chichibabin's hydrocarbon with perfluoro aryl linker (**3.4**).

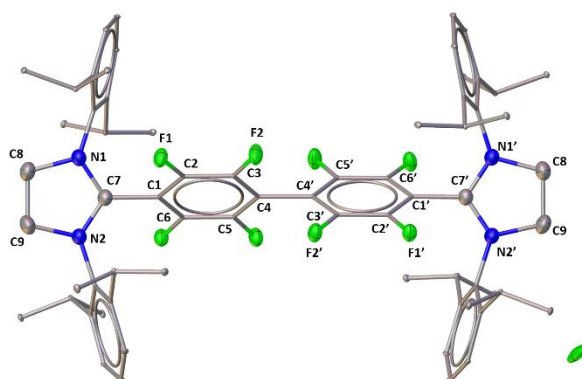


Figure 3.7. The molecular structure of **3.3**. The hydrogen atoms are not shown for clarity. Selected bond lengths (Å) and angles (°): C7-N1 1.309(6), C7-N2 1.340(6), C1-C7 1.493(6), C1-C2 1.359(7), C2-C3 1.406(7), C3-C4 1.356(7), C4-C5 1.351(7), C5-C6 1.392(7), C6-C1 1.360(7), C4-C4' 1.515(9), C2-F1 1.334(5), C3-F2 1.348(6); N1-C7-N2 113.0(4), N1-C7-C1 124.3(4), N2-C7-C1 126.1(3).

3.3 is crystalized in the triclinic *P*-1 space group (Figure 3.7). The central C7/C7' atoms adopt a trigonal geometry with an average angle of 113.0(4)° (N1-C1-N2/N1'-C7'-N2'). The average C-C bond distance of the backbone in the imidazolium rings (C9-C8) is 1.497(8)Å, which is comparable with starting compound, 5-SIDipp ([1.5144(19) Å].⁶⁴ and other reported imidazolium salts. The average C-C bond lengths in the octafluoro-biphenyl (C₆F₄-C₆F₄) linker is 1.37 Å, which is similar with the aryl ring. The C1/C1'-C7/C7' bond lengths are 1.493(6) Å, characteristics for a C-C single bond. The linker octa-fluorobiphenylene ring is twisted by 58.3° (av) from the plane of the imidazolin rings and two tetrafluorophenyl rings are twisted by 55.3° (av).

In order to reduce **3.3**, we have added two equivalents of cobaltocene with the fluoride salt in THF at -78 °C and the yellow color was immediately changed to a dark green solution (Scheme 3.3). The reaction was continued for another three hours at that temperature. Green

colored crystals of **3.4** were obtained after keeping the toluene solution of the reaction mixture at room temperature for 2 days and subjected to an X-ray diffraction study. The cobaltocene ($19 e^{-1}$) is oxidized to a stable $\text{Co(III)Cp}_2\text{F}$ ($18 e^{-1}$) species by capturing two fluoride anions and is precipitated out from the system. We have recorded the NMR spectrum of **3.4**, but observed peak broadening most likely due to the monoradical impurities, which we have observed for NHC based Thiele's hydrocarbon in the previous section. The molecular ion peak was observed at m/z 1077.4828 with the highest relative intensity. **3.4** is stable in the solid state under inert atmosphere.

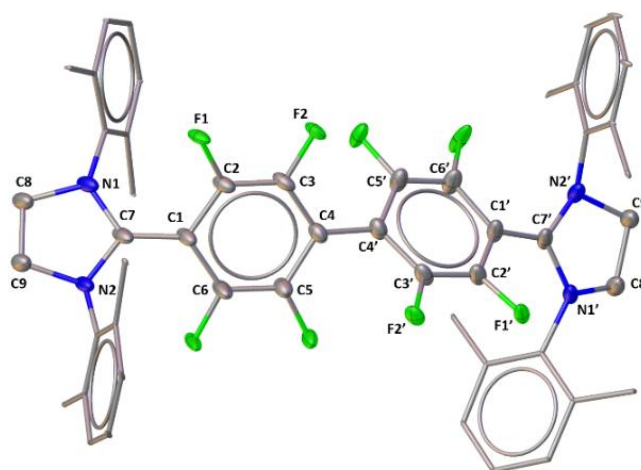


Figure 3.8. Molecular structure of **3.4**. The methyl groups of Dipp moieties and the hydrogen atoms are not shown for clarity. Selected bond lengths (\AA), angles and torsion angles (deg): C7-N1 1.379(4), C7-N2 1.382(3), C1-C7 1.402(4), C1-C2 1.430(4), C2-C3 1.346(4), C3-C4 1.429(4), C4-C5 1.353(4), C5-C6 1.426(4), C6-C1 1.434(4), C4-C4' 1.415(5), C2-F1 1.359(3), C3-F2 1.354(3); N1-C7-N2 108.6(3), N1-C7-C1 125.3(3), N2-C7-C1 126.1(3); N1-C7-C1-C2 23.6(2), N2-C7-C1-C6 $-157.4(4)$.

3.4 crystallized in the monoclinic $C2/c$ space group. The molecular structure of **3.4** (Figure 3.8) reveals the trigonal planar geometry at the C7/C7' carbon atom with a N1-C7-N2 angle of

108.6(3)°, which is in between 5-SIDipp and its imidazolium salt (**3.3**). The C7-N1/N2 [1.380 (av) Å] bond lengths are elongated compared to those in **2** (C7-N1/N2 1.318 (av) Å). The bond lengths of C1-C7/C1'-C7' is 1.402(4) Å, which is much shorter compared to those in the dicationic fluoride salt, **3.3** (1.493(6) Å). There are some bond alternations in the octafluoro-biphenyl linker across C_{ortho} - C_{ipso} , which suggests that the unpaired electrons are delocalized into the aryl ring. (av. C_{ortho} 1.429 Å and av. C_{ipso} 1.349 Å). The imidazolin rings of **3.4** are twisted by 25.9° (av) from the plane of the bridging phenylene ring and two C_6F_4 rings are twisted by 40.6°(av) from the plane of the imidazolium rings, which is considerably smaller than those in **3.3**, indicating of enhanced quinoidal character in **3.4**. These geometric parameters suggest a close-shell singlet state is the ground state for **3.4**. Further conformation for the quinoidal character of **3.4** comes from the pyramidalization of the nitrogen atoms in the imidazolium rings [the sum of the angles at the nitrogen atom ($\Sigma N = 350.6^\circ$)], while **3.3** is almost planar with the sum of the angles at the nitrogen atom ($\Sigma N = 358.2^\circ$).⁶⁵

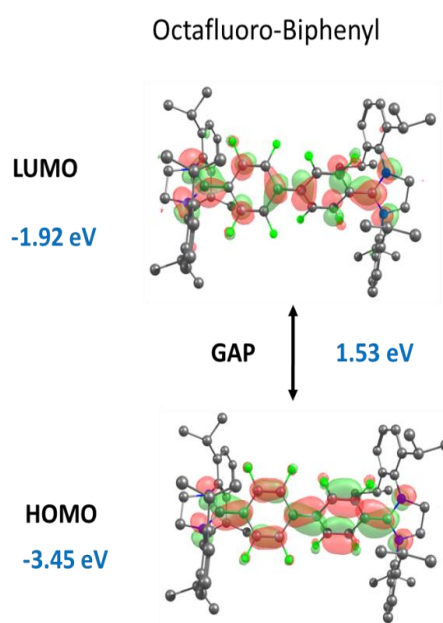


Figure 3.9. HOMO-LUMO Energy gap calculations for **3.4**.

In order to get the electronic structure and to understand the bonding scenario in compound **3.2**, DFT calculations were performed at B3LYP/def2-SVP level of theory (Figure 3.9). Computed electronic states of **3.2** reveal that close-shell singlet remains the electronic ground state with singlet-triplet energy difference ($\Delta E_{S\rightarrow T}$) of -3.7 kcal mol⁻¹. The computed bond lengths and angles of singlet state are in good agreement with the experimentally obtained X-ray crystal structure of those of the triplet state, which can be seen from the alignment and superposition plot of the conformers. It is of note here that the replacement of H by F led to decrease of S \rightarrow T gap by 7 kcal mol⁻¹. Our calculated results reveal 0.61 diradical character (Y) which is also increased compare to its hydrogen analogue ($Y = 0.40$).

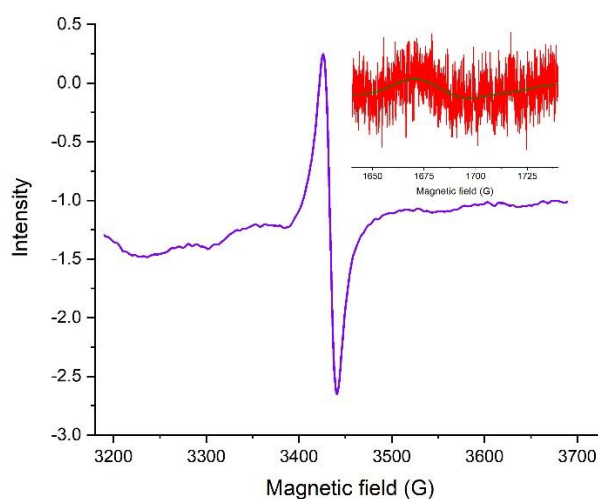


Figure 3.10. Solid state X-band EPR Spectrum of Chichibabin's hydrocarbon, **3.4** with inset showing the half field signal.

The calculated small ($\Delta E_{S\rightarrow T}$) -3.7 kcal mol⁻¹ suggest that the triplet state maybe populated to some extent at room temperature. A doublet EPR spectrum was observed in the solid state at 298K (Figure 3.10). This situation is very similar to the mysterious controversy over the magnetic properties of Chichibabin's hydrocarbon; which is known as "biradical paradox" as

the weak intensity triplet can be masked even with less than 0.1% impurity of a monoradical species, thereby showing a doublet-like spectrum. Interestingly, a half-field signal was detected for **3.4** at 298 K (Figure 3.10) for the forbidden $\Delta M_s = 2$ transition, which is characteristic for triplets.

After observing a strong visible luminescence under UV lamp, we have studied the photo-physical phenomenon of **3.4**, which shows a very intense absorption band at 697 nm (Figure 3.11). We have also studied concentration dependent UV spectra in THF solution of **3.4** ($\epsilon = 1.7 \times 10^5 \text{ M}^{-1}\text{cm}^{-1}$).

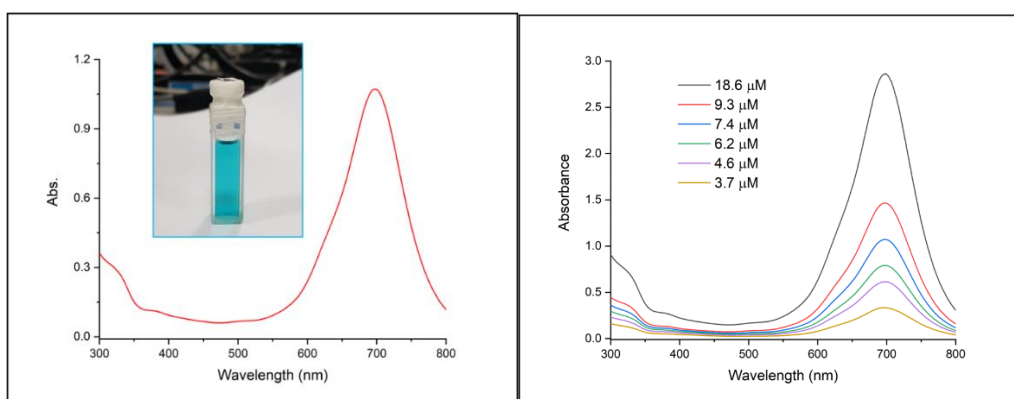


Figure 3.11. UV/Vis spectra of **3.4** in THF at different concentrations.

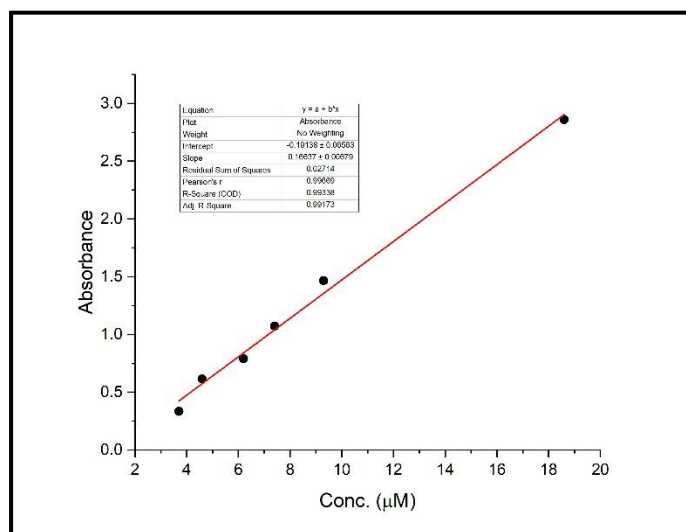
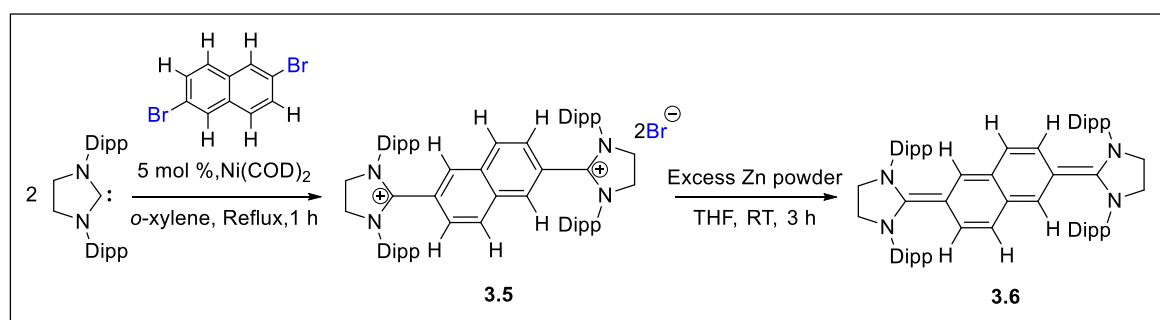


Figure 3.12. Linear regression of **3.4** at 697 nm.

3.4: Closed-Shell Kekulé Diradicaloids Spanned by Naphthalene and its Perfluoro Spacer:

In order to achieve the desired molecule, we first prepared the starting material, **3.5** from the direct two folds carbenylation of 2,6 dibromo-naphthalene with 5-SIDipp under Ni-catalysis (Scheme 3.4). The off-white solid is characterized by NMR spectroscopy, mass spectrometry and single crystal X-ray studies (Figure 3.13). The C-C bond lengths in the perfluoro naphthalene linker is unsymmetrical which is in agreement with that expected for the reported naphthyl ring. The $C_{carbene}$ adopts a trigonal planar geometry with an average angle of $111.7(2)^\circ$ (N1-C11-N2). The distance between the imidazolium ring and the $C_{10}H_6$ ring is $1.474(3) \text{ \AA}$ indicating a C-C single bond, which is similar with recently reported imidazolium salts. The bridging naphthyl ring of **3.5** is planar and twisted by 41.85 (average value) from the plane (torsion angles (deg) N1-C11-C8-C7 $-42.3(3)$, N2-C11-C8-C9 $-41.4(3)$) of the imidazole rings.

The reduction of **3.5** with excess Zn powder in toluene at room temperature gives the expected naphthalene based Kekulé based diradicaloid structure, **3.6** (Scheme 3.4). Upon extraction in toluene solution **3.6** is isolated as an air-sensitive pink colored solid powder in a 55% yield. **3.6** is stable in solution and solid phase under inert gas atmosphere. Single crystals of **3.6** suitable for X-ray diffraction were grown by storing the concentrated toluene solution at $-35\text{ }^{\circ}\text{C}$ for 3-4 days. The solid-state molecular structure of **3.6** is shown in figure 3.14. The molecular structure of **3.6** reveals the trigonal planar geometry at the C6 carbon atom with a N1-C6-N2 angle of $107.43(14)^{\circ}$, which is in between of 5-SIDipp and its imidazolium salt (**3.5**). The C6-N1/N2 [$1.399(2)$ (av) Å] bond lengths are significantly longer compared to those in **3.5** (C11-N1/N2 1.328 (av) Å). The mean bond lengths of C6-C5 is $1.381(2)$ Å, which is much shorter compared to those in the dicationic salt, **3.5** ($1.474(3)$ Å). There are some bond alternations in the C_{10}H_6 linker across C_{ortho} - C_{ipso} which suggests that the unpaired electrons are delocalized into the aryl ring. (av. C_{ortho} 1.447Å and av. C_{ipso} 1.360Å). The imidazole rings of **3.6** are twisted 12.9° (av) from the plane of the bridging phenylene ring, which is substantially lesser than those in **3.5**, indicating a significant contribution of the quinoid resonance form in the former.



Scheme 3.4. Synthesis of naphthalene based Kekulé diradicaloid, **3.6**.

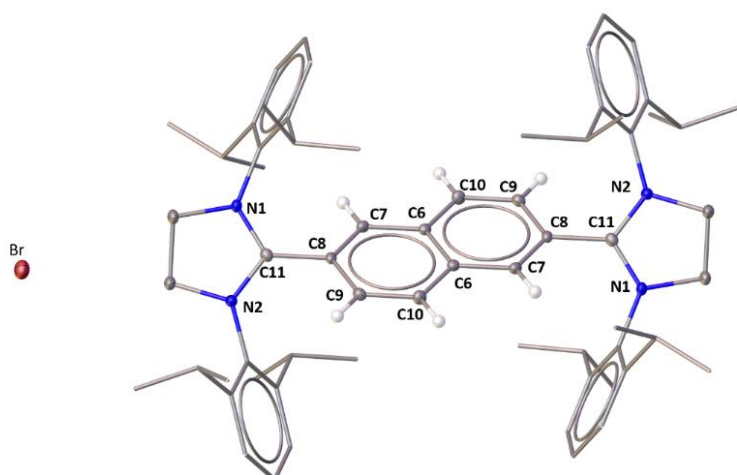


Figure 3.13. The molecular structures of **3.5**. Hydrogen atoms except the protons attached to boron are omitted for the clarity. Selected bond distances (Å) and bond angles (deg): C11-N1 1.327(3), C11-N2 1.330(3), C11-C8 1.474(3), C8-C7 1.375(3), C7-C6 1.415(3); N1-C11-N2 111.7(2), N1-C11-C8 123.9(2), N2-C11-C8 124.5(2); N1-C11-C8-C7 $-42.3(3)$, N2-C11-C8-C9 $-41.4(3)$.

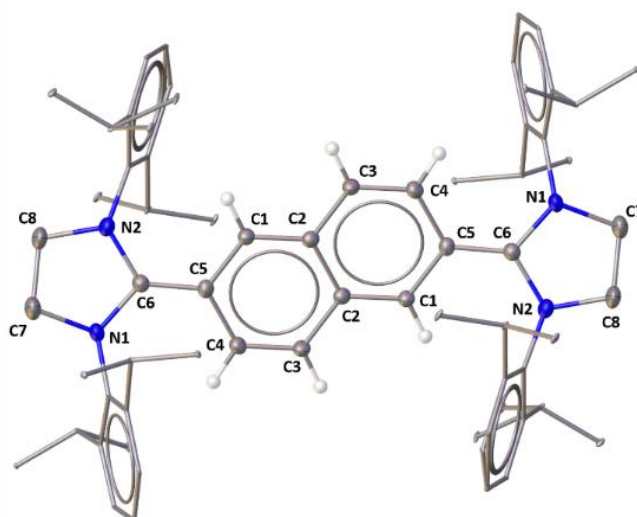
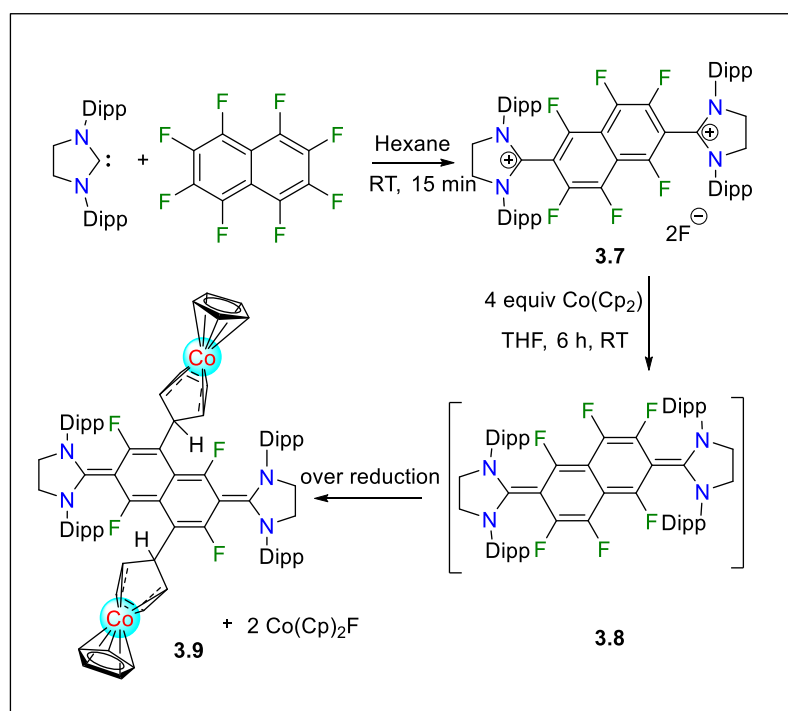


Figure 3.14. The molecular structures of **3.6**. Hydrogen atoms except the protons attached to boron are omitted for the clarity. Selected bond distances (Å) and bond angles (deg): C6-N1 1.399(2), C6-N2 1.399(2), C6-C5 1.381(2), C5-C1 1.450(2), C1-C2 1.354(2), C2-C3 1.440(2),

C3-C4 1.367(2), C4-C5 1.445(2); N1-C6-N2 107.43(14), N1-C6-C5 125.59(15), N2-C6-C5 126.96(15); N1-C6-C5-C4 12.3(3), N2-C6-C5-C1 13.4 (3).

In order to get the electronic structure and to understand the bonding scenario in compound **3.6**, DFT calculations were performed at B3LYP/def2-SVP level of theory. Computed electronic states of **3.6** reveal that close-shell singlet remains the electronic ground state with singlet-triplet energy difference ($\Delta E_{S \rightarrow T}$) of $-15.8 \text{ kcal mol}^{-1}$ (gas phase). The computed bond lengths and angles of singlet state are in good agreement with the experimentally obtained X-ray crystal structure of those of the triplet state, which can be seen from the alignment and super position plot of the conformers. It is of note here that the extension of one more phenylene linker from benzene to naphthalene linker led to the decrease of S \rightarrow T gap by $7.5 \text{ kcal mol}^{-1}$.



Scheme 3.5. Stepwise synthesis of fluorine substituted naphthalene based Kekulé biradical **3.9**.

Next, we sought to replace the hydrogen atoms of naphthalene with fluorine atoms and study whether it has any impact in the diradical character. An attractive strategy to replace the hydrogen with fluorine is to exploit the C-F bond activation tactic by NHC. Therefore, we have treated two equivalents of 5-SIDipp with one equivalent of octafluoro-naphthalene in toluene at ambient condition, which yielded the red colored dicationic salt **3.7** with two fluoride ions as counter anions (Scheme 3.5) within 15 min stirring. Interestingly, the double C-F activation of octafluoronaphthalene is not reported with any NHCs. **3.7** is well characterized via single crystal X-ray studies, NMR spectroscopy, and mass spectrometry. In the ^{19}F NMR spectrum, the signals at δ -114.14, -132.13 ppm characteristics for the four *ortho* fluorine atoms and -141.51 and -143.33 ppm for the two *meta* fluorine atoms in the naphthalene ring. The resonance at δ -175.98 ppm corresponds to the two fluoride anions. The molecular ion peak at m/z 556.2871 in the HRMS supports the formation of **3.7**.

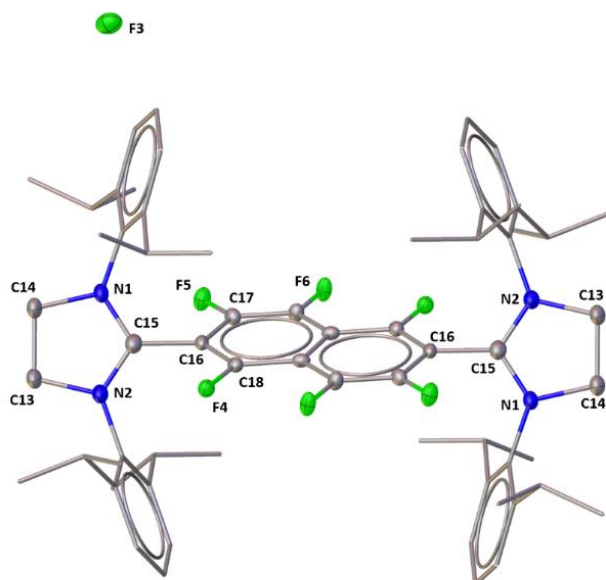


Figure 3.15. The molecular structure of **3.7**. Hydrogen atoms are omitted for clarity. Selected bond distances (Å) and angles (deg): C15-N1 1.316(3), C15-N2 1.320(3), C14N1 1.487(3),

C13-N2 1.488(3), C15-C16 1.483(3), C17-F5 1.299(3); N1-C15-N2 113.97(18), C13-N2-C15 109.49(17), N1-C15-C16 109.70(17), N2-C15-C16 124.23(19); N1-C15-C16-C17 54.9(3), N2-C15-C16-C18 58.3(3).

The molecular structure of **3.7** (Figure 3.15) has been determined by single crystal X-ray diffraction studies. The C-C bond lengths in the perfluoro naphthalene linker is unsymmetrical, which is in agreement with that expected for the reported naphthyl ring. The C_{carbene} adopts a trigonal planar geometry with an average angle of 113.9° (N1-C15-N2). The distance between the imidazolium ring and the $C_{10}F_6$ ring is 1.483(3) Å indicating a C-C single bond, which is similar with recently reported imidazolium salts. The bridging hexafluoro naphthyl ring of **3.7** is planar and twisted by 56.63° (average value) from the plane (torsion angles (deg) N1-C15-C16-C17 54.9(3), N2-C15-C16-C18 58.3(3)) of the imidazole rings.

Treatment of **3.7** with the four equivalents of cobaltocene at -30°C temperature in THF led to the unprecedented formation of an over reduced product **3.9** via the formation of the intermediate **3.8**. In **3.9**, two *meta*-C-F bonds of the naphthalene moiety have been replaced by cobaltocene and forms two C-C bonds. One of the cyclopentadiene ring which connects with the meta carbon of the naphthyl ring lost the planarity and binds with the four electrons at the cobalt atom and Co(II) oxidised to stable Co(III) centre. The side products $\text{Co}(\text{Cp})_2\text{F}$ was separated as brown precipitate from the system by extracting the product in *n*-hexane with 28 % yield. In 2017, the group of Bertrand and co-workers has shown the insertion of CoCp ring in the alkyne salt to trap the radical in the reduction with cobaltocene. The selective reduction of **3.7** with 2 equivalents of cobaltocene to isolate **3.8** was unsuccessful. **3.9** is only characterized by single crystal X-ray diffraction studies and mass spectrometry. Attempt to characterize **3.9** with NMR spectroscopy only results broadening of the spectrum due to

presence of the presence of mono radical impurities, which is very common for Kekulé type of biradicaloid species.

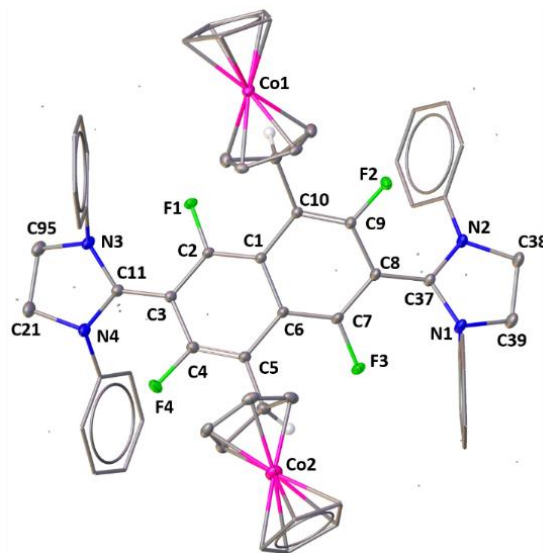


Figure 3.16. The molecular structure of **3.9**. Hydrogen atoms except one on the cp ring and the isopropyl groups of Dipp moieties are omitted for clarity of the figure. Selected bond distances (Å), bond angles (deg) and torsion angles (deg): C11-N3 1.3912(14), C11-N4 1.3893(14), C37-N1 1.3881(14), C37-N2 1.3852(14), C11-C3 1.3897(15), C37-C8 1.3896(14), C3-C2 1.4400(15), C2-C1 1.3636(14), C1-C6 1.4610(14), C6-C5 1.3641(15), C5-C4 1.3515(15), C4-C3 1.4486(15); C2-F1 1.3589(12), C10-C70 1.5426(15), C5-C74 1.5330(16); N3-C11-N4 107.82(9), N1-C37-N2 108.07(9), N3-C11-C3 125.10(10), N4-C11-C3 127.08(10); N3-C11-C3-C2 -21.9(2), N4-C11-C3-C4 -25.5(2), N2-C37-C8-C9 -24.4(2), N1-C37-C8-C7 -24.6(2).

The single crystals of **3.9** were grown by keeping the concentrated *n*-hexane solution of **3.9** at room temperature for 2 days. The molecular structure of **3** (Figure 3.16) reveals the trigonal planar geometry at the C11/C37 carbon atom with a N3-C11-N4/N1-C37-N2 angle of 107.82(9)°/ 108.07(9)°, which is in between of 5-SIDipp and its imidazolium salt, **3.7**. The C11-N3/N4 [1.390(av) Å]. and C37-N1/N2 [1.386 (av) Å] bond lengths are significantly longer

compared to those in **3.7** (C15-N1/N2 1.318 (av) Å). The mean bond lengths of C11-C3/C37-C8 is 1.389 Å, which is shorter compared to those in the dicationic salt, **3.7** (1.483(3) Å). There are some bond alternations in the C₁₀F₆ linker across C_{ortho}-C_{ipso} which suggests that the unpaired electrons are delocalized into the aryl ring. (av. C_{ortho} 1.444 Å and av. C_{ipso} 1.357 Å). The imidazole rings of **3.9** are twisted 24.1° (av) from the plane of the bridging phenylene ring, which is substantially lesser than those in **3.7**, indicating a significant contribution of the quinoid resonance form in the former. These geometric parameters suggest a close-shell singlet state is the ground state for **3.9**. Further conformation for the quinoidal character of **3.9** comes from the slight pyramidalization of one of the nitrogen atoms in the NHC units (the sum of the angles at the nitrogen atom { $\Sigma N = 350.7^\circ$ })

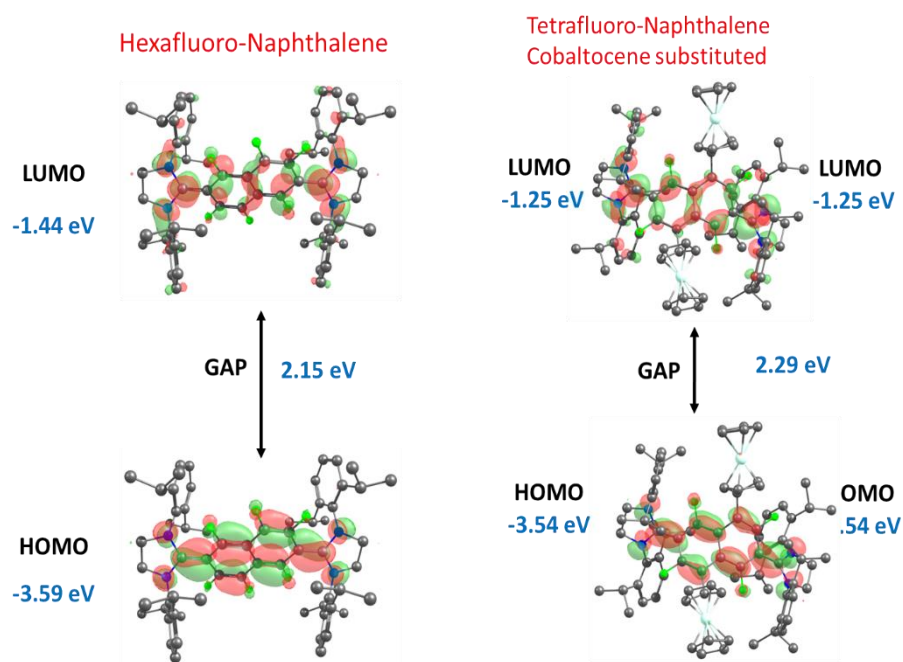


Figure 3.14. The HOMO-LUMO energy gap calculations of **3.8** and **3.9**.

In order to get the electronic structure and to understand the bonding scenario in compound **3.8** and **3.9**, DFT calculations were performed at B3LYP/def2-SVP level of theory. Computed

electronic states of both reveal that close-shell singlet remains the electronic ground state with singlet-triplet energy difference ($\Delta E_{S\rightarrow T}$) of $-17.1 \text{ kcal mol}^{-1}$. The computed bond lengths and angles of singlet state are in good agreement with the experimentally obtained X-ray crystal structure. It is of note here that the replacement of H by F in the naphthalene linker led to increase of S \rightarrow T gap by $1.3 \text{ kcal mol}^{-1}$.

3.5. Conclusion:

Herein, we have demonstrated a new synthetic pathway to obtain the NHC based Kekulé di-radicaloids. To prepare the NHC analogue of Thiele's hydrocarbon we have exploited the C-F activation of hexafluorobenzene and the replacement of hydrogen atoms with fluorines reduce the $\Delta E_{S\rightarrow T}$ by $5.4 \text{ kcal mol}^{-1}$. Further, we have prepared the NHC analogue of Chichibabin's hydrocarbon from the reduction of the dicationic imidazolium salt, **3.3**. The extension of fluorine based phenylene spacer to a biphenylene spacer reduced the $\Delta E_{S\rightarrow T}$ to $-3.7 \text{ kcal mol}^{-1}$ with a higher diradical character ($y = 0.61$). Subsequently, we have prepared for the first time the naphthalene based Kekulé hydrocarbons. For this purpose, we have chosen the octafluoronaphthalene and 2,6-dibromonaphthalene as precursors. The theoretical calculations reveal that the introduction of the fused ring in the spacer decreases the S-T energy gaps significantly ($\Delta E_{S\rightarrow T}$ for **3.6**: $-15.8 \text{ kcal mol}^{-1}$ and $\Delta E_{S\rightarrow T}$ of **3.9**: $-17.1 \text{ Kcal mol}^{-1}$) from that of phenylene.

3.6 References:

1. Abe, M., Diradicals. *Chem. Rev.* **2013**, *113*, 7011-7088.
2. Salem, L.; Rowland, C., The Electronic Properties of Diradicals. *Angew. Chem. Int. Ed.* **1972**, *11*, 92-111.
3. Breher, F., Stretching bonds in main group element compounds—Borderlines between biradicals and closed-shell species. *Coord. Chem. Rev.* **2007**, *251*, 1007-1043.
4. Grützmacher, H.; Breher, F., Odd-Electron Bonds and Biradicals in Main Group Element Chemistry. *Angew. Chem. Int. Ed.* **2002**, *41*, 4006-4011.
5. Jung, Y.; Head-Gordon, M., How Diradicaloid Is a Stable Diradical? *ChemPhysChem* **2003**, *4*, 522-525.
6. Kamada, K.; Ohta, K.; Kubo, T.; Shimizu, A.; Morita, Y.; Nakasuji, K.; Kishi, R.; Ohta, S.; Furukawa, S.-i.; Takahashi, H.; Nakano, M., Strong Two-Photon Absorption of Singlet Diradical Hydrocarbons. *Angew. Chem. Int. Ed.* **2007**, *46*, 3544-3546.
7. Morita, Y.; Suzuki, S.; Sato, K.; Takui, T., Synthetic organic spin chemistry for structurally well-defined open-shell graphene fragments. *Nat. Chem.* **2011**, *3*, 197-204.
8. Nakano, M.; Champagne, B., Theoretical Design of Open-Shell Singlet Molecular Systems for Nonlinear Optics. *J. Phys. Chem. Lett.* **2015**, *6*, 3236-3256.
9. Sun, Z.; Ye, Q.; Chi, C.; Wu, J., Low band gap polycyclic hydrocarbons: from closed-shell near infrared dyes and semiconductors to open-shell radicals. *Chem. Soc. Rev.* **2012**, *41*, 7857-7889.
10. Arnold, P. L.; Liddle, S. T., Deprotonation of N-heterocyclic carbenes to afford heterobimetallic organolanthanide complexes. *Organometallics* **2006**, *25*, 1485-1491.
11. Barry, B. M.; Soper, R. G.; Hurmalainen, J.; Mansikkamäki, A.; Robertson, K. N.; McClellan, W. L.; Veinot, A. J.; Roemmele, T. L.; Werner-Zwanziger, U.; Boéré, R. T.; Tuononen, H. M.; Clyburne, J. A. C.; Masuda, J. D., Mono- and Bis(imidazolidinium ethynyl)

Cations and Reduction of the Latter To Give an Extended Bis-1,4-([3]Cumulene)-p-carboquinoid System. *Angew. Chem. Int. Ed.* **2018**, *57*, 749-754.

12. Jiang, C.; Bang, Y.; Wang, X.; Lu, X.; Lim, Z.; Wei, H.; El-Hankari, S.; Wu, J.; Zeng, Z., Tetrabenzo-Chichibabin's hydrocarbons: substituent effects and unusual thermochromic and thermomagnetic behaviours. *Chem. Commun.* **2018**, *54*, 2389-2392.

13. Kikuchi, A.; Iwahori, F.; Abe, J., Definitive Evidence for the Contribution of Biradical Character in a Closed-Shell Molecule, Derivative of 1,4-Bis-(4,5-diphenylimidazol-2-ylidene)cyclohexa-2,5-diene. *J. Am. Chem. Soc.* **2004**, *126*, 6526-6527.

14. Maiti, A.; Zhang, F.; Krummenacher, I.; Bhattacharyya, M.; Mehta, S.; Moos, M.; Lambert, C.; Engels, B.; Mondal, A.; Braunschweig, H.; Ravat, P.; Jana, A., Anionic Boron- and Carbon-Based Hetero-Diradicaloids Spanned by a p-Phenylene Bridge. *J. Am. Chem. Soc.* **2021**, *143*, 3687-3692.

15. Ni, Y.; Gordillo-Gómez, F.; Peña Alvarez, M.; Nan, Z.; Li, Z.; Wu, S.; Han, Y.; Casado, J.; Wu, J., A Chichibabin's Hydrocarbon-Based Molecular Cage: The Impact of Structural Rigidity on Dynamics, Stability, and Electronic Properties. *J. Am. Chem. Soc.* **2020**, *142*, 12730-12742.

16. Rottschäfer, D.; Busch, J.; Neumann, B.; Stammler, H.-G.; van Gastel, M.; Kishi, R.; Nakano, M.; Ghadwal, R. S., Diradical Character Enhancement by Spacing: N-Heterocyclic Carbene Analogues of Müller's Hydrocarbon. *Chem. Eur. J.* **2018**, *24*, 16537-16542.

17. Chitnis, S. S.; Krischer, F.; Stephan, D. W., Catalytic Hydrodefluorination of C-F Bonds by an Air-Stable P-III Lewis Acid. *Chem. Eur. J.* **2018**, *24*, 6543-6546.

18. Chu, T.; Boyko, Y.; Korobkov, I.; Nikonov, G. I., Transition Metal-like Oxidative Addition of C-F and C-O Bonds to an Aluminum(I) Center. *Organometallics* **2015**, *34*, 5363-5365.

19. Jana, A.; Samuel, P. P.; Tavcar, G.; Roesky, H. W.; Schulzke, C., Selective Aromatic C-F and C-H Bond Activation with Silylenes of Different Coordinate Silicon. *J. Am. Chem. Soc.* **2010**, *132*, 10164-10170.
20. Mallov, I.; Johnstone, T. C.; Burns, D. C.; Stephan, D. W., A model for C-F activation by electrophilic phosphonium cations. *Chem. Commun.* **2017**, *53*, 7529-7532.
21. Mallov, I.; Ruddy, A. J.; Zhu, H.; Grimme, S.; Stephan, D. W., C-F Bond Activation by Silylium Cation/Phosphine Frustrated Lewis Pairs: Mono-Hydrodefluorination of PhCF₃, PhCF₂H and Ph₂CF₂. *Chem. Eur. J.* **2017**, *23*, 17692-17696.
22. Mondal, T.; De, S.; Koley, D., DFT Study on C-F Bond Activation by Group 14 Dialkylamino Metalylenes: A Competition between Oxidative Additions versus Substitution Reactions. *Inorg. Chem.* **2017**, *56*, 10633-10643.
23. Sen, S. S.; Roesky, H. W., Silicon-fluorine chemistry: from the preparation of SiF₂ to C-F bond activation using silylenes and its heavier congeners. *Chem. Commun.* **2018**, *54*, 5046-5057.
24. Swamy, V.; Parvin, N.; Raj, K. V.; Vanka, K.; Sen, S. S., C(sp³)-F, C(sp²)-F and C(sp³)-H bond activation at silicon(II) centers. *Chem. Commun.* **2017**, *53*, 9850-9853.
25. Emerson-King, J.; Hauser, S. A.; Chaplin, A. B., C-F bond activation of perfluorinated arenes by a bioxazoline-derived N-heterocyclic carbene. *Org. Biomol. Chem.* **2017**, *15*, 787-789.
26. Kim, Y.; Lee, E., Activation of C-F bonds in fluoroarenes by N-heterocyclic carbenes as an effective route to synthesize abnormal NHC complexes. *Chem. Commun.* **2016**, *52*, 10922-10925.
27. Kuhn, N.; Fahl, J.; Boese, R.; Henkel, G., On the reaction of 2,3-dihydroimidazol-2-ylidenes with pentafluoropyridine: Carbenes as reactants in nucleophilic aromatic substitution. *Z.Naturforsch.(B)* **1998**, *53*, 881-886.

28. Mallah, E.; Kuhn, N.; Maichle-Mossmer, C.; Steimann, M.; Strobele, M.; Zeller, K. P., Nucleophilic Aromatic Substitution with 2,3-Dihydro-1,3-diisopropyl-4,5-dimethylimidazol-2-ylidene. *Z.Naturforsch.(B)* **2009**, *64*, 1176-1182.
29. Paul, U. S. D.; Radius, U., Ligand versus Complex: C–F and C–H Bond Activation of Polyfluoroaromatics at a Cyclic (Alkyl)(Amino)Carbene. *Chem. Eur. J.* **2017**, *23*, 3993-4009.
30. Styra, S.; Melaimi, M.; Moore, C. E.; Rheingold, A. L.; Augenstein, T.; Breher, F.; Bertrand, G., Crystalline Cyclic (Alkyl)(amino)carbene-tetrafluoropyridyl Radical. *Chem. Eur. J.* **2015**, *21*, 8441-8446.
31. Bissinger, P.; Braunschweig, H.; Damme, A.; Krummenacher, I.; Phukan, A. K.; Radacki, K.; Sugawara, S., Isolation of a Neutral Boron-Containing Radical Stabilized by a Cyclic (Alkyl)(Amino) Carbene. *Angew. Chem. Int. Ed.* **2014**, *53*, 7360-7363.
32. Braunschweig, H.; Krummenacher, I.; Legare, M. A.; Matler, A.; Radacki, K.; Ye, Q., Main-Group Metallomimetics: Transition Metal-like Photolytic CO Substitution at Boron. *J. Am. Chem. Soc.* **2017**, *139*, 1802-1805.
33. Deissenberger, A.; Welz, E.; Drescher, R.; Krummenacher, I.; Dewhurst, R. D.; Engels, B.; Braunschweig, H., A New Class of Neutral Boron-Based Diradicals Spanned by a Two-Carbon-Atom Bridge. *Angew. Chem. Int. Ed.* **2019**, *58*, 1842-1846.
34. Hansmann, M. M.; Melaimi, M.; Bertrand, G., Crystalline Monomeric Allenyl/Propargyl Radical. *J. Am. Chem. Soc.* **2017**, *139*, 15620-15623.
35. Hansmann, M. M.; Melaimi, M.; Bertrand, G., Organic Mixed Valence Compounds Derived from Cyclic (Alkyl)(amino)carbenes. *J. Am. Chem. Soc.* **2018**, *140*, 2206-2213.
36. Hansmann, M. M.; Melaimi, M.; Munz, D.; Bertrand, G., Modular Approach to Kekule Diradicaloids Derived from Cyclic (Alkyl)(amino)carbenes. *J. Am. Chem. Soc.* **2018**, *140*, 2546-2554.

37. Kinjo, R.; Donnadiou, B.; Celik, M. A.; Frenking, G.; Bertrand, G., Synthesis and Characterization of a Neutral Tricoordinate Organoboron Isoelectronic with Amines. *Science* **2011**, *333*, 610-613.
38. Kundu, S.; Sinhababu, S.; Chandrasekhar, V.; Roesky, H. W., Stable cyclic (alkyl)(amino)carbene (cAAC) radicals with main group substituents. *Chem. Sci.* **2019**, *10*, 4727-4741.
39. Li, Y.; Mondal, K. C.; Samuel, P. P.; Zhu, H.; Orben, C. M.; Panneerselvam, S.; Dittrich, B.; Schwederski, B.; Kaim, W.; Mondal, T.; Koley, D.; Roesky, H. W., C4 Cumulene and the Corresponding Air-Stable Radical Cation and Dication. *Angew. Chem. Int. Ed.* **2014**, *53*, 4168-4172.
40. Li, Z. S.; Hou, Y. F.; Li, Y. Q.; Hinz, A.; Harmer, J. R.; Su, C. Y.; Bertrand, G.; Grutzmacher, H., L3C3P3: Tricarbontriphosphide Tricyclic Radicals and Cations Stabilized by Cyclic (alkyl)(amino)carbenes. *Angew. Chem. Int. Ed.* **2018**, *57*, 198-202.
41. Mahoney, J. K.; Jazzar, R.; Royal, G.; Martin, D.; Bertrand, G., The Advantages of Cyclic Over Acyclic Carbenes To Access Isolable C-Centered Radicals. *Chem. Eur. J.* **2017**, *23*, 6206-6212.
42. Mahoney, J. K.; Martin, D.; Moore, C. E.; Rheingold, A. L.; Bertrand, G., Bottleable (Amino)(Carboxy) Radicals Derived from Cyclic (Alkyl)(Amino) Carbenes. *J. Am. Chem. Soc.* **2013**, *135*, 18766-18769.
43. Mahoney, J. K.; Martin, D.; Thomas, F.; Moore, C. E.; Rheingold, A. L.; Bertrand, G., Air-Persistent Monomeric (Amino)(carboxy) Radicals Derived from Cyclic (Alkyl)(Amino) Carbenes. *J. Am. Chem. Soc.* **2015**, *137*, 7519-7525.
44. Martin, C. D.; Soleilhavoup, M.; Bertrand, G., Carbene-stabilized main group radicals and radical ions. *Chem. Sci.* **2013**, *4*, 3020-3030.

45. Melaimi, M.; Jazzar, R.; Soleilhavou, M.; Bertrand, G., Cyclic (Alkyl)(amino)carbenes (CAACs): Recent Developments. *Angew. Chem. Int. Ed.* **2017**, *56*, 10046-10068.
46. Mondal, K. C.; Roesky, H. W.; Schwarzer, M. C.; Frenking, G.; Tkach, I.; Wolf, H.; Kratzert, D.; Herbst-Irmer, R.; Niepotter, B.; Stalke, D., Conversion of a Singlet Silylene to a stable Biradical. *Angew. Chem. Int. Ed.* **2013**, *52*, 1801-1805.
47. Mondal, K. C.; Roy, S.; Roesky, H. W., Silicon based radicals, radical ions, diradicals and diradicaloids. *Chem. Soc. Rev.* **2016**, *45*, 1080-1111.
48. Munz, D.; Chu, J.; Melaimi, M.; Bertrand, G., NHC-CAAC Heterodimers with Three Stable Oxidation States. *Angew. Chem. Int. Ed.* **2016**, *55*, 12886-12890.
49. Paul, S. D. U.; Radius, U., What Wanzlick Did Not Dare To Dream: Cyclic (Alkyl)(amino) carbenes (cAACs) as New Key Players in Transition-Metal Chemistry. *Eur. J. Inorg. Chem.* **2017**, 3362-3375.
50. Roy, S.; Stuckl, A. C.; Demeshko, S.; Dittrich, B.; Meyer, J.; Maity, B.; Koley, D.; Schwederski, B.; Kaim, W.; Roesky, H. W., Stable Radicals from Commonly Used Precursors Trichlorosilane and Diphenylchlorophosphine. *J. Am. Chem. Soc.* **2015**, *137*, 4670-4673.
51. Messelberger, J.; Grünwald, A.; Pinter, P.; Hansmann, M. M.; Munz, D., Carbene derived diradicaloids – building blocks for singlet fission? *Chem. Sci.* **2018**, *9*, 6107-6117.
52. Rottschäfer, D.; Ho, N. K. T.; Neumann, B.; Stammler, H.-G.; van Gastel, M.; Andrada, D. M.; Ghadwal, R. S., N-Heterocyclic Carbene Analogues of Thiele and Chichibabin Hydrocarbons. *Angew. Chem. Int. Ed.* **2018**, *57*, 5838-5842.
53. Rottschäfer, D.; Neumann, B.; Stammler, H.-G.; Andrada, D. M.; Ghadwal, R. S., Kekulé diradicaloids derived from a classical N-heterocyclic carbene. *Chem. Sci.* **2018**, *9*, 4970-4976.

54. Rottschäfer, D.; Neumann, B.; Stammler, H.-G.; van Gastel, M.; Andrada, D. M.; Ghadwal, R. S., Crystalline Radicals Derived from Classical N-Heterocyclic Carbenes. *Angew. Chem. Int. Ed.* **2018**, *57*, 4765-4768.
55. Munz, D., Pushing Electrons-Which Carbene Ligand for Which Application? *Organometallics* **2018**, *37*, 275-289.
56. Tschitschibabin, A. E., Über das Triphenylmethyl. *Ber. Dtsch. Chem. Ges.* **1907**, *40*, 3056-3058.
57. Maiti, A.; Chandra, S.; Sarkar, B.; Jana, A., Acyclic diaminocarbene-based Thiele, Chichibabin, and Müller hydrocarbons. *Chem. Sci.* **2020**, *11*, 11827-11833.
58. Maiti, A.; Sobottka, S.; Chandra, S.; Jana, D.; Ravat, P.; Sarkar, B.; Jana, A., Diamidocarbene-Based Thiele and Tschitschibabin Hydrocarbons: Carbonyl Functionalized Kekulé Diradicaloids. *J. Org. Chem.* **2021**, *86*, 16464-16472.
59. Maiti, A.; Stubbe, J.; Neuman, N. I.; Kalita, P.; Duari, P.; Schulzke, C.; Chandrasekhar, V.; Sarkar, B.; Jana, A., CAAC-Based Thiele and Schlenk Hydrocarbons. *Angew. Chem. Int. Ed.* **2020**, *59*, 6729-6734.
60. Loh, Y. K.; Vasko, P.; McManus, C.; Heilmann, A.; Myers, W. K.; Aldridge, S., A crystalline radical cation derived from Thiele's hydrocarbon with redox range beyond 1 V. *Nat. Commun.* **2021**, *12*, 7052.
61. Talavera, M.; von Hahmann, C. N.; Muller, R.; Ahrens, M.; Kaupp, M.; Braun, T., C-H and C-F Bond Activation Reactions of Fluorinated Propenes at Rhodium: Distinctive Reactivity of the Refrigerant HFO-1234yf. *Angew. Chem. Int. Ed.* **2019**, *58*, 10688-10692.
62. Huber, S. M.; Heinemann, F. W.; Audebert, P.; Weiss, R., 4,5-Bis(dialkylamino)-Substituted Imidazolium Systems: Facile Access to N-Heterocyclic Carbenes with Self-Umpolung Option. *Chem. Eur. J.* **2011**, *17*, 13078-13086.

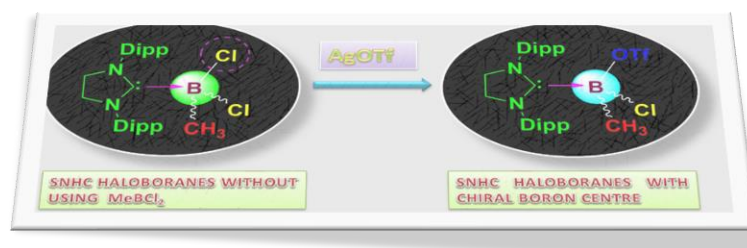
63. Gorodetsky, B.; Ramnial, T.; Branda, N. R.; Clyburne, J. A. C., Electrochemical reduction of an imidazolium cation: a convenient preparation of imidazol-2-ylidenes and their observation in an ionic liquid. *Chem. Commun.* **2004**, 1972-1973.
64. Giffin, N. A.; Hendsbee, A. D.; Masuda, J. D., 1,3-Bis(2,6-diisopropylphenyl)imidazolidin-2-ylidene. *Acta Crystallographica Section E* **2010**, *66*, o2194.
65. Schoeller, W. W.; Eisner, D., The 1,4-Diphosphabuta-1,3-diene Ligand for Coordination of Divalent Group 13 and 14 Elements: A Density Functional Study. *Inorg. Chem.* **2004**, *43*, 2585-2589.
66. Kamada, K.; Ohta, K.; Shimizu, A.; Kubo, T.; Kishi, R.; Takahashi, H.; Botek, E.; Champagne, B.; Nakano, M., Singlet Diradical Character from Experiment. *J. Phys. Chem. Lett.* **2010**, *1*, 937-940.
67. Kanzaki, Y.; Shiomi, D.; Sato, K.; Takui, T., Biradical Paradox Revisited Quantitatively: A Theoretical Model for Self-Associated Biradical Molecules as Antiferromagnetically Exchange Coupled Spin Chains in Solution. *J. Phys. Chem. B* **2012**, *116*, 1053-1059.
68. Ravat, P.; Baumgarten, M., "Tschitschibabin type biradicals": benzenoid or quinoid? *Phys. Chem. Chem. Phys.* **2015**, *17*, 983-991.
69. Su, Y.; Wang, X.; Zheng, X.; Zhang, Z.; Song, Y.; Sui, Y.; Li, Y.; Wang, X., Tuning Ground States of Bis(triarylamine) Dications: From a Closed-Shell Singlet to a Diradicaloid with an Excited Triplet State. *Angew. Chem. Int. Ed.* **2014**, *53*, 2857-2861.
70. Su, Y. T.; Wang, X. Y.; Li, Y. T.; Song, Y.; Sui, Y. X.; Wang, X. P., Nitrogen Analogues of Thiele's Hydrocarbon. *Angew. Chem. Int. Ed.* **2015**, *54*, 1634-1637.
71. Tan, G. W.; Wang, X. P., Isolable Bis(triarylamine) Dications: Analogues of Thiele's, Chichibabin's, and Muller's Hydrocarbons. *Accounts Chem. Res.* **2017**, *50*, 1997-2006.

72. Wang, J.; Xu, X.; Phan, H.; Herng, T. S.; Gopalakrishna, T. Y.; Li, G.; Ding, J.; Wu, J., Stable Oxindolyl-Based Analogues of Chichibabin's and Müller's Hydrocarbons. *Angew. Chem. Int. Ed.* **2017**, *56*, 14154-14158.
73. Zeng, Z. B.; Shi, X. L.; Chi, C. Y.; Navarrete, J. T. L.; Casado, J.; Wu, J. S., Pro-aromatic and anti-aromatic pi-conjugated molecules: an irresistible wish to be diradicals. *Chem. Soc. Rev.* **2015**, *44*, 6578-6596.

Chapter-4

Stepwise Nucleophilic Substitution to Access Saturated N-heterocyclic Carbene-haloboranes with Boron–methyl Bonds

Abstract: Compounds of boranes with N-heterocyclic carbenes (NHCs) are known, yet little attention has been paid to NHC compounds of



boron bearing a methyl and halogen moieties together. The reason for the less attention can be attributed to the hazardous methyldichloroborane (MeBCl₂), which ignites in air. In this chapter, we have used a saturated five-membered N-Heterocyclic carbene for the synthesis of SNHC-haloboranes adducts and their further nucleophilic substitutions to put unusual functional groups at the central boron atom. The reaction of 5-SIDipp with BR₃, BCl₃ and R'BCl₂ yields Lewis-base adducts, 5-SIDipp·BR₃ [R = H (**4.1**), C₆F₅ (**4.2**)], 5-SIDipp·BCl₃ (**4.3**) and 5-SIDipp·R'BCl₂ [R' = H (**4.4**), Ph (**4.5**)]. The hydrolysis of **4.4** gives the NHC stabilized boric acid, 5-SIDipp·B(OH)₃ (**4.6**), selectively. Replacement of chlorine atoms from **4.4** and **4.5** with one equivalent of AgOTf led to the formation of 5-SIDipp·HBCl(OTf) (**4.7**) and 5-SIDipp·PhBCl(OTf) (**4.8**). The addition of two equivalents of AgNO₃ to **4.5** leads to the formation of rare *di*-nitro substituted 5-SIDipp·BPh(NO₃)₂ (**4.10**). We describe here convenient solution-phase access to 5-SIDipp·MeBCl₂ (**4.11**) by salt metathesis reaction of 5-SIDipp·BCl₃ (**4.3**) with MeLi. Replacement of chlorine atoms from **4.11** with stepwise addition of AgOTf led to the formation of 5-SIDipp·MeBCl(OTf) (**4.12**), and 5-SIDipp·MeB(OTf)₂ (**4.13**). In the cases of **4.6**, **4.9** and **4.12** all the substituents on the boron atom are different. Further, the reaction of 5-SIDipp with B(C₆F₅)₃ in tetrahydrofuran and diethyl ether shows a frustrated Lewis pair type small molecule activated products, **4.14** and **4.15**.

4.1. Introduction:

The combination of an N-heterocyclic carbene (NHC) with a borane usually results in a complex called NHC·borane. Although before 2008, there was not many reports on NHC·borane complexes, significant advances have been made in the subsequent years. Early work on NHC·boranes was centered on the complexes of simple boranes such as BH_3 , BF_3 that were prepared by direct complexation of the NHC with the corresponding borane.¹⁻⁵ Subsequently, the synthesis of more than two dozen NHC·borane complexes of composition $\text{NHC}\cdot\text{BX}_3$, $\text{NHC}\cdot\text{BHX}_2$, $\text{NHC}\cdot\text{BH}_2\text{X}$, etc. have been reported, mainly from the groups of Curran, Braunschweig, Robinson, Tamm, and others.⁶⁻¹⁶ In an elegant review on NHC·borane adducts,¹⁰ Curran and co-workers noted that the field is still open and concluded by posing a question what other NHC·boranes can be made? Interestingly, a survey of known $\text{NHC}\cdot\text{RBX}_2$ with different R groups reveal that the common functional groups in carbon chemistry like methyl groups are rarely found bound to boron atoms in NHC·borane adducts. For example, $\text{NHC}\cdot\text{BCl}_2\text{Ph}$ is known,¹⁷ but $\text{NHC}\cdot\text{BCl}_2\text{Me}$ is unknown. One reason could be the needed borane (MeBCl_2) is not widely available. It is prepared from the reaction of Me_3SnCl with excess BCl_3 that gives rise to a mixture of products (eqn. 1). MeBCl_2 has a boiling point of $11\text{ }^\circ\text{C}$, ignites in contact with air, and should be stored in a Schlenk tube equipped with a grease-free stopcock at a temperature below $-30\text{ }^\circ\text{C}$.¹⁸ So, *handling of MeBCl_2 under laboratory condition is non-trivial*. The other reason is that in carbon chemistry the methyl group behaves as electron donor (+I effect), while in boron chemistry the methyl groups are electron-withdrawing (-I effect) due to the difference in electronegativity between carbon (2.5) and boron (2.0).¹⁹ To our knowledge, no structural information is available on NHC·methylhaloborane compounds to date and $\text{IDipp}\cdot\text{BCl}_2\text{iPr}$ is the only known alkylhaloborane adduct prepared by Braunschweig and coworkers.²⁰ So, we were interested to

make NHC·haloborane adducts, where one of the substituents of the boron atom is a methyl group. It is of note here that MeBCl₂ was detected as an intermediate in the chemical vapor deposition synthesis of boron carbide,²¹ and studying the chemistry of MeBCl₂ might provide a deeper understanding of its chemical reactivity.

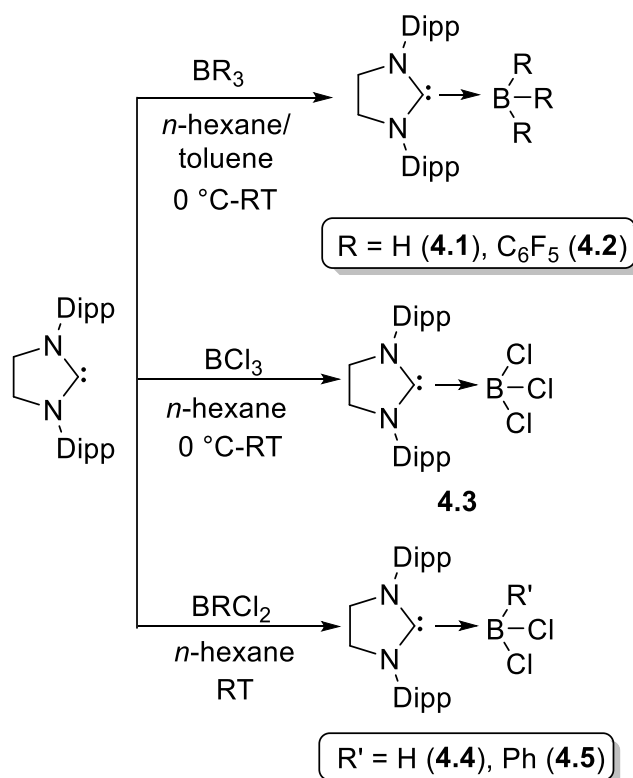


In 2007, Robinson and co-workers introduced IDipp ligand for making the IDipp·BBr₃ adduct and subsequent stabilization of compounds with B–B single and double bonds.¹⁵ The same NHC was later employed by Braunschweig and co-workers for the isolation of a compound with a B≡B triple bond.²² Curran and co-workers reported a series of NHC·boranes with the same NHC by means of nucleophilic substitution reaction.¹² In view of our current interest in saturated NHCs, we have chosen the saturated version of IDipp, known as 5-SIDipp for our study. We have noted that the contribution of saturated NHCs in boron chemistry is rather cursory. Nonetheless, the Braunschweig group isolated a B-B triply bound compound using 5-SIDipp as a ligand [SIDipp→B≡B←SIDipp].²³

Herein we demonstrate a detailed study of nucleophilic substitution reactions of 5-SIDipp·haloboranes. 5-SIDipp·BCl₃ compound (**4.3**), which led to 5-SIDipp·BMeCl₂ adduct (**4.11**). This is the first carbene·BMeCl₂ adduct, and it does not require the use of hazardous MeBCl₂. Removal of another chlorine from **4.3** with the trifluoromethanesulfonate (OTf) group resulted in an unusual NHC·borane, 5-SIDipp·B(Me)(Cl)(OTf) (**4.12**), where the three groups attached to the boron center are different. Subsequent removal of another chloride by OTf moiety led to 5-SIDipp·B(Me)(OTf)₂ (**4.13**). We have also studied the substitution reactions of 5-SIDipp·BHCl₂, **4.4** and 5-SIDipp·BPhCl₂, **4.5** with AgOTf, AgNO₃, and water to attach rare functional groups on the boron atom. Furthermore, we have shown that the combination 5-SIDipp and B(C₆F₅)₃ led to the activation of THF and diethyl ether via frustrated Lewis pair (FLP) way.

4.2. Preparation of 5-SIDipp-boranes and haloborane adducts:

We started our investigation by reacting 5-SIDipp with simple commercially available boron compounds. The addition of one equivalent of $\text{BH}_3 \cdot \text{ether}$ in the *n*-hexane solution of 5-SIDipp at low temperature led to the formation of **4.1** (Scheme 4.1). The latter was previously characterized by NMR spectroscopy by the group of Curran in 2010,²⁴ but was not structurally characterized. Storing the concentrated toluene solution at $-35\text{ }^\circ\text{C}$ in a freezer afforded the colorless crystals of **4.1** suitable for single crystal X-ray analysis. It crystallizes in the monoclinic space group, $P2_1/n$ (Figure 4.1) The formation of the adduct resulted in pyramidalization of the boron atom leading to a distorted tetrahedral geometry, with a change in hybridization at boron from approximately sp^2 to sp^3 . The distance between the boron and the carbene carbon atom is $1.594(4)\text{ \AA}$, which is comparable with those in the previously reported $\text{NHC} \cdot \text{BH}_3$ adducts.²⁵



Scheme 4.1. Synthesis of **4.1-4.5**

5-SIDipp·B(C₆F₅)₃ (**4.2**) is synthesized by the treatment of tris(pentafluorophenyl)borane in toluene solution of 5-SIDipp with at very low temperature. Colorless crystals of **4.2** are isolated by keeping the solution at -36 °C for in a day. **4.2** Crystallizes in the monoclinic *P*-1 space group. The molecular structure of **4.2** is shown in figure 4.2. The distance between carbene carbon atom C27 and B atom 1.696(3) Å, which is longer than normal IDipp·B(C₆F₅)₃ adduct (1.663(5) Å).²⁶ This bond elongation is probably a consequence of the enhanced steric bulk at the tetracoordinated boron center. One of the pentafluoroarene rings is co-planar with the Dipp arene ring, stabilized through the π arene interaction. The ¹¹B NMR spectrum of **4.2** shows one signal at -15.5 ppm, which is in accordance with the recently reported a *a*NHC adduct of B(C₆F₅)₃.²⁷ Similar to IDipp·B(C₆F₅)₃, **4.2** is not stable in solution at room temperature and hence we were unable to satisfactorily characterize by NMR spectroscopy.

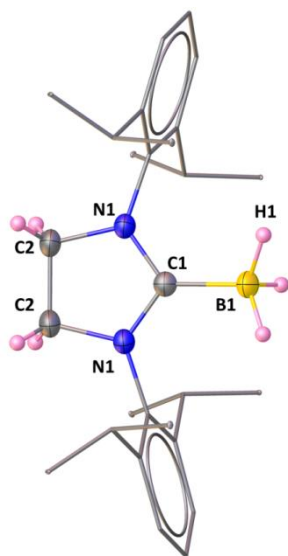


Figure 4.1. The molecular structure of **4.1**, there is only half molecule in the asymmetric unit (except hydrogen atoms attached to the boron atom and the carbene backbone, other hydrogen atoms are omitted for the clarity of the picture). Selected bond lengths [Å] and angles [deg]: C2–C2 1.517(4), C2–N1 1.465(2), C1–N1 1.338(2), C1–B1 1.593(4), B1–H1 1.0851; N1–C1–N1 108.5(2), N1–C1–B1 125.73(11), C1–B1–H1 111.1.

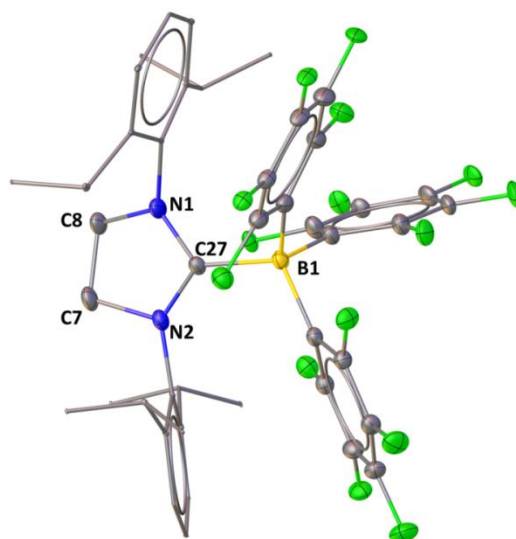


Figure 4.2. The molecular structure of **4.2** (hydrogen atoms are omitted for the clarity of the picture). Selected bond lengths [Å] and angles [deg]: C7–C8 1.483(4), C8–N1 1.484(3), C7–N2 1.477(3), C27–N2 1.355(3), C27–N1 1.343(3), C27–B1 1.696(3); N1–C27–N2 107.69(18), N1–C27–B1 130.5(2), N2–C27–B1 121.42(18).

The addition of BHCl_2 -dioxane in the solution of 5-SIDipp in *n*-hexane gives the white precipitation of 5-SIDipp· BHCl_2 , **4.4** at room temperature (Scheme 1). The precipitate was further dissolved in toluene and dichloromethane to afford the colorless crystals of **4.4** at -36 °C. The ^{11}B NMR spectrum of **4.4** displays a resonance at 6.9 ppm as a sharp singlet. The backbone four protons appeared at 4.08 ppm in the ^1H NMR spectrum. **4.4** is characterized by single-crystal X-ray diffraction studies (Figure 4.3). **4.4** is crystalized in the monoclinic $P2_1/n$ space group. The B–C bond length in **4.4** [1.628(7) Å] is considerably longer compared to that in the 5-SIDipp· BH_3 [1.593(4) Å]. The increase in the bond length can be ascribed to the enhancement of steric hindrance at the central boron atom. The average B–Cl distance is 1.86 Å, which matches with the previously reported carbene-haloborane adducts ($\text{NHC}\cdot\text{BCl}_3$, $\text{NHC}\cdot\text{BRCl}_2$, and $\text{NHC}\cdot\text{BR}_2\text{Cl}$).

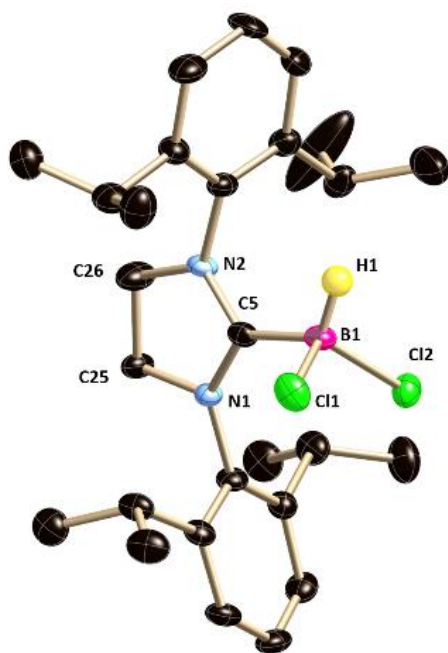


Figure 4.3. The molecular structure of **4.4** (hydrogen atoms except at the boron atom in **1** are omitted for clarity). Selected bond lengths [\AA] or angles [deg]: C5–N1 1.337(5), C5–N2 1.329(6), C25–N1 1.491(6), C26–N2 1.477(6), C5–B1 1.628(7), B1–Cl1 1.865(5), B1–Cl2 1.869(5); N1–C5–N2 109.2(4), N1–C5–B1 128.9(4), N2–C5–B1 121.9(4), Cl1–B1–Cl2 110.1(3).

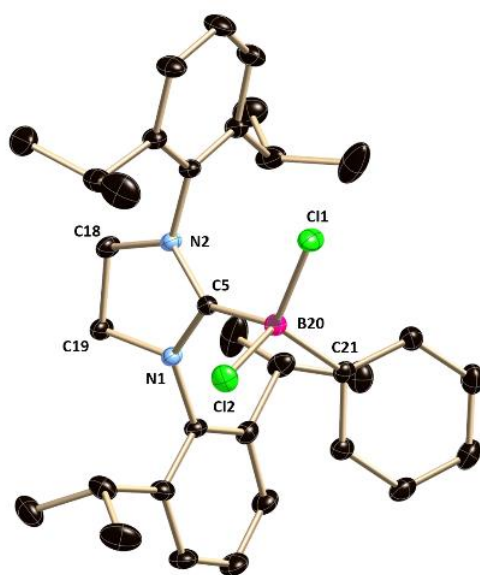
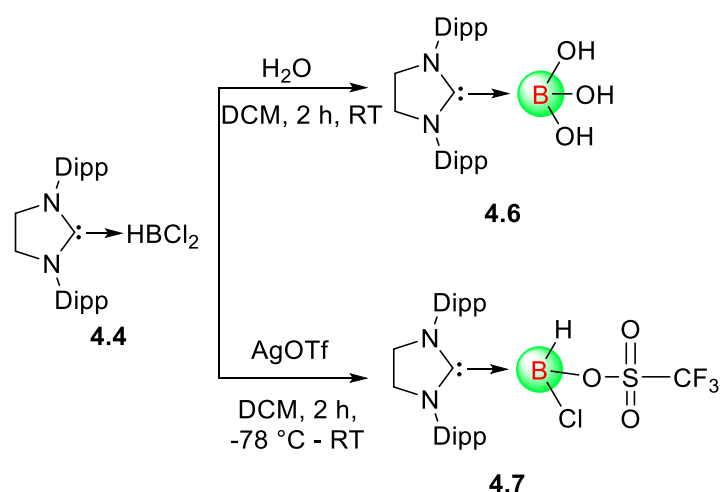


Figure 4.4. The molecular structure of **4.5**. Hydrogen atoms are omitted for clarity. Selected bond lengths [\AA] or angles [deg]: C5–N1 1.3403(8), C5–N2 1.3443(8), C19–N1 1.4810(9),

C18–N2 1.4756(9), C5–B20 1.6661(10), B20–C21 1.6204(10), B20–Cl1 1.8992(8), B20–Cl2 1.8698(8); N1–C5–N2 108.63(6), N1–C5–B20 127.41(6), N2–C5–B20 123.20(6), C5–B20–Cl1 100.88(4), C5–B20–C21 110.99(5), Cl1–B20–Cl2 106.42(4).

The reaction of 1.1 equivalent of PhBCl₂ with 5-SIDipp in *n*-hexane gives an immediate white precipitate formation of 5-SIDipp·PhBCl₂ (**4.5**) (Scheme 4.1). The ¹¹B NMR spectrum of **4.5** shows one resonance at 1.8 ppm. **4.5** crystallizes in the monoclinic *P*2₁/*n* space group (Figure 4.4). The carbene carbon atom C5 is tri-coordinated and features a trigonal-planar geometry, and the boron atom connected with the C5 atom adopts a tetrahedral geometry. The B–C_{NHC} bond distance is 1.6661(10) Å, which is slightly longer in comparison to that in **4.4** due to the steric congestion rendered by the phenyl group at the boron center. The B–Cl bonds are 1.8992(8) Å and 1.8698(8) Å, which are in good agreement with the previously reported B–Cl bond distance.

4.3. Nucleophilic substitution at the tetracoordinate 5-SIDipp-haloborane centre:



Scheme 4.2. Reactivity of **4.4** with H₂O and AgOTf.

Treatment of 1.05 equivalents of water in a dichloromethane solution of **4.4** hydrolyses all the B–H and B–Cl bonds and forms NHC-stabilized boric acid, 5-SIDipp·B(OH)₃, **4.6** (Scheme 4.2) exclusively. Replacement of the chloride and the hydride groups by hydroxide moieties in **4.4** is accompanied by an upfield shift in the ¹¹B NMR spectrum (–1.6 ppm) from that of **4.1**. **4.4** crystallizes in the monoclinic *P*2₁/*c* space group (Figure 4.5). The central boron-carbon distance is 1.650(5) Å and the average B–O bond distances are 1.38 Å.

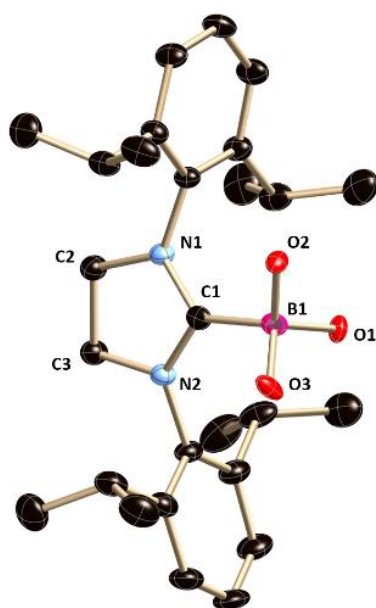


Figure 4.5. The molecular structure of **4.6**. Hydrogen atoms are omitted for clarity. Selected bond lengths [Å] or angles [deg]: N1–C1 1.316(4), N2–C1 1.337(4), C2–N1 1.471(4), C3–N2 1.478(4), C1–B1 1.650(5), B1–O1 1.375(4), B1–O2 1.386(4); N1–C1–N2 113.2(3), N1–C1–B1 125.4(3), N2–C1–B1 125.0(3), C1–B1–O1 110.4(3), C1–B1–O2 108.5(3), O1–B1–O2 111.1(3).

Further, we added silver triflate (AgOTf) to a dichloromethane solution of **4.4** at –78 °C, which replaced one of the labile chlorine atoms by the triflate group (Scheme 4.2). In the ¹¹B NMR

spectrum of **4.7**, the resonance for the central boron atom appears at -3.4 ppm. The resonance at -76.7 ppm in the ^{19}F NMR is characteristic of the triflate group attached to the central boron atom. Colorless crystals of **4.7** suitable for X-ray diffraction studies were grown from a saturated toluene solution at 4 °C. The constitution of **4.7** was authenticated by a single-crystal X-ray study (Figure 4.6). **4.7** crystallizes in the monoclinic space group $P2_1/n$. The relevant bond length and angles are given in the legend of figure 4.6. All the four substituents on the central boron atom are different in **4.7**. The central boron atom (B1) lies slightly below the plane of an imidazolium ring (torsion angles (deg): C2–N1–C1–B1 = $174.4(2)$ and C3–N2–C1–B1 $-166.5(2)$) and the B–O bond is not orthogonal to the plane of the imidazolium ring with the torsion angles N1–C1–B1–O1 = $-41.6(2)^\circ$ and N2–C1–B1–O1 = $148.4(2)^\circ$. The B–OTf bond length is $1.515(2)$ Å, which is in good agreement with the B–O bond length in our previously reported 5-SIDipp·BMeOTfCl (B1–O3 $1.503(3)$ Å).

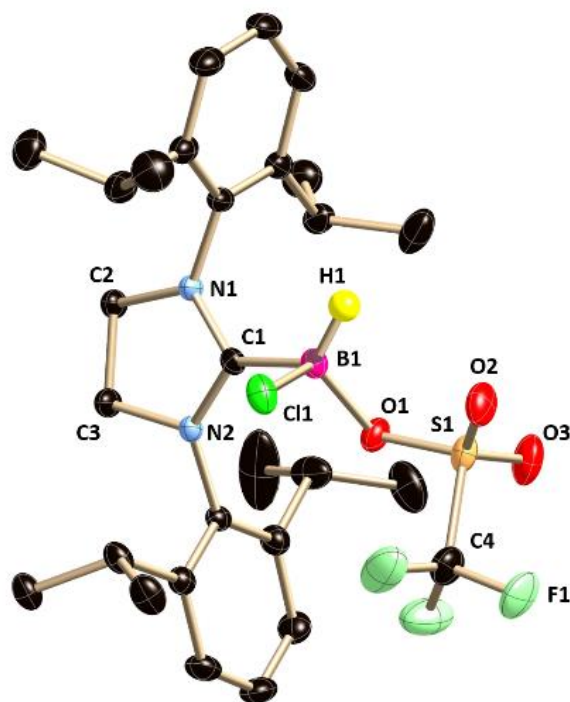
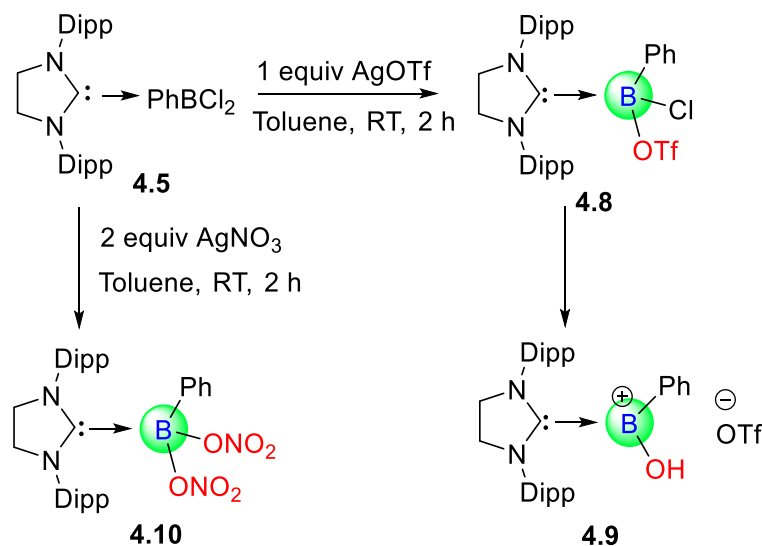


Figure 4.6. The molecular structure of **4.7**. Hydrogen atom except H1 are omitted for clarity. Selected bond lengths [Å] or angles [deg]: N1–C1 1.316(4), N2–C1 1.337(4), C2–N1 1.471(4), C3–N2 1.478(4), C1–B1 1.650(5), B1–O1 1.375(4); N1–C1–N2 113.2(3), N1–C1–B1 125.4(3), N2–C1–B1 125.0(3), C1–B1–O1 110.4(3).

Treatment of one and two equivalents of AgOTf and AgNO₃ with **4.5** in toluene afforded *mono*-triflate and *di*-nitro substituted 5-SIDipp-boranes, respectively. Substitution of one and two chlorine atoms from the tetra coordinated boron atom of **4.5** resulted in the formation of 5-SIDipp·BPhCl(OTf), **4.8**, and 5-SIDipp·BPh(ONO₂)₂, **4.10** (Scheme 4.3). The functional groups such as nitrate and triflate are rarely found to bind with the boron atom.²⁸⁻³⁴ **4.8** crystallizes in the monoclinic *P*2₁/*n* space group (Figure 4.7). The boron atom lies on a tetrahedral geometry, which can be confirmed from the bond angles around the boron atoms in **4.8** (C5–B2–Cl1 100.54(11), C5–B2–O1 106.51(13), and C5–B2–C7 118.55(14)). The B–C_{NHC} bond length in **4.8** (1.648(2) Å) is in well agreement with that in **4.5**. The B–O and B–Cl

bonds in **4.8** are almost orthogonal to the plane (torsion angle: N1–C5–B2–Cl1 76.96(17)°, N2–C5–B2–Cl1 –89.6(2)° and torsion angle: N1–C5–B2–O1 –170.96(14)°, N2–C5–B2–O1 22.5(2)°, respectively).



Scheme 4.3. Nucleophilic substitution of **4.5** with AgOTf and AgNO₃.

However, the spectroscopic characterization of **4.8** becomes complicated because of solvent-mediated slow hydrolysis. The only signal in the ¹¹B NMR spectra of the product, **4.9** appears at 30.9 ppm as a singlet, which is indicative of a three-coordinated boron center, instead of a four-coordinated boron, as expected in **4.8**. We regrow the crystals from the NMR tube and realized that there is hydrolysis taking place at the B–Cl bond with adventitious water leading to 5-SIDipp stabilized borenium cation, with a triflate as a counter anion (**4.9**). The constitution of **4.9** rationalizes the resonance at 30.9 ppm in the ¹¹B NMR spectrum. Although the formation of the **4.9** clearly can be seen from the molecular structure, but due to low-quality data we refrain from discussing its structural parameters. However, even after repeated attempts, we were unable to stop this hydrolysis and hence, could not characterize **4.8** spectroscopically. The CF₃ group of the triflate moiety in **4.9** resonates at –78.6 ppm in the ¹⁹F NMR, which is

slightly different from the resonances of triflates bound to the boron atom (-76.7 ppm in **4.6**) and is characteristic of the free triflate anion.

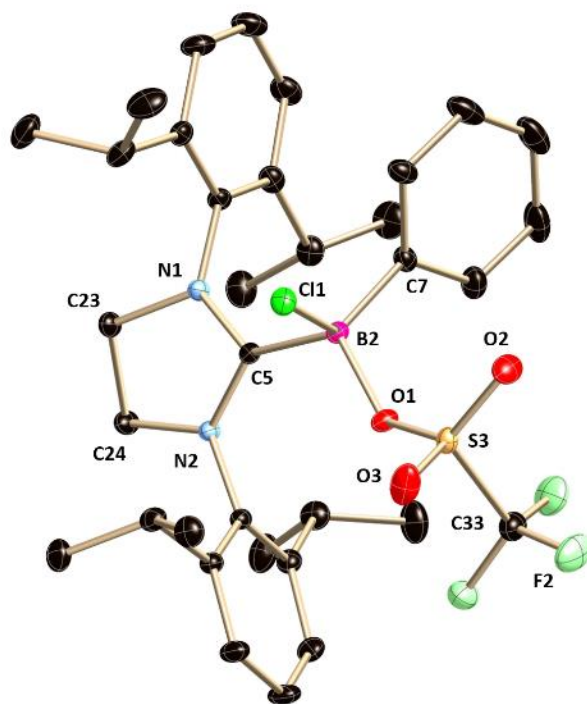


Figure 4.7. The molecular structure of **4.8**. Hydrogen atoms are omitted for clarity. Selected bond lengths [\AA] or angles [deg]: N1–C5 1.341(2), N2–C5 1.330(2), C23–N1 1.485(2), C24–N2 1.482(2), C5–B2 1.648(2), B2–Cl1 1.8948(19), B2–O1 1.532(2); N1–C5–N2 109.30(14), N1–C5–B2 123.00(14), N2–C5–B2 126.57(14), C5–B2–Cl1 100.54(11), C5–B2–O1 106.51(13), C5–B2–C7 118.55(14).

In the ^{11}B NMR, **4.10** shows resonance at 4.2 ppm shifted slightly low-field with respect to that in **4.5** (1.9 ppm), which is presumably due to electron-withdrawing nature of the ONO_2 moieties. The solid-state structure of **4.10** also was confirmed by X-ray crystal analysis. **4.10** crystallizes in the monoclinic $P2_1/c$ space group with important structural parameters are given in the legend of figure 4.8.

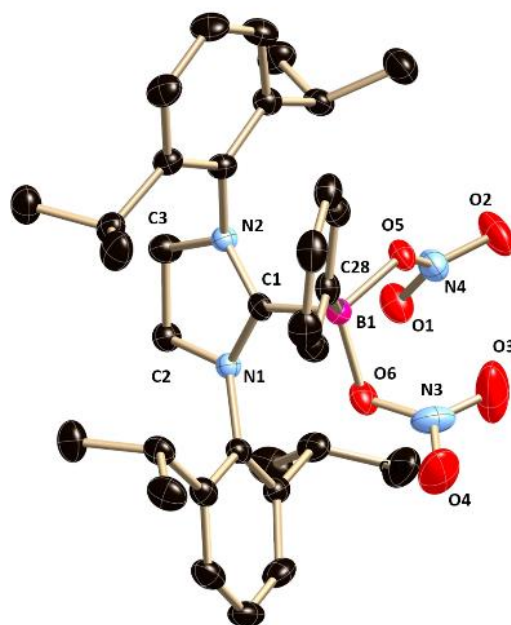
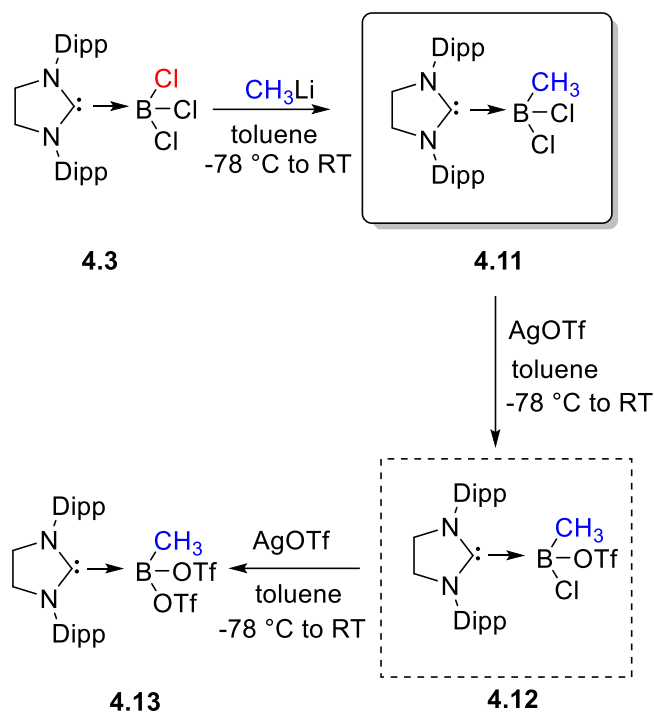


Figure 4.8. The molecular structure of **4.10**. Hydrogen atoms are omitted for clarity. Selected bond lengths [Å] or angles [deg]: N1–C1 1.337(3), C1–N2 1.340(3), N1–C2 1.480(3), N2–C3 1.484(3), C1–B1 1.662(4), B1–O5 1.535(4), B1–O6 1.522(3); N1–C1–N2 112.4(2), C1–N1–C2 112.4(2), C1–N2–C3 111.8(2), C1–B1–O5 101.59(19), C1–B1–O6 109.7(2), O5–B1–O6 111.3(2), C1–B1–C28 118.4(2).

4.4. Preparation of first carbene·MeBCl₂ adduct and its stepwise nucleophilic substitution:

Subsequently, we have also prepared SIDipp·BCl₃ adduct (**4.3**) which was characterized by the NMR spectroscopy. The addition of an equivalent of MeLi in the toluene solution of **4.3** at -78 °C cleanly afforded the monosubstituted product **4.11** (Scheme 4.4). After filtration of the lithium chloride precipitate, the concentrated toluene solution was kept for crystallization at 4 °C, which afforded colourless crystals of **4.11** after 1 day in a 60% yield. This is to the best of our knowledge the first methylchloroborane adduct of any carbene because no

$cAAC \cdot B(Me)Cl_2$ adduct is also reported. We have also attempted the analogous metathesis reaction with $IDipp \cdot BCl_3$, which was not successful and leading to a mixture of products, which we could not identify.



Scheme 4.4. Synthesis of 5-SIDipp·MeBCl₂ adduct and its stepwise nucleophilic substitution with AgOTf

The molecular structure of **4.11** is shown in figure 4.9 along with the important bond lengths and angles. **4.11** crystallizes in the monoclinic space group, $P2_1/n$. The carbene carbon atom C5 is tri-coordinated and featured a trigonal planar geometry and the boron atom connected with the C5 atom forms a tetrahedral geometry. The B1–C5 bond distance is 1.6261(19) Å, which is slightly longer compared to that in **4.1** (1.59(4) Å). There is a disorder in the methyl position of **4.11** (for clarity we are showing only one carbon atom). The C5 atom is associated with 78 % occupancy and the C2 atom is associated with 28 % occupancy. The B1–C1 distance (1.844(3) Å) is little higher compared to the B1–C2 distance (1.610(6) Å).

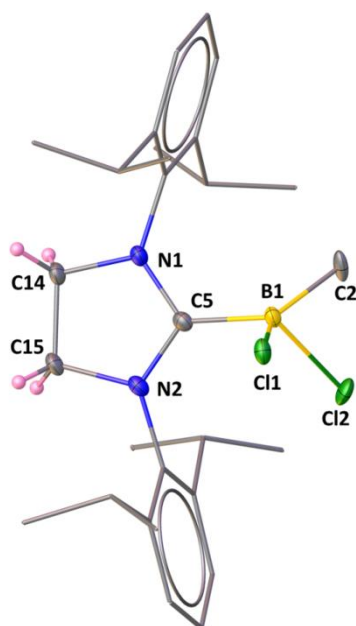


Figure 4.9. The molecular structure of **4.11** (hydrogen atoms except the back protons are omitted for the clarity of the picture). Selected bond lengths [Å] and angles [deg]: C14–C15 1.516(2), C5–N1 1.3307(17), C15–N2 1.4806(19), C5–N1 1.3338(16), C5–B1 1.6261(19), B1–C2 1.610(6), B1–Cl1 1.844(3), B1–Cl2 1.822(2); N1–C5–N2 109.93(11), N1–C5–B1 121.23(11), N2–C5–B1 128.40(12), C2–B1–Cl1 132.0(3).

In order to study the reactivity of **4.11**, we have added silver triflate into the toluene solution of **4.11** at $-78\text{ }^{\circ}\text{C}$ temperature, which led to a nucleophilic substitution of one of the chlorine atoms with the triflate group (Scheme 4.4). Colorless crystals of **4.12** suitable for X-ray diffraction studies were grown from the saturated toluene solution at $4\text{ }^{\circ}\text{C}$. **4.12** is one of the rare NHC stabilized boron compounds, where the four groups are different on the central boron atom.³⁵⁻³⁸ Further addition of one more equivalent of silver triflate to the toluene solution of **4.12** replaces another chlorine atom from the boron core with the triflate group and gives **4.12** with two triflate groups and one methyl at the centre boron atom.

The molecular structure of **4.12** is in agreement with the data obtained in solution and is depicted in figure 4.10 together with the important geometrical parameters. The chiral boron atom exhibits a distorted tetrahedral geometry. The distance between the methyl group from

the boron atom is B1–C26 1.682(3) Å, which is significantly shorter than that in **4.11** presumably due to the electron withdrawing nature of the triflate group. The boron atom (B1) lies little below in the plane of an imidazolium ring (torsion angles (deg): C15–N1–C5–B1 166.53(16), C16–N2–C5–B1–173.64(15)) and the B–O bond is not orthogonal to the plane of imidazolium ring with a torsion angle (deg) N1–C5–B1–O3 41.58, N2–C5–B1–O3 -148.93. The B–OTf bond length is 1.503(3) Å, which is in good agreement with the B–O bond length in Curran's IDipp·BH₂OTs (1.522(7) Å, OTs = tosylate).¹²

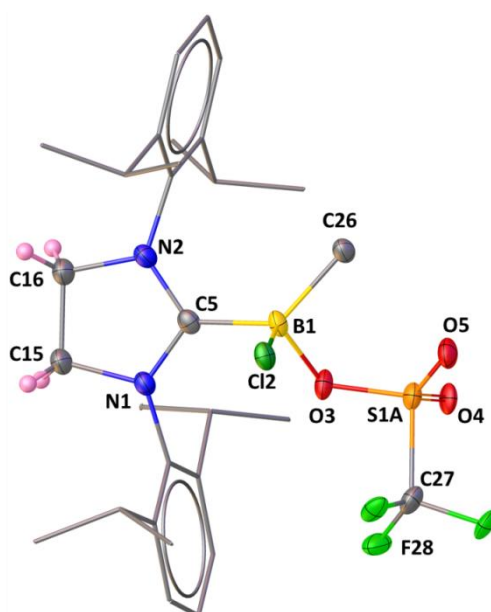
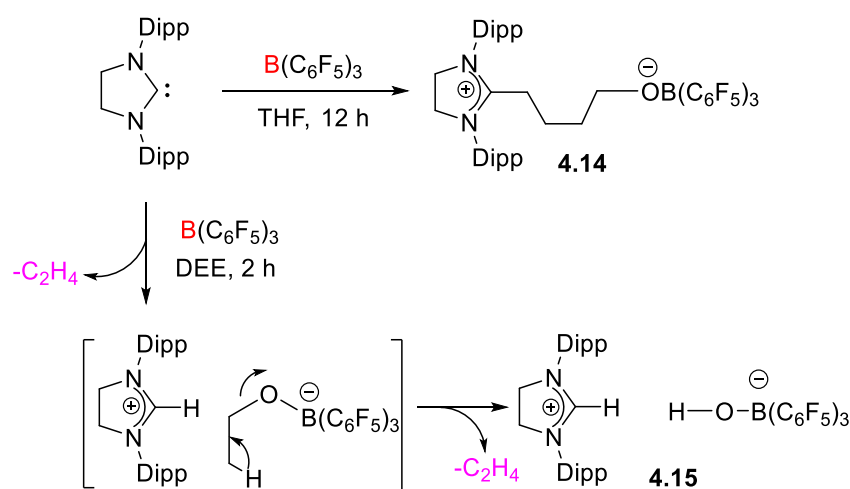


Figure 4.10. The molecular structure of **4.12** (hydrogen atoms except the back protons are omitted for the clarity of the picture). There is a disorder associated with the fluorine, oxygen and sulfur atoms in the triflate group; for clarity we are not showing the disordered atoms. Selected bond lengths [Å] and angles [deg]: C15–C16 1.525(3), C5–B1 1.617(3), B1–Cl2 1.880(3), B1–C26 1.682(3), B1–O3 1.503(3), O3–S1A 1.515(16), S1A–O5 1.427(2); N1–C5–N2 110.21(15), Cl2–B1–C26 115.59(16), B1–O3–S1A 124.16(14), O3–S1A–C27 97.94(15).

The NMR spectra of compounds **4.11-4.13** were compatible with their molecular structures. The ¹¹B NMR spectrum of **4.11** shows a resonance at 1.98 ppm, which is downfield

than that in **4.3** (1.28 ppm). The presence of the methyl group bound to the boron atom is reflected from the resonance at 1.24 ppm in the ^1H NMR spectrum of **4.11**. Replacement of another chloride atom by the triflate moiety in **4.12** led to upfield shift in the ^{11}B NMR spectrum (-2.54 ppm). The methyl protons of **4.12** bound to the boron atom resonate at 1.29 ppm in the ^1H NMR. In the ^{19}F NMR spectrum of **4.12**, the $-\text{CF}_3\text{SO}_3$ group appears at -78.21 ppm. Substitution of the last chloride atom by another triflate moiety led to further upfield shift in the ^{11}B NMR of **4.13** (-6.62 ppm). The ^{19}F NMR spectrum of **4.13** shows a broad signal at δ -76.99 ppm, which is shifted to marginally low-field than that in **4.12**.

4.5. Lewis pair mediated tetrahydrofuran and diethyl ether activation:



Scheme 4.5. 5-SIDipp·B(C₆F₅)₃ Lewis pair mediated tetrahydrofuran and diethyl ether activation at room temperature

The combination of N-heterocyclic carbene and B(C₆F₅)₃ has been exploited in frustrated Lewis pair (FLP) chemistry.³⁹ We have also demonstrated the adduct formation between 5-SIDipp and B(C₆F₅)₃ in toluene (*vide supra*). When we performed the same reaction in THF or diethyl ether, it led to the activation of those etheral solvents. The THF solution of the 5-SIDipp·B(C₆F₅)₃ was kept for 12 h at room temperature, which afforded the zwitterionic

species **4.14** in quantitative yield as a white solid (Scheme 4.5). The molecular structure of **4.14** was established by X-ray diffraction analysis (Figure 4.11). **4.14** crystallizes in the triclinic $P1^-$ space group. One of the C–O bonds in the THF molecule is cleaved, and as a result, the THF ring becomes acyclic and inserts between the Lewis pairs. Similar to the case for 5-SIDipp·B(C₆F₅)₃, **4.14** is not stable in solution at room temperature, so we were unable to satisfactorily characterize it by NMR spectroscopy. The ¹¹B NMR resonance at –2.8 ppm is similar to those established for the tetra-coordinated boron compounds. The C5 atom adopts a trigonal planar geometry, which is confirmed by the sum of the bond angles [N1–C5–N2 112.29(15)°, N1–C5–C6 125.21(15)°, N2–C5–C6 122.50(14)°]. The C5–C6 bond distance is marginally shorter compared to the adjacent C–C bond (C5–C6 1.501(2) Å and C6–C7 1.539(2) Å). The boron atom adopts a tetrahedral geometry. The C–O (1.404(2) Å) and the B–O (1.453(2) Å) bond distances are similar to the other previously reported structures.⁴⁰ This reactivity was extended to diethyl ether (DEE), which resulted in the isolation of imidazolinium salt with a borate counter-anion (**4.15**). This compound presumably results from activation of the C–O bond of the diethyl ether with concomitant elimination of two ethylene molecules (Scheme 4.5). A signal at 8.9 ppm in the ¹H NMR spectrum confirms the presence of an imidazolinium cation. The ¹¹B NMR displays the characteristic resonance at –4.2 ppm, which can be assigned to a tetrahedral [(HO)B(C₆F₅)₃] anion. X-ray crystallographic analysis later confirmed the structure of **4.15** (Figure 4.12).

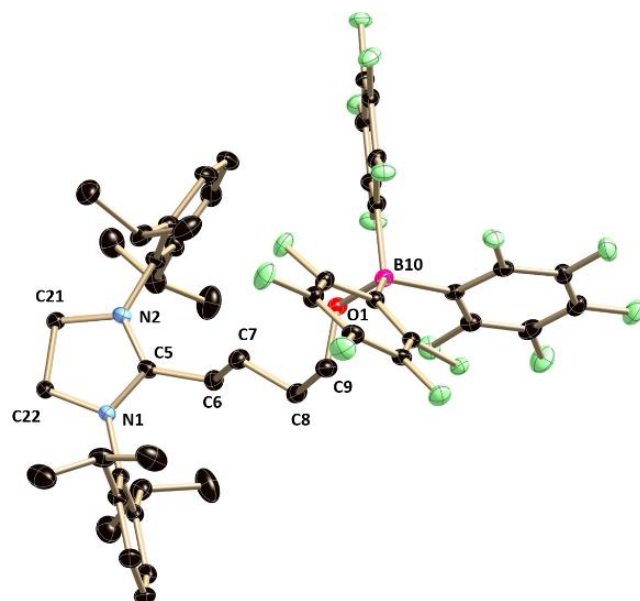


Figure 4.11. The molecular structure of **4.14**. Hydrogen atoms are omitted for clarity. Selected bond lengths [\AA] or angles [deg]: N2–C5 1.322(2), N1–C5 1.327(2), N1–C22 1.479(2), N2–C21 1.484(2), C5–C6 1.501(2), C6–C7 1.539(2), C9–O1 1.404(2), O1–B10 1.453(2); N1–C5–N2 112.29(15), N1–C5–C6 125.21(15), N2–C5–C6 122.50(14), C9–O1–B10 117.96(13).

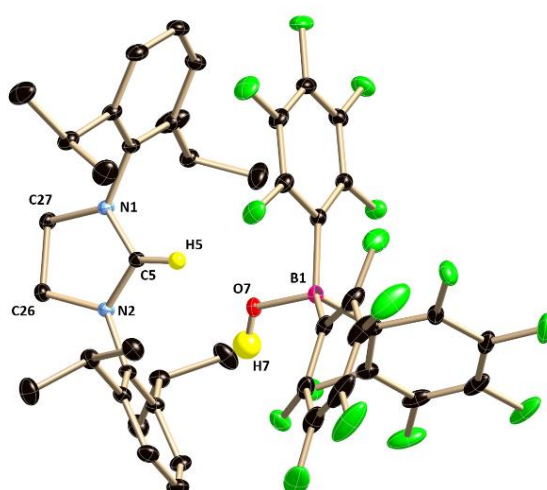


Figure 4.12. The molecular structure of **4.15**. Hydrogen atoms except the H5 and H7 are omitted for clarity. Selected bond lengths [\AA] or angles [deg]: N1–C5 1.3156(11), N2–C5 1.3174(12), C5–H5 0.950, N1–C27 1.4810(13), N2–C26 1.4817(12), B1–O7 1.4696(12), O7–

H1 0.83(2); N1–C5–N2 112.94(8), C27–N1–C5 110.17(8), C26–N2–C5 109.91(8), B1–O7–H7 114.3(15).

4.6. Conclusions

NHC·boranes are typically readily accessible, but we have mentioned in the introduction that no NHC adduct of MeBCl₂ has been known. The hesitance of the chemistry community probably stems from the synthetic routes, which are tedious and require special techniques. Here we have prepared saturated N-Heterocyclic carbene boranes bearing methyl groups by simple salt metathesis reaction starting from 5-SIDipp·BCl₃ (**4.3**). **4.11** is the first carbene·MeBCl₂ adduct and its preparation does not require the hazardous MeBCl₂. **4.6**, **4.9** and **4.12** are rare examples of NHC coordinated boron compounds, where all three substituents of the boron atom are different. Further, we have shown the selective nucleophilic substitution at the tetra-coordinated boron center to obtain several boranes with rare functional groups such as –ONO₂, –OTf, –OH etc. The combination of 5-SIDipp and B(C₆F₅)₃ were shown to affect the C–O bond cleavage differently for THF and diethyl ether. As expected, the 5-SIDipp/B(C₆F₅)₃ combination in THF resulted in ring opening of the THF to produce borate **4.14**. In the case of diethyl ether, the rupture of the C–O bond takes place along with the elimination of two molecules of ethylene, leading to the formation of an imidazolinium cation with tris (pentafluorophenyl) hydroxy borate as the counter anion (**4.15**).

4.7. References:

1. Arduengo, A. J.; Davidson, F.; Krafczyk, R.; Marshall, W. J.; Schmutzler, R., Carbene Complexes of Pnictogen Pentafluorides and Boron Trifluoride. *Monatsh. Chem.* **2000**, *131*, 251-265.

2. Kuhn, N.; Henkel, G.; Kratz, T.; Kreuzberg, J.; Boese, R.; Maulitz, A. H., Derivate des Imidazols, VI. Stabile Carben-Borane. *Chem. Ber.* **1993**, *126*, 2041-2045.
3. Nielsen, D. J.; Cavell, K. J.; Skelton, B. W.; White, A. H., Tetrafluoroborate Anion B–F Bond Activation—Unusual Formation of a Nucleophilic Heterocyclic Carbene:BF₃ Adduct. *Inorg. Chim. Acta* **2003**, *352*, 143-150.
4. Ramnial, T.; Jong, H.; McKenzie, I. D.; Jennings, M.; Clyburne, J. A. C., An imidazol-2-ylidene borane complex exhibiting inter-molecular [C–Hδ⁺···Hδ[–]–B] dihydrogen bonds. *Chem. Commun.* **2003**, 1722-1723.
5. Yamaguchi, Y.; Kashiwabara, T.; Ogata, K.; Miura, Y.; Nakamura, Y.; Kobayashi, K.; Ito, T., Synthesis and reactivity of triethylborane adduct of N-heterocyclic carbene: versatile synthons for synthesis of N-heterocyclic carbene complexes. *Chem. Commun.* **2004**, 2160-2161.
6. Bissinger, P.; Braunschweig, H.; Damme, A.; Dewhurst, R. D.; Kraft, K.; Kramer, T.; Radacki, K., Base-stabilized boryl and cationic haloborylene complexes of iron. *Chem. - Eur. J.* **2013**, *19*, 13402-13407.
7. Bissinger, P.; Braunschweig, H.; Kraft, K.; Kupfer, T., Trapping the Elusive Parent Borylene. *Angew. Chem., Int. Ed.* **2011**, *50*, 4704-4707.
8. Brahmi, M. M.; Monot, J.; Desage-El Murr, M.; Curran, D. P.; Fensterbank, L.; Lacote, E.; Malacria, M., Preparation of NHC Borane Complexes by Lewis Base Exchange with Amine– and Phosphine–Boranes. *J. Org. Chem.* **2010**, *75*, 6983-6985.
9. Chase, P. A.; Stephan, D. W., Hydrogen and Amine Activation by a Frustrated Lewis Pair of a Bulky N-Heterocyclic Carbene and B(C₆F₅)₃. *Angew. Chem., Int. Ed.* **2008**, *47*, 7433-7437.

10. Curran, D. P.; Solovyev, A.; MakhlofBrahmi, M.; Fensterbank, L.; Malacria, M.; Lacôte, E., Synthesis and Reactions of N-Heterocyclic Carbene Boranes. *Angew. Chem., Int. Ed.* **2011**, *50*, 10294.
11. Doddi, A.; Peters, M.; Tamm, M., N-Heterocyclic Carbene Adducts of Main Group Elements and Their Use as Ligands in Transition Metal Chemistry. *Chem. Rev.* **2019**, *119*, 6994-7112.
12. Solovyev, A.; Chu, Q.; Geib, S. J.; Fensterbank, L.; Malacria, M.; Lacôte, E.; Curran, D. P., Substitution Reactions at Tetracoordinate Boron: Synthesis of N-Heterocyclic Carbene Boranes with Boron-Heteroatom Bonds. *J. Am. Chem. Soc.* **2010**, *132*, 15072-15080.
13. Tamm, M.; Lügger, T.; Hahn, E. F., Isocyanide and Ylidene Complexes of Boron: Synthesis and Crystal Structures of (2-(Trimethylsiloxy)phenylisocyanide)-Triphenylborane and (1,2-Dihydrobenzoxazol-2-ylidene)-Triphenylborane. *Organometallics* **1996**, *15*, 1251-1256.
14. Ueng, S. H.; Makhlof Brahmi, M.; Derat, É.; Fensterbank, L.; Lacôte, E.; Malacria, M.; Curran, D. P., Complexes of Borane and N-Heterocyclic Carbenes: A New Class of Radical Hydrogen Atom Donor. *J. Am. Chem. Soc.* **2008**, *130*, 10082-10083.
15. Wang, Y.; Quillian, B.; Wei, P.; Wannere, C. S.; Xie, Y.; King, R. B.; Schaefer, H. F.; Schleyer, P. v. R.; Robinson, G. H., A Stable Neutral Diborene Containing a B=B Double Bond. *J. Am. Chem. Soc.* **2007**, *129*, 12412.
16. Wang, Y.; Quillian, B.; Wei, P.; Xie, Y.; Wannere, C. S.; King, R. B.; Schaefer, H. F.; Schleyer, P. v. R.; Robinson, G. H., Planar, Twisted, and Trans-Bent: Conformational Flexibility of Neutral Diborenes. *J. Am. Chem. Soc.* **2008**, *130*, 3298.
17. Braunschweig, H.; Claes, C.; Damme, A.; Deibenberger, A.; Dewhurst, R. D.; Hörl, C.; Kramer, T., A facile and selective route to remarkably inert monocyclic NHC-stabilized boriranes. *Chem. Commun.* **2015**, *51*, 1627.

18. Nöth, H.; Rojas-Lima, S.; Troll, A., The Structural Chemistry of N-Monolithium Borazines. *Eur. J. Inorg. Chem.* **2005**, *2005*, 1895-1906.
19. Teixidor, F.; Barberà, G.; Vaca, A.; Kivekäs, R.; Sillanpää, R.; Oliva, J.; Viñas, C., Are Methyl Groups Electron-Donating or Electron-Withdrawing in Boron Clusters? Permethylated o-Carborane. *J. Am. Chem. Soc.* **2005**, *127*, 10158-10159.
20. Bissinger, P.; Braunschweig, H.; Damme, A.; Hörl, C.; Krummenacher, I.; Kupfer, T., Boron as a Powerful Reductant: Synthesis of a Stable Boron-Centered Radical-Anion Radical-Cation Pair. *Angew. Chem., Int. Ed.* **2015**, *54*, 359-362.
21. Reinisch, G.; Patel, S.; Chollon, G.; Leyssale, J. M.; Alotta, D.; Bertrand, N.; Vignoles, G. L., *J. Nanosci. Nanotechnol.* **2011**, *11*, 8323-8327.
22. Braunschweig, H.; Dewhurst, R. D.; Hammond, K.; Mies, J.; Radacki, K.; Vargas, A., Ambient-Temperature Isolation of a Compound with a Boron-Boron Triple Bond. *Science* **2012**, *336*, 1420-1422.
23. Böhnke, J.; Braunschweig, H.; Dellermann, T.; Ewing, W. C.; Hammond, K.; Jimenez-Halla, J. O. C.; Kramer, T.; Mies, J., The Synthesis of B₂(SIDip)₂ and its Reactivity Between the Diboracumulenic and Diborynic Extremes. *Angew. Chem., Int. Ed.* **2015**, *54*, 13801-13805.
24. Walton, J. C.; Brahmi, M. M.; Fensterbank, L.; Lacôte, E.; Malacria, M.; Chu, Q.; Ueng, S. H.; Solov'yev, A.; Curran, D. P., EPR Studies of the Generation, Structure, and Reactivity of N-Heterocyclic Carbene Borane Radicals. *J. Am. Chem. Soc.* **2010**, *132*, 2350-2358.
25. Bissinger, P.; Braunschweig, H.; Kupfer, T.; Radacki, K., Monoborane NHC Adducts in the Coordination Sphere of Transition Metals. *Organometallics* **2010**, *29*, 3987-3990.

26. Kronig, S.; Theuergarten, E.; Holschumacher, D.; Bannenberg, T.; Daniliuc, C. G.; Jones, P. G.; Tamm, M., Dihydrogen Activation by Frustrated Carbene-Borane Lewis Pairs: An Experimental and Theoretical Study of Carbene Variation. *Inorg. Chem.* **2011**, *50*, 7344.
27. Thakur, A.; Vardhanapu, P. K.; Vijaykumar, G.; Bhatta, S. R., Investigation on reactivity of non-classical carbenes with sterically hindered Lewis acid, B(C₆F₅)₃ under inert and open conditions. *J. Chem. Sci.* **2016**, *128*, 613-620.
28. Becker, M.; Schulz, A.; Villinger, A.; Voss, K., Stable sulfate and nitrate borane-adduct anions. *RSC Advances* **2011**, *1*, 128-134.
29. Berkeley, E. R.; Ewing, W. C.; Carroll, P. J.; Sneddon, L. G., Synthesis, Structural Characterization, and Reactivity Studies of 5-CF₃SO₃-B₁₀H₁₃. *Inorg. Chem.* **2014**, *53*, 5348-5358.
30. Guibert, C. R.; Marshall, M. D., Synthesis of the Tetranitratoborate Anion. *J. Am. Chem. Soc.* **1966**, *88*, 189-190.
31. Hawthorne, M. F.; Mavunkal, I. J.; Knobler, C. B., Electrophilic reactions of protonated closo-B₁₀H₁₀2- with arenes, alkane carbon-hydrogen bonds, and triflate ion forming aryl, alkyl, and triflate nido-6-X-B₁₀H₁₃ derivatives. *J. Am. Chem. Soc.* **1992**, *114*, 4427-4429.
32. Solovyev, A.; Chu, Q.; Geib, S. J.; Fensterbank, L.; Malacria, M.; Lacôte, E.; Curran, D. P., Substitution Reactions at Tetracoordinate Boron: Synthesis of N-Heterocyclic Carbene Boranes with Boron-Heteroatom Bonds. *J. Am. Chem. Soc.* **2010**, *132*, 15072-15080.
33. Titova, K. V.; Rosolovskii, V. Y., Reaction of nitrates of monovalent cations with BCl₃. *Bulletin of the Academy of Sciences of the USSR, Division of chemical science* **1975**, *24*, 2246-2248.
34. Zelenov, V. P.; Gorshkov, E. Y.; Zavaruev, M. V.; Dmitrienko, A. O.; Troyan, I. A.; Pivkina, A. N.; Khakimov, D. V.; Pavlikov, A. V., Synthesis and mutual transformations of

nitronium tetrakis(nitrooxy)- and tetrakis(2,2,2-trifluoroacetoxy)borates. *New J. Chem.* **2020**, *44*, 13944-13951.

35. Aupic, C.; Mohamed, A. A.; Figliola, C.; Nava, P.; Tuccio, B.; Chouraqui, G.; Parrain, J. L.; Chuzel, O., Highly Diastereoselective Preparation of Chiral NHC-boranes Stereogenic at the Boron Atom. *Chem. Sci.* **2019**, *10*, 6524-6530.

36. Kawamoto, T.; Geib, S.; Curran, D. P., Radical Reactions of N-Heterocyclic Carbene Boranes with Organic Nitriles: Cyanation of NHC-Boranes and Reductive Decyanation of Malononitriles. *J. Am. Chem. Soc.* **2015**, *137*, 8617-8622.

37. Li, X.; Curran, D. P., Insertion of Reactive Rhodium Carbenes into Boron–Hydrogen Bonds of Stable N-Heterocyclic Carbene Boranes. *J. Am. Chem. Soc.* **2013**, *135*, 12076-12081.

38. Taniguchi, T.; Curran, D. P., Hydroboration of Arynes with N-Heterocyclic Carbene Boranes. *Angew. Chem., Int. Ed.* **2014**, *53*, 13150-13154.

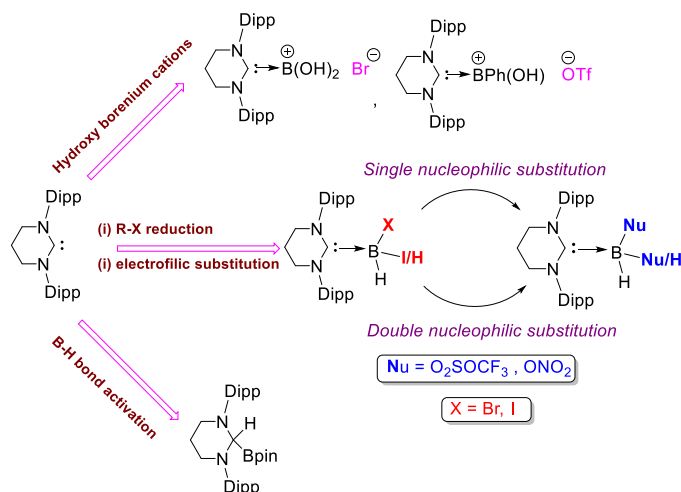
39. Stephan, D. W.; Erker, G., Frustrated Lewis Pairs: Metal-free Hydrogen Activation and More. *Angew. Chem. Int. Ed.* **2010**, *49*, 46-76.

40. Kronig, S.; Theuergarten, E.; Holschumacher, D.; Bannenberg, T.; Daniliuc, C. G.; Jones, P. G.; Tamm, M., Dihydrogen Activation by Frustrated Carbene-Borane Lewis Pairs: An Experimental and Theoretical Study of Carbene Variation. *Inorg. Chem.* **2011**, *50*, 7344-7359.

Chapter-5

The chemistry of six-membered N-heterocyclic carbene boranes

Abstract: The chemistry of NHC-boranes is of fundamental interest from the perspectives of main-group chemistry. The NHC-borane chemistry has been restricted to typical imidazol-2-ylidene classes of carbenes. Herein, we have undertaken



the reactivity of a variety of boranes with a 6-membered saturated NHC, which has been unexplored so far. The lower HOMO–LUMO gap along with a higher HOMO of 6-SIDipp compared to other typical five-membered NHCs encouraged us to study such chemistry. The stoichiometric reactions of BH₃ and other haloboranes (BRCl₂) (R = H, Ph) with 6-SIDipp led to mono-SNHC adducts **5.1**, **5.10** and **5.16**. Similar adduct formation (**5.11**) was observed with 9-borabicyclo [3.3.1] nonane (9-BBN) but it is not so stable and undergoes ring expansion at mild conditions to give a seven membered NCBNC₃ ring, **5.12**. Further, we have prepared 6-SIDipp·BH₂X (X= Br (**5.8**) and I (**5.6**)) by reacting **5.1** with alkyl halides (R-X) and CBr₄. Direct electrophilic halogenation of **5.1** with a stoichiometric amount of I₂ led to NHC boryl iodides, 6-SIDipp·BH₂I (**5.2**) and 6-SIDipp·BHI₂ (**5.3**), which were further reacted towards various nucleophiles to give novel 6-SIDipp based mono and disubstituted boranes with OTf (**5.4** and **5.5**) or ONO₂ (**5.6** and **5.7**) functional groups. Interestingly, the reaction of HBpin with 6-SIDipp led to the oxidative addition of the B-H bond at the carbene carbon (**5.13**), which is the first example of a B-H bond insertion at the NHC-carbon atom. The addition of Br₂/H₂O

to **5.1** smoothly results in forming of a three-coordinate dihydroxyborenum cation (**5.21**). The addition of triflic acid to **5.16** gives the monohydroxyborenum cation (**5.18**), the first isolated cationic analogue of the phenylborinic acid.

5.1. Introduction:

Although NHC complexes of boranes were first detected in 1968,¹ little chemistry involving NHC-boranes was known until Robinson prepared, 5-IDipp·BH₃.² Since then, there is an increasing interest in the synthesis and reactivity of carbene·borane complexes. Especially, the substitution reaction of carbene·borane adducts led to very rare classes of boron compounds with unusual functional groups such as azide, nitro, etc. attached to the boron atom.³ As of now, mainly two classes of carbene have been employed for such studies. While the works from the groups of Fensterbank, Lacôte, Malacria, and Curran mainly concentrated on typical “Arduengo type” carbenes,⁴⁻⁹ Braunschweig and co-workers recently reported nucleophilic addition and substitution of cAAC·BH₃ adduct.¹⁰ So, it is apparent that the expansion in carbene·borane chemistry took place from borane perspective, not much from carbene side. In fact, in a recent review, Curran et al. concluded by posing a question on what other NHC-boranes can be made.

It is known that an increase in the carbene angle by an increase in the ring size from a five- to a six-membered ring usually diminishes the HOMO–LUMO gap and renders a more reactive NHC (Figure 5.1). The higher HOMO and lower HOMO-LUMO gap ($\Delta E = 3.9$ eV) of the six-membered saturated NHC (6-SIDipp) anticipates more reactivity.¹¹ However, the reports of six-membered carbenes are limited in literature partly due to their less thermal stability and structural rigidity. Nonetheless, Aldridge and co-workers reported stable adduct formation of 6-SIDipp with AlH₃.¹² Subsequently, Jones and Stasch isolated monomeric complexes of 6-SIDipp and group-15 element trichlorides.¹³ Besides, Tamm and co-workers used 6-SIDipp as a Lewis base component in a FLP for the activation of dihydrogen.¹⁴

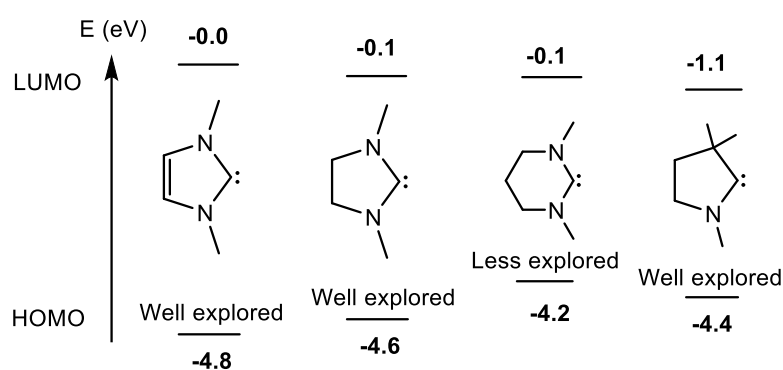


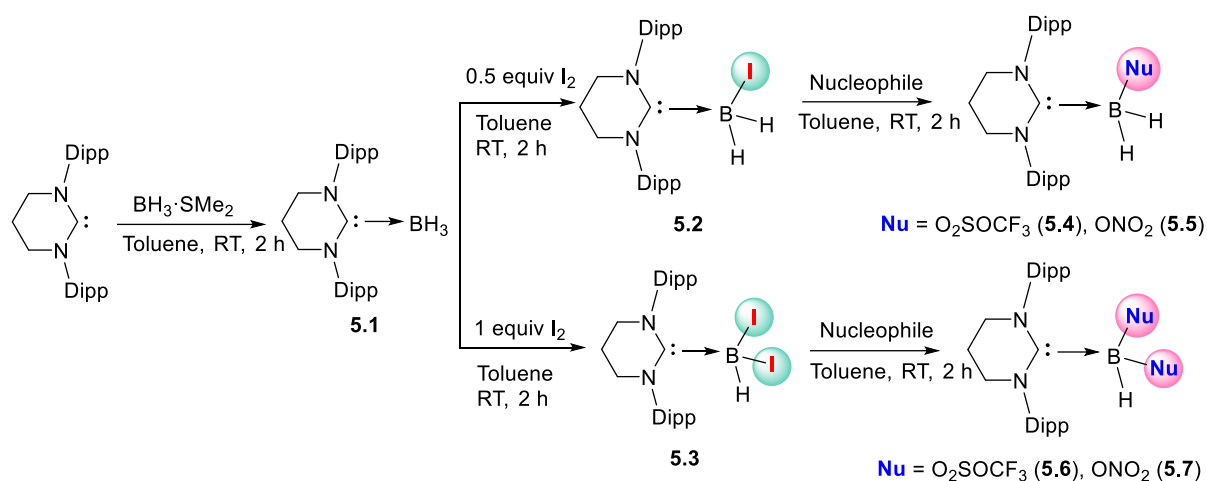
Figure 5.1. HOMO-LUMO energy gap of NHCs and CAAC.¹¹

Given our current interest in boron chemistry,¹⁵⁻¹⁷ we have undertaken the reactivity study of saturated six-membered N-heterocyclic carbene (6-SIDipp) with various boranes. While BH_3 , HBCl_2 , PhBCl_2 , and 9-BBN form the corresponding adducts with 6-SIDipp, the unprecedented 1,1-activation of HBpin at the NHC carbene center was observed. Interestingly, 6-SIDipp· BH_3 is amenable to further functionalization via halogenation using alkyl bromide, CBr_4 as well as I_2 , which provide access to NHC mono and diboryl halides, selectively. Despite having a formal negative charge on the boron, 6-SIDipp· BH_2I and 6-SIDipp· BHI_2 undergo nucleophilic substitution reactions with AgOTf and AgNO_3 to give boron compounds with OTf and ONO_2 functionalities. Dihydroxyborenum cations, the cationic analogues of phenylboronic acid and phenylhydroxyborenum cation, the cationic analogue of phenyl borinic acid, are difficult to prepare due to the lack of any R group.¹⁸ Here, we have prepared a range of mono and dihydroxyborenum cations starting from 6-SIDipp· RBCl_2 .

5.2. Selective electrophilic *mono-* and *di-*iodination at 6-SIDipp· BH_3 Center:

The addition of $\text{BH}_3\cdot\text{SMe}_2$ to 6-SIDipp in *n*-hexane and toluene mixture at -30°C gives an adduct (**5.1**) as a white precipitate (Scheme 5.1). The quartet at -31.3 ppm ($J_{\text{B-H}} = 84.04$ Hz) in the ^{11}B NMR indicates the presence of a tetra-coordinated boron atom. The $^1\text{H}\{^{11}\text{B}\}$ NMR shows a sharp singlet at 0.25 ppm for the BH_3 protons. The molecular-ion peak was observed

at m/z 419.3409 in the high resolution mass spectrum with the highest relative intensity. The B–C bond length in **5.1** is 1.602(3) Å, slightly longer than those in the previously known NHC·BH₃ adducts, presumably due to the enhanced steric crowding around the BH₃ unit (Figure 5.2).



Scheme 5.1. Synthesis and halogenation of **5.1** and subsequent nucleophilic substitution reactions.

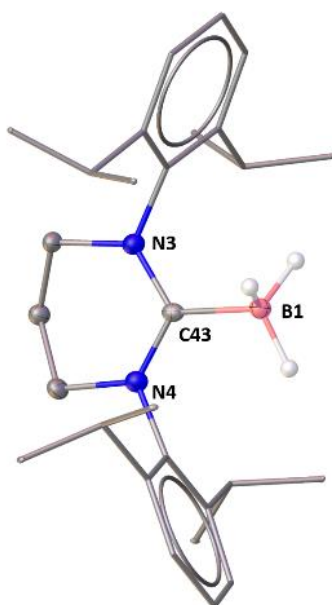


Figure 5.2. The molecular structures of **5.1** (hydrogen atoms except on the boron atoms are omitted for the clarity of the picture). Selected bond lengths (Å) and angles (deg): C43–N3

1.340(2), C43-N4 1.348(2), B1-C43 1.602(3); N3-C43-N4 117.17(17), N3-C43-B1 122.75(16), N4-C43-B1 120.08(16).

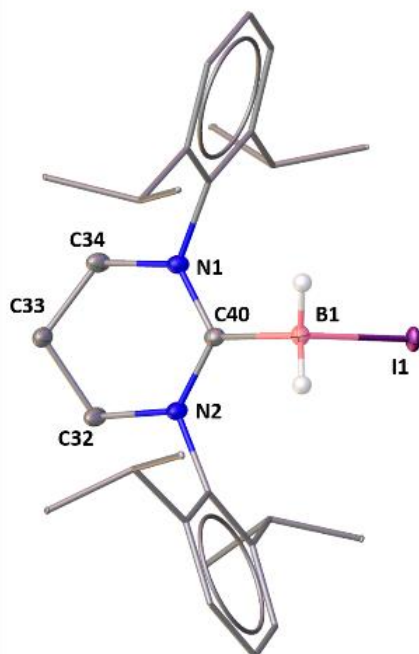


Figure 5.3. The molecular structures of **5.2** (hydrogen atoms except on the boron atoms are omitted for the clarity of the picture). Selected bond lengths (Å), angles (deg) and torsion angle (deg): C40-N1 1.3424(13), N2-C40 1.3433(13), B1-C40 1.6145(16), B1-I1 2.3005(13); N2-C40-N1 118.29(9), N1-C40-B1 120.86(9), C40-B1-I1 106.79(7); C34-N1-C40-B1 -175.7(1), C32-N2-C40-B1 178.3(1), N1-C40-B1-I1 -91.1(1), N2-C40-B1-I1 -90.4(1).

Direct electrophilic halogenation of NHC·boranes to access NHC boryl halide products has a modicum of precedence. Treatment of **5.1** with 0.5 equiv of I₂ at room temperature selectively replaces only one hydrogen atom to give rise **5.2**, which exhibits a broad signal at -30.2 ppm in the ¹¹B NMR spectrum. When one equivalent of I₂ was used, double iodination at 6-BH₃ center was achieved in 88% yield (**5.3**). The *di*-iodination was detected by the rapid disappearance of quartet of **5.1** and the appearance of a signal at -39.4 ppm in the ¹¹B NMR spectrum. The ¹H{¹¹B} NMR spectra of **5.2** and **5.3** show a sharp singlet at 1.6 and 2.38 ppm for the boron bound protons. The molecular structures of **5.2** and **5.3** are shown in Figures 5.3

and **5.4**. The boron atom lies in the plane of the tetrahydropyrimidinium ring for **5.2** and the B-I bond [2.3005(13) Å] is perfectly orthogonal to the plane [torsion angle (deg) N1-C40-B1-I1 -91.1(1), N2-C40-B1-I1 -90.4(1)]. The B-C bond distance in **5.3** [1.643(4) Å] is marginally longer than that in **5.2** [1.6145(16) Å]. The I1-B1-I2 angle in **5.3** is 111.54(11), which confirms a nearly perfect tetrahedral geometry around the boron atom. The B1-I1 bond is almost orthogonal to the plane, while the B1-I2 is not orthogonal to the plane [torsion angle (deg) N1-C2-B1-I2 138.73(18), N2-C2-B1-I2 -48.0(3)]. The B-I (2.3 Å) bond in **5.2** is little longer compare to the B-I bond in **5.3** (av 2.27 Å). For comparison, we have studied the disubstitution reaction of I₂ with 5-IDipp·BH₃, but the reaction led to formation of a mixture of *mono*-iodide, *di*-iodide, and *tri*-iodide (minor), as evaluated from ¹¹B NMR spectroscopy.²

Next, we hypothesized that **5.2** and **5.3** can react with nucleophiles to displace the iodide ligand and give various substituted NHC-boranes. Iodides of both **5.2** and **5.3** could be replaced smoothly to afford the corresponding boranes with OTf (**5.4** and **5.6**) and ONO₂ (**5.5** and **5.7**) functionalities (Figures 5.5-5.7). The B1-C2 bond (1.629(2) Å) distance in **5.4** is little increased compare to **5.1** (1.60). The torsion angles of plane C2-B1-O1-S1 and N1-C2-B1-O1 are 150.07(11) and 6.3(2) which suggest that the B1-O1 bond is not orthogonal to the respective planes. To our knowledge, the ONO₂ functional group in NHC-Borane chemistry is not known so far.

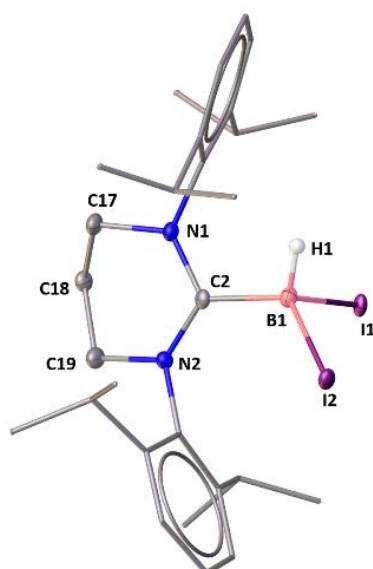


Figure 5.4. The molecular structures of **5.3** (hydrogen atoms except on the boron atoms are omitted for the clarity of the picture). Selected bond lengths (Å), angles (deg) and torsion angle (deg): C2-N1 1.350(3), N2-C2 1.357(3), B1-C2 1.643(4), B1-I1 2.279(3), B1-I2 2.264(3), B1-H1 1.0000; N2-C2-N1 118.2(2), N1-C2-B1 115.01(19), N2-C2-B1 126.4(2), C2-B1-I1 103.74(15), C2-B1-I2 120.81(17) I1-B1-I2 111.54(11); N1-C2-B1-I1 $-95.4(2)$, N2-C2-B1-I1 $77.9(3)$, N1-C2-B1-I2 $138.73(18)$, N2-C2-B1-I2 $-48.0(3)$.

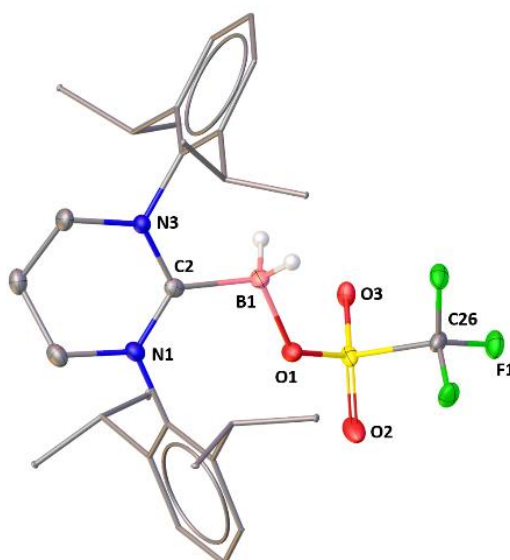


Figure 5.5. The molecular structures of **5.4** (hydrogen atoms except on the boron atoms are omitted for the clarity of the picture). Selected bond lengths (Å), angles (deg) and torsion angle

(deg): N3-C2 1.3426(19), N1-C2 1.3386(19), B1-C2 1.629(2), B1-O1 1.551(2), S1-O1 1.5014(15), C26-F1 1.327(2); N3-C2-N1 118.53(13), N3-C2-B1 114.90(12), C2-B1-O1 113.04(12); C2-B1-O1-S1 150.07(11), N1-C2-B1-O1 6.3(2), N3-C2-B1-O1 -174.30(12), B1-O1-S1-C17 81.86(14).

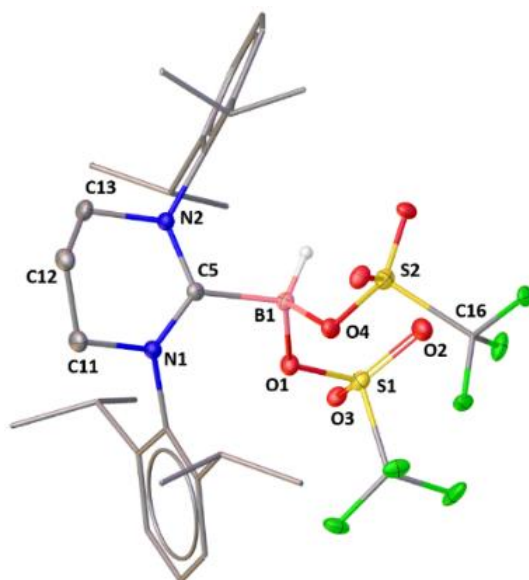


Figure 5.6. The molecular structures of **5.6** (hydrogen atoms except on the boron atoms are omitted for the clarity of the picture). Selected bond lengths (Å), angles (deg) and torsion angle (deg): N2-C5 1.3421(13), N1-C5 1.3521(13), B1-C5 1.6621(15), B1-O1 1.5394(14), B1-O4 1.4943(13); N1-C5-B1 123.54(9), N2-C5-B1 117.98(9), C5-B1-O1 106.91(8), O1-B1-O4 105.64(8); C5-B1-O1-S1 -105.82(9), C5-B1-O4-S2 168.34(7), N1-C5-B1-O1 -61.57(12), N2-C5-B1-O1 113.79(10).

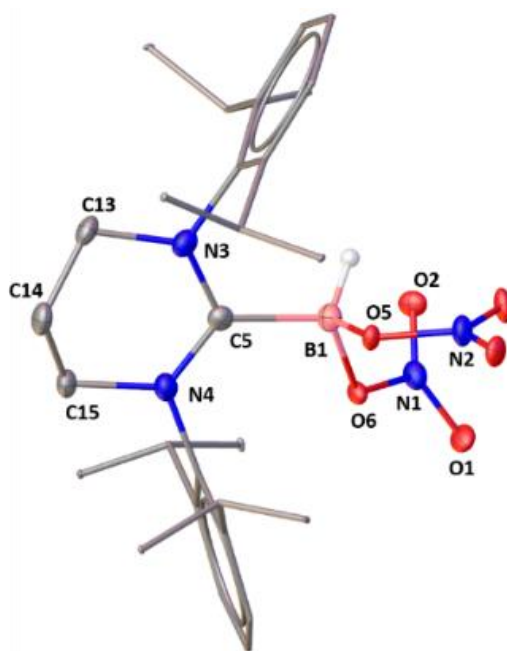


Figure 5.7. The molecular structures of **5.7**. Hydrogen atoms except the protons attached to boron are omitted for the clarity. Selected bond distances (Å) and bond and torsion angles (deg): C5-N3 1.3381(17), N4-C5 1.3341(18), B1-C5 1.659(2), B1-O5 1.4961(18), B1-O6 1.5166(19), N1-O1 1.2169(19), N1-O2 1.2269(19); N3-C5-N4 118.50(12), N4-C5-B1 124.07(12), N3-C5-B1 117.25(12), C5-B1-O6 102.92(10), C5-B1-O5 112.39(11), O5-B1-O6 106.35(12), O1-N1-O2 126.26(14); N4-C5-B1-O6 102.02(14), N4-C5-B1-O5 -11.98(19), N3-C5-B1-O5 163.11(12), N3-C5-B1-O6 -82.88(14).

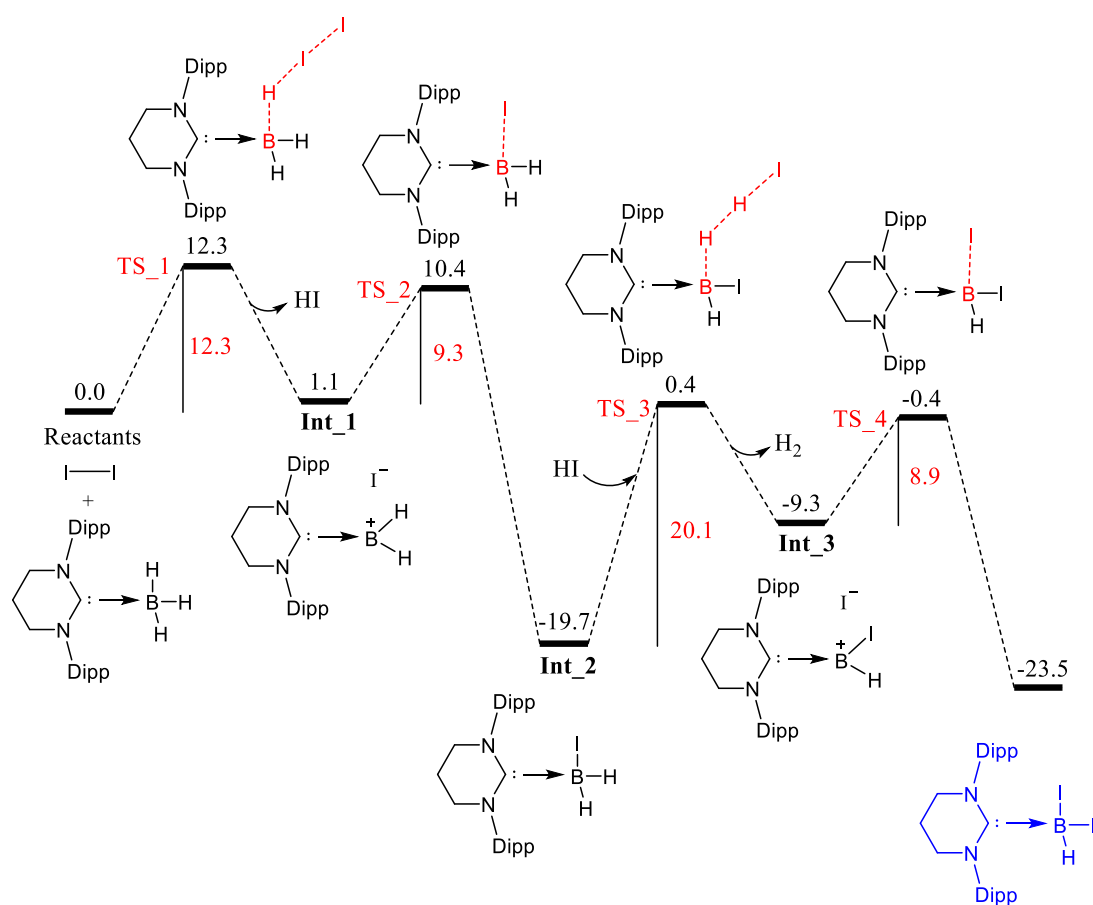
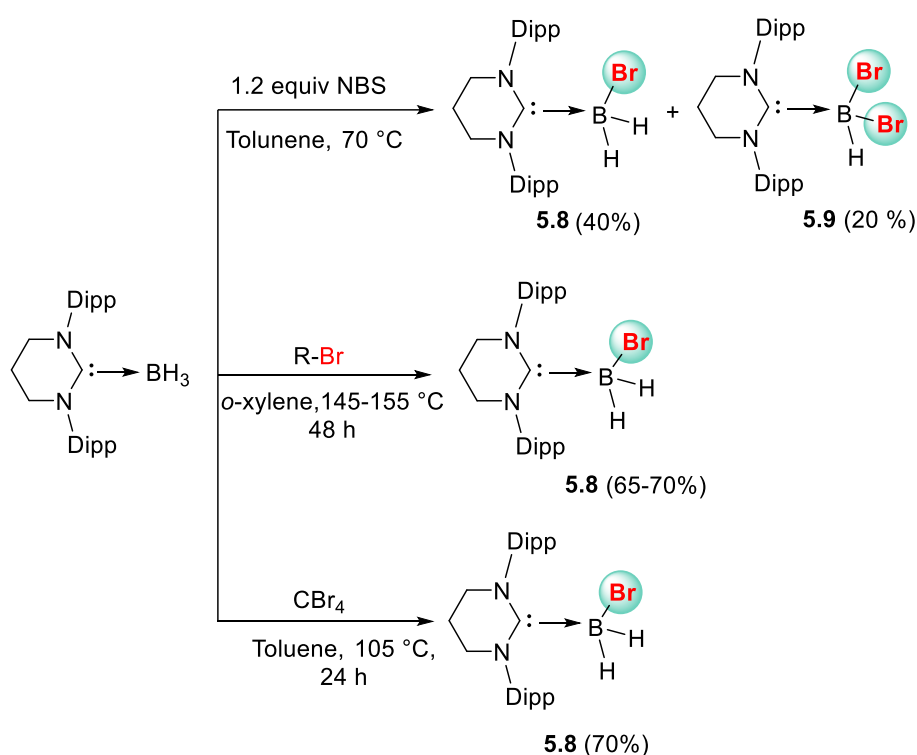


Figure 5.8. The free energy profile for the disubstitution reaction of **5.1** with iodine molecule (energy values are in kcal/mol).

We have studied the mechanism (Figure 5.8) for the disubstitution reaction of **5.1** by the iodine molecule using density functional theory (DFT) calculations. In the first step, the reaction goes through a barrier (**TS_1**) of 12.3 kcal/mol, where the B-H and I-I bonds break and the H-I bond forms, leading to the formation of HI and **Int_1** (consisting of a boron cation and an iodide ion). It is followed by the second barrier (**TS_2**) of 9.3 kcal/mol, where the B-I bond forms, leading to the formation of the *mono*-substituted **Int_2**. Then, the reaction proceeds through **TS_3**, with a barrier of 20.1 kcal/mol, in which the B-H and the H-I bonds break, and the H-H bond forms. **TS_3** leads to the formation of H₂ and **Int_3**. In the last step, the reaction crosses an 8.9 kcal/mol barrier (**TS_4**), where the B-I bond forms, leading to the final disubstituted product. Calculations also suggest that the 5-IDipp·BH₃ would result in disubstituted products.

However, both the barriers (**TS_3** and **TS_4**) for the conversion of the *mono*-substituted intermediate to the disubstituted product are higher for 5-IDipp·BH₃ (23.2 kcal/mol and 9.9 kcal/mol, respectively) than for 6-SIDipp·BH₃ (20.1 kcal/mol and 8.9 kcal/mol, respectively), which is why the disubstituted product is exclusively observed only for 6-SIDipp case, while 5-IDipp gives a mixture of *mono*- and *di*-substituted products.

5.3. *Mono*- and *di*-bromination at 6-SIDipp·BH₃ center:



Scheme 5.2. Synthesis of 6-SIDipp·BH₂Br (**5.8**) and 6-SIDipp·BHBr₂ (**5.9**).

In order to get the selective bromination, we have added 1.2 equivalents of N-bromosuccinimide (NBS) to the toluene solution of 6-SIDipp·BH₃ at 70 °C temperature, but it afforded the dibromo product, **5.9** with 20% yield along with the *mono*-bromo product (**5.8**) in 40% yield (Scheme 5.2). The formation of both **5.8** and **5.9** were indicated by ¹¹B NMR spectroscopy with the appearance of two new peaks at -20.1 ppm and -14.7 ppm, which are shifted downfield with respect to that in 6-SIDipp·BH₃ (-31.3 ppm). We were unable to get

the pure ^1H NMR spectrum of **5.9** due to the formation of mixture of products. However, we were able to get the single crystals of **5.9** suitable for X-ray studies, which confirms its constitution (Figure 5.10). Compound **5.9** was crystallized in the monoclinic $P2_1/n$ space group. The C5-B1 bond length in **5.9** is 1.639(4) Å, which is slightly longer than that in 6-SIDipp·BH₃ [1.602(3) Å].

To selectively prepare **5.8**, we reacted the 6-SIDipp·BH₃ with *n*-octyl, *n*-decyl, and *n*-dodecyl bromides in *o*-xylene at 145 °C for a fixed time period of 48 h, which led to 65-70% conversion of borane to bromoborane, **5.8**. Table 5.1 summarizes the results from this series of experiments. A more facile route to obtain **5.8** involved heating of 6-SIDipp·BH₃ in CBr₄ in toluene at 105 °C for 24 h (entry 5, table 5.1). We obtained the single crystals of **5.8** from the latter methodology (Figure 5.9). **5.8** crystallizes in monoclinic $P2_1/n$ space group. The C5–B1 bond lengths in **5.8** [1.619(6) Å] is shorter compared to that in **5.9** [1.639(4) Å]. The molecular ion peaks for **5.8** and **5.9** were detected in the HRMS spectra with *m/z* 497.2541 and 575.1605, respectively.

Table 5.1: Formation of 6-SIDipp·BH₂Br (**5.8**) from the reduction of CBr₄ and alkyl halides

Entry	R-Br	Equivalents	Solvent	Temperature (°C)	Time	Yield (%)
1	C ₈ H ₁₇ Br	1.5	<i>o</i> -Xylene	145	48 h	68
2	C ₁₀ H ₂₁ Br	1.5	<i>o</i> -Xylene	145	48 h	70
3	C ₁₂ H ₂₅ Br	1.5	<i>o</i> -Xylene	145	48 h	65
4	CBr ₄	1.2	Toluene	95	48 h	36
5	CBr ₄	2	Toluene	105	24 h	70

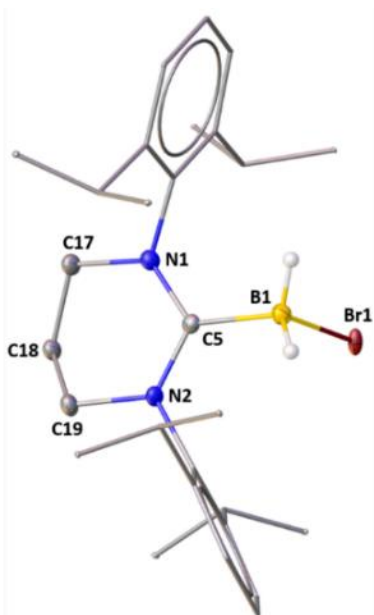


Figure 5.9. The molecular structures of **5.8** (hydrogen atoms except on the boron atom are omitted for the clarity of the picture). Selected bond lengths (Å), angles (deg) and torsion angle (deg): C5-N1 1.349(6), N2-C5 1.342(4), B1-C5 1.619(6), B1-Br1 2.102(9); N1-C5-B1 120.70(17), N2-C5-B1 118.2(2), C5-B1-Br1 104.01(14); C17-N1-C5-B1 -174.72(15), C19-N2-C5-B1 -173.13(15), N1-C5-B1-Br1 -85.48(18), N2-C5-B1-Br1 93.62(17).

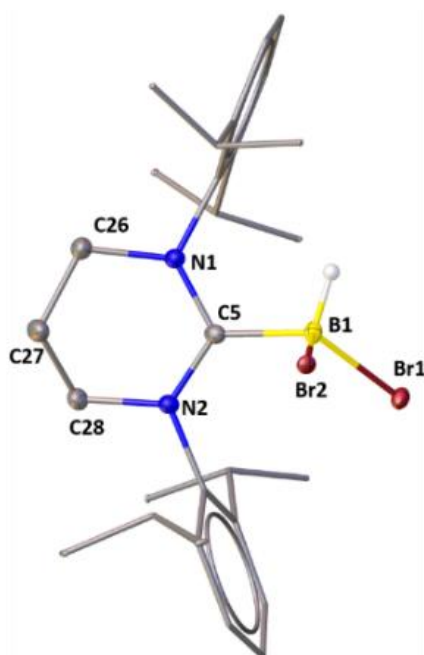
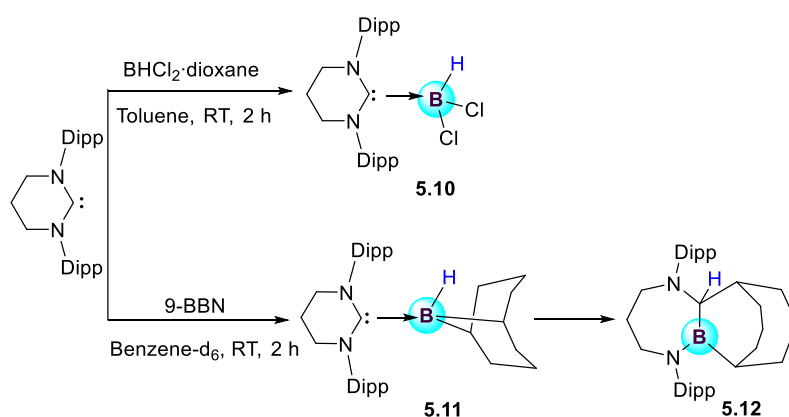


Figure 5.10. The molecular structures of **5.9** (hydrogen atoms except on the boron atoms are omitted for the clarity of the picture). Selected bond lengths (Å), angles (deg) and torsion angle

(deg): C5-N1 1.356(3), N2-C5 1.348(3), B1-C5 1.639(4), B1-Br1 2.048(3), B1-Br2 2.018(3), B1-H1 1.000; N2-C5-N1 117.9(2), N1-C5-B1 116.1(2), N2-C5-B1 117.9(2), C5-B1-Br1 117.86(19), C5-B1-Br2 104.09(19) Br1-B1-Br2 115.36(16); N2-C5-B1-Br1 56.0(3), N1-C5-B1-Br1 -133.9(2), N1-C5-B1-Br2 96.9(2), N2-C5-B1-Br2 -73.2(3), C26-N1-C5-B1 -158.8(3), C28-N2-C5-B1 172.7(2).

5.4. Reactivity of 6-SIDipp with 9-BBN and ring expansion of 6-NHC:

Following the isolation of 6-SIDipp·BH₃, we were curious to study the reactions of 6-SIDipp with other boranes. The reactions of 6-SIDipp with one equivalent of BHCl₂ form Lewis acid base adduct (**5.10**) (Scheme 5.3), which shows resonance at -7.4 ppm in the ¹¹B NMR spectrum. Inspection of the molecular structures of **5.10** reveals that the B-C bond lengths in **5.10** [1.6438(12) Å] is longer than that of 6-SIDipp·BH₃ [1.602(3) Å], which is thought to be due to increased steric congestion at the boron center (Figure 5.11). The other important bond lengths and angles are given in the legends of the Figure 5.11. In the HRMS spectrum, the molecular ion peaks were found at m/z 509.2636 for **5.10**.



Scheme 5.3. Lewis acid-base adduct formation of 6-SIDipp with HBCl₂ and 9-BBN.

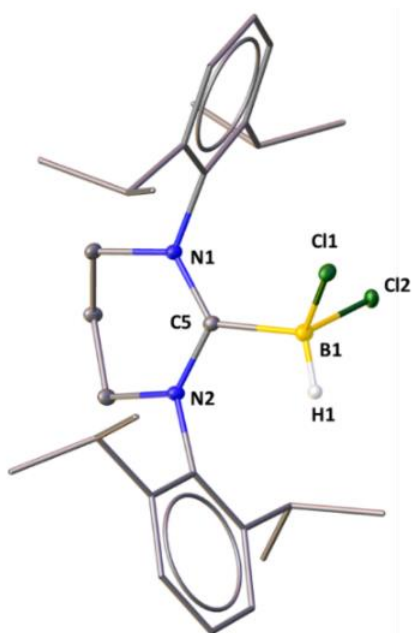


Figure 5.11. The molecular structures of **5.10** (hydrogen atoms except the proton on the central boron atom are omitted for the clarity of the picture). Selected bond lengths (\AA) and angles (deg): C5-N1 1.349(10), C5-N2 1.345(10), C5-B1 1.643(12), B1-Cl1 1.886(10), B1-Cl2 1.876(9), B1-H1 1.000; N1-C5-N2 118.29(7), N1-C5-B1 116.03(6), N2-C5-B1 125.08(7), Cl2-B1-Cl1 110.74(5).

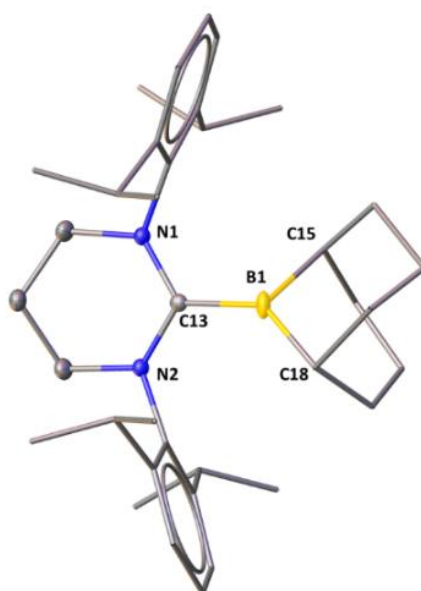


Figure 5.12. The molecular structures of **5.11** (hydrogen atoms are omitted for the clarity of the picture). Selected bond lengths (\AA) and angles (deg): C13-N1 1.351(2), N2-C13 1.348(5),

B1-C13 1.647(4), B1-C15 1.713(8), B1-C18 1.536(7); N1-C13-N2 116.4(2), N1-C13-B1 123.1(4), N2-C13-B1 120.5(4).

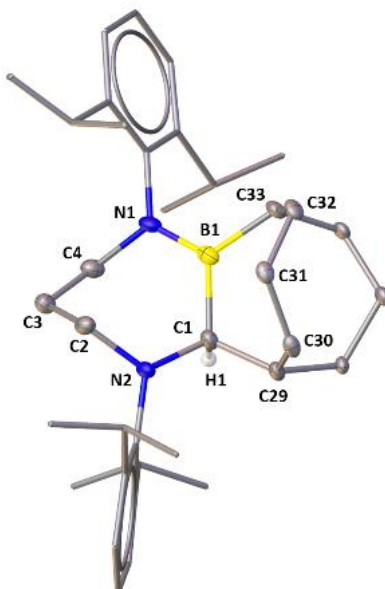


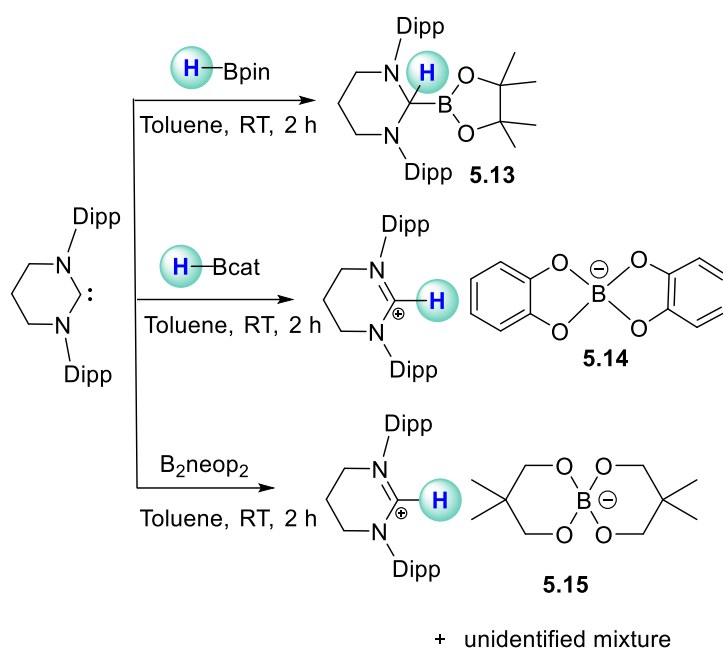
Figure 5.13. The molecular structures of **5.12** (hydrogen atoms except the C4 atom are omitted for the clarity of the picture). Selected bond lengths (Å) and angles (deg): N1-B1 1.411(3), N1-C4 1.484(2), N2-C2 1.447(2), C2-C3 1.524(3), C3-C4 1.530(3), N2-C1 1.476(2), B1-C1 1.612(3), B1-C33 1.588(3), C1-C29 1.546(3); N1-B1-C1 118.90(16), N2-C1-B1 115.39(15), N2-C1-C29 110.40(15), N1-B1-C33 120.53(17), C2-C3-C4 113.19(16).

The reaction of 6-SIDipp with 9-BBN led to the formation of an adduct (**5.11**), which is not very stable and underwent ring expansion at room temperature to afford an unusual seven membered BCNC₃N ring (**5.12**) (Scheme 5.3). The conversion of **5.11** to **5.12** was monitored by ¹¹B NMR. After 30 minutes of the reaction, a doublet appears at -13.3 ppm ($J_{B-H} = 63.81$ Hz) in the ¹¹B NMR spectrum, which is characteristics for the tetra-coordinated boron center in **5.11**. After 6 h of reaction, the latter resonance disappears, and a new resonance is detected at 49.1 ppm, which is a characteristic for the tri-coordinated boron atom. It is of note here that the group of Stephan demonstrated that five-membered N-heterocyclic carbene with PR₂ (R =

*t*Bu, NiPr₂) at the wingtip positions underwent ring expansion with 9-BBN,¹⁹ while the typical 5-IDipp was shown to form a stable adduct with 9-BBN.²⁰ While the ring expansion of 5-NHCs in presence of *s/p*-block hydrides are well-established,²¹⁻²⁵ there is only one literature precedence of ring expansion of 6-SIMes to a seven-membered ring in presence of PhSiH₃, which required 3 days and 110 °C.²⁶ Though we did not perform any theoretical studies, it can be postulated from the literature that the mechanism proceeds via initial coordination of the NHC to the boron center of 9-BBN (**5.11**). Afterwards, the hydrogen atom attached with the boron atom migrates to the electron deficient carbene carbon atom. This hydride migration prompted the attack of one of the adjacent nitrogen atoms to the boron atom, and thereby resulting the C–N bond cleavage and the C–C bond formation. Despite of varying the reaction parameters, we were unsuccessful to obtain **5.11** and **5.12** separately in preparative reasonable amounts that can permit their full characterization. However, we were able to grow the single crystals of **5.11** and **5.12** (Figures 5.12 and 5.13). The B–C bond length in **5.11** is 1.647(4) Å. Upon ring expansion, the same B–C bond length is slightly shortened to 1.612(3) Å.

5.5. 6-SIDipp mediated B-H activation of HBpin, HBcat and B₂neop₂:

The 1,1-addition of a B–H bond of HBpin to any NHC is not known. In 2010, Bertrand and co-workers studied the reaction of HBpin and 5-SIDipp and isolated an unexpected dimer via the ring cleavage of NHC.²⁷ On the other hand, the similar reaction with CAAC^{Me} afforded 1,1-activation product,^{27,28} which was rationalized by the increased nucleophilic character over 5-SIDipp. As 6-SIDipp is more nucleophilic than 5-SIDipp,^{11,29} we studied its reaction with HBpin. Gratifyingly, the reaction led to the 1,1-addition of the B–H bond of HBpin at the carbene carbon (Scheme 5.4).



Scheme 5.4. B-H activation of HBpin, HBcat, B₂Neop₂ with 6-SIDipp.

Storing the reaction mixture for a day at room temperature led to the colorless crystal of **5.13**, which was analyzed by single crystal X-ray method (Figure 5.14). **5.13** crystallizes in the monoclinic space group, $P2_1/n$. The oxidative addition of the B-H bond of HBpin forms a tetrahedral geometry at the carbene center. The solid-state structure of **5.13** shows that the six membered NHC ring adopts a perfect chair conformation. The distance between the B1 and C5 atom is 1.592(2) Å, which is significantly longer than CAAC^{Me} mediated B-H activated products (1.55 Å),²⁷ but shorter compared to those in the aforementioned NHC·borane adducts. The constitution of **5.13** was further confirmed by ¹H, ¹¹B, and ¹³C, NMR spectroscopy, and mass spectrometry. The broad signal at 30.9 ppm in ¹¹B NMR spectra indicates the insertion of the carbene-carbon atom into the B-H bond. The same carbon atom displays a broad resonance at 82.4 ppm in the ¹³C{¹H} NMR spectrum, which indicates *sp*³-hybridized carbon atom. The hydrogen atom attached to the carbene carbon atom gives a peak at 4.87 ppm. The molecular ion peak was detected at *m/z* 533.4267 in the HRMS spectrum.

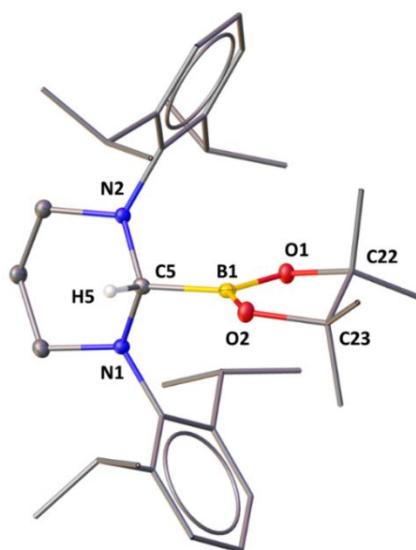


Figure 5.14. The molecular structure of **5.13** (except for hydrogen atom attached to the carbene carbon atom, other hydrogen atoms are omitted for the clarity of the picture). Selected bond lengths (Å) and angles (deg): B1-C5 1.592(2), B1-O1 1.360(2), B1-O2 1.361(2), C5-H5 1.0000, C5-N1 1.471(2), C5-N2 1.463(2); N1-C5-N2 106.99(12), N2-C5-B1 112.89(13), N1-C5-B1 111.89(13), O1-B1-O2 114.25(14).

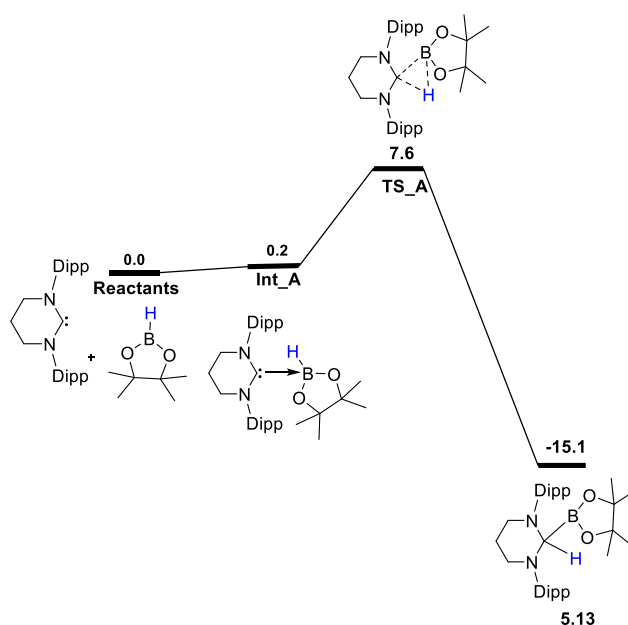


Figure 5.15. The reaction energy profile diagram for the oxidative addition of HBpin with 6-SIDipp. The values (in kcal/mol) have been calculated at the PBE/TZVP level of theory with DFT.

In order to understand the mechanism of oxidative addition of HBpin with six-membered NHC, we have done the full quantum chemical calculations (Figure 5.15) using the density functional theory (DFT). 6-SIDipp reacts with HBpin to give the adduct **Int_A**, which is thermodynamically unstable by 0.2 kcal/mol, with the bond distance of 1.66 Å between NHC carbon and boron of HBpin. In the next step, **Int_A** was transformed into **5.13** via a three-membered transition state **TS_A** with the activation free energy barrier (ΔG^\ddagger) 7.6 kcal/mol and reaction free energy (ΔG) being -15.1 kcal/mol. The bond distance of 1.59 Å was found between NHC carbon and boron of HBpin in **5.17**. We have also studied why 5-SIDipp does not undergo 1,1-oxidative addition with HBpin. It was found that the oxidative addition with 6-SIDipp was favourable by ~15 kcal/mol than 5-SIDipp.

NHCs form adducts with HBcat, while CAAC gives the B-H bond activated product. However, 6-SIDipp does not lead to an adduct formation in the reaction with HBcat. Instead, a pyrimidinium salt with [Bcat₂]⁻ counter anion was obtained. It can be assumed that 6-SIDipp undergoes B-H bond activation leading to the formation of **5.14** (Scheme 5.4). Subsequently, another molecule of HBcat attacks the C–B bond resulting in the formation of **5.14**. The formation of such [Bcat₂]⁻ anion arises from the nucleophile-promoted degradation of HBcat, and subsequent substituent redistribution are documented in the literature.³⁰⁻³² Colorless crystals of **5.14** were isolated after storing the solution for a day at room temperature. **5.14** crystallizes in the monoclinic *P2₁/c* space group (Figure 5.16). The ¹¹B NMR spectrum of **5.14** shows one signal at 14.3 ppm for tetra-coordinated boron center. The proton attached to the pyrimidinium salt gives a signal at 7.48 ppm in the ¹H NMR spectrum. The formation of **5.14** was further confirmed from the molecular ion peaks at *m/z* 405.3260 ([M-C₁₂H₈BO₄]⁺) and 226.9510 ([M-C₂₈H₄₁N₂]⁺) for the two separate ions in the HRMS spectrum.

The reaction of B₂neop₂ with 6-SIDipp in toluene at room temperature results an unprecedented pyrimidinium salt formation along with [Bneop₂]⁻ anion, **5.15** (Scheme 5.4), which was obtained

as colorless crystals after keeping the toluene solution at 4 °C for one day. The solid-state structure of **5.15** is shown in Figure 5.17. The ^{11}B NMR spectrum of **5.15** displays one sharp signal at 1.85 ppm for the tetra coordinated borate anion. The peak at 7.48 ppm is characteristic for the pyrimidinium proton. The question on the source of the proton is very difficult to answer; it could be moisture or solvent. Similar reactivities were also seen for $i\text{Pr}_2\text{Im}$ and $\text{Me}_2\text{Im}^{\text{Me}}$ carbene in the reaction with B_2eg_3 by the groups of Radius and Marder, though structural isolation of the spiro borate anion remained elusive in their cases.

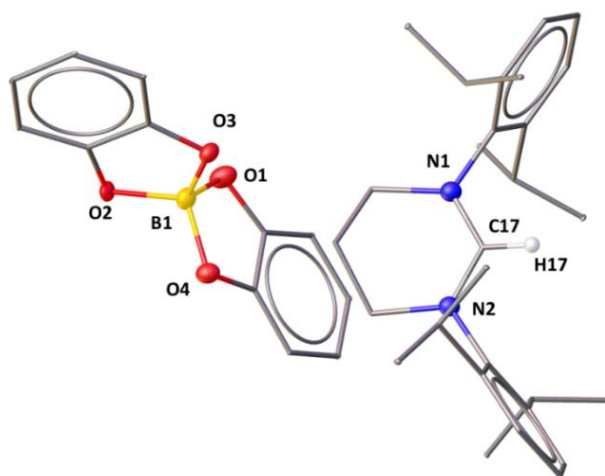


Figure 5.16. The molecular structure of **5.14** (hydrogen atoms except on C17 are omitted for clarity of the picture). Selected bond lengths (Å) and angles (deg): N1-C17 1.307(2), C17-N2 1.310(2), C17-H17 0.9500, B1-O1 1.475(2), B1-O2 1.481(2); N1-C17-N2 123.10(15), O1-B1-O2 104.65(15).

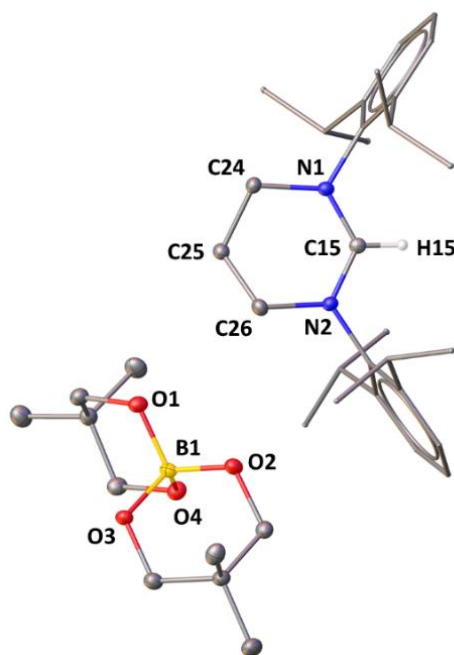


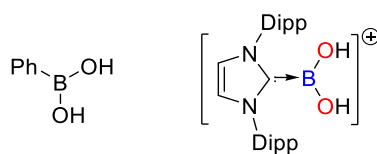
Figure 5.17. The molecular structure of **5.15** (hydrogen atoms except the proton on C15 are omitted for the clarity of the picture). Selected bond lengths (Å) and angles (deg): N1-C15 1.315(4), C15-N2 1.325(4), C15-H15 0.9300, B1-O1 1.453(4), B1-O2 1.467(4), B1-O3 1.492(4), B1-O4 1.487(4); N1-C15-N2 124.2(3), O1-B1-O2 107.6(3), O3-B1-O4 110.3(3).

5.6. 6-SIDipp stabilized borenium cations; isolation of a cationic analogue of borinic Acid and its reactivity:

While phenylboronic acid ($\text{PhB}(\text{OH})_2$) is ubiquitous in organic chemistry such as in Suzuki–Miyaura, Chan–Evans–Lam cross coupling reactions, Petasis reaction etc.,³³⁻³⁵ diphenylborinic acid [$\text{Ph}_2\text{B}(\text{OH})$] is very less illustrated due to its instability.³⁶⁻³⁸ Though diphenylborinic acid was disputably first prepared in 1894 by Michaelis by hydrolysis of diphenylchloroborane,³⁹ the first structurally characterized borinic acid [$\text{Mes}_2\text{B}(\text{OH})$,] was reported by Power in 1987, almost after a century.⁴⁰ Displacement of the phenyl group by a strong σ -donor neutral ligand like N-heterocyclic carbenes (NHCs) in phenylboronic acid resulted in the dihydroxyborenium cations, $[\text{LB}(\text{OH})_2]^+$, the cationic analogues of phenylboronic acid, which have been

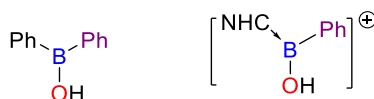
structurally authenticated first by the group of Curran¹⁸ and recently by ourselves. In the same line, removal of one phenyl group from diphenylborinic acid should furnish a three-coordinate monohydroxy borenium cation of composition $[\text{LB}(\text{Ph})(\text{OH})]^+$, however, no such compound has been realized till to date (Scheme 5.5).

*Phenylboronic acid and its cationic analogue:
dihydroxyborenium cation*



Curran (2012)

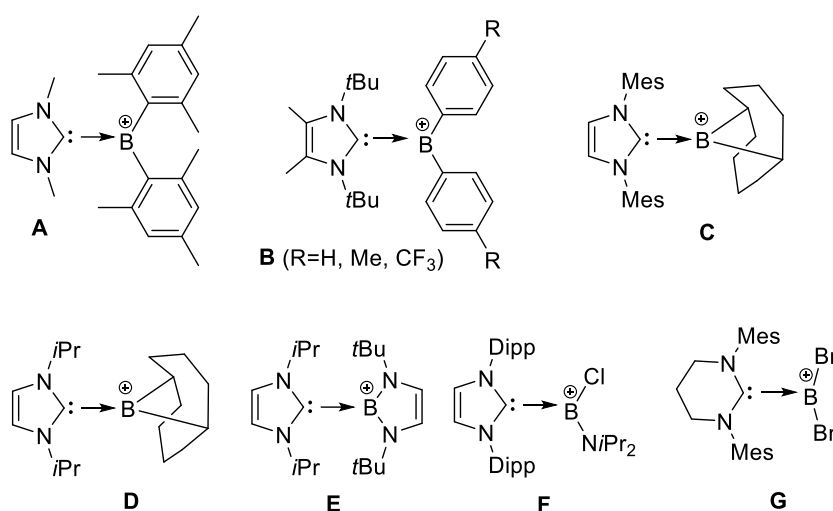
*Diphenylborinic acid and its cationic analogue:
monohydroxyborenium cation*



Structurally not known

Scheme 5.5. Phenylboronic, diphenylborinic acid and their NHC supported cationic analogues.

Though NHC supported borenium cations with different substituents at boron such as diarylborenium by Gabbaï's (**A**)⁴¹ and Tamm (**B**),⁴² dialkylborenium by Lindsay (**C**)⁴³ and Stephan (**D**),²⁰ diamino borenium (**E**) by Weber,⁴⁴ aminochloroborenium (**F**) by Robinson,⁴⁵ and dibromoborenium (**G**) by Aldridge⁴⁶ have been reported (Scheme 5.5), a seemingly simple compound such as $[\text{NHC}\cdot\text{B}(\text{Ph})\text{Cl}]^+$ has still not been isolated. Ingleson and co-workers isolated $[(2\text{-DMAP})\text{B}(\text{Ph})\text{Cl}]^+$ cation by the sequential addition of 2-DMAP and AlCl_3 to PhBCl_2 ,⁴⁷ but the coordination number of the boron atom in the cation is four. So, according to Nöth's classification,^{48,49} it is a boronium cation, and not a borenium cation. It must be noted here that Cade and Ingleson reported an $\text{ArOB}(\text{L})\text{Ph}$ cation, which can be considered as a cationic analogue of a borinic ester.⁵⁰



Scheme 5.6. Selected examples of previously reported NHC-stabilized borenium cations (excluding dihydroxyborenium cations). Counter anions are not shown for clarity of the scheme.

We have synthesized the adduct **5.16** by reacting 6-SIDipp with PhBCl₂ in toluene (Scheme 5.7). The ¹¹B NMR spectrum of **5.16** displays a resonance at 3.4 ppm as a broad singlet. The molecular structure of **5.16** is determined by single-crystal X-ray studies (Figure 5.18). The B–C bond length in **5.1** (1.691(3) Å) is quite longer compared to the 6-SIDipp·BH₃ adduct (1.602(3) Å). The B–Cl bond distances (1.8861(10) and 1.8769(9) Å) are in good agreement with the previously reported carbene-chloroborane adducts.⁵¹ The X-ray structural studies of **5.16** show that the phenyl ring on the boron atom lies parallel to the plane of one Dipp-arene ring. The molecular ion peak was detected at *m/z* 563.3173 for **5.16** with the highest relative intensity.

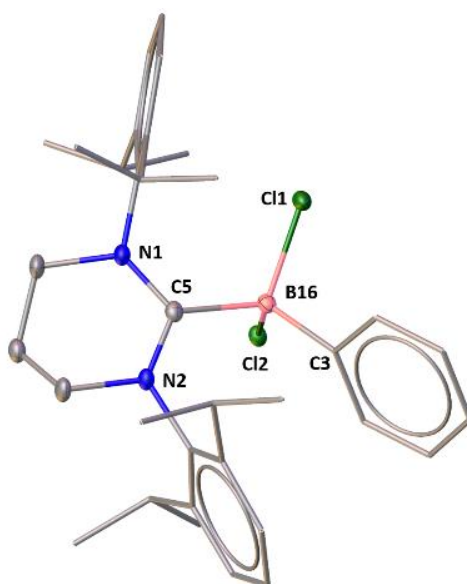
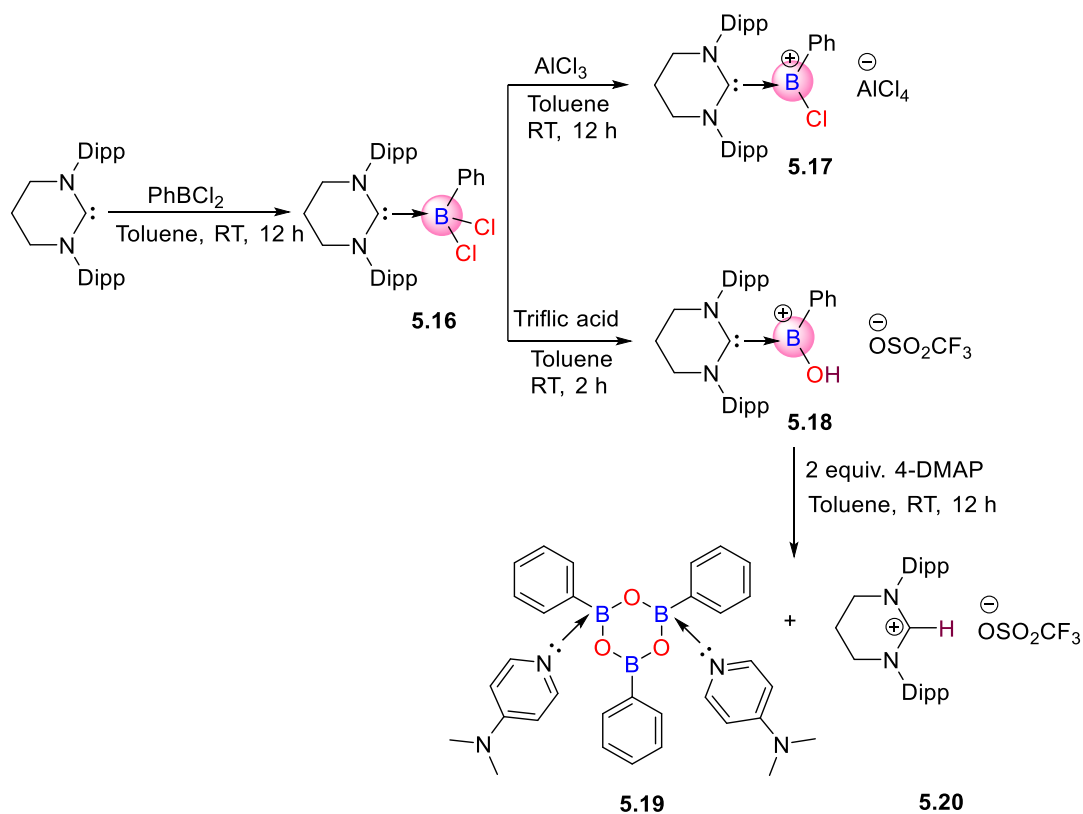


Figure 5.18. The molecular structure of **5.16**. Hydrogen atoms are omitted for clarity. Selected bond distances (Å) and bond angles (deg): C5-N1 1.352(3), C5-N2 1.344(3), B16-C5 1.691(3), B16-Cl1 1.889(2), B16-Cl2 1.910(2), B16-C3 1.620(3); N1-C5-N2 116.38(17), N1-C5-B16 122.30(17), N2-C5-B16 120.57(16), Cl1-B16-Cl2 105.77(11).



Scheme 5.7. Synthesis of phenylchloroborenium (**5.17**) and phenylhydroxyborenium (**5.18**).

We reckon that the displacement of one chloride ligand from **5.16** should result in NHC stabilized phenylchloroborenium cation. Adopting Ingleson's strategy,⁴⁷ we reacted **5.16** with one equivalent of AlCl₃ in toluene, which led to [6-SIDipp·B(Ph)(Cl)]⁺ (**5.17**) with AlCl₄⁻ as the counter anion (Scheme 5.7). The ¹¹B NMR spectrum indicates the generation of the borenium cation, which displays a resonance at 29.5 ppm. It is in good agreement with Robinson's [5-IDipp·B(NiPr₂)(Cl)]⁺ (**C**), but substantially upfield with respect to Aldridge's [6-SIDipp·BBr₂]⁺ (**E**) (51.4 ppm).^{45,46} The molecular structure of **5.17** is shown in figure 5.19. **5.17** crystallizes in the monoclinic *P2/c* space group. The B–C_{NHC} distance (1.628(11) Å) is significantly reduced from that in **5.16** (1.691(3) Å) apparently due to the change in the hybridization of the boron atom from *sp*³ (in **5.16**) to *sp*² (in **5.17**). Due to the π -stacking interaction, the phenyl ring on the boron atom is parallel with one of the Dipp arene ring leading to different B–C_{ipso} contacts (2.77 and 2.92 Å), which are common to the borenium cations for bending of the flanking arene rings towards the boron center. The B–Cl distance (1.737(9) Å) is 0.15 Å shorter compared to **5.16** due to the electron donation from the chlorine atom to the electrophilic boron center in **5.17**.

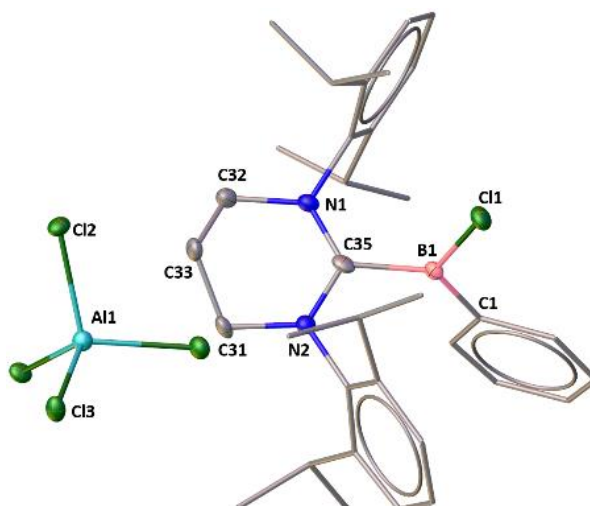


Figure 5.19. The molecular structure of **5.17**. Hydrogen atoms are omitted for clarity. Selected bond distances (Å), bond angles (deg) and torsion angles (deg): C35-N2 1.338(9), C35-N1 1.320(9), N2-C31 1.470(9), N1-C32 1.468(10), C35-B1 1.628(11), B1-C1 1.523(12), B1-Cl1 1.737(9), Cl2-Al1 2.136(3), Cl3-Al1 2.131(3); N1-C35-N2 121.0(6), N2-C35-B1 116.7(6), N1-C35-B1 122.2(6), Cl1-B1-C35 115.4(6), C35-B1-C1 126.2(7), Cl1-B1-C1 118.4(6); N1-C35-B1-C1 -108.6(9), N2-C35-B1-C1 69(1), N1-C35-B1-C11 72.0(8), N2-C35-B1-C11 -110.8(7).

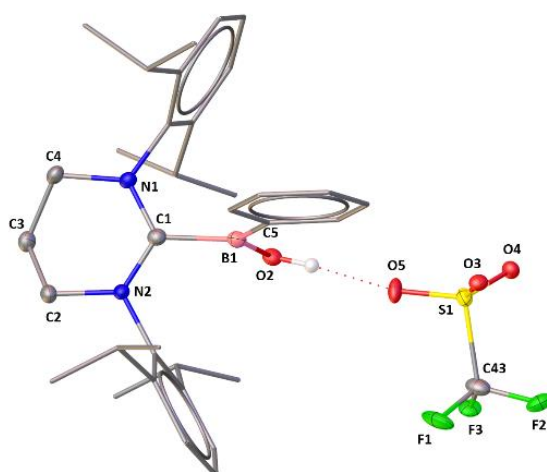


Figure 5.20. The molecular structure of **5.18**. Hydrogen atoms except on O2 atom are omitted for clarity. Selected bond distances (Å), bond angles (deg) and torsion angles (deg): N1-C1 1.3330(13), N2-C1 1.3333(14), N1-C4 1.4811(15), N2-C2 1.4783(14), B1-C1 1.6231(16), B1-

O2 1.3830(15), B1-C5 1.5580(17), S1-O5 1.4497(11), C43-F1 1.335(2); N1-C1-N2 121.43(10), N2-C1-B1 119.14(9), N1-C1-B1 119.43(9), C5-B1-O2 124.65(10); N1-C1-B1-O2 91.08(12), N2-C1-B1-O2 89.20(12), N1-C1-B1-C5 88.81(13), N2-C1-B1-C5 -90.91(12).

Encouraged by this result, we decided to test the viability of isolating our target compound, $[\text{B}(\text{Ph})\text{OH}]^+$ using 6-SIDipp. Deliberate hydrolysis of **5.17** did not furnish the target compound. In 2014, Curran and co-workers reported the generation of dihydroxyborenum cation $[\text{5-IDipp}\cdot\text{B}(\text{OH})_2][\text{OTf}]$ by reacting $[\text{5-IDipp}\cdot\text{B}(\text{X})(\text{OTf})]$ ($\text{X} = \text{Cl}, \text{OTf}$) with triflic acid, and concluded that the hydrolysis happened by the adventitious water.¹⁸ So, we reacted **5.16** with triflic acid and to our delight, the reaction afforded the 6-SIDipp stabilized phenyl hydroxy borenum cation (**5.18**) with triflate as a counter anion. The dropwise addition of triflic acid into the toluene solution of **5.16** at low temperature forms a turbid solution immediately. The reaction mixture was continued stirring for another two hours at room temperature and dried completely to give a white precipitate. The colourless crystals of **5.18** were grown from the concentrated toluene solution at 4 °C and characterized by single crystal X-ray as well as NMR spectroscopy, and mass spectrometry. The ¹¹B NMR of **5.18** gives a resonance at 28.9 ppm. The peak at -78.2 ppm in the ¹⁹F NMR confirms the presence of the triflate group as the counter anion. The molecular ion peak with the highest intensity at m/z 509.3700 further confirms the formation of **5.18**. The stretching frequency for the O-H group in **5.18** appears at 3438 cm⁻¹. Figure 5.20 depicts the molecular structure of **5.18**, which is, to our knowledge, the first isolated compound containing a phenylhydroxyborenum cation. **5.18** crystallizes in the monoclinic $P2_1/n$ space group. The B-C_{NHC} distance is 1.6231(16) Å, which is comparable with that in **5.16** and the previously reported $[\text{6-SIDipp}\cdot\text{B}(\text{OH})]^+$ (1.614(7) Å). The dearth of -R group is compensated by the hydrogen bonding of the oxygen atom of the triflate group with

the hydroxyl group at the boron center with a O–H···O distance 2.736 Å. The average B–C_{ipso} contacts are 2.86 Å, which is marginally longer compared to the Aldridge's dibromoborenium (2.786(7) and 2.798(8) Å).⁴⁶ Both B–O and the B–C_{Ph} bonds are lying perfectly orthogonal to the planes (torsion angle: N1–C1–B1–O2 91.08(12)°, N2–C1–B1–O2 89.20(12)°, N1–C1–B1–C5 88.81(13)°, N2–C1–B1–C5 –90.91(12)°.

Cation **5.18** readily reacts with 4-dimethylaminopyridine (4-DMAP) to give 4-DMAP stabilized boroxine (**5.19**) at room temperature along with the tetrahydro-pyrimidinium salt with a triflate anion, **5.20**. Though PhB(OH)₂ is known to undergo dehydration reaction at 110 °C for 6 h,⁵² generation of a boroxine derivative at room temperature from a cationic analogue of borinic acid is not known. It must be noted here that Braunschweig and co-workers recently reported the isolation of a cAAC stabilized boroxine by reacting cAAC stabilized diborene with CO₂.⁵³ The separation of **5.19** and **5.20** was done via fractional crystallization. The molecular structure of **5.19** is shown in figure 5.21. **5.19** crystallizes in the monoclinic *P*-1 space group. The coordination geometry of the boron atoms in boroxine ring is not equal because two boron atoms are four-coordinated, while the third one is three-coordinated. As a result, the B–O bond lengths in **5.20** are not same. As a matter of fact, attempts to prepare boroxine derivative where all boron atoms are coordinated to DMAP was not successful even when excess amount of 4-DMAP was used. The B–O bond lengths in **5.19**, where the boron atom is coordinated to DMAP (1.4334(19) and 1.4696(19) Å) are longer than B–O bond lengths, where the boron atom is three coordinated (1.358(2) and 1.355(2) Å). The B–N bond lengths (1.677(2) and 1.648(2) Å) are marginally longer than Alcarazo's carbodiphosphorane and DMAP stabilized boronium cation.⁵⁴ In the ¹¹B NMR, **5.19** gives a resonance at 20.5 ppm for due to a fast exchange of the two DMAP molecules across the three boron centers. In the HRMS spectrum, the molecular ion peak at *m/z* 405.3256 approves the formation of **5.19**.

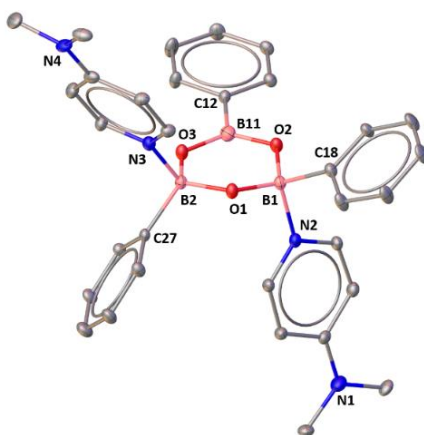
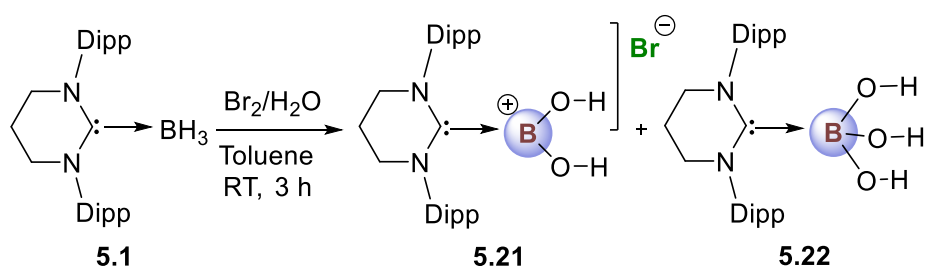


Figure 5.21. The molecular structure of **5.19**. Hydrogen atoms are omitted for clarity. Selected bond distances (Å) and bond angles (deg): B1-O1 1.419(2), B2-O1 1.4334(19), B2-O3 1.4696(19), O2-B1 1.4766(19), O2-B11 1.358(2), B11-O3 1.355(2), B1-N2 1.677(2), B2-C27 1.627(2), B1-C18 1.623(2), B2-N3 1.648(2), B11-C12 1.588(2); B1-O2-B11 119.12(12), B2-O3-B11 121.12(12), B1-O1-B2 122.26(11).

5.7. 6-SIDipp stabilized dihydroxyborenium cations:

The preparation of borenium cations relies on two main approaches: (a) the replacement of X in R_2B-X by a free NHC or (b) by reacting an acid (HX) with $NHC \cdot BR_2H$. The Curran's group reported the dihydroxyborenium cation by treating 5-IDipp·BH(X)OTf (X = Cl, OTf) with excess TfOH in 5 days.¹⁸ Here, we have isolated a new dihydroxyborenium cation **5.21**; the cationic analogue of phenyl boric acid, in a seemingly simple way by reacting **5.1** with Br_2/H_2O .



Scheme 5.8. Preparation of a dihydroxy borenium cation **5.21** in a single step from **5.1**.

The reaction of **5.1** with bromine water led to an immediate color change from colorless to yellow and afforded a 6-SIDipp stabilized dihydroxyboreonium cation (**5.21**) at room temperature in 3 h (Scheme 5.8). Yellow color crystals were grown from the saturated toluene solution at 4 °C. Along with 55% of the yellow crystals of **5.21**, a 7% yield of colorless crystals was found, which was the 6-SIDipp·B(OH)₃ adduct, **5.22**. Both the compounds are separated by fractional crystallization. There is no report of the formation of NHC·B(OH)₃ type Lewis adducts so far. Both **5.21** and **5.22** were characterized with single-crystal X-ray studies (Figures 5.22 and 5.23). The ¹¹B NMR spectrum gives a singlet at 25.4 ppm for **5.21** and -5.2 ppm for **5.22**. The cyclic voltammogram of **5.21** exhibits reversible redox wave at $E_{p, red} = -1.7$ V, and oxidation at $E_{p, oxd} = 0.56$ V, respectively.

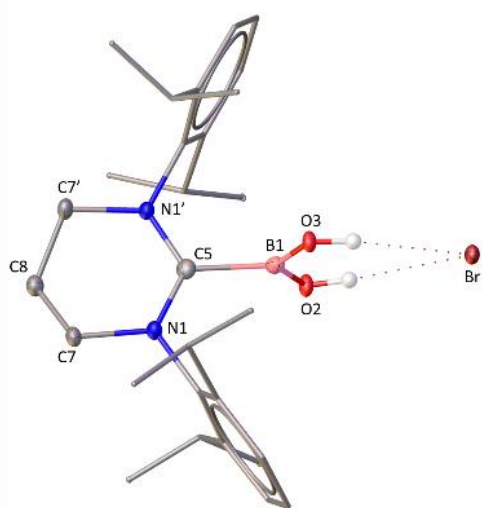


Figure 5.22. The molecular structure of **5.21** (except hydrogen atoms attached to the oxygen atom, other hydrogen atoms are omitted for the clarity of the picture). Selected bond lengths (Å), angles (deg) and torsion angles (deg): N1-C5 1.321(4), C5-B1 1.614(7), B1-O2 1.344(7), B1-O3 1.341(7), O2/O3-H2/H3 0.80(7); N1-C5-N1' 121.5(4), N1-C5-B1 119.2(2), O3-B1-O2 127.7(5); N1-C5-B1-O2 -90.4(4), N1'-C5-B1-O2 90.4(4), N1-C5-B1-O3 89.6(4), N1'-C5-B1-O3 -89.6(4).

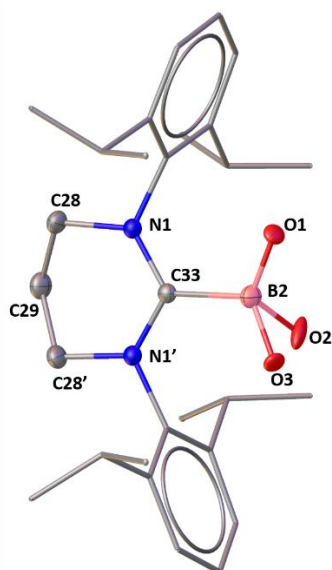
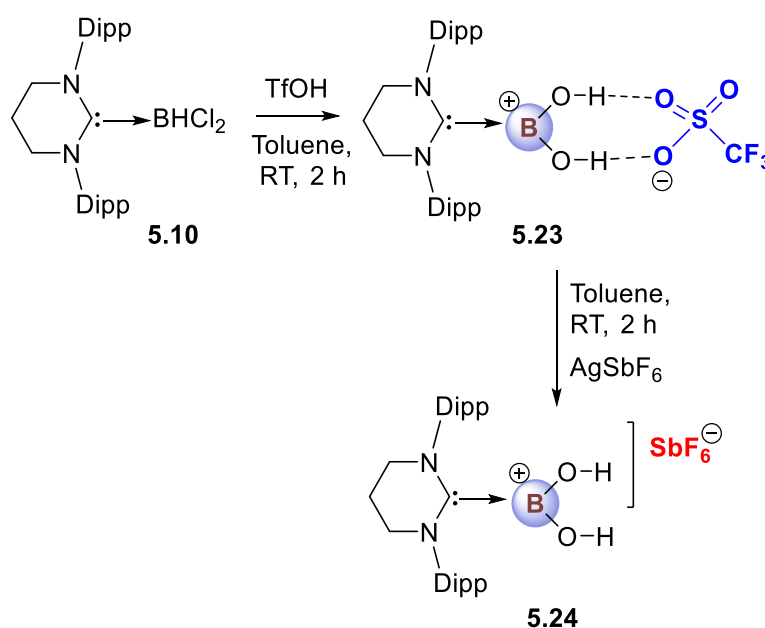


Figure 5.23. The molecular structures of **5.22** (hydrogen atoms are omitted for the clarity of the picture). Selected bond lengths (Å), angles (deg): N1-C33 1.3338(17), C33-B2 1.683(4), B2-O1 1.326(5), B2-O2 1.282(4), B2-O3 1.381(4); N1-C33-N1', 118.74(19), C33-B2-O1 110.6(3), O1-B2-O2 115.1(4).

5.21 crystallizes in the orthorhombic *Pnma* space group (Figure 5.22). The boron atom adopts a trigonal planar (O3-B1-O2 bond angle is 127.7(5)°) environment with the B-O distances of 1.344(7) and 1.341(7) Å, which are substantially shorter than the typical B-O single bond (>1.5 Å). The B-O bonds are perfectly orthogonal to the plane (torsion angles (deg) N1-C5-B1-O2 – 90.4(4), N1'-C5-B1-O2 90.4(4), N1-C5-B1-O3 89.6(4), N1'-C5-B1-O3 –89.6(4)). The hydroxyl groups attached to the boron atom in **5.21** involve in hydrogen bonding with the bromide anion, which presumably stabilizes the dihydroxyborenum cation via formation of a six-membered ring with O-H...Br bond distances of 2.422 and 2.466 Å.

With **5.10** in hand, we attempted its reaction with two equivalents of TfOH, which smoothly afforded a stable dihydroxyborenum cation with a triflate anion [6-SIDipp·B(OH)₂]⁺OTf⁻, **5.23** (Scheme 5.9) within only 2 h. Colorless crystals of **5.23**, which crystallizes in the orthorhombic *Pbca* space group were grown from the saturated toluene solution (Figure 5.24).

5.23 is air-stable, but gradually decomposes in the presence of THF and Et₂O to [6-SIDipp-H]⁺OTf⁻. The ¹¹B NMR chemical shift for **5.23** was detected at 21.08 ppm, reflecting a tri-coordinate boron environment. The molecular ion peak for **5.23** was identified at *m/z* 599.3036 in the HRMS spectrum. Anion exchange reaction of **5.23** with AgSbF₆ in CH₂Cl₂ at low temperature led to the replacement of the OTf⁻ anion with the SbF₆⁻ moiety (**5.24**). Unlike **5.23**, the latter is not very stable and decomposes with time to tetrahydropyrimidinium salt with SbF₆⁻ as a counter anion as confirmed by single-crystal X-ray studies. In the molecular structure of **5.24** (Figure 5.25), there are two molecules among which one belongs to **5.24**, and another one is the decomposed pyrimidinium salt.



Scheme 5.9. Preparation of a dihydroxy borenium cation **5.23** with a triflate anion and its anion exchange reactivity.

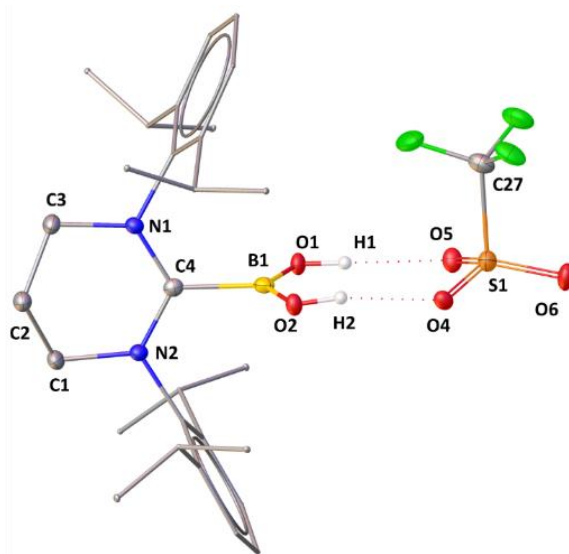


Figure 5.24. The molecular structure of **5.23** (except hydrogen atoms attached to the oxygen boron atom, other hydrogen atoms are omitted for the clarity of the picture). Selected bond lengths (Å), angles (deg) and torsion angles (deg): N1-C4 1.325(3), N2-C4 1.330(3), B1-C4 1.610(4), B1-O1 1.347(3), B1-O2 1.337(3), O1/O2-H1/H2 0.8400, S1-O4 1.4585(19), S1-O5 1.4365(19), S1-O6 1.427(2); N1-C4-N2 120.9(2), N1-C4-B1 120.0(2), N2-C4-B1 119.1(2), O1-B1-O2 129.7(3); N1-C4-B1-O1 -85.5(3), N1-C4-B1-O2 94.1(3), N2-C4-B1-O1 96.3(3), N2-C4-B1-O2 -84.1(3).

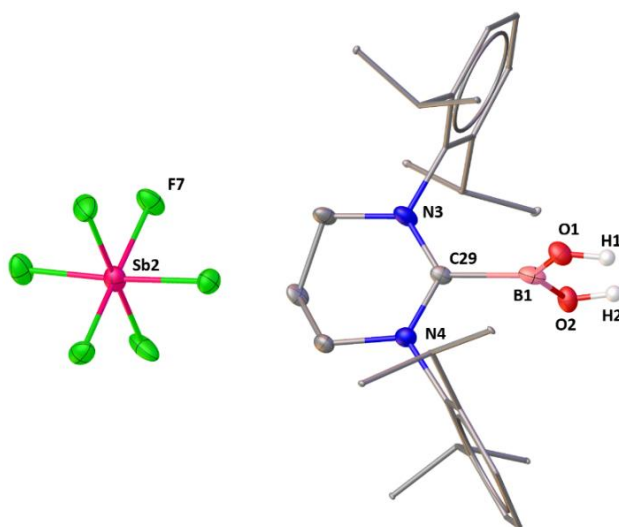
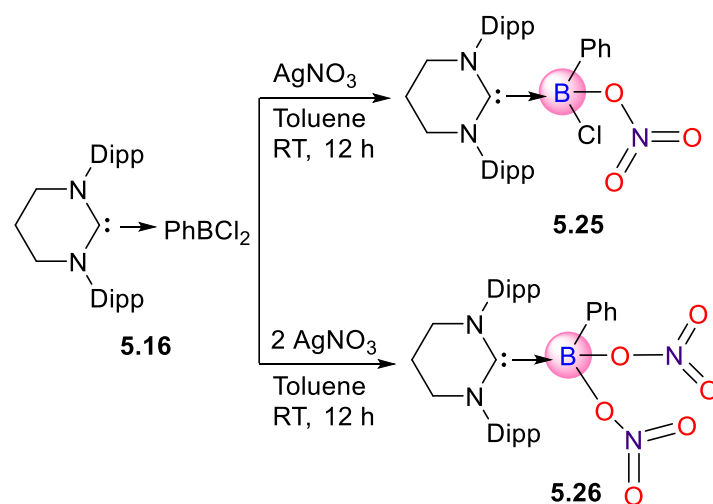


Figure 5.25. The molecular structures of **5.24**. Selected bond lengths (Å), angles (deg): N3-C29 1.324(11), N4-C29 1.460(10), C29-B1 1.636(14), B1-O1 1.347(12), B1-O2 1.336(13),

Sb2-F7 1.869(7); N3-C29-N4 121.9(8), N3-C29-B1 117.0(8), N4-C29-B1 121.0(8), C29-B1-O1 116.1(8), O1-B1-O2 129.7(10).



Scheme 5.10. Nucleophilic substitution reaction of **5.16** with AgNO_3 .

5.8. Nucleophilic substitution at 6-SIDipp- PhBCl_2 center:

Treatment of **5.16** with one and two equivalents of AgNO_3 in toluene afforded good yield of *mono*- and *di*- nitrate substituted 6-SIDipp-boranes, respectively (**5.25** and **5.26**, Scheme 5.10). It must be noted here that functional group such as ONO_2 is seldom found bonded to boron atoms. The ^{11}B NMR of **5.25** display characteristic resonance signal at 5.7 ppm. The ^{11}B NMR of **5.26** exhibits a resonance at -1.4 ppm in the solid-state NMR along with the formation of very minor peak at 19.4 ppm, which is indicative of a three-coordinated boron species. Despite repetitive attempts, we could not observe any other upfield resonance. We assume that **5.26** undergoes slow degradation to an unknown three coordinate boron species that we could not identify. The solid-state structures of **5.25** and **5.26** were confirmed by X-ray crystallographic analysis. **5.25** crystallizes in the monoclinic space $P2/n$ space group (Figure 5.26). The B-Cl bond length in **5.25** ($1.955(7)$ Å) is little longer compared to those in **5.16**, and it is orthogonal to the plane (torsion angle: $\text{N1-C7-B1-C11 } -87.7(3)^\circ$, $\text{N2-C7-B1-C11 } 81.8(3)^\circ$).

5.26 crystallizes in the triclinic *P*-1 space group (Figure 5.27). The B-O distances in **5.26** (1.5197(17) and 1.5019(17) Å) are marginally longer than that in **5.25** (1.479(4) Å). In the HRMS mass spectrum, the molecular ion peak with the highest intensity at *m/z* 590.3353 is the characteristics for **5.25**.

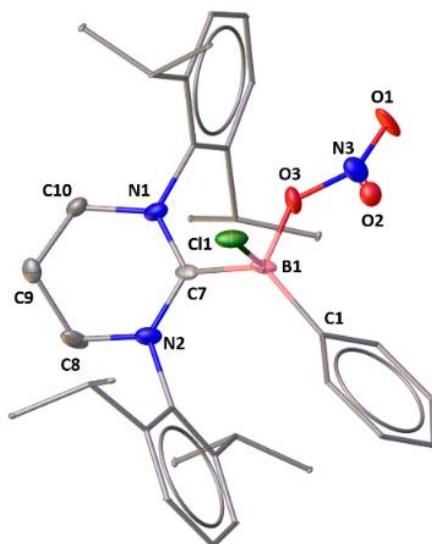


Figure 5.26. The molecular structure of **5.25**. Hydrogen atoms are omitted for clarity. Selected bond distances (Å), bond angles (deg), and torsion angles (deg): C7-N1 1.347(4), C7-N2 1.337(4), N1-C10 1.478(4), N2-C8 1.465(4), B1-C7 1.671(5), B1-Cl1 1.955(7), B1-C1 1.617(5), B1-O3 1.479(4), N3-O2 1.220(4), N3-O1 1.204(4), N3-O3 1.319(4); N1-C7-N2 117.7(3), N2-C7-B1 120.0(2), N1-C7-B1 121.5(2), C7-B1-O3 102.2(2), C7-B1-Cl1 96.9(3), O1-N3-O2 123.7(4); N1-C7-B1-Cl1 -87.7(3), N2-C7-B1-Cl1 81.8(3), N1-C7-B1-O3 25.5(4), N2-C7-B1-O3 -165.0(3).

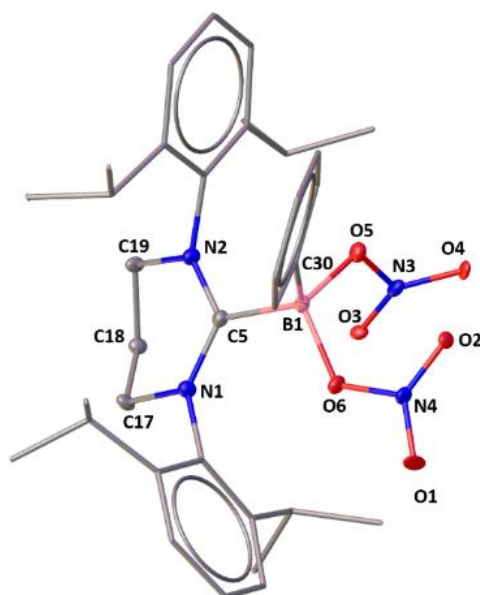


Figure 5.27. The molecular structure of **5.26**. Hydrogen atoms are omitted for clarity. Selected bond distances (Å), bond angles (deg), and torsion angles (deg): C5-N1 1.3502(17), C5-N2 1.3406(17), B1-C5 1.6942(19), N2-C19 1.4858(17), N1-C17 1.4835(17), B1-C30 1.603(2), B1-O6 1.5197(17), B1-O5 1.5019(17), N3-O5 1.3798(15), N4-O6 1.3604(15), N3-O3 1.214(5), N4-O1 1.2126(16); N1-C5-N2 118.09(12), N1-C5-B1 117.41(11), N2-C5-B1 124.15(11), C5-B1-O6 108.07(11), C5-B1-O5 103.05(10), C5-B1-C30 119.50(11), O5-B1-O6 109.04(11); C17-N1-C5-B1 162.71(12), C19-N2-C5-B1 -166.92(12), N2-C5-B1-C30 -108.04(15), N1-C5-B1-C30 78.92(16), N1-C5-B1-O6 -41.36(15), N1-C5-B1-O5 -156.69(11), N2-C5-B1-O5 16.35(17), N2-C5-B1-O6 131.68(12).

5.9. Conclusion:

While the body of work on carbene-borane chemistry is growing, the carbene component has been restricted to two classes of carbenes: (a) Arduengo type five-membered NHC and (b) cAAC. Here, we have introduced a new NHC, 6-SIDipp for NHC·borane chemistry, and described a detailed study of substitution reactions of 6-SIDipp·BH₃ (**5.1**). These results have uncovered the facile substitution to the coordinatively saturated *sp*³ boron atom in 6-

SIDipp·BH₃ with a range of functional groups such as bromide (**5.8**, **5.9**), iodide (**5.2** and **5.3**), triflate (**5.4** and **5.6**), ONO₂ (**5.5** and **5.7**) chloride. It is interesting to note that prototypical Arduengo type NHCs do not yield such double substitution upon halogenation. **5.1** was also found to generate a novel dihydroxyborenium ion (**5.21**) just by reacting with bromine water at room temperature in 3 h. We have also demonstrated the ability of a six-membered NHC (6-SIDipp) for stabilizing borenium cations. For this purpose, we have first prepared 6-SIDipp·PhBCl₂ adduct (**5.16**). The reaction of **5.16** with AlCl₃ led to the first borenium cation of composition [6-SIDipp·B(Ph)(Cl)]⁺ (**5.17**). Analogous reaction with triflic acid resulted in [6-SIDipp·B(Ph)(OH)]⁺ (**5.18**), which can be considered as the cationic analogue of less illustrated phenylborinic acid. Attempts to do the Lewis base exchange reaction with 4-DMAP led to the formation of an unusual boroxine (**5.19**) where the boron atoms are differently coordinated. **5.16** is also amenable towards nucleophilic substitution reaction with AgNO₃ furnishing 6-SIDipp·PhBCl(ONO₂) (**5.25**) and 6-SIDipp·PhB(ONO₂)₂ (**5.26**). It can be mentioned that examples of structurally characterized boranes with ONO₂ functionality are relatively scarce. Interestingly, 9-BBN forms an adduct with 6-SIDipp (**5.11**) which undergoes ring expansion to a seven membered ring (**5.12**) at room temperature. Finally, the stronger nucleophilic properties of six-membered NHC (6-SIDipp) than those of typical five-membered NHCs was epitomized in the 1,1-activation of the B-H bond of HBpin (**5.13**) at the carbene carbon. Although CAAC was shown to exhibit such reactivity, no NHC has been known to add the B-H bond of HBpin in this fashion.

5.10: References:

1. Bittner, G.; Witte, H.; Hesse, G., Nitrile-Ylide From Isonitriletriphenylborane Adducts. *Annalen Der Chemie-Justus Liebig* **1968**, *713*, 1-9.
2. Wang, Y.; Quillian, B.; Wei, P.; Wannere, C. S.; Xie, Y.; King, R. B.; Schaefer, H. F.; Schleyer, P. v. R.; Robinson, G. H., A Stable Neutral Diborene Containing a BB Double Bond. *J. Am. Chem. Soc.* **2007**, *129*, 12412-12413.
3. Curran, D. P.; Solovyev, A.; Brahmi, M. M.; Fensterbank, L.; Malacria, M.; Lacote, E., Synthesis and Reactions of N-Heterocyclic Carbene Boranes. *Angew. Chem. Int. Ed.* **2011**, *50*, 10294-10317.
4. Biahmi, M. M.; Monot, J.; Desage-El Murr, M.; Curran, D. P.; Fensterbank, L.; Lacote, E.; Malacria, M., Preparation of NHC Borane Complexes by Lewis Base Exchange with Amine-and Phosphine-Boranes. *J. Org. Chem.* **2010**, *75*, 6983-6985.
5. Dai, W.; Geib, S. J.; Curran, D. P., Reactions of N-Heterocyclic Carbene Boranes with 5-Diazo-2,2-dimethyl-1,3-dioxane-4,6-dione: Synthesis of Mono- and Bishydrazonyl NHC-Boranes. *J. Org. Chem.* **2018**, *83*, 8775-8779.
6. Nozaki, K.; Aramaki, Y.; Yamashita, M.; Ueng, S. H.; Malacria, M.; Lacote, E.; Curran, D. P., Boryltrihydroborate: Synthesis, Structure, and Reactivity as a Reductant in Ionic, Organometallic, and Radical Reactions. *J. Am. Chem. Soc.* **2010**, *132*, 11449-11451.
7. Solovyev, A.; Chu, Q.; Geib, S. J.; Fensterbank, L.; Malacria, M.; Lacôte, E.; Curran, D. P., Substitution Reactions at Tetracoordinate Boron: Synthesis of N-Heterocyclic Carbene Boranes with Boron-Heteroatom Bonds. *J. Am. Chem. Soc.* **2010**, *132*, 15072-15080.
8. Solovyev, A.; Ueng, S. H.; Monot, J.; Fensterbank, L.; Malacria, M.; Lacote, E.; Curran, D. P., Estimated Rate Constants for Hydrogen Abstraction from N-Heterocyclic Carbene-Borane Complexes by an Alkyl Radical. *Org. Lett.* **2010**, *12*, 2998-3001.

9. Ueng, S. H.; Makhoulf Brahmi, M.; Derat, É.; Fensterbank, L.; Lacôte, E.; Malacria, M.; Curran, D. P., Complexes of Borane and N-Heterocyclic Carbenes: A New Class of Radical Hydrogen Atom Donor. *J. Am. Chem. Soc.* **2008**, *130*, 10082-10083.
10. Auerhammer, D.; Arrowsmith, M.; Braunschweig, H.; Dewhurst, R. D.; Jimenez-Halla, J. O. C.; Kupfer, T., Nucleophilic addition and substitution at coordinatively saturated boron by facile 1,2-hydrogen shuttling onto a carbene donor. *Chem. Sci.* **2017**, *8*, 7066-7071.
11. Munz, D., Pushing Electrons-Which Carbene Ligand for Which Application? *Organometallics* **2018**, *37*, 275-289.
12. Abdalla, J. A. B.; Riddlestone, I. M.; Tirfoin, R.; Phillips, N.; Bates, J. I.; Aldridge, S., Al-H sigma-bond coordination: expanded ring carbene adducts of AlH₃ as neutral bi- and tri-functional donor ligands. *Chem. Commun.* **2013**, *49*, 5547-5549.
13. Sidiropoulos, A.; Osborne, B.; Simonov, A. N.; Dange, D.; Bond, A. M.; Stasch, A.; Jones, C., Expanded ring N-heterocyclic carbene adducts of group 15 element trichlorides: synthesis and reduction studies. *Dalton Trans.* **2014**, *43*, 14858-14864.
14. Kronig, S.; Theuergarten, E.; Holschumacher, D.; Bannenberg, T.; Daniliuc, C. G.; Jones, P. G.; Tamm, M., Dihydrogen Activation by Frustrated Carbene-Borane Lewis Pairs: An Experimental and Theoretical Study of Carbene Variation. *Inorg. Chem.* **2011**, *50*, 7344-7359.
15. Bisai, M. K.; Sharma, V.; Gonnade, R. G.; Sen, S. S., Reactivities of Silaimines with Boranes: From Cooperative B-H Bond Activation to Donor Stabilized Silyl Cation. *Organometallics* **2021**, *40*, 2133-2138.
16. Bisai, M. K.; Swamy, V.; Raj, K. V.; Vanka, K.; Sen, S. S., Diverse Reactivity of Hypersilylsilylene with Boranes and ThreeComponent Reactions with Aldehyde and HBpin. *Inorg. Chem.* **2021**, *60*, 1654-1663.

17. Swamy, V.; Raj, K. V.; Vanka, K.; Sen, S. S.; Roesky, H. W., Silylene induced Cooperative B-H Bond Activation and Unprecedented Aldehyde C-H Bond Splitting with Amidinate Ring Expansion. *Chem. Commun.* **2019**, *55*, 3536-3539.
18. Solovyev, A.; Geib, S. J.; Lacote, E.; Curran, D. P., Reactions of Boron-Substituted N-Heterocyclic Carbene Boranes with Triflic Acid. Isolation of a New Dihydroxyborenium Cation. *Organometallics* **2012**, *31*, 54-56.
19. Wang, T.; Stephan, D. W., Carbene-9-BBN Ring Expansions as a Route to Intramolecular Frustrated Lewis Pairs for CO₂ Reduction. *Chem. Eur. J.* **2014**, *20*, 3036-3039.
20. Farrell, J. M.; Hatnean, J. A.; Stephan, D. W., Activation of Hydrogen and Hydrogenation Catalysis by a Borenium Cation. *J. Am. Chem. Soc.* **2012**, *134*, 15728-15731.
21. Al-Rafia, S. M. I.; McDonald, R.; Ferguson, M. J.; Rivard, E., Preparation of Stable Low-Oxidation-State Group 14 Element Amidohydrides and Hydride-Mediated Ring-Expansion Chemistry of N-Heterocyclic Carbenes. *Chem. Eur. J.* **2012**, *18*, 13810-13820.
22. Arrowsmith, M.; Hill, M. S.; Kociok-Köhn, G.; MacDougall, D. J.; Mahon, M. F., Beryllium-Induced C–N Bond Activation and Ring Opening of an N-Heterocyclic Carbene. *Angew. Chem. Int. Ed.* **2012**, *51*, 2098-2100.
23. Bose, S. K.; Fucke, K.; Liu, L.; Steel, P. G.; Marder, T. B., Zinc-Catalyzed Borylation of Primary, Secondary and Tertiary Alkyl Halides with Alkoxy Diboron Reagents at Room Temperature. *Angew. Chem. Int. Ed.* **2014**, *53*, 1799-1803.
24. Schmidt, D.; Berthel, J. H. J.; Pietsch, S.; Radius, U., C–N Bond Cleavage and Ring Expansion of N-Heterocyclic Carbenes using Hydrosilanes. *Angew. Chem. Int. Ed.* **2012**, *51*, 8881-8885.
25. Schneider, H.; Hock, A.; Bertermann, R.; Radius, U., Reactivity of NHC Alane Adducts towards N-Heterocyclic Carbenes and Cyclic (Alkyl)(amino)carbenes: Ring Expansion, Ring Opening, and Al–H Bond Activation. *Chem. Eur. J.* **2017**, *23*, 12387-12398.

26. García, L.; Al Furaiji, K. H. M.; Wilson, D. J. D.; Dutton, J. L.; Hill, M. S.; Mahon, M. F., Ring expansion of a ring expanded carbene. *Dalton Trans.* **2017**, *46*, 12015-12018.
27. Frey, G. D.; Masuda, J. D.; Donnadiou, B.; Bertrand, G., Activation of Si–H, B–H, and P–H Bonds at a Single Nonmetal Center. *Angew. Chem. Int. Ed.* **2010**, *49*, 9444-9447.
28. Gautam, N.; Logdi, R.; Sreejyothi, P.; Rajendran, N. M.; Tiwari, A. K.; Mandal, S. K., Bicyclic (alkyl)(amino)carbene (BICAAC) as a metal-free catalyst for reduction of nitriles to amines. *Chem. Commun.* **2022**, *58*, 3047-3050.
29. Dröge, T.; Glorius, F., The Measure of All Rings—N-Heterocyclic Carbenes. *Angew. Chem. Int. Ed.* **2010**, *49*, 6940-6952.
30. Würtemberger-Pietsch, S.; Schneider, H.; Marder, T. B.; Radius, U., Adduct Formation, B–H Activation and Ring Expansion at Room Temperature from Reactions of HBcat with NHCs. *Chem. Eur. J.* **2016**, *22*, 13032-13036.
31. Eck, M.; Würtemberger-Pietsch, S.; Eichhorn, A.; Berthel, J. H. J.; Bertermann, R.; Paul, U. S. D.; Schneider, H.; Friedrich, A.; Kleeberg, C.; Radius, U.; Marder, T. B., B–B bond activation and NHC ring-expansion reactions of diboron(4) compounds, and accurate molecular structures of B₂(NMe₂)₄, B₂eg₂, B₂neop₂ and B₂pin₂. *Dalton Trans.* **2017**, *46*, 3661-3680.
32. Westcott, S. A.; Blom, H. P.; Marder, T. B.; Baker, R. T.; Calabrese, J. C., Nucleophile promoted degradation of catecholborane: consequences for transition metal-catalyzed hydroborations. *Inorg. Chem.* **1993**, *32*, 2175-2182.
33. Miyaura, N.; Suzuki, A. Stereoselective Synthesis of Arylated (E)-Alkenes by the Reaction of Alk-1-enylboranes with Aryl halides in the Presence of Palladium Catalyst. *J. Chem. Soc., Chem. Commun.* **1979**, *19*, 866-867.
34. Petasis, N. A.; Zavialov, I. A., A New and Practical Synthesis of α -Amino Acids from Alkenyl Boronic Acids. *J. Am. Chem. Soc.* **1997**, *119*, 445-446.

35. Sakai, M.; Ueda, M.; Miyaura, N., Rhodium-Catalyzed Addition of Organoboronic Acids to Aldehydes. *Angew. Chem. Int. Ed.* **1998**, *37*, 3279-3281.
36. Lee, D.; Taylor, M. S., Borinic Acid-Catalyzed Regioselective Acylation of Carbohydrate Derivatives. *J. Am. Chem. Soc.* **2011**, *133*, 3724-3727.
37. Lee, D.; Williamson, C. L.; Chan, L.; Taylor, M. S., Regioselective, Borinic Acid-Catalyzed Monoacylation, Sulfonylation and Alkylation of Diols and Carbohydrates: Expansion of Substrate Scope and Mechanistic Studies. *J. Am. Chem. Soc.* **2012**, *134*, 8260-8267.
38. Wang, G.; Garrett, G. E.; Taylor, M. S., Borinic Acid-Catalyzed, Regioselective Ring Opening of 3,4-Epoxy Alcohols. *Org. Lett.* **2018**, *20*, 5375-5379.
39. Michaelis, A. Untersuchungen über aromatische Borverbindungen. *Ber.* **1894**, *27*, 244-262.
40. Weese, K. J.; Bartlett, R. A.; Murray, B. D.; Olmstead, M. M.; Power, P. R., Synthesis and spectroscopic and structural characterization of derivatives of the quasi-alkoxide ligand [OBMes₂] (Mes = 2,4,6-Me₃C₆H₂). *Inorg. Chem.* **1987**, *26*, 2409-2413.
41. Matsumoto, T.; Gabbai, F. P., A Borenum Cation Stabilized by an N-Heterocyclic Carbene Ligand. *Organometallics* **2009**, *28*, 4252-4253.
42. Silva Valverde, M. F.; Schweyen, P.; Gisinger, D.; Bannenberg, T.; Freytag, M.; Kleeberg, C.; Tamm, M., N-Heterocyclic Carbene Stabilized Boryl Radicals. *Angew. Chem. Int. Ed.* **2017**, *56*, 1135-1140.
43. McArthur, D.; Butts, C. P.; Lindsay, D. M., A dialkylborenum ion via reaction of N-heterocyclic carbene-organoboranes with Bronsted acids-synthesis and DOSY NMR studies. *Chem. Commun.* **2011**, *47*, 6650-6652.

44. Weber, L.; Dobbert, E.; Stammler, H.-G.; Neumann, B.; Boese, R.; Bläser, D., Reaction of 1,3-Dialkyl-4,5-dimethylimidazol-2-ylidenes with 2-Bromo-2,3-dihydro-1H-1,3,2-diazaboroles (Alkyl=*i*Pr and *t*Bu). *Chem. Ber.* **1997**, *130*, 705-710.
45. Wang, Y.; Robinson, G. H., Carbene Stabilization of Highly Reactive Main-Group Molecules. *Inorg. Chem.* **2011**, *50*, 12326-12337.
46. Mansaray, H. B.; Rowe, A. D. L.; Phillips, N.; Niemeyer, J.; Kelly, M.; Addy, D. A.; Bates, J. I.; Aldridge, S., Modelling fundamental arene-borane contacts: spontaneous formation of a dibromoborenium cation driven by interaction between a borane Lewis acid and an arene pi system. *Chem. Commun.* **2011**, *47*, 12295-12297.
47. Lawson, J. R.; Clark, E. R.; Cade, I. A.; Solomon, S. A.; Ingleson, M. J., Haloboration of Internal Alkynes with Boronium and Borenium Cations as a Route to Tetrasubstituted Alkenes. *Angew. Chem. Int. Ed.* **2013**, *52*, 7518-7522.
48. Koelle, P.; Nöth, H., The chemistry of Borinium and Borenium ions. *Chem. Rev.* **1985**, *85*, 399-418.
49. Piers, W. E.; Bourke, S. C.; Conroy, K. D., Borinium, Borenium, and Boronium Ions: Synthesis, Reactivity, and Applications. *Angew. Chem. Int. Ed.* **2005**, *44*, 5016-5036.
50. Cade, I. A.; Ingleson, M. J., syn-1,2-Carboboration of Alkynes with Borenium Cations. *Chem. Eur. J.* **2014**, *20*, 12874-12880.
51. Bissinger, P.; Braunschweig, H.; Damme, A.; Hörl, C.; Krummenacher, I.; Kupfer, T., Boron as a Powerful Reductant: Synthesis of a Stable Boron-Centered Radical-Anion Radical-Cation Pair. *Angew. Chem., Int. Ed.* **2015**, *54*, 359-362.
52. Wu, X.; Liu, X.; Zhao, G., Catalyzed asymmetric aryl transfer reactions to aldehydes with boroxines as aryl source. *Tetrahedron: Asymmetry* **2005**, *16*, 2299-2305.
53. Stoy, A.; Härterich, M.; Dewhurst, R. D.; Jiménez-Halla, J. O. C.; Endres, P.; Eyßlein, M.; Kupfer, T.; Deissenberger, A.; Thiess, T.; Braunschweig, H., Evidence for Borylene

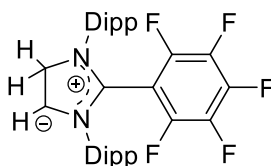
Carbonyl (LHB=C=O) and Base-Stabilized (LHB=O) and Base-Free Oxoborane (RB=O) Intermediates in the Reactions of Diborenes with CO₂. *J. Am. Chem. Soc.* **2022**, *144*, 3376-3380.

54. Inés, B.; Patil, M.; Carreras, J.; Goddard, R.; Thiel, W.; Alcarazo, M., Synthesis, Structure, and Reactivity of a Dihydrido Borenium Cation. *Angew. Chem. Int. Ed.* **2011**, *50*, 8400-8403.

6.1: Experimental details for chapter-2

6.1.1. Synthesis and Characterization of Compounds 2.1-2.11

Synthesis and Characterization of Compound 2.1



2.1

Benzene (10 mL) was charged in a Schlenk flask containing **5-SIPr** (0.2 g, 0.51 mmol) and C₆F₆ (0.190 g, 1.02 mmol). The reaction mixture was stirred at room temperature for 15 min. The color of the reaction mixture was changed from yellow to brown. A greenish yellow precipitate was separated through cannula filtration from the reaction mixture. The volatiles were removed in vacuum and the resulting residue was washed with *n*-hexane (5 mL) to give **2.1** as a greenish yellow solid. **2.1** was dissolved in CHCl₃ (3 mL) and was kept at 4 °C in a freezer for 5-7 days to afford colorless crystals suitable for single crystal X-ray analysis. Yield: 0.22 g (77.8 %). MP: 198.6 °C.

¹H NMR (400 MHz, 298 K, CDCl₃): δ = 1.18 (d, J = 6.62 Hz, 12H, CH(CH₃)₂), 1.25 (d, J = 7.39 Hz, 12H, CH(CH₃)₂), 2.98 (br sept, J = 6.73 Hz, 4H, CHCH₃), 4.34 (s, 3H, N-CH₂CH-N), 7.21 (d, J = 7.42 Hz, 4H, *meta*-Ar-H), 7.39 (t, J = 6.95 Hz, 2H, *para*-Ar-H) ppm

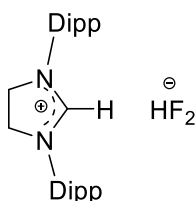
¹³C{¹H} NMR (101 MHz, 298 K, CDCl₃): δ = 23.12, 26.81 (H_{CM_{e2}}), 29.59 (H_{CM_{e2}}), 53.15 (N-CH₂CH-N), 125.34, 130.94, 132.13 (Ar-C₆H₃), 146.17 (*ipso*-C₆H₃) ppm, C(C₆F₅) and C(C₆F₅) were not detected due to signal broadening (¹⁹F coupling)

¹⁹F{¹H} NMR (377 MHz, 298 K, CDCl₃): δ = -113.29 (s, 1F, *para*-Ar-F), -141.90 (d, J_{FF} = 18.31 Hz, 2F, *ortho*-Ar-F), -166.89 (d, J_{FF} = 18.31 Hz, 2F, *meta*-Ar-F) ppm

HRMS (CH₃CN): *m/z* Calcd. for C₃₃H₃₇F₅N₂ [M]⁺ 556.1871, found 556.3005

Elemental analysis: Calcd. C, 71.20; H, 6.70; N, 5.03; Found. C, 70.5; H, 6.27; N, 4.89. Due to the sensitivity of the crystals the analytical values show deviations from the calculated one.

Synthesis and Characterization of Compound 2.2



2.2

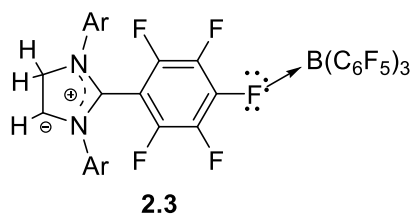
C₆F₆ (0.190 g, 1.02 mmol) was added to 3 ml benzene solution of **5-SIPr** (0.2 g, 0.51 mmol) at room temperature. After 15 min the reaction mixture was again cooled to -30 °C and 0.5 equivalent of 2 ml benzene solution of **5-SIPr** (0.1 g, 0.26 mmol) was added to the reaction mixture. The reaction was kept for 2-3 h at room temperature and a precipitate was formed. 5 ml of dichloromethane was added to dissolve the precipitate. Finally, it was concentrated and kept for crystallization at 4 °C. Colorless crystals of **2.2** were isolated after 2 days which was characterized by single crystal X-ray study. Yield: 0.140 g (64.2 %). MP: 198.6 °C.

¹H NMR (400 MHz, 298 K, CDCl₃): δ = 0.75-1.29 (m, 24H, 2CH(CH₃)₂), 2.79 (br sept, *J* = 6.73 Hz, 4H, CHCH₃), 4.92 (s, 4H, N-CH₂CH₂-N), 8.09 (s, 1H, N-CH-N), 15.89 (s, 2H, HF₂⁻) ppm

¹⁹F{¹H} NMR (377 MHz, 298 K, CDCl₃): δ = -162.42 (s, 2F, HF₂⁻) ppm

HRMS (CH₃CN): *m/z* Calcd. for C₂₇H₄₀F₂N₂[M]⁺ 430.3108, found [M-HF₂⁻] 391.3105.

Synthesis and Characterization of Compound 2.3



Dichloromethane (5 mL) solution of **2.1** (0.2 g, 0.36 mmol) was added to the THF (5 mL) solution of $B(C_6F_5)_3$ (0.185 g, 0.36 mmol) drop by drop at $-78\text{ }^\circ\text{C}$. The reaction mixture was allowed to come at room temperature to give rise a golden yellow solution in 12 h. The volatiles were removed in vacuum and extracted with THF (5 mL). Concentration of the THF solution resulted in the crystals of **2.3**. Yield: 0.32 g (85.34 %). MP: $141.6\text{ }^\circ\text{C}$.

^1H NMR (400 MHz, 298 K, DMSO- d_6): $\delta = 1.00\text{--}1.35$ (m, 24H, $\text{CH}(\text{CH}_3)_2$), 2.91, 3.08 (br sept, $J = 6.73$ Hz, 4H, CHCH_3), 4.53 (s, 2H, N- CH_2 -CH-N), 4.64 (s, 1H, N- CH_2 -CH-N), 7.32 (m, 4H, Ar-H), 7.43 (m, 2H, Ar-H) ppm

$^{13}\text{C}\{^1\text{H}\}$ NMR (101 MHz, 298 K, DMSO- d_6): $\delta = 21.80, 25.09$ (HCM_{e2}), 26.80, 28.04 (HCM_{e2}), 53.89, 54.78 (CH_2CH), 125.50, 127.66, 132.09 (Ar- C_6H_3), 146.61 (*ipso*-Ar- C_6H_3) ppm, $\text{C}(\text{C}_6\text{F}_5)$ and $\text{C}(\text{C}_6\text{F}_5)$ were not detected due to signal broadening (^{19}F coupling)

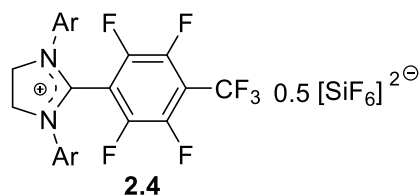
$^{19}\text{F}\{^1\text{H}\}$ NMR (377 MHz, 298 K, DMSO- d_6): $\delta = -134.56$ to -134.92 (m, 6F, *ortho*- C_6F_5), -136.88 (d, $J_{\text{FF}} = 16.02$ Hz, 2F, *ortho*- C_6F_4), -155.98 (d, $J_{\text{FF}} = 20.60$, 1F, bridging F), -158.91 (t, $J_{\text{FF}} = 22.89$, 2F, *meta*- C_6F_4), -160.62 (t, $J_{\text{FF}} = 22.89$, 3F, *para*- C_6F_5), -165.06 to -165.50 (m, 6F, *meta*- C_6F_5) ppm

$^{11}\text{B}\{^1\text{H}\}$ NMR (128 MHz, 298 K, DMSO- d_6): -0.81 (d, $J = 79.41$ Hz, 1B, $\text{B}(\text{C}_6\text{F}_5)_3$) ppm

HRMS (CH_3CN): m/z Calcd. for $\text{C}_{51}\text{H}_{37}\text{BF}_{20}\text{N}_2 + \text{Na}^+$ $[\text{M}+\text{Na}^+]$ 1091.2623, found 1091.2629

Elemental analysis: Calcd. (%) for $C_{51}H_{37}BF_{20}N_2$ [$1068.27 \text{ g mol}^{-1}$]: C 57.32, H 3.49, N 2.51; found: C 57.27, H 3.58, N 2.62

Synthesis and Characterization of Compound 2.4



In a Schlenk tube, **5-SIPr** (0.2 g, 0.51 mmol) was dissolved in benzene (5 mL) and $C_6F_5(CF_3)$ (0.12 g, 0.51 mmol) was added to the solution at -30°C . The reaction was instantaneously changed to green and finally yellow after 1h. The volatiles were removed in vacuum and the resulting residue was washed with *n*-hexane (5 mL) to give **2.4** as a yellow solid. Benzene (2 mL) solution of **2.4** was kept at room temperature to afford a colorless crystal of **2.4** suitable for X-ray analysis. Yield: 0.28 g (79.0%), MP: 155.3°C .

^1H NMR (400 MHz, 298 K, DMSO- d_6): $\delta = 1.15$ (d, $J = 6.10$ Hz, 12H, $\text{CH}(\text{CH}_3)_2$), 1.30 (d, $J = 6.71$ Hz, 12H, $\text{CH}(\text{CH}_3)_2$), 3.03 (br sept, 4H, CHCH_3), 4.58, 4.76 (s, 4H, $\text{N-CH}_2\text{CH}_2\text{-N}$), 7.40 (m, 4H, *meta*-Ar-H), 7.53 (t, 2H, $J = 7.93$ Hz, *para*-Ar-H) ppm

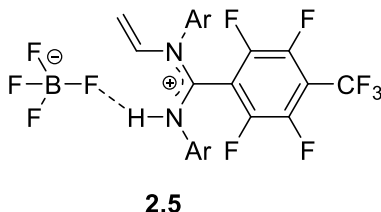
$^{13}\text{C}\{^1\text{H}\}$ NMR (101 MHz, 298 K, DMSO- d_6): $\delta = 22.23$, 26.67 (HCMe_2), 28.34 (HCMe_2), 54.80 (CH_2CH), 125.57, 128.52, 131.79 (Ar- C_6H_3), 145.83 (*ipso*-Ar- C_6H_3) ppm, $\text{C}(\text{C}_6\text{F}_5)$ and $\text{C}(\text{C}_6\text{F}_5)$ were not detected due to signal broadening (^{19}F coupling)

$^{19}\text{F}\{^1\text{H}\}$ NMR (377 MHz, 298K, DMSO- d_6): $\delta = -56.42$ (t, $J_{\text{FF}} = 27.47$ Hz, 3F, CF_3), -124.62 (s, 6F, SiF_6^{2-}), -131.82 (s, 2F, *ortho*-Ar-F), -137.11 (m, $J_{\text{FF}} = 9.15$ Hz, 2F, *meta*-Ar-F) ppm

HRMS (CH_3CN): m/z Calcd. for $\text{C}_{34}\text{H}_{38}\text{F}_7\text{N}_2$ [$\text{M}-0.5 \text{ SiF}_6$] 607.2918, found 607.2921

Elemental Analysis: Calcd. C, 67.20; H, 6.30; N, 4.61; Found. C, 67.75; H, 6.56; N, 4.57

Synthesis and Characterization of Compound 2.5



To a solution of **5-SIPr** (0.2 g, 0.18 mmol) in 5 mL of benzene, $C_6F_5(CF_3)$ (0.12 g, 0.51 mmol) was added at $-30\text{ }^\circ\text{C}$. The mixture was stirred for 30 min and trifluoroborane diethyl etherate (0.062 mL, 0.51 mmol) was added drop by drop at $-30\text{ }^\circ\text{C}$ to the reaction mixture. The resulting solution color was changed to light greenish immediately with the formation of a white precipitate. After stirring for further 1 h at room temperature, the volatiles were removed under vacuum and extracted through the frit filtration with dichloromethane (5 mL). Colorless crystals appeared after keeping the dichloromethane (2 mL) solution at $4\text{ }^\circ\text{C}$ for 1 day. Yield 0.3 g (85 %), MP: $141.6\text{ }^\circ\text{C}$.

^1H NMR (200 MHz, 298 K, CDCl_3): $\delta = 1.17$ (d, $J = 6.10$ Hz, 12H, $\text{CH}(\text{CH}_3)_2$), 1.35 (d, $J = 6.10$ Hz, 12H, $\text{CH}(\text{CH}_3)_2$), 3.00 (sept, $J = 5.49$, 4H, CHCH_3), 3.57 (s, 1H, NH), 4.82 (s, 3H, $\text{CH}_2=\text{CH}$), 7.25 (d, $J = 7.93$ Hz, 4H, Ar-H), 7.462 (t, $J = 7.32$, 2H, Ar-H) ppm

$^{13}\text{C}\{^1\text{H}\}$ NMR (101 MHz, 298 K, DMSO-d_6): $\delta = 22.72$, (HCM_{e2}), 26.78 , 29.09 (HCM_{e2}), 55.12 (CH_2CH), 125.51 , 128.45 , 132.08 (Ar- C_6H_3), 146.37 (*ipso*-Ar- C_6H_3) ppm, $\text{C}(\text{C}_6\text{F}_5)$ and $\text{C}(\text{C}_6\text{F}_5)$ were not detected due to signal broadening (^{19}F coupling)

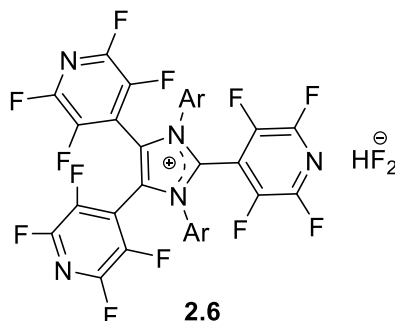
$^{19}\text{F}\{^1\text{H}\}$ NMR (377 MHz, 298 K, DMSO-d_6): $\delta = -56.70$ (t, $J = 22.89$ Hz, 3F, CF_3), -129.49 (m, 2F, *ortho*-Ar-CF), 134.95 (m, 2F, *meta*-Ar-CF), -149.65 (s, 1F, BF_4 , attached with N-H via H bonding), -152.30 (s, 3 F, BF_4 , remaining 3F) ppm

$^{11}\text{B}\{^1\text{H}\}$ NMR (128 MHz, 298 K, DMSO-d_6): 4.26 (s, 1B, BF_4^-) ppm

HRMS (CH₃CN): *m/z* calculated for C₃₄H₃₈BF₁₁N₂ 694.4816, found 607.2916 (M-BF₄⁻)

Elemental Analysis: Calcd. C, 58.80; H, 5.52; N, 4.03; Found. C, 58.63; H, 5.45; N, 4.41

Synthesis and Characterization of Compound 2.6



Pentafluoropyridine (0.261 g, 1.53 mmol) was added to a solution of IDipp (0.2 g, 0.51 mmol) at 0 °C, in 10 mL of toluene and *n*-hexane mixture. An immediate formation of yellow precipitate was noticed after coming to room temperature. The resulting mixture was stirred for 15 minutes and the precipitate was filtered through a cannula followed by washing with *n*-hexane and diethyl ether. The solution was dried in vacuum and kept for crystallization with the mixture of tetrahydrofuran (5 mL) and toluene (2 mL). Yellow crystals came after keeping this solution at 4 °C for 2-3 days with a yield of 0.468 g (56 %). MP: decomposition at 120 °C.

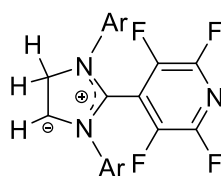
¹H NMR (200 MHz, 298 K, CDCl₃): δ = 1.26-1.16 (m, 24 H, CH(CH₃)₂), 2.41 (sept, *J* = 6.87 Hz, 4 H, CH(CH₃)₂), 7.33 (d, *J* = 8.39 Hz, 4 H, *meta*-Ar-H), 7.58 (t, *J* = 7.63 Hz, 2 H, *para*-Ar-H), 15.05 (br s, 1H, HF₂⁻) ppm

¹³C{¹H} NMR (101 MHz, 298 K, CDCl₃): δ = 15.21 (CH₃, diethyl ether) 22.65, 26.92 (HCM₂), 29.08 (HCM₂), 65.84 (CH₂O, diethyl ether), 55.31 (tetrahydrofuran), 125.02 (NCH=CHN) 125.54, 128.13, 132.24 (Ar-C₆H₃), 125.40, 127.67, 128.58, 129.04, 131.59, 131.83 (C₅F₄N), 146.25 (*ipso*-C₆H₃), 157.14 (NCN) ppm

$^{19}\text{F}\{^1\text{H}\}$ NMR (377 MHz, 298 K, CDCl_3): $\delta = -168.49$ (br s, 2 F, HF_2^-), -135.04 (m), -133.77 (m), -123.52 (m), -120.18 (d = 27.62 Hz), -83.82 (m), -82.48 (d, $J = 31.57$ Hz) ppm

Elemental analysis: calcd (%) for $\text{C}_{42}\text{H}_{35}\text{F}_{12}\text{N}_5$ [837.27 gmol^{-1}]: C 60.22, H 4.21, N 8.36; found: C 60.47, H 4.01, N 8.21

Synthesis and Characterization of Compound 2.7



2.7

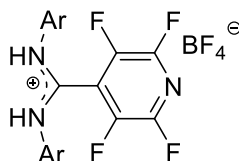
Pentafluoropyridine (0.17 g, 1.02 mmol) was added to a hexane solution of SIDipp (0.2 g, 0.51 mmol) at 0°C . An immediate formation of yellow precipitate was noticed after coming to room temperature. The resulting mixture was stirred for 1 hour at that temperature. The precipitate was filtered through a cannula followed by washing with *n*-hexane. The solution was dried in vacuum. Yellow powder of **2.7** was collected with a yield of 0.350 g (65%). MP: decomposition at 120°C . **^1H NMR (500 MHz, 298 K, CDCl_3):** $\delta = 1.30$ - 1.16 (m, 12H, $\text{CH}(\text{CH}_3)_2$), 3.00 (sept, $J = 6.38$ Hz, 4H, $\text{CH}(\text{CH}_3)_2$), 4.65 (s, 1H, N- CH_2CH -N), 5.00 (s, 2H, N- CH_2CH -N), 7.19-7.43 (m, 6H, Ar-*H*) ppm

$^{13}\text{C}\{^1\text{H}\}$ NMR (101 MHz, 298 K, CDCl_3): $\delta = 22.65$, 23.67 ($\text{H}\text{C}\text{M}\text{e}_2$), 26.88, 28.99 ($\text{H}\text{C}\text{M}\text{e}_2$), 54.42, 56.03 (CH_2CH), 125.43, 128.37, 132.04 (Ar- C_6H_3), 124.80, 125.07, 129.77, 130.98, 131.31 ($\text{C}_5\text{F}_4\text{N}$), 146.25 (*ipso*- C_6H_3) ppm

$^{19}\text{F}\{^1\text{H}\}$ NMR (377 MHz, 298 K, CDCl_3): $\delta = -132.93$ (s, 2F, *meta*-Ar- $\text{C}_5\text{F}_4\text{N}$) -83.74 (s, 2F, *ortho*-Ar- $\text{C}_5\text{F}_4\text{N}$) ppm

Elemental analysis: calcd (%) for $C_{32}H_{37}F_4N_3$ [539.66 gmol^{-1}]: C 71.22, H 6.91, N 7.79; found: C 71.27, H 6.58, N 7.62

Synthesis and Characterization of Compound 2.8



2.8

Pentafluoropyridine (0.086 g, 0.51 mmol) was added to a solution of SIDipp (0.2 g, 0.51 mmol) at 0°C , in 10 mL of THF. The resulting mixture was stirred for 30 minutes at room temperature and trifluoroborane diethyl etherate (0.065 mL, 0.051 mmol) was added drop wise at -78°C . The solution became colorless immediately. After stirring the reaction mixture for further 30 minutes at room temperature, the solution was dried in vacuum and extracted through a frit with the mixture of tetrahydrofuran and dichloromethane. Colorless crystals came after keeping this solution mixture at -36°C for 4–5 days with a yield of 0.29 g (48 %). MP: decomposition at 72°C .

^1H NMR (200 MHz, 298 K, CDCl_3): $\delta = 1.19$ (d, $J = 6.10$ Hz, 12H, $\text{CH}(\text{CH}_3)_2$), 1.37 (d, $J = 6.87$ Hz, 12H, $\text{CH}(\text{CH}_3)_2$), 3.01 (sept, $J = 6.87$ Hz, 4H, $\text{CH}(\text{CH}_3)_2$), 4.87 (bs, 2H, NH), 7.23 (d, $J = 8.39$ Hz, 4H, *meta*-Ar-H), 7.47 (t, $J = 7.63$ Hz, *para*-Ar-H) ppm

$^{13}\text{C}\{^1\text{H}\}$ NMR (101 MHz, 298 K, CDCl_3): $\delta = 22.63, 23.72$ ($\text{H}(\text{CMe}_2)$), 26.86, 29.08 ($\text{H}(\text{CMe}_2)$), 55.31 (CH_2Cl_2 , dichloromethane) 125.55, 128.16, 132.24 (Ar- C_6H_3), 124.44, 136.40, 139.11 ($\text{C}_5\text{F}_4\text{N}$), 146.34 (*ipso*- C_6H_3), 157.14 (NCN) ppm

$^{19}\text{F}\{^1\text{H}\}$ NMR (377 MHz, 298 K, CDCl_3): $\delta = -153.18$ (s, 4F, 2BF_4^-), -132.86 (s, 2F, *meta*-Ar- $\text{C}_5\text{F}_4\text{N}$), -83.61 (s, 2F, *ortho*-Ar- $\text{C}_5\text{F}_4\text{N}$) ppm

$^{11}\text{B}\{^1\text{H}\}$ NMR (128 MHz, 298 K, CDCl_3): -1.05 (br s, 1B, BF_4) ppm

Elemental analysis: calcd (%) for $\text{C}_{30}\text{H}_{36}\text{F}_8\text{BN}_3$ [$601.43 \text{ g mol}^{-1}$]: C 59.91, H 6.03, N 6.99; found: C 59.11, H 5.61, N 6.12

Synthesis and Characterization of Compound 2.9

Pentafluoropyridine (0.85 g, 0.51 mmol) and $\text{B}(\text{C}_6\text{F}_5)_3$ (0.52 g, 1.02 mmol) were added to a toluene solution (20 mL) of SIDipp (0.60 g, 1.53 mmol) at 0 °C. The resulting solution was changed to pink color after coming to room temperature. After stirring for further 1 hour at room temperature, we have collected an aliquot of 0.5 mL to monitor the reaction by NMR spectroscopy, which revealed multiple product formation. The solution was subsequently filtered through a frit. Storing the solution at 4 °C for 2-3 days resulted in colorless crystals of **2.9**. Yield 0.26 g (28 %).

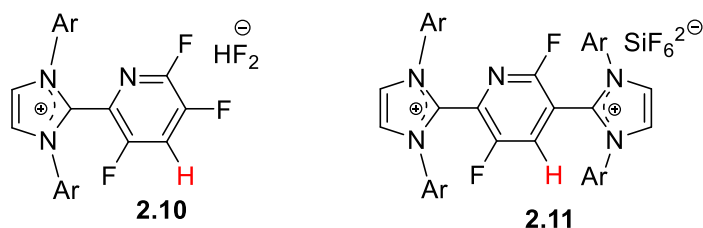
^1H NMR (500 MHz, 298 K, CDCl_3): δ = 1.20-1.35 (m, 12H, $\text{CH}(\text{CH}_3)_2$), 2.87 (sept, J = 6.5 Hz, 4H, $\text{CH}(\text{CH}_3)_2$), 4.41 (s, 4H, N- CH_2CH_2 -N), 7.31-7.53 (m, 12H, Ar- H), 8.78 (s, 1H, N-CH-N) ppm

$^{13}\text{C}\{^1\text{H}\}$ NMR (101 MHz, 298 K, CDCl_3): δ = 23.84, 24.48 (H CMe_2), 28.15, 29.37 (H CMe_2), 53.59, 55.19 (CH_2CH_2), 122.38, 123.38, 124.90, 129.48, 134.13, 135.41, 137.24, 146.69, 147.47, 148.53 ($3^*\text{C}_6\text{F}_5$), 125.18, 128.57, 131.95 (Ar- C_6H_3), 145.63 (*ipso*- C_6H_3), 160.06 (N-CH-N) ppm

$^{19}\text{F}\{^1\text{H}\}$ NMR (377 MHz, 298 K, CDCl_3): δ = -109.91, -119.91, -124.85, -127.78, -130.91, -133.50, -135.65, -158.47, -162.62, -164.62, -166.19, -166.99 (15 F, $3^*\text{C}_6\text{F}_5$) -135.73 (d, J = 31.21 Hz, 1 F, B- F) ppm

$^{11}\text{B}\{^1\text{H}\}$ NMR (128 MHz, 298 K, CDCl_3): -15.55 (SIDipp- $\text{B}(\text{C}_6\text{F}_5)_3$), -4.19 (s, 1B, $\text{FB}(\text{C}_6\text{F}_5)_3$) ppm.

Synthesis and Characterization of Compounds 2.10 and 2.11



Tetrafluoropyridine (0.038 g, 0.255 mmol) was added to a solution of IDipp (0.2 g, 0.51 mmol) at 0 °C, in 10 mL of toluene and hexane mixture. An immediate formation of yellow precipitate was noticed after coming to room temperature. The resulting mixture was stirred for 15 minutes at that temperature. The precipitate was filtered through a cannula followed by washing with pentane. The saturated dichloromethane solution (5 mL) was kept for crystallization at 4 °C. Yellow crystals of **2.11** along with few crystals of **2.10** came after 2-3 days.

¹H NMR (500 MHz, 298 K, CDCl₃): δ = 1.24-1.02 (m, 48H, CH(CH₃)₂), 2.44 (m, 8H, CH(CH₃)₂), 7.59 (m, 1H, C₅F₂HN), 8.49-9.06 (s, 4H, 2*CH=CH) ppm; 7.43-7.16 (m, 12H, Ar-H) ppm

¹³C{¹H} NMR (101 MHz, 298 K, CDCl₃): δ = 22.37, 25.49 (HCM_{e2}), 29.23 (HCM_{e2}), 124.42, 124.78 (NCH=CHN), 128.18, 128.99, 132.05, 132.37 (Ar-C₆H₃), 125.25, 128.01, 127.67, 128.85, 130.35, 131.37 (C₅F₂HN), 146.23 (*ipso*-C₆H₃)

¹⁹F{¹H} NMR (377 MHz, 298 K, CDCl₃): δ = -130.14 (br s, 6F, SiF₆²⁻), -124.07 (d, *J* = 27.62 Hz, 1F), -84.60 (d, *J* = 27.62 Hz, 1F) ppm.

6.1.2. Crystallographic data for the structural analysis of compounds 2.1-2.6, 2.8, and 2.11:

Single crystals of **2.1** and **2.4** were mounted on a Super Nova Dual Source X-ray Diffractometer system (Agilent Technologies) equipped with a CCD area detector and the X-ray generator was operated at 50 kV and 0.8 mA to generate Mo-K α radiation (λ = 0.71073 Å) and Cu-K α radiation

($\lambda = 1.54178 \text{ \AA}$) at 100(2) K. Data reduction was performed using CrysAlisPro software.¹ Remaining crystals (**2.2**, **2.3**, **2.5**, **2.6**, **2.8**, **2.9**, and **2.11**) were mounted on a Bruker SMART APEX II single crystal X-ray CCD diffractometer having graphite monochromatised (Mo-K $\alpha = 0.71073 \text{ \AA}$) radiation at low temperature 100 K. The X-ray generator was operated at 50 kV and 30 mA. The X-ray data acquisition was monitored by APEX2 program suit. The data were corrected for Lorentz-polarization and absorption effects using SAINT and SADABS programs which are an integral part of APEX2 package.² The structures were solved by direct methods and refined by full matrix least squares, based on F^2 , using SHELXL. Crystal structures were refined using Olex2-1.0 software. Anisotropic refinement was performed for all non-H atom. The C-H hydrogen atoms were calculated using the riding model.^{3,4} The structures were examined using the ADSYM subroutine of PLATON to assure that no additional symmetry could be applied to the models. The molecular weight of each structure mentioned herein has been calculated considering the solvent molecules trapped in the crystal. Mercury software was used to prepare packing diagrams and molecular interactions.⁴

Crystal Data for Compound 2.1 (CCDC 1868728). $C_{35}H_{39}F_5N_2Cl_6$ (**2.1**·2CHCl₃), $M = 795.38$, colorless, $0.28 \times 0.25 \times 0.21 \text{ mm}^3$, triclinic, space group $P-1$, $a = 10.5133(4) \text{ \AA}$, $b = 19.4207(9) \text{ \AA}$, $c = 20.7354(9) \text{ \AA}$, $\alpha = 74.723(4)^\circ$, $\beta = 79.836(4)^\circ$, $\gamma = 89.317(4)^\circ$, $V = 4017.3(3) \text{ \AA}^3$, $Z = 4$, $T = 100 \text{ K}$, $2\theta_{\max} = 50^\circ$, $D_{\text{calc}} (\text{g cm}^{-3}) = 1.315$, $F(000) = 1640$, $\mu (\text{mm}^{-1}) = 0.48$, 14122 reflections collected, 32048 unique reflections ($R_{\text{int}} = 0.029$), 9830 observed ($I > 2\sigma(I)$) reflections, multi-scan absorption correction, $T_{\min} = 0.875$, $T_{\max} = 0.905$, 346 refined parameters, $S = 1.099$, $R1 = 0.078$, $wR2 = 0.303$ (all data $R = 0.1057$, $wR2 = 0.2626$), maximum and minimum residual electron densities; $\Delta\rho_{\max} = 1.18$, $\Delta\rho_{\min} = -0.81 (\text{e}\text{\AA}^{-3})$.

Crystal Data for Compound 2.2 (CCDC 1872249). $C_{29}H_{44}Cl_4F_2N_2$, $M = 600.46$, colorless, $0.10 \times 0.10 \times 0.08 \text{ mm}^3$, Monoclinic, space group $P2_1/c$, $a = 10.817(3) \text{ \AA}$, $b = 16.139(4) \text{ \AA}$, $c = 18.616(5) \text{ \AA}$, $\alpha = \gamma = 90^\circ$, $\beta = 97.246(13)^\circ$, $V = 3224.1(15) \text{ \AA}^3$, $Z = 4$, $T = 100 \text{ K}$, $2\theta_{\max} = 54.2^\circ$, $D_{\text{calc}} (\text{g cm}^{-3}) = 1.237$, $F(000) = 1272$, $\mu (\text{mm}^{-1}) = 0.400$, 49988 reflections collected, 7013 unique reflections ($R_{\text{int}} = 0.025$), 6510 observed ($I > 2\sigma(I)$) reflections, multi-scan absorption correction, $T_{\min} = 0.705$, $T_{\max} = 0.746$, 355 refined parameters, $S = 1.11$, $RI = 0.036$, $wR2 = 0.120$ (all data $R = 0.0487$, $wR2 = 0.1367$), maximum and minimum residual electron densities; $\Delta\rho_{\max} = 0.62$, $\Delta\rho_{\min} = -0.86 (\text{e\AA}^{-3})$.

Crystal Data for Compound 2.3 (CCDC 1868731). $C_{114}H_{90}B_2F_{40}N_4O_3$, colorless, $0.20 \times 0.17 \times 0.13 \text{ mm}^3$, monoclinic, space group $P2_1/c$, $a = 11.923(5) \text{ \AA}$, $b = 14.962(6) \text{ \AA}$, $c = 30.699(14) \text{ \AA}$, $\alpha = \gamma = 90^\circ$, $\beta = 100.096(18)$, $V = 5391(4) \text{ \AA}^3$, $Z = 2$, $T = 100 \text{ K}$, $2\theta_{\max} = 50.00^\circ$, $D_{\text{calc}} (\text{g cm}^{-3}) = 1.455$, $F(000) = 2396$, $\mu (\text{mm}^{-1}) = 0.13$, 86407 reflections collected, 9483 unique reflections ($R_{\text{int}} = 0.065$), 7573 observed ($I > 2\sigma(I)$) reflections, multi-scan absorption correction, $T_{\min} = 0.6676$, $T_{\max} = 0.7461$, 747 refined parameters, $S = 1.16$, $RI = 0.051$, $wR2 = 0.141$ (all data $R = 0.0694$, $wR2 = 0.1286$), maximum and minimum residual electron densities; $\Delta\rho_{\max} = 0.59$, $\Delta\rho_{\min} = -0.79 (\text{e\AA}^{-3})$.

Crystal Data for Compound 2.4 (CCDC 1868732). $C_{166}H_{190}F_{34}N_8O_4Si \cdot (2.4 \cdot H_2O)_4$, yellow, $0.27 \times 0.20 \times 0.16 \text{ mm}^3$, Triclinic, space group $P-1$, $a = 11.252(7) \text{ \AA}$, $b = 19.515(12) \text{ \AA}$, $c = 20.392(11) \text{ \AA}$, $\alpha = 116.63(3)$, $\beta = 104.14(5)$, $\gamma = 91.96(3)$, $V = 3828(4) \text{ \AA}^3$, $Z = 1$, $T = 100(2) \text{ K}$, $2\theta_{\max} = 49.6^\circ$, $D_{\text{calc}} (\text{g cm}^{-3}) = 1.317$, $F(000) = 1594$, $\mu (\text{mm}^{-1}) = 0.11$, 148250 reflections collected, 15719 unique reflections ($R_{\text{int}} = 0.052$), 9305 observed ($I > 2\sigma(I)$) reflections, multi-scan absorption correction, $T_{\min} = 0.973$, $T_{\max} = 0.982$, 1045 refined parameters, $S = 1.03$, $R1 = 0.064$, $wR2 = 0.137$

(all data $R = 0.150$, $wR2 = 0.113$), maximum and minimum residual electron densities; $\Delta\rho_{\max} = 0.64$, $\Delta\rho_{\min} = -0.31$ ($\text{e}\text{\AA}^{-3}$).

Crystal Data for Compound 2.5 (CCDC 1868733) $\text{C}_{34}\text{H}_{40}\text{BF}_{11}\text{N}_2\text{Cl}_2$, $M = 779.40$, colorless, $0.15 \times 0.15 \times 0.1$ mm^3 , orthorhombic, space group $Pbca$, $a = 18.032(9)$ \AA , $b = 19.755(10)$ \AA , $c = 20.827(12)$ \AA , $\alpha = \beta = \gamma = 90^\circ$, $V = 7419(7)$ \AA^3 , $Z = 8$, $T = 100(2)$ K, $2\theta_{\max} = 52.80^\circ$, D_{calc} (g cm^{-3}) = 1.396 , $F(000) = 3216$, μ (mm^{-1}) = 0.258 , 53759 reflections collected, 7261 unique reflections ($R_{\text{int}} = 0.066$), 5644 observed ($I > 2\sigma(I)$) reflections, multi-scan absorption correction, $T_{\min} = 0.5948$, $T_{\max} = 0.7454$, 493 refined parameters, $S = 1.063$, $R1 = 0.062$, $wR2 = 0.182$ (all data $R = 0.0809$, $wR2 = 0.1664$), maximum and minimum residual electron densities; $\Delta\rho_{\max} = 1.07$, $\Delta\rho_{\min} = -0.950$ ($\text{e}\text{\AA}^{-3}$).

Crystal Data for Compound 2.6 (CCDC 2055788). $\text{C}_{49}\text{H}_{44}\text{F}_{15}\text{N}_5$, yellow, $0.2 \times 0.12 \times 0.1$ mm^3 , monoclinic, space group $P2_1/n$, $a = 12.4788(17)$ \AA , $b = 19.2697(19)$ \AA , $c = 18.877(3)$ \AA , $\alpha = \gamma = 90^\circ$, $\beta = 90.694(8)$, $V = 4538.9(11)$ \AA^3 , $Z = 4$, $T = 100(2)$ K, $2\theta_{\max} = 144.74^\circ$, D_{calc} (g cm^{-3}) = 1.446 , $F(000) = 2032$, μ (mm^{-1}) = 1.125 , 201625 reflections collected, 7877 unique reflections ($R_{\text{int}} = 0.16$), 8937 observed ($I > 2\sigma(I)$) reflections, multi-scan absorption correction, $T_{\min} = 0.6293$, $T_{\max} = 0.7536$, 649 refined parameters, $S = 1.099$, $R1 = 0.0638$, $wR2 = 0.1272$ (all data $R = 0.0740$, $wR2 = 0.1394$), maximum and minimum residual electron densities; $\Delta\rho_{\max} = 0.45$, $\Delta\rho_{\min} = -0.37$ ($\text{e}\text{\AA}^{-3}$).

Crystal Data for Compound 2.8 (CCDC 2055789). $\text{C}_{31}\text{H}_{35}\text{BCl}_2\text{F}_8\text{N}_3$, colorless, $0.35 \times 0.32 \times 0.27$ mm^3 , monoclinic, space group $P2_1/n$, $a = 10.7352(3)$ \AA , $b = 17.7450(5)$ \AA , $c = 18.4206(5)$ \AA , $\alpha = \gamma = 90^\circ$, $\beta = 100.624(2)$, $V = 3448.90(17)$ \AA^3 , $Z = 4$, $T = 100(2)$ K, $2\theta_{\max} = 56.68^\circ$, D_{calc} (g cm^{-3}) = 1.321 , $F(000) = 1412$, μ (mm^{-1}) = 0.257 , 59318 reflections collected, 8556 unique reflections

($R_{\text{int}} = 0.042$), 6946 observed ($I > 2\sigma(I)$) reflections, multi-scan absorption correction, $T_{\text{min}} = 0.5546$, $T_{\text{max}} = 0.7457$, 439 refined parameters, $S = 0.978$, $R1 = 0.0623$, $wR2 = 0.1771$ (all data $R = 0.0748$, $wR2 = 0.1895$), maximum and minimum residual electron densities; $\Delta\rho_{\text{max}} = 0.88$, $\Delta\rho_{\text{min}} = -0.72$ ($\text{e}\text{\AA}^{-3}$).

Crystal Data for Compound 2.9 (CCDC 2055790). ($\text{C}_{57}\text{H}_{51}\text{BF}_{16}\text{N}_2$), colorless, $0.22 \times 0.12 \times 0.1$ mm^3 , triclinic, space group $P-1$, $a = 10.350(2)$ \AA , $b = 11.9292(18)$ \AA , $c = 22.376(12)$ \AA , $\alpha = 83.095(18)^\circ$, $\beta = 83.19(2)^\circ$, $\gamma = 70.263(12)^\circ$, $V = 2572.5(15)$ \AA^3 , $Z = 2$, $T = 100(2)$ K, $2\theta_{\text{max}} = 52.08^\circ$, D_{calc} (g cm^{-3}) = 1.393, $F(000) = 1112$, μ (mm^{-1}) = 0.121, 36581 reflections collected, 10656 unique reflections ($R_{\text{int}} = 0.032$), 8721 observed ($I > 2\sigma(I)$) reflections, multi-scan absorption correction, $T_{\text{min}} = 0.6846$, $T_{\text{max}} = 0.7454$, 693 refined parameters, $S = 1.097$, $R1 = 0.0622$, $wR2 = 0.1492$ (all data $R = 0.0783$, $wR2 = 0.1573$), maximum and minimum residual electron densities; $\Delta\rho_{\text{max}} = 0.48$, $\Delta\rho_{\text{min}} = -0.52$ ($\text{e}\text{\AA}^{-3}$).

Crystal Data for Compound 2.11 (CCDC 2070006). ($\text{C}_{59}\text{H}_{73}\text{F}_2\text{N}_5\text{F}_6\text{Si} \cdot 6(\text{CH}_2\text{Cl}_2)$), yellow, $0.12 \times 0.09 \times 0.08$ mm^3 , monoclinic, space group $P2_1/n$, $a = 15.6778(15)$ \AA , $b = 19.214(2)$ \AA , $c = 26.770(3)$ \AA , $\alpha = \gamma = 90^\circ$, $\beta = 105.888(3)^\circ$, $V = 7755.9(14)$ \AA^3 , $Z = 4$, $T = 100(2)$ K, $2\theta_{\text{max}} = 49.32^\circ$, D_{calc} (g cm^{-3}) = 1.32, $F(000) = 3200$, μ (mm^{-1}) = 0.503, 309048 reflections collected, 13648 unique reflections ($R_{\text{int}} = 0.16$), 9882 observed ($I > 2\sigma(I)$) reflections, multi-scan absorption correction, $T_{\text{min}} = 0.6324$, $T_{\text{max}} = 0.961$, 854 refined parameters, $S = 1.058$, $R1 = 0.0861$, $wR2 = 0.2161$ (all data $R = 0.1100$, $wR2 = 0.2342$), maximum and minimum residual electron densities; $\Delta\rho_{\text{max}} = 0.097$, $\Delta\rho_{\text{min}} = -0.903$ ($\text{e}\text{\AA}^{-3}$).

6.1.3. Details of the theoretical computational for Compound 2.1

All the calculations in this study have been performed with density functional theory (DFT), with the aid of the Turbomole 7.1 suite of programs,⁶ using the PBE functional.⁷ The TZVP⁸ basis set has been employed. The resolution of identity (RI),⁹ along with the multipole accelerated resolution of identity (marij)¹⁰ approximations have been employed for an accurate and efficient treatment of the electronic Coulomb term in the DFT calculations. Solvent correction were incorporated with optimization calculations using the COSMO model,¹¹ with benzene ($\epsilon = 2.27$) or hexane-toluene mixture ($\epsilon = 2.99$) as the solvent. The values reported are ΔG values, with zero point energy corrections, internal energy and entropic contributions included through frequency calculations on the optimized minima with the temperature taken to be 298.15 K. Harmonic frequency calculations were performed for all stationary points to confirm them as a local minima or transition state structures.

Care was taken to ensure that the obtained transition state structures possessed only one imaginary frequency corresponding to the correct normal mode. The validity of the obtained transition states was further confirmed by doing IRC^[S10, S11] calculations: the correct reactant and product structures were obtained for every transition state obtained. To do the IRC calculations, Turbomole 7.1 was employed.

Details of minima and TS search. Stationary points are places on the potential energy surface (PES) with a zero gradient, i.e. zero first derivatives of the energy with respect to atomic coordinates. Two types of stationary points are of special importance to chemists. These are minima (reactants, products, intermediates) and first-order saddle points (transition states). These two types of stationary points can be characterized by the curvature of the PES. At a minimum the

Hessian matrix (second derivatives of energy with respect to atomic coordinates) is positive, that is the curvature is positive in all directions. If there is only one negative curvature, the stationary point is a transition state (TS). Because vibrational frequencies are basically the square roots of the curvatures, a minima has all real frequencies, and a saddle point has one imaginary vibrational “frequency”. Structure optimizations are most efficiently done by so-called quasi-Newton–Raphson methods.^[S12] For TS optimizations the TRIM (Trust Radius Image Minimization) method implemented in Turbomole 7.1 software packages, tries to maximize the energy along one of the Hessian eigen vectors, while minimizing it in all other directions. Thus, one “follows” one particular eigen vector, hereafter called the “transition” vector. After computing the Hessian for the guess structure one have to identify which vector to follow. For a good TS guess, this is the eigenvector with negative eigen value, or imaginary frequency.

6.1.4. Cyclic Voltammetry of 2.1.

Cyclic voltammetry (CV) measurements were carried out using a PGSTAT 101 electrochemical workstation (METROHM). All experiments were carried out under an atmosphere of argon in degassed and anhydrous acetonitrile solution containing *n*-Bu₄NPF₆ (0.1 M) at a scan rate of 0.10 mV s⁻¹. The setup consisted of a glassy carbon working electrode (surface area = 0.04 cm²), a glassy carbon counter electrode, and a silver wire immersed in a saturated LiCl solution in EtOH and 0.1 M *n*-Bu₄NPF₆ solution in acetonitrile as the reference electrode. The recorded voltammograms were referenced to the internal standard Fc⁺/Fc (ferrocenium/ferrocene) couple.

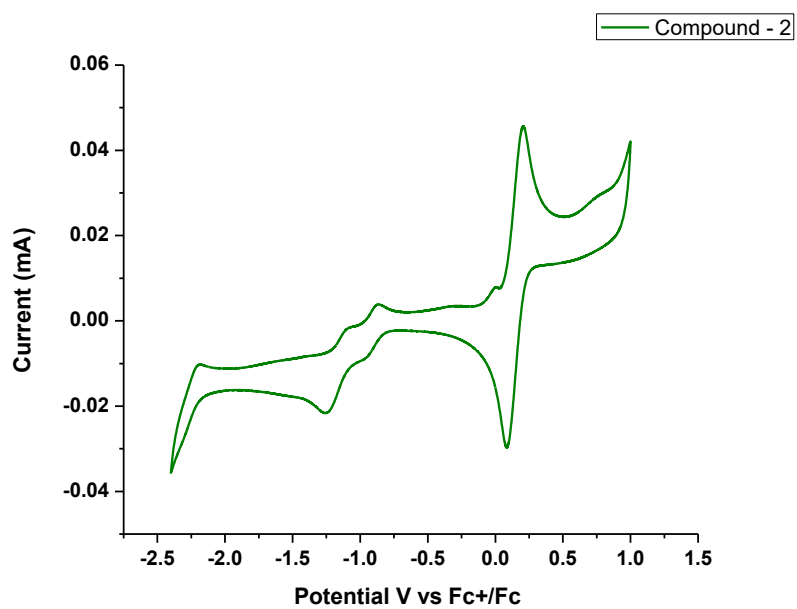
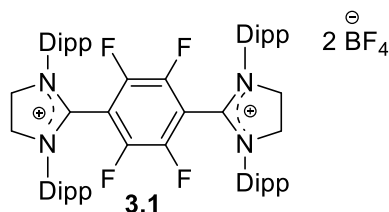


Figure S30. Cyclic voltammogram of compound **2.1** recorded at 0.1 mV s^{-1} .

6.2: Experimental details for chapter-3

6.2.1. Synthesis and Characterization of Compounds 3.1-3.9

Synthesis and Characterization of Compound 3.1



To a solution of SIPr (0.2 g, 0.051 mmol) in 10 mL of benzene, hexafluorobenzene (0.19 g, 1.02 mmol) was added at 0 °C. The mixture was stirred for 15 min at room temperature and trifluoroborane diethyl etherate (0.065 mL, 0.051 mmol) was added dropwise at -78 °C. The resulting solution color was changed to orange immediately with the formation of a white precipitate. After stirring the reaction mixture for further 1 h at room temperature, the solution was dried in vacuum and extracted through the frit filtration with the mixture of tetrahydrofuran and dichloromethane. Colorless crystals came after keeping this solution mixture at 4 °C for 2-3 days with a yield of 0.315 g (56 %). MP: decomposition at 210.6 °C.

¹H NMR (500 MHz, 298 K, DMSO-*d*₆): δ = 1.30-0.71 (m, 2x24H, CH(CH₃)₂), 2.81 (sept, 4H, CH(CH₃)₂), 3.03 (sept, 4H, CH(CH₃)₂), 4.69 (s, 4H, N-CH₂CH₂-N), 4.73 (s, 4H, N-CH₂CH₂-N), 7.54-7.27 (m, 12H, Ar-*H*) ppm

¹³C{¹H} NMR (101 MHz, 298K, DMSO-*d*₆): δ = 21.97, 22.48 (HCM_{e2}), 28.26, 28.59 (HCM_{e2}), 54.18, 54.90 (CH₂CH₂), 125.47, 125.69, 127.83, 129.65, 131.55, 132.36 (Ar-C₆H₃), 146.03, 155.98 (*ipso*-C₆H₃) ppm, C(C₆F₅) were not detected due to signal broadness (¹⁹F coupling), due to heavy molecular weight of **3.1** we could not get high intensity ¹³C NMR spectra.

$^{19}\text{F}\{^1\text{H}\}$ NMR (377 MHz, 298K, DMSO- d_6): $\delta = -146.22$ (s, 4F, Ar- C_6F_4), -148.37 (s, 8F, 2BF_4^-) ppm

$^{11}\text{B}\{^1\text{H}\}$ NMR (128 MHz, 298K, DMSO- d_6): -1.1 (br s, 1B, BF_4) ppm

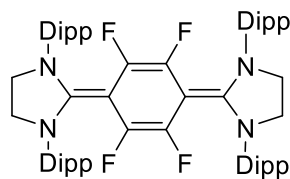
IR (ATR, cm^{-1}): 2975, 2876 (C-H stretching), 1599, 1565 (C=C), 1365, 1378 (C-H bending), 1052 (C-F), 798 (C-Cl)

UV-Vis (solid state, λ_{max} (nm)): 356, 450, 510

Elemental analysis: calcd (%) for $\text{C}_{60}\text{H}_{76}\text{B}_2\text{F}_{12}\text{N}_4$ [$1102.61 \text{ g mol}^{-1}$]: C 65.34, H 6.95, N 5.08; found: C 66.27, H 6.58, N 5.62

HRMS (CH_3CN): m/z calcd for $[\text{C}_{60}\text{H}_{76}\text{B}_2\text{F}_{12}\text{N}_4\text{-BF}_4]^{++}$ 464.3003 found 464.3034; $[\text{C}_{60}\text{H}_{76}\text{F}_4\text{N}_4]$ 928.5987 found $[\text{C}_{60}\text{H}_{76}\text{F}_4\text{N}_4 + \text{H}^+]$ found 929.6081; $[\text{C}_{60}\text{H}_{76}\text{F}_4\text{N}_4 + \text{NH}_4^+]$ 946.6070

Synthesis and Characterization of Compound 3.2



3.2b

THF (20 mL) was added to a mixture of lithium (0.005 g, 0.068 mmol) and **3.1** (0.5 g, 0.045 mmol) at -60 °C. The reaction mixture was slowly allowed to come to room temperature and was stirred for 1 hour at room temperature. The solvent was removed in vacuo, and the residue was extracted with THF (10 mL). After evaporation and drying under vacuum, yellow crystals of **3.2** were obtained at 4 °C after one day. Yield 0.26 g (62 %)

Alternative method: Hexafluorobenzene (0.190 g, 1.02 mmol) was added to a solution of SIPr (0.2 g, 0.51 mmol) in 10 mL of THF at 0 °C. After stirring for 30 min at room temperature, the reaction

mixture was again added to a THF solution (10 mL) of Mg powder (0.030 g, 1.25 mmol) at 0 °C. The resulting solution color was changed to black after coming to room temperature. After stirring for further 1h at room temperature; the solution was extracted through the frit filtration. Yellow crystals came after keeping this THF solution mixture at 4 °C for 1 day. Yield 0.23 g (68 %). MP: decomposition at 164 °C.

¹H NMR: Due to the presence of a paramagnetic impurity, we were unable to obtain a well-resolved NMR spectrum of **3.2**.

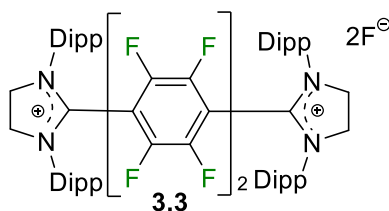
IR (ATR, cm⁻¹): 2962, 2858 (C-H_{stretching}), 1461, 1565 (C=C), 1386,1320 (C-H_{bending}), 1027 (C-F), 798 (C-Cl)

UV-Vis (c = 2 * 10⁻⁴ M THF, λ (nm) (ε (M⁻¹ cm⁻¹)): 384 (13634), 476 (14352), 769 (43324)

Elemental analysis: calcd (%) for C₆₀H₇₆F₄N₄ [929.29 gmol⁻¹]: C 77.55, H 8.24, N 6.03; found: C 75.27, H 6.58, N 5.84; Due to the sensitivity of the crystals of **3.2** the analytical values show some deviation from the calcd one

HRMS (THF): m/z calcd for C₆₀H₇₆F₄N₄ [M] 928.6008, found 928.6006

Synthesis and Characterization of Compound 3.3



To a solution 10 ml solution of SIDipp (0.4 g, 1.04 mmol), 10 ml solution of decafluorobiphenyl (0.170 g, 0.052 mmol) was added at room temperature. The resulting solution color was changed to orange immediately with the formation of a yellow precipitate. After stirring the reaction

mixture for further 1 h at room temperature, the filtrate was filtered through cannula and the precipitate was dried in vacuum. Yellow color crystals came after keeping the 3-4 ml dichloromethane solution mixture at 4 °C for 2-3 days with a yield of 0.315 g (65 %).

¹H NMR (400 MHz, 298 K, CDCl₃): δ = 1.18-1.42 (m, 2x24H, CH(CH₃)₂), 3.07 (m, 4Hx2, CH(CH₃)₂), 3.03 (sept, 4H, CH(CH₃)₂), 4.90 (s, 4H, N-CH₂CH₂-N), 4.98 (s, 4H, N-CH₂CH₂-N), 7.22-7.49 (m, 12H, Ar-H) ppm

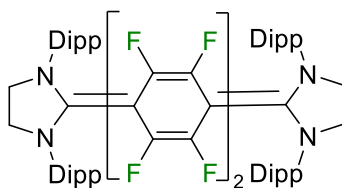
¹³C{¹H} NMR (101 MHz, 298 K, CDCl₃): δ = 22.8, 23.5, 24.2, 26.7, 26.9, 28.8, 29.1, 53.1, 54.2, 54.5, 55.3, 55.6, 122.4, 122.8, 123.6, 124.3, 124.5, 125.1, 125.4, 128.7, 128.9, 130.2, 131.7, 132, 132.1, 145.4, 146.3, 146.3, 147.3 ppm

¹⁹F{¹H} NMR (377 MHz, 298 K, CDCl₃): δ = -130.1, -131.2, -132.2, -133.2, -133.4, -134.7, -135.9, -139.5 (8F, Ar-C₆F₄), -218.6 (s, 2F, 2F⁻) ppm

UV-Vis (solid state, λ_{\max} (nm)): 435 and 385

ESI (CH₃CN): *m/z* calcd for [C₆₆H₇₇F₁₀N₄-F₂]⁺⁺ 1077.4828 found 1077.60158

Synthesis and Characterization of Compound 3.4



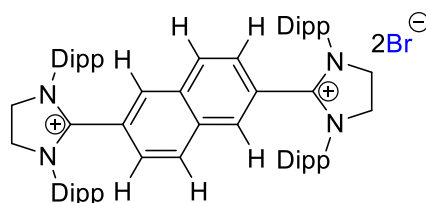
3.4b

5 ml THF solution of cobaltocene (0.17 g, 0.045 mmol) was added to 15 ml THF solution of **3.3** (0.5 g, 0.045 mmol) dropwise at 0 °C temperature over 15 min. The reaction mixture was slowly allowed to come to room temperature and was stirred for another 1 hour at room temperature. The solvent was removed in vacuo, and the residue was extracted with toluene (10 mL). Green color

crystals of **3.4** were obtained after keeping the concentrated toluene solution at room temperature for one day. Yield 0.26 g (30 %).

UV-Vis ($c = 7.4 * 10^{-6} \text{ M THF}$), λ (nm): 697.

Synthesis and Characterization of Compound 3.5



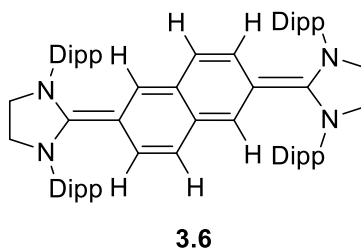
3.5

In a dry Schlenk flask, SIDipp (1.5 g, 0.39 mmol) and 2,6-Dibromonaphthalene (0.56 g, 0.18 mmol) were added in presence of 5 mol% Ni(COD)₂ and 30 mL of ortho-xylene was added to it. The solution was refluxed for 1 h. Yellow color precipitate was filtered through cannula filtration and the dried under vacuum. The solid was further washed with toluene and colorless crystals were grown from the dichloromethane solution of the product at 4 °C after 1 day with a yield of 1.3 g (62%).

¹H NMR (500 MHz, 298 K, DMSO-d₆): δ = 0.79-1.29 (m, 2x24H, CH(CH₃)₂), 3.03 (sept, 4H, CH(CH₃)₂), 3.03 (sept, 8H, CH(CH₃)₂), 4.62 (s, 8H, N-CH₂CH₂-N), 6.92-7.76 (m, 18H, Ar-H)

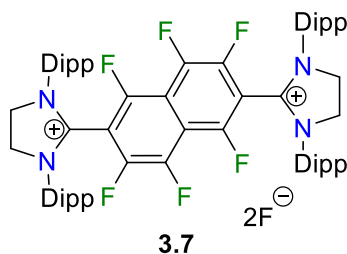
¹³C{¹H} NMR (101 MHz, 298 K, DMSO-d₆): δ = 22.6, 25.6, 28.2, 53.71, 121.4, 124.7, 125.6, 129.65, 130.1, 131.3, 131.7, 145.1, 146

Synthesis and Characterization of Compound 3.6



THF (20 mL) was added to a mixture of magnesium (0.092 g, 0.135 mmol) and **3.5** (0.5 g, 0.045 mmol) at $-30\text{ }^{\circ}\text{C}$. The reaction mixture was slowly allowed to come to room temperature and was stirred for 3 hours at room temperature. The solvent was removed in vacuo, and the residue was extracted with toluene (10 mL). Pink color crystals of **3.6** were obtained after keeping the 5 ml concentrated toluene solution at $-36\text{ }^{\circ}\text{C}$ for 10 days. Yield 0.12 g (26 %). **3.6** is NMR silent due to the presence of mono-radical impurities.

Synthesis and Characterization of Compound 3.7

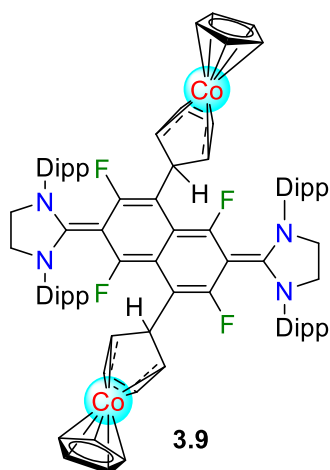


To a solution 10 ml solution of SIDipp (0.4 g, 0.104 mmol), 10 ml solution of octafluoronaphthalene (0.147 g, 0.052 mmol) was added at room temperature. The resulting solution color was changed to red immediately with the formation of a red precipitate. After stirring the reaction mixture for further 15 min at room temperature, the filtrate was filtered through cannula and the precipitate was dried in vacuum. Red color crystals came after keeping the 3-4 ml dichloromethane solution mixture at $-36\text{ }^{\circ}\text{C}$ for 7 days with a yield of 0.343 g (65 %).

^1H NMR (400 MHz, 298 K, CDCl_3): δ = 0.91-1.27 (m, 2x24H, $\text{CH}(\text{CH}_3)_2$), 2.99 (sept, 8H, $\text{CH}(\text{CH}_3)_2$), 4.74 (s, 8H, N- CH_2CH_2 -N), 7.28-7.45 (m, 12H, Ar-H)

$^{19}\text{F}\{^1\text{H}\}$ NMR (377 MHz, 298 K, CDCl_3): δ = -114.3 (2F, *ortho*-Ar- C_6F_4), -132.2 (2F, *para*-Ar- C_6F_4), -141.5, -143.8 (2F, *meta*-Ar- C_6F_4), -176.2 (2F, 2F^-).

Synthesis and Characterization of Compound 3.9



5 ml THF solution of cobaltocene (0.38 g, 0.188 mmol) was added to 15 ml THF solution of **3.7** (0.5 g, 0.047 mmol) dropwise at $-30\text{ }^\circ\text{C}$ temperature over 15 min. The reaction mixture was slowly allowed to come to room temperature and was stirred for another 6 hours at room temperature. The solvent was removed in vacuo, and the residue was extracted with hexane (10 mL). Red color crystals of **3.7** were obtained after keeping the concentrated hexane solution (4 ml) at room temperature for one day. Yield 0.14 g (26%). **3.9** is NMR silent due to the presence of mono-radical impurities.

6.2.2. Crystallographic data for the structural analysis of compounds 3.3-3.9

Single crystals of suitable size were mounted on a Bruker SMART APEX II single crystal X-ray CCD diffractometer having graphite monochromatised (Mo-K α = 0.71073 Å) radiation at low temperature 100 K. The X-ray generator was operated at 50 kV and 30 mA. The X-ray data acquisition was monitored by APEX2 program suit. The data were corrected for Lorentz-polarization and absorption effects using SAINT and SADABS programs which are an integral part of APEX2 package.^[S2] The structures were solved by direct methods and refined by full matrix least squares, based on F^2 , using SHELXL Crystal structures were refined using Olex2-1.0 software. Anisotropic refinement was performed for all non-H atom. The C-H hydrogen atoms were calculated using the riding model.^[S3,S4] The structures were examined using the ADSYM subroutine of PLATON to assure that no additional symmetry could be applied to the models. The molecular weight of each structure mentioned herein has been calculated considering the solvent molecules trapped in the crystal. Mercury software was used to prepare packing diagrams and molecular interactions.^[S5] Crystallographic information files are available at www.ccdc.cam.ac.uk/data with the mentioned accession numbers.

Crystal Data for Compound 3.1 (CCDC 1868729): C₁₃₆H₁₆₄B₄Cl₁₂F₂₄N₈O₂, colorless, 0.19 × 0.15 × 0.1 mm³, monoclinic, space group $P2_1/n$, $a = 15.370(8)$ Å, $b = 39.968(19)$ Å, $c = 23.287(11)$ Å, $\alpha = \gamma = 90^\circ$, $\beta = 92.65(2)$, $V = 14290(12)$ Å³, $Z = 2$, $T = 100$ K, $2\theta_{\max} = 52.8^\circ$, D_{calc} (g cm⁻³) = 1.33, $F(000) = 5956$, μ (mm⁻¹) = 0.32, 305294 reflections collected, 29113 unique reflections ($R_{\text{int}} = 0.067$), 21434 observed ($I > 2\sigma(I)$) reflections, multi-scan absorption correction, $T_{\min} = 0.6943$, $T_{\max} = 0.7454$, 1798 refined parameters, $S = 1.08$, $R1 = 0.086$, $wR2 = 0.245$ (all data $R = 0.1099$, $wR2 = 0.2468$), maximum and minimum residual electron densities; $\Delta\rho_{\max} = 0.79$, $\Delta\rho_{\min} = -1.02$ (eÅ⁻³).

Crystal Data for Compound 3.2 (CCDC 1951186): $C_{60}H_{76}F_4N_4$, $M = 929.24$, Yellow, $0.15 \times 0.12 \times 0.1 \text{ mm}^3$, monoclinic, space group $P2_1/c$, $a = 10.45(3) \text{ \AA}$, $b = 25.95(6) \text{ \AA}$, $c = 19.75(5) \text{ \AA}$, $\alpha = \gamma = 90^\circ$, $\beta = 102.94(10)$, $V = 5220(21) \text{ \AA}^3$, $Z = 4$, $T = 100 \text{ K}$, $2\theta_{\max} = 52.6^\circ$, $D_{\text{calc}} (\text{g cm}^{-3}) = 1.182$, $F(000) = 2000$, $\mu (\text{mm}^{-1}) = 0.078$, 90636 reflections collected, 10586 unique reflections ($R_{\text{int}} = 0.063$), 7574 observed ($I > 2\sigma(I)$) reflections, multi-scan absorption correction, $T_{\min} = 0.634$, $T_{\max} = 0.745$, 629 refined parameters, $S = 1.042$, $R1 = 0.0526$, $wR2 = 0.1110$ (all data $R = 0.0828$, $wR2 = 0.1244$), maximum and minimum residual electron densities; $\Delta\rho_{\max} = 0.28$, $\Delta\rho_{\min} = -0.25 (\text{e}\text{\AA}^{-3})$.

Crystal Data for Compound 3.3: $C_{66}H_{76}F_{10}N_4$, $M = 1115.35$, Yellow, $0.2 \times 0.2 \times 0.2 \text{ mm}^3$, monoclinic, space group $C2/c$, $a = 20.123(5) \text{ \AA}$, $b = 21.977(6) \text{ \AA}$, $c = 20.646(5) \text{ \AA}$, $\alpha = \gamma = 90^\circ$, $\beta = 95.924(10)$, $V = 9082(4) \text{ \AA}^3$, $Z = 4$, $T = 200 \text{ K}$, $2\theta_{\max} = 53^\circ$, $D_{\text{calc}} (\text{g cm}^{-3}) = 0.816$, $F(000) = 2361.7$, $\mu (\text{mm}^{-1}) = 0.062$, 140412 reflections collected, 9286 unique reflections ($R_{\text{int}} = 0.1458$), 7574 observed ($I > 2\sigma(I)$) reflections, multi-scan absorption correction, $T_{\min} = 0.988$, $T_{\max} = 0.745$, 370 refined parameters, $S = 1.608$, $R1 = 0.1377$, $wR2 = 0.3982$ (all data $R = 0.1966$, $wR2 = 0.4714$), maximum and minimum residual electron densities; $\Delta\rho_{\max} = 1.03$, $\Delta\rho_{\min} = -0.61 (\text{e}\text{\AA}^{-3})$.

Crystal Data for Compound 3.4: $C_{66}H_{76}F_8N_4$, $M = 1077.353$, Dark green, $0.2 \times 0.2 \times 0.15 \text{ mm}^3$, monoclinic, space group $C2/c$, $a = 29.005(3) \text{ \AA}$, $b = 13.5928(15) \text{ \AA}$, $c = 20.342(4) \text{ \AA}$, $\alpha = \gamma = 90^\circ$, $\beta = 126.388(2)$, $V = 6456.3(15) \text{ \AA}^3$, $Z = 4$, $T = 100 \text{ K}$, $2\theta_{\max} = 56.74^\circ$, $D_{\text{calc}} (\text{g cm}^{-3}) = 1.108$, $F(000) = 2289.6$, $\mu (\text{mm}^{-1}) = 0.080$, 158185 reflections collected, 8049 unique reflections ($R_{\text{int}} = 0.0785$), 7574 observed ($I > 2\sigma(I)$) reflections, multi-scan absorption correction, $T_{\min} = 0.634$, $T_{\max} = 0.745$, 361 refined parameters, $S = 1.077$, $R1 = 0.1037$, $wR2 = 0.2919$ (all data $R = 0.1337$, $wR2 = 0.3371$), maximum and minimum residual electron densities; $\Delta\rho_{\max} = 0.88$, $\Delta\rho_{\min} = -0.68 (\text{e}\text{\AA}^{-3})$.

Crystal Data for Compound 3.5: $C_{37}H_{46}BrCl_{15}N_2$, $M = 1130.42$, Colorless, $0.28 \times 0.24 \times 0.12$ mm³, monoclinic, space group $P2_1/n$, $a = 14.6550(13)$ Å, $b = 23.548(2)$ Å, $c = 14.9100(12)$ Å, $\alpha = \gamma = 90^\circ$, $\beta = 102.290(3)$, $V = 5027.4(7)$ Å³, $Z = 4$, $T = 100$ K, $2\theta_{\max} = 58.62^\circ$, D_{calc} (g cm⁻³) = 1.493, $F(000) = 2288$, μ (mm⁻¹) = 1.644, 275302 reflections collected, 9286 unique reflections ($R_{\text{int}} = 0.1458$), 7574 observed ($I > 2\sigma(I)$) reflections, multi-scan absorption correction, $T_{\min} = 0.5104$, $T_{\max} = 0.7457$, 537 refined parameters, $S = 1.231$, $R1 = 0.0425$, $wR2 = 0.1051$ (all data $R = 0.0453$, $wR2 = 0.1101$), maximum and minimum residual electron densities; $\Delta\rho_{\max} = 0.94$, $\Delta\rho_{\min} = -0.82$ (eÅ⁻³).

Crystal Data for Compound 3.6: $C_{64}H_{82}N_4$, $M = 907.33$, Colorless, $0.19 \times 0.14 \times 0.08$ mm³, monoclinic, space group $P2_1/n$, $a = 15.6821(10)$ Å, $b = 12.2442(7)$ Å, $c = 18.5784(13)$ Å, $\alpha = \gamma = 90^\circ$, $\beta = 108.907(2)$, $V = 3374.9(4)$ Å³, $Z = 2$, $T = 100$ K, $2\theta_{\max} = 56.63^\circ$, D_{calc} (g cm⁻³) = 0.893, $F(000) = 988$, μ (mm⁻¹) = 0.051, 92545 reflections collected, 8404 unique reflections ($R_{\text{int}} = 0.1458$), 7574 observed ($I > 2\sigma(I)$) reflections, multi-scan absorption correction, $T_{\min} = 0.6479$, $T_{\max} = 0.7457$, 335 refined parameters, $S = 1.093$, $R1 = 0.0738$, $wR2 = 0.2213$ (all data $R = 0.0980$, $wR2 = 0.2424$), maximum and minimum residual electron densities; $\Delta\rho_{\max} = 0.37$, $\Delta\rho_{\min} = -0.50$ (eÅ⁻³).

Crystal Data for Compound 3.7: $C_{68}H_{76}Cl_8F_{12}N_4$, $M = 1473.02$, Colorless, $0.16 \times 0.12 \times 0.10$ mm³, monoclinic, space group $P2_1/c$, $a = 14.6927(8)$ Å, $b = 18.5978(11)$ Å, $c = 14.5593(8)$ Å, $\alpha = \gamma = 90^\circ$, $\beta = 112.463(2)$, $V = 3676.5(4)$ Å³, $Z = 2$, $T = 100$ K, $2\theta_{\max} = 56.68^\circ$, D_{calc} (g cm⁻³) = 1.331, $F(000) = 1536$, μ (mm⁻¹) = 0.378, 61641 reflections collected, 8404 unique reflections ($R_{\text{int}} = 0.1458$), 7574 observed ($I > 2\sigma(I)$) reflections, multi-scan absorption correction, $T_{\min} = 0.6799$, $T_{\max} = 0.7457$, 441 refined parameters, $S = 1.073$, $R1 = 0.0652$, $wR2 = 0.1714$ (all data $R = 0.0759$,

$wR2 = 0.1818$), maximum and minimum residual electron densities; $\Delta\rho_{\max} = 1.49$, $\Delta\rho_{\min} = -0.71$ ($e\text{\AA}^{-3}$).

6.2.3. Cyclic voltammetry of compound 3.1

All experiments were carried out under an atmosphere of argon in degassed and anhydrous acetonitrile solution containing $n\text{-Bu}_4\text{NPF}_6$ (0.1 M) at a scan rate of 0.70 V s^{-1} . The set up consisted of a glassy carbon working electrode (surface area = 0.04 cm^2), Pt counter electrode, Ag/AgCl reference electrode and 0.1 M $n\text{-Bu}_4\text{NPF}_6$ solution in acetonitrile as the electrolyte.

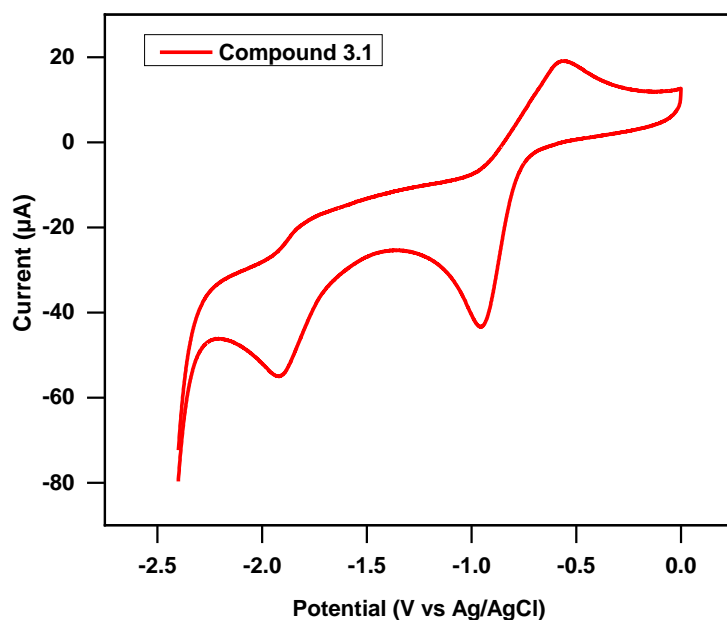


Figure 6.2.1. Cyclic voltammogram of **3.1** recorded at 0.7 V s^{-1} .

6.2.4. IR spectra of 3.1 and 3.2

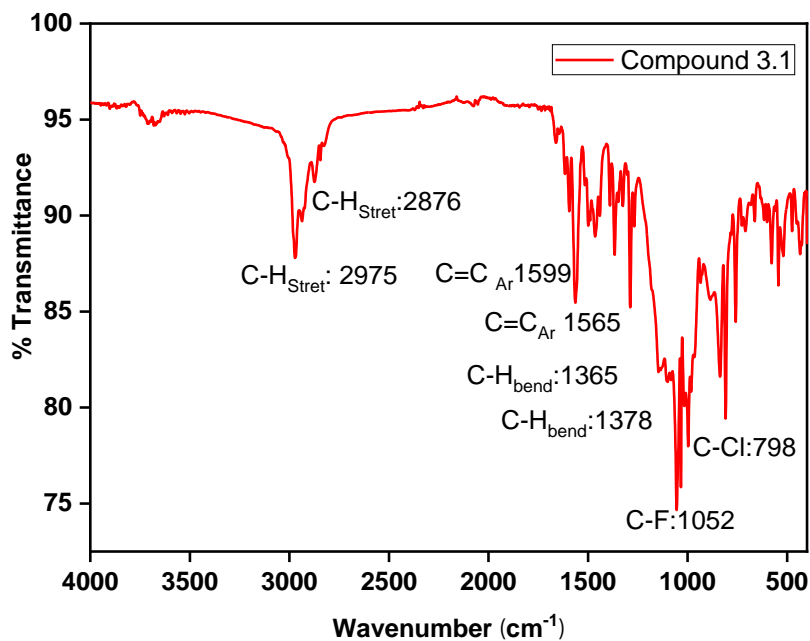


Figure 6.2.2. IR spectrum of 3.1.

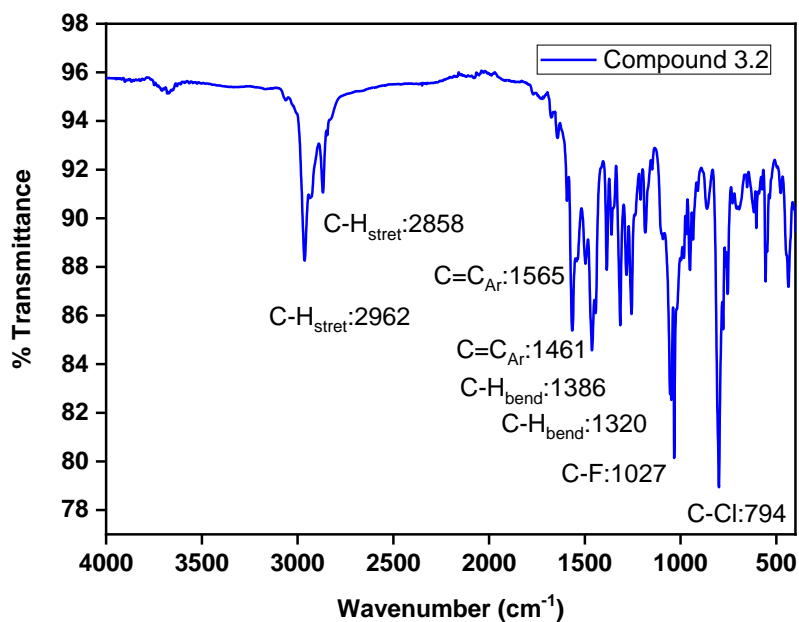


Figure 6.2.3. IR spectrum of 3.2.

6.2.5. Solid state absorption and emission spectra of 3.1

Absorption spectrum of 3.1

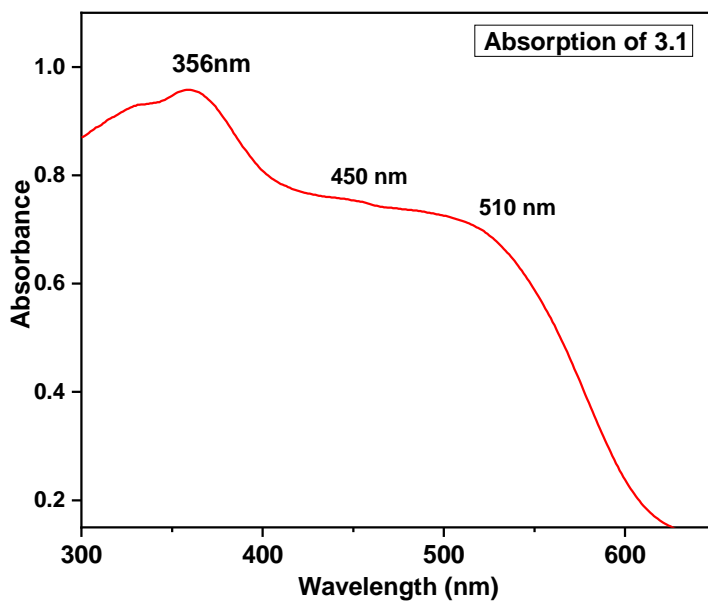


Figure 6.3.4. Solid state UV-Visible spectrum of 3.1.

Emission spectrum of 3.1

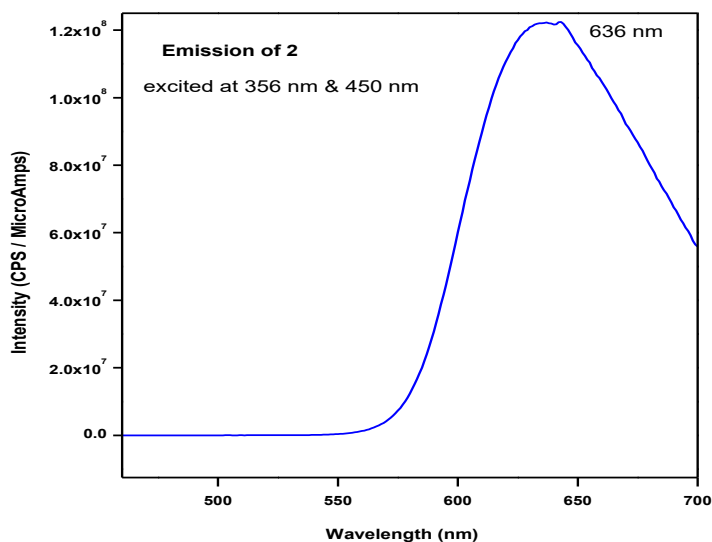


Figure 6.3.5. Solid state emission spectrum of **3.1** at absorption 356 nm and 450 nm.

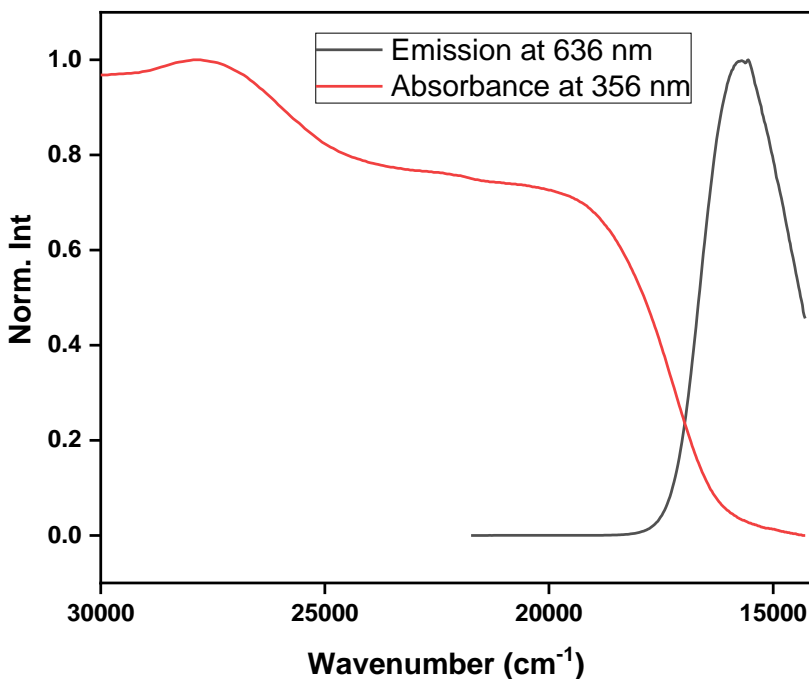


Figure 6.3.6. Calculation of Stokes shift from absorption at 356 nm of **3.1** (Stokes shift ca. 12080 cm^{-1}).

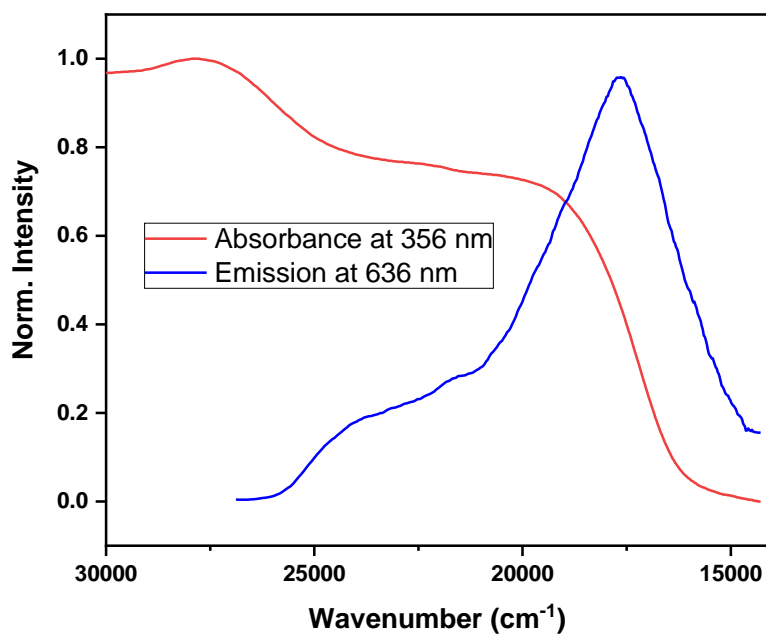


Figure 6.3.7. Calculation of Stokes shift from absorption at 510 nm of **3.1** (Stokes shift ca. 2056 cm⁻¹).

6.2.6. Lifetime measurement of 3.1

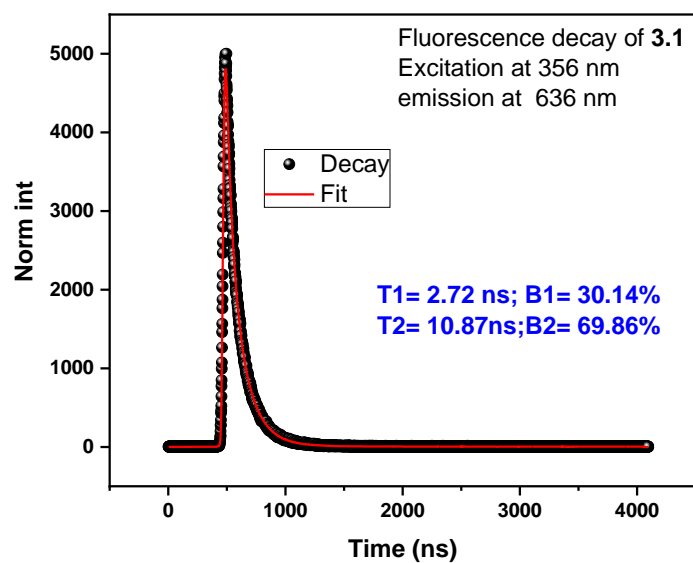


Figure 6.3.8. Lifetime measurement of **3.1** in solid state at emission 636 nm.

6.2.7. Absorption spectrum of **3.2**

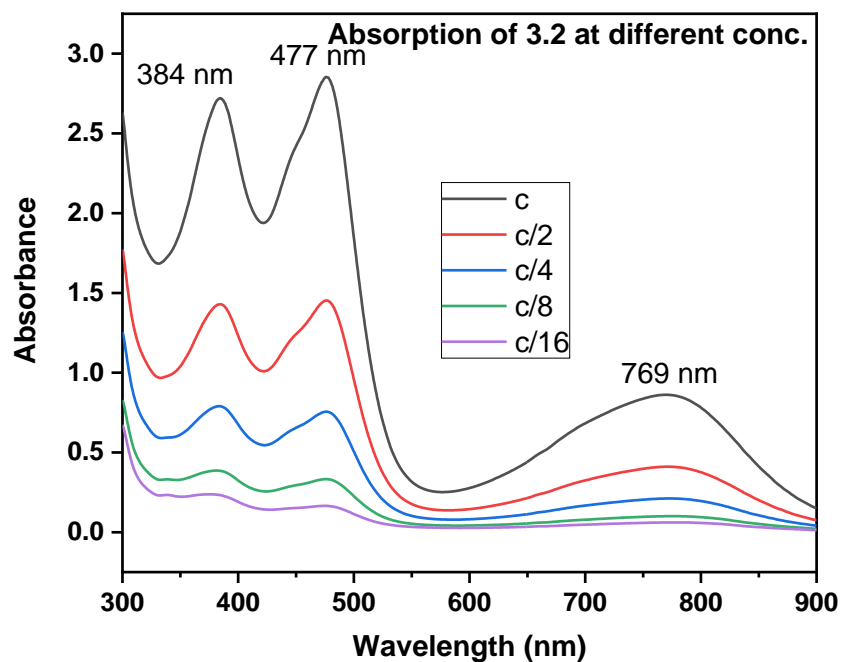


Figure 6.2.8. UV-Visible spectra of 3.2 at different concentration recorded in THF ($c = 2 \times 10^{-4}$).

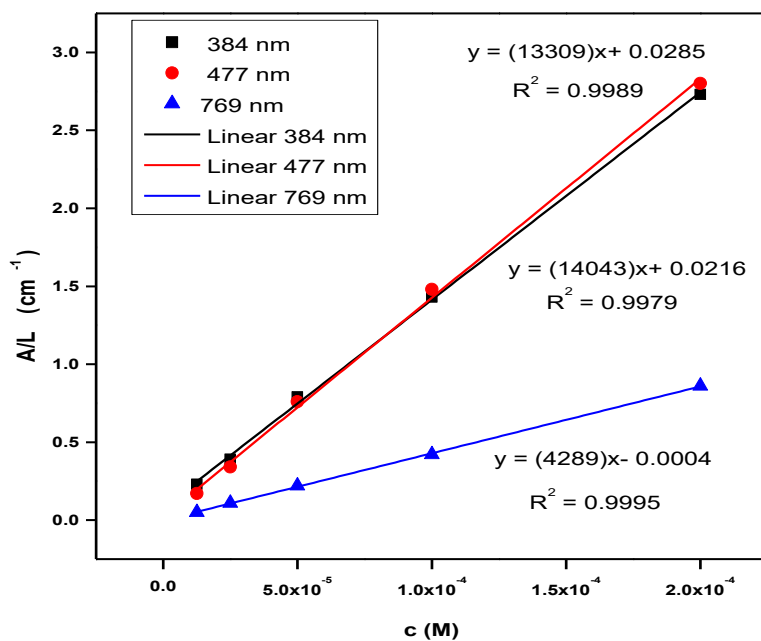
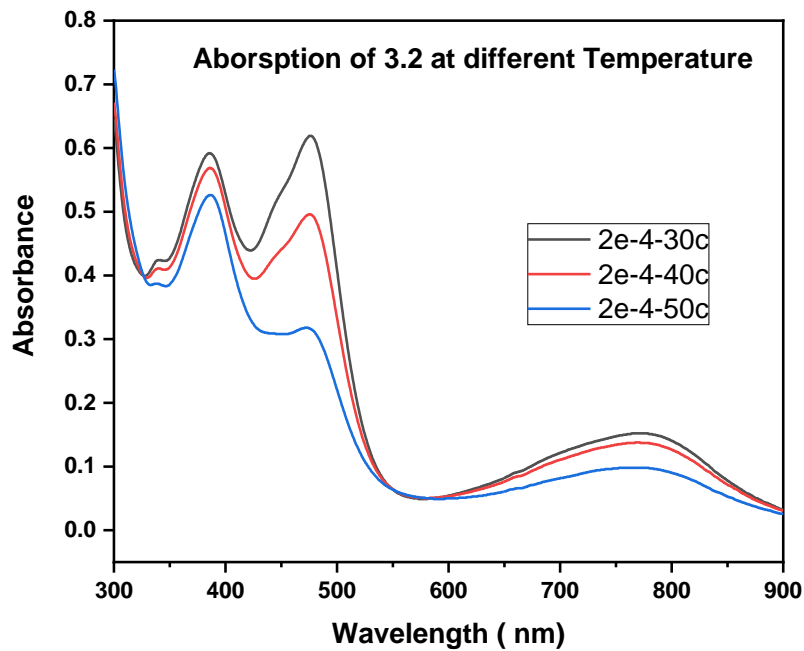


Figure 6.2.9. Plot of absorption/L vs. concentration.**Figure 6.2.10.** UV-Visible spectra of **3.2** ($c = 10^{-4}$ M THF solution) with variable temperature.

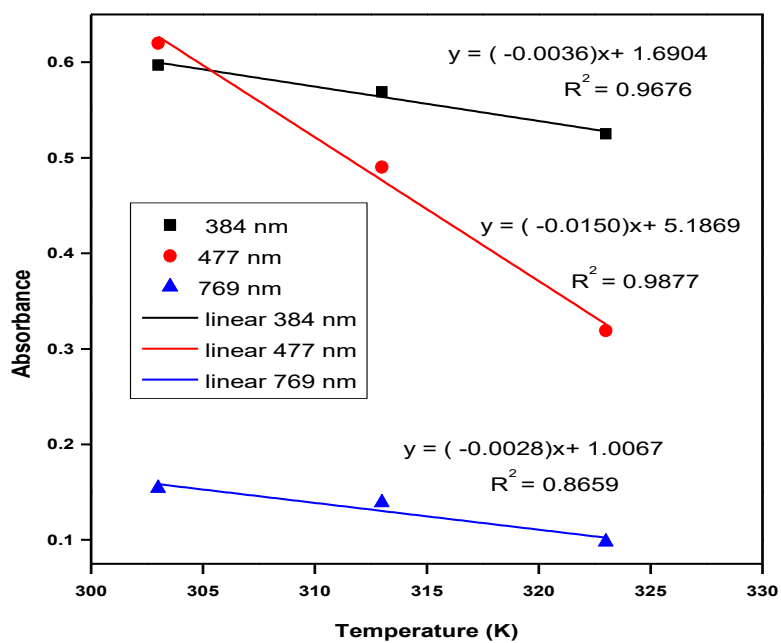


Figure 6.2.11. Temperature dependency of the UV-Vis transitions of **3.2**.

6.3.9. EPR spectrum of 3 at 298 K and 77 K

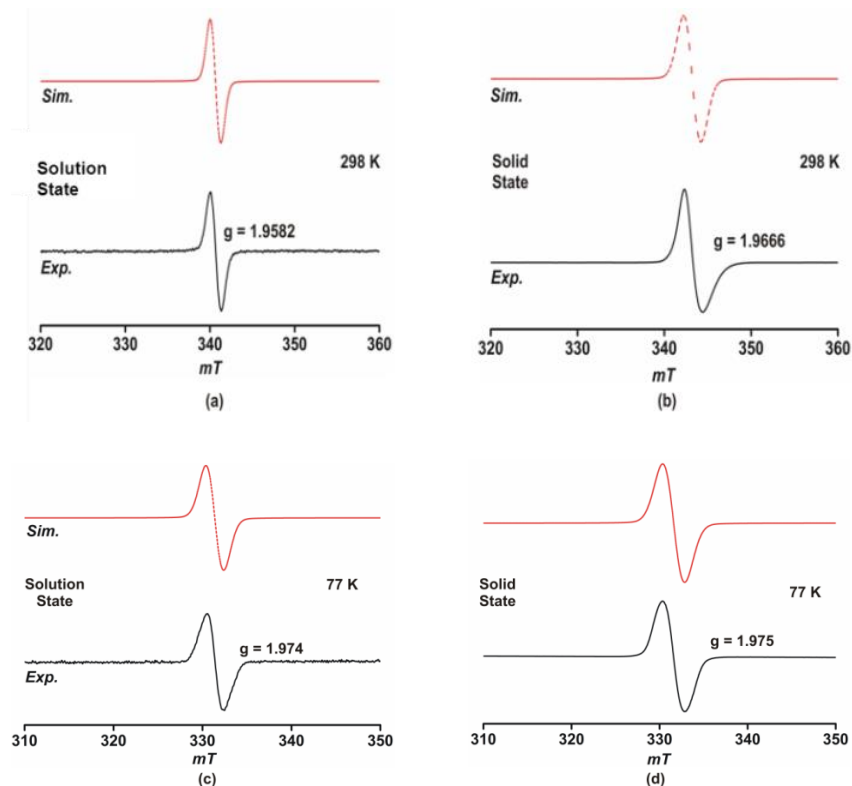


Figure 6.2.12. X-band EPR spectra of **3.3** at 298 K (a) in solution (5 mM in THF) and (b) in the solid state; at 77 K (c) in solution (5 mM in THF) and (d) in the solid state. Microwave frequency 9.41 GHz, power 0.995 mW, modulation frequency 100 KHz, amplitude 100 mT.

6.3.10. Details of the theoretical computational for Compound 3.2

All computations reported in this article were performed by density functional theory (DFT) method using Gaussian 09 (G09) program package.^[S6] Geometry optimizations were carried out using the exchange-correlation functional, R/U-B3LYP (Becke, three parameter, Lee-Yang-Parr)^[S7] in conjugation with def2-SVP basis set^[S8] for all atoms without symmetry constraints. Natural bond orbital (NBO) analysis^[S9] and Wiberg bond indices (WBI)^[S10] were performed at the

B3LYP/def2-TZVPP^[S11]//B3LYP/def2-SVP level using the *NBO* Version 3.1 program implemented in the Gaussian package.

According to the multi-configurational (MC)-SCF theory, the weight of the doubly excited configuration is expressed as the diradical character which is formally defined in the spin-projected UHF(PUHF) theory as^[S12]

$$y_i = 1 - \frac{2T_i}{1 + T_i^2} \quad (1)$$

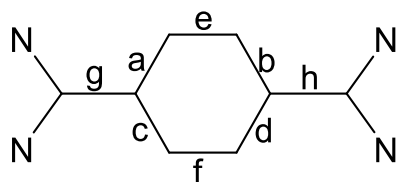
Where, T_i is the orbital overlap between the orbital pairs which can also be demonstrated by the occupations numbers (n_i) of the UHF natural orbitals (UNOs) [Eq 2]:

$$T_i = \frac{n_{HOMO-i} - n_{LUMO+i}}{2} \quad (2)$$

The calculation of the diradical character were performed from the occupation number of the lowest unoccupied natural orbital (LUNO) at UHF/6-31G(d,p) level of theory.

TDDFT calculations were accomplished in a tetrahydrofuran (THF) solvent using CPCM model^[S13] to calculate excitation energies as implemented in Gaussian program. We used CAM-B3LYP^[S14] functional in conjugation with the def2-SVP basis set. Orbital diagrams are rendered in the Chemcraft visualization software.^[S15]

Table 6.3.1. Selected experimental and calculated bond lengths (Å), BLA of compound **3.2**.



	Avg of a, b, c, and d	Avg of e and f	Avg of g and h	Avg of \angle N-C-N	Σ N	BLA ^[b]

3.2 ^[a]	1.448	1.346	1.384	108.5	350.5	0.10
CS	1.452	1.360	1.394	108.2	355.3	0.09
T	1.418	1.388	1.446	109.4	355.4	0.03

^[a] X-ray crystal data: the bond lengths [Å] and angles [°]; ^[b] BLA = Bond Length Alteration i.e., the difference between the average of length of longitudinal bonds (a, b, c and d) and the average of length of transverse bonds (e and f). [CS = Close shell singlet, T = Triplet]

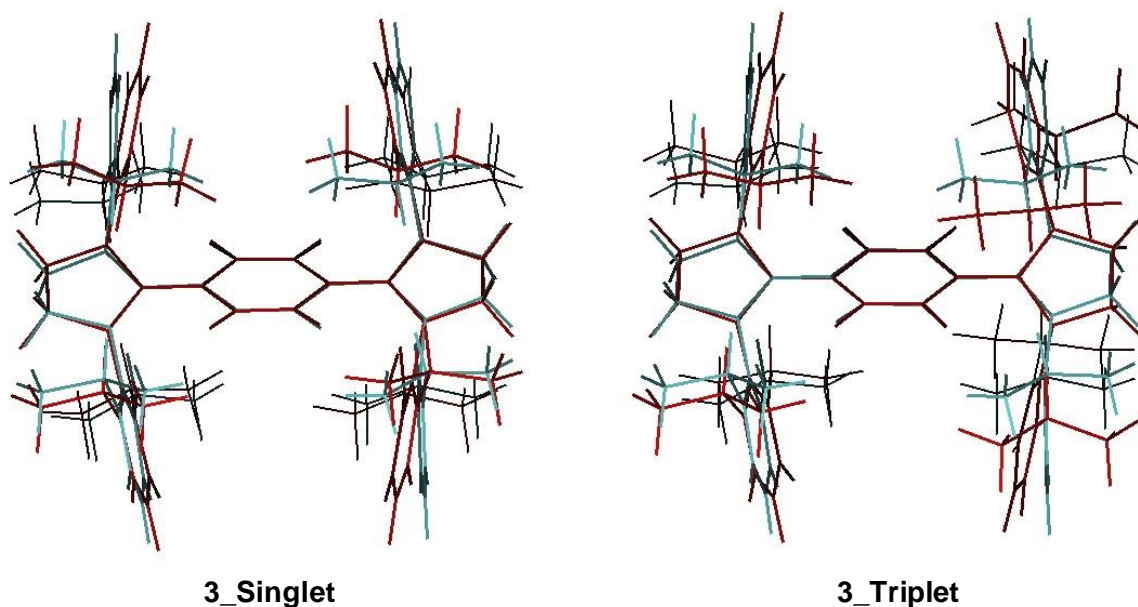


Figure 6.3.13. Superposition of crystal structure of **3.2** with optimized geometries of different spin states at R/U-B3LYP/def2-SVP level

Table 6.3.2. Calculated geometrical parameters [distances (d) are in Å and angles (A) are in degree (°)] of **3.2** (in Closed shell singlet and triplet electronic states)

3.2	Crystal Structure	R/U-B3LYP/def2-SVP	
		Singlet	Triplet

d(C5-N1)	1.390	1.396	1.399
d(C5-N4)	1.404	1.396	1.399
d(N2-C10)	1.398	1.398	1.403
d(N3-C10)	1.402	1.398	1.403
d(C5-C6)	1.385	1.394	1.440
d(C10-C9)	1.384	1.394	1.452
d(C9-C35)	1.449	1.453	1.415
d(C35-C34)	1.344	1.360	1.388
d(C34-C6)	1.451	1.451	1.420
d(C7-F2)	1.356	1.349	1.345
d(C35-F4)	1.358	1.349	1.345
d(C34-F3)	1.360	1.349	1.345
d(C7-C8)	1.348	1.360	1.388
d(C8-C9)	1.444	1.453	1.415
d(C8-F1)	1.363	1.349	1.345
A(N1-C5-N4)	108.3	108.4	109.2
A(N2-C10-N3)	108.6	107.9	109.5
A(C9-C10-N2)	126.6	126.0	125.3
A(C9-C10-N3)	124.8	126.0	125.3
A(C8-C9-C35)	110.3	111.7	113.9
A(C7-C6-C34)	110.2	111.9	113.7
A(C6-C5-N1)	126.7	125.8	125.4

A(C6-C5-N4)	125.0	125.8	125.4
-------------	-------	-------	-------

Table 6.3.3 Results of the NBO analysis of **3.2** at B3LYP/def2-TZVPP//B3LYP/def2-SVP level

Compound	Bond	Bond type	Occupancy (e)	Atomic contribution. hybridization	WBI ^[a]
3.2	C5-C6	σ	1.973	C5: 48.9%, sp1.51 C6: 51.1 %, sp1.60	1.394
		π	1.776	C5: 40.9%, p C6: 59.1%, p	
	C9-C10	σ	1.973	C9: 51.0%, sp1.60 C10: 49.0%, sp1.51	1.403
		π	1.784	C9: 58.6%, p C10: 41.4%, p	

^[a]Wiberg Bond Index**Table 6.3.4** TDDFT result of **3.2** at CAM-B3LYP/def2-SVP(CPCM)//B3LYP/def2-SVP level.

Total no. of states in the calculation: 20

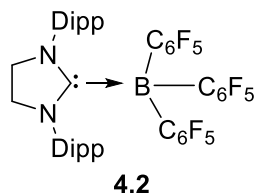
Compound	λ (nm) ^[a]	$f^{[b]}$	$\Delta E(\text{cm}^{-1})^{[c]}$	Transitions ^[d]
3.2	446	1.1079	22405.4	HOMO→LUMO (97%)
	332	0.0635	30050.0	HOMO→LUMO+2 (90%)

^[a]Wavelength of the transition. ^[b]The oscillator strength of the transition. ^[c]Excitation energies for each transition. ^[d]Molecular orbitals involved in the transitions.

6.3: Experimental details for chapter-4

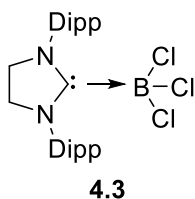
6.3.1. Synthesis and Characterization of Compounds 4.2-4.15

Synthesis of 4.2



To a solution of $B(C_6F_5)_3$ (0.26 g, 0.51 mmol) in 5 mL of toluene was added 10 mL of a toluene solution of SIDipp (0.2 g, 0.51 mmol) dropwise at $-78\text{ }^\circ\text{C}$. The mixture was warmed to room temperature and stirred for 1 h. The resulting colorless solution was filtered through cannula filtration. The filtrate toluene solution was concentrated to 3–4 mL and kept for crystallization at $-35\text{ }^\circ\text{C}$ in a freezer, which afforded colorless crystals of **4.2**. The compound was not very stable, and hence we are unable to give proper spectroscopic evidence.

Synthesis and characterization of 4.3



To a solution of SIDipp (0.2 g, 0.51 mmol) in 10 mL of *n*-hexane was added BCl_3 (0.42 mL, 0.51 mmol) dropwise at $-78\text{ }^\circ\text{C}$. The mixture was warmed to room temperature and stirred for 1 h. The formation of a white precipitate was observed, which was filtered through cannula filtration. After the precipitate was washed one to two times with *n*-hexane, it was dried under high vacuum. The isolated yield of the white powdered compound was 70%. MP = $295\text{ }^\circ\text{C}$.

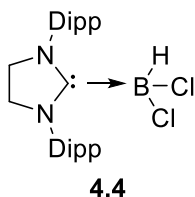
^1H NMR (400 MHz, 298 K, CDCl_3): δ 1.35 (d, $J = 6.63$ Hz, 12H, $\text{CH}(\text{CH}_3)_2$), 1.46 (d, $J = 6.88$ Hz, 12H, $\text{CH}(\text{CH}_3)_2$), 3.25 (sept, $J = 6.76$ Hz, 4H, $\text{CH}(\text{CH}_3)_2$), 4.13 (s, 4H, N- CH_2CH_2 -N), 7.25–7.43 (m, 12H, Ar- H)

$^{13}\text{C}\{^1\text{H}\}$ NMR (101 MHz, 298 K, CDCl_3): δ 23.47, 26.04 ($\text{H}\text{C}\text{M}\text{e}_2$), 29.11 ($\text{H}\text{C}\text{M}\text{e}_2$), 53.70 (CH_2CH_2), 124.42, 129.83, 134.61 (Ar- C_6H_3), 145.82 (ipso- C_6H_3)

$^{11}\text{B}\{^1\text{H}\}$ NMR (128 MHz, 298 K, CDCl_3): 1.28 (s, 1B, BCl_3)

Elemental analysis: Anal. Calcd for $\text{C}_{27}\text{H}_{38}\text{BCl}_3\text{N}_2$ [506.22 g mol^{-1}]: C, 63.87; H, 7.54; N, 5.52. Found: C, 63.85; H, 7.58; N, 5.48

Synthesis and characterization of 4.4



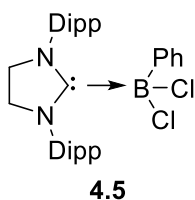
A slightly excess of $\text{BHCl}_2 \cdot \text{dioxane}$ (0.20 ml, 0.58 mmol) was added to a 10 ml hexane solution of 5-SIDipp (0.20 g, 0.48 mmol) at room temperature in a flask. Stirring the resulted mixture for further 2 hours at room temperature accessed a white precipitate. Colourless crystals of **4.4** were isolated after keeping the white powder in the mixture of 1 ml dichloromethane and 2 ml toluene solution. Yield = 0.20 g (90 %).

^1H NMR (400 MHz, 298 K, CDCl_3): $\delta = 1.29$ (d, $J = 6.88$ Hz, 12H, $\text{CH}(\text{CH}_3)_2$), 1.40 (d, $J = 6.63$ Hz, 12H, $\text{CH}(\text{CH}_3)_2$), 3.17 (sept, $J = 6.75$ Hz, 4H, $\text{CH}(\text{CH}_3)_2$), 4.08 (s, 4H, N CH_2CH_2 N), 7.23 (d, $J = 7.75$ Hz, 4H, Ar- H), 7.40 (t, $J = 7.75$ Hz, 2H, Ar- H) ppm

$^{13}\text{C}\{^1\text{H}\}$ NMR (101 MHz, 298 K, CDCl_3): $\delta = 23.4, 26.0, 28.9, 53.1, 124.4, 129.8, 133.2, 146.1$ ppm

$^{11}\text{B}\{^1\text{H}\}$ NMR (128 MHz, 298 K, CDCl_3): $\delta = 6.9$ (s, 1B, BHCl_2) ppm

Synthesis and characterization of 4.5



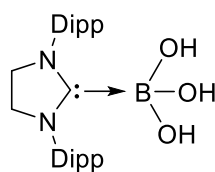
A slightly excess of BPhCl_2 -dioxane (0.090 g, 0.58 mmol) was added to a 10 ml hexane solution of 5-SIDipp (0.20 g, 0.48 mmol) at room temperature in a flask. Stirring the resulted mixture for further 2 hours at room temperature accessed a white precipitate. Colorless crystals of **4.5** were isolated after keeping the white powder in the mixture of 1 ml dichloromethane and 2 ml toluene solution. Yield = 0.24 g (90 %).

^1H NMR (400 MHz, 298 K, CDCl_3): $\delta = 1.42$ (d, $J = 6.72$ Hz, 12 H, $\text{CH}(\text{CH}_3)_2$), 1.51 (d, $J = 6.65$ Hz, 12 H, $\text{CH}(\text{CH}_3)_2$), 3.39 (sept, $J = 6.75$ Hz, 4H, $\text{CH}(\text{CH}_3)_2$), 4.22 (s, 4 H, $\text{NCH}_2\text{CH}_2\text{N}$), 6.95 (d, $J = 6.88$ Hz, 2H, *ortho-H* of B-Ph), 7.25 (d, $J = 7.75$ Hz, 4H, Ar-H), 7.26 (bs, 1H, *para-H* of B-Ph), 7.44 (t, $J = 7.73$ Hz, 2H, Ar-H), 7.49 (t, $J = 7.88$ Hz, *meta-H* of B-Ph) ppm

$^{13}\text{C}\{^1\text{H}\}$ NMR (101 MHz, 298 K, CDCl_3): $\delta = 23.2, 26.2, 28.9, 53.9, 124.2, 129.6, 133.5, 135.2, 145.7$ ppm

$^{11}\text{B}\{^1\text{H}\}$ NMR (128 MHz, 298 K, CDCl_3): $\delta = 1.8$ (s, 1B, BPhCl_2) ppm

Synthesis and characterization of 4.6



4.6

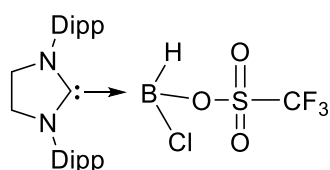
1.05 equivalent of water (0.01 g, 0.54 mmol) was added drop by drop to a 15 mL dichloromethane solution of **4.4** (0.20 g, 0.53 mmol) at room temperature in a flask. Stirring the resulted mixture for further 2 h at room temperature accessed a clear solution. The reaction mixture was concentrated to 5 mL and kept at 4 °C to obtain the colorless crystals of **4.6**. Yield = 0.36 g (80%).

$^1\text{H NMR}$ (400 MHz, 298 K, CDCl_3): δ = 1.31 (d, J = 6.97 Hz, 12H, $\text{CH}(\text{CH}_3)_2$), 1.35 (d, J = 6.85 Hz, 12H, $\text{CH}(\text{CH}_3)_2$), 3.07 (sept, J = 6.85 Hz, 4H, $\text{CH}(\text{CH}_3)_2$), 4.06 (s, 4H, $\text{NCH}_2\text{CH}_2\text{N}$), 7.23 (d, J = 7.70 Hz, 4H, Ar- H), 7.39 (t, J = 7.75 Hz, 2H, Ar- H) ppm

$^{13}\text{C}\{^1\text{H}\}$ NMR (101 MHz, 298 K, CDCl_3): δ = 23.4, 25.4, 28.9, 53.3, 67.9, 124.2, 129.6, 133.1, 146.0 ppm

$^{11}\text{B}\{^1\text{H}\}$ NMR (128 MHz, 298 K, CDCl_3): δ = -1.6 (s, 1B, $\text{B}(\text{OH})_3$) ppm

Synthesis and characterization of 4.7



4.7

A DCM solution (20 mL) of **4.4** (0.47 g, 1 mmol) was added dropwise to a DCM solution (20 mL) of previously weighed AgOTf (0.25 g, 1 mmol) at -78 °C in the absence of light. A white precipitate of AgCl was formed immediately, and it was filtered through frit filtration after the reaction mixture was warmed to room temperature. The colorless toluene solution was

concentrated (5 mL) and kept for crystallization at 4 °C, which afforded colorless crystals of **4.7** after 1–2 day(s). Yield = 0.48 g (82%).

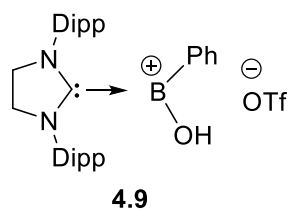
¹H NMR (400 MHz, 298 K, CDCl₃): δ = 1.31 (d, J = 6.88 Hz, 12H, CH(CH₃)₂), 1.40 (d, J = 6.63 Hz, 12H, CH(CH₃)₂), 3.13 (sept, J = 7.63 Hz, 4H, CH(CH₃)₂), 4.11 (s, 4H, NCH₂CH₂N), 7.20 (d, J = 7.38 Hz, 4H, Ar-H), 7.42 (t, J = 7.63 Hz, 2H, Ar-H) ppm

¹³C{¹H} NMR (101 MHz, 298 K, CDCl₃): δ = 21.4, 23.2, 25.9, 26.3, 28.9, 53.4, 124.7, 128.2, 130.2, 132.4, 137.8, 145.7, 145.9 ppm

¹¹B{¹H} NMR (128 MHz, 298 K, CDCl₃): δ = 3.4 (s, 1B, BH(OTf)Cl) ppm).

¹⁹F{¹H} NMR (377 MHz, 298 K, CDCl₃): δ = -76.7 (s, 3F, OSO₂CF₃) ppm

Synthesis and characterization of **4.9**



A toluene solution (20 mL) of **4.5** (0.55 g, 1 mmol) was added dropwise to a toluene solution (20 mL) of previously weighed AgOTf (0.25 g, 1 mmol) at -30 °C in the absence of light. A white precipitate of AgCl formed immediately, and it was filtered through frit filtration after the reaction mixture was warmed to room temperature. The colorless toluene solution was concentrated (5 mL) and was kept for crystallization at 4 °C, which afforded colorless crystals of **4.9** after 1 day. Yield = 0.25 g (45%).

¹H NMR (400 MHz, 298 K, CDCl₃): δ = 1.24 (d, J = 6.88 Hz, 12H, CH(CH₃)₂), 1.38 (d, J = 6.63 Hz, 12H, CH(CH₃)₂), 2.99 (sept, J = 6.75 Hz, 4H, CH(CH₃)₂), 4.59 (s, 4H, NCH₂CH₂N), 7.29 (d,

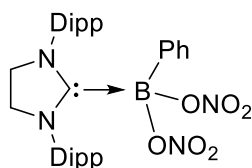
$J = 7.75$ Hz, 4H, Ar-*H*), 7.48 (t, $J = 7.75$ Hz, 2H, Ar-*H*), 7.52 (t, $J = 7.50$ Hz, 2H, meta-*H* of B-*Ph*), 7.61 (t, $J = 7.38$ Hz, para-*H* of B-*Ph*), 8.25 (d, $J = 6.75$ Hz, 2H, ortho-*H* of B-*Ph*) ppm

$^{13}\text{C}\{^1\text{H}\}$ NMR (101 MHz, 298 K, CDCl_3): $\delta = 21.4, 23.8, 25.1, 29.2, 54.7, 125.0, 127.9, 129.0, 135.6, 137.8, 146.2$ ppm

$^{11}\text{B}\{^1\text{H}\}$ NMR (128 MHz, 298 K, CDCl_3): $\delta = 30.9$ (s, 1B, BPh(OH)) ppm

$^{19}\text{F}\{^1\text{H}\}$ NMR (377 MHz, 298 K, CDCl_3): $\delta = -78.6$ (s, 3F, OSO_2CF_3) ppm

Synthesis and characterization of 4.10



4.10

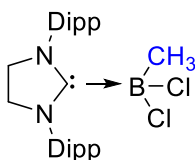
A toluene solution (20 mL) of **4.5** (0.55 g, 1 mmol) was added dropwise to a toluene solution (20 mL) of previously weighed AgNO_3 (0.34 g, 2 mmol) at -30 °C in the absence of light. A white precipitate of AgCl was formed slowly, and it was filtered via frit filtration after 6 h. The colorless toluene solution was concentrated (5 mL) and was kept for crystallization at 4 °C, which afforded colorless crystals of **4.10** after 2 days. Yield = 0.37 g (62%).

^1H NMR (400 MHz, 298 K, CDCl_3): $\delta = 1.12$ (d, $J = 6.75$ Hz, 12H, $\text{CH}(\text{CH}_3)_2$), 1.20 (d, $J = 6.75$ Hz, 12H, $\text{CH}(\text{CH}_3)_2$), 3.13 (sept, $J = 6.75$ Hz, 4H, $\text{CH}(\text{CH}_3)_2$), 4.15 (s, 4H, $\text{NCH}_2\text{CH}_2\text{N}$), 6.50 (d, $J = 6.88$ Hz, 2H, ortho-*H* of B-*Ph*), 6.89 (t, $J = 7.38$ Hz, 2H, meta-*H* of B-*Ph*), 7.01 (t, $J = 7.25$ Hz, para-*H* of B-*Ph*), 7.24 (d, $J = 7.88$ Hz, 4H, Ar-*H*), 7.46 (t, $J = 7.75$ Hz, 2H, Ar-*H*), ppm

$^{13}\text{C}\{^1\text{H}\}$ NMR (101 MHz, 298 K, CDCl_3): $\delta = 22.4, 26.8, 28.8, 53.8, 124.6, 127.1, 131.6, 134.5, 146.2$ ppm

$^{11}\text{B}\{^1\text{H}\}$ NMR (128 MHz, 298 K, CDCl_3): $\delta = 4.2$ (s, 1B, $\text{BPh}(\text{NO}_3)_2$) ppm

Synthesis and characterization of 4.11



4.11

One equivalent of MeLi (0.61 ml, 1.1 mmol) was added dropwise to the toluene solution of **4.3** (0.506 g, 1 mmol) at $-78\text{ }^\circ\text{C}$. The reaction mixture was allowed to come to room temperature and stirred for 12 h, which resulted in the generation of the white precipitate of the lithium chloride. It was further filtered through frit filtration. The toluene solution of the filtrate was concentrated and was kept for crystallization at $4\text{ }^\circ\text{C}$, which afforded colourless crystals of **4.11** after 1 day in a 60% (0.29 g) yield. MP: decomposes at $200\text{ }^\circ\text{C}$

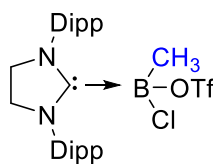
^1H NMR (400 MHz, 298K, C_6D_6): $\delta = 1.11$ (d, $J = 6.49$ Hz, 12H, $\text{CH}(\text{CH}_3)_2$), 1.49 (d, $J = 6.87$ Hz, 12H, $\text{CH}(\text{CH}_3)_2$), 1.24 (s, 3H, $\text{B}(\text{CH}_3)\text{Cl}_2$), 3.27 (sept, $J = 6.49$ Hz, 4H, $\text{CH}(\text{CH}_3)_2$), 3.46 (s, 4H, N- CH_2CH_2 -N), 7.04-7.19 (m, 12H, Ar-H) ppm

$^{13}\text{C}\{^1\text{H}\}$ NMR (101 MHz, 298K, C_6D_6): $\delta = 24.32$, 26.56 (HCMe_2), 29.81 (HCMe_2), 53.69 (CH_2CH_2), 125.30, 130.70, 134.59 (Ar- C_6H_3), 146.97 (*ipso*- C_6H_3) ppm

$^{11}\text{B}\{^1\text{H}\}$ NMR (128 MHz, 298K, C_6D_6): 1.98 (s, 1B, BMeCl_2) ppm

Elemental analysis: calcd (%) for $\text{C}_{29}\text{H}_{41}\text{BCl}_2\text{N}_2$ [486.27 g mol^{-1}]: C 69.01, H 8.48, N 5.75; found: C 58.88, H 8.40, N 5.69

Synthesis and characterization of 4.12

**4.12**

Toluene solution (20 mL) of **4.11** (0.48 g, 1 mmol) was added dropwise to the toluene solution (20 mL) of previously weighted AgOTf (0.25 g, 1 mmol) at -78 °C in absence of light. Immediate formation of white precipitate of AgCl was filtered through frit filtration after allowing the reaction mixture to come at room temperature. The colorless toluene solution was concentrated (5 mL) and was kept for crystallization at 4 °C, which afforded colourless crystals of **4.12** after 1-2 day(s) in a 68 % (0.41 g) yield. MP = 158 °C

¹H NMR (400 MHz, 298K, C₆D₆): δ = 1.12 (d, J = 6.63 Hz, 12H, CH(CH₃)₂), 1.43 (d, J = 6.88 Hz, 12H, CH(CH₃)₂), 1.29 (s, 3H, B(CH₃)Cl₂), 3.27 (sept, J = 6.75 Hz, 4H, CH(CH₃)₂), 3.51 (s, 4H, N-CH₂CH₂-N), 7.06-7.18 (m, 12H, Ar-H) ppm

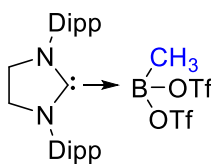
¹³C{¹H} NMR (101 MHz, 298K, C₆D₆): δ = 24.37, 26.61 (H_CMe₂), 29.85 (H_CMe₂), 53.88 (CH₂CH₂), 125.33, 130.73, 134.62 (Ar-C₆H₃), 147.06 (*ipso*-C₆H₃) ppm

¹¹B{¹H} NMR (128 MHz, 298K, C₆D₆-d₆): -2.54 (br s, 1B, BCl(Me)OTf) ppm

¹⁹F{¹H} NMR (128 MHz, 298K, C₆D₆): -78.21 (br s, 3F, BCl(Me)OSO₂CF₃) ppm

Elemental analysis: calcd (%) for C₂₉H₄₁BClF₃N₂O₃S₄ [600.26 g mol⁻¹]: C 57.96, H 6.88, N 4.66; found: C 56.88, H 6.05, N 4.62

Synthesis and characterization of 4.13



4.13

Toluene solution of **4.12** (0.60 g, 1 mmol) was added dropwise to the toluene solution of previously weighed AgOTf (0.25 g, 1 mmol) at -78°C in absence of light. Immediate formation of white precipitate of AgCl was filtered through frit filtration after coming the reaction mixture at room temperature. The colorless toluene solution was dried under vacuum and afforded white powder of **4.13** in 56 % (0.39 g) yield. MP: decomposes at 147°C

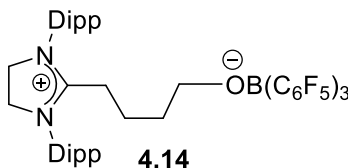
^1H NMR (400 MHz, 298K, C_6D_6): δ = 1.06 (s, 3H, $\text{B}(\text{CH}_3)\text{Cl}_2$), 1.17 (d, J = 6.63 Hz, 12H, $\text{CH}(\text{CH}_3)_2$), 1.40 (d, J = 6.63 Hz, 12H, $\text{CH}(\text{CH}_3)_2$), 3.22 (sept, J = 6.75 Hz, 4H, $\text{CH}(\text{CH}_3)_2$), 3.71 (s, 4H, N- CH_2CH_2 -N), 6.96-7.04 (m, 12H, Ar- H) ppm

$^{13}\text{C}\{^1\text{H}\}$ NMR (101 MHz, 298K, C_6D_6): δ = 24.31, 26.60 (HCMe_2), 29.81 (HCMe_2), 54.06 (CH_2CH_2), 125.26, 130.72, 134.47 (Ar- C_6H_3), 147.08 (*ipso*- C_6H_3); **$^{11}\text{B}\{^1\text{H}\}$ NMR (128 MHz, 298K, C_6D_6):** -6.62 (br s, 1B, $\text{BCl}(\text{Me})\text{OTf}$) ppm

$^{19}\text{F}\{^1\text{H}\}$ NMR (128 MHz, 298K, C_6D_6): -76.99 (br s, $\text{BClMe}(\text{OSO}_2\text{CF}_3)_2$) ppm

Elemental analysis: calcd (%) for $\text{C}_{30}\text{H}_{41}\text{BF}_6\text{N}_2\text{O}_6\text{S}_2$ [$714.24 \text{ g mol}^{-1}$]: C 50.42, H 5.78, N 3.92; found: C 50.27, H 5.41, N 3.83

Synthesis and characterization of 4.14

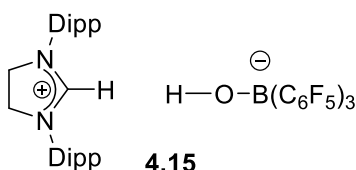


4.14

A THF solution (5 mL) of 5-SIDipp (0.382 g, 1 mmol) was added dropwise to a THF solution (20 mL) of previously weighed $B(C_6F_5)_3$ (0.512 g, 1 mmol) at room temperature. The reaction mixture turned to a clear colorless solution immediately and run for 12 h. The solution was dried completely and 3 mL of toluene solution was added to dissolve the white solid product. Colorless crystals of **4.14** were afforded after keeping the toluene solution for crystallization at 4 °C after 2 days. Yield = 0.45 g (46%). The formation of **4.14** was accompanied by some other side products, which could not be identified. Hence, we did not have a spectroscopically pure product to record the 1H and ^{13}C NMR.

$^{11}B\{^1H\}$ NMR (128 MHz, 298 K, $CDCl_3$): $\delta = -2.8$ (s, 1B, $B(C_6F_5)_3$) ppm.

Synthesis and characterization of 4.15



A diethyl ether solution (5 mL) of 5-SIDipp (0.382 g, 1 mmol) was added dropwise to a diethyl ether solution (5 mL) of previously weighed $B(C_6F_5)_3$ (0.512 g, 1 mmol) at room temperature. The reaction mixture turned to a clear colorless solution immediately and run for 12 h. The solution was dried completely and 3 mL of toluene solution was added to dissolve the white solid product. Colorless crystals of **4.15** were afforded after keeping the toluene solution for crystallization at 4 °C after 1 day. Yield = 0.78 g (85%).

1H NMR (400 MHz, 298 K, $CDCl_3$): $\delta = 1.20$ (d, $J = 6.88$ Hz, 12H, $CH(CH_3)_2$), 1.35 (d, $J = 6.88$ Hz, 12H, $CH(CH_3)_2$), 2.87 (sept, $J = 6.75$ Hz, 4H, $CH(CH_3)_2$), 4.39 (s, 4H, NCH_2CH_2N), 7.29 (d, $J = 7.75$ Hz, 4H, Ar-H), 7.54 (t, $J = 7.88$ Hz, 2H, Ar-H), 8.90 (s, 1H, N-CH-N) ppm

$^{13}\text{C}\{^1\text{H}\}$ NMR (101 MHz, 298 K, CDCl_3): $\delta = 23.9, 24.4, 29.4, 53.6, 60.8, 125.2, 128.6, 131.9, 145.6, 160.3$ ppm

$^{11}\text{B}\{^1\text{H}\}$ NMR (128 MHz, 298 K, CDCl_3): $\delta = -4.2$ (s, 1B, $\text{HO-B}(\text{C}_6\text{F}_5)_3$) ppm

$^{19}\text{F}\{^1\text{H}\}$ NMR (377 MHz, 298 K, CDCl_3): $\delta = -135.6, -162.4, -166.1$ (15F, $\text{B}(\text{C}_6\text{F}_5)_3$) ppm

6.3.2. Crystallographic data for the structural analysis of compounds 4.1-2.6, 2.8, and 2.11:

Single crystals of **1a**, **4.2**, **4.11**, **4.12**, were mounted on a Bruker SMART APEX II single crystal X-ray CCD diffractometer having graphite monochromatised ($\text{Mo-K}\alpha = 0.71073 \text{ \AA}$) radiation at low temperature 100 K. The X-ray generator was operated at 50 kV and 30 mA. The X-ray data acquisition was monitored by APEX2 program suit. The data were corrected for Lorentz-polarization and absorption effects using SAINT and SADABS programs which are an integral part of APEX2 package. The structures were solved by direct methods and refined by full matrix least squares, based on F^2 , using SHELXL Crystal structures were refined using Olex2-1.0 software. Anisotropic refinement was performed for all non-H atom. The C-H hydrogen atoms were calculated using the riding model. The structures were examined using the ADSYM subroutine of PLATON to assure that no additional symmetry could be applied to the models. The molecular weight of each structure mentioned herein has been calculated considering the solvent molecules trapped in the crystal. Crystallographic information files are available at www.ccdc.cam.ac.uk/data with the mentioned CCDC numbers.

Crystal Data for Compound 4.1 (CCDC 2040725): ($\text{C}_{27}\text{H}_{41}\text{BN}_2$), colorless, $0.17 \times 0.15 \times 0.1$ mm³, monoclinic, space group $Pnma$, $a = 11.953(4) \text{ \AA}$, $b = 20.524(7) \text{ \AA}$, $c = 10.910(3) \text{ \AA}$, $\alpha = \gamma = \beta = 90$, $V = 2676.5(15) \text{ \AA}^3$, $Z = 4$, $T = 105 \text{ K}$, $2\theta_{\text{max}} = 40.7^\circ$, $D_{\text{calc}} (\text{g cm}^{-3}) = 1.004$, $F(000) = 888$, $\mu (\text{mm}^{-1}) = 0.057$, 30029 reflections collected, 3486 unique reflections ($R_{\text{int}} = 0.067$), 1867

observed ($I > 2\sigma(I)$) reflections, multi-scan absorption correction, $T_{\min} = 0.636$, $T_{\max} = 0.746$, 143 refined parameters, $S = 1.022$, $R1 = 0.099$, $wR2 = 0.1937$ (all data $R = 0.1476$, $wR2 = 0.226$), maximum and minimum residual electron densities; $\Delta\rho_{\max} = 0.229$, $\Delta\rho_{\min} = -0.221$ ($\text{e}\text{\AA}^{-3}$).

Crystal Data for Compound 4.2 (CCDC 2040726): ($\text{C}_{45}\text{H}_{38}\text{BF}_{15}\text{N}_2$), colorless, $0.4 \times 0.34 \times 0.18$ mm^3 , monoclinic, space group $P-1$, $a = 9.2054(8)$ \AA , $b = 12.0369(11)$ \AA , $c = 19.8417(17)$ \AA , $\alpha = 78.184(4)$, $\beta = 86.061(4)$, $\gamma = 74.567(4)$, $V = 2074.1(3)$ \AA^3 , $Z = 2$, $T = 267(2)$ K, $2\theta_{\max} = 56.58^\circ$, D_{calc} (g cm^{-3}) = 1.445, $F(000) = 924$, μ (mm^{-1}) = 0.131, 79662 reflections collected, 10321 unique reflections ($R_{\text{int}} = 0.0549$), 5975 observed ($I > 2\sigma(I)$) reflections, multi-scan absorption correction, $T_{\min} = 0.948$, $T_{\max} = 0.977$, 576 refined parameters, $S = 1.019$, $R1 = 0.0632$, $wR2 = 0.1352$ (all data $R = 0.1193$, $wR2 = 0.1686$), maximum and minimum residual electron densities; $\Delta\rho_{\max} = 0.236$, $\Delta\rho_{\min} = -0.235$ ($\text{e}\text{\AA}^{-3}$).

Crystal Data for Compound 4.4 (CCDC 2180189): ($\text{C}_{39}\text{H}_{51}\text{BCl}_2\text{N}_2$), colorless, $0.14 \times 0.13 \times 0.06$ mm^3 , monoclinic, space group $P2_1/n$, $a = 12.3193(19)$ \AA , $b = 14.797(3)$ \AA , $c = 20.094(3)$ \AA , $\alpha = \gamma = 90$, $\beta = 94.984(5)$, $V = 3649.0(10)$ \AA^3 , $Z = 4$, $T = 100$ K, $2\theta_{\max} = 49.996^\circ$, D_{calc} (g cm^{-3}) = 1.146, $F(000) = 1352$, μ (mm^{-1}) = 0.206, 156159 reflections collected, 6392 unique reflections ($R_{\text{int}} = 0.1716$), multi-scan absorption correction, $T_{\min} = 0.746$, $T_{\max} = 0.629$, 405 refined parameters, $S = 1.151$, $R1 = 0.0933$, $wR2 = 0.2291$ (all data $R = 0.1166$, $wR2 = 0.2441$), maximum and minimum residual electron densities; $\Delta\rho_{\max} = 0.42$, $\Delta\rho_{\min} = -0.52$ ($\text{e}\text{\AA}^{-3}$).

Crystal Data for Compound 4.5 (CCDC 2180190): ($\text{C}_{33}\text{H}_{43}\text{BCl}_2\text{N}_2$), colorless, $0.12 \times 0.12 \times 0.08$ mm^3 , monoclinic, space group $P2_1/n$, $a = 11.8231(7)$ \AA , $b = 18.7331(11)$ \AA , $c = 14.2604(8)$ \AA , $\alpha = \gamma = 90$, $\beta = 106.906(2)$, $V = 3021.9(3)$ \AA^3 , $Z = 4$, $T = 100$ K, $2\theta_{\max} = 72.752^\circ$, D_{calc} (g cm^{-3}) = 1.208, $F(000) = 1176$, μ (mm^{-1}) = 0.239, 134803 reflections collected, 14650 unique

reflections ($R_{\text{int}}=0.0564$), multi-scan absorption correction, $T_{\text{min}}=0.693$, $T_{\text{max}}=0.747$, 351 refined parameters, $S=1.107$, $R1=0.0349$, $wR2=0.0984$ (all data $R=0.0424$, $wR2=0.1074$), maximum and minimum residual electron densities; $\Delta\rho_{\text{max}}=0.61$, $\Delta\rho_{\text{min}}=-0.53$ ($\text{e}\text{\AA}^{-3}$).

Crystal Data for Compound 4.6 (CCDC 2180191): ($\text{C}_{27}\text{H}_{42}\text{BN}_2\text{O}_3$), colorless, $0.2 \times 0.2 \times 0.2$ mm^3 , monoclinic, space group $P2_1/c$, $a=12.8167(19)$ \AA , $b=15.081(3)$ \AA , $c=14.254(3)$ \AA , $\alpha=\gamma=90$, $\beta=108.660(3)$, $V=2612.1(6)$ \AA^3 , $Z=4$, $T=296.15$ K, $2\theta_{\text{max}}=56.96^\circ$, D_{calc} (g cm^{-3}) = 1.153, $F(000)=988$, μ (mm^{-1}) = 0.2074, 113995 reflections collected, 6560 unique reflections ($R_{\text{int}}=0.3107$), $S=1.043$, $R1=0.0985$, $wR2=0.1721$ (all data $R=0.2309$, $wR2=0.2185$), maximum and minimum residual electron densities; $\Delta\rho_{\text{max}}=0.32$, $\Delta\rho_{\text{min}}=-0.42$ ($\text{e}\text{\AA}^{-3}$).

Crystal Data for Compound 4.7 (CCDC 2180197): ($\text{C}_{35}\text{H}_{47}\text{BClF}_3\text{N}_2\text{O}_3\text{S}$), colorless, $0.15 \times 0.12 \times 0.09$ mm^3 , monoclinic, space group $P2_1/n$, $a=12.286(3)$ \AA , $b=14.731(3)$ \AA , $c=20.644(4)$ \AA , $\alpha=\gamma=90$, $\beta=104.789(9)$, $V=3612.8(13)$ \AA^3 , $Z=4$, $T=100$ K, $2\theta_{\text{max}}=52.998^\circ$, D_{calc} (g cm^{-3}) = 1.248, $F(000)=1440$, μ (mm^{-1}) = 0.215, 53931 reflections collected, 7489 unique reflections ($R_{\text{int}}=0.0481$), multi-scan absorption correction, $T_{\text{min}}=0.644$, $T_{\text{max}}=0.746$, 424 refined parameters, $S=1.058$, $R1=0.0541$, $wR2=0.1529$ (all data $R=0.0580$, $wR2=0.1580$), maximum and minimum residual electron densities; $\Delta\rho_{\text{max}}=1.35$, $\Delta\rho_{\text{min}}=-0.84$ ($\text{e}\text{\AA}^{-3}$).

Crystal Data for Compound 4.8 (CCDC 2180198): ($\text{C}_{41}\text{H}_{51}\text{BClF}_3\text{N}_2\text{O}_3\text{S}$), colorless, $0.26 \times 0.22 \times 0.2$ mm^3 , monoclinic, space group $P2_1/n$, $a=16.0556(5)$ \AA , $b=22.2837(7)$ \AA , $c=23.3059(7)$ \AA , $\alpha=\gamma=90$, $\beta=107.6690(10)$, $V=7945.0(4)$ \AA^3 , $Z=8$, $T=100$ K, $2\theta_{\text{max}}=49.998^\circ$, D_{calc} (g cm^{-3}) = 1.263, $F(000)=3200$, μ (mm^{-1}) = 0.203, 196375 reflections collected, 13881 unique reflections ($R_{\text{int}}=0.0508$), multi-scan absorption correction, $T_{\text{min}}=0.701$, $T_{\text{max}}=0.746$, 976 refined

parameters, $S = 1.136$, $R1 = 0.0463$, $wR2 = 0.1329$ (all data $R = 0.0508$, $wR2 = 0.1386$), maximum and minimum residual electron densities; $\Delta\rho_{\max} = 1.11$, $\Delta\rho_{\min} = -0.43$ ($\text{e}\text{\AA}^{-3}$).

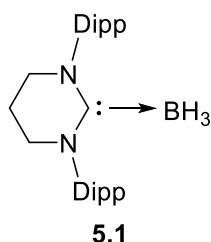
Crystal Data for Compound 4.10 (CCDC 2180199): ($\text{C}_{33}\text{H}_{43}\text{BN}_4\text{O}_6$), colorless, $0.14 \times 0.13 \times 0.06$ mm^3 , monoclinic, space group $P2_1/c$, $a = 10.1256(5)$ \AA , $b = 16.8204(13)$ \AA , $c = 18.9207(16)$ \AA , $\alpha = \gamma = 90$, $\beta = 98.178(2)$, $V = 3189.7(4)$ \AA^3 , $Z = 4$, $T = 160$ K, $2\theta_{\max} = 59.156^\circ$, D_{calc} (g cm^{-3}) = 1.255, $F(000) = 1288$, μ (mm^{-1}) = 0.086, 21918 reflections collected, 7552 unique reflections ($R_{\text{int}} = 0.1113$), multi-scan absorption correction, $T_{\min} = 0.683$, $T_{\max} = 0.746$, 405 refined parameters, $S = 0.995$, $R1 = 0.0693$, $wR2 = 0.1688$ (all data $R = 0.1607$, $wR2 = 0.2175$), maximum and minimum residual electron densities; $\Delta\rho_{\max} = 0.51$, $\Delta\rho_{\min} = -0.76$ ($\text{e}\text{\AA}^{-3}$).

Crystal Data for Compound 4.11 (CCDC 2040731): ($\text{C}_{28}\text{H}_{38}\text{BC}_{12}\text{N}_2$), colorless, $0.25 \times 0.1 \times 0.1$ mm^3 , monoclinic, space group $P 2_1/c$, $a = 13.5240(10)$ \AA , $b = 14.8694(10)$ \AA , $c = 14.9855(9)$ \AA , $\alpha = \gamma = 90$, $\beta = 113.028(2)$, $V = 2773.4(3)$ \AA^3 , $Z = 4$, $T = 100(2)$ K, $2\theta_{\max} = 61.09^\circ$, D_{calc} (g cm^{-3}) = 1.160, $F(000) = 1036$, μ (mm^{-1}) = 0.252, 113554 reflections collected, 9811 unique reflections ($R_{\text{int}} = 0.1478$), 8448 observed ($I > 2\sigma(I)$) reflections, multi-scan absorption correction, $T_{\min} = 0.970$, $T_{\max} = 0.975$, 325 refined parameters, $S = 1.082$, $R1 = 0.0485$, $wR2 = 0.1346$ (all data $R = 0.0594$, $wR2 = 0.1478$), maximum and minimum residual electron densities; $\Delta\rho_{\max} = 0.698$, $\Delta\rho_{\min} = -0.617$ ($\text{e}\text{\AA}^{-3}$).

Crystal Data for Compound 4.12 (CCDC 2040732): ($\text{C}_{36}\text{H}_{48}\text{BClF}_3\text{N}_2\text{O}_3\text{S}$) Sum formula, colorless, $0.16 \times 0.15 \times 0.12$ mm^3 , monoclinic, space group $P2_1/n$, $a = 12.2563(12)$ \AA , $b = 14.7943(14)$ \AA , $c = 20.6918(18)$ \AA , $\alpha = \gamma = 90$, $\beta = 104.604(4)$ \AA , $V = 3630.7(6)$ \AA^3 , $Z = 4$, $T = 100(2)$ K, $2\theta_{\max} = 61.18^\circ$, D_{calc} (g cm^{-3}) = 1.266, $F(000) = 1468.0$, μ (mm^{-1}) = 0.215, 269370 reflections collected, 11118 unique reflections ($R_{\text{int}} = 0.056$), 9675 observed ($I > 2\sigma(I)$) reflections,

multi-scan absorption correction, $T_{\min} = 0.966$, $T_{\max} = 0.975$, 500 refined parameters, $S = 1.121$, $R1 = 0.0679$, $wR2 = 0.2003$ (all data $R = 0.0780$, $wR2 = 0.2129$), maximum and minimum residual electron densities; $\Delta\rho_{\max} = 0.791$, $\Delta\rho_{\min} = -1.248$ ($\text{e}\text{\AA}^{-3}$).

Crystal Data for Compound 4.14 (CCDC 2180200): ($\text{C}_{52}\text{H}_{49}\text{BF}_{15}\text{N}_2\text{O}$), colorless, $0.3 \times 0.15 \times 0.1$ mm³, triclinic, space group $P-1$, $a = 9.4393(13)$ Å, $b = 14.568(2)$ Å, $c = 17.814(3)$ Å, $\alpha = 97.195(6)$, $\beta = 97.145(5)$, $\gamma = 99.872(5)$, $V = 2367.6(6)$ Å³, $Z = 2$, $T = 100$ K, $2\theta_{\max} = 62.2^\circ$, D_{calc} (g cm^{-3}) = 1.146, $F(000) = 1352$, μ (mm^{-1}) = 0.206, 156159 reflections collected, 6392 unique reflections ($R_{\text{int}} = 0.1716$), $S = 1.151$, $R1 = 0.0933$, $wR2 = 0.2291$ (all data $R = 0.1166$, $wR2 = 0.2441$), maximum and minimum residual electron densities; $\Delta\rho_{\max} = 0.42$, $\Delta\rho_{\min} = -0.52$ ($\text{e}\text{\AA}^{-3}$).

6.4: Experimental details for chapter-5**6.4.1. Synthesis and Characterization of Compounds 5.1-5.11****Synthesis and Characterization of Compound 5.1**

BH₃·SMe₂ (0.05 ml, 0.70 mmol) was added to a solution of 6-SIDipp (0.2 g, 0.50 mmol) in 5 ml toluene solvent at -36 °C. The resulting mixture was stirred for 2 hours at room temperature. Colorless crystals of **5.1** were isolated from the concentrated toluene solution with a yield of 0.15 g (70 %).

¹H NMR (400 MHz, 298 K, CDCl₃): δ = 0.25 (s, 3H, BH₃), 1.30 (d, *J* = 6.97 Hz, 12H, CH(CH₃)₂), 1.36 (d, *J* = 6.72, 12H, CH(CH₃)₂), 2.33 (q, *J* = 5.88 Hz, 2H, NCH₂CH₂CH₂N), 3.06 (sept, *J* = 6.88 Hz, 4H, CH(CH₃)₂), 3.52 (t, *J* = 5.87 Hz, 4H, NCH₂CH₂CH₂N), 7.18 (d, *J* = 7.70 Hz, 4H, Ar-*H*), 7.32 (t, *J* = 7.70 Hz, 2 H, Ar-*H*) ppm

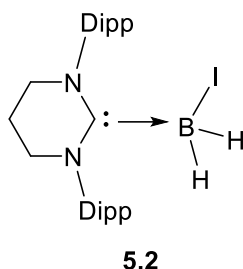
¹³C{¹H} NMR (101 MHz, 298 K, CDCl₃): δ = 20.5, 23.5, 25.3, 28.7, 49.3, 124.1, 128.2, 142.0, 144.3 ppm

¹¹B{¹H} NMR (128 MHz, 298 K, CDCl₃): δ = -31.3 (q, 1B, BH₃) ppm

ESI-MS (CH₃CN): m/z Calcd. for C₂₈H₄₃BN₂ [M+H]⁺ 419.3592, found 419.3409

Elemental Analysis: calcd. C, 80.36; H, 10.36; N, 6.69; found: C, 80.41; H, 10.53; N, 6.61

Synthesis and Characterization of Compound 5.2



0.5 equivalent of Iodine (I_2) (0.061 g, 0.24 mmol) and **5.1** (0.2 g, 0.48 mmol) were taken in a Schlenk flask and 5 ml of toluene was added to the reaction mixture. The reaction was run for 1 h at room temperature. The toluene solution was concentrated and filtered through cannula. Colorless crystals of **5.2** were isolated after keeping the solution at 4 °C for a day with a yield of 0.22 g (85 %).

1H { ^{11}B } NMR (400 MHz, 298 K, $CDCl_3$): δ = 1.28 (d, J = 6.88 Hz, 12H, $CH(CH_3)_2$), 1.47 (d, J = 6.63 Hz, 12H, $CH(CH_3)_2$), 1.60 (s, 2 H, BH_2I), 2.30 (quintet, J = 5.40 Hz, 2H, $NCH_2CH_2CH_2N$), 3.14 (sept, J = 6.16 Hz, 4H, $CH(CH_3)_2$), 3.64 (t, J = 5.67 Hz, 4H, $NCH_2CH_2CH_2N$), 7.19 (m, 4H, Ar-H), 7.33 (t, J = 7.75 Hz, 2H, Ar-H) ppm

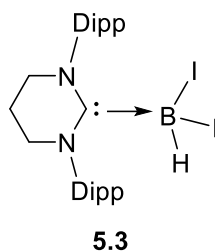
^{13}C { 1H } NMR (101 MHz, 298 K, $CDCl_3$): δ = 19.5, 24.0, 26.1, 28.6, 50.9, 124.4, 128.8, 140.8, 144.5 ppm

^{11}B { 1H } NMR (127 MHz, 298 K, $CDCl_3$): δ = -30.2 (bs, 1B, BH_2I) ppm

ESI-MS (CH_3CN): m/z Calcd. for $C_{28}H_{42}N_2BI$ [$M+H$] $^+$ 545. 2558, found 545. 3156

Elemental Analysis: Calcd. C, 61.78; H, 7.78; N, 5.15; found C, 61.72; H, 7.68; N, 5.13

Synthesis and Characterization of Compound 5.3



1.0 equivalent of iodine (I_2) (0.12 g, 0.48 mmol) and **5.1** (0.2 g, 0.48 mmol) were taken in a Schlenk flask and 5 ml of benzene was added to the reaction mixture. The reaction was run for an hour at room temperature. The benzene solution was concentrated and filtered through cannula. Colorless crystals of **5.3** were isolated after storing the solution at 4 °C for a day with a yield of 0.3 g (88 %).

1H { ^{11}B } NMR (400 MHz, 298 K, $CDCl_3$): δ = 1.29 (d, J = 6.88 Hz, 12H, $CH(CH_3)_2$), 1.51 (d, J = 6.65 Hz, 12 H, $CH(CH_3)_2$), 2.38 (s, 1H, BHI_2), 2.40 (quintet, J = 5.63 Hz, 2H, $NCH_2CH_2CH_2N$), 3.25 (sept, J = 6.75 Hz, 4H, $CH(CH_3)_2$), 3.72 (t, J = 5.62 Hz, 4H, $NCH_2CH_2CH_2N$), 7.22 (m, 4H, Ar-H), 7.37 (t, J = 7.75 Hz, 2H, Ar-H) ppm

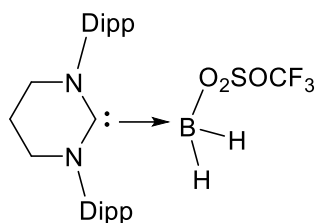
^{13}C { 1H } NMR (101 MHz, 298 K, $CDCl_3$): δ = 20.2, 24.5, 26.3, 28.9, 52.6, 125.1, 129.4, 140.8, 145.0 ppm

^{11}B { 1H } NMR (128 MHz, 298 K, $CDCl_3$): δ = -39.4 (bs, 1B, BHI_2) ppm

ESI-MS (CH_3CN): m/z Calcd. for $C_{28}H_{41}N_2BI_2$ $[M+H]^+$ 671.1525, found 670.8353

Elemental Analysis: Calcd. C, 50.18; H, 6.17; N, 4.18; found C, 50.15; H, 6.12; N, 4.24

Synthesis and Characterization of Compound 5.4



5.4

One equivalent of $\text{AgOSO}_2\text{CF}_3$ (0.10 g, 0.37 mmol) and **5.2** (0.2 g, 0.37 mmol) were taken in a Schlenk flask and 5 ml of toluene was added to the reaction mixture. The reaction was run for 4 h at room temperature. The yellow precipitate of AgI was filtered through frit and the reaction mixture was concentrated. Colorless crystals of **5.4** were isolated after keeping the solution at room temperature for a day with a yield of 0.12 g (55 %).

$^1\text{H}\{^{11}\text{B}\}$ NMR (400 MHz, 298 K, CDCl_3): δ = 1.31 (d, J = 6.88 Hz, 12H, $\text{CH}(\text{CH}_3)_2$), 1.36 (d, J = 6.63 Hz, 12H, $\text{CH}(\text{CH}_3)_2$), 2.34 (quintet, J = 5.50 Hz, 2H, $\text{NCH}_2\text{CH}_2\text{CH}_2\text{N}$), 2.37 (bs, 2H, $\text{BH}_2\text{OSO}_2\text{CF}_3$), 2.98 (sept, J = 6.75 Hz, 4H, $\text{CH}(\text{CH}_3)_2$), 3.56 (t, J = 5.75 Hz, 4H, $\text{NCH}_2\text{CH}_2\text{CH}_2\text{N}$), 7.18 (m, 4H, Ar-H), 7.35 (t, J = 7.75 Hz, 2H, Ar-H) ppm

$^{13}\text{C}\{^1\text{H}\}$ NMR (101 MHz, 298 K, CDCl_3): δ = 23.6, 26.2, 26.1, 29.0, 51.9, 124.3, 129.1, 140.1, 144.9 ppm

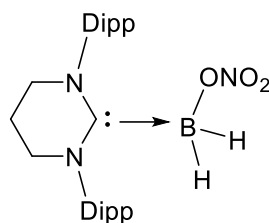
$^{11}\text{B}\{^1\text{H}\}$ NMR (128 MHz, 298 K, CDCl_3): δ = -7.1 (bs, 1B, $\text{BH}_2\text{OSO}_2\text{CF}_3$) ppm

$^{19}\text{F}\{^1\text{H}\}$ NMR (377 MHz, 298 K, CDCl_3): δ = -78.2 (s, 3F, $\text{BH}_2\text{OSO}_2\text{CF}_3$) ppm

ESI-MS (CH_3CN): m/z Calcd. for $\text{C}_{29}\text{H}_{42}\text{N}_2\text{BF}_3\text{SO}_3$ $[\text{M}+\text{Na}]^+$ 579.2839, found 597.2588

Elemental Analysis: Calcd. C, 61.48; H, 7.47; N, 4.94; found C, 61.32; H, 7.62; N, 4.88

Synthesis and Characterization of Compound 5.5



5.5

One equivalent of AgNO₃ (0.07 g, 0.38 mmol) and **5.2** (0.2 g, 0.37 mmol) were taken in a Schlenk flask and 5 ml of toluene was added to the reaction mixture. The reaction was run for 4 h at room temperature. The yellow precipitate of AgI was filtered through frit and the reaction mixture was concentrated. Colorless crystals of **5.5** were isolated after keeping the solution at room temperature for a day with a yield of 0.085 g (48 %).

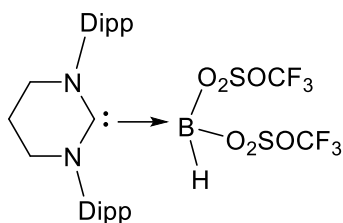
¹H{¹¹B} NMR (400 MHz, 298 K, CDCl₃): δ = 1.28 (d, J = 6.88 Hz, 12H, CH(CH₃)₂), 1.38 (d, J = 6.75 Hz, 12H, CH(CH₃)₂), 2.32 (s, 2H, BH₂ONO₂), 2.37 (m, 2H, NCH₂CH₂CH₂N), 3.04 (sept, J = 6.88 Hz, 4H, CH(CH₃)₂), 3.59 (t, J = 5.88 Hz, 4H, NCH₂CH₂CH₂N), 7.19 (m, 4H, Ar-H), 7.33 (t, J = 7.75 Hz, 2H, Ar-H) ppm

¹³C{¹H} NMR (101 MHz, 298 K, CDCl₃): δ = 19.8, 23.2, 25.9, 28.9, 50.2, 124.3, 125.2, 129.0, 139.9, 144.4 ppm

ESI-MS (CH₃CN): m/z Calcd. for C₂₈H₄₂N₂BN₃O₃ [M+Na]⁺ 507.3375, found 507.3315

Elemental Analysis: Calcd. C, 70.14; H, 8.83; N, 8.76; found C, 70.24; H, 8.79; N, 8.71

Synthesis and Characterization of Compound 5.6



5.6

Two equivalents of $\text{AgOSO}_2\text{CF}_3$ (0.23 g, 0.90 mmol) and **5.3** (0.3 g, 0.45 mmol) were taken in a Schlenk flask and 5 ml of toluene was added to the reaction mixture. The reaction was run for 4 h at room temperature. The yellow precipitate of AgI was filtered through frit and the reaction mixture was concentrated. Colorless crystals of **5.6** were isolated after keeping the solution at -36°C temperature for 3 days with a yield of 0.17 g (54 %).

$^1\text{H NMR}$ (400 MHz, 298 K, CDCl_3): $\delta = 1.28$ (d, $J = 6.88$ Hz, 12H, $\text{CH}(\text{CH}_3)_2$), 1.31 (d, $J = 6.63$ Hz, 12H, $\text{CH}(\text{CH}_3)_2$), 2.34 (s, 1H, $\text{BH}(\text{OSO}_2\text{CF}_3)_2$), 2.46 (quintet, $J = 5.25$ Hz, 2H, $\text{NCH}_2\text{CH}_2\text{CH}_2\text{N}$), 2.96 (sept, $J = 6.75$ Hz, 4H, $\text{CH}(\text{CH}_3)_2$), 3.68 (t, $J = 5.75$ Hz, 4H, $\text{NCH}_2\text{CH}_2\text{CH}_2\text{N}$), 7.20 (m, 4H, Ar-H), 7.42 (t, $J = 7.75$ Hz, 2H, Ar-H) ppm

$^{13}\text{C}\{^1\text{H}\}$ NMR (101 MHz, 298 K, CDCl_3): $\delta = 22.4, 26.3, 29.1, 48.2, 124.9, 130.1, 136.0, 146.1$ ppm

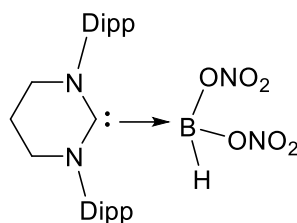
$^{11}\text{B}\{^1\text{H}\}$ NMR (128 MHz, 298 K, CDCl_3): $\delta = -3.24$ (bs, 1B, $\text{BH}(\text{OSO}_2\text{CF}_3)_2$) ppm

$^{19}\text{F}\{^1\text{H}\}$ NMR (377 MHz, 298 K, CDCl_3): $\delta = -78.9$ (s, $2 \times 3\text{F}$, $\text{BH}(\text{OSO}_2\text{CF}_3)_2$) ppm

ESI-MS (CH_3CN): m/z Calcd. for $\text{C}_{30}\text{H}_{41}\text{N}_2\text{BF}_6\text{S}_2\text{O}_6$ $[\text{M}+\text{Na}]^+$ 715.2476, found 715.2108

Elemental Analysis: Calcd. C, 50.42; H, 5.78; N, 3.92; found C, 50.32; H, 5.65; N, 3.88

Synthesis and Characterization of Compound 5.7

**5.7**

Two equivalents of AgNO_3 (0.152 g, 0.90 mmol) and **5.3** (0.3 g, 0.45 mmol) were taken in a Schlenk flask and 5 ml of toluene was added to the reaction mixture. The reaction was run for 12 h at room temperature. The yellow precipitate of AgI was filtered through frit and the reaction mixture was concentrated. Colorless crystals of **5.7** were isolated after keeping the solution at 4 °C temperature for a day with a yield of 0.11 g (46 %).

$^1\text{H}\{^{11}\text{B}\}$ NMR (400 MHz, 298 K, CDCl_3): δ = 1.27 (d, J = 6.88 Hz, 12H, $\text{CH}(\text{CH}_3)_2$), 1.39 (d, J = 6.75 Hz, 12H, $\text{CH}(\text{CH}_3)_2$), 2.37, (s, 1H, $\text{BH}(\text{NO}_3)_2$), 2.39 (m, 2 H, $\text{NCH}_2\text{CH}_2\text{CH}_2\text{N}$), 3.06 (sept, J = 6.88 Hz, 4H, $\text{CH}(\text{CH}_3)_2$), 3.67 (t, J = 5.75 Hz, 4H, $\text{NCH}_2\text{CH}_2\text{CH}_2\text{N}$), 7.23 (m, 4H, Ar-H), 7.38 (t, J = 7.75 Hz, 2 H, Ar-H) ppm

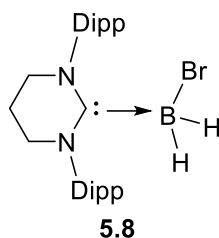
$^{13}\text{C}\{^1\text{H}\}$ NMR (101 MHz, 298 K, CDCl_3): δ = 14.1, 22.6, 26.5, 29.0, 31.6, 51.3, 124.4, 124.6, 129.7, 144.7 ppm

$^{11}\text{B}\{^1\text{H}\}$ NMR (128 MHz, 298 K, CDCl_3): δ = -0.98 (bd, 1B, $\text{BH}(\text{NO}_3)_2$) ppm

ESI-MS (CH_3CN): m/z Calcd. for $\text{C}_{28}\text{H}_{41}\text{N}_4\text{BO}_6$ $[\text{M}]^+$ 540.3114, found 540.3331

Elemental Analysis: Calcd. C, 62.23; H, 7.65; N, 10.37; found C, 60.24; H, 7.29; N, 9.89

Synthesis and Characterization of Compound 5.8



Two equivalents of carbon tetrabromide (CBr_4) (0.32 g, 0.96 mmol) and 6-SIDipp- BH_3 (0.2 g, 0.48 mmol) were taken in a Schlenk flask and 5 ml of toluene was added to it. The reaction mixture was then heated to 105 °C for 24 h. Colorless crystals of **5.8** were isolated from the flask after keeping the solution at room temperature for a day with a yield of 0.17 g (70%).

Alternatively, 1.5 equivalents of *n*-octyl bromide (0.14 g, 0.72 mmol) or *n*-decyl bromide (0.16 g, 0.72 mmol) or *n*-dodecyl bromide (0.18 g, 0.72 mmol) were added to 6-SIDipp- BH_3 (0.2 g, 0.48 mmol) in 5 ml *o*-xylene solvent and at 145 °C for a fixed time period of 48 h. The reaction mixtures were dried completely and 3 ml toluene solvent were added to it. colorless crystal of **5.8** came after keeping the toluene solution for one day at room temperature with a yield of 65%-70%.

Table 6.5.1: Formation of 6-SIDipp- BH_2Br from the reduction of CBr_4 and alkyl halides

Entry	R-Br	Equivalent	Solvent	Temperature (°C)	Time	Yield (%)
1	$\text{C}_8\text{H}_{17}\text{Br}$	1.5	<i>o</i> -Xylene	145	48 h	68
2	$\text{C}_{10}\text{H}_{21}\text{Br}$	1.5	<i>o</i> -Xylene	145	48 h	70
3	$\text{C}_{12}\text{H}_{25}\text{Br}$	1.5	<i>o</i> -Xylene	145	48 h	65

4	CBr ₄	1.2	Toluene	95	48 h	36
5	CBr ₄	2	Toluene	105	24 h	70

¹H NMR (400 MHz, 298 K, CDCl₃): δ = 1.27 (d, J = 6.88 Hz, 12H, CH(CH₃)₂), 1.43 (d, J = 6.63 Hz, 12H, CH(CH₃)₂), 1.56, (s, 2H, BH₂Br), 2.35 (quintet, J = 5.38 Hz, 2H, NCH₂CH₂CH₂N), 3.12 (sept, J = 6.75 Hz, 4H, CH(CH₃)₂), 3.65 (t, J = 5.88 Hz, 4H, NCH₂CH₂CH₂N), 7.20) (d, J = 7.75 Hz, 4H, Ar-*H*), 7.33 (t, J = 7.75 Hz, 2H, Ar-*H*) ppm

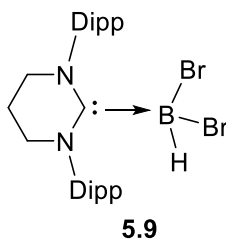
¹³C{¹H} NMR (101 MHz, 298 K, CDCl₃): δ = 19.7 (CH₂CH₂CH₂), 23.7 (CH(CH₃)₂), 26.0 (CH(CH₃)₂), 28.8 (CH(CH₃)₂), 50.5 (NCH₂), 124.4 (Ar-C), 128.9 (Ar-C), 140.8 (Ar-C), 144.6 (Ar-C) ppm, NCN signal not observed

¹¹B{¹H} NMR (128 MHz, 298 K, CDCl₃): δ = -20.1 (bs, 1B, BH₂Br) ppm

HRMS (CH₃CN): m/z Calcd. for C₂₈H₄₂N₂BBR [M-H]⁺ 495.2534, found 497.2541

Elemental Analysis: Calcd. C, 67.62; H, 8.51; N, 5.63; found C, 67.58; H, 8.43; N, 5.41

Synthesis and Characterization of Compound 5.9



1.2 equivalent of N-bromosuccinamide (NBS) (0.102 g, 0.58 mmol) and 6-SIDipp-BH₃ (0.2 g, 0.48 mmol) were taken in a Schlenk flask and 5 ml of toluene was added to the reaction mixture. The reaction was continued for 12 h at 70 °C temperature. Colorless crystals of **5.8** and **5.9** were isolated after keeping the solution at 4 °C for a day, where **5.8** was observed to be the major product

with 40% NMR yield along with 20% NMR yield for **5.9**. As both **5.8** and **5.9** were crystallized in similar reaction condition it's very difficult to separate both the products. Hence the NMRs spectra are given for mixture of products.

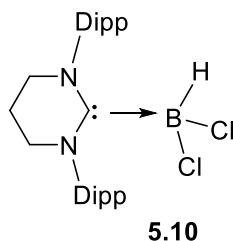
¹H NMR (400 MHz, 298 K, CDCl₃) of 5.9: δ = 1.29 (d, J = 6.63 Hz, 12 H, CH(CH₃)₂), 1.48 (d, J = 6.63 Hz, 12 H, CH(CH₃)₂), 2.37 (quintet, 2 H, NCH₂CH₂CH₂N), 2.76 (s, 4 H, NCH₂CH₂N, NBS), 3.22 (m, 4 H, CH(CH₃)₂), 3.68 (m, J = 5.62 Hz, 4 H, NCH₂CH₂CH₂N), 7.23 (m, 4 H, Ar-H), 7.36 (t, J = 7.75 Hz, 2 H, Ar-H) ppm

¹³C{¹H} NMR (101 MHz, 298 K, CDCl₃) of 5.9: δ = 19.7 (CH₂CH₂CH₂), 23.9 (CH(CH₃)₂), 26.2 (CH(CH₃)₂), 29.5 (N-CH₂CH₂N, NBS), 28.9 (CH(CH₃)₂), 52.3 (NCH₂), 124.6 (Ar-C), 129.1 (Ar-C), 140.3 (Ar-C), 144.8 (Ar-C) ppm, NCN signal not observed

¹¹B{¹H} NMR (128 MHz, 298 K, CDCl₃) 5.8 and 5.9: δ = -14.3 (bs, 1 B, BHBr₂), -20.1 (bs, 1 B, BH₂Br) ppm

HRMS (CH₃CN) of 5.9: m/z Calcd. for C₂₈H₄₁N₂BBr₂ [M+H]⁺ 575.1802, found 575.1605

Synthesis and Characterization of Compound 5.10



A slightly excess of BHCl₂·dioxane (0.05 ml, 0.70 mmol) was added to a 5 ml toluene and 3 ml hexane solution of 6-SIDipp (0.20 g, 0.50 mmol) at room temperature in a flask. Stirring the resulted reaction mixture for further 2 hours at room temperature accessed a white precipitate.

Colorless crystals of **5.10** were isolated after keeping the white powder in the mixture of 1 ml dichloromethane and 2 ml toluene solution for overnight. Yield 0.17 g (68%).

^1H NMR (400 MHz, 298 K, CDCl_3): δ = 1.27 (d, J = 6.85 Hz, 12H, $\text{CH}(\text{CH}_3)_2$), 1.43 (d, J = 6.60 Hz, 12H, $\text{CH}(\text{CH}_3)_2$), 2.35 (q, J = 4.52 Hz, 2H, $\text{NCH}_2\text{CH}_2\text{CH}_2\text{N}$), 3.16 (sept, J = 6.72 Hz, 4H, $\text{CH}(\text{CH}_3)_2$), 3.65 (t, J = 5.87 Hz, 4H, $\text{NCH}_2\text{CH}_2\text{CH}_2\text{N}$), 7.20 (d, J = 7.70 Hz, 4H, Ar- H), 7.34 (t, J = 7.70 Hz, 2H, Ar- H) ppm

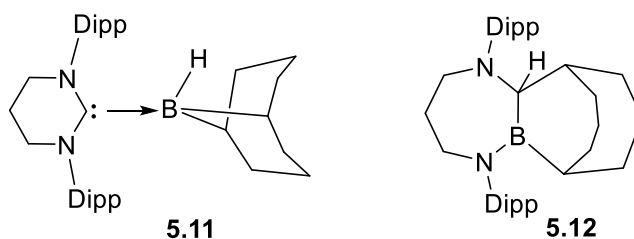
$^{13}\text{C}\{^1\text{H}\}$ NMR (101 MHz, 298 K, CDCl_3): δ = 19.7 ($\text{CH}_2\text{CH}_2\text{CH}_2$), 23.6 ($\text{CH}(\text{CH}_3)_2$), 26.2 ($\text{CH}(\text{CH}_3)_2$), 28.9 ($\text{CH}(\text{CH}_3)_2$), 51.9 (NCH_2), 124.3 (Ar-C), 129.1(Ar-C), 140.1(Ar-C), 144.9 (Ar-C) ppm, NCN signal not observed

$^{11}\text{B}\{^1\text{H}\}$ NMR (128 MHz, 298 K, CDCl_3): δ = -7.4 (s, 1B, BHCl_2) ppm

HRMS (CH_3CN): m/z Calcd. for $\text{C}_{28}\text{H}_{41}\text{BCl}_2\text{N}_2$ [$\text{M}+\text{Na}$] $^+$ 509.2632, found 509.2636

Elemental Analysis: Calcd. C, 68.45; H, 8.48; N, 5.75; found: C, 68.88; H, 8.53; N, 5.48

Synthesis and Characterization of Compounds **5.11** and **5.12**



6-SIDipp (0.20 g, 0.50 mmol) was dissolved in benzene- d_6 (5 mL) in a vial and 9-BBN (0.061 g, 0.50 mmol) was added to this solution at room temperature. The resulting mixture was directly kept at -4 °C to get the crystals of **5.11** after 1 day. When the same resulting mixture was kept at room temperature it gives the colorless crystals of **5.12** after 2 days. We have monitored the conversion of **5.11** to **5.12** via time dependent ^{11}B NMR spectra. **5.11** is unstable at room

temperature and converts to the ring expansion product within 6 hours which is shown below. We have attempted many times but could not get better ^1H and ^{13}C spectrum due to the mixture of product formations.

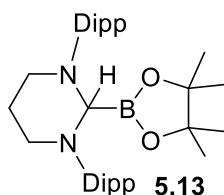
$^{11}\text{B}\{^1\text{H}\}$ NMR (128 MHz, 298 K, C_6D_6) after 30 min reaction: $\delta = -13.3$ (bs, 1B, 9-BBN), 27.9 (bs, 1B, excess 9-BBN) ppm

$^{11}\text{B}\{^1\text{H}\}$ NMR (128 MHz, 298 K, C_6D_6) after 3 h reaction: $\delta = -13.3$ (bs, 1B, 9-BBN), 48.9 (bs, 1 B, NBCNC₃) ppm

$^{11}\text{B}\{^1\text{H}\}$ NMR (128 MHz, 298 K, CDCl_3) after 6 h reaction: $\delta = 49.1$ (bs, 1B, NBCNC₃), 31.9 (bs, 1B, excess 9-BBN), ppm

HRMS (CH_3CN) of **5.12**: m/z Calcd. for $\text{C}_{36}\text{H}_{55}\text{BN}_2$ $[\text{M}+\text{H}]^+$ 527.4531, found 527.4514

Synthesis and Characterization of Compound 5.13



To a benzene- d_6 solution (5 mL) of 6-SIDipp (0.2 g, 0.50 mmol) in a Schlenk flask, one equivalent of HBpin (0.06 g, 0.50 mmol) was added at room temperature. Colorless crystals of **5.13** were isolated from the same flask after keeping the solution at room temperature for a day, with a yield of 0.17 g (65%).

^1H NMR (400 MHz, 298 K, CDCl_3): $\delta = 0.39$ (s, 12H, 2* $\text{C}(\text{CH}_3)_2$ in Bpin), 1.17 (d, $J = 6.88$ Hz, 6H, $\text{CH}(\text{CH}_3)_2$), 1.24 (d, $J = 6.75$ Hz, 6H, $\text{CH}(\text{CH}_3)_2$), 1.31 (d, 6H, $J = 7.00$ Hz, 6H, $\text{CH}(\text{CH}_3)_2$), 1.35 (d, 6H, $J = 6.88$ Hz, 6H, $\text{CH}(\text{CH}_3)_2$), 3.12 (m, 1H, $\text{NCH}_2\text{CH}_2\text{CH}_2\text{N}$), 3.15 (m, 1H,

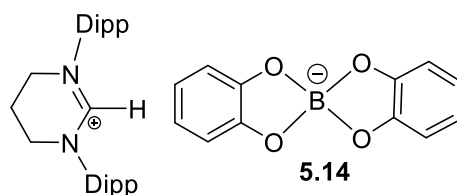
NCH₂CH₂CH₂N), 3.32 (m, 2H, CH(CH₃)₂), 3.36 (m, 2H, CH(CH₃)₂), 4.41 (m, *J* = 5.62 Hz, 4H, NCH₂CH₂CH₂N), 4.88 (s, 1H, N-CH-N), 6.98-7.10 (m, 6H, Ar-*H*) ppm

¹³C{¹H} NMR (101 MHz, 298 K, CDCl₃): δ = 14.1 (C(CH₃)₂; Bpin), 22.3 (CH₂CH₂CH₂), 22.7 (CH₂CH₂CH₂), 23.1 (C(CH₃)₂; Bpin), 23.6 (C(CH₃)₂; Bpin), 25.7 CH(CH₃)₂, 26.2 CH(CH₃)₂, 27.7 CH(CH₃)₂, 28.1 CH(CH₃)₂, 29.3 (CH(CH₃)₂), 31.6 CH(CH₃)₂, 53.7 (NCH₂), 82.7 (NCN), 122.9 (Ar-C), 123.9 (Ar-C), 126.4 (Ar-C), 145.6 (Ar-C), 150.5 (Ar-C), 151.5 (Ar-C) ppm

¹¹B{¹H} NMR (127 MHz, 298 K, CDCl₃): δ = 30.9 (q, 1B, Bpin) ppm

HRMS (CH₃CN): *m/z* Calcd. for C₃₄H₅₃BO₂N₂ [M+H]⁺ 533.4273, found 533.4267

Synthesis and Characterization of Compound 5.14



HBcat (0.072 g, 0.61 mmol) was added to a benzene-*d*₆ solution (4 mL) of 6-SIDipp (0.2 g, 0.50 mmol) in a Schlenk flask at room temperature. Keeping the reaction mixture for 2-3 hours at room temperature produced the crystals of **5.14** with a yield of 0.14 g (46%).

¹H NMR (400 MHz, 298 K, CDCl₃): δ = 1.22 (d, *J* = 6.84 Hz, 12H, CH(CH₃)₂), 1.31 (d, *J* = 6.72 Hz, 12H, CH(CH₃)₂), 2.45 (q, *J* = 5.14 Hz, 2H, NCH₂CH₂CH₂N), 2.83 (sept, *J* = 6.85 Hz, 4H, CH(CH₃)₂), 3.76 (t, *J* = 5.62 Hz, 4H, NCH₂CH₂CH₂N), 6.58-6.61 (m, 8H, Ar-*H*-Bcat), 7.25 (doublet, 4H, Ar-*H*), 7.46 (t, 2H, Ar-*H*), 7.48 (s, 1H, NCHN) ppm

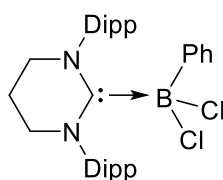
¹³C{¹H} NMR (101 MHz, 298 K, CDCl₃): δ = 18.8 (CH₂CH₂CH₂), 24.6 (CH(CH₃)₂), 28.9 (CH(CH₃)₂), 48.9 (NCH₂), 67.9 (NCN), 108.4 (Ar-C), 117.6 (Ar-C), 125.2 (Ar-C), 128.2 (Ar-C), 128.9 (Ar-C), 131.4 (Ar-C), 135.5 (Ar-C), 145.2 (Ar-C), 151.9 (Ar-C), 153.1 (Ar-C) ppm

$^{11}\text{B}\{^1\text{H}\}$ NMR (377 MHz, 298 K, CDCl_3): $\delta = 14.3$ (s, 1B, $\text{B}(\text{cat})_2$) ppm

HRMS (CH_3CN): m/z Calcd. for $\text{C}_{28}\text{H}_{41}\text{N}_2$ $[\text{M}-\text{C}_{12}\text{H}_8\text{BO}_4]^+$ 405.3264, found 405.3260 and $\text{C}_{12}\text{H}_8\text{BO}_4$ $[\text{M}-\text{C}_{28}\text{H}_{41}\text{N}_2]^+$ 227.0510, found 226.9510

Elemental Analysis: Calcd. C, 75.94; H, 7.81; N, 4.43; found Calcd. C, 75.23; H, 7.52; N, 4.21.

Synthesis and Characterization of Compound 5.16



5.16

6-SIDipp (0.20 g, 0.50 mmol) was dissolved in toluene (5 mL) in a Schlenk flask and toluene solution of PhBCl_2 (0.08 g, 0.50 mmol) was added to it drop by drop at low temperature. The resulting mixture was kept on stirring for 3 h and then allowed to come to room temperature. After completion of the reaction, all the volatiles were completely removed under vacuum and the residue was washed with *n*-hexane. Crystallization of the resulting solid in toluene at 4 °C yielded the colorless crystals of **5.16** with a yield of 0.17 g (61 %). MP = 134 °C.

^1H NMR (400 MHz, 298 K, CDCl_3): $\delta = 1.24$ (d, 12H, $J = 6.75$ Hz, $\text{CH}(\text{CH}_3)_2$), 1.44 (d, $J = 6.63$ Hz, 12H, $\text{CH}(\text{CH}_3)_2$), 2.37 (q, $J = 5.75$ Hz, 2H, $\text{NCH}_2\text{CH}_2\text{CH}_2\text{N}$), 3.34 (sept, $J = 6.75$ Hz, 4H, $\text{CH}(\text{CH}_3)_2$), 3.70 (t, $J = 5.88$ Hz, 4H, $\text{NCH}_2\text{CH}_2\text{CH}_2\text{N}$), 6.71-6.73 (m, 3H, *meta* and *para* H of B-*Ph*), 6.99 (d, $J = 7.63$ Hz, 4H, *ortho*-H of Dipp), 7.04-7.06 (m, 2H, *ortho*-H of B-*Ph*), 7.17 (t, $J = 7.63$ Hz, 2H, *para*-H of Dipp) ppm

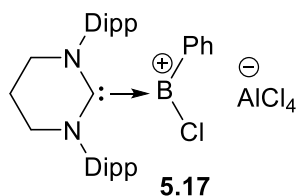
$^{13}\text{C}\{^1\text{H}\}$ NMR (101 MHz, 298 K, CDCl_3): $\delta = 19.2, 24.7, 28.9, 48.8, 125.1, 127.2, 129.9, 131.2, 134.2, 135.7, 145.6, 152.9$ ppm

$^{11}\text{B}\{^1\text{H}\}$ NMR (128 MHz, 298 K, CDCl_3): $\delta = 3.4$ (s, 1B, BPhCl_2) ppm

HRMS (CH_3CN): m/z Calcd. for $\text{C}_{34}\text{H}_{45}\text{BCl}_2\text{N}_2$ $[\text{M}+\text{H}]^+$ 563.3126, found 563.3173

Elemental analysis: Calcd. C, 72.48; H, 8.05; N, 4.97; found C, 71.95; H, 7.75; N, 4.56

Synthesis and Characterization of Compound 5.17



5.16 (0.30 g, 0.53 mmol) and AlCl_3 (0.07 g, 0.53 mmol) were taken in a Schlenk flask and added 10 mL toluene to it at low room temperature and stirred the reaction mixture for 4 h. The resulting solution was filtered through canula. Concentrating and storing the reaction mixture at $-4\text{ }^\circ\text{C}$ afforded crystals of **5.17** with a yield of 0.24 g (65 %). MP = $196\text{ }^\circ\text{C}$.

^1H NMR (400 MHz, 298 K, CDCl_3): $\delta = 1.24$ (d, 12H, $J = 5.88$ Hz, $\text{CH}(\text{CH}_3)_2$), 1.39 (d, $J = 5.24$ Hz, 12H, $\text{CH}(\text{CH}_3)_2$), 2.80 (bs, 2H, $\text{NCH}_2\text{CH}_2\text{CH}_2\text{N}$), 3.05 (sept, $J = 6.75$ Hz, 4H, $\text{CH}(\text{CH}_3)_2$), 4.22 (bs, 4H, $\text{NCH}_2\text{CH}_2\text{CH}_2\text{N}$), 7.26 (d, $J = 7.25$ Hz, 4H, *ortho*-H of Dipp), 7.46 (t, $J = 7.63$ Hz, 2H, *para*-H of Dipp), 7.52 (t, $J = 7.25$ Hz, 2H, *meta*-H of B-Ph), 7.61 (t, $J = 7.38$, 1H, *para*-H of B-Ph), 8.25 (d, $J = 6.75$ Hz, 2H, *ortho*-H of B-Ph) ppm

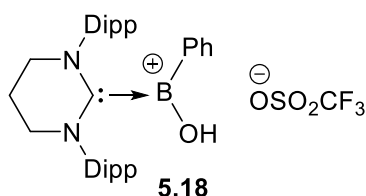
$^{13}\text{C}\{^1\text{H}\}$ NMR (101 MHz, 298 K, CDCl_3): $\delta = 19.1, 21.4, 24.6, 29.0, 48.4, 125.2, 127.9, 131.4, 135.6, 145.5, 153.4$ ppm

$^{11}\text{B}\{^1\text{H}\}$ NMR (128 MHz, 298 K, CDCl_3): $\delta = 29.5$ (s, 1B, BPhCl) ppm

HRMS (CH_3CN): m/z Calcd. for $\text{C}_{34}\text{H}_{45}\text{BClN}_2$ $[(\text{M}-\text{AlCl}_4)+\text{Na}]^+$ 550.3257, found 550.4354

Elemental Analysis: Calcd. C, 58.61; H, 6.51; N, 4.02; found C, 58.28; H, 6.71; N, 4.30

Synthesis and Characterization of Compound 5.18



5.16 (0.09 g, 0.53 mmol) was dissolved in 10 mL toluene in a Schlenk flask and triflic acid (0.05 mL, 0.54 mmol) was added drop by drop to it at 0 °C. The reaction mixture was allowed to come to room temperature and stirred for another 2 h. After that the solution was dried completely and washed with *n*-hexane to remove all the volatiles. Then 8 ml of toluene was added and the reaction mixture was filtered through canula, concentrated and kept at 4 °C, which yielded colorless crystals of **5.18** with a yield of 0.28 g (80 %). MP = 83 °C.

¹H NMR (400 MHz, 298 K, CDCl₃): δ = 1.24 (d, 12H, J = 5.88 Hz, CH(CH₃)₂), 1.40 (d, J = 5.25 Hz, 12H, CH(CH₃)₂), 2.76 (bs, 2H, NCH₂CH₂CH₂N), 3.02 (sept, J = 6.88 Hz, 4H, CH(CH₃)₂), 4.11 (bs, 4H, NCH₂CH₂CH₂N), 7.29 (d, J = 7.25 Hz, 4H, *ortho*-H of Dipp), 7.47 (t, J = 7.63 Hz, 2H, *para*-H of Dipp), 7.52 (t, J = 7.50 Hz, 2H, *meta*-H of B-Ph), 7.61 (t, J = 7.38, 1H, *para*-H of B-Ph), 8.25 (d, J = 6.75 Hz, 2H, *ortho*-H of B-Ph) ppm

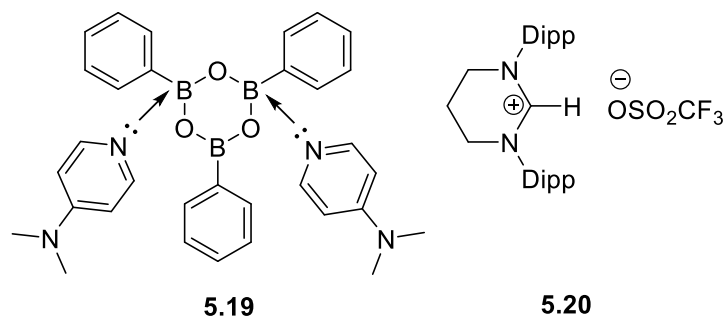
¹³C{¹H} NMR (101 MHz, 298 K, CDCl₃): δ = 19.2, 21.4, 23.8, 24.8, 25.3, 28.9, 48.7, 123.6, 125.3, 129.0, 131.4, 135.5, 137.9, 145.5, 153.2 ppm

¹¹B{¹H} NMR (128 MHz, 298 K, CDCl₃): δ = 28.8 (s, 1B, BPhOH) ppm

¹⁹F{¹H} NMR (377 MHz, 298 K, CDCl₃): δ = -78.2 (s, 3F, OSO₂CF₃) ppm

HRMS (CH₃CN): m/z Calcd. for C₃₄H₄₆BN₂O [M(M'-OTf)]⁺ 509.3698, found 509.3700

Synthesis and Characterization of Compound 5.19 and 5.20



10 mL toluene was added to a Schlenk flask containing **5.18** (0.30 g, 0.46 mmol) and 4-DMAP (0.112 g, 0.92 mmol) and the reaction mixture was stirred for 12 h at room temperature. The reaction mixture was filtered through canula and stored it at 4 °C to give mixture of colorless crystals of compound **5.19** and **5.20** after one day.

¹H NMR of 5.19 (400 MHz, 298 K, CDCl₃): δ = 3.04 (s, 12 H, *CH*₃*NCH*₃(DMAP)), 6.52-8.29 (m, 24 H, H of B-*Ph*) ppm

¹³C{¹H} NMR of 5.19 (101 MHz, 298 K, CDCl₃): δ = 39.3, 106.5, 127.3, 129.1, 133.5, 145.9, 155.1 ppm

¹¹B{¹H} NMR (128 MHz, 298 K, CDCl₃): δ = 20.7 (s, 1B, BOPh), -5.2 (bs, 2B, -O-B(Ph)(DMAP)) ppm

¹⁹F{¹H} NMR (377 MHz, 298 K, CDCl₃): δ = -78.2 (s, 3F, OSO₂CF₃) ppm

HRMS (CH₃CN): *m/z* Calcd. for C₃₂H₃₅B₃O₃N₄ [M+H]⁺ 556.2983, found 556.2556

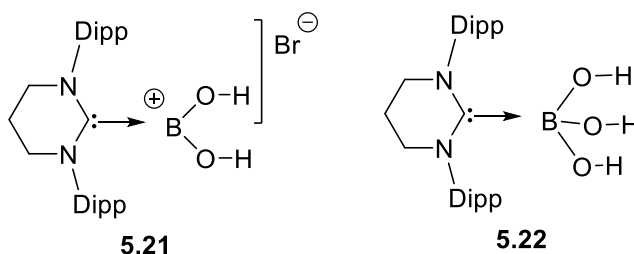
Characterization of Compound 5.20

¹H NMR (400 MHz, 298 K, CDCl₃): δ = 1.22 (d, 12 H, *J* = 6.75 Hz, CH(CH₃)₂), 1.37 (d, *J* = 6.75 Hz, 12 H, CH(CH₃)₂), 2.76 (q, *J* = 5.25 Hz, 2 H, NCH₂CH₂CH₂N), 3.04 (sept, *J* = 6.88 Hz, 4 H, CH(CH₃)₂), 4.26 (t, *J* = 5.63 Hz, 4 H, NCH₂CH₂CH₂N), 7.24 (d, *J* = 7.75 Hz, 4 H, *ortho*-H of Dipp), 7.44 (t, *J* = 7.75 Hz, 2H, *meta*-H of Dipp), 7.56 (*para*-H of Dipp) ppm

$^{13}\text{C}\{^1\text{H}\}$ NMR (101 MHz, 298 K, CDCl_3): $\delta = 19.1, 24.5, 28.6, 48.6, 124.9, 130.9, 135.3, 145.2, 152.7$ ppm

HRMS (CH_3CN): m/z Calcd. for $\text{C}_{28}\text{H}_{41}\text{N}_2$ $[\text{M-OTf}]^+$ 405.3264, found 405.3256

Synthesis and Characterization of Compound 5.21



1.2 equivalent of bromine-water ($\text{Br}_2/\text{H}_2\text{O}$) (0.05 uL, 0.58 mmol) was added to the toluene solution (5 ml) of **5.1** (0.2 g, 0.48 mmol) at low temperature. The reaction was run for 3 h at room temperature. The toluene solution was concentrated and filtered through cannula. Colorless crystals of **5.21** were isolated after keeping the solution at 4 °C for a day with a yield of 0.14 g (55%). The remaining solution was again further kept for recrystallization and colorless crystal of **5.22** were isolated with 7% (16 mg) yield.

^1H NMR (400 MHz, 298 K, CDCl_3): $\delta = 1.26$ (d, $J = 5.88$ Hz, 12H, $\text{CH}(\text{CH}_3)_2$), 1.32 (d, $J = 6.38$ Hz, 12H, $\text{CH}(\text{CH}_3)_2$), 2.48 (bs, 2H, $\text{NCH}_2\text{CH}_2\text{CH}_2\text{N}$), 2.95 (sept, $J = 5.88$ Hz, 4H, $\text{CH}(\text{CH}_3)_2$), 3.71 (bs, 4H, $\text{NCH}_2\text{CH}_2\text{CH}_2\text{N}$), 4.50 (s, 2H, $\text{B}-(\text{OH})_2$), 7.19 (m, 4H, Ar-H), 7.38 (t, $J = 7.58$ Hz, 2H, Ar-H) ppm

$^{13}\text{C}\{^1\text{H}\}$ NMR (101 MHz, 298 K, CDCl_3): $\delta = 19.2, 22.9, 26.8, 29.3, 33.8, 49.1, 125.1, 129.0, 129.2, 131.3, 136.3, 137.9, 146.3$ ppm

$^{11}\text{B}\{^1\text{H}\}$ NMR (127 MHz, 298 K, CDCl_3): $\delta = 25.4$ (bs, 1B, $\text{B}(\text{OH})_2$) ppm

ESI-MS (CH_3CN): m/z Calcd. for $\text{C}_{28}\text{H}_{42}\text{BO}_2\text{N}_2$ $[\text{M}+\text{H}]^+$ 449.3334, found 449.3254

Elemental Analysis: Calcd. C, 63.53; H, 8.00; N, 5.29; found C, 63.42; H, 8.31; N, 5.38

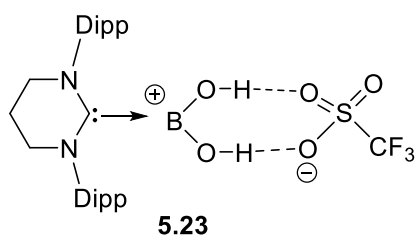
Characterization of Compound 5.22

^1H $\{^{11}\text{B}\}$ NMR (400 MHz, 298 K, CDCl_3): δ = 1.27 (d, J = 6.85 Hz, 12H, $\text{CH}(\text{CH}_3)_2$), 1.42 (d, J = 6.72 Hz, 12H, $\text{CH}(\text{CH}_3)_2$), 2.36 (quintet, J = 4.75 Hz, 2H, $\text{NCH}_2\text{CH}_2\text{CH}_2\text{N}$), 3.16 (sept, J = 6.75 Hz, 4H, $\text{CH}(\text{CH}_3)_2$), 3.63 (t, J = 5.62 Hz, 4H, $\text{NCH}_2\text{CH}_2\text{CH}_2\text{N}$), 7.19 (m, 4H, Ar-H), 7.34 (t, J = 7.5, 2H, Ar-H) ppm

$^{13}\text{C}\{^1\text{H}\}$ NMR (101 MHz, 298 K, CDCl_3): δ = 19.6, 23.5, 26.1, 28.9, 51.9, 124.2, 125.1, 129.0, 131.2, 140.1, 144.8 ppm

$^{11}\text{B}\{^1\text{H}\}$ NMR (127 MHz, 298 K, CDCl_3): δ = -5.2 (s, 1B, $\text{B}(\text{OH})_3$) ppm

Synthesis and Characterization of Compound 5.23



Two equivalents of triflic acid (0.150 g, 1.0 mmol) were added to the DCM solution of **5.10** (0.3 g, 0.5 mmol) at low temperature. The reaction was run for 12 h at room temperature. The reaction mixture was dried completely and washed with hexane for 2 times. Then 5 ml of toluene was added to the reaction mixture and filtered through frit. The reaction mixture was concentrated and colorless crystals of **5.23** were isolated after keeping the solution at room temperature for a day with a yield of 0.11 g (35%).

^1H NMR (400 MHz, 298 K, CDCl_3): δ = 1.27 (d, J = 6.88 Hz, 12H, $\text{CH}(\text{CH}_3)_2$), 1.32 (d, J = 6.75 Hz, 12H, $\text{CH}(\text{CH}_3)_2$), 2.48 (quintet, J = 5.63 Hz, 2H, $\text{NCH}_2\text{CH}_2\text{CH}_2\text{N}$), 2.97 (sept, J = 6.75 Hz, 4H, $\text{CH}(\text{CH}_3)_2$), 3.69 (t, J = 5.75 Hz, 4H, $\text{NCH}_2\text{CH}_2\text{CH}_2\text{N}$), 7.21 (m, J = 7.88 Hz, 4H, Ar- H), 7.43 (t, J = 7.75 Hz, 2H, Ar- H) 7.64 (bs, 2H, $\text{B}(\text{OH})_2$) ppm

$^{13}\text{C}\{^1\text{H}\}$ NMR (101 MHz, 298 K, CDCl_3): δ = 18.7 ($\text{CH}_2\text{CH}_2\text{CH}_2$), 22.5 ($\text{CH}(\text{CH}_3)_2$), 26.3 ($\text{CH}(\text{CH}_3)_2$), 29.2 ($\text{CH}(\text{CH}_3)_2$), 48.2 (NCH_2), 124.9 (Ar-C), 128.2 (Ar-C), 129.0 (Ar-C), 131.1 (Ar-C), 136.1 (Ar-C), 146.1 (Ar-C) ppm, NCN signal not observed

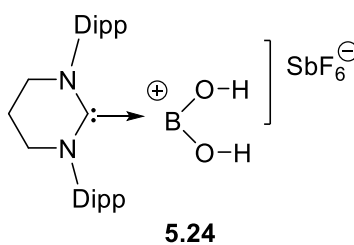
$^{11}\text{B}\{^1\text{H}\}$ NMR (128 MHz, 298 K, CDCl_3): δ = 24.6 (q, 1B, $\text{B}(\text{OH})_2$) ppm

$^{19}\text{F}\{^1\text{H}\}$ NMR (377 MHz, 298 K, CDCl_3): δ = -78.9 (s, 3F, CF_3) ppm

HRMS (CH_3CN): m/z Calcd. for $\text{C}_{29}\text{H}_{42}\text{BF}_3\text{O}_5\text{N}_2\text{S}$ $[\text{M}+\text{H}]^+$ 599.2932, found 599.3036

Elemental Analysis: Calcd. C, 58.20; H, 7.07; N, 4.68; found C, 58.60; H, 7.21; N, 4.53

Synthesis and Characterization of Compound 5.24



One equivalent silver hexafluoroantimonate (AgSbF_6) (0.171 g, 0.50 mmol) was added to the toluene solution of **5.10** (0.3 g, 0.50 mmol) at low temperature. The reaction was run for 4 h at room temperature. The reaction mixture was dried completely and washed with hexane. Then 5 ml of toluene was added to the reaction mixture and filtered through frit. The reaction mixture was concentrated and colorless crystals of **5.24** were isolated after keeping the solution at $-36\text{ }^\circ\text{C}$ temperature for a day with a yield of 0.14 g (42%).

^1H NMR (400 MHz, 298 K, CDCl_3): δ = 1.32 (d, J = 6.88 Hz, 12H, $\text{CH}(\text{CH}_3)_2$), 1.38 (d, J = 6.75 Hz, 12H, $\text{CH}(\text{CH}_3)_2$), 2.33 (q, J = 5.63 Hz, 2H, $\text{NCH}_2\text{CH}_2\text{CH}_2\text{N}$), 3.06 (sept, J = 6.75 Hz, 4H, $\text{CH}(\text{CH}_3)_2$), 3.55 (t, J = 5.75 Hz, 4H, $\text{NCH}_2\text{CH}_2\text{CH}_2\text{N}$), 7.21 (d, J = 7.63 Hz, 4H, Ar- H), 7.36 (t, J = 7.75 Hz, 2H, Ar- H) ppm

$^{13}\text{C}\{^1\text{H}\}$ NMR (101 MHz, 298 K, CDCl_3): δ = 19.6 ($\text{CH}_2\text{CH}_2\text{CH}_2$), 23.3 ($\text{CH}(\text{CH}_3)_2$), 25.7 ($\text{CH}(\text{CH}_3)_2$), 28.9 ($\text{CH}(\text{CH}_3)_2$), 50.5 (NCH_2), 123.9 (Ar-C), 128.8 (Ar-C), 140.4 (Ar-C), 144.7 (Ar-C) ppm, NCN signal not observed

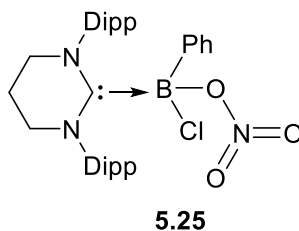
$^{11}\text{B}\{^1\text{H}\}$ NMR (127 MHz, 298 K, CDCl_3): δ = 24.5 (m, 1B, $\text{B}(\text{OH})_2$) and -0.03 (doublet, unknown tetraborate anion fragment due to the decomposition of the **5.24** with time) ppm

$^{19}\text{F}\{^1\text{H}\}$ NMR (377 MHz, 298 K, CDCl_3): δ = -130.7 (s, 6F, SbF_6) ppm

HRMS (CH_3CN): m/z Calcd. for $\text{C}_{28}\text{H}_{42}\text{N}_2\text{O}_2\text{B}$ $[\text{M}+\text{H}]^+$ 450.3412, found 450.3474

Elemental Analysis: Calcd. C, 49.08; H, 6.18; N, 4.09; found C, 49.12; H, 6.68; N, 4.18

Synthesis and Characterization of Compound 5.25



The equimolar amount of **5.16** (0.30 g, 0.53 mmol) and AgNO_3 (0.090 g, 0.53 mmol) (covered in aluminum foil) was taken in a Schlenk flask and dissolved in 10 mL dichloromethane. The reaction was stirred for 12 h at room temperature. Subsequently, the reaction mixture was dried completely and 8 ml of toluene was added to the reaction mixture. After frit filtration, the filtrate was

concentrated and the colorless crystals of **5.25** were isolated after storing the solution at 4 °C for 2 days with a yield of 0.15 g (41%). MP: 162 °C.

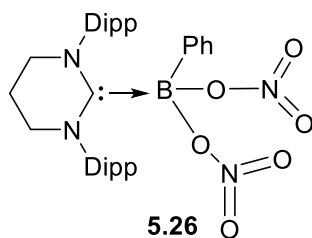
$^1\text{H NMR}$ (400 MHz, 298 K, CDCl_3): $\delta = 1.24$ (d, 12H, $J = 6.50$ Hz, $\text{CH}(\text{CH}_3)_2$), 1.37 (d, $J = 6.38$ Hz, 12H, $\text{CH}(\text{CH}_3)_2$), 2.73 (bs, 4H, $\text{NCH}_2\text{CH}_2\text{CH}_2\text{N}$), 2.97 (sept, $J = 6.38$ Hz, 4H, $\text{CH}(\text{CH}_3)_2$), 4.10 (bs, 4H, $\text{NCH}_2\text{CH}_2\text{CH}_2\text{N}$), 7.25 (d, $J = 7.63$ Hz, 4H, *ortho*-H of Dipp), 7.34 (t, $J = 7.63$ Hz, 2H, *meta*-H of B-Ph), 7.45 (t, $J = 7.93$ Hz, 2H, *para*-H of Dipp), 7.63 (bs, 1H, *para*-H of B-Ph), 7.84 (d, $J = 7.13$ Hz, 2H, *ortho*-H of B-Ph) ppm

$^{13}\text{C}\{^1\text{H}\}$ NMR (101 MHz, 298 K, CDCl_3): $\delta = 19.1, 24.6, 28.8, 48.5, 125.1, 131.3, 135.4, 145.3, 153.2$ ppm

$^{11}\text{B}\{^1\text{H}\}$ NMR (128 MHz, 298 K, CDCl_3): $\delta = 4.7$ (s, 1B, BPhNO₃Cl) ppm

HRMS (CH_3CN): m/z Calcd. for $\text{C}_{34}\text{H}_{45}\text{BClN}_3\text{O}_3$ $[\text{M}+\text{H}]^+$ 589.3237, found 589.3318

Synthesis and Characterization of Compound 5.26



5.16 (0.30 g, 0.53 mmol) and AgNO_3 (0.180 g, 1.06 mmol) were taken in a Schlenk flask in 1:2 ratio and dissolved in 10 mL dichloromethane. The reaction was stirred for 12 h at room temperature. The reaction mixture was dried completely and 8 ml of toluene was added to the reaction mixture. After frit filtration, the filtrate was concentrated and colorless crystals of **5.26** were isolated after storing the solution at room temperature for 4 days with a yield of 0.92 g (28%). MP = 136 °C.

¹H NMR (400 MHz, 298 K, CDCl₃): δ = 1.25 (d, 12H, J = 6.10 Hz, CH(CH₃)₂), 1.38 (d, J = 5.49 Hz, 12 H, CH(CH₃)₂), 2.76 (q, J = 5.19 Hz, 4 H, NCH₂CH₂CH₂N), 3.02 (sept, J = 6.71 Hz, 4 H, CH(CH₃)₂), 4.19 (t, J = 5.19 Hz, 4 H, NCH₂CH₂CH₂N),), 7.25 (d, J = 8.24 Hz, 4 H, *ortho*-H of Dipp), 7.31 (t, J = 7.32 Hz, 2 H, *meta*-H of B-Ph), 7.38 (t, J = 7.32, 1 H, *para*-H of B-Ph), 7.45 (t, J = 7.63 Hz, 2 H, *para*-H of Dipp), 7.85 (d, J = 6.71 Hz, 2 H, *ortho*-H of B-Ph) ppm

6.4.2. Crystallographic data for the structural analysis of compounds 5.1-5.4, 5.6-5.19, 5.21-5.22, 5.25-5.26:

Single crystals were mounted on a Bruker SMART APEX II single crystal X-ray CCD diffractometer having graphite monochromatised (Mo-K α = 0.71073 Å) radiation at low temperature 100 K and 298 K. The X-ray generator was operated at 50 kV and 30 mA. The X-ray data acquisition was monitored by APEX2 program suit. The data were corrected for Lorentz-polarization and absorption effects using SAINT and SADABS programs which are an integral part of APEX2 package. The structures were solved by direct methods and refined by full matrix least squares, based on F^2 , using SHELXL Crystal structures were refined using Olex2-1.0 software. Anisotropic refinement was performed for all non-H atom. The C-H hydrogen atoms were calculated using the riding model. The structures were examined using the ADSYM subroutine of PLATON to assure that no additional symmetry could be applied to the models. The molecular weight of each structure mentioned herein has been calculated considering the solvent molecules trapped in the crystal. Crystallographic information is available at www.ccdc.cam.ac.uk/data with the mentioned CCDC number.

Crystal Data for Compound 5.1 (CCDC 2102132): (C₂₈H₄₃BN₂), colorless, 0.12 × 0.12 × 0.07 mm³, orthorhombic, space group *Pbcn*, a = 19.167(2) Å, b = 14.1542(17) Å, c = 39.176(5) Å, α

$= \beta = \gamma = 90$, $V = 10628(2) \text{ \AA}^3$, $Z = 16$, $T = 100(2) \text{ K}$, $2\theta_{\max} = 48.22^\circ$, $D_{\text{calc}} (\text{g cm}^{-3}) = 1.046$, $F(000) = 3680$, $\mu (\text{mm}^{-1}) = 0.059$, 465420 reflections collected, 10905 unique reflections ($R_{\text{int}} = 0.1436$), 8657 observed ($I > 2\sigma(I)$) reflections, multi-scan absorption correction, $T_{\min} = 0.6275$, $T_{\max} = 0.7454$, 599 refined parameters, $S = 1.145$, $R1 = 0.0644$, $wR2 = 0.1465$ (all data $R = 0.0902$, $wR2 = 0.1612$), maximum and minimum residual electron densities; $\Delta\rho_{\max} = 0.295$, $\Delta\rho_{\min} = -0.483 (\text{e\AA}^{-3})$.

Crystal Data for Compound 5.2 (CCDC 2125724): ($\text{C}_{28}\text{H}_{42}\text{BIN}_2 \cdot \text{C}_7\text{H}_7$), colorless, $0.25 \times 0.15 \times 0.12 \text{ mm}^3$, monoclinic, space group $C2/c$, $a = 30.7004(15) \text{ \AA}$, $b = 13.6937(5) \text{ \AA}$, $c = 18.6768(8) \text{ \AA}$, $\alpha = \gamma = 90$, $\beta = 118.551(3)$, $V = 6896.9(5) \text{ \AA}^3$, $Z = 8$, $T = 100(2) \text{ K}$, $2\theta_{\max} = 66.64^\circ$, $D_{\text{calc}} (\text{g cm}^{-3}) = 1.224$, $F(000) = 2648$, $\mu (\text{mm}^{-1}) = 0.952$, 325196 reflections collected, 16717 unique reflections ($R_{\text{int}} = 0.0516$), 14908 observed ($I > 2\sigma(I)$) reflections, multi-scan absorption correction, $T_{\min} = 0.6797$, $T_{\max} = 0.7471$, 379 refined parameters, $S = 1.124$, $R1 = 0.0345$, $wR2 = 0.0929$ (all data $R = 0.0409$, $wR2 = 0.1005$), maximum and minimum residual electron densities; $\Delta\rho_{\max} = 3.047$, $\Delta\rho_{\min} = -2.301 (\text{e\AA}^{-3})$.

Crystal Data for Compound 5.3 (CCDC 2123602): ($\text{C}_{28}\text{H}_{41}\text{BI}_2\text{N}_2$), colorless, $0.1 \times 0.06 \times 0.05 \text{ mm}^3$, monoclinic, space group $P2_1/n$, $a = 9.5036(4) \text{ \AA}$, $b = 19.9724(6) \text{ \AA}$, $c = 16.0540(6) \text{ \AA}$, $\alpha = \gamma = 90$, $\beta = 103.2450(10)$, $V = 2966.15(19) \text{ \AA}^3$, $Z = 4$, $T = 100(2) \text{ K}$, $2\theta_{\max} = 68.59^\circ$, $D_{\text{calc}} (\text{g cm}^{-3}) = 1.501$, $F(000) = 1336$, $\mu (\text{mm}^{-1}) = 2.43$, 119156 reflections collected, 10349 unique reflections ($R_{\text{int}} = 0.0482$), 9558 observed ($I > 2\sigma(I)$) reflections, multi-scan absorption correction, $T_{\min} = 0.5564$, $T_{\max} = 0.7467$, 306 refined parameters, $S = 1.222$, $R1 = 0.0350$, $wR2 = 0.1352$ (all data $R = 0.0431$, $wR2 = 0.1510$), maximum and minimum residual electron densities; $\Delta\rho_{\max} = 2.177$, $\Delta\rho_{\min} = -3.068 (\text{e\AA}^{-3})$.

Crystal Data for Compound 5.4 (CCDC 2123596): ($C_{29}H_{42}BF_3N_2O_3S$), colorless, $0.24 \times 0.12 \times 0.1 \text{ mm}^3$, triclinic, space group $P-1$, $a = 9.601(6) \text{ \AA}$, $b = 9.604(6) \text{ \AA}$, $c = 18.081(11) \text{ \AA}$, $\alpha = 97.88(2)$, $\beta = 90.02(2)$, $\gamma = 108.16(3)$, $V = 1567.4(17) \text{ \AA}^3$, $Z = 2$, $T = 100(2) \text{ K}$, $2\theta_{\max} = 60.42^\circ$, $D_{\text{calc}} (\text{g cm}^{-3}) = 1.200$, $F(000) = 604$, $\mu (\text{mm}^{-1}) = 0.152$, 102707 reflections collected, 11185 unique reflections ($R_{\text{int}} = 0.0811$), 7314 observed ($I > 2\sigma(I)$) reflections, multi-scan absorption correction, $T_{\min} = 0.6558$, $T_{\max} = 0.7465$, 360 refined parameters, $S = 1.076$, $R1 = 0.0579$, $wR2 = 0.1627$ (all data $R = 0.1096$, $wR2 = 0.1912$), maximum and minimum residual electron densities; $\Delta\rho_{\max} = 0.719$, $\Delta\rho_{\min} = -1.218 (\text{e\AA}^{-3})$.

Crystal Data for Compound 5.6 (CCDC 2123605): ($C_{30}H_{41}BF_6N_2O_6S_2$), colorless, $0.22 \times 0.12 \times 0.09 \text{ mm}^3$, monoclinic, space group $P2_1/c$, $a = 17.311(3) \text{ \AA}$, $b = 11.1748(15) \text{ \AA}$, $c = 17.490(3) \text{ \AA}$, $\alpha = \gamma = 90$, $\beta = 96.691(7)$, $V = 3360.5(9) \text{ \AA}^3$, $Z = 4$, $T = 100(2) \text{ K}$, $2\theta_{\max} = 50.48^\circ$, $D_{\text{calc}} (\text{g cm}^{-3}) = 1.412$, $F(000) = 1496$, $\mu (\text{mm}^{-1}) = 0.236$, 113806 reflections collected, 12070 unique reflections ($R_{\text{int}} = 0.0487$), 9829 observed ($I > 2\sigma(I)$) reflections, multi-scan absorption correction, $T_{\min} = 0.6731$, $T_{\max} = 0.7467$, 432 refined parameters, $S = 1.129$, $R1 = 0.0361$, $wR2 = 0.1029$ (all data $R = 0.0537$, $wR2 = 0.1211$), maximum and minimum residual electron densities; $\Delta\rho_{\max} = 0.918$, $\Delta\rho_{\min} = -0.884 (\text{e\AA}^{-3})$.

Crystal Data for Compound 5.7 (CCDC 2123606): ($C_{28}H_{41}BN_4O_6$), colorless, $0.22 \times 0.11 \times 0.08 \text{ mm}^3$, monoclinic, space group $P2_1/c$, $a = 18.736(3) \text{ \AA}$, $b = 8.3227(19) \text{ \AA}$, $c = 18.866(3) \text{ \AA}$, $\alpha = \gamma = 90$, $\beta = 96.145(5)$, $V = 2925.0(10) \text{ \AA}^3$, $Z = 4$, $T = 100(2) \text{ K}$, $2\theta_{\max} = 62.78^\circ$, $D_{\text{calc}} (\text{g cm}^{-3}) = 1.227$, $F(000) = 1160$, $\mu (\text{mm}^{-1}) = 0.086$, 90856 reflections collected, 9543 unique reflections ($R_{\text{int}} = 0.0487$), 7541 observed ($I > 2\sigma(I)$) reflections, multi-scan absorption correction, $T_{\min} = 0.6465$, $T_{\max} = 0.7462$, 432 refined parameters, $S = 1.152$, $R1 = 0.0637$, $wR2 = 0.1651$ (all data $R = 0.0875$,

$wR2 = 0.1820$), maximum and minimum residual electron densities; $\Delta\rho_{\max} = 0.683$, $\Delta\rho_{\min} = -0.476$ ($\text{e}\text{\AA}^{-3}$).

Crystal Data for Compound 5.16 (CCDC 2102134): ($\text{C}_{34}\text{H}_{45}\text{BCl}_2\text{N}_2\cdot\text{C}_6\text{H}_6$) Sum formula, colorless, $0.14 \times 0.12 \times 0.10 \text{ mm}^3$, monoclinic, space group $P2_1/n$, $a = 14.805(6) \text{ \AA}$, $b = 15.822(6) \text{ \AA}$, $c = 17.997(6) \text{ \AA}$, $\alpha = \gamma = 90$, $\beta = 98.638(18)$, $V = 4168(3) \text{ \AA}^3$, $Z = 4$, $T = 100(2) \text{ K}$, $2\theta_{\max} = 56.38^\circ$, $D_{\text{calc}} (\text{g cm}^{-3}) = 1.022$, $F(000) = 1376$, $\mu (\text{mm}^{-1}) = 0.182$, 118273 reflections collected, 10300 unique reflections ($R_{\text{int}} = 0.083$), 8078 observed ($I > 2\sigma(I)$) reflections, multi-scan absorption correction, $T_{\min} = 0.6622$, $T_{\max} = 0.7457$, 414 refined parameters, $S = 1.091$, $R1 = 0.0552$, $wR2 = 0.1639$ (all data $R = 0.0733$, $wR2 = 0.1808$), maximum and minimum residual electron densities; $\Delta\rho_{\max} = 0.782$, $\Delta\rho_{\min} = -0.430$ ($\text{e}\text{\AA}^{-3}$).

Crystal Data for Compound 5.17 (CCDC 2153463): ($\text{C}_{34}\text{H}_{45}\text{AlBCl}_5\text{N}_2$), colorless, $0.12 \times 0.1 \times 0.07 \text{ mm}^3$, monoclinic, space group $P 2_1/c$, $a = 10.6046(15) \text{ \AA}$, $b = 18.021(2) \text{ \AA}$, $c = 19.456(3) \text{ \AA}$, $\alpha = \gamma = 90$, $\beta = 96.127(4)$, $V = 3696.9(9) \text{ \AA}^3$, $Z = 4$, $T = 100 \text{ K}$, $2\theta_{\max} = 51.4^\circ$, $D_{\text{calc}} (\text{g cm}^{-3}) = 1.252$, $F(000) = 1464$, $\mu (\text{mm}^{-1}) = 0.442$, 142086 reflections collected, 6486 unique reflections ($R_{\text{int}} = 0.0782$), 5469 observed ($I > 2\sigma(I)$) reflections, multi-scan absorption correction, $T_{\min} = 0.6609$, $T_{\max} = 0.7453$, 416 refined parameters, $S = 1.090$, $R1 = 0.1206$, $wR2 = 0.3536$ (all data $R = 0.1355$, $wR2 = 0.3744$), maximum and minimum residual electron densities; $\Delta\rho_{\max} = 0.990$, $\Delta\rho_{\min} = -1.042$ ($\text{e}\text{\AA}^{-3}$).

Crystal Data for Compound 5.18 (CCDC 2153464): ($\text{C}_{42}\text{H}_{54}\text{BF}_3\text{N}_2\text{O}_4\text{S}$), colorless, $0.15 \times 0.12 \times 0.08 \text{ mm}^3$, monoclinic, space group $P2_1/c$, $a = 12.0999(9) \text{ \AA}$, $b = 19.0144(14) \text{ \AA}$, $c = 18.1852(13) \text{ \AA}$, $\alpha = \gamma$, $\beta = 104.995(3)$, $V = 4041.4(5) \text{ \AA}^3$, $Z = 4$, $T = 100 (2) \text{ K}$, $2\theta_{\max} = 69.48^\circ$, $D_{\text{calc}} (\text{g cm}^{-3}) = 1.234$, $F(000) = 1600$, $\mu (\text{mm}^{-1}) = 0.136$, 149282 reflections collected, 17799 unique reflections

($R_{\text{int}} = 0.0636$), 14547 observed ($I > 2\sigma(I)$) reflections, multi-scan absorption correction, $T_{\text{min}} = 0.6601$, $T_{\text{max}} = 0.7469$, 487 refined parameters, $S = 1.082$, $R1 = 0.060$, $wR2 = 0.1655$ (all data $R = 0.0751$, $wR2 = 0.1776$), maximum and minimum residual electron densities; $\Delta\rho_{\text{max}} = -0.766$, $\Delta\rho_{\text{min}} = 1.104$ ($\text{e}\text{\AA}^{-3}$).

Crystal Data for Compound 5.19 (CCDC 2153465): ($\text{C}_{46}\text{H}_{51}\text{B}_3\text{N}_4\text{O}_3$), colorless, $0.26 \times 0.12 \times 0.06$ mm^3 , triclinic, space group $P-1$, $a = 10.8369(16)$ \AA , $b = 14.0568(19)$ \AA , $c = 14.774(2)$ \AA , $\alpha = 86.965(5)$, $\beta = 82.058(5)$, $\gamma = 77.879(5)$, $V = 2178.6(5)$ \AA^3 , $Z = 2$, $T = 100(2)$ K, $2\theta_{\text{max}} = 65.5^\circ$, D_{calc} (g cm^{-3}) = 1.129, $F(000) = 788$, μ (mm^{-1}) = 0.069, 49360 reflections collected, 7574 unique reflections ($R_{\text{int}} = 0.071$), 6725 observed ($I > 2\sigma(I)$) reflections, multi-scan absorption correction, $T_{\text{min}} = 0.6064$, $T_{\text{max}} = 0.7465$, 576 refined parameters, $S = 1.030$, $R1 = 0.0500$, $wR2 = 0.1322$ (all data $R = 0.0553$, $wR2 = 0.1376$), maximum and minimum residual electron densities; $\Delta\rho_{\text{max}} = 0.459$, $\Delta\rho_{\text{min}} = -0.348$ ($\text{e}\text{\AA}^{-3}$).

Crystal Data for Compound 5.21 (CCDC 2123612): ($\text{C}_{28}\text{H}_{42}\text{BBrN}_2\text{O}_2$), colorless, $0.15 \times 0.12 \times 0.06$ mm^3 , orthorhombic, space group $Pnma$, $a = 16.517(10)$ \AA , $b = 20.453(9)$ \AA , $c = 8.264(3)$ \AA , $\alpha = \beta = \gamma = 90$, $V = 2792(2)$ \AA^3 , $Z = 4$, $T = 100(2)$ K, $2\theta_{\text{max}} = 42.30^\circ$, D_{calc} (g cm^{-3}) = 1.259, $F(000) = 1120$, μ (mm^{-1}) = 1.499, 64957 reflections collected, 2527 unique reflections ($R_{\text{int}} = 0.194$), 1755 observed ($I > 2\sigma(I)$) reflections, multi-scan absorption correction, $T_{\text{min}} = 0.6212$, $T_{\text{max}} = 0.7457$, 173 refined parameters, $S = 1.071$, $R1 = 0.0412$, $wR2 = 0.0855$ (all data $R = 0.0795$, $wR2 = 0.1063$), maximum and minimum residual electron densities; $\Delta\rho_{\text{max}} = 0.558$, $\Delta\rho_{\text{min}} = -0.659$ ($\text{e}\text{\AA}^{-3}$).

Crystal Data for Compound 5.22 (CCDC 2123642): ($\text{C}_{28}\text{H}_{40}\text{BN}_2\text{O}_4$), colorless, $0.15 \times 0.10 \times 0.08$ mm^3 , orthorhombic, space group $Pnma$, $a = 12.325(3)$ \AA , $b = 20.525(5)$ \AA , $c = 10.920(3)$ \AA , $\alpha = \beta = \gamma = 90$, $V = 2762.4(12)$ \AA^3 , $Z = 4$, $T = 293(2)$ K, $2\theta_{\text{max}} = 59.66^\circ$, D_{calc} (g cm^{-3}) = 1.153,

$F(000) = 1036$, μ (mm^{-1}) = 0.076, 215531 reflections collected, 4981 unique reflections ($R_{\text{int}} = 0.100$), 3797 observed ($I > 2\sigma(I)$) reflections, multi-scan absorption correction, $T_{\text{min}} = 0.6965$, $T_{\text{max}} = 0.7463$, 176 refined parameters, $S = 1.110$, $R1 = 0.0979$, $wR2 = 0.2878$ (all data $R = 0.1463$, $wR2 = 0.3238$), maximum and minimum residual electron densities; $\Delta\rho_{\text{max}} = 0.720$, $\Delta\rho_{\text{min}} = -1.319$ ($\text{e}\text{\AA}^{-3}$).

Crystal Data for Compound 5.25 (CCDC 2153460): ($\text{C}_{34}\text{H}_{45}\text{BClN}_{3.25}\text{O}_3$), colorless, $0.15 \times 0.11 \times 0.08$ mm^3 , monoclinic, space group $P2_1/n$, $a = 12.8105(15)$ \AA , $b = 17.071(2)$ \AA , $c = 15.1302(17)$ \AA , $\alpha = \gamma = 90$, $\beta = 98.179(4)$, $V = 3275.1(7)$ \AA^3 , $Z = 4$, $T = 100(2)$ K, $2\theta_{\text{max}} = 52.7^\circ$, D_{calc} (g cm^{-3}) = 1.204, $F(000) = 1271$, μ (mm^{-1}) = 0.154, 138965 reflections collected, 6728 unique reflections ($R_{\text{int}} = 0.0893$), 5527 observed ($I > 2\sigma(I)$) reflections, multi-scan absorption correction, $T_{\text{min}} = 0.7070$, $T_{\text{max}} = 0.7454$, 401 refined parameters, $S = 1.134$, $R1 = 0.0768$, $wR2 = 0.1992$ (all data $R = 0.0986$, $wR2 = 0.2188$), maximum and minimum residual electron densities; $\Delta\rho_{\text{max}} = 0.461$, $\Delta\rho_{\text{min}} = -0.855$ ($\text{e}\text{\AA}^{-3}$).

Crystal Data for Compound 5.26 (CCDC 2153461): ($\text{C}_{37.50}\text{H}_{48.50}\text{BN}_4\text{O}_6$), colorless, $0.22 \times 0.16 \times 0.07$ mm^3 , triclinic, space group $P-1$, $a = 9.3097(5)$ \AA , $b = 10.3396(6)$ \AA , $c = 20.4624(11)$ \AA , $\alpha = 84.254(2)$, $\beta = 84.315(2)$, $\gamma = 63.441(2)$, $V = 1749.71(17)$ \AA^3 , $Z = 2$, $T = 100(2)$ K, $2\theta_{\text{max}} = 72.54^\circ$, D_{calc} (g cm^{-3}) = 1.257, $F(000) = 709$, μ (mm^{-1}) = 0.085, 82311 reflections collected, 6140 unique reflections ($R_{\text{int}} = 0.0971$), 5300 observed ($I > 2\sigma(I)$) reflections, multi-scan absorption correction, $T_{\text{min}} = 0.4948$, $T_{\text{max}} = 0.7476$, 461 refined parameters, $S = 1.036$, $R1 = 0.0384$, $wR2 = 0.0969$ (all data $R = 0.0452$, $wR2 = 0.1015$), maximum and minimum residual electron densities; $\Delta\rho_{\text{max}} = 0.330$, $\Delta\rho_{\text{min}} = -0.297$ ($\text{e}\text{\AA}^{-3}$).

6.4.3. Details of theoretical calculations for the formation of 5.3 and 5.13

All the calculations in this study have been performed with density functional theory (DFT), with the aid of the Turbomole 7.5 suite of programs,⁴ using the PBE functional,⁵ along with dispersion correction (DFT-D3) for **5.3**.⁶ The def-TZVP basis set⁷ has been employed. The resolution of identity (RI),⁸ along with the multipole accelerated resolution of identity (marij)⁹ approximations have been employed for an accurate and efficient treatment of the electronic Coulomb term in the DFT calculations. Solvent correction was incorporated with optimization calculations using the COSMO model,¹⁰ with toluene ($\epsilon = 2.374$) as the solvent. The values reported are ΔG values, with zero-point energy corrections, internal energy and entropic contributions were included through frequency calculations on the optimized minima, with the temperature taken to be 298.15 K. The translational entropy term in the calculated structures was corrected through a free volume correction introduced by Mammen *et al.*¹¹ This volume correction is to account for the unreasonable enhancement in translational entropy that is generally observed in computational software. Harmonic frequency calculations were performed for all stationary points to confirm them as local minima or transition state structures.

Energy profile for the disubstitution reaction of 5-IDipp·BH₃:

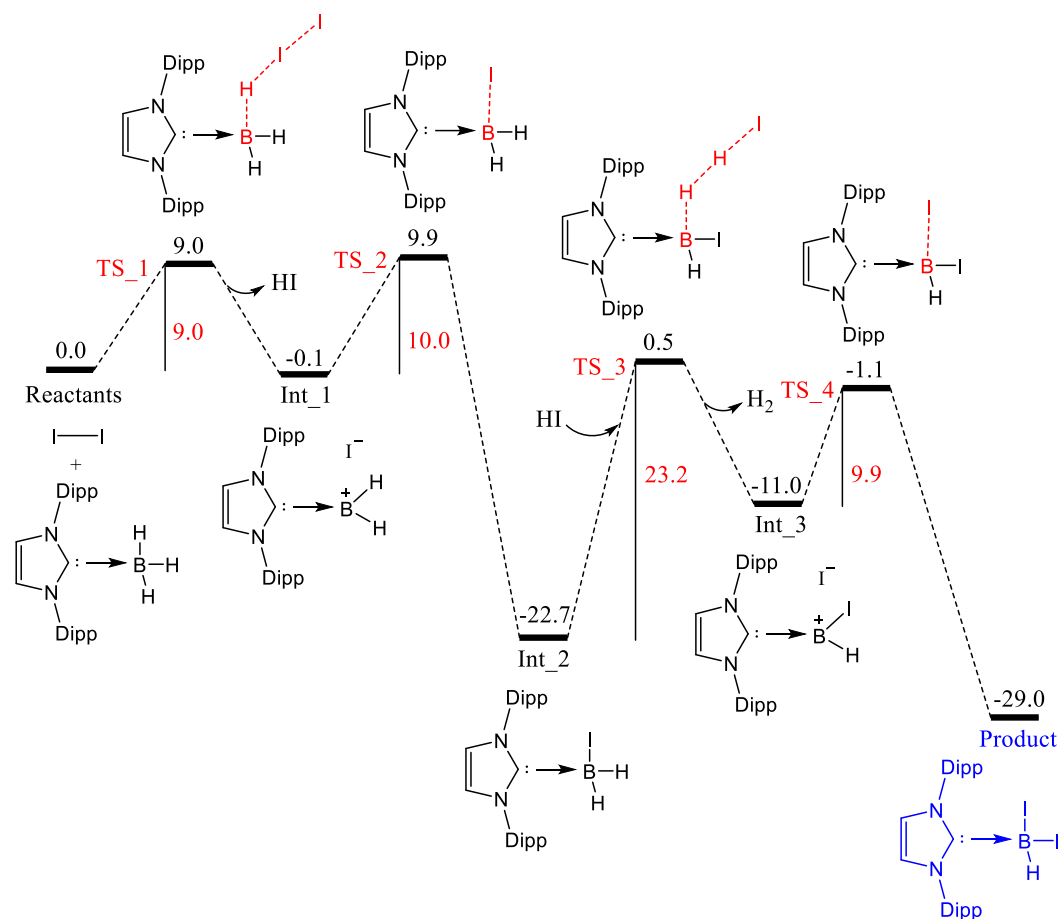


Figure 6.5.1. The free energy profile for the disubstitution reaction of 5-IDipp·BH₃ by the iodine molecule. Values are in kcal/mol.

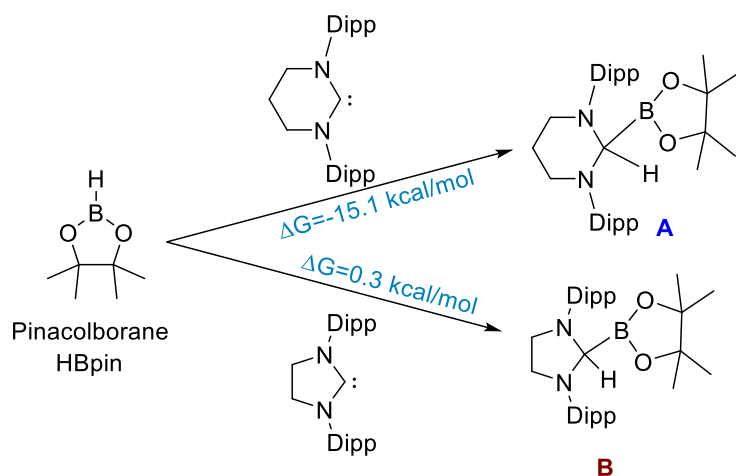


Figure 6.5.2. The comparison between six-membered NHC and five-membered NHC after oxidative addition of HBpin. The values (in kcal/mol) have been calculated at the PBE/TZVP level of theory with DFT.

6.4.4. Cyclic voltammogram of 5.21

All experiments were carried out under an atmosphere of argon in degassed and anhydrous acetonitrile solution containing $n\text{-Bu}_4\text{NPF}_6$ (0.1 M) at a scan rate of 0.70 V s^{-1} . The set up consisted of a glassy carbon working electrode (surface area = 0.04 cm^2), Pt counter electrode, Ag/AgCl reference electrode and 0.1 M $n\text{-Bu}_4\text{NPF}_6$ solution in acetonitrile as the electrolyte.

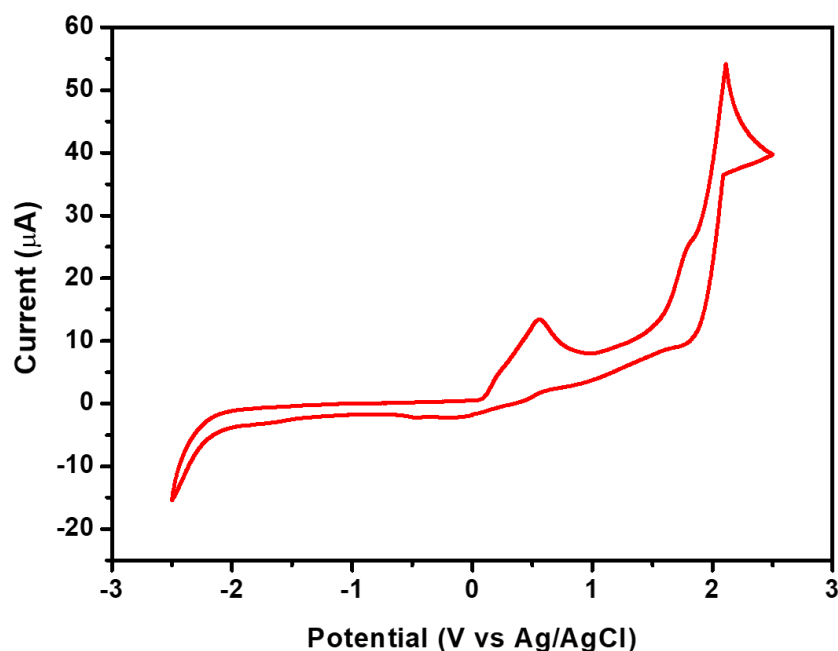


Figure 6.5.3. The cyclic voltammogram of 5.21 were recorded at 0.7 V s^{-1} .

ABSTRACT

Name of the Student: Gargi Kundu

Registration No.: 10CC17A26014

Faculty of Study: Chemical Science

Year of Submission: 2022

AcSIR academic centre/CSIR Lab: CSIR-NCL **Name of the Supervisor:** Dr. Sakya S. Sen

Title of the thesis: An excursion into the chemistry of more nucleophilic saturated N-heterocyclic carbenes

This thesis covers the work to develop cheap and biocompatible metal complexes that can be used as an alternative to transition metal complexes. Transition metal chemistry forms the heart of small molecule activation due to the availability of partially filled d-orbitals, allowing fast and reversible changes in the metal's oxidation states. The last two decades have witnessed that main group metal complexes, especially N-heterocyclic carbenes were used as the alternative to transition metal complexes. NHCs have been reported and made the chemistry rich with their novel and unprecedented bonding and reactivity studies. In this regard, saturated NHCs represent a special class due to their more nucleophilic character compared to their unsaturated analogues. Higher HOMOs of the SNHCs results in the lower HOMO-LUMO gap compared to the unsaturated NHCs. In the same vein, the six-membered saturated NHC possesses more nucleophilicity than 5-membered NHCs and CAACs. *Chapter 2* accounts the deprotonation of 5-SIDipp by the C-F bond of C₆F₆ and it affords a mesoionic compound with concomitant elimination of HF. Neither, NHCs nor CAACs are known to generate such mesoionic compounds by such a single-step C-F bond activation. *Chapter 3* illustrates a new synthetic pathway to prepare the NHC based Kekulé di-radicaloids. To prepare the NHC analogue of Thiele's and Chichibabin's hydrocarbon we have exploited the C-F activation strategy. The replacement of the hydrogens with fluorines reduce the singlet-triplet energy gap and increase the diradical character. *Chapter 4* described the NHC·borane chemistry with 5-SIDipp. NHC·boranes are typically readily accessible, but no NHC adduct of MeBCl₂ has been known. Herein, we have prepared the first N-Heterocyclic carbene boranes bearing methyl groups by simple salt metathesis reaction starting from 5-SIDipp·BCl₃. *Chapter 5* represents the reactivity of 6-SNHC in boron chemistry. Herein, we have shown the NHC mediated 1, 1 B-H activation of HBpin, ring expansion of 6-NHC and substitution at tetra-coordinated boron centre.

**List of publication(s) in SCI Journal(s) (published & accepted) emanating
from the thesis work, with complete bibliographic details**

1. **Gargi Kundu**, Ruchi Dixit, Srinu Tothadi, Kumar Vanka, Sakya S. Sen*: Versatile chemistry of six-membered NHC with boranes: bromination at sp^3 borane, activation of B–H bond of HBpin, and formation of dihydroxyborenium cation. *Dalton Transactions*, **2022**. (Just accepted)
2. **Gargi Kundu**, Kajal Balayan, Srinu Tothadi, Sakya S. Sen*: Six-membered Saturated NHC Stabilized Borenium Cations: Isolation of a Cationic Analogue of Borinic Acid. *Inorganic Chemistry*, **2022**. (DOI: 10.1021/acs.inorgchem.2c00611)
3. **Gargi Kundu**, V. S. Ajithkumar, K. Vipin Raj, Kumar Vanka, Srinu Tothadi, Sakya S. Sen*, Substitution at sp^3 Boron of a Six-membered NHC-BH₃: Convenient Access to a Dihydroxyborenium Cation. *Chemical Communications* **2022**, 58, 3873–3876.
4. **Gargi Kundu**, Srinu Tothadi, Sakya S. Sen*: Nucleophilic Substitution at a Coordinatively Saturated Five-membered SNHC·haloborane Centre. *Inorganics* **2022**, 10, 97. (Invited article for the Special Issue "Fifth Element: The Current State of Boron Chemistry")
5. **Gargi Kundu**, V. S. Ajithkumar, Milan Kumar Bisai, Srinu Tothadi, Tamal Das, Kumar Vanka, Sakya S. Sen*: Diverse Reactivity of Carbenes and Silylenes towards Fluoropyridines. *Chemical Communications* **2021**, 57, 4428–4431.
6. **Gargi Kundu**, Sanjukta Pahar, Srinu Tothadi, Sakya S. Sen*: Stepwise Nucleophilic Substitution to Access Saturated N-heterocyclic Carbene Haloboranes with Boron–Methyl Bonds. *Organometallics* **2020**, 39, 4696–4703.
7. **Gargi Kundu**, Sriman De, Srinu Tothadi, Abhisek Das, Debasis Koley*, Sakya S. Sen*: Saturated N-Heterocyclic Carbene Based Thiele's Hydrocarbon with a Tetrafluorophenylene Linker. *Chemistry – A European Journal* **2019**, 25, 16533–16537. (Selected as a Hot paper)
8. Moumita Pait[†], **Gargi Kundu**[†], Srinu Tothadi, Suvendu Karak, Shaila Jain, Kumar Vanka, Sakya Singha Sen*: C–F Bond Activation by a Saturated N-Heterocyclic Carbene: Mesoionic Compound Formation and Adduct Formation with B(C₆F₅)₃. *Angewandte Chemie International Edition* **2019**, 58, 2804–2808. ([†]: Equal contribution).

**List of papers with abstract presented (oral/poster) at
national/international conferences/seminars with complete details**

1. Presented a poster on National Science Day Celebrations at CSIR-National Chemical Laboratory, Pune, India, February 2019. **(Received best poster award)**
Title: *NHC Mediated C–F Bond Activation and Subsequent Derivatization*
2. Presented a research poster at “International Conference on Structural and Inorganic Chemistry-II” (ICSIC-II), held during 17-18 March, 2019 at IISER Pune, India. **(Received best poster award)**
Title: *N-Heterocyclic Carbene Mediated C–F Bond Activation and subsequent Derivatization*
3. Presented a research poster in “MODERN TRENDS IN INORGANIC CHEMISTRY-XVIII” (MTIC-XVIII), held in December, 2019 at Indian Institute of Technology Guwahati, India.
Title: *NHC Mediated C–F Bond Activation and Subsequent Derivatization*
4. Presented a poster on National Science Day Celebrations at CSIR-National Chemical Laboratory, Pune, India, February, 2020. **(Received best poster award)**
Title: *N-Heterocyclic Carbene Mediated C-F Bond Activation and subsequent Derivatization*
5. Presented poster at “#LatinXChem Twitter Conference 2020” held on September 7th, 2020 on twitter. (Gargi Kundu and Sakya Singha Sen) **(Ranked 4th in the honorable mention)**
Title: *NHC mediated C-F Bond Activation of perfluoroarenes*
6. Presented a poster on National Science Day Celebrations at CSIR-National Chemical Laboratory, Pune, India, February 2021.
Title: *N-heterocyclic Carbene reactivity with boranes: B-H activation vs Adduct formation*
7. Presented a poster at “RSC Poster Twitter Conference 2021” held on March 2–3, 2021.
Title: *NHC Mediated C-F bond Activation and Subsequent Derivatization*
8. Proster at “#LatinXChem Twitter Conference 2020” held on September 20th, 2021 on twitter.
Title: *Saturated N-heterocyclic Carbene reactivity with boranes: B-H activation vs Adduct formation*

9. Presented poster at “International Conference on Main-group Molecules to Materials-II (MMM-II)” held during 13–15 December, 2021, organized virtually by NISER, Bhubaneswar. **(Received best poster award)**

Title: *Substitution at Coordinatively Saturated Boron Center*

10. Presented poster at the “58th Annual Convention of Chemists” (ACC-2021) & International Conference on “Recent Trends in Chemical Sciences” (RTCS-2021)’ organized by the Indian Chemical Society, Kolkata, India held online during 21–24 December, 2021. **(Adjudged for the ‘Indian Chemical Society Research Excellence Award’)**

Title: *Substitution at Coordinatively Saturated Boron Center*

11. Presented a research poster at “RSC Poster Twitter Conference 2021” held during 2–3 March, 2022. **(Received 2nd best poster award)**

Title: *Substitution at Coordinatively Saturated Boron Center*

Carbenes

International Edition: DOI: 10.1002/anie.201814616
German Edition: DOI: 10.1002/ange.201814616**C–F Bond Activation by a Saturated N-Heterocyclic Carbene: Mesoionic Compound Formation and Adduct Formation with B(C₆F₅)₃**Moumita Pait⁺, Gargi Kundu⁺, Srinu Tothadi, Suvendu Karak, Shailja Jain, Kumar Vanka, and Sakya S. Sen*

Dedicated to Professor Vadapalli Chandrasekhar on the occasion of his 60th birthday

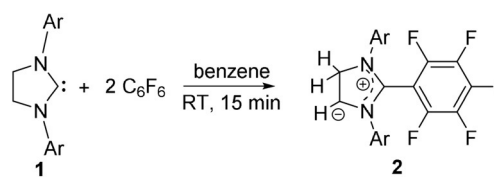
Abstract: The reaction of SIPr, [1,3-bis(2,6-diisopropylphenyl)-imidazolin-2-ylidene] (**1**), with C₆F₆ led to the formation of an unprecedented mesoionic compound (**2**). The formation of **2** is made accessible by deprotonation of the SIPr backbone with simultaneous elimination of HF. The C–F bond para to the imidazolium ring in **2** is only of 1.258(4) Å, which is the one of the shortest structurally authenticated C–F bonds known to date. The liberation of HF during the reaction is unequivocally proved by the addition of one more equivalent of SIPr, which leads to the imidazolium salt with the HF₂[−] anion. To functionalize **2**, the latter reacted with B(C₆F₅)₃ to give an unusual donor–acceptor compound, where the fluoride atom from the C₆F₅ moiety coordinates to B(C₆F₅)₃ and the carbanion moiety remains unaffected. Such coordination susceptibility of the fluoride atom of a nonmetallic system to a main-group Lewis acid (F_{non-metal} → BR₃) is quite unprecedented.

Since Robinson's seminal work on deprotonation of IPr (1,3-bis(2,6-diisopropylphenyl)-imidazol-2-ylidene) at C4 (alkenic backbone) with *n*BuLi,^[1] there has been a flurry of research activity on deprotonation from the N-heterocyclic carbenes (NHC) backbone and subsequent C4 metallation thanks to extensive work from the groups of Hevia, Mulvey, Braunstein, Braunschweig, and others.^[2–7] The deprotonation of saturated NHCs, however, led to rearranged products through C–N bond activation and ring cleavage.^[8,9]

Given our recent interest, as well as that of others in C–F bond activation by compounds with low-valent main-group

elements,^[10–19] we intended to explore saturated NHCs for C–F bond activation. While both cyclic alkyl amino carbenes (cAACs) and IPr have been recently explored for C–F bond activation,^[14–17] their different electronic properties are reflected in their mode of C–F bond activation. We have observed herein that the reaction of SIPr (**1**; for structure see Scheme 1) with C₆F₆ has led to the activation of one of the C–F bonds with concomitant deprotonation from the backbone, resulting in the formation of an unprecedented mesoionic compound (**2**) along with HF elimination. The HF elimination is confirmed by adding one more equivalent of **1**, which forms an imidazolium salt with HF₂[−] as the counter anion (**3**; for structure see Scheme 2). Subsequent to the isolation of **2**, we intended to derivatize this mesoionic compound by reaction with B(C₆F₅)₃, but it forms a donor–acceptor adduct (**4**; for structure see Scheme 3), where the fluoride atom of the C₆F₅ moiety coordinates to boron, leaving the carbanion moiety intact. Such behavior displaying the Lewis basicity of a fluoride atom of the C₆F₅ ligand in a metal-free system is unprecedented.

The reaction of C₆F₆ with **1** at 60 °C for 14 hours led to the formation of **2** as a greenish-yellow solid. However, when C₆F₆ was added to **1** in benzene in 2:1 ratio at room temperature, the formation of **2** was detected in 15 minutes (Scheme 1). The formation of **2** is indicated in the ¹⁹F NMR



Scheme 1. C–F bond activation of C₆F₆ by SIPr (**1**) and subsequent deprotonation (Ar = 2,6-*i*-Pr₂C₆H₃).

spectrum, which shows signals at $\delta = -113.29$ ppm for the *para*-fluorine atom, $\delta = -141.93$ and $\delta = -166.92$ ppm for the *ortho*- and *meta*-fluorine atoms respectively. Colorless crystals of **2** were isolated from a saturated CDCl₃ solution maintained at 4 °C for 5–7 days, and they revealed the formation of a mesoionic compound. The molecular structure of **2** (Figure 1) reveals the C2–C3 bond length is 1.468(6) Å, which is shorter than the standard C2–C3 bond length in **1** [1.5144(19) Å].^[20] The ¹H NMR spectrum shows only one singlet at $\delta = 4.34$ ppm with an integration for three hydrogen

[*] Dr. M. Pait,^[†] G. Kundu,^[†] Dr. S. S. Sen
Inorganic Chemistry and Catalysis Division, CSIR-National Chemical Laboratory, Dr. Homi Bhabha Road, Pashan, Pune 411008 (India)
E-mail: ss.sen@ncl.res.in

G. Kundu,^[†] S. Karak, S. Jain, Dr. K. Vanka, Dr. S. S. Sen
Academy of Scientific and Innovative Research (AcSIR)
Ghaziabad 201002 (India)

Dr. S. Tothadi
Organic Chemistry Division, CSIR-National Chemical Laboratory
Dr. Homi Bhabha Road, Pashan, Pune 411008 (India)

S. Karak, S. Jain, Dr. K. Vanka
Physical and Material Chemistry Division, CSIR-National Chemical Laboratory, Dr. Homi Bhabha Road, Pashan, Pune 411008 (India)

[†] These authors contributed equally to this work.

Supporting information and the ORCID identification number(s) for the author(s) of this article can be found under:
<https://doi.org/10.1002/anie.201814616>.

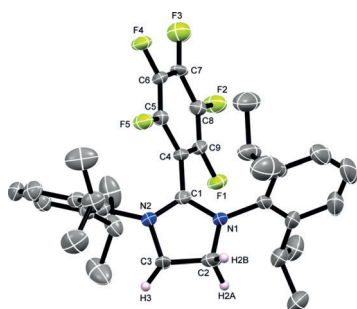
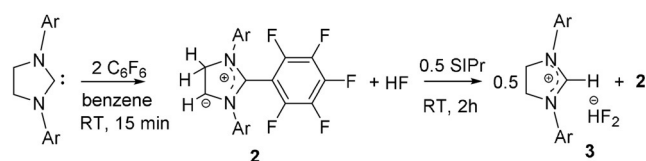


Figure 1. Molecular structure (ORTEP) of **2** with anisotropic displacement parameters drawn at 50% probability level.^[37] Hydrogen atoms (except in the SIPr backbone) are not shown for clarity. Selected bond lengths [Å] and angles [°]: C1–N1 1.320(4), C1–N2 1.334(4), C2–N1 1.472(5), C2–C3 1.468(6), C1–C4 1.451(5), C7–F3 1.258(4); N1–C1–N2 111.8(3), C3–C2–N1 104.6(3), N1–C1–C4 123.7(3), N2–C1–C4 124.5(3), C9–C4–C5 114.7(3).

atoms. The molecular-ion peak at m/z 556.2871 in the HRMS supports the deprotonation from the backbone. The C–F bond length *para* to the imidazolium moiety is determined to be 1.258(4) Å, which is one of the shortest C–F single bonds known to date (the C–F bond length in perfluoroalkanes is of about 1.3 Å).^[21] The bond length is very close to the C=F bond calculated for [MeC(F)=F]⁺ (1.259 Å) and [F₂C=F]⁺ (1.243 Å).^[22] This value is the consequence of the delocalization of the lone pairs of the *para*-F atom over the aryl ring. The other C–F bond lengths range from 1.348(4)–1.359(4) Å. The C–C bond lengths in the C₆F₅ moiety vary from 1.351(5)–1.427(5) Å, indicating the partial delocalization over the aryl ring. The cyclic voltammogram (CV) of **2** (see Figure S30 in the Supporting Information) exhibits a reversible one-electron reduction and oxidation process where the reduction peak potential ($E_{p,red}$) appears at –0.95 V and the oxidation peak potential ($E_{p,oxd}$) is found at –0.87 V. Along with the reversible process, an irreversible one-electron reduction ($E_{p,red} = -1.25$ V) and irreversible oxidation ($E_{p,oxd} = -1.09$ V) are also observed.

Recently, Tavčar and co-workers showed the reactions of IPr with different sources of HF.^[23] To unambiguously prove the liberation of HF during the C–F bond activation, we reasoned that the addition of one more equivalent of **1** to the reaction mixture might react with the liberated HF. Indeed, the addition of another equivalent of **1** in the mixture of **1** and C₆F₆ (Scheme 2) led to the formation of the imidazolium bifluoride **3**. The formation of the latter stands as a proof of HF elimination during the C–F bond activation. As the solubilities of **2** and **3** are very similar, we were unable to satisfactorily characterize **3** by NMR spectroscopy. The ¹H NMR spectrum of **3** shows a broad singlet at $\delta =$



Scheme 2. Trapping of the HF molecule by the formation of the monocationic salt with HF₂[–] as a counter anion (**3**).

15.88 ppm, which is a characteristic resonance for HF₂[–] and in accordance with those reported by Tavčar and co-workers for [IPrH][HF₂].^[23] A singlet at $\delta = -162.42$ ppm in the ¹⁹F NMR spectrum can also be seen. The molecular structure of **3** (Figure 2) reveals the trigonal-planar geometry at C5 with a N1–C5–N2 angle of 112.91(13)°. The C2–C3 bond length is 1.544(2) Å, which is in accordance with the C2–C3 bond length in **1** (1.5144(19) Å).^[20]

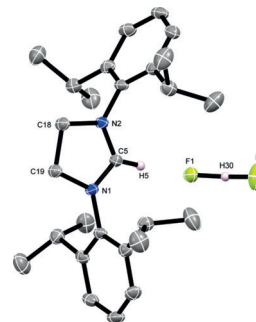


Figure 2. Molecular structure (ORTEP) of **3** with anisotropic displacement parameters drawn at 50% probability level.^[37] Hydrogen atoms (except HF₂[–]) are not shown for clarity. Selected bond lengths [Å] and angles [°]: C5–N2 1.3137(18), C5–N1 1.3152(18), N2–C18 1.4844(18), N1–C19 1.4874(18), C18–C19 1.544(2), C5–H5 0.9300, F1–H30 1.233(18); N1–C5–N2 112.91(13), C19–C18–N2 102.57(11), C18–N2–C5 111.06(12).

To understand the mechanism for the C–F bond activation of C₆F₆, quantum chemical calculations were performed using density-functional theory (DFT) methods at the PBE/TZVP level of theory (Figure 3). The approach of C₆F₆ to the

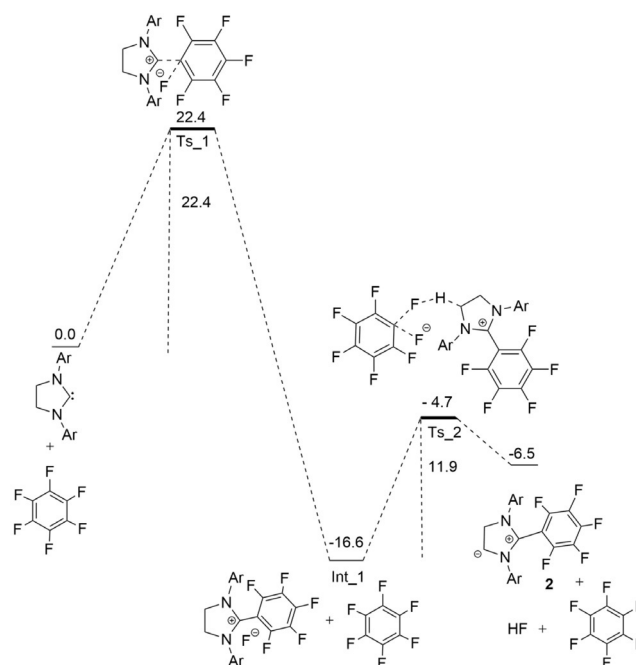
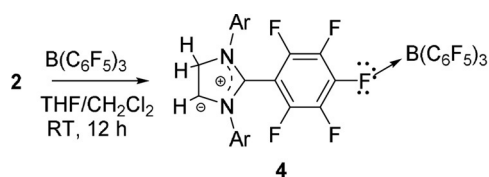


Figure 3. Reaction energy profile diagram for the C–F bond activation of C₆F₆ by SIPr. The values (in kcal mol^{–1}) have been calculated at the PBE/TZVP level of theory with DFT.

carbene leads to the formation of **Int_1** via **Ts_1**, which is a very stable intermediate ($\Delta G = -16.6 \text{ kcal mol}^{-1}$). The barrier for this step is $22.4 \text{ kcal mol}^{-1}$. Subsequent to this step, calculations suggest that a molecule of C_6F_6 acts as a “fluoride shuttle”, transferring a fluoride to the backbone carbon center (see **Ts_2**) to yield the experimentally observed product (**2**). This mediating role of C_6F_6 was deemed important, for it was seen that without the fluoride transferring assistance of C_6F_6 , it was difficult to break the C–H bond to eliminate HF from the intermediate **Int_1**. This role is in line with our observation on why the reaction takes place at room temperature in presence of excess C_6F_6 . Note that, Kuhn and co-workers also used a huge excess of C_6F_6 in the presence of BF_3 for carbene mediated C–F bond activation.^[24]

With **2** in hand, we sought to derivatize the backbone with a Lewis acid. Hence, we reacted **2** with $\text{B}(\text{C}_6\text{F}_5)_3$ (Scheme 3).



Scheme 3. Reaction of **2** with $\text{B}(\text{C}_6\text{F}_5)_3$ and formation of a donor-acceptor adduct. THF = tetrahydrofuran.

Surprisingly, it led to a donor-acceptor adduct (**4**), wherein the fluoride atom *para* to the imidazolium moiety coordinates to $\text{B}(\text{C}_6\text{F}_5)_3$, leaving the carbanion moiety intact. Despite the Lewis-acidic nature of $\text{B}(\text{C}_6\text{F}_5)_3$, compounds that feature $\text{F} \rightarrow \text{B}(\text{C}_6\text{F}_5)_3$ donor-acceptor interactions are very rare. Parkin and co-workers reported the reaction of a terminal zinc fluoride with $\text{B}(\text{C}_6\text{F}_5)_3$ and it led to the adduct $[\kappa^4\text{-Tptm}]\text{ZnF} \rightarrow \text{B}(\text{C}_6\text{F}_5)_3$.^[25] However, such a donor-acceptor interaction from the fluoride atom of a metal-free system to borane is thus far not known. The molecular structure of **4** is shown in Figure 4. The $\text{F} \rightarrow \text{B}$ bond in **4** [$1.512(3) \text{ \AA}$] is substantially longer than that in $[\kappa^4\text{-Tptm}]\text{ZnF} \rightarrow \text{B}(\text{C}_6\text{F}_5)_3$ [$1.476(6) \text{ \AA}$]^[25] and the average value for the $[(\text{C}_6\text{F}_5)_3\text{BF}]^-$ anion (1.434 \AA)^[26] in non-metal-containing salts. Coordination of the C–F moiety through the fluoride atom is indicated by the increase in the C–F bond length [$1.308(2) \text{ \AA}$] relative to that in **2** [$1.258(4) \text{ \AA}$], but it is shorter than the other C–F bond lengths [$1.339(2)$ – $1.344(2) \text{ \AA}$]. The mesoionic nature of the compound is illustrated from the ^1H NMR studies, which show two resonances for the backbone protons at $\delta = 4.64$ and 4.53 ppm , integrating for one and two protons, respectively. A broad signal appears at $\delta = -0.81 \text{ ppm}$ in the ^{11}B NMR spectrum, which is substantially shifted from that of $\text{B}(\text{C}_6\text{F}_5)_3$ ($\delta = 61.5 \text{ ppm}$). The fluoride coordinated to $\text{B}(\text{C}_6\text{F}_5)_3$ resonates at $\delta = -155.98 \text{ ppm}$, which is downfield compared to the BF fragment in $[\text{FB}(\text{C}_6\text{F}_5)_3]^-$, which typically resonates between $\delta = -185$ and -192 ppm .^[26,27]

The elimination of HF during the C–F bond activation was further manifested in the reaction of SIPr with $\text{C}_6\text{F}_5\text{CF}_3$. The reaction led to the activation of the *para* C–F bond relative to the CF_3 group, resulting in the formation of an

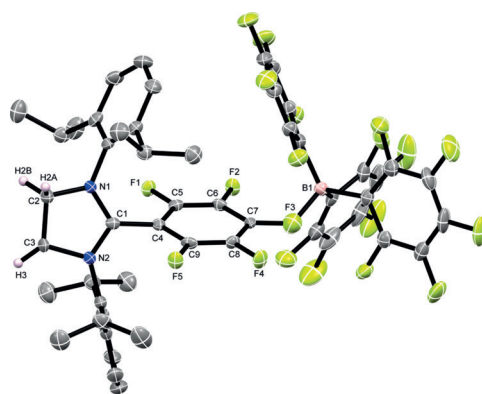
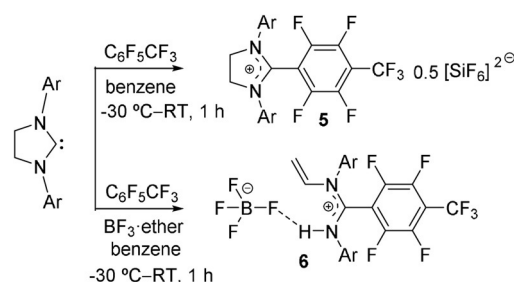


Figure 4. Molecular structure (ORTEP) of **4**.^[37] The anisotropic displacement parameters are drawn at 50% probability level. Hydrogen atoms (except in the SIPr backbone) are not shown for clarity. Selected bond lengths [\AA] and angles [$^\circ$]: C1–N1 $1.326(3)$, C1–N2 $1.324(3)$, C2–N1 $1.480(3)$, C3–C2 $1.527(4)$, C4–C1 $1.467(3)$, C7–F3 $1.308(3)$, B1–F3 $1.512(3)$; N1–C1–N2 $112.7(2)$, C3–C2–N1 $102.27(19)$, N1–C1–C4 $123.1(2)$, N2–C1–C4 $124.2(2)$, C9–C4–C5 $115.7(2)$.

imidazolium salt along with $[\text{SiF}_6]^{2-}$ as the counter anion, **5** (Scheme 4). The molecular structure of **5** is shown in Figure 5. The ^{19}F NMR spectrum of **5** shows a peak at $\delta = -124.61 \text{ ppm}$, which is in good agreement with that reported by the groups of Tavčar^[28] and Atwood.^[29] The C1–C4 bond length is $1.485(4) \text{ \AA}$, which is in good agreement with that in **2**. The source of $[\text{SiF}_6]^{2-}$ can be attributed to the glass surface, which can react with the in situ liberated HF from the



Scheme 4. C–F bond activation of $\text{C}_6\text{F}_5\text{CF}_3$ by SIPr (**1**).

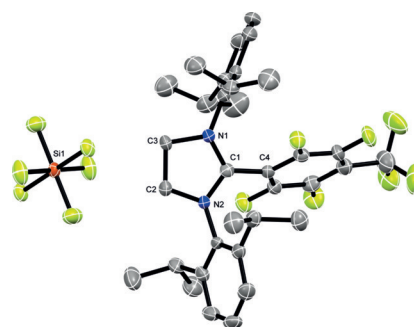


Figure 5. Molecular structure (ORTEP) of **5**.^[37] Anisotropic displacement parameters are depicted at the 50% probability level. Hydrogen atoms are not shown for clarity. Selected bond lengths [\AA] and angles [$^\circ$]: C1–N2 $1.324(3)$, C1–N1 $1.318(3)$, C3–N1 $1.484(3)$, C1–C4 $1.485(4)$, C2–C3 $1.519(4)$; N1–C1–N2 $113.1(2)$, N1–C3–C2 $102.1(2)$, N1–C1–C4 $121.6(2)$, N2–C1–C4 $125.1(2)$.

system.^[30] We could not stop the reaction of HF with the glass vessel even when performing the reaction at -30°C .

To prohibit the reaction of in situ generated HF with the glass vessel by fluoride abstraction, we added BF_3 to the reaction mixture of **1** and $\text{C}_6\text{F}_5\text{CF}_3$ after 30 minutes at low temperature, and it led to the formation of the NHC ring-opening product **6** (Figure 6), where HF is captured by

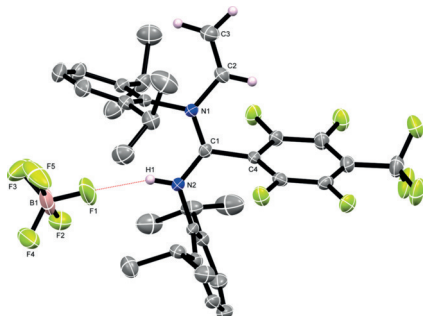


Figure 6. Molecular structure (ORTEP) of **6**.^[37] Anisotropic displacement parameters are depicted at the 50% probability level. Hydrogen atoms (except at N2 atom) are not shown for clarity. In crystal packing one F atom of BF_4^- shows disorder and occupied in two different sites with 40% and 60% occupancy. Selected bond lengths [Å] and angles [°]: C1–N1 1.327(3), C1–N2 1.322(3), C1–C4 1.504(4), C2–C3 1.314(4), F3–B1 1.312(5); N1–C1–N2 122.3(2), C2–N1–C1 121.8(2), N1–C1–C4 118.1(2), F3–B1–F2 98.2(3).

hydrogen bonding. The C–C single bond is oxidized to a C=C bond (Scheme 4). There are recent reports on ring expansion of NHCs using either BeH_2 ^[31] or hydrosilanes,^[32] and C–N bond activation by transition metals,^[33,34] as well as by main-group compounds.^[16] However, in all these cases, the $\text{C}_{\text{carbene}}-\text{N}$ bond activation takes place and the backbone of the NHC moiety remains intact. Only Filippou et al. have observed the formation of an imine compound, $\text{CH}_2=\text{CH}-\text{N}(\text{dipp})-\text{CH}=\text{N}(\text{dipp})$, as a minor product while treating (SIPrH)Br with $\text{Na}(\text{SiMe}_3)_2$.^[35] Very recently, Harder and co-workers reported the reaction of saturated an N-heterocyclic alkene with $n\text{BuLi}$ in the presence of TMEDA, and it leads to ring opening by cleavage of one of the cyclic C–N bonds from the backbone.^[36] The tetrafluoroborate anion serves as an effective hydrogen-bond acceptor. The ^{11}B NMR spectrum gives a signal at $\delta = 4.26$ ppm for BF_4^- . The C2–C3 bond length was determined to be 1.314(4) Å, confirming the double-bond formation.

In conclusion, we report the deprotonation of SIPr by a C–F bond of C_6F_6 , and it affords a mesoionic compound (**2**) with concomitant elimination of HF. Neither NHCs nor cAACs are known to generate such mesoionic compounds by such a single-step C–F bond activation. The formation of HF during the reaction is supported by the addition of another molecule of SIPr in the reaction medium, and leads to the imidazolium bifluoride **3**. **2** possesses one of the shortest structurally authenticated C–F bonds [1.258(4) Å]. The reaction of **2** with $\text{B}(\text{C}_6\text{F}_5)_3$ results in the donor–acceptor adduct **4**, where the Lewis basicity of the fluoride atom of the C_6F_5 moiety is illustrated by its coordination to $\text{B}(\text{C}_6\text{F}_5)_3$. Such

a donor–acceptor interaction from the fluoride atom of a metal-free system to borane is unprecedented.

Experimental Section

Synthetic methods, characterization data, computational details, and details of single-crystal X-ray studies, as well as cif files of **2–6** are given in the Supporting Information.

Acknowledgements

S.S.S., K.V., M.P. and S.T. thank DST-SERB (SB/S1/IC-10/2014), DST (EMR/2014/000013), SERB NPDF (PDF/2016/002059) and (PDF/2017/000047) for providing financial assistance for this work. G.K., S.J. thank CSIR-India and S.K. thanks UGC, India for their research fellowships. SSS thanks Prof. Dr. Fabian Dielmann, Westfälische Wilhelms-Universität, Münster for his useful suggestions to prepare SIPr in high yield. We are grateful to the reviewers for their critical insights to improve the quality of the manuscript.

Conflict of interest

The authors declare no conflict of interest.

Keywords: carbanions · C–F activation · N-heterocyclic carbenes · structure elucidation · ylides

How to cite: *Angew. Chem. Int. Ed.* **2019**, *58*, 2804–2808
Angew. Chem. **2019**, *131*, 2830–2834

- [1] Y. Wang, Y. Xie, M. Y. Abraham, P. Wei, H. F. Schaefer III, P. v. R. Schleyer, G. H. Robinson, *J. Am. Chem. Soc.* **2010**, *132*, 14370–14372.
- [2] L. C. H. Maddock, T. Cadenbach, A. R. Kennedy, I. Borilovic, G. Aromí, E. Hevia, *Inorg. Chem.* **2015**, *54*, 9201–9210.
- [3] M. Uzelac, A. R. Kennedy, A. Hernán-Gómez, M. A. Fuentes, E. Hevia, *Z. Anorg. Allg. Chem.* **2016**, *642*, 1241–1244.
- [4] D. R. Armstrong, S. E. Baillie, V. L. Blair, N. G. Chabloz, J. Diez, J. Garcia-Alvarez, A. R. Kennedy, S. D. Robertson, E. Hevia, *Chem. Sci.* **2013**, *4*, 4259–4266.
- [5] A. J. Martínez-Martínez, M. A. Fuentes, A. Hernán-Gómez, E. Hevia, A. R. Kennedy, R. E. Mulvey, C. T. O'Hara, *Angew. Chem. Int. Ed.* **2015**, *54*, 14075–14079; *Angew. Chem.* **2015**, *127*, 14281–14285.
- [6] A. A. Danopoulos, P. Braunstein, E. Rezabal, G. Frison, *Chem. Commun.* **2015**, *51*, 3049–3052.
- [7] H. Braunschweig, C. Claes, A. Damme, A. Deisenberger, R. D. Dewhurst, C. Hörl, T. Kramer, *Chem. Commun.* **2015**, *51*, 1627–1630.
- [8] A. Hernán-Gómez, A. R. Kennedy, E. Hevia, *Angew. Chem. Int. Ed.* **2017**, *56*, 6632–6635; *Angew. Chem.* **2017**, *129*, 6732–6735.
- [9] Y. Wang, G. H. Robinson, *Inorg. Chem.* **2011**, *50*, 12326–12337.
- [10] A. Jana, P. P. Samuel, G. Tavčar, H. W. Roesky, C. Schulzke, *J. Am. Chem. Soc.* **2010**, *132*, 10164–10170.
- [11] R. Azhakar, H. W. Roesky, H. Wolf, D. Stalke, *Chem. Commun.* **2013**, *49*, 1841–1843.
- [12] V. S. V. S. N. Swamy, N. Parvin, K. V. Raj, K. Vanka, S. S. Sen, *Chem. Commun.* **2017**, *53*, 9850–9853.
- [13] T. Chu, Y. Boyko, I. Korobkov, G. I. Nikonov, *Organometallics* **2015**, *34*, 5363–5365.

- [14] U. S. D. Paul, U. Radius, *Chem. Eur. J.* **2017**, *23*, 3993–4009.
- [15] S. Styra, M. Melaimi, C. E. Moore, A. L. Rheingold, T. Augenstein, F. Breher, G. Bertrand, *Chem. Eur. J.* **2015**, *21*, 8441–8446.
- [16] Y. Kim, E. Lee, *Chem. Commun.* **2016**, *52*, 10922–10925.
- [17] M. C. Leclerc, S. I. Gorelsky, B. M. Gabidullin, I. Korobkov, R. T. Baker, *Chem. Eur. J.* **2016**, *22*, 8063–8067.
- [18] S. S. Sen, H. W. Roesky, *Chem. Commun.* **2018**, *54*, 5046–5057.
- [19] T. Stahl, H. F. T. Klare, M. Oestreich, *ACS Catal.* **2013**, *3*, 1578–1587.
- [20] N. A. Giffin, A. D. Hendsbee, J. D. Masuda, *Acta Crystallogr. Sect. E* **2010**, *66*, o2194.
- [21] J. L. Kiplinger, T. G. Richmond, C. E. Osterberg, *Chem. Rev.* **1994**, *94*, 373–431.
- [22] E. Kraka, D. Cremer, *ChemPhysChem* **2009**, *10*, 686–698.
- [23] B. Alič, G. Tavčar, *J. Fluorine Chem.* **2016**, *192*, 141–146.
- [24] E. Mallah, N. Kuhn, C. Maichle-Moßmer, M. Steimann, M. Ströbele, K.-P. Zeller, *Z. Naturforsch. B* **2009**, *64*, 1176–1182.
- [25] W. Sattler, S. Ruccolo, G. Parkin, *J. Am. Chem. Soc.* **2013**, *135*, 18714–18717.
- [26] C. B. Caputo, D. W. Stephan, *Organometallics* **2012**, *31*, 27–30.
- [27] A. J. V. Marwitz, J. L. Dutton, L. G. Mercier, W. E. Piers, *J. Am. Chem. Soc.* **2011**, *133*, 10026–10029.
- [28] B. Alič, M. Tramšek, A. Kokalj, G. Tavčar, *Inorg. Chem.* **2017**, *56*, 10070–10077.
- [29] B. D. Conley, B. C. Yearwood, S. Parkin, D. A. Atwood, *J. Fluorine Chem.* **2002**, *115*, 155–160.
- [30] H. Baumgarth, G. Meier, T. Braun, B. Braun-Cula, *Eur. J. Inorg. Chem.* **2016**, 4565–4572.
- [31] M. Arrowsmith, M. S. Hill, G. Kociok-Köhn, D. J. MacDougall, M. Mahon, *Angew. Chem. Int. Ed.* **2012**, *51*, 2098–2100; *Angew. Chem.* **2012**, *124*, 2140–2142.
- [32] D. Schmidt, J. H. J. Berthel, S. Pietsch, U. Radius, *Angew. Chem. Int. Ed.* **2012**, *51*, 8881–8885; *Angew. Chem.* **2012**, *124*, 9011–9015.
- [33] A. Kaiho, H. Suzuki, *Angew. Chem. Int. Ed.* **2012**, *51*, 1408–1411; *Angew. Chem.* **2012**, *124*, 1437–1440.
- [34] S. K. Bose, A. Deibenberger, A. Eichhorn, P. G. Steel, Z. Lin, T. B. Marder, *Angew. Chem. Int. Ed.* **2015**, *54*, 11843–11847; *Angew. Chem.* **2015**, *127*, 12009–12014.
- [35] A. C. Filippou, O. Chernov, G. Schakenburg, *Chem. Eur. J.* **2011**, *17*, 13574–13583.
- [36] T. X. Gentner, G. Ballmann, J. Pahl, H. Elsen, S. Harder, *Organometallics* **2018**, *37*, 4473–4480.
- [37] CCDC 1868728 (2), 1872249 (3), 1868731 (4), 1868732 (5), and 1868733 (6) contain the supplementary crystallographic data for this paper. These data can be obtained free of charge from The Cambridge Crystallographic Data Centre.

Manuscript received: December 25, 2018

Accepted manuscript online: January 2, 2019

Version of record online: January 29, 2019

WILEY-VCH

 **Chemistry
Europe**

European Chemical
Societies Publishing

Take Advantage and Publish Open Access



By publishing your paper open access, you'll be making it immediately freely available to anyone everywhere in the world.

That's maximum access and visibility worldwide with the same rigor of peer review you would expect from any high-quality journal.

Submit your paper today.



www.chemistry-europe.org

C–F Activation | Hot Paper |

Saturated N-Heterocyclic Carbene Based Thiele's Hydrocarbon with a Tetrafluorophenylene Linker

Gargi Kundu,^[a, b] Sriman De,^[c] Srinu Tothadi,^[d] Abhishek Das,^[e] Debasis Koley,^{*[c]} and Sakya S. Sen^{*[a, b]}

Dedicated to Dr. Amitava Das on the occasion of his 60th Birthday

Abstract: The synthesis of a **SIPr** [1,3-bis(2,6-diisopropylphenyl)-imidazolin-2-ylidene] derived Kekulé diradicaloid with a tetrafluorophenylene spacer (**3**) has been described. Two synthetic routes have been reported to access **3**. The cleavage of C–F bond of C₆F₆ by **SIPr** in the presence of BF₃ led to double C–F activated compound with two tetrafluoro borate counter anions (**2**), which upon reduction by lithium metal afforded **3**. Alternatively, **3** can be directly accessed in one step by reacting **SIPr** with C₆F₆ in presence of Mg metal. Compounds **2** and **3** were well characterized spectroscopically and by single-crystal X-ray diffraction studies. Experimental and computational studies support the cumulenic closed-shell singlet state of **3** with a singlet-triplet energy gap (ΔE_{S-T}) of 23.7 kcal mol⁻¹.

The activation of C–F bonds of perfluoroarenes by compounds with Si^{II}, P^{III}, Al^I atoms has become an increasingly popular topic of research over the last years thanks to pioneering works by Stephan, Roesky, Nikonov and many others.^[1] The group of Kuhn, and later the groups of Lee and Radius investi-

gated the C–F bond activation by using N-heterocyclic carbenes (NHCs).^[2] In 2015, Bertrand and co-workers reported the activation of the C–F bond of C₅F₅N by a cyclic (alkyl)(amino)-carbene (cAAC) and subsequently isolated a (cAAC)-tetrafluoropyridyl radical by reducing the C–F bond activated product.^[3] In fact, the cAAC moieties are excellent for stabilizing a variety of organic, main-group and transition-metal radical species, as demonstrated from the extensive studies by the groups of Bertrand, Roesky, Braunschweig, and others.^[4,5] In contrast, radicals derived from N-heterocyclic carbenes (NHCs) are astoundingly small,^[6] although very recently NHC derivatives of Kekulé diradicaloids have been realized by Ghadwal and co-workers.^[6d–f]

Due to lower HOMO–LUMO energy gap of saturated NHCs than their unsaturated counterparts,^[7] the capability of saturated NHCs to stabilize organic radicals should be better.^[6g] Recently, we have studied the reactivity of C₆F₆ and C₆F₅CF₃ with **SIPr**.^[8] In this work, we show the utilization of C–F bond activation of C₆F₆ chemistry to realize a **SIPr**-based Thiele's hydrocarbon spanned by a C₆F₄ linker. The question remains whether the four substituted fluorine atoms at the central phenylene ring of **3** would destabilize the quinoid state and stabilize the biradical state. A further impetus comes from the works of Abe and co-workers who showed the increase in the biradical character in 1,4-bis-(4,5-diphenylimidazol-2-ylidene) tetrafluoro cyclohexa-2,5-diene (tf-BDPI-2Y) from parent BDPI-2Y.^[6h] Although tf-BDPI-2Y was not structurally characterized, they were able to obtain the single-crystal structure of the dimerized product (tf-BDPI-2YD).^[6h]

We have performed the reaction of **SIPr** and C₆F₆, but have added BF₃-ether to the reaction mixture after 15 min for the isolation of the orange colored dicationic salt **2** with two BF₄⁻ molecules as the counter anions (Scheme 1).^[10] Interestingly, the addition of BF₃ led to double C–F bond activation from C₆F₆. The activation of another C–F bond is reflected in the ¹⁹F NMR spectrum, which shows signals at $\delta = -142.22$ ppm for the four fluorine atoms and at -148.37 ppm for the eight fluorine atoms of two BF₄ moieties. The ¹¹B NMR spectrum exhibits a signal at $\delta = -1.11$ ppm. In the HRMS, the molecular ion peak was found at *m/z* 464.3034 with the highest relative intensity, which supports the formation of **2**. The cyclic voltammogram of **2** (see Figure 2) exhibits two reversible redox waves at $E_{p,red} = -0.95$ V and -1.91 V and oxidation at $E_{p,oxd} = -0.57$ V and -1.79 V, respectively. The reduction potential of **2** is significantly lower compared to the related C2-protonated

[a] G. Kundu,[†] Dr. S. S. Sen
Inorganic Chemistry and Catalysis Division
CSIR-National Chemical Laboratory
Dr. Homi Bhabha Road, Pashan, Pune 411008 (India)
E-mail: ss.sen@ncl.res.in

[b] G. Kundu,[†] Dr. S. S. Sen
Academy of Scientific and Innovative Research (AcSIR)
New Ghaziabad 201002 (India)

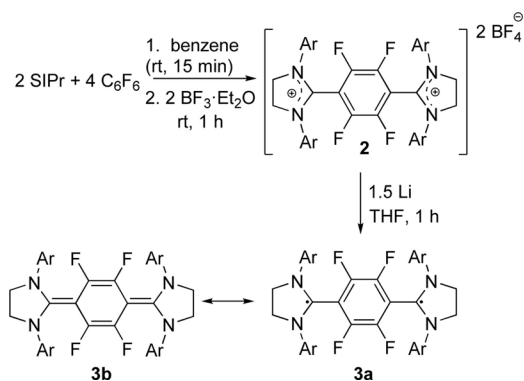
[c] S. De,[†] Dr. D. Koley
Department of Chemical Sciences
Indian Institute of Science Education and Research (IISER) Kolkata
Mohanpur, 741246 (India)
E-mail: koley@iiserkol.ac.in

[d] Dr. S. Tothadi
Organic Chemistry Division, CSIR-National Chemical Laboratory
Dr. Homi Bhabha Road, Pashan, Pune 411008 (India)

[e] A. Das
Indian Association for the Cultivation of Science
2A & 2B Raja S. C. Mullick Road Kolkata 700032 (India)

[†] These authors contributed equally to this work.

Supporting information and the ORCID identification number(s) for the author(s) of this article can be found under:
<https://doi.org/10.1002/chem.201904421>.



Scheme 1. Stepwise access to **3**. C_6F_6 was used in 1:2 ratio with **SIPr** to perform the reaction at room temperature. A larger amount of C_6F_6 acts as a “fluoride shuttle”;^[9] Ar = 2,6-*i*Pr₂-C₆H₃.

imidazolium salts (ca. -2.3 V)^[11] of NHCs, presumably due to the electron withdrawing effect of the fluoride atoms.

The molecular structure of **2** (Figure 1) reveals that the C2–C3 bond distance in the imidazolium rings is 1.530(6) Å, a value similar to that in **SIPr** [1.5144(19) Å].^[12] and other report-

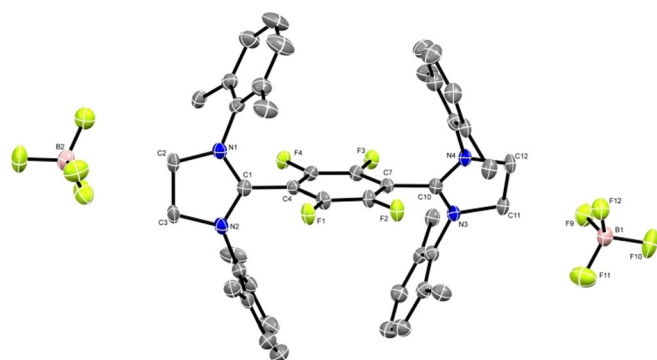


Figure 1. The molecular structure (ORTEP) of **2** with anisotropic displacement parameters drawn at 50% probability level. The methyl groups and the hydrogen atoms are not shown for clarity. Selected bond lengths (Å) and angles (°): C1–N1 1.313(5), C1–N2 1.324(5), C2–N1 1.488(5), C2–C3 1.530(6), C1–C4 1.486(5); N1–C1–N2 114.6(4), C3–C2–N1 102.9(3), N1–C1–C4 122.0(4), N2–C1–C4 123.2(4).

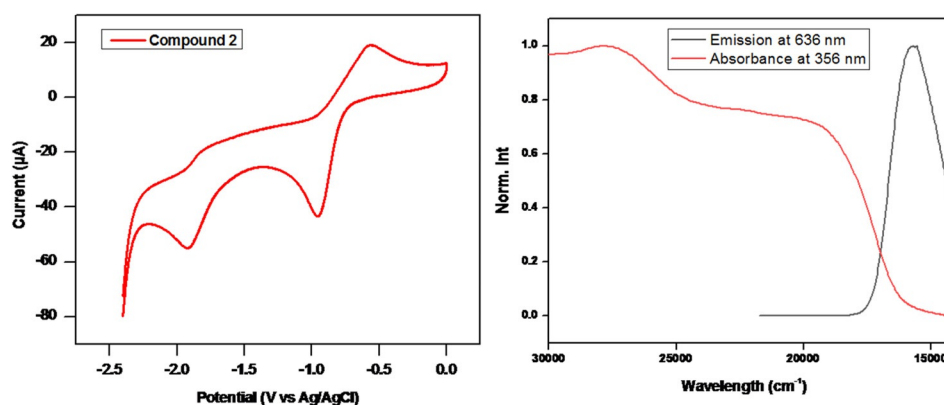


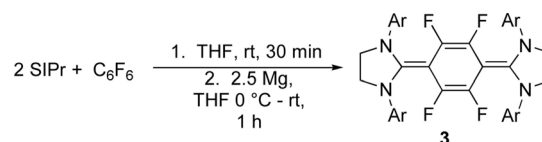
Figure 2. The cyclic voltammogram of **2** recorded at 0.7 V s⁻¹ (left). Absorption (red lines) and emission (black lines) spectra of **2** at room temperature in the solid state.

ed imidazolium salts. The average C–C bond length in the C_6F_4 linker is 1.38 Å, which is in agreement with that expected for the aryl ring. The C1/C10 carbene carbon adopts a trigonal planar geometry with an average angle of 114° (N1–C1–N2/N3–C10–N4). The C1–C4 bond length is 1.486(5) Å, indicating a C–C single bond. The bridging tetrafluorophenylene ring of **2** are planar and twisted by 65.9° (average value) from the plane of the imidazole rings.

After observing a strong visible luminescence under UV lamp, we have studied the photo-physical phenomenon of **2**, which shows a very intense absorption band at 356 nm along with weaker, broad bands at higher energy region. Upon excitation at λ_{max} 356 nm and 450 nm, **2** gives a strong emissive band at 636 nm with a huge Stokes shift, about 12079 cm⁻¹, and upon excitation at $\lambda_{\text{max}}=510$ nm excitation it shows small Stokes shift, around 2056 cm⁻¹. The lifetime measurement of **2** shows very short lifetimes 2.72 ns (B1 = 30.12%) and 10.87 ns (B2 = 69.86%) with bi-exponential in character; which is indicative of fluorescence.

Based on the cyclic voltammetry data (Figure 2), we wonder whether the reduction of **2** can serve as a precursor to access the **SIPr**-mediated carbon diradical or tetrafluoro-substituted quinoid hydrocarbon. Gratifyingly, the addition of lithium metal to the THF solution of **2** resulted in an immediate color change from yellow–orange to black and the compound **3** was obtained as black solid in 62% yield along with the formation of an imine, $CH_2=CH-N(Ar)-CH=N(Ar)$ (Ar = 2,6-*i*Pr₂-C₆H₃).

Surprisingly, in situ addition of Mg powder at 0°C in the reaction mixture of **SIPr** and C_6F_6 in THF led to the formation of **3** (Scheme 2) in one step. The Mg is oxidized to Mg^{II} by capturing two fluoride anions and is precipitated out as MgF_2 from the system. The generation of MgF_2 also inhibits the HF elimination. The molecular ion peak was observed at m/z 928.6006



Scheme 2. One-step methodology to access **3**.

with the highest relative intensity (See Supporting Information, section S4). To the best of our knowledge, there is no report so far on such a single-step access to any NHC-based diradicaloid. Compound **3** is stable in the solid state under inert atmosphere. However, in the solution state, we have observed gradual formation of the aforementioned imine after 2–3 days.

The single crystals of **3** were grown by keeping the THF solution of **3** at 4 °C for 2–3 days. The molecular structure of **3** (Figure 3) reveals the trigonal planar geometry at the C5/C10

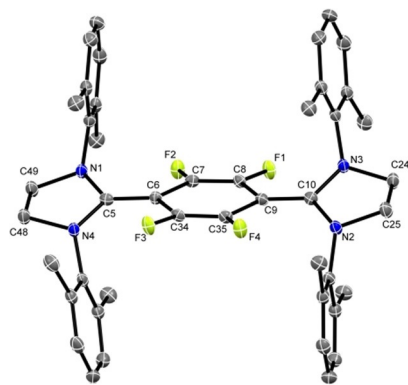


Figure 3. Molecular structure (ORTEP) of **3** with anisotropic displacement parameters drawn at 50% probability level. The methyl groups and the hydrogen atoms are not shown for clarity. Selected bond lengths (Å) and angles (°): C5–N1 1.390(4), C5–N4 1.404(3), N2–C10 1.398(4), N3–C10 1.402(3), C5–C6 1.385(4), C10–C9 1.384(4), C9–C35 1.449(3), C35–C34 1.344(4), C34–C6 1.451(4), C7–F2 1.356(3); N1–C5–N4 108.3(2), N2–C10–N3 108.6(2), C9–C10–N2 126.60(17), C8–C9–C35 110.3(2).

carbon atom with a N1–C5–N4/N3–C10–N2 angle of 108.3(2)°/108.6(2)° which is in between the values for **SIPr** and its imidazolium salt (**2**). The C5–N4/N1 (1.397 Å average) and C10–N2/N3 (1.40 Å, average) bond lengths are significantly longer compared to those in **2** (C1–N1/N2 1.318 Å and C10–N3/N4 1.326 Å, average values). The mean bond lengths of C5–C6/C9–C10 is 1.385 Å, which is much shorter compared to those in the dicationic salt, **2** (1.482 Å). There are some bond alternations in the C₆F₄ linker across C_{ortho}–C_{ipso} which suggests that the unpaired electrons are delocalized into the aryl ring (average values: C_{ortho} 1.450 Å and C_{ipso} 1.346 Å). The imidazole rings of **3** are twisted 23.6° (average) from the plane of the bridging phenylene ring, which is substantially lesser than those in **2**, indicating a significant contribution of the quinoid resonance form in the former. These geometric parameters suggest a close-shell singlet state is the ground state for **3**. Further conformation for the quinoidal character of **3** comes from the slight pyramidalization of one of the nitrogen atoms in the NHC units [the sum of the angles at the nitrogen atom (ΣN = 350.7°), Table S1, Supporting Information].^[13]

In order to get the electronic structure and to understand the bonding scenario in compound **3**, DFT calculations were performed at B3LYP/def2-SVP level of theory (see the Computational Details section in the Supporting Information). Computed electronic states of **3** reveal that close-shell singlet remains the electronic ground state with singlet-triplet energy

difference ($\Delta E_{S \rightarrow T}$) of 23.7 kcal mol⁻¹. The computed bond lengths and angles of singlet state are in good agreement with the experimentally obtained X-ray crystal structure of those of the triplet state, which can be seen from the alignments and superposition plot of the conformers (see Supporting Information, Figure S18 and Table S2). It is worth noting that the replacement of H by F led to decrease of S→T gap by 5.4 kcal mol⁻¹.^[6d]

To gain insight into the bonding nature in **3**, we have also performed natural bond orbital (NBO) analysis at the B3LYP/def2-TZVPP//B3LYP/def2-SVP level of theory. NBO population analysis entails that C5–C6/C9–C10 bonds in **3** shows a double bond character with σ and π occupancies of 1.973/1.973 e and 1.776/1.784 e, respectively (Table S3, Supporting Information). The σ bond is formed mainly from the overlap of sp²-hybridized orbital of C5/C9 and sp²-hybridized orbital of C6/C10 atoms, whereas the π -bond is originated by the sideways overlap of pure p orbital of both the bonding partners. Calculated Wiberg bond indices (WBI) of C5–C6/C9–C10 bonds are 1.394 and 1.403 respectively, indicating significant double bond characters in both cases. Thus, from the NBO results, we can predict the quinoidal bond nature in compound **3**. Additionally, we have measured the diradical character of **3** as described by Nakano and co-workers,^[14] but our calculated results reveal absence of any diradical character.

The room-temperature UV/Vis spectrum of a THF solution of **3** (Figure S9) features two intense absorption bands at λ_{\max} 384 and 476 nm with a shoulder at 769 nm (log ϵ = 4.13–4.63 m⁻¹ cm⁻¹). Subsequently, we have carried out time-dependent density functional theory calculations (TDDFT) to analyze the UV/Vis spectral signatures of **3** (Table S4, Supporting Information). The compound **3** in the close-shell configuration gives two main absorption bands at 446 and 332 nm, respectively. The higher-lying signal corresponds to the highest occupied molecular orbital (HOMO)→lowest unoccupied molecular orbital (LUMO) excitation with an oscillator strength of 1.1079, whereas the lower-lying signal designates the HOMO→LUMO+2 transition (f=0.0635). The HOMO represents the π orbital of C5–C6/C9–C10 bonds delocalized over benzene moiety, whereas the LUMO and LUMO+2 designate the lone pair of the carbene carbon and the π^* orbital of the -Dipp groups bonded to the nitrogen atoms, respectively. The selected KS-MOs of **3** are depicted in Figure 4.

Though our single-crystal data and calculated result indicate a close-shell ground state for **3**, but the latter displays a doublet EPR signal characteristics of a monoradical impurity,^[15,16] which could not be isolated (Figure S17, Supporting Information). Due to the presence of this paramagnetic impurity, we were unable to obtain well resolved ¹H and ¹³C NMR resonances.

In conclusion, we have described a route to prepare tetrafluorophenylene substituted Thiele's hydrocarbon (**3**) by exploiting the C–F bond activation of C₆F₆ using **SIPr** in a one-step as well as two step procedure. Single-crystal X-ray data and DFT calculations suggest a close-shell singlet ground state for **3** with a singlet-triplet energy gap 23.7 kcal mol⁻¹. No diradical character was found for **3** indicating the quinoidal bond

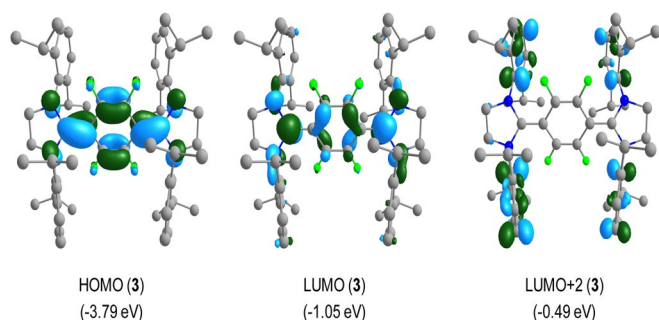


Figure 4. Selected KS-MOs of **3** (isosurface = 0.045 a.u.) at the B3LYP/def2-TZVPP//B3LYP-def2-SVP level of theory. Hydrogen atoms are omitted for clarity.

nature. Ongoing studies are focused on extending the C–F bond activation to other NHC derived diradicaloids.

Experimental Section

Crystallographic data: CCDC 1868729 (**2**) and 1951186 (**3**) contain the supplementary crystallographic data for this paper. These data are provided free of charge by The Cambridge Crystallographic Data Centre.

Acknowledgements

We are grateful to the Science and Engineering Research Board (SERB), India (CRG/2018/000287) (SSS) and SERB NPDF(PDF/2017/000047) (ST) for providing financial assistance. G.K. and A.D. thank CSIR-India and SD thanks UGC for fellowships. D.K. acknowledges the funding from bilateral DST-DFG (INT/FRG/DFG/P-05/2017) Scheme and thank IISER Kolkata for computational facility. We are thankful to Prof. Tapan Kanti Paine from IACS, Kolkata for helping us in EPR measurement and fruitful discussions. We are thankful to the referees for their critical input to improve the quality of the manuscript.

Conflict of interest

The authors declare no conflict of interest.

Keywords: C–F activation • density functional calculations • fluorine • Kekulé diradicaloids • saturated NHC

- [1] a) For C–F bond activation by Si^{II} , P^{III} , Al^{I} compounds, please see: A. Jana, P. P. Samuel, G. Tavčar, H. W. Roesky, C. Schulzke, *J. Am. Chem. Soc.* **2010**, *132*, 10164–10170; b) V. S. V. S. N. Swamy, N. Parvin, K. V. Raj, K. Vanka, S. S. Sen, *Chem. Commun.* **2017**, *53*, 9850–9853; c) I. Mallov, T. C. Johnstone, D. C. Burns, D. W. Stephan, *Chem. Commun.* **2017**, *53*, 7529–7532; d) I. Mallov, A. J. Ruddy, H. Zhu, S. Grimme, D. W. Stephan, *Chem. Eur. J.* **2017**, *23*, 17692–17696; e) S. S. Chitnis, F. Krischer, D. W. Stephan, *Chem. Eur. J.* **2018**, *24*, 6543–6546; f) T. Chu, Y. Boyko, I. Korobkov, G. I. Nikonov, *Organometallics* **2015**, *34*, 5363–5365; g) T. Mondal, S. De, D. Koley, *Inorg. Chem.* **2017**, *56*, 10633–10643; h) S. S. Sen, H. W. Roesky, *Chem. Commun.* **2018**, *54*, 5046–5057.
- [2] a) N. Kuhn, J. Fahl, R. Boese, G. Henkel, *Z. Naturforsch. B. Chem. Sci.* **1998**, *53*, 881–886; b) E. Mallah, N. Kuhn, C. Maichle-Mößner, M. Stei-

- mann, M. Ströbele, K.-P. Zeller, *Z. Naturforsch. B* **2009**, *64*, 1176–1182; c) Y. Kim, E. Lee, *Chem. Commun.* **2016**, *52*, 10922–10925; d) U. S. D. Paul, U. Radius, *Chem. Eur. J.* **2017**, *23*, 3993–4009; e) J. Emerson-King, S. A. Hauser, A. B. Chaplin, *Org. Biomol. Chem.* **2017**, *15*, 787–789.
- [3] S. Styra, M. Melaimi, C. E. Moore, A. L. Rheingold, T. Augenstein, F. Brehner, G. Bertrand, *Chem. Eur. J.* **2015**, *21*, 8441–8446.
- [4] a) For selected examples on CAAC stabilized main-group and transition metal radicals, please see: R. Kinjo, B. Donnadiu, M. A. Celik, G. Frenking, G. Bertrand, *Science* **2011**, *333*, 610–613; b) J. K. Mahoney, D. Martin, C. E. Moore, A. L. Rheingold, G. Bertrand, *J. Am. Chem. Soc.* **2013**, *135*, 18766–18769; c) K. C. Mondal, H. W. Roesky, M. C. Schwarzer, G. Frenking, I. Tkach, H. Wolf, D. Kratzert, R. Herbst-Irmer, B. Niepötter, D. Stalke, *Angew. Chem. Int. Ed.* **2013**, *52*, 1801–1805; *Angew. Chem.* **2013**, *125*, 1845–1850; d) Y. Li, K. C. Mondal, P. P. Samuel, H. Zhu, C. M. Orben, S. Panneerselvam, B. Dittich, B. Schwederski, W. Kaim, T. Mondal, D. Koley, H. W. Roesky, *Angew. Chem. Int. Ed.* **2014**, *53*, 4168–4172; *Angew. Chem.* **2014**, *126*, 4252–4256; e) P. Bissinger, H. Braunschweig, A. Damme, I. Krummenacher, A. K. Phukan, K. Radacki, S. Sugawara, *Angew. Chem. Int. Ed.* **2014**, *53*, 7360–7363; *Angew. Chem.* **2014**, *126*, 7488–7491; f) J. K. Mahoney, D. Martin, F. Thomas, C. E. Moore, A. L. Rheingold, G. Bertrand, *J. Am. Chem. Soc.* **2015**, *137*, 7519–7525; g) S. Roy, A. C. Stückl, S. Demeshko, B. Dittich, J. Meyer, B. Maity, D. Koley, B. Schwederski, W. Kaim, H. W. Roesky, *J. Am. Chem. Soc.* **2015**, *137*, 4670–4673; h) D. Munz, J. Chu, M. Melaimi, G. Bertrand, *Angew. Chem. Int. Ed.* **2016**, *55*, 12886–12890; *Angew. Chem.* **2016**, *128*, 13078–13082; i) J. K. Mahoney, R. Jazzar, G. Royal, D. Martin, G. Bertrand, *Chem. Eur. J.* **2017**, *23*, 6206–6212; j) M. M. Hansmann, M. Melaimi, G. Bertrand, *J. Am. Chem. Soc.* **2017**, *139*, 15620–15623; k) U. S. D. Paul, U. Radius, *Eur. J. Inorg. Chem.* **2017**, 3362–3375; l) H. Braunschweig, I. Krummenacher, M.-A. Légaré, A. Matler, K. Radacki, Q. Ye, *J. Am. Chem. Soc.* **2017**, *139*, 1802–1805; m) M. M. Hansmann, M. Melaimi, G. Bertrand, *J. Am. Chem. Soc.* **2018**, *140*, 2206–2213; n) M. M. Hansmann, M. Melaimi, D. Munz, G. Bertrand, *J. Am. Chem. Soc.* **2018**, *140*, 2546–2554; o) A. Deissenberger, E. Welz, R. Drescher, I. Krummenacher, R. D. Dewhurst, B. Engels, H. Braunschweig, *Angew. Chem. Int. Ed.* **2019**, *58*, 1842–1846; *Angew. Chem.* **2019**, *131*, 1857–1861; p) Z. Li, Y. Hou, Y. Li, A. Hinz, J. R. Harmer, C.-Y. Su, G. Bertrand, H. Grützmacher, *Angew. Chem. Int. Ed.* **2018**, *57*, 198–202; *Angew. Chem.* **2018**, *130*, 204–208.
- [5] a) For reviews on the stabilization of radicals by cAACs: C. D. Martin, M. Soleilhavoup, G. Bertrand, *Chem. Sci.* **2013**, *4*, 3020–3030; b) K. C. Mondal, S. Roy, H. W. Roesky, *Chem. Soc. Rev.* **2016**, *45*, 1080–1111; c) M. Melaimi, R. Jazzar, M. Soleilhavoup, G. Bertrand, *Angew. Chem. Int. Ed.* **2017**, *56*, 10046–10068; *Angew. Chem.* **2017**, *129*, 10180–10203; d) S. Kundu, S. Sinhababu, V. Chandrasekhar, H. W. Roesky, *Chem. Sci.* **2019**, *10*, 4727–4741.
- [6] a) P. L. Arnold, S. T. Liddle, *Organometallics* **2006**, *25*, 1485–1491; b) D. Rottschäfer, B. Neumann, H.-G. Stammler, M. v. Gastel, D. Andrada, R. S. Ghadwal, *Angew. Chem. Int. Ed.* **2018**, *57*, 4765–4768; *Angew. Chem.* **2018**, *130*, 4855–4858; c) B. Barry, G. Soper, J. Hurlmalainen, A. Mansikkamäki, K. N. Robertson, W. L. McClennan, A. J. Veinot, T. L. Roemmele, U. Werner-Zwanziger, R. T. Boeré, H. M. Tuononen, J. Clyburne, J. D. Masuda, *Angew. Chem. Int. Ed.* **2018**, *57*, 749–754; *Angew. Chem.* **2018**, *130*, 757–762; d) D. Rottschäfer, B. Neumann, H. G. Stammler, D. M. Andrada, R. S. Ghadwal, *Chem. Sci.* **2018**, *9*, 4970–4976; e) D. Rottschäfer, N. K. T. Ho, B. Neumann, H. G. Stammler, M. v. Gastel, D. M. Andrada, R. S. Ghadwal, *Angew. Chem. Int. Ed.* **2018**, *57*, 5838–5842; *Angew. Chem.* **2018**, *130*, 5940–5944; f) D. Rottschäfer, J. Busch, B. Neumann, H. G. Stammler, M. v. Gastel, R. Kishi, M. Nakano, R. S. Ghadwal, *Chem. Eur. J.* **2018**, *24*, 16537–16542; g) J. Messelberger, A. Grünwald, P. Pinter, M. M. Hansmann, D. Munz, *Chem. Sci.* **2018**, *9*, 6107–6117; h) A. Kikuchi, F. Iwahori, J. Abe, *J. Am. Chem. Soc.* **2004**, *126*, 6526–6527.
- [7] D. Munz, *Organometallics* **2018**, *37*, 275–289.
- [8] M. Pait, G. Kundu, S. Tothadi, S. Karak, S. Jain, K. Vanka, S. S. Sen, *Angew. Chem. Int. Ed.* **2019**, *58*, 2804–2808; *Angew. Chem.* **2019**, *131*, 2830–2834.
- [9] M. Talavera, C. N. v. Hahmann, R. Müller, M. Ahrens, M. Kaupp, T. Braun, *Angew. Chem. Int. Ed.* **2019**, *58*, 10688–10692; *Angew. Chem.* **2019**, *131*, 10798–10802.
- [10] a) E. Mallah, N. Kuhn, C. Maichle-Mößner, M. Steimann, M. Ströbele, K.-P. Zeller, *Z. Naturforsch. B* **2009**, *64*, 1176–1182; b) S. M. Huber, F. W. Heinemann, P. Audebert, R. Weiss, *Chem. Eur. J.* **2011**, *17*, 13078–13086.

- [11] B. Gorodetsky, T. Ramnial, N. R. Branda, J. A. C. Clyburne, *Chem. Commun.* **2004**, 1972–1973.
- [12] N. A. Giffin, A. D. Hendsbee, J. D. Masuda, *Acta Crystallogr. Sect. E* **2010**, *66*, o2194.
- [13] W. W. Schoeller, D. Eisner, *Inorg. Chem.* **2004**, *43*, 2585–2589.
- [14] K. Kamada, K. Ohta, A. Shimizu, T. Kubo, R. Kishi, H. Takahashi, E. Botek, B. Champagne, M. Nakano, *J. Phys. Chem. Lett.* **2010**, *1*, 937–940.
- [15] a) Y. Kanzaki, D. Shiomi, K. Sato, T. Takui, *J. Phys. Chem. B* **2012**, *116*, 1053–1059; b) P. Ravat, M. Baumgarten, *Phys. Chem. Chem. Phys.* **2015**, *17*, 983–991.
- [16] a) G. Tan, X. Wang, *Acc. Chem. Res.* **2017**, *50*, 1997–2006; b) Z. Zeng, X. Shi, C. Chi, J. T. Lopez Navarrete, J. Casado, J. Wu, *Chem. Soc. Rev.* **2015**, *44*, 6578–6596; c) J. Wang, X. Xu, H. Phan, T. S. Herng, T. Y. Gopalakrishna, G. Li, J. Ding, J. Wu, *Angew. Chem. Int. Ed.* **2017**, *56*, 14154–14158; *Angew. Chem.* **2017**, *129*, 14342–14346; d) Y. Su, X. Wang, Y. Li, Y. Sui, X. Wang, *Angew. Chem. Int. Ed.* **2015**, *54*, 1634–1637; *Angew. Chem.* **2015**, *127*, 1654–1657; e) Y. Su, X. Wang, X. Zheng, Z. Zhang, Y. Song, Y. Sui, Y. Li, X. Wang, *Angew. Chem. Int. Ed.* **2014**, *53*, 2857–2861; *Angew. Chem.* **2014**, *126*, 2901–2905.

 Manuscript received: September 25, 2019

Revised manuscript received: October 6, 2019

Accepted manuscript online: October 14, 2019

Version of record online: November 28, 2019

Stepwise Nucleophilic Substitution to Access Saturated N-heterocyclic Carbene Haloboranes with Boron–Methyl Bonds

Gargi Kundu, Sanjukta Pahar, Srinu Tothadi, and Sakya S. Sen*

Cite This: *Organometallics* 2020, 39, 4696–4703

Read Online

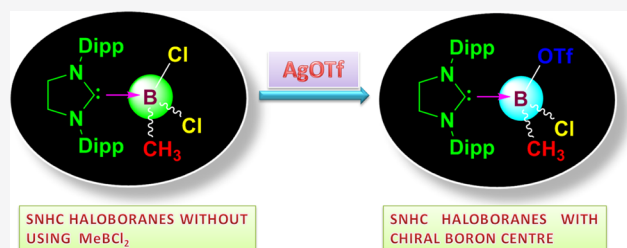
ACCESS |

Metrics & More

Article Recommendations

Supporting Information

ABSTRACT: Compounds of boranes with N-heterocyclic carbenes are known, yet little attention has been paid to NHC compounds of boron bearing methyl and halogen moieties together. The reason can be attributed to the hazardous methylchloroborane (MeBCl_2), which ignites in air. We describe here convenient solution-phase access to $\text{SIDipp}\cdot\text{MeBCl}_2$ ($\text{SIDipp} = 1,3\text{-bis}(2,6\text{-diisopropylphenyl})\text{imidazolin-2-ylidene}$) (**3**) by a salt metathesis reaction of $\text{SIDipp}\cdot\text{BCl}_3$ (**2**) with MeLi . Replacement of the chlorine atoms of **3** with stepwise addition of AgOTf led to the formation of $\text{SIDipp}\cdot\text{MeBCl}(\text{OTf})$ (**4**) and $\text{SIDipp}\cdot\text{MeB}(\text{OTf})_2$ (**5**). In the case of **4**, all of the substituents on the boron atom are different. Subsequently, we extended our synthetic approach to the amidinate system and prepared $\text{PhC}(\text{NtBu})_2\text{B}(\text{Me})\text{Cl}$ (**7**) from the reaction of $\text{PhC}(\text{NtBu})_2\text{BCl}_2$ (**6**) with MeLi .



INTRODUCTION

The combination of an N-heterocyclic carbene (NHC) with a borane usually results in a complex called an NHC-borane. Although before 2008 there were not many reports on NHC-borane complexes, significant advances have been made in the subsequent years. Early work on NHC-boranes was centered on complexes of simple boranes such as BH_3 and BF_3 that were prepared by direct complexation of the NHC with the corresponding borane.¹ Subsequently, the synthesis of more than two dozen NHC-borane complexes with the compositions $\text{NHC}\cdot\text{BX}_3$, $\text{NHC}\cdot\text{BHX}_2$, $\text{NHC}\cdot\text{BH}_2\text{X}$, etc. have been reported, mainly from the groups of Curran, Braunschweig, Robinson, Tamm, and others.^{2,3} In an elegant review of NHC-borane adducts,^{3a} Curran and co-workers noted that the field is still open and concluded by posing this question: what other NHC-boranes can be made? Interestingly, a survey of known $\text{NHC}\cdot\text{RBX}_2$ species with different R groups reveals that common functional groups in carbon chemistry such as methyl groups are rarely found bound to boron atoms in NHC-borane adducts. For example, $\text{NHC}\cdot\text{BCl}_2\text{Ph}$ is known,⁴ but $\text{NHC}\cdot\text{BCl}_2\text{Me}$ is unknown. One reason could be the needed borane (MeBCl_2) is not widely available. It is prepared from the reaction of Me_3SnCl with excess BCl_3 , which gives rise to a mixture of products (eq 1). MeBCl_2 has a boiling point of 11 °C, ignites in contact with air, and should be stored in a Schlenk tube equipped with a grease-free stopcock at a temperature below −30 °C.⁵ Thus, the handling of MeBCl_2 under laboratory conditions is nontrivial. The other reason is that in carbon chemistry the methyl group behaves as an electron donor (+I effect), while in boron chemistry the methyl group, contrary to the common conviction, are electron withdrawing (−I effect) due to the difference in electronegativity between

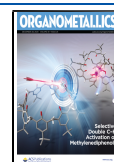
carbon (2.5) and boron (2.0).⁶ As a result, no structural information is available on NHC-methylhaloborane compounds to date. To the best of our knowledge, $\text{IDipp}\cdot\text{BCl}_2i\text{Pr}$ ($\text{IDipp} = 1,3\text{-bis}(2,6\text{-diisopropylphenyl})\text{imidazol-2-ylidene}$) is the only known alkylhaloborane adduct, which was prepared by Braunschweig and co-workers.⁷ Thus, we were interested to make NHC-haloborane adducts, where one of the substituents of the boron atom is a methyl group. It is of note here that MeBCl_2 was detected as an intermediate in the chemical vapor deposition synthesis of boron carbide⁸ and studying the chemistry of MeBCl_2 might provide a deeper understanding of its chemical reactivity.



In 2007, Robinson and co-workers introduced the ligand IDipp to make the $\text{IDipp}\cdot\text{BBR}_3$ adduct and subsequently stabilize compounds with B–B single and double bonds.^{2c} The same NHC was later employed by Braunschweig and co-workers for the isolation of a compound with a $\text{B}\equiv\text{B}$ triple bond.⁹ Curran and co-workers reported a series of NHC-boranes with the same NHC by means of nucleophilic substitution reactions.^{2a} In view of our current interest in saturated NHCs,¹⁰ we have chosen the saturated version of IDipp , known as SIDipp ($\text{SIDipp} = 1,3\text{-bis}(2,6\text{-diisopropylphenyl})\text{imidazolin-2-ylidene}$).

Received: October 27, 2020

Published: December 15, 2020



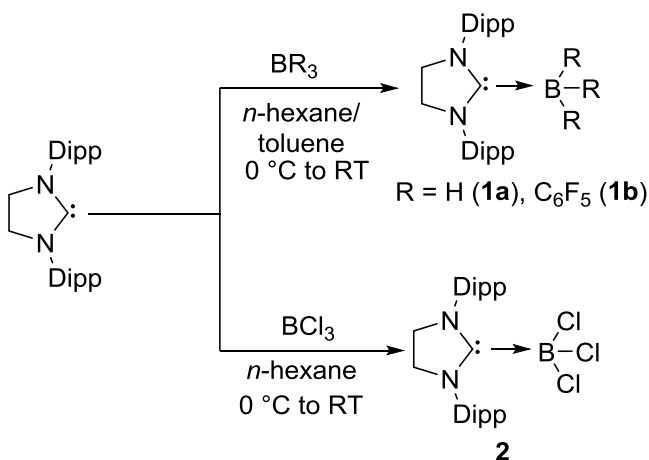
diisopropylphenyl)imidazolin-2-ylidene) for our study. We have noted that the contribution of saturated NHCs to boron chemistry is rather cursory. Nonetheless, the Braunschweig group isolated a B–B triply bound compound using the SIDipp ligand (SIDipp→B≡B←SIDipp).¹¹

Herein we demonstrate a detailed study of nucleophilic substitution reactions of SIDipp·BCl₃ (2), which led to the adduct SIDipp·BMeCl₂ (3). This is the first carbene·BMeCl₂ adduct, and it does not require the use of hazardous MeBCl₂. Removal of another chlorine from 3 with the trifluoromethanesulfonate (OTf) group resulted in an unusual NHC·borane, SIDipp·B(Me)(Cl)(OTf) (4), where the three groups attached to the boron center are different. Subsequent removal of another chloride by an OTf moiety led to SIDipp·B(Me)(OTf)₂ (5). We further extended the nucleophilic substitution reaction to the amidinate boron system.

RESULTS AND DISCUSSION

We started our investigation by reacting SIDipp with simple commercially available boron compounds. The addition of 1 equiv of BH₃·ether in a hexane solution of SIDipp at low temperature led to the formation of 1a (Scheme 1). The latter

Scheme 1. Synthesis of 1a,b and 2



was previously characterized by NMR spectroscopy by the Curran's group in 2010,¹² but was not structurally characterized. Storing the concentrated toluene solution at −35 °C in a freezer afforded colorless crystals of 1a suitable for single-crystal X-ray analysis. It crystallizes in the monoclinic space group *P*2₁/*n* (Figure 1). The formation of the adduct resulted in pyramidalization of the boron atom, leading to a distorted tetrahedral geometry, with a change in hybridization at boron from approximately sp² to sp³. The distance between the boron and the carbene carbon atom is 1.593(4) Å, which is comparable with those in the previously reported NHC·BH₃ adducts.^{13a}

SIDipp·B(C₆F₅)₃ (1b) was synthesized by the treatment of tris(pentafluorophenyl)borane with a toluene solution of SIDipp at very low temperature. Colorless crystals of 1b were isolated by keeping the solution at −36 °C for 1 day. 1b crystallizes in the monoclinic space group *P*1̄. The molecular structure of 1b is shown in Figure 2. The distance between carbene carbon atom C27 and the B atom is 1.696(3) Å, which is longer than that for a normal IDipp·B(C₆F₅)₃ adduct (1.663(5) Å).^{13b} This bond elongation is probably a consequence of the enhanced steric bulk at the tetracoordi-

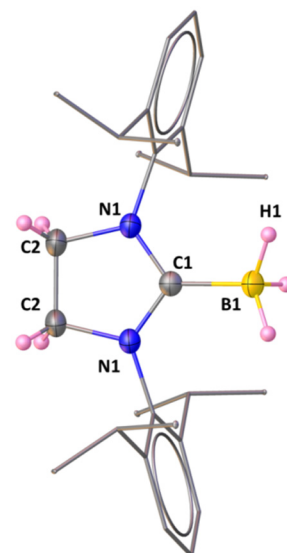


Figure 1. Molecular structure of 1a, with only a half-molecule in the symmetric unit. Except for hydrogen atoms attached to the boron atom and the carbene backbone, other hydrogen atoms are omitted for clarity. Selected bond lengths (Å) and angles (deg): C2–C2 1.517(4), C2–N1 1.465(2), C1–N1 1.338(2), C1–B1 1.593(4), B1–H1 1.085(1); N1–C1–N1 108.5(2), N1–C1–B1 125.73(11), C1–B1–H1 111.1.

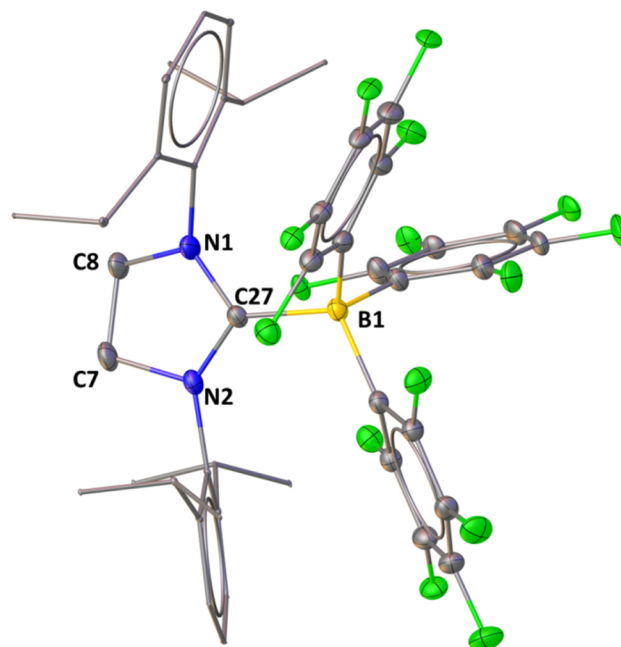


Figure 2. Molecular structure of 1b. Hydrogen atoms are omitted for clarity. Selected bond lengths (Å) and angles (deg): C7–C8 1.483(4), C8–N1 1.484(3), C7–N2 1.477(3), C27–N2 1.355(3), C27–N1 1.343(3), C27–B1 1.696(3); N1–C27–N2 107.69(18), N1–C27–B1 130.5(2), N2–C27–B1 121.42(18).

nated boron center. One of the pentafluoroarene rings is coplanar with the Dipp arene ring; this is stabilized through a π –arene interaction. The ¹¹B NMR spectrum of 1b shows one signal at −15.5 ppm, which is in accordance with the recently reported aNHC adduct of B(C₆F₅)₃.¹⁴ Similar to the case for IDipp·B(C₆F₅)₃, 1b is not stable in solution at room

temperature and hence we were unable to satisfactorily characterize it by NMR spectroscopy.

Subsequently, we have also prepared the adduct $\text{SiDipp}\cdot\text{BCl}_3$ (**2**), which was characterized by NMR spectroscopy. The addition of 1 equiv of MeLi to a toluene solution of **2** at -78°C cleanly afforded the monosubstituted product **3**. After filtration of the lithium chloride precipitate, the concentrated toluene solution was kept for crystallization at 4°C , which afforded colorless crystals of **3** after 1 day in 60% yield. To the best of our knowledge, this is the first methylchloroborane adduct of any carbene because no $\text{cAAC}\cdot\text{B}(\text{Me})\text{Cl}_2$ adduct has been reported. We have also attempted the analogous metathesis reaction with $\text{IDipp}\cdot\text{BCl}_3$, which was not successful and led to a mixture of products, which we could not identify.

The molecular structure of **3** is shown in Figure 3 along with the important bond lengths and angles. **3** crystallizes in the

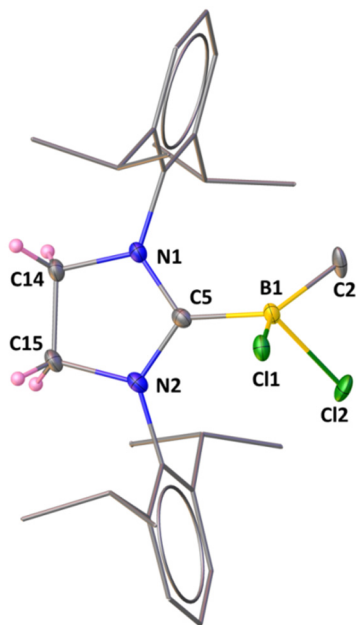
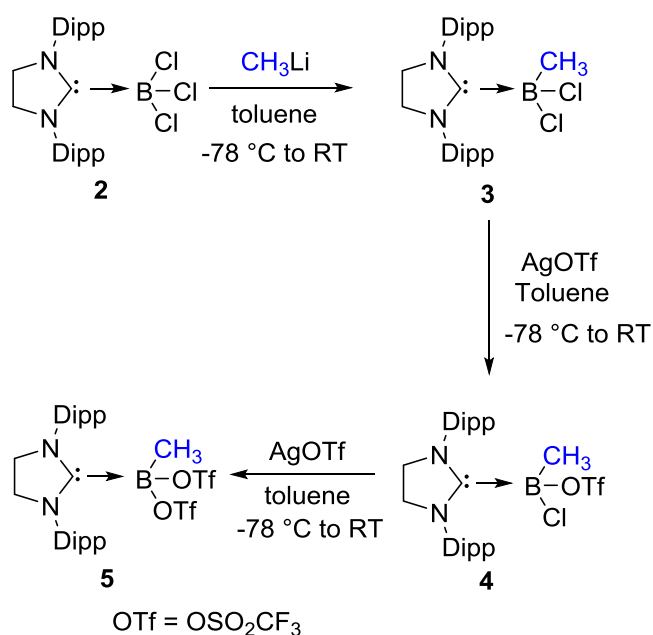


Figure 3. Molecular structure of **3**. Hydrogen atoms except for the back protons are omitted for clarity. Selected bond lengths (Å) and angles (deg): C14–C15 1.516(2), C5–N1 1.3307(17), C15–N2 1.4806(19), C5–N2 1.3338(16), C5–B1 1.6261(19), B1–C2 1.610(6), B1–C1 1.844(3), B1–Cl1 1.822(2); N1–C5–N2 109.93(11), N1–C5–B1 121.23(11), N2–C5–B1 128.40(12), C2–B1–Cl1 132.0(3).

monoclinic space group $P2_1/n$. The carbene carbon atom C5 is tricoordinated and features a trigonal-planar geometry, and the boron atom connected with the C5 atom forms a tetrahedral geometry. The B1–C5 bond distance is 1.6261(19) Å, which is slightly longer in comparison to that in **1a** (1.59(4) Å). There is a disorder in the methyl position of **3** (for clarity we are showing only one carbon atom). The C5 atom is associated with 78% occupancy, and the C2 atom is associated with 28% occupancy. The B1–C1 distance (1.844(3) Å) is slightly higher in comparison to the B1–C2 distance (1.610(6) Å).

In order to study the reactivity of **3**, we added silver triflate to a toluene solution of **3** at -78°C , which led to a nucleophilic substitution of one of the labile chlorine atoms by a triflate group (Scheme 2). Colorless crystals of **4** suitable for X-ray diffraction studies were grown from a saturated toluene solution at 4°C . **4** is one of the rare NHC-stabilized boron

Scheme 2. Synthesis of **3–5**



compounds where the four groups on the central boron atom are different.^{15–18} Further addition of 1 equiv more of silver triflate to a toluene solution of **4** results in replacement of another chlorine atom from the boron core by a triflate group and gives **5** with two triflate groups and one methyl group at the center boron atom.

The molecular structure of **4** is in agreement with the data obtained in solution and is depicted in Figure 4 together with the important geometrical parameters. The chiral boron atom exhibits a distorted-tetrahedral geometry. The distance between the methyl and the boron is B1–C26 1.682(3) Å, which is significantly shorter than that in **3** presumably due to the electron-withdrawing nature of the triflate group. The boron atom (B1) lies slightly below the plane of an imidazolium ring (torsion angles (deg): C(15)–N(1)–C(5)–B(1) 166.53(16) and C(16)–N(2)–C(5)–B(1) –173.64(15)) and the B–O bond is not orthogonal to the plane of the imidazolium ring with the torsion angles N1–C5–B1–O3 41.58° and N2–C5–B1–O3 –148.93. The B–OTf bond length is 1.503(3) Å, which is in good agreement with the B–O bond length in Curran's $\text{IDipp}\cdot\text{BH}_2\text{OTs}$ (1.522(7) Å, Ts = tosylate).^{2a}

Compounds **3–5** were characterized by NMR spectroscopy (Table 1), and the NMR spectra obtained were compatible with their structures. The ^{11}B NMR spectrum of **3** shows a resonance at 1.98 ppm, which is downfield from that in **2** (1.28 ppm). The presence of a methyl group bound to the boron atom is reflected by the resonance at 1.24 ppm in the ^1H NMR spectrum of **3**. Replacement of another chlorine ligand by a triflate moiety in **4** led to an upfield shift in the ^{11}B NMR spectrum (–2.54 ppm). The methyl protons of **4** bound to boron resonate at 1.29 ppm in the ^1H NMR. In the ^{19}F NMR spectrum of **4**, the SO_3CF_3 group appears at –78.21 ppm. Substitution of the last chlorine ligand by another triflate moiety led to a further upfield shift in the ^{11}B NMR of **5** (–6.62 ppm). The ^{19}F NMR spectrum of **5** shows a broad signal at δ –76.99 ppm, which is shifted to marginally lower field from that in **4**.

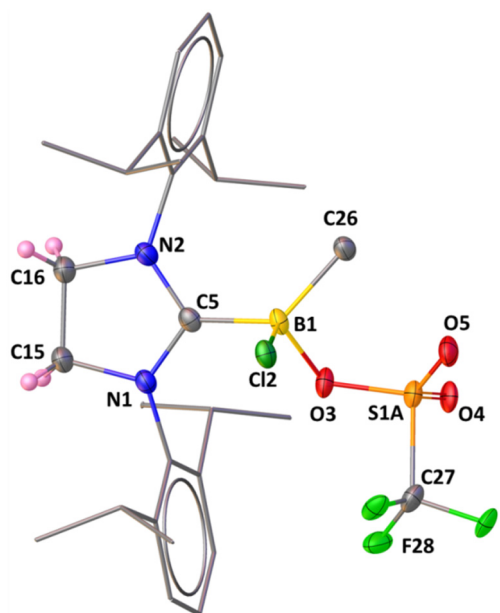


Figure 4. Molecular structure of **4**. Hydrogen atoms except for the back protons are omitted for clarity. There is a disorder associated with the fluorine, oxygen, and sulfur atoms in the triflate group; for clarity we are not showing the disordered atoms. Selected bond lengths (Å) and angles (deg): C15–C16 1.525(3), C5–B1 1.617(3), B1–Cl2 1.880(3), B1–C26 1.682(3), B1–O3 1.503(3), O3–S1A 1.515(16), S1A–O5 1.427(2); N1–C5–N2 110.21(15), Cl2–B1–C26 115.59(16), B1–O3–S1A 124.16(14), O3–S1A–C27 97.94(15).

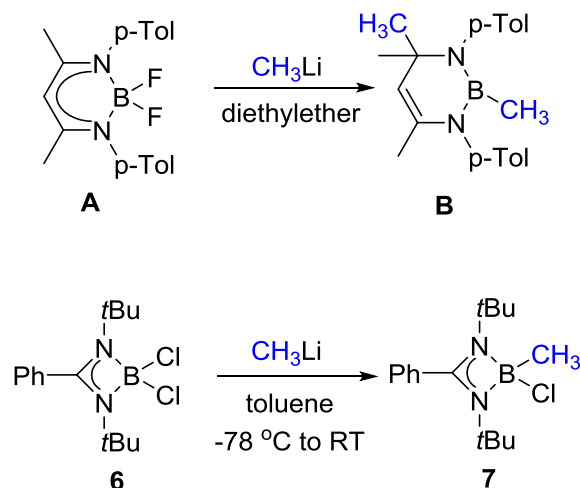
Table 1. Comparison of $C_{\text{SIDipp}} \rightarrow B$ Bond Lengths (Å) and ^{11}B NMR of SIDipp-borane Adducts

compound	$C_{\text{SIDipp}} \rightarrow B$ bond length (Å)	^{11}B NMR (ppm)
1a	1.593(4)	−36.0 ¹⁰
1b	1.696(3)	−15.53
2		1.28
3	1.6261(19)	1.98
4	1.617(3)	−2.54
5		−6.62

A nucleophilic substitution reaction was also attempted on an amidinate boron system. In 1999, Smith and co-workers reported that the reaction of (Tolylnacnac)BF₂ (**A**) with MeLi resulted in [η^2 -(Me)₂C(Ntolyl)CH=C(Ntolyl)Me]BMe (**B**) (Scheme 3).¹⁹ In fact, Aldridge and co-workers also reported that the reaction of PhC{(N*t*Pr)₂BBr₂} with Yamashita's boryllithium reagent (thf)₂Li{B(NDippCH)₂}²⁰ did not lead to a metathetical product but afforded an alternative product stemming from the nucleophilic attack at the remote C center rather than the B center.²¹ However, the reaction of PhC{(N*t*Bu)₂BCl₂} (**6**) (Figure 5) with 1 equiv of MeLi led to the monosubstituted product **7** (Scheme 3). The methyl protons attached to boron atom show a new peak at 1.19 ppm in the ¹H NMR spectrum. The ¹¹B NMR spectrum of **7** gives a resonance at 6.20 ppm for the tetracoordinate boron atom.

Storing a concentrated toluene solution of **7** at −30 °C in a freezer afforded colorless crystals of **7** suitable for X-ray analysis within 1 day. **7** crystallizes in the orthorhombic space group *Pbca*. In the four-membered BNCN ring, the N1–B1–N2 angle and the B–N distances are 82.60(13)° and average 1.571 Å, respectively, which are similar to those for the other

Scheme 3. Previous Attempt of the Nucleophilic Substitution Reaction of Boron Difluoride (**A**) with MeLi (Top)¹⁹ and Our Work on the Synthesis of **6** and **7** (bottom)



reported amidinoborane complexes.²² The distance between the tetracoordinate boron and the methyl carbon is 1.646(5) Å, which is slightly longer than that in **3**.

CONCLUSION

NHC-boranes are typically readily accessible, but we have mentioned in the Introduction that no NHC adduct of MeBCl₂ has been known. The hesitance of the chemistry community probably stems from the synthetic routes, which are tedious and require special techniques. Here we have prepared saturated N-heterocyclic carbene–boranes bearing methyl groups by a simple salt metathesis reaction starting from SIDipp-BCl₃ (**2**). The resulting products **3–5** are thermally stable, and **3** and **4** have been characterized by X-ray crystallography. **3** is the first carbene–MeBCl₂ adduct, and its preparation does not require the hazardous MeBCl₂. **4** is a rare example of an NHC-coordinated boron compound where all three substituents of the boron atom are different. Further chemistry with **3** and **4** is currently ongoing and will be reported in due course.

EXPERIMENTAL DETAILS

General Procedures and Instrumentation. All manipulations were carried out under an inert atmosphere of argon using standard Schlenk techniques in a argon-filled glovebox. The solvents, especially tetrahydrofuran, dichloromethane, and hexane, were purified by an MBRAUN MB SPS-800 solvent purification system. Other chemicals were purchased from Sigma-Aldrich and TCI Chemicals and were used without further purification. The starting material SIDipp was synthesized by using a literature procedure.²³ ¹H, ¹³C, ¹⁹F, and ¹¹B NMR spectra were recorded in C₆D₆ and CDCl₃, using a Bruker Avance DPX 200, a Bruker Avance DPX 400, or a Bruker Avance DPX 500 spectrometer referenced to external SiMe₄. Elemental analyses for compounds **2–7** were performed at the CSIR National Chemical Laboratory, Pune, India. Due to the sensitivity of the crystals the analytical values show some deviation from the calculated values for **3**, **4**, and **7**. Melting points were measured in a sealed glass tube on a Stuart SMP-30 melting point apparatus and were uncorrected.

Synthesis of 1b. To a solution of B(C₆F₅)₃ (0.26 g, 0.51 mmol) in 5 mL of toluene was added 10 mL of a toluene solution of SIDipp (0.2 g, 0.51 mmol) dropwise at −78 °C. The mixture was warmed to room temperature and stirred for 1 h. The resulting colorless solution

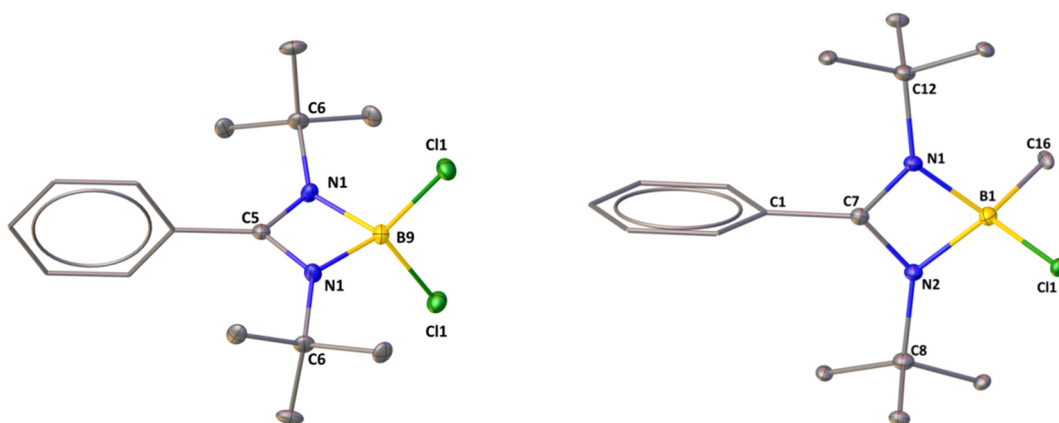


Figure 5. Molecular structures of (left) **6** and (right) **7**. Hydrogen atoms are omitted for clarity. For the molecular structure and labeling diagram of **6**, there is only a half-molecule in the symmetric unit. Selected bond lengths (Å) and angles (deg): for **6**, C5–N1 1.337(2), N1–B9 1.568(3), N1–C6 1.476(2), B9–C11 1.8281(17), N1–C5–N1 101.5(2), N1–B9–N1 82.61(18), N1–B9–C11 114.22(7), N1–B9–C11 114.22(7); for **7**, C1–C7 1.484(2), N1–B1 1.571(3), N2–B1 1.570(3), C7–N1 1.336(2), C7–N2 1.341(2), B1–C11 1.850(2), B1–C16 1.646(5), N1–C7–N2 101.54(15), N1–B1–N2 82.60(13), N1–B1–C11 116.30(14), C11–B1–C16 108.74(19).

was filtered through cannula filtration. The filtrate toluene solution was concentrated to 3–4 mL and kept for crystallization at $-35\text{ }^{\circ}\text{C}$ in a freezer, which afforded colorless crystals of **1b**. The compound was not very stable, and hence we are unable to give proper spectroscopic evidence.

Synthesis of 2. To a solution of SIDipp (0.2 g, 0.51 mmol) in 10 mL of *n*-hexane was added BCl_3 (0.42 mL, 0.51 mmol) dropwise at $-78\text{ }^{\circ}\text{C}$. The mixture was warmed to room temperature and stirred for 1 h. The formation of a white precipitate was observed, which was filtered through cannula filtration. After the precipitate was washed one to two times with *n*-hexane, it was dried under high vacuum. The isolated yield of the white powdered compound was 70%.

^1H NMR (400 MHz, 298 K, CDCl_3): δ 1.35 (d, $J = 6.63$ Hz, 12H, $\text{CH}(\text{CH}_3)_2$), 1.46 (d, $J = 6.88$ Hz, 12H, $\text{CH}(\text{CH}_3)_2$), 3.25 (sept, $J = 6.76$ Hz, 4H, $\text{CH}(\text{CH}_3)_2$), 4.13 (s, 4H, $\text{N-CH}_2\text{CH}_2\text{-N}$), 7.25–7.43 (m, 12H, Ar-H). $^{13}\text{C}\{^1\text{H}\}$ NMR (101 MHz, 298 K, CDCl_3): δ 23.47, 26.04 (H CMe_2), 29.11 (H CMe_2), 53.70 (CH_2CH_2), 124.42, 129.83, 134.61 (Ar- C_6H_3), 145.82 (*ipso*- C_6H_3). $^{11}\text{B}\{^1\text{H}\}$ NMR (128 MHz, 298 K, CDCl_3): 1.28 (s, 1B, BCl_3). Melting point: $295\text{ }^{\circ}\text{C}$ dec. Anal. Calcd for $\text{C}_{27}\text{H}_{38}\text{BCl}_3\text{N}_2$ [506.22 g mol^{-1}]: C, 63.87; H, 7.54; N, 5.52. Found: C, 63.85; H, 7.58; N, 5.48.

Synthesis of 3. One equivalent of MeLi (0.61 mL, 1.1 mmol) was added dropwise to a toluene solution of **2** (0.506 g, 1 mmol) at $-78\text{ }^{\circ}\text{C}$. The reaction mixture was warmed to room temperature and stirred for 12 h, which resulted in the generation of a white precipitate of lithium chloride. It was further filtered through frit filtration. The toluene solution of the filtrate was concentrated and was kept for crystallization at $4\text{ }^{\circ}\text{C}$, which afforded colorless crystals of **3** after 1 day in a 60% (0.29 g) yield.

^1H NMR (400 MHz, 298 K, C_6D_6): δ 1.11 (d, $J = 6.49$ Hz, 12H, $\text{CH}(\text{CH}_3)_2$), 1.49 (d, $J = 6.87$ Hz, 12H, $\text{CH}(\text{CH}_3)_2$), 1.24 (s, 3H, $\text{B}(\text{CH}_3)_2$), 3.27 (sept, $J = 6.49$ Hz, 4H, $\text{CH}(\text{CH}_3)_2$), 3.46 (s, 4H, $\text{N-CH}_2\text{CH}_2\text{-N}$), 7.04–7.19 (m, 12H, Ar-H). $^{13}\text{C}\{^1\text{H}\}$ NMR (101 MHz, 298 K, C_6D_6): δ 24.32, 26.56 (H CMe_2), 29.81 (H CMe_2), 53.69 (CH_2CH_2), 125.30, 130.70, 134.59 (Ar- C_6H_3), 146.97 (*ipso*- C_6H_3). $^{11}\text{B}\{^1\text{H}\}$ NMR (128 MHz, 298 K, C_6D_6): 1.98 (s, 1B, BMeCl_2). Melting point: $200\text{ }^{\circ}\text{C}$ dec. Anal. Calcd for $\text{C}_{29}\text{H}_{41}\text{BCl}_2\text{N}_2$ [486.27 g mol^{-1}]: C, 69.01; H, 8.48; N, 5.75. Found: C, 58.88; H, 8.40; N, 5.69.

Synthesis of 4. A toluene solution (20 mL) of **3** (0.48 g, 1 mmol) was added dropwise to a toluene solution (20 mL) of previously weighed AgOTf (0.25 g, 1 mmol) at $-78\text{ }^{\circ}\text{C}$ in the absence of light. A white precipitate of AgCl formed immediately, and it was filtered through frit filtration after the reaction mixture was warmed to room temperature. The colorless toluene solution was concentrated (5 mL) and was kept for crystallization at $4\text{ }^{\circ}\text{C}$, which afforded colorless crystals of **4** after 1–2 day(s) in a 68% (0.41 g) yield.

^1H NMR (400 MHz, 298 K, C_6D_6): δ 1.12 (d, $J = 6.63$ Hz, 12H, $\text{CH}(\text{CH}_3)_2$), 1.43 (d, $J = 6.88$ Hz, 12H, $\text{CH}(\text{CH}_3)_2$), 1.29 (s, 3H, $\text{B}(\text{CH}_3)_2$), 3.27 (sept, $J = 6.75$ Hz, 4H, $\text{CH}(\text{CH}_3)_2$), 3.51 (s, 4H, $\text{N-CH}_2\text{CH}_2\text{-N}$), 7.06–7.18 (m, 12H, Ar-H). $^{13}\text{C}\{^1\text{H}\}$ NMR (101 MHz, 298 K, C_6D_6): δ 24.37, 26.61 (H CMe_2), 29.85 (H CMe_2), 53.88 (CH_2CH_2), 125.33, 130.73, 134.62 (Ar- C_6H_3), 147.06 (*ipso*- C_6H_3). $^{11}\text{B}\{^1\text{H}\}$ NMR (128 MHz, 298 K, C_6D_6): -2.54 (br s, 1B, $\text{BCl}(\text{Me})\text{OTf}$). $^{19}\text{F}\{^1\text{H}\}$ NMR (128 MHz, 298 K, C_6D_6): -78.21 (br s, 3F, $\text{BCl}(\text{Me})\text{OSO}_2\text{CF}_3$). Melting point: $158\text{ }^{\circ}\text{C}$. Anal. Calcd for $\text{C}_{29}\text{H}_{41}\text{BClF}_3\text{N}_2\text{O}_3\text{S}_4$ [600.26 g mol^{-1}]: C, 57.96; H, 6.88; N, 4.66. Found: C, 56.88; H, 6.05; N, 4.62.

Synthesis of 5. A toluene solution of **4** (0.60 g, 1 mmol) was added dropwise to a toluene solution of previously weighed AgOTf (0.25 g, 1 mmol) at $-78\text{ }^{\circ}\text{C}$ in the absence of light. A white precipitate of AgCl was formed immediately, and it was filtered through frit filtration after the reaction mixture was warmed to room temperature. The colorless toluene solution was dried under vacuum and afforded a white powder of **5** in 56% (0.39 g) yield.

^1H NMR (400 MHz, 298 K, C_6D_6): δ 1.06 (s, 3H, $\text{B}(\text{CH}_3)_2$), 1.17 (d, $J = 6.63$ Hz, 12H, $\text{CH}(\text{CH}_3)_2$), 1.40 (d, $J = 6.63$ Hz, 12H, $\text{CH}(\text{CH}_3)_2$), 3.22 (sept, $J = 6.75$ Hz, 4H, $\text{CH}(\text{CH}_3)_2$), 3.71 (s, 4H, $\text{N-CH}_2\text{CH}_2\text{-N}$), 6.96–7.04 (m, 12H, Ar-H). $^{13}\text{C}\{^1\text{H}\}$ NMR (101 MHz, 298 K, C_6D_6): δ 24.31, 26.60 (H CMe_2), 29.81 (H CMe_2), 54.06 (CH_2CH_2), 125.26, 130.72, 134.47 (Ar- C_6H_3), 147.08 (*ipso*- C_6H_3). $^{11}\text{B}\{^1\text{H}\}$ NMR (128 MHz, 298 K, C_6D_6): -6.62 (br s, 1B, $\text{BCl}(\text{Me})\text{OTf}$). $^{19}\text{F}\{^1\text{H}\}$ NMR (128 MHz, 298 K, C_6D_6): -76.99 (br s, $\text{BClMe}(\text{OSO}_2\text{CF}_3)_2$). Melting point: $147\text{ }^{\circ}\text{C}$ dec. Anal. Calcd for $\text{C}_{30}\text{H}_{41}\text{BF}_6\text{N}_2\text{O}_6\text{S}_2$ [714.24 g mol^{-1}]: C, 50.42; H, 5.78; N, 3.92. Found: C, 50.27; H, 5.41; N, 3.83.

Synthesis of 6. PhLi (5.4 mL, 10.25 mmol, 1.9 M in diethyl ether) was added to a solution of $t\text{BuN}=\text{C}=\text{N}t\text{Bu}$ (1.55 g, 10.0 mmol) in toluene (50 mL) in a 100 mL Schlenk flask at $-78\text{ }^{\circ}\text{C}$. The solution was warmed to ambient temperature and stirred for 4 h. Then BCl_3 (12.5 mL, 12.5 mmol, 1.0 M in hexane) was added drop by drop to the reaction mixture at $-78\text{ }^{\circ}\text{C}$. The reaction mixture was warmed to room temperature and stirred for another 18 h. The white precipitate of the reaction mixture was filtered through Celite. The resultant toluene solvent was removed under reduced pressure, concentrated to 10–12 mL, and stored at $-30\text{ }^{\circ}\text{C}$ in a freezer, which afforded colorless crystals of **6** suitable for X-ray analysis within 1 day. Yield: 3.09 g (98.4%).

^1H NMR (400 MHz, C_6D_6 , 298 K): δ 1.19 (s, 18 H), 6.85–6.93 (m, 5 H) ppm. ^{13}C NMR (101 MHz, C_6D_6 , 298 K): δ 30.88, 54.89, 128.07, 128.15, 128.63, 128.70, 130.87 ppm. $^{11}\text{B}\{^1\text{H}\}$ NMR (128 MHz, 298 K, C_6D_6): 6.22 (s, 1B, BCl_2). Melting point: $189\text{ }^{\circ}\text{C}$ dec.

Anal. Calcd for $C_{15}H_{24}BCl_2N_2$ [$313.14 \text{ g mol}^{-1}$]: C, 57.36; H, 7.70; N, 8.92. Found: C, 57.82; H, 7.79; N, 8.52.

Synthesis of 7. One equivalent of MeLi (0.33 mL, 1.02 mmol, 3.1 M in diethoxymethane) was added dropwise to a toluene solution of **6** (0.315 g, 1 mmol) at $-78 \text{ }^\circ\text{C}$, and the reaction mixture was slowly warmed to room temperature. After the mixture was stirred for another 12 h at room temperature, a white precipitate of lithium chloride was formed, which was further filtered through frit filtration. The toluene filtrate solution was concentrated to 5–6 mL and was kept for crystallization at $-30 \text{ }^\circ\text{C}$, which afforded colorless crystals of **7** within 1 day in 32% (0.095 g) yield.

^1H NMR (400 MHz, C_6D_6 , 298 K): δ 1.13 (s, 18 H) 1.19 (s, 3 H) 6.84–6.98 (m, 5 H) ppm. ^{13}C NMR (101 MHz, C_6D_6 , 298 K): δ 30.87, 31.19, 53.58, 128.20, 128.58, 130.54, 132.31, 170.85 ppm. $^{11}\text{B}\{^1\text{H}\}$ NMR (128 MHz, 298 K, C_6D_6): 6.20 (s, 1B, $BMeCl_2$), 0.87 ppm. Melting point: $105 \text{ }^\circ\text{C}$. Anal. Calcd for $C_{16}H_{27}BCl_2N_2$ [$293.20 \text{ g mol}^{-1}$]: C, 65.44; H, 9.27; N, 9.54. Found: C, 65.38; H, 9.59; N, 9.30.

Crystallographic Data for the Structural Analysis of Compounds 1a, 1b, 3, 4, 6, and 7. Single crystals of **1a**, **1b**, **3**, **4**, **6**, and **7** were mounted on a Bruker SMART APEX II single crystal X-ray CCD diffractometer having graphite-monochromated (Mo $K\alpha = 0.71073 \text{ \AA}$) radiation at a low temperature of 100 K. The X-ray generator was operated at 50 kV and 30 mA. The X-ray data acquisition was monitored by the APEX2 program suite. The data were corrected for Lorentz–polarization and absorption effects using the SAINT and SADABS programs, which are an integral part of the APEX2 package.²⁴ The structures were solved by direct methods and refined by full-matrix least squares, based on F^2 , using SHELXL. Crystal structures were refined using Olex2-1.0 software. Anisotropic refinement was performed for all non-H atoms. The C–H hydrogen atoms were calculated using the riding model.²⁵ The structures were examined using the ADSYM subroutine of PLATON to ensure that no additional symmetry could be applied to the models. The molecular weight of each structure mentioned herein has been calculated considering the solvent molecules trapped in the crystal. Crystallographic information is available at www.ccdc.cam.ac.uk/data or as part of the Supporting Information.

1a: $C_{27}H_{41}BN_2$, colorless, $0.17 \times 0.15 \times 0.1 \text{ mm}^3$, monoclinic, space group $Pnma$, $a = 11.953(4) \text{ \AA}$, $b = 20.524(7) \text{ \AA}$, $c = 10.910(3) \text{ \AA}$, $\alpha = \gamma = \beta = 90^\circ$, $V = 2676.5(15) \text{ \AA}^3$, $Z = 4$, $T = 105 \text{ K}$, $2\theta_{\text{max}} = 40.7^\circ$, $D_{\text{calc}} = 1.004 \text{ g cm}^{-3}$, $F(000) = 888$, $\mu = 0.057 \text{ mm}^{-1}$, 30029 reflections collected, 3486 unique reflections ($R_{\text{int}} = 0.067$), 1867 observed ($I > 2\sigma(I)$) reflections, multiscan absorption correction, $T_{\text{min}} = 0.636$, $T_{\text{max}} = 0.746$, 143 refined parameters, $S = 1.022$, $R1 = 0.099$, $wR2 = 0.1937$ (all data $R1 = 0.1476$, $wR2 = 0.226$), maximum and minimum residual electron densities $\Delta\rho_{\text{max}} = 0.229 \text{ e \AA}^{-3}$, $\Delta\rho_{\text{min}} = -0.221 \text{ e \AA}^{-3}$. CCDC: 2040725.

1b: $C_{45}H_{38}BF_5N_2$, colorless, $0.4 \times 0.34 \times 0.18 \text{ mm}^3$, monoclinic, space group $P1$, $a = 9.2054(8) \text{ \AA}$, $b = 12.0369(11) \text{ \AA}$, $c = 19.8417(17) \text{ \AA}$, $\alpha = 78.184(4)^\circ$, $\beta = 86.061(4)^\circ$, $\gamma = 74.567(4)^\circ$, $V = 2074.1(3) \text{ \AA}^3$, $Z = 2$, $T = 267(2) \text{ K}$, $2\theta_{\text{max}} = 56.58^\circ$, $D_{\text{calc}} = 1.445 \text{ g cm}^{-3}$, $F(000) = 924$, $\mu (\text{mm}^{-1}) = 0.131$, 79662 reflections collected, 10321 unique reflections ($R_{\text{int}} = 0.0549$), 5975 observed ($I > 2\sigma(I)$) reflections, multiscan absorption correction, $T_{\text{min}} = 0.948$, $T_{\text{max}} = 0.977$, 576 refined parameters, $S = 1.019$, $R1 = 0.0632$, $wR2 = 0.1352$ (all data $R1 = 0.1193$, $wR2 = 0.1686$), maximum and minimum residual electron densities $\Delta\rho_{\text{max}} = 0.236 \text{ e \AA}^{-3}$, $\Delta\rho_{\text{min}} = -0.235 \text{ e \AA}^{-3}$. CCDC: 2040726.

3: $C_{28}H_{38}BCl_2N_2$, colorless, $0.25 \times 0.1 \times 0.1 \text{ mm}^3$, monoclinic, space group $P2_1/c$, $a = 13.5240(10) \text{ \AA}$, $b = 14.8694(10) \text{ \AA}$, $c = 14.9855(9) \text{ \AA}$, $\alpha = \gamma = 90^\circ$, $\beta = 113.028(2)^\circ$, $V = 2773.4(3) \text{ \AA}^3$, $Z = 4$, $T = 100(2) \text{ K}$, $2\theta_{\text{max}} = 61.09^\circ$, $D_{\text{calc}} = 1.160 \text{ g cm}^{-3}$, $F(000) = 1036$, $\mu = 0.252 \text{ mm}^{-1}$, 113554 reflections collected, 9811 unique reflections ($R_{\text{int}} = 0.1478$), 8448 observed ($I > 2\sigma(I)$) reflections, multiscan absorption correction, $T_{\text{min}} = 0.970$, $T_{\text{max}} = 0.975$, 325 refined parameters, $S = 1.082$, $R1 = 0.0485$, $wR2 = 0.1346$ (all data $R1 = 0.0594$, $wR2 = 0.1478$), maximum and minimum residual electron densities $\Delta\rho_{\text{max}} = 0.698 \text{ e \AA}^{-3}$, $\Delta\rho_{\text{min}} = -0.617 \text{ e \AA}^{-3}$. CCDC: 2040731.

4: $C_{36}H_{48}BClF_3N_2O_3S$ sum formula, colorless, $0.16 \times 0.15 \times 0.12 \text{ mm}^3$, monoclinic, space group $P2_1/n$, $a = 12.2563(12) \text{ \AA}$, $b = 14.7943(14) \text{ \AA}$, $c = 20.6918(18) \text{ \AA}$, $\alpha = \gamma = 90^\circ$, $\beta = 104.604(4)^\circ$, $V = 3630.7(6) \text{ \AA}^3$, $Z = 4$, $T = 100(2) \text{ K}$, $2\theta_{\text{max}} = 61.18^\circ$, $D_{\text{calc}} = 1.266 \text{ g cm}^{-3}$, $F(000) = 1468.0$, $\mu = 0.215 \text{ mm}^{-1}$, 269370 reflections collected, 11118 unique reflections ($R_{\text{int}} = 0.056$), 9675 observed ($I > 2\sigma(I)$) reflections, multiscan absorption correction, $T_{\text{min}} = 0.966$, $T_{\text{max}} = 0.975$, 500 refined parameters, $S = 1.121$, $R1 = 0.0679$, $wR2 = 0.2003$ (all data $R1 = 0.0780$, $wR2 = 0.2129$), maximum and minimum residual electron densities $\Delta\rho_{\text{max}} = 0.791 \text{ e \AA}^{-3}$, $\Delta\rho_{\text{min}} = -1.248 \text{ e \AA}^{-3}$. CCDC: 2040732.

6: $C_{15}H_{23}BCl_2N_2$, colorless, $0.15 \times 0.12 \times 0.12 \text{ mm}^3$, monoclinic, space group $C2/c$, $a = 14.3073(5) \text{ \AA}$, $b = 10.6719(4) \text{ \AA}$, $c = 12.4297(7) \text{ \AA}$, $\alpha = \gamma = 90^\circ$, $\beta = 116.9710(10)^\circ$, $V = 1691.43(13) \text{ \AA}^3$, $Z = 4$, $T = 100(2) \text{ K}$, $2\theta_{\text{max}} = 61.04^\circ$, $D_{\text{calc}} = 1.229 \text{ g cm}^{-3}$, $F(000) = 664.0$, $\mu = 0.376 \text{ mm}^{-1}$, 8773 reflections collected, 1546 unique reflections ($R_{\text{int}} = 0.034$), 1525 observed ($I > 2\sigma(I)$) reflections, multiscan absorption correction, $T_{\text{min}} = 0.947$, $T_{\text{max}} = 0.956$, 96 refined parameters, $S = 1.127$, $R1 = 0.0442$, $wR2 = 0.1259$ (all data $R1 = 0.0445$, $wR2 = 0.1261$), maximum and minimum residual electron densities $\Delta\rho_{\text{max}} = 0.405 \text{ e \AA}^{-3}$, $\Delta\rho_{\text{min}} = -0.408 \text{ e \AA}^{-3}$. CCDC: 2040733.

7: $C_{31}H_{49}B_2Cl_2N_4$ sum formula, colorless, $0.38 \times 0.28 \times 0.18 \text{ mm}^3$, orthorhombic, space group $Pbca$, $a = 10.3728(6) \text{ \AA}$, $b = 13.9814(10) \text{ \AA}$, $c = 22.0596(15) \text{ \AA}$, $\alpha = \gamma = \beta = 90^\circ$, $V = 3199.2(4) \text{ \AA}^3$, $Z = 4$, $T = 100 \text{ K}$, $2\theta_{\text{max}} = 56.58^\circ$, $D_{\text{calc}} = 1.184 \text{ g cm}^{-3}$, $F(000) = 1228$, $\mu = 0.229 \text{ mm}^{-1}$, 85885 reflections collected, 3932 unique reflections ($R_{\text{int}} = 0.103$), 3110 observed ($I > 2\sigma(I)$) reflections, multiscan absorption correction, $T_{\text{min}} = 0.926$, $T_{\text{max}} = 0.960$, 188 refined parameters, $S = 1.065$, $R1 = 0.0721$, $wR2 = 0.1435$ (all data $R1 = 0.1236$, $wR2 = 0.1527$), maximum and minimum residual electron densities $\Delta\rho_{\text{max}} = 0.509 \text{ e \AA}^{-3}$, $\Delta\rho_{\text{min}} = -0.491 \text{ e \AA}^{-3}$. CCDC: 2040734.

■ ASSOCIATED CONTENT

Supporting Information

The Supporting Information is available free of charge at <https://pubs.acs.org/doi/10.1021/acs.organomet.0c00691>.

Representative NMR spectra of **2–7** (PDF)

Accession Codes

CCDC 2040725–2040726 and 2040731–2040734 contain the supplementary crystallographic data for this paper. These data can be obtained free of charge via www.ccdc.cam.ac.uk/data_request/cif, or by emailing data_request@ccdc.cam.ac.uk, or by contacting The Cambridge Crystallographic Data Centre, 12 Union Road, Cambridge CB2 1EZ, UK; fax: +44 1223 336033.

■ AUTHOR INFORMATION

Corresponding Author

Sakya S. Sen – Inorganic Chemistry and Catalysis Division, CSIR-National Chemical Laboratory, Pune 411008, India; Academy of Scientific and Innovative Research (AcSIR), Ghaziabad 201002, India; orcid.org/0000-0002-4955-5408; Email: ss.sen@ncl.res.in

Authors

Gargi Kundu – Inorganic Chemistry and Catalysis Division, CSIR-National Chemical Laboratory, Pune 411008, India; Academy of Scientific and Innovative Research (AcSIR), Ghaziabad 201002, India

Sanjukta Pahar – Inorganic Chemistry and Catalysis Division, CSIR-National Chemical Laboratory, Pune 411008, India; Academy of Scientific and Innovative Research (AcSIR), Ghaziabad 201002, India

Srinu Tothadi – Organic Chemistry Division, CSIR-National Chemical Laboratory, Pune 411008, India; orcid.org/0000-0001-6840-6937

Complete contact information is available at:
<https://pubs.acs.org/10.1021/acs.organomet.0c00691>

Notes

The authors declare no competing financial interest.

ACKNOWLEDGMENTS

Science and Engineering Research Board (SERB) of India (CRG/2018/000287) (S.S.S.) is acknowledged for providing financial assistance. G.K. thanks the Council of Scientific and Industrial Research (CSIR) of India for a research fellowship. S.P. thanks the DST of India for an INSPIRE Fellowship (IF160314). S.T. is grateful to the CSIR-HRDG for an SRA fellowship (Pool No. 9119).

REFERENCES

- (1) (a) Kuhn, N.; Henkel, G.; Kratz, T.; Kreutzberg, J.; Boese, R.; Maulitz, A. H. Derivate des Imidazols, VI. Stabile Carben-Borane. *Chem. Ber.* **1993**, *126*, 2041–2045. (b) Ramnial, T.; Jong, H.; McKenzie, I. D.; Jennings, M.; Clyburne, J. A. C. An imidazol-2-ylidene borane complex exhibiting inter-molecular [C–H^{δ+}...H^{δ-}–B] dihydrogen bonds. *Chem. Commun.* **2003**, 1722–1723. (c) Yamaguchi, Y.; Kashiwabara, T.; Ogata, K.; Miura, Y.; Nakamura, Y.; Kobayashi, K.; Ito, T. Synthesis and reactivity of triethylborane adduct of N-heterocyclic carbene: versatile synthons for synthesis of N-heterocyclic carbene complexes. *Chem. Commun.* **2004**, 2160–2161. (d) Arduengo, A. J., III; Davidson, F.; Kracczyk, R.; Marshall, W. J.; Schmutzler, R. Carbene Complexes of Pnictogen Pentafluorides and Boron Trifluoride. *Monatsh. Chem.* **2000**, *131*, 0251–0265. (e) Nielsen, D. J.; Cavell, K. J.; Skelton, B. W.; White, A. H. Tetrafluoroborate Anion B–F Bond Activation—Unusual Formation of a Nucleophilic Heterocyclic Carbene:BF₃ Adduct. *Inorg. Chim. Acta* **2003**, *352*, 143–150.
- (2) (a) Solovyyev, A.; Chu, Q.; Geib, S. J.; Fensterbank, L.; Malacria, M.; Lacôte, E.; Curran, D. P. Substitution Reactions at Tetracoordinate Boron: Synthesis of N-Heterocyclic Carbene Boranes with Boron-Heteroatom Bonds. *J. Am. Chem. Soc.* **2010**, *132*, 15072–15080. (b) Brahmi, M. M.; Monot, J.; Desage-El Murr, M.; Curran, D. P.; Fensterbank, L.; Lacote, E.; Malacria, M. Preparation of NHC Borane Complexes by Lewis Base Exchange with Amine- and Phosphine-Boranes. *J. Org. Chem.* **2010**, *75*, 6983–6985. (c) Bissinger, P.; Braunschweig, H.; Kraft, K.; Kupfer, T. Trapping the Elusive Parent Borylene. *Angew. Chem., Int. Ed.* **2011**, *50*, 4704–4707. (d) Bissinger, P.; Braunschweig, H.; Damme, A.; Dewhurst, R. D.; Kraft, K.; Kramer, T.; Radacki, K. Base-stabilized boryl and cationic haloborylene complexes of iron. *Chem. - Eur. J.* **2013**, *19*, 13402–13407. (e) Wang, Y.; Quillian, B.; Wei, P.; Wannere, C. S.; Xie, Y.; King, R. B.; Schaefer, H. F., III; Schleyer, P. v. R.; Robinson, G. H. A Stable Neutral Diborene Containing a B=B Double Bond. *J. Am. Chem. Soc.* **2007**, *129*, 12412–12413. (f) Wang, Y.; Quillian, B.; Wei, P.; Xie, Y.; Wannere, C. S.; King, R. B.; Schaefer, H. F.; Schleyer, P. v. R.; Robinson, G. H. Planar, Twisted, and Trans-Bent: Conformational Flexibility of Neutral Diborenes. *J. Am. Chem. Soc.* **2008**, *130*, 3298–3299. (g) Tamm, M.; Lügger, T.; Hahn, E. F. Isocyanide and Ylidene Complexes of Boron: Synthesis and Crystal Structures of (2-(Trimethylsilyloxy)phenylisocyanide)–Triphenylborane and (1,2-Dihydrobenzoxazol-2-ylidene)–Triphenylborane. *Organometallics* **1996**, *15*, 1251–1256. (h) Chase, P. A.; Stephan, D. W. Hydrogen and Amine Activation by a Frustrated Lewis Pair of a Bulky N-Heterocyclic Carbene and B(C₆F₅)₃. *Angew. Chem., Int. Ed.* **2008**, *47*, 7433–7437. (i) Ueng, S.-H.; Makhlof Brahmī, M.; Derat, É.; Fensterbank, L.; Lacôte, E.; Malacria, M.; Curran, D. P. Complexes of Borane and N-Heterocyclic Carbenes: A New Class of Radical Hydrogen Atom Donor. *J. Am. Chem. Soc.* **2008**, *130*, 10082–10083.
- (3) (a) Curran, D. P.; Solovyyev, A.; Makhlof Brahmī, M.; Fensterbank, L.; Malacria, M.; Lacôte, E. Synthesis and Reactions of N-Heterocyclic Carbene Boranes. *Angew. Chem., Int. Ed.* **2011**, *50*, 10294–10317. (b) Doddi, A.; Peters, M.; Tamm, M. N-Heterocyclic Carbene Adducts of Main Group Elements and Their Use as Ligands in Transition Metal Chemistry. *Chem. Rev.* **2019**, *119*, 6994–7112.
- (4) Braunschweig, H.; Claes, C.; Damme, A.; Deifsenberger, A.; Dewhurst, R. D.; Hörl, C.; Kramer, T. A facile and selective route to remarkably inert monocyclic NHC-stabilized boriranes. *Chem. Commun.* **2015**, *51*, 1627–1630.
- (5) Nöth, H.; Rojas-Lima, S.; Troll, A. The Structural Chemistry of N-Monolithium Borazines. *Eur. J. Inorg. Chem.* **2005**, *2005*, 1895–1906.
- (6) Teixidor, F.; Barberà, G.; Vaca, A.; Kivekäs, R.; Sillanpää, R.; Oliva, J.; Viñas, C. Are Methyl Groups Electron-Donating or Electron-Withdrawing in Boron Clusters? Permethylation of *o*-Carborane. *J. Am. Chem. Soc.* **2005**, *127*, 10158–10159.
- (7) Bissinger, P.; Braunschweig, H.; Damme, A.; Hörl, C.; Krummenacher, I.; Kupfer, T. Boron as a Powerful Reductant: Synthesis of a Stable Boron-Centered Radical-Anion Radical-Cation Pair. *Angew. Chem., Int. Ed.* **2015**, *54*, 359–362.
- (8) Reinisch, G.; Patel, S.; Chollon, G.; Leyssale, J.-M.; Alotta, D.; Bertrand, N.; Vignoles, G. L. *J. Nanosci. Nanotechnol.* **2011**, *11*, 8323–8327.
- (9) Braunschweig, H.; Dewhurst, R. D.; Hammond, K.; Mies, J.; Radacki, K.; Vargas, A. Ambient-Temperature Isolation of a Compound with a Boron-Boron Triple Bond. *Science* **2012**, *336*, 1420–1422.
- (10) (a) Pait, M.; Kundu, G.; Tothadi, S.; Karak, S.; Jain, S.; Vanka, K.; Sen, S. C–F Bond Activation by a Saturated N-Heterocyclic Carbene: Mesoionic Compound Formation and Adduct Formation with B(C₆F₅)₃. *Angew. Chem., Int. Ed.* **2019**, *58*, 2804–2808. (b) Kundu, G.; De, S.; Tothadi, S.; Das, A.; Dey, A.; Sen, S. Saturated N-Heterocyclic Carbene Based Thiele's Hydrocarbon with a Tetrafluorophenylene Linker. *Chem. - Eur. J.* **2019**, *25*, 16533–16537.
- (11) Böhne, J.; Braunschweig, H.; Dellermann, T.; Ewing, W. C.; Hammond, K.; Jimenez-Halla, J. O. C.; Kramer, T.; Mies, J. The Synthesis of B₂(SIDip)₂ and its Reactivity Between the Diboracumulenic and Diborynic Extremes. *Angew. Chem., Int. Ed.* **2015**, *54*, 13801–13805.
- (12) Walton, J. C.; Brahmī, M. M.; Fensterbank, L.; Lacôte, E.; Malacria, M.; Chu, Q.; Ueng, S.-H.; Solovyyev, A.; Curran, D. P. EPR Studies of the Generation, Structure, and Reactivity of N-Heterocyclic Carbene Borane Radicals. *J. Am. Chem. Soc.* **2010**, *132*, 2350–2358.
- (13) (a) Bissinger, P.; Braunschweig, H.; Kupfer, T.; Radacki, K. Monoborane NHC Adducts in the Coordination Sphere of Transition Metals. *Organometallics* **2010**, *29*, 3987–3990. (b) Kronig, S.; Theuergarten, E.; Holschumacher, D.; Bannenberg, T.; Daniliuc, C. G.; Jones, P. G.; Tamm, M. Dihydrogen Activation by Frustrated Carbene-Borane Lewis Pairs: An Experimental and Theoretical Study of Carbene Variation. *Inorg. Chem.* **2011**, *50*, 7344–7359.
- (14) Thakur, A.; Vardhanapu, P. K.; Vijaykumar, G.; Bhatta, S. R. Investigation on reactivity of non-classical carbenes with sterically hindered Lewis acid, B(C₆F₅)₃ under inert and open conditions. *J. Chem. Sci.* **2016**, *128*, 613–620.
- (15) Kawamoto, T.; Geib, S.; Curran, D. P. Radical Reactions of N-Heterocyclic Carbene Boranes with Organic Nitriles: Cyanation of NHC-Boranes and Reductive Decyanation of Malononitriles. *J. Am. Chem. Soc.* **2015**, *137*, 8617–8622.
- (16) Taniguchi, T.; Curran, D. P. Hydroboration of Arynes with N-Heterocyclic Carbene Boranes. *Angew. Chem., Int. Ed.* **2014**, *53*, 13150–13154.
- (17) Li, X.; Curran, D. P. Insertion of Reactive Rhodium Carbenes into Boron–Hydrogen Bonds of Stable N-Heterocyclic Carbene Boranes. *J. Am. Chem. Soc.* **2013**, *135*, 12076–12081.
- (18) Aupic, C.; Mohamed, A. A.; Figliola, C.; Nava, P.; Tuccio, B.; Chouraqui, G.; Parrain, J.-L.; Chuzel, O. Highly Diastereoselective

Preparation of Chiral NHC-boranes Stereogenic at the Boron Atom. *Chem. Sci.* **2019**, *10*, 6524–6530.

(19) Qian, B.; Baek, S. W.; Smith, M. R., III Synthesis, Structure, and Reactivity of β -Diketiminato Boron(III) Complexes. *Polyhedron* **1999**, *18*, 2405–2414.

(20) Segawa, Y.; Yamashita, M.; Nozaki, K. Boryllithium: Isolation, Characterization, and Reactivity as a Boryl Anion. *Science* **2006**, *314*, 113–115.

(21) Protchenko, A. V.; Urbano, J.; Abdalla, J. A. B.; Campos, J.; Vidovic, D.; Schwarz, A. D.; Blake, M. P.; Mountford, P.; Jones, C.; Aldridge, S. Electronic Delocalization in Two and Three Dimensions: Differential Aggregation in Indium “Metalloid” Clusters. *Angew. Chem., Int. Ed.* **2017**, *56*, 15098–15102.

(22) (a) Dureen, M. A.; Stephan, D. W. Reactions of Boron Amidinates with CO₂ and CO and Other Small Molecules. *J. Am. Chem. Soc.* **2010**, *132*, 13559–13568. (b) Hill, N. J.; Findlater, M.; Cowley, A. H. Synthetic and structural chemistry of amidinate-substituted boron halides. *Dalton Trans.* **2005**, 3229–3234.

(23) Filippou, A. C.; Chernov, O.; Schakenburg, G. Chromium-Silicon Multiple Bonds: The Chemistry of Terminal N-Heterocyclic-Carbene-Stabilized Halosilylidyne Ligands. *Chem. - Eur. J.* **2011**, *17*, 13574–13583.

(24) APEX3, SAINT-Plus and SADABS; Bruker AXS Inc.: Madison, WI, USA, 2006. (b) Apex CCD and SAINT v8.30C; Bruker AXS Inc.: Madison, WI, USA, 2013.

(25) (a) Sheldrick, G. M. A short history of SHELX. *Acta Crystallogr., Sect. A: Found. Crystallogr.* **2008**, *A64*, 112–122. (b) Krause, L.; Herbst-Irmer, R.; Sheldrick, G. M.; Stalke, D. Comparison of silver and molybdenum microfocus X-ray sources for single-crystal structure determination. *J. Appl. Crystallogr.* **2015**, *48*, 3–10. (c) Krause, L.; Herbst-Irmer, R.; Stalke, D. An empirical correction for the influence of low-energy contamination. *J. Appl. Crystallogr.* **2015**, *48*, 1907–1913.



Diverse reactivity of carbenes and silylenes towards fluoropyridines†

 Gargi Kundu,^{ab} V. S. Ajithkumar,^{ab} Milan Kumar Bisai,^{ab} Srinu Tothadi,^{id c}
 Tamal Das,^{bd} Kumar Vanka^{id bd} and Sakya S. Sen^{id *ab}

 Cite this: *Chem. Commun.*, 2021, 57, 4428

 Received 15th March 2021,
 Accepted 24th March 2021

DOI: 10.1039/d1cc01401c

rsc.li/chemcomm

The reaction of IDipp with C₅F₅N led to functionalization of all three carbon atoms of the imidazole ring with HF₂[−] as the counter-anion (1). Reactivity with 2,3,5,6-tetrafluoropyridine gives only C–F bond activation leaving C–H bonds intact (5b). The reaction of SIDipp with C₅F₅N in the presence of BF₃ afforded the ring cleavage product (3). Analogous reactions with silylene led to oxidative addition at the Si(II) center.

The activation of C–F bonds provides a direct and efficient strategy for the functionalization of perfluoroarenes. The importance of C–F activation has mothered the invention of a plethora of transition metal free-mediated methodologies involving compounds with main group elements such as carbenes,^{1–11} N-heterocyclic olefins,¹² boryl lithium,¹³ silylenes,^{14–17} Al(I),^{18–20} Mg(I),^{21,22} P(III)^{23–25} compounds *etc.* In fact, several main group compounds such as alumanyl anion,²⁶ LMg(C₆H₆)MgL (L = (CH[C(CH₃)N-Ar]₂, Ar = 2,6-diisopentylphenyl),²⁷ or Mg(I) dimer²¹ have been reported to cleave the C–F bond of inert fluorobenzene, which is a formidable task because decreasing fluorination increases the C–F bond activation barrier. Among the main-group species, the activation of the C–F bonds by carbenes is at the forefront. Since the seminal publication from Bertrand's group² on the activation of the *para*-C–F bond of C₅F₅N by a cyclic alkyl amino carbene (CAAC), several other groups have reported C–F bond activation of perfluoroarenes by different carbenes, such as those of Radius, Turner, Lee, Baker, Chaplin, and others.^{4–11} Typically, NHC mediated activations are mostly found

to undergo in a 1 : 1 ratio leading to mono functionalization at the C-2 position. In 2016, Lee and coworkers reported the sequential C–F bond cleavage of two C₆F₅CF₃ moieties, where one perfluoro substituent was bound to the former carbene carbon atom, and the other one to the backbone of the NHC, leading to a tetra-substituted imidazolium salt.⁵ However, functionalization of all three carbon atoms of the imidazole moiety starting from an NHC through C–F bond activation is still not in synthetic chemists' repertoire.

The reaction of IDipp (IDipp = 1,3-bis(2,6-diisopropylphenyl)-imidazole-2-ylidene) with C₅F₅N in toluene produced 'penta-substituted' imidazolium bifluoride salt, **1** along with the liberation of one molecule HF (Scheme 1). Yellow crystals of **1** were grown from the toluene and THF mixture. **1** crystallizes in the monoclinic *P*₂₁/*n* space group (Fig. 1). The ¹H NMR spectrum shows a broad signal at 15.05 ppm for a HF₂[−] proton. The peak at −168.49 ppm assigned to ¹⁹F NMR is characteristic of the two fluorine atoms of HF₂[−]. The melting point of **1** is 120 °C, indicating its potential to be used as an ionic liquid.²⁸

Full quantum chemical calculations were done with density functional theory (DFT) at the dispersion and solvent corrected PBE/TZVP level of theory in order to understand the mechanism (Fig. 2). In the first step of the reaction, C₅F₅N approaches towards NHC and the carbene carbon of NHC attacks the *para*-carbon centre of C₅F₅N; formation of the C–C single bond and, subsequently, C–F bond activation occurs *via* **TS1** (N···C···C···F) leading to the formation of **Int1**. The reaction free energy (Δ*G*) and the activation free energy (Δ*G*[#]) values for this step are −24.6 kcal mol^{−1} and 13.7 kcal mol^{−1}, respectively. In the next step, another molecule of C₅F₅N reacts with **Int1** *via* a concerted mechanism leading to the formation of the C–C bond and the simultaneous breaking of the C–F bond *via* **TS2**, forming **Int2**, and the expulsion of HF. The Δ*G* and Δ*G*[#] values for this step are −30.5 kcal mol^{−1} and 21.7 kcal mol^{−1}, respectively. Now in the final step, **Int2** reacts with the third molecule of C₅F₅N, with F[−] abstracting the remaining proton from **Int2**. As a result, the carbanion attacks the *para*-carbon center of C₅F₅N, and the formation of another C–C bond,

^a Inorganic Chemistry and Catalysis Division, CSIR-National Chemical Laboratory, Dr Homi Bhabha Road, Pashan, Pune 411008, India. E-mail: ss.sen@ncl.res.in

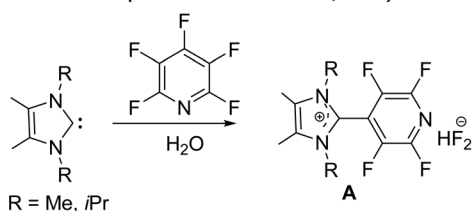
^b Academy of Scientific and Innovative Research (AcSIR), Ghaziabad-201002, India

^c Organic Chemistry Division, CSIR-National Chemical Laboratory, Dr Homi Bhabha Road, Pashan, Pune 411008, India

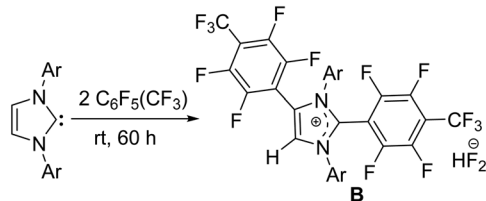
^d Physical and Material Chemistry Division, CSIR-National Chemical Laboratory, Dr Homi Bhabha Road, Pashan, Pune 411008, India

† Electronic supplementary information (ESI) available: Experimental & computational details, CIFs of **1**, **3**, **4**, **5b** and **6**, and Checkcif. CCDC 2055788 (**1**), 2055789 (**3**), 2055790 (**4**), 2070006 (**5b**) and 2055791 (**6**). For ESI and crystallographic data in CIF or other electronic format see DOI: 10.1039/d1cc01401c

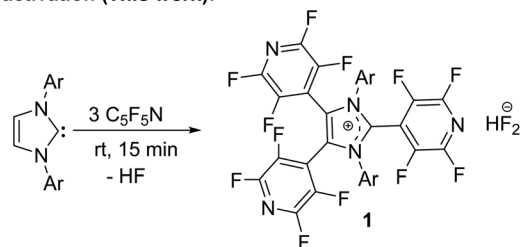
Single C-F activation (Kuhn and coworkers, 1998):



Double C-F activation (Lee and coworkers, 2016):



Triple C-F activation (This work):



Scheme 1 Previous examples of single and double C–F activation of perfluoroarenes by NHCs. This work describes the triple C–F bond activation and synthesis of **1** (Ar = 2,6-*i*Pr₂-C₆H₃).

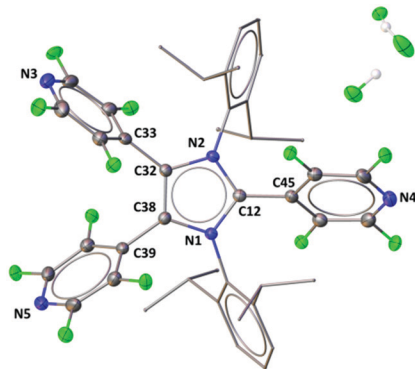


Fig. 1 Molecular structure of **1** (only hydrogen atoms of HF and HF₂[−] moieties are shown for clarity). Selected bond lengths (Å) and bond angles (°): C12–N1 1.349(2), C12–N2 1.348(2), C12–C45 1.477(2), N1–C38 1.392(2), N2–C32 1.392(2), C32–C38 1.356(2), C12–C45 1.477(2); N1–C12–N2 109.08(14), N1–C12–C45 125.32(15), N2–C12–C45 125.35(15), C38–N1–C12 107.89(14), C32–N2–C12 107.88(14).

as well as a third C–F bond activation occurs *via* **TS3**, leading to the functionalization of all three carbon atoms of the imidazole ring along with the generation of HF₂[−] as the counter-anion. The calculated ΔG and ΔG^\ddagger values for this step are -15.6 kcal mol^{−1} and 17.3 kcal mol^{−1} respectively. The ΔG (-30.5 kcal mol^{−1}) value for the slowest step is quite favorable and the activation energy (ΔG^\ddagger) barrier corresponding to the transition state is 21.7 kcal mol^{−1}.

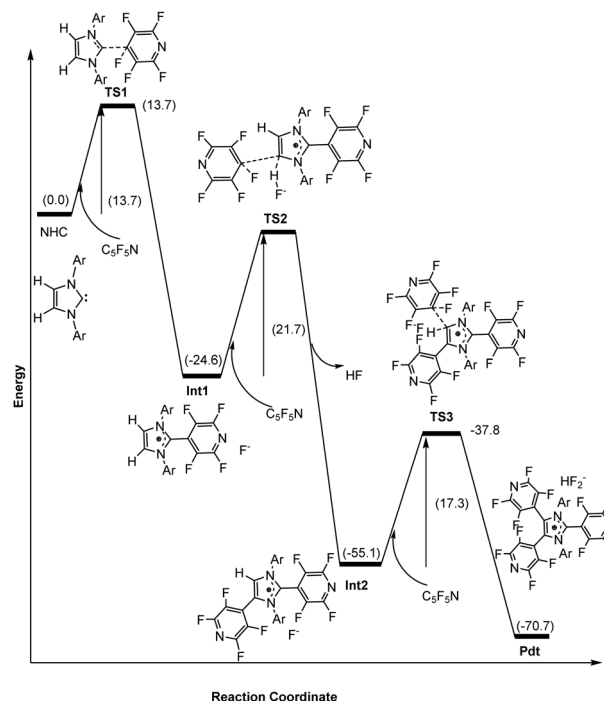
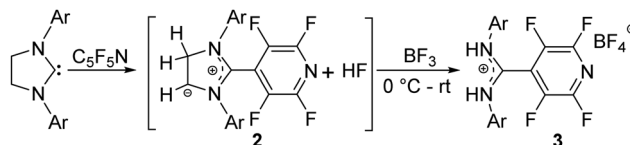


Fig. 2 The reaction energy profile diagram for the NHC mediated C–F bond activation of C₆F₅N. The values (in kcal mol^{−1}) have been calculated at the PBE/TZVP level of theory with DFT.

The analogous C–F bond activation of C₆F₅N with SIDipp (SIDipp = 1,3-bis(2,6-diisopropylphenyl)-imidazolin-2-ylidene) presumably led to a mesoionic intermediate (**2**) through the deprotonation from the backbone^{29,30} with concomitant elimination of HF (Scheme 2). The formation of **2** is only indicated by spectroscopic studies. The ¹H NMR spectrum revealed two distinct signals for the backbone protons at 5.0 and 4.6 ppm in 2 : 1 integration (ESI,† Fig. S4). In the ¹⁹F NMR spectrum, the *ortho* fluorines show a resonance at -83.7 ppm, while the *meta* fluorines are assigned at -132.9 ppm (ESI,† Fig. S6). No detection of the *para* fluorine also indicates the formation of **2**. The molecular-ion peak at *m/z* 540.3014 in the HRMS supports the formation of intermediate **2** (Fig. S7, ESI†). The addition of BF₃ to the reaction mixture led to the cleavage of the ring. We are not aware of such complete cleavage of NHC and subsequent formation of an amidinium salt or diaminocarbocation. The molecular structure of **3** is shown in Fig. 3. The C1 atom is three-coordinate and features a trigonal planar geometry. From the crystal structure of **3**, we can see that the distance between H1 and F7 is 1.91 Å, which is shorter than the sum of the van der Waals radii of both H and F (vdw of H: 1.2 Å and vdw of F: 1.47 Å). Hence, a strong hydrogen bonding can be envisaged



Scheme 2 Synthesis of **3**.

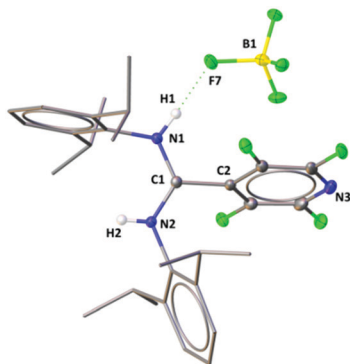
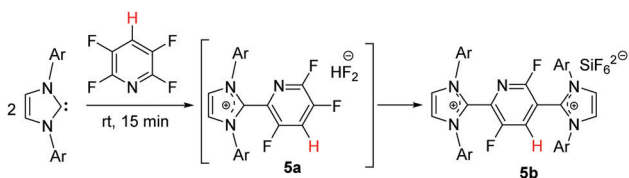


Fig. 3 The molecular structure of **3** (hydrogen atoms except NH protons are not shown for clarity). Selected bond lengths (Å) and bond angles (°): C1–C2 1.494(2), C1–N1 1.317(2), C1–N2 1.318(2), B1–F7 1.416(2), B1–F5 1.371(4); N1–C1–N2 123.25(15), N1–C1–C2 116.22(15), N2–C1–C2 120.51(14).

between H1 and F7, as N–H works as a strong donor side and B–F behaves as a strong acceptor.³¹

The generation of HF during the C–F bond activation of C₅F₅N by SIDipp was further confirmed when the analogous reaction was performed in the presence of B(C₆F₅)₃. The reaction afforded compound **4**, where the *in situ* generated HF is trapped between SIDipp and B(C₆F₅)₃. **4** was unable to be satisfactorily characterized using spectroscopy because of the formation of SIDipp·B(C₆F₅)₃³² and intermediate **2** as side products. Moreover, SIDipp·B(C₆F₅)₃ decomposes after some time at room temperature.³² Fortunately, we were able to grow colorless crystals of **4**. The synthetic scheme (Scheme S1, ESI[†]) and molecular structure (Fig. S16, ESI[†]) of **4** is given in the ESI.[†]

The introduction of C–H bonds into the fluoroarenes brings competition between the C–F and C–H oxidative addition. The activation of C–F bonds with tetrafluoro-pyridine is not reported with any main group elements. The reaction of tetrafluoro-pyridine with IDipp led to the activation of *ortho*-fluorine and generated **5a**. The presence of HF₂[−] as the counter anion was indicated from the NMR data. The latter underwent further C–F bond activation in the presence of another equivalent of IDipp to give the dicationic salt, **5b** (Scheme 3). The formation of SiF₆^{2−} as the counter anion can be attributed to the reaction of glass with extrinsic HF generated from side reactions. The C–H bond remained intact during the reaction as opposed to the C–H bond cleavage of 2,3,5,6-tetrafluoropyridine by Pt(PCy₃)₂.³³ The saturated DCM solution mainly yields crystals of **5b** (Fig. 4) along with a few crystals of **5a**. However, the data quality of **5a** was too poor to allow a detailed analysis of the structural parameters.



Scheme 3 Synthesis of **5b**.

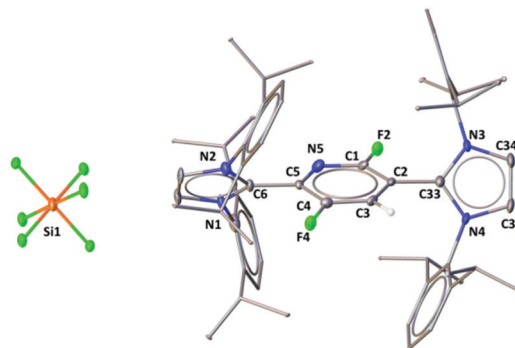
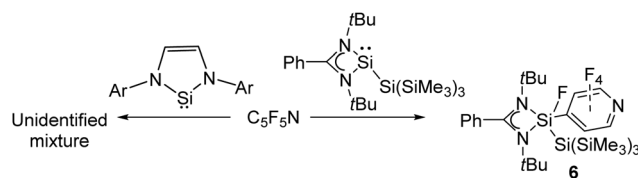


Fig. 4 The molecular structure of **5b** (hydrogen atoms except perfluoro-CH protons are not shown for clarity). F attached to C1 has disorder at two positions with atom site occupancies ~74% (F2) and ~26% (F1). Similarly, F attached to C4 has disorder at two positions with atom site occupancies ~75% (F4) and ~25% (F3). Selected bond lengths (Å) and bond angles (°): C5–C6 1.469(6), C5–N5 1.352(6), C1–F2 1.356(5), C2–C33 1.458(6); C5–N5–C1 119.1(4), N1–C6–N2 108.0(3), N3–C33–N4 108.1(4).

The scope of C–F bond activation of C₅F₅N was further studied with two different types of silylenes: (a) Denk's two coordinate silylene (NHSi) with dipp substituents on the N atom³⁴ as they are isostructural with NHCs and (b) three-coordinate amidinato hypersilylsilylene, PhC(N*t*Bu)₂SiSi(SiMe₃)₃.^{35,36} The reaction of NHSi with C₅F₅N is not very conclusive (see ESI,[†] Fig S24–S27), while the reaction of C₅F₅N with our recently reported hypersilylsilylene,³² PhC(N*t*Bu)₂SiSi(SiMe₃)₃ afforded the oxidative addition product **6** (Scheme 4). The reason to choose PhC(N*t*Bu)₂SiSi(SiMe₃)₃ as a substrate is due to the presence of three types of Si atoms, however, only the Si(II) center selectively reacts with C₅F₅N. The resonance in the ²⁹Si NMR spectrum detected at −76.96 ppm (*J*_{Si–F} = 333.06 Hz) as a doublet indicates the formation of a penta-coordinate silicon compound. The ¹⁹F NMR spectrum revealed three signals: −50.41 ppm for Si–F, −140.08 ppm for two *ortho* fluorines, and −157.18 ppm for two *meta* fluorine atoms. The geometry of the central silicon atom is a distorted trigonal bipyramidal with a terminal Si–F bond of 1.65 Å (Fig. 5). The Si1–Si2 bond length is 2.39 Å, which is slightly shorter than that in the parent hypersilylsilylene (2.43 Å).³⁴

In summary, the C–F bond activation of C₅F₅N by IDipp led to the functionalization of all three positions of the imidazole ring. However, the analogous reaction with SIDipp led to a mesoionic intermediate, which underwent ring cleavage upon the addition of BF₃. 2,3,5,6-Tetrafluoropyridine activates only the C–F bond leaving the C–H bond intact. The reactions with hypersilylsilylene resulted in the oxidative addition of the C–F bond at the Si(II) center.



Scheme 4 Synthesis of **6**.

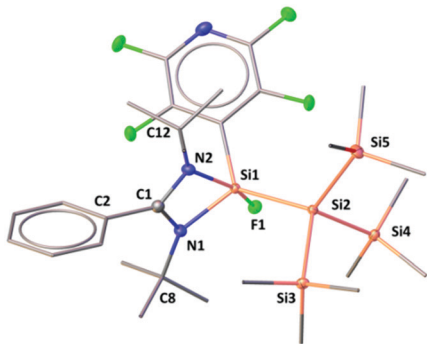


Fig. 5 The molecular structure of **6** (hydrogen atoms are not shown for clarity). Selected bond lengths (Å) and bond angles (°): C1–C2 1.494(3), N1–Si1 1.8199(16), N2–Si1 2.0186(16), Si1–F1 1.6528(12), Si1–Si2 2.3960(7); N1–C1–N2 107.33(16), N1–Si1–N2 67.86(7), Si2–Si1–F1 95.13(4).

Science and Engineering Research Board (SERB), India (CRG/2018/000287) (SSS) is acknowledged for providing financial assistance. GK, MKB, and TD thank CSIR, India for providing their research fellowships. VSA is thankful to DST, India for the INSPIRE Fellowship (IF190035). ST is grateful to CSIR-HRDG for providing the SRA fellowship (Pool No. 9119). The authors are thankful to the reviewers for their critical inputs to improve the quality of the manuscript.

Conflicts of interest

There are no conflicts to declare.

Notes and references

- N. Kuhn, J. Fahl, R. Boese and G. Henkel, *Z. Naturforsch., B: J. Chem. Sci.*, 1998, **53b**, 881–886.
- E. Mallah, N. Kuhn, C. Maichle-Moßmer, M. Steimann, M. Ströbele and K.-P. Zeller, *Z. Naturforsch., B: J. Chem. Sci.*, 2009, **64b**, 1176–1182.
- S. Styra, M. Melaimi, C. E. Moore, A. L. Rheingold, T. Augenstein, F. Breher and G. Bertrand, *Chem. – Eur. J.*, 2015, **21**, 8441–8446.
- Z. R. Turner, *Chem. – Eur. J.*, 2016, **22**, 11461–11468.
- Y. Kim and E. Lee, *Chem. Commun.*, 2016, **52**, 10922–10925.
- M. C. Leclerc, S. I. Gorelsky, B. M. Gabidullin, I. Korobkov and R. T. Baker, *Chem. – Eur. J.*, 2016, **22**, 8063–8067.
- M. C. Leclerc, B. M. Gabidullin, J. G. Da Gama, S. L. Daifuku, T. E. Iannuzzi, M. L. Neidig and R. T. Baker, *Organometallics*, 2017, **36**, 849–857.
- M. Pait, G. Kundu, S. Tothadi, S. Karak, S. Jain, K. Vanka and S. S. Sen, *Angew. Chem., Int. Ed.*, 2019, **58**, 2804–2808.
- G. Kundu, S. De, S. Tothadi, A. Das, D. Koley and S. S. Sen, *Chem. – Eur. J.*, 2019, **25**, 16533–16537.
- U. S. D. Paul and U. Radius, *Chem. – Eur. J.*, 2017, **23**, 3993–4009.
- J. Emerson-King, S. A. Hauser and A. B. Chaplin, *Org. Biomol. Chem.*, 2017, **15**, 787–789.
- D. Mandal, S. Chandra, N. I. Neuman, A. Mahata, A. Sarkar, A. Kundu, S. Anga, H. Rawat, C. Schulzke, K. R. Mote, B. Sarkar, V. Chandrasekhar and A. Jana, *Chem. – Eur. J.*, 2020, **26**, 5951–5955.
- S. Ito, N. Kato and K. Mikami, *Chem. Commun.*, 2017, **53**, 5546–5548.
- A. Jana, P. P. Samuel, G. Tavčar, H. W. Roesky and C. Schulzke, *J. Am. Chem. Soc.*, 2010, **132**, 10164–10170.
- R. Azhakar, H. W. Roesky, H. Wolf and D. Stalke, *Chem. Commun.*, 2013, **49**, 1841–1843.
- V. S. V. S. N. Swamy, N. Parvin, K. V. Raj, K. Vanka and S. S. Sen, *Chem. Commun.*, 2017, **53**, 9850–9853.
- S. S. Sen and H. W. Roesky, *Chem. Commun.*, 2018, **54**, 5046–5057.
- T. Chu, Y. Boyko, I. Korobkov and G. I. Nikonov, *Organometallics*, 2015, **34**, 5363–5365.
- M. R. Crimmin, M. J. Butler and A. J. P. White, *Chem. Commun.*, 2015, **51**, 15994–15996.
- O. Kysliak, H. Görls and R. Kretschmer, *Chem. Commun.*, 2020, **56**, 7865–7868.
- D. D. L. Jones, I. Douair, L. Maron and C. Jones, *Angew. Chem., Int. Ed.*, 2021, **60**, 7087–7092.
- C. Bakewell, A. J. P. White and M. R. Crimmin, *J. Am. Chem. Soc.*, 2016, **138**, 12763–12766.
- I. Mallov, T. C. Johnstone, D. C. Burns and D. W. Stephan, *Chem. Commun.*, 2017, **53**, 7529–7532.
- I. Mallov, A. J. Ruddy, H. Zhu, S. Grimme and D. W. Stephan, *Chem. – Eur. J.*, 2017, **23**, 17692–17696.
- S. S. Chitnis, F. Krischer and D. W. Stephan, *Chem. – Eur. J.*, 2018, **24**, 6543–6546.
- J. Hicks, P. Vasko, J. M. Goicoechea and S. Aldridge, *Angew. Chem., Int. Ed.*, 2021, **60**, 1707–1713.
- T. X. Gentner, B. Rösch, G. Ballmann, J. Langer, H. Elsen and S. Harder, *Angew. Chem., Int. Ed.*, 2018, **57**, 607–611.
- P. K. Maji, S. Sauerbrey, G. Schnakenburg, A. J. Arduengo, III and R. Streubel, *Inorg. Chem.*, 2012, **51**, 10408–10416.
- T. Brückner, M. Arrowsmith, M. Heß, K. Hammond, M. Müller and H. Braunschweig, *Chem. Commun.*, 2019, **55**, 6700–6703.
- T. X. Gentner, G. Ballmann, J. Pahl, H. Elsen and S. Harder, *Organometallics*, 2018, **37**, 4473–4480.
- G. R. Desiraju, *Acc. Chem. Res.*, 1996, **29**, 441–449.
- G. Kundu, S. Pahar, S. Tothadi and S. S. Sen, *Organometallics*, 2020, **39**, 4696–4703.
- N. A. Jasim, R. N. Perutz, A. C. Whitwood, T. Braun, J. Izundu, B. Neumann, S. Rothfeld and H.-G. Stammer, *Organometallics*, 2004, **23**, 6140–6149.
- P. Zark, A. Schäfer, A. Mitra, D. Haase, W. Saak, R. West and T. Müller, *J. Organomet. Chem.*, 2010, **695**, 398–408.
- M. K. Bisai, V. S. V. S. N. Swamy, T. Das, K. Vanka, R. G. Gonnade and S. S. Sen, *Inorg. Chem.*, 2019, **58**, 10536–10542.
- M. K. Bisai, V. S. V. S. N. Swamy, K. V. Raj, K. Vanka and S. S. Sen, *Inorg. Chem.*, 2021, **60**, 1654–1663.


 Cite this: *Chem. Commun.*, 2022, 58, 3783

 Received 3rd December 2021,
 Accepted 16th February 2022

DOI: 10.1039/d1cc06816d

rsc.li/chemcomm

Substitution at sp^3 boron of a six-membered NHC·BH₃: convenient access to a dihydroxyborenium cation†‡

 Gargi Kundu,^{ab} V. S. Ajithkumar,^{ab} K. Vipin Raj,^{ib, bc} Kumar Vanka,^{ib, bc}
 Srinu Tothadi^{ib, bd} and Sakya S. Sen^{ib, *ab}

Herein, we have undertaken the synthesis and investigated the reactivity of a 6-membered saturated NHC borane adduct (**1**). Direct electrophilic halogenation of **1** with a stoichiometric amount of I₂ led to NHC boryl iodides, 6-SIDipp-BH₂I (**2**) and 6-SIDipp-BHI₂ (**3**), which were further reacted with various nucleophiles to give novel 6-SIDipp based mono and disubstituted boranes with OTf (**4** and **6**) or ONO₂ (**5** and **7**) functional groups. The addition of Br₂/H₂O to **1** smoothly results in a dihydroxyborenium cation (**8**).

Although NHC complexes of boranes were first detected in 1968,¹ little chemistry involving NHC-boranes was known until Robinson prepared 1,3-bis-(2,6-diisopropylphenyl)imidazol-2-ylidene borane (5-IDipp·BH₃).² Since then, there has been increasing interest in the synthesis and reactivity of carbene-borane complexes. In particular, the substitution reaction of carbene-borane led to very rare classes of boron compounds with unusual functional groups such as azide, nitro, *etc.* attached to the boron atom.³ As of now, mainly two classes of carbene have been employed for such studies. While the works from the groups of Fensterbank, Lacôte, Malacria, and Curran mainly concentrated on typical Arduengo type carbenes,^{4–9} Braunschweig and coworkers recently reported nucleophilic addition and substitution of a cyclic alkyl amino carbene (CAAC) BH₃ adduct.¹⁰ So, it is apparent that the expansion in carbene-borane chemistry took place from a borane perspective, and not much from the carbene side. In fact, in a

recent review, Curran *et al.* concluded by posing a question on what other NHC-boranes can be made.³

The reports of six-membered carbenes are limited in the literature partly due to their less thermal stability and structural rigidity, though they feature a higher HOMO and lower HOMO–LUMO gap compared to typical five-membered NHCs.¹¹ Nonetheless, Aldridge and coworkers reported stable adduct formation of 6-SIDipp with AlH₃.¹² Subsequently, Jones and Stasch isolated monomeric complexes of 6-SIDipp and group 15 element trichlorides.¹³ Besides, Tamm and coworkers used 6-SIDipp as a Lewis base component in an FLP for the activation of dihydrogen.¹⁴

Due to our current interest in boron chemistry,^{15,16} we have studied the synthesis and reactivity of a saturated six-membered N-heterocyclic carbene (6-SIDipp) borane (**1**) adduct. **1** is amenable to further functionalization *via* iodination, providing access to NHC mono and diboryl iodides (**2** and **3**), selectively, which undergo nucleophilic substitution reactions with AgOTf and AgNO₃ to give boron compounds with OTf (**4** and **6**) and ONO₂ (**5** and **7**) functionalities. **5** and **7** represent the first NHC-boranes with an ONO₂ functional group. Dihydroxyborenium cations, the cationic analogues of phenylboronic acid, are difficult to prepare due to the lack of any R group.¹⁷ Herein, we have prepared a dihydroxyborenium cation (**8**) conveniently by reacting **1** with bromine-water.

The addition of BH₃·SME₂ to 6-SIDipp in *n*-hexane and toluene mixture at –30 °C gives an adduct, **1** as a white precipitate (Scheme 1). The quartet at –31.3 ppm (*J*_{B–H} = 84.04 Hz) in the ¹¹B NMR indicates the presence of a tetra-coordinated boron atom. The ¹H{¹¹B} NMR shows a sharp singlet at 0.25 ppm for the BH₃ protons. The molecular-ion peak was observed at *m/z* 419.3409 in the mass spectrum with the highest relative intensity. The B–C bond length in **1** is 1.602(3) Å, slightly longer than those in the previously known NHC·BH₃ adducts, presumably due to the enhanced steric crowding around the BH₃ unit (Fig. 1).

Direct electrophilic halogenation of NHC-boranes to access NHC boryl halide products has a modicum of precedence. The

^a *Inorganic Chemistry and Catalysis Division, CSIR-National Chemical Laboratory, Dr. Homi Bhabha Road, Pashan, Pune 411008, India. E-mail: ss.sen@ncl.res.in*

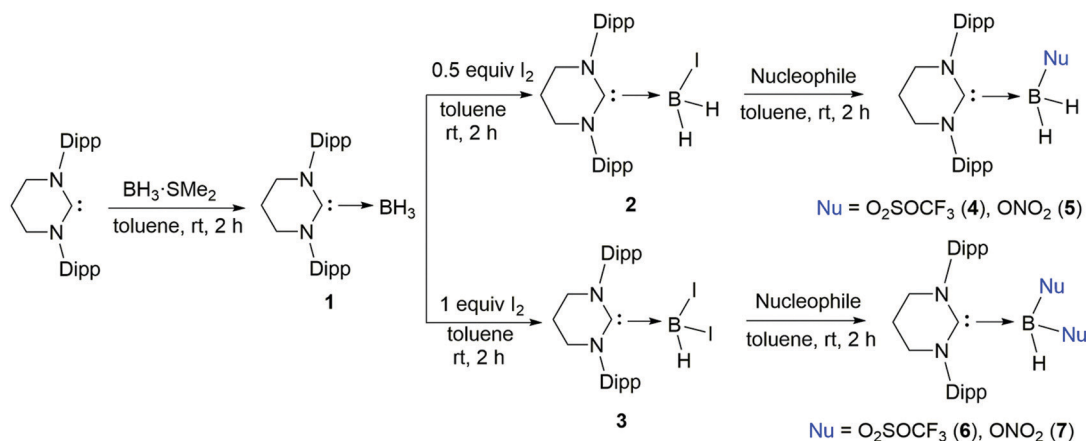
^b *Academy of Scientific and Innovative Research (AcSIR), Ghaziabad-201002, India*

^c *Physical and Material Chemistry Division, CSIR-National Chemical Laboratory, Dr. Homi Bhabha Road, Pashan, Pune 411008, India*

^d *Analytical and Environmental Sciences Division and Centralized Instrumentation Facility, CSIR-Central Salt and Marine Chemicals Research Institute, Gijubhai Badheka Marg, Bhavnagar-364002, India*

† Dedicated to Professor Debashis Ray on the occasion of his 60th birthday.

‡ Electronic supplementary information (ESI) available: Complete synthesis, characterization and X-ray data. CCDC 2102132 (**1**), 2125724 (**2**), 2123602 (**3**), 2123596 (**4**), 2123605 (**6**), 2123606 (**7**), 2123612 (**8**), 2123642 (**9**). For ESI and crystallographic data in CIF or other electronic format see DOI: 10.1039/d1cc06816d



Scheme 1 Synthesis and halogenation of **1** and subsequent nucleophilic substitution reactions (Dipp = Ar = 2,6-*i*Pr₂C₆H₃).

treatment of **1** with 0.5 equiv. of I₂ at room temperature selectively replaces only one hydrogen atom to give rise to **2**, which exhibits a broad signal at -30.2 ppm in the ¹¹B NMR spectrum. When one equivalent of I₂ was used, double iodination at the 6-BH₃ center was achieved in 88% yield (**3**). The diiodination was detected by the rapid disappearance of the quartet of **1** and the appearance of a signal at -39.4 ppm in the ¹¹B NMR. The ¹H{¹¹B} NMR shows a sharp singlet at 1.6 and 2.38 ppm for the boron bound protons. The molecular structures of **2** and **3** are shown in Fig. 1. The boron atom lies in the plane of the tetrahydropyrimidinium ring for **2** and the B-I bond [2.3005(13) Å] is perfectly orthogonal to the plane [torsion angle (deg) N1-C40-B1-I1 -91.1(1), N2-C40-B1-I1 -90.4(1)]. The B-C bond distance in **3** [1.643(4) Å] is marginally longer than that in **2** [1.6145(16) Å]. The I1-B1-I2 angle in **3** is 111.54(11), which confirms a nearly perfect tetrahedral

geometry around the boron atom. The B1-I1 bond is almost orthogonal to the plane, while the B1-I2 is not orthogonal to the plane [torsion angle (deg) N1-C2-B1-I2 138.73(18), N2-C2-B1-I2 -48.0(3)]. The B-I [2.3 Å] bond in **2** is little longer compared to the B-I bonds in **3** [av 2.27 Å]. For comparison, we have studied the disubstitution reaction of I₂ with 5-IDipp-BH₃, but the reaction led to the formation of a mixture of monoiodide, diiodide, and triiodide (minor), as evaluated from ¹¹B NMR spectroscopy (Fig. S45 and S48, ESI†).

Next, we assume that **2** and **3** can react with nucleophiles to displace iodide and give various substituted NHC-boranes. Iodides of both **2** and **3** could be smoothly replaced to afford the corresponding boranes with OTf (**4** and **6**) and ONO₂ (**5** and **7**) functionalities (Fig. 1 and 2). The B1-C2 bond [1.629(2) Å] distance in **4** is little increased compared to **1** [1.60 Å]. The torsion angles (deg) of plane C2-B1-O1-S1 and N1-C2-B1-O1

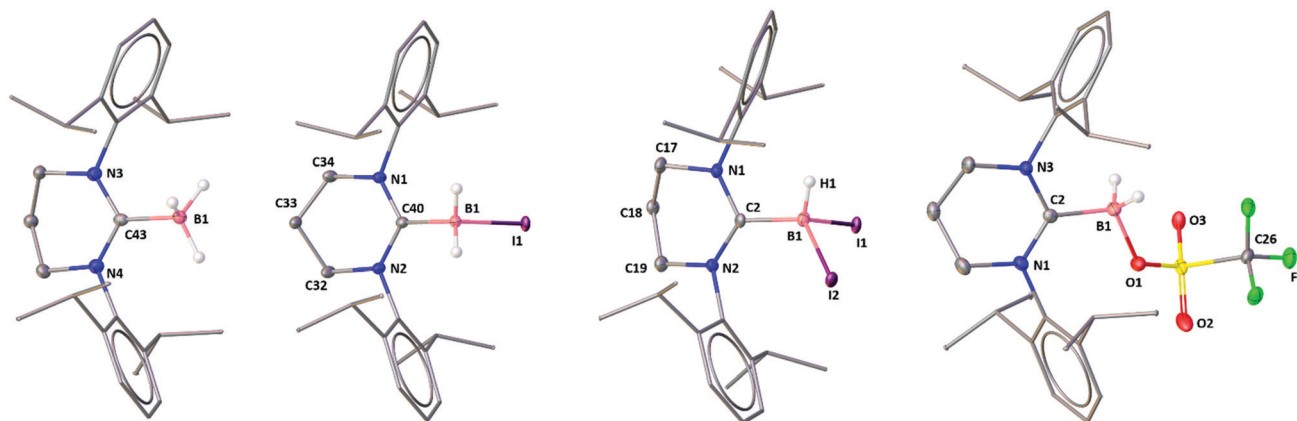


Fig. 1 The molecular structures of **1–4** (left to right, hydrogen atoms except on the boron atoms are omitted for the clarity of the picture). Selected bond lengths [Å], bond angles and torsion angles [deg]: **1**: C43–N3 1.340(2), C43–N4 1.348(2), B1–C43 1.602(3); N3–C43–N4 117.17(17), N3–C43–B1 122.75(16), N4–C43–B1 120.08(16); **2**: C40–N1 1.3424(13), N2–C40 1.3433(13), B1–C40 1.6145(16), B1–I1 2.3005(13); N2–C40–N1 118.29(9), N1–C40–B1 120.86(9), C40–B1–I1 106.79(7); C34–N1–C40–B1 -175.7(1), C32–N2–C40–B1 178.3(1), N1–C40–B1–I1 -91.1(1), N2–C40–B1–I1 -90.4(1); **3**: C2–N1 1.350(3), N2–C2 1.357(3), B1–C2 1.643(4), B1–I1 2.279(3), B1–I2 2.264(3), B1–H1 1.0000; N2–C2–N1 118.2(2), N1–C2–B1 115.01(19), N2–C2–B1 126.4(2), C2–B1–I1 103.74(15), C2–B1–I2 120.81(17) I1–B1–I2 111.54(11); N1–C2–B1–I1 -95.4(2), N2–C2–B1–I1 77.9(3), N1–C2–B1–I2 138.73(18), N2–C2–B1–I2 -48.0(3); **4**: N3–C2 1.3426(19), N1–C2 1.3386(19), B1–C2 1.629(2), B1–O1 1.551(2), S1–O1 1.5014(15), C17–F1 1.327(2); N3–C2–N1 118.53(13), N3–C2–B1 114.90(12), C2–B1–O1 113.04(12); C2–B1–O1–S1 150.07(11), N1–C2–B1–O1 6.3(2), N3–C2–B1–O1 -174.30(12), B1–O1–S1–C17 81.86(14).

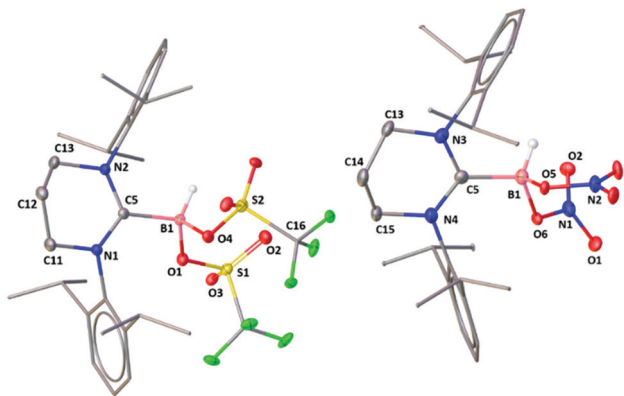


Fig. 2 The molecular structures of **6** (left) and **7** (right). Hydrogen atoms except the protons attached to boron are omitted for clarity. Selected bond distances [Å], bond angles and torsion angles [deg] for **6**: N2–C5 1.3421(13), N1–C5 1.3521(13), B1–C5 1.6621(15), B1–O1 1.5394(14), B1–O4 1.4943(13); N1–C5–B1 123.54(9), N2–C5–B1 117.98(9), C5–B1–O1 106.91(8), O1–B1–O4 105.64(8); C5–B1–O1–S1 –105.82(9), C5–B1–O4–S2 168.34(7), N1–C5–B1–O1 –61.57(12), N2–C5–B1–O1 113.79(10); **7**: C3–N5 1.3381(17), N4–C5 1.3341(18), B1–C5 1.659(2), B1–O5 1.4961(18), B1–O6 1.5166(19), N1–O1 1.2169(19), N1–O2 1.2269(19); N3–C5–N4 118.50(12), N4–C5–B1 124.07(12), N3–C1–B1 117.25(12), C5–B1–O6 102.92(10), C5–B1–O5 112.39(11), O5–B1–O6 106.35(12), O1–N1–O2 126.26(14); N4–C5–B1–O6 102.02(14), N4–C5–B1–O5 –11.98(19), N3–C5–B1–O5 163.11(12), N3–C5–B1–O6 –82.88(14).

are 150.07(11) and 6.3(2), which suggests that the B1–O1 bond is not orthogonal to the respective planes. To our knowledge, the ONO₂ functional group in NHC–borane chemistry is not known so far. The nucleophilic substitution of 6-SIDipp–BH₂ (**3**) is unique because the analogous disubstitution reaction with 5-IDipp was not reported.

We have studied the mechanism (Fig. 3) for the disubstitution reaction of **1** by the iodine molecule using density functional theory (DFT) calculations (see the ESI† for details). In the first step, the reaction goes through a barrier (TS₁) of 12.3 kcal mol^{−1},

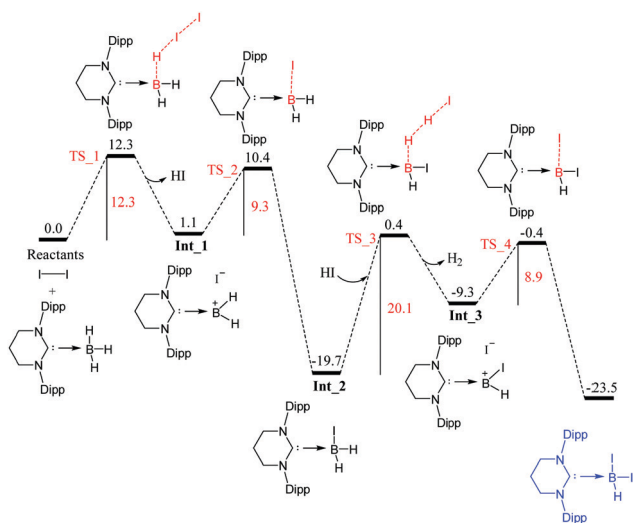
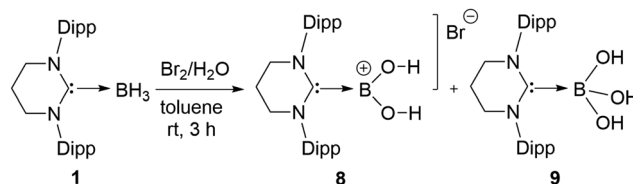


Fig. 3 The free energy profile for the disubstitution reaction of **1** by the iodine molecule. Values are in kcal mol^{−1}.

where the B–H and I–I bonds break and the H–I bond forms, leading to the formation of HI and **Int**₁ (consisting of a boron cation and an iodide ion). This is followed by the second barrier (TS₂) of 9.3 kcal mol^{−1}, where the B–I bond forms, leading to the formation of the monosubstituted **Int**₂. Then, the reaction proceeds through TS₃, with a barrier of 20.1 kcal mol^{−1}, in which the B–H and the H–I bonds break, and the H–H bond forms. TS₃ leads to the formation of H₂ and **Int**₃. In the last step, the reaction crosses an 8.9 kcal mol^{−1} barrier (TS₄), where the B–I bond forms, leading to the final disubstituted product. Calculations also suggest that the 5-IDipp–BH₃ would result in disubstituted products. However, both the barriers (TS₃ and TS₄) for the conversion of the monosubstituted intermediate to the disubstituted product are higher for 5-IDipp–BH₃ [23.2 kcal mol^{−1} and 9.9 kcal mol^{−1}, respectively] (Fig. S51, ESI†) than for 6-SIDipp–BH₃ [20.1 kcal mol^{−1} and 8.9 kcal mol^{−1}, respectively], which is why the disubstituted product is exclusively observed only for the 6-SIDipp case, while 5-IDipp gives a mixture of mono- and disubstituted products.

The preparation of borenium cations relies on two main approaches: (a) the replacement of X in R₂B–X by a free NHC or (b) by reacting an acid (HX) with NHC–BR₂H. These procedures allow for the preparation of several NHC-based borenium cations thanks to pioneering work by the groups of Gabbaï, Stephan, Robinson, Lindsay, Curran, Vedejs, and others.^{17–23} All these groups used typical 5-IDipp as the NHC. Only Aldridge's group has recently reported a dibromoborenium cation stabilized by 6-SIDipp.²⁴ Among them, only Curran's group reported the dihydroxyborenium cation by treating 5-IDipp–BH(X)OTf (X = Cl, OTf) with excess TfOH in 5 days.¹⁷ Here, we have isolated a new dihydroxyborenium cation **8** in a seemingly simple way by reacting **1** with Br₂/H₂O.

The reaction of **1** with bromine water led to an immediate color change from colorless to yellow and afforded a 6-SIDipp stabilized dihydroxyborenium cation (**8**) at room temperature in 3 h (Scheme 2). Yellow color crystals were grown from the saturated toluene solution at 4 °C. Along with 55% of the yellow crystals of **8**, a 7% yield of colorless crystals was found, which was the 6-SIDipp–B(OH)₃ adduct, **9**. Both the compounds are separated by fractional crystallization. There is no report of the formation of NHC–B(OH)₃ type Lewis adducts so far. Both **8** and **9** were characterized with single-crystal X-ray studies (Fig. 4 and Fig. S50, ESI†). The ¹¹B NMR spectrum gives a singlet at 25.4 ppm for **8** and −5.2 ppm for **9**. The cyclic voltammogram of **8** exhibits a reversible redox wave at E_{p,red} = −1.7 V, and oxidation at E_{p,oxd} = 0.56 V, respectively (Fig. S49, ESI†). For **9**,



Scheme 2 Preparation of a dihydroxyborenium cation **8** in a single step from **1**.

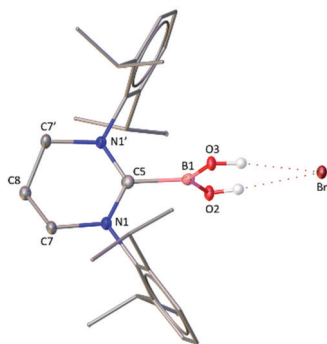


Fig. 4 The molecular structure of **8** (except hydrogen atoms attached to the oxygen atom, other hydrogen atoms are omitted for the clarity of the picture). Selected bond lengths [Å], bond angles and torsion angles [deg]: N1–C5 1.321(4), C5–B1 1.614(7), B1–O2 1.344(7), B1–O3 1.341(7), O2/O3–H2/H3 0.80(7), N1–C5–N1' 121.5(4), N1–C5–B1 119.2(2), O3–B1–O2 127.7(5); N1–C5–B1–O2 –90.4(4), N1'–C5–B1–O2 90.4(4), N1–C5–B1–O3 89.6(4), N1–C5–B1–O3 –89.6(4).

the detailed characterization along with the molecular structure and bond lengths are described in the ESI† (Fig. S50).

8 crystallizes in the orthorhombic *Pnma* space group. The boron atom adopts a trigonal planar [O3–B1–O2 bond angle is 127.7(5) deg] environment with the B–O distances of 1.344(7) and 1.341(7) Å, which are substantially shorter than the typical B–O single bond [> 1.5 Å]. The B–O bonds are perfectly orthogonal to the plane [torsion angles (deg) N1–C5–B1–O2 –90.4(4), N1'–C5–B1–O2 90.4(4), N1–C5–B1–O3 89.6(4), N1–C5–B1–O3 –89.6(4)]. The hydroxyl groups attached to the boron atom in **8** are involved in hydrogen bonding with the bromide anion, which presumably stabilizes the dihydroxyborenum cation *via* the formation of a six-membered ring with O–H...Br bond distances of 2.422 and 2.466 Å.

While the body of work on carbene-borane chemistry is growing, the carbene component is mainly restricted to two classes of carbenes: (a) Arduengo type five-membered NHC and (b) CAAC. Here, we have introduced a new NHC, 6-SIDipp for NHC-borane chemistry, and described a detailed study of substitution reactions of 6-SIDipp-BH₃ (**1**). These results have uncovered the facile substitution to the coordinatively saturated sp³ boron atom in 6-SIDipp-BH₃ with a range of functional groups, such as iodide (**2**), triflate (**4**), and ONO₂ (**5**). Apart from mono substitution, we have also shown that **1** readily undergoes a double substitution reaction with iodine to give **3**, and those iodide atoms of **3** can be replaced with other nucleophiles to generate novel NHC-boranes (**6** and **7**). **1** was also found to generate a novel dihydroxyborenum ion (**8**) by reacting with bromine water at room temperature.

Science and Engineering Research Board (SERB), India (CRG/2018/000287) (SSS) is acknowledged for providing financial assistance. G. K. and K. V. R. thank the Council of Scientific and Industrial Research (CSIR), India for a research fellowship. V. S. A. thanks D. S. T., India for the INSPIRE Fellowship

(IF190035). S. T. is grateful to AESD&CIF, CSIR-CSMCR for instrumentation facilities and infrastructure.

Conflicts of interest

There are no conflicts to declare.

Notes and references

- G. Bittner, H. Witte and G. Hesse, *Justus Liebigs Ann. Chem.*, 1968, **713**, 1–11.
- Y. Wang, B. Quillian, P. Wei, C. S. Wannere, Y. Xie, R. B. King, H. F. Schaefer, P. V. R. Schleyer and G. H. Robinson, *J. Am. Chem. Soc.*, 2007, **129**, 12412–12413.
- D. P. Curran, A. Solovyeu, M. M. Brahmi, L. Fensterbank, M. Malacria and E. Lacôte, *Angew. Chem., Int. Ed.*, 2011, **50**, 10294–10317.
- S.-H. Ueng, M. M. Brahmi, É. Derat, L. Fensterbank, E. Lacôte, M. Malacria and D. P. Curran, *J. Am. Chem. Soc.*, 2008, **130**, 10082–10083.
- A. Solovyeu, Q. Chu, S. J. Geib, L. Fensterbank, M. Malacria, E. Lacôte and D. P. Curran, *J. Am. Chem. Soc.*, 2010, **132**, 15072–15080.
- K. Nozaki, Y. Aramaki, M. Yamashita, S.-H. Ueng, M. Malacria, E. Lacôte and D. P. Curran, *J. Am. Chem. Soc.*, 2010, **132**, 11449–11451.
- A. Solovyeu, S.-H. Ueng, J. Monot, L. Fensterbank, M. Malacria, E. Lacôte and D. P. Curran, *Org. Lett.*, 2010, **12**, 2998–3001.
- W. Dai, S. J. Geib and D. P. Curran, *J. Org. Chem.*, 2018, **83**, 8775–8779.
- M. Makhlof Brahmi, J. Monot, M. Desage-El Murr, D. P. Curran, L. Fensterbank, E. Lacôte and M. Malacria, *J. Org. Chem.*, 2010, **75**, 6983–6985.
- D. Auerhammer, M. Arrowsmith, H. Braunschweig, R. D. Dewhurst, J. O. C. Jiménez-Halla and T. Kupfer, *Chem. Sci.*, 2017, **8**, 7066–7071.
- D. Munz, *Organometallics*, 2018, **37**, 275–289.
- J. A. B. Abdalla, I. M. Riddlestone, R. Tirfoin, N. Phillips, J. I. Bates and S. Aldridge, *Chem. Commun.*, 2013, **49**, 5547–5549.
- A. Sidiropoulos, B. Osborne, A. N. Simonov, D. Dange, A. M. Bond, A. Stasch and C. Jones, *Dalton Trans.*, 2014, **43**, 14858–14864.
- S. Kronig, E. Theuergarten, D. Holschumacher, T. Bannenberg, C. G. Daniliuc, P. G. Jones and M. Tamm, *Inorg. Chem.*, 2011, **50**, 7344–7359.
- G. Kundu, S. Pahar, S. Tothadi and S. S. Sen, *Organometallics*, 2020, **39**, 4696–4703.
- (a) V. S. V. S. N. Swamy, K. V. Raj, K. Vanka, S. S. Sen and H. W. Roesky, *Chem. Commun.*, 2019, **55**, 3536–3539; (b) M. K. Bisai, V. S. V. S. N. Swamy, K. V. Raj, K. Vanka and S. S. Sen, *Inorg. Chem.*, 2021, **60**, 1654–1663; (c) M. K. Bisai, V. Sharma, R. G. Gonnade and S. S. Sen, *Organometallics*, 2021, **40**, 2133–2138.
- A. Solovyeu, S. J. Geib, E. Lacôte and D. P. Curran, *Organometallics*, 2012, **31**, 54–56.
- T. Matsumoto and F. P. Gabbaï, *Organometallics*, 2009, **28**, 4252–4253.
- D. McArthur, C. P. Butts and D. M. Lindsay, *Chem. Commun.*, 2011, **47**, 6650–6652.
- J. M. Farrell, J. A. Hatnean and D. W. Stephan, *J. Am. Chem. Soc.*, 2012, **134**, 15728–15731.
- Y. Wang, M. Y. Abraham, R. J. Gilliard, Jr., D. R. Sexton, P. Wei and G. H. Robinson, *Organometallics*, 2013, **32**, 6639–6642.
- S. Muthaiah, D. C. H. Do, R. Ganguly and D. Vidović, *Organometallics*, 2013, **32**, 6718–6724.
- A. Prokofjevs, J. W. Kampf, A. Solovyeu, D. P. Curran and E. Vedejs, *J. Am. Chem. Soc.*, 2013, **135**, 15686–15689.
- H. B. Mansaray, A. D. L. Rowe, N. Phillips, J. Niemeyer, M. Kelly, D. A. Addy, J. I. Bates and S. Aldridge, *Chem. Commun.*, 2011, **47**, 12295–12297.

Six-Membered Saturated NHC-Stabilized Borenium Cations: Isolation of a Cationic Analogue of Borinic Acid

Gargi Kundu, Kajal Balayan, Srinu Tothadi, and Sakya S. Sen*



Cite This: *Inorg. Chem.* 2022, 61, 12991–12997



Read Online

ACCESS |



Metrics & More

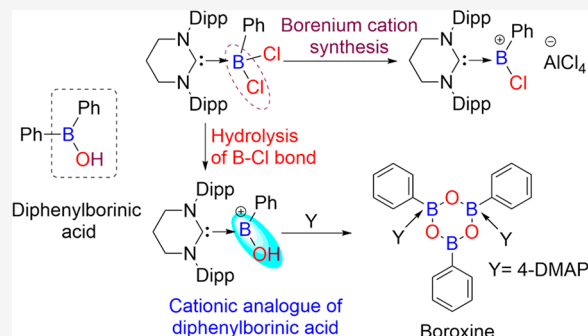


Article Recommendations



Supporting Information

ABSTRACT: The reaction of six-membered saturated NHC [1,3-di(2,6-diisopropylphenyl) tetrahydropyrimidine-2-ylidene; henceforth abbreviated as 6-SIDipp] with PhBCl_2 yields a Lewis base adduct, 6-SIDipp- PhBCl_2 (**1**), which readily undergoes nucleophilic substitution reaction with AgNO_3 , leading to the single (**2**) and double (**3**) substitution of both chlorides with ONO_2 moieties at the boron atom. The reaction of **1** with 1 equiv of AlCl_3 resulted in a borenium cation of composition $[\text{6-SIDipp-B(Ph)Cl}]^+$ (**4**) with AlCl_4^- as the counteranion. Although borenium cations with different substituents on boron have been reported, a structurally characterized phenylchloroborenium cation remains unknown. Similarly, the reaction of **1** with triflic acid provides the first representative of a new class of borenium cations bearing one hydroxyl and one phenyl group on boron (**5**), a cationic analogue of borinic acid.



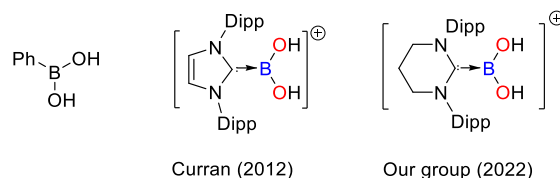
INTRODUCTION

Although phenylboronic acid $[\text{PhB(OH)}_2]$ is ubiquitous in organic chemistry such as in Suzuki–Miyaura, Chan–Evans–Lam cross-coupling reactions, Petasis reaction, and so on,¹ diphenylboronic acid $[\text{Ph}_2\text{B(OH)}]$ is very less illustrated due to its instability.^{2–4} Although diphenylboronic acid was probably first prepared in 1894 by Michaelis by hydrolysis of diphenylchloroborane,⁵ the first structurally characterized borinic acid $[\text{Mes}_2\text{B(OH)}]$, Mes = 2,4,6-Me₃C₆H₂ was reported by Power in 1987, almost after a century.⁶ Displacement of the phenyl group with a strong σ -donor neutral ligand like N-heterocyclic carbenes (NHCs) in phenylboronic acid resulted in dihydroxyborenium cations, $[\text{LB(OH)}_2]^+$, the cationic analogues of phenylboronic acid, which were structurally authenticated first by the group of Curran⁷ and recently by us.⁸ On the same line, removal of one phenyl group from diphenylboronic acid should furnish a three-coordinated monohydroxy borenium cation of composition $[\text{LB(Ph)(OH)}]^+$; however, no such compound has been realized to date (Scheme 1).

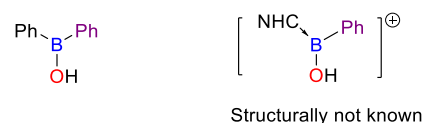
Inspired by the pioneering studies on carbene–borane chemistry by Fensterbank, Lacôte, Malacria, Curran, Braunschweig, and others,^{9–15} we have recently demonstrated the preparation of the 6-SIDipp-BH₃ adduct and studied its substitution reaction with iodine, which resulted in monoiodides and diboryl iodides.⁸ The latter two are amenable for nucleophilic substitution reaction, which allowed us to introduce $\text{OSO}_2\text{CF}_3^-$ and ONO_2^- -functionalized 6-SIDipp borane compounds.⁸ Here, we describe the isolation of the 6-SIDipp- PhBCl_2 adduct (**1**). The reactions of **1** with AgNO_3 leads to the formation of 6-SIDipp- $\text{PhBCl(ONO}_2)$ (**2**) and 6-

Scheme 1. Phenylboronic, Diphenylboronic Acid, and Their NHC-Supported Cationic Analogues (Dipp = 2,6-*i*Pr₂-C₆H₃)

Phenylboronic acid and its cationic analogue: dihydroxyborenium cation



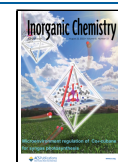
Diphenylboronic acid and its cationic analogue: monohydroxyborenium cation



SIDipp- $\text{PhB(ONO}_2)_2$ (**3**). The isolation of a 6-SIDipp-phenylchloroborenium cation (**4**) is achieved by reacting **1**

Received: February 23, 2022

Published: August 5, 2022

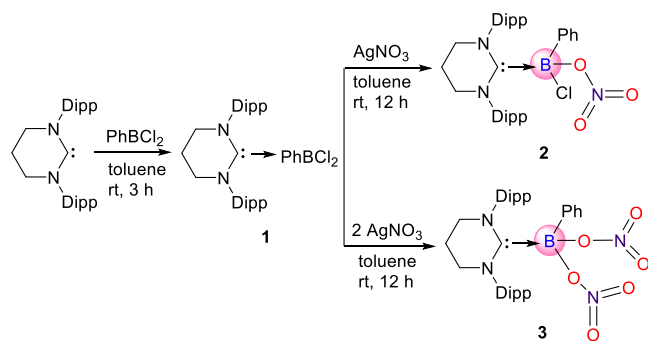


with AlCl_3 . Finally, the synthesis of $[\text{6-SIDipp-B(Ph)(OH)}]^+$ (**5**) is reported for the first time.

RESULTS AND DISCUSSION

Our studies began with the synthesis of adduct **1**, which was obtained by reacting 6-SIDipp with PhBCl_2 in toluene (Scheme 2). The ^{11}B NMR spectrum of **1** displays a resonance

Scheme 2. Synthesis of **1** and Its Nucleophilic Substitution Reaction with AgNO_3



signal at 3.4 ppm as a broad singlet. The molecular structure of **1** is determined by single-crystal X-ray studies (Figure 1). The

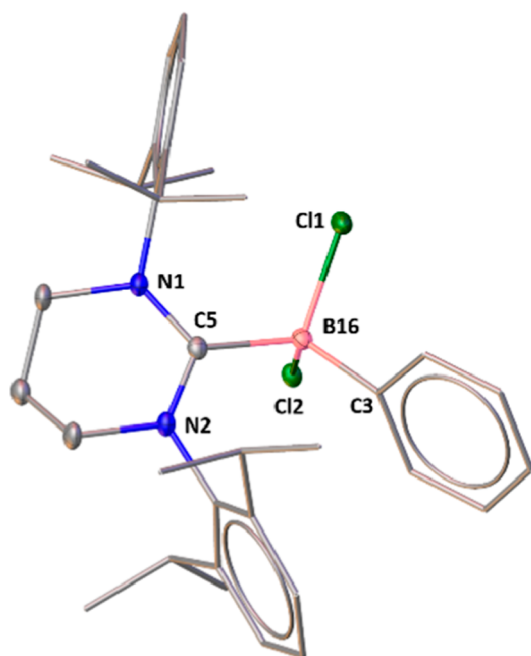


Figure 1. Molecular structure of **1**. Hydrogen atoms are omitted for clarity. Selected bond distances (Å) and bond angles (deg): C5–N1 1.352(3), C5–N2 1.344(3), B16–C5 1.691(3), B16–Cl1 1.889(2), B16–Cl2 1.910(2), B16–C3 1.620(3); N1–C5–N2 116.38(17), N1–C5–B16 122.30(17), N2–C5–B16 120.57(16), and Cl2–B16–Cl1 105.77(11).

B–C bond length in **1** (1.691(3) Å) is quite longer compared to that in the 6-SIDipp- BH_3 adduct (1.602(3) Å).⁸ The B–Cl bond distances (1.8861(10) and 1.8769(9) Å) are in good agreement with the previously reported carbene–chloroborane adducts.^{16,17} The X-ray structural studies of **1** show that the phenyl ring on the boron atom lies parallel to the plane of one

Dipp-arene ring. The molecular ion peak was detected at m/z 563.3173 for **1** with the highest relative intensity.

Treatment of **1** and **2** equiv of AgNO_3 with **1** in toluene afforded mono- and di-nitrate-substituted 6-SIDipp-boranes, **2** and **3**, in good yields. It must be noted here that functional groups such as ONO_2 are seldom found bonded to boron atoms.⁸ The ^{11}B NMR spectrum of **2** displays a characteristic resonance signal at 4.7 ppm. The ^{11}B NMR spectrum of **3** exhibits a resonance signal at 30 ppm in CDCl_3 as well as in toluene- d_8 , which is indicative of a three-coordinated boron species. The ^1H NMR spectrum of **3** with minimal exposure in the solution phase shows the purity of the complex to be approximately 85%. We surmise that **3** undergoes slow degradation to an unknown three-coordinated boron species that we could not identify. Hence, we have recorded the solid-state ^{11}B NMR spectrum of **3**, which exhibits a resonance signal at -1.4 ppm, reflecting a four-coordinated boron in **3** (see Figure S11). The solid-state structures of **2** and **3** were confirmed by X-ray crystal analysis. **2** crystallizes in the monoclinic space $P2_1/n$ space group (Figure 2). The B–Cl

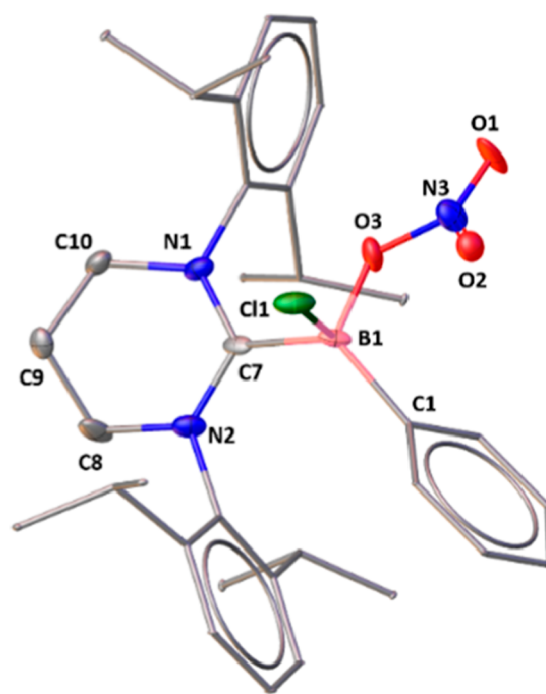


Figure 2. Molecular structure of **2**. Hydrogen atoms are omitted for clarity. Selected bond distances (Å), bond angles (deg), and torsion angles (deg): C7–N1 1.347(4), C7–N2 1.337(4), N1–C10 1.478(4), N2–C8 1.465(4), B1–C7 1.671(5), B1–Cl1 1.955(7), B1–C1 1.617(5), B1–O3 1.479(4), N3–O2 1.220(4), N3–O1 1.204(4), N3–O3 1.319(4); N1–C7–N2 117.7(3), N2–C7–B1 120.0(2), N1–C7–B1 121.5(2), C7–B1–O3 102.2(2), C7–B1–Cl1 96.9(3), O1–N3–O2 123.7(4); N1–C7–B1–Cl1 $-87.7(3)$, N2–C7–B1–Cl1 81.8(3), N1–C7–B1–O3 25.5(4), and N2–C7–B1–O3 $-165.0(3)$.

bond length (1.955(7) Å) is little longer compared to that in **1**, and it is orthogonal to the plane (torsion angle: N1–C7–B1–Cl1 $-87.7(3)^\circ$ and N2–C7–B1–Cl1 $81.8(3)^\circ$). **3** crystallizes in the triclinic $P-1$ space group (Figure 3). The B–O distances in **3** (1.5197(17) and 1.5019(17) Å) are marginally longer than those in **2** (1.479(4) Å). In the HRMS mass spectrum,

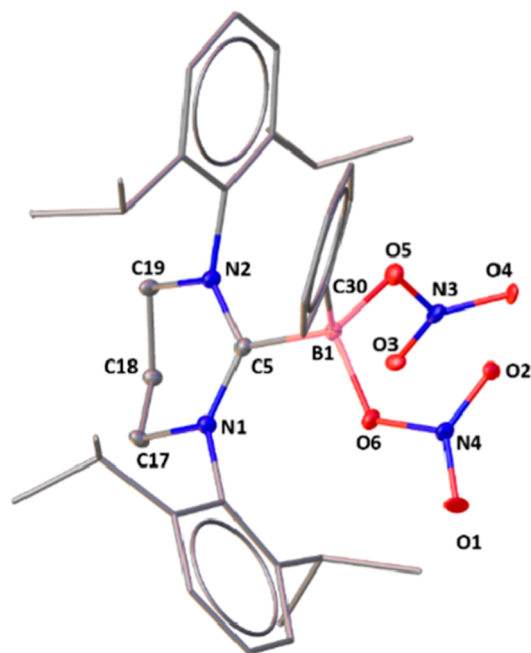


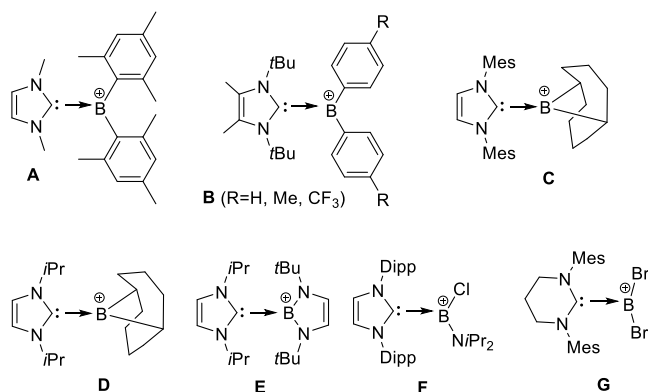
Figure 3. Molecular structure of **3**. Hydrogen atoms are omitted for clarity. Selected bond distances (Å), bond angles (deg), and torsion angles (deg): C5–N1 1.3502(17), C5–N2 1.3406(17), B1–C5 1.6942(19), N2–C19 1.4858(17), N1–C17 1.4835(17), B1–C30 1.603(2), B1–O6 1.5197(17), B1–O5 1.5019(17), N3–O5 1.3798(15), N4–O6 1.3604(15), N3–O3 1.214(5), N4–O1 1.2126(16); N1–C5–N2 118.09(12), N1–C5–B1 117.41(11), N2–C5–B1 124.15(11), C5–B1–O6 108.07(11), C5–B1–O5 103.05(10), C5–B1–C30 119.50(11), O5–B1–O6 109.04(11); C17–N1–C5–B1 162.71(12), C19–N2–C5–B1 –166.92(12), N2–C5–B1–C30 –108.04(15), N1–C5–B1–C30 78.92(16), N1–C5–B1–O6 –41.36(15), N1–C5–B1–O5 –156.69(11), N2–C5–B1–O5 16.35(17), and N2–C5–B1–O6 131.68(12).

the molecular ion peak with the highest intensity at m/z 590.3353 is characteristic of **2**.

Although NHC-supported borenium cations with different substituents at boron such as diarylborenium by Gabbaï's (**A**)¹⁸ and Tamm (**B**),¹⁹ dialkylborenium by Lindsay (**C**)²⁰ and Stephan (**D**),²¹ diamino borenium (**E**) by Weber,²² aminochloroborenium (**F**) by Robinson,²³ and dibromoborenium (**G**) by Aldridge²⁴ have been reported (Scheme 3), a seemingly simple compound such as [NHC·B(Ph)Cl]⁺ has still not been isolated. Ingleson and co-workers isolated the [(2-DMAP)B(Ph)Cl]⁺ cation by the sequential addition of 2-DMAP and AlCl₃ to PhBCl₂,²⁵ but the coordination number of the boron atom in the cation is 4. Therefore, according to Nöth's classification,^{26,27} it is a boronium cation and not a borenium cation. It must be noted here that Cade and Ingleson reported an ArOB(L)Ph cation, which can be considered as a cationic analogue of a borinic ester.²⁸

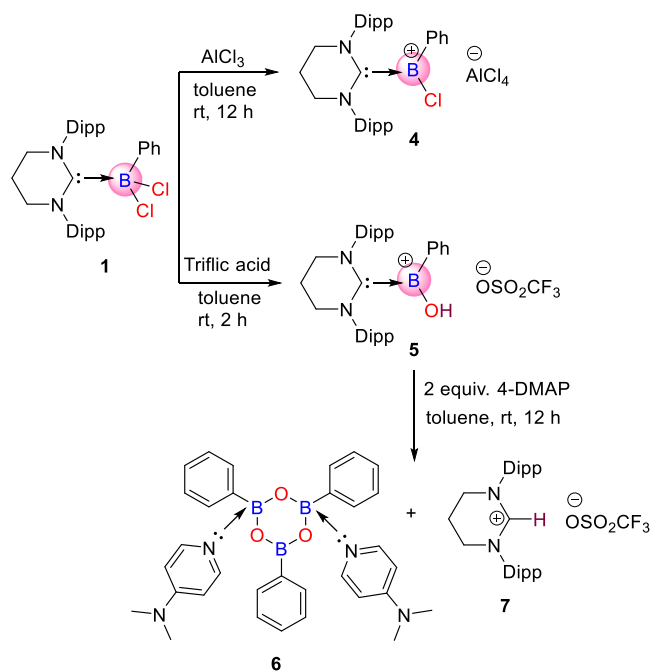
We reckon that displacement of one chloride ligand from **1** should result in a NHC-stabilized phenylchloroborenium cation. By adopting Ingleson's strategy,²⁵ we reacted **1** with 1 equiv of AlCl₃ in toluene, which led to the formation of [6-SIDipp·B(Ph)(Cl)]⁺ (**4**) with AlCl₄[−] as the counteranion (Scheme 4). The ¹¹B NMR spectrum indicates the generation of the borenium cation, which displays a resonance signal at 29.5 ppm. It is in good agreement with Robinson's [5-IDipp·B(NiPr₂)(Cl)]⁺ (**F**) but substantially upfield with respect to Aldridge's [6-SIDipp·BBr₂]⁺ (**G**) (51.4 ppm). The molecular

Scheme 3. Selected Examples of Previously Reported NHC-Stabilized Borenium Cations (Excluding Dihydroxyborenium Cations)^a



^aAnions have not been given.

Scheme 4. Synthesis of Phenylchloroborenium (**4**) and Phenylhydroxyborenium (**5**)



structure of **4** is shown in Figure 4. **4** crystallizes in the monoclinic $P2_1/c$ space group. The B–C_{NHC} distance (1.628(11) Å) is significantly reduced from that in **1** (1.691(3) Å), apparently due to the change in the hybridization of the boron atom from sp³ (in **1**) to sp² (in **4**). Due to the π -stacking interaction, the phenyl ring on the boron atom is parallel with one of the dipp arene rings, leading to different B–C_{ipso} contacts (2.77 and 2.92 Å), which are common to the borenium cations for bending of the flanking arene rings toward the boron center. The B–Cl distance (1.737(9) Å) is 0.15 Å shorter compared to that in **1** due to the electron donation from the chlorine atom to the electrophilic boron center in **4**.

Encouraged by this result, we decided to test the viability of isolating our target compound, [B(Ph)OH]⁺, using 6-SIDipp. Deliberate hydrolysis of **4** did not furnish the target compound. In 2014, Curran and co-workers reported the

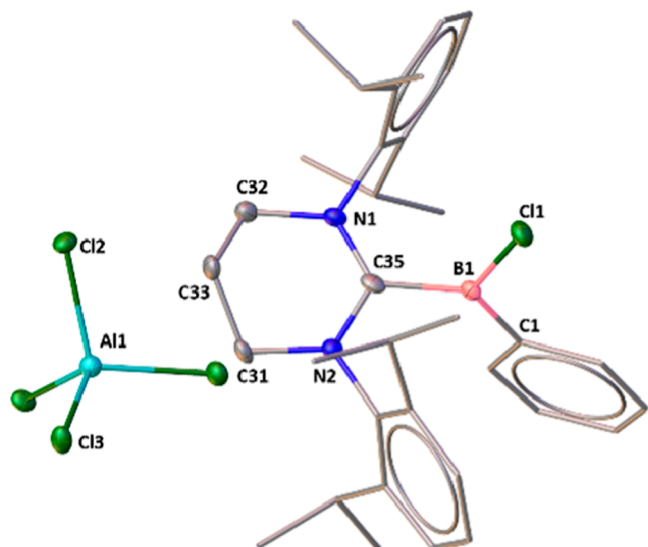


Figure 4. Molecular structure of **4**. Hydrogen atoms are omitted for clarity. Selected bond distances (Å), bond angles (deg), and torsion angles (deg): C35–N2 1.338(9), C35–N1 1.320(9), N2–C31 1.470(9), N1–C32 1.468(10), C35–B1 1.628(11), B1–C1 1.523(12), B1–Cl1 1.737(9), Cl2–Al1 2.136(3), Cl3–Al1 2.131(3); N1–C35–N2 121.0(6), N2–C35–B1 116.7(6), N1–C35–B1 122.2(6), Cl1–B1–C35 115.4(6), C35–B1–C1 126.2(7), Cl1–B1–C1 118.4(6); N1–C35–B1–C1 –108.6(9), N2–C35–B1–C1 69(1), N1–C35–B1–Cl1 72.0(8), and N2–C35–B1–Cl1 –110.8(7).

generation of dihydroxyborenium cation [5-IDipp·B(OH)₂]⁺[OTf][–] by reacting [5-IDipp·B(X)(OTf)]⁺ (X = Cl and OTf)

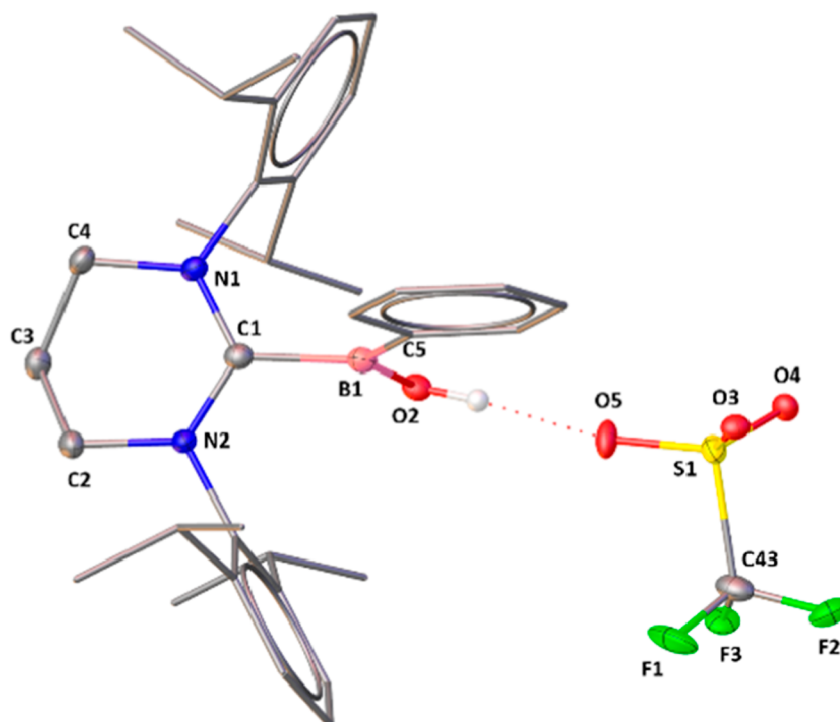


Figure 5. Molecular structure of **5**. Hydrogen atoms except the O2 atom are omitted for clarity. Selected bond distances (Å), bond angles (deg) and torsion angles (deg): N1–C1 1.3330(13), N2–C1 1.3333(14), N1–C4 1.4811(15), N2–C2 1.4783(14), B1–C1 1.6231(16), B1–O2 1.3830(15), B1–C5 1.5580(17), S1–O5 1.4497(11), C43–F1 1.335(2); N1–C1–N2 121.43(10), N2–C1–B1 119.14(9), N1–C1–B1 119.43(9), C5–B1–O2 124.65(10); N1–C1–B1–O2 91.08(12), N2–C1–B1–O2 89.20(12), N1–C1–B1–C5 88.81(13), and N2–C1–B1–C5 –90.91(12).

with triflic acid and concluded that the hydrolysis happened with adventitious water.⁷ Therefore, we reacted **1** with triflic acid, and to our delight, the reaction afforded the 6-SIDipp-stabilized phenyl hydroxy borenium cation (**5**) with triflate as a counteranion. The dropwise addition of triflic acid into the toluene solution of **1** at low temperature formed a turbid solution immediately. The reaction mixture was run for another 2 h at room temperature and dried completely to give a white precipitate. The colorless crystals of **5** were grown in concentrated toluene solution at 4 °C and characterized by single-crystal X-ray as well as NMR spectroscopy and mass spectrometry. The ¹¹B NMR spectrum of **5** shows a resonance signal at 28.9 ppm. The peak at –78.2 ppm in the ¹⁹F NMR spectrum confirms the presence of the triflate group as the counteranion. The molecular ion peak with the highest intensity at *m/z* 509.3700 further confirms the formation of **5**. The stretching frequency for the O–H group in **5** appears at 3438 cm^{–1}.

Figure 5 depicts the molecular structure of **5**, which is, to our knowledge, the first isolated compound containing a phenylhydroxyborenium cation. **5** crystallizes in the monoclinic *P*2₁/*c* space group. The B–C_{NHC} distance is 1.6231(16) Å, which is comparable with that in **4** and the previously reported [6-SIDipp·B(OH)]⁺ cation (1.614(7) Å).⁸ The dearth of the R group is compensated by the hydrogen bonding of the oxygen atom of the triflate group with the hydroxyl group at the boron center with a O–H⋯O distance of 2.736 Å. The average B–C_{ipso} contact is 2.86 Å, which is marginally longer compared to that in Aldridge's dibromoborenium (2.786(7) and 2.798(8) Å).²⁴ Both B–O and B–C_{Ph} bonds lie perfectly orthogonal to the planes [torsion angle:

N1-C1-B1-O2 $91.08(12)^\circ$, N2-C1-B1-O2 $89.20(12)^\circ$, N1-C1-B1-C5 $88.81(13)^\circ$, and N2-C1-B1-C5 $-90.91(12)^\circ$].

Cation **5** readily reacts with 4-dimethylaminopyridine (4-DMAP) to give DMAP-stabilized boroxine (**6**) at room temperature along with tetrahydropyrimidinium salt with a triflate anion, **7**. Although PhB(OH)_2 is known to undergo dehydration reaction at 110°C for 6 h,²⁹ generation of a boroxine derivative at room temperature from a cationic analogue of borinic acid is not known. It must be noted here that Braunschweig and co-workers recently reported the isolation of a cyclic alkyl amino carbene (CAAC)-stabilized boroxine by reacting CAAC-stabilized diborene with CO_2 .³⁰ The separation of **6** and **7** was carried out via fractional crystallization. The molecular structure of **6** is shown in Figure 6. **6** crystallizes in the triclinic *P*-1 space group. The

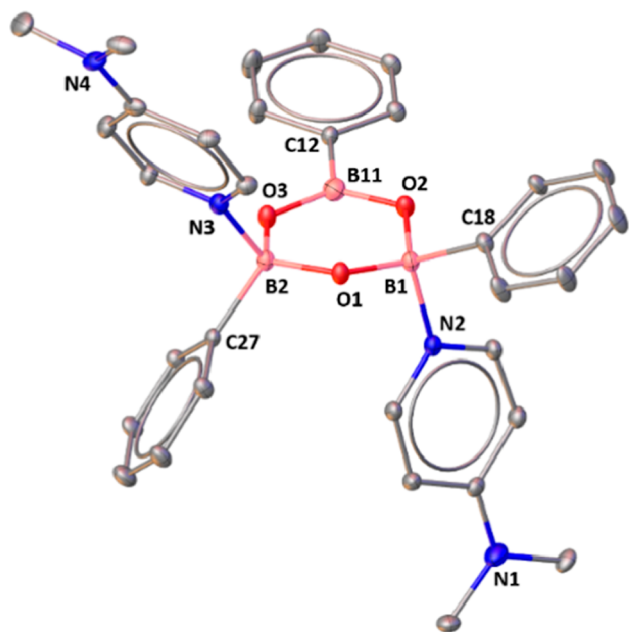


Figure 6. Molecular structure of **6**. Hydrogen atoms are omitted for clarity. Selected bond distances (Å) and bond angles (deg): B1–O1 1.419(2), B2–O1 1.4334(19), B2–O3 1.4696(19), O2–B1 1.4766(19), O2–B11 1.358(2), B11–O3 1.355(2), B1–N2 1.677(2), B2–C27 1.627(2), B1–C18 1.623(2), B2–N3 1.648(2), B11–C12 1.588(2); B1–O2–B11 119.12(12), B2–O3–B11 121.12(12), and B1–O1–B2 122.26(11).

coordination geometry of the boron atoms in the boroxine ring is not equivalent because two boron atoms are four-coordinated, while the third one is three-coordinated. As a result, the B–O bond lengths in **6** are not the same. As a matter of fact, attempts to prepare boroxine derivatives where all boron atoms are coordinated to DMAP were not successful even when excess amount of 4-DMAP was used. The B–O bond lengths in **6**, where the boron atom is coordinated to DMAP (1.4334(19) and 1.4696(19) Å), are longer than B–O bond lengths, where the boron atom is three-coordinated (1.358(2) and 1.355(2) Å). The B–N bond lengths (1.677(2) and 1.648(2) Å) are marginally longer than those in Alcarazo's carbodiphosphorane and DMAP-stabilized boronium cations.³¹ In the ^{11}B NMR spectrum, **6** shows a resonance signal at 20.5 ppm due to a fast exchange of the two DMAPs across the three boron centers. In the mass spectrum, the molecular

ion peak at m/z 405.3256 approves the formation of **7**. The molecular structure of **7** is provided in the Supporting Information (see Figure S30).

CONCLUSIONS

In summary, we have demonstrated the ability of a six-membered NHC (6-SIDipp) for stabilizing boronium cations. For this purpose, we have first prepared the 6-SIDipp- PhBCl_2 adduct (**1**). The reaction of **1** with AlCl_3 led to the formation of the first boronium cation of composition $[\text{6-SIDipp-B(Ph)(Cl)}]^+$ (**4**). Analogous reaction with triflic acid resulted in $[\text{6-SIDipp-B(Ph)(OH)}]^+$ (**5**), which can be considered as the cationic analogue of less-illustrated phenylborinic acid. Attempts to carry out the Lewis base exchange reaction with 4-DMAP led to the formation of an unusual boroxine (**6**), where the boron atoms are differently coordinated. **1** is also amenable toward nucleophilic substitution reaction with AgNO_3 , furnishing 6-SIDipp- $\text{PhBCl(ONO}_2)$ (**2**) and 6-SIDipp- $\text{PhB(ONO}_2)_2$ (**3**). It can be mentioned that examples of structurally characterized boranes with ONO_2 are relatively scarce.

EXPERIMENTAL SECTION

All manipulations were carried out in an inert atmosphere of argon using standard Schlenk techniques and in an argon-filled glovebox. The solvents, especially toluene, tetrahydrofuran, dichloromethane, and *n*-hexane, were purified using a MBRAUN solvent purification system MB SPS-800. The chemicals used in this study were purchased from Sigma-Aldrich and TCI Chemicals and were used without further purification. The starting material, 6-SIDipp, was synthesized by using a literature procedure.³² The ^1H , ^{13}C , ^{11}B , and ^{19}F NMR spectra were recorded in CDCl_3 , using a Bruker Avance DPX 400 and Bruker Avance DPX 500 spectrometer. Chemical shifts (δ) are given in ppm. NMR spectra were referenced to external SiMe_4 (^1H and ^{13}C), $\text{BF}_3\cdot\text{OEt}_2$ (^{11}B), and CFCl_3 (^{19}F). Mass spectra (ESI-MS) were obtained using a Q Exactive Thermo Scientific system at the CSIR National Chemical Laboratory, Pune. Elemental analyses were performed at the CSIR National Chemical Laboratory, Pune, India. Melting points were measured in a sealed glass tube on a Stuart SMP-30 melting point apparatus and were uncorrected.

Synthesis of 1. 6-SIDipp (0.20 g, 0.50 mmol) was dissolved in toluene (5 mL) in a Schlenk flask, and toluene solution of PhBCl_2 (0.08 g, 0.50 mmol) was added to it drop by drop at low temperature. The resulting mixture was kept for stirring for 3 h and then allowed to come to room temperature. After completion of the reaction, all the volatiles were completely removed under vacuum and the residue was washed with *n*-hexane. Crystallization of the resulting solid in toluene at 4°C yielded the colorless crystals of **1** with a yield of 0.17 g (61%). mp 134°C . ^1H NMR (400 MHz, 298 K, CDCl_3): δ 1.24 (d, 12H, $J = 6.75$ Hz, $\text{CH}(\text{CH}_3)_2$), 1.44 (d, $J = 6.63$ Hz, 12H, $\text{CH}(\text{CH}_3)_2$), 2.37 (q, $J = 5.75$ Hz, 2H, $\text{NCH}_2\text{CH}_2\text{CH}_2\text{N}$), 3.34 (sept, $J = 6.75$ Hz, 4H, $\text{CH}(\text{CH}_3)_2$), 3.70 (t, $J = 5.88$ Hz, 4H, $\text{NCH}_2\text{CH}_2\text{CH}_2\text{N}$), 6.71–6.73 (m, 3H, *meta* and *para* H of B-Ph), 6.99 (d, $J = 7.63$ Hz, 4H, *ortho*-H of Dipp), 7.04–7.06 (m, 2H, *ortho*-H of B-Ph), 7.17 (t, $J = 7.63$ Hz, 2H, *para*-H of Dipp) ppm. $^{13}\text{C}\{^1\text{H}\}$ NMR (101 MHz, 298 K, CDCl_3): δ 19.2, 24.7, 28.9, 48.8, 125.1, 127.2, 129.9, 131.2, 134.2, 135.7, 145.6, 152.9 ppm. $^{11}\text{B}\{^1\text{H}\}$ NMR (128 MHz, 298 K, CDCl_3): δ 3.4 (s, 1B, BPhCl_2) ppm. HRMS (CH_3CN): m/z calcd for $\text{C}_{34}\text{H}_{45}\text{BCl}_2\text{N}_2$ $[\text{M} + \text{H}]^+$, 563.3126; found, 563.3173. Elemental analysis: Calcd C, 72.48; H, 8.05; N, 4.97. Found: C, 71.95; H, 7.75; N, 4.56.

Synthesis of 2. An equimolar amount of **1** (0.30 g, 0.53 mmol) and AgNO_3 (0.090 g, 0.53 mmol) (covered in aluminum foil) was taken in a Schlenk flask and dissolved in 10 mL of dichloromethane. The reaction was stirred for 12 h at room temperature. Subsequently, the reaction mixture was dried completely, and 8 mL of toluene was added to the reaction mixture. After frit filtration, the filtrate was

concentrated, and the colorless crystals of **2** were isolated after storing the solution at 4 °C for 2 days with a yield of 0.15 g (41%). mp 162 °C. ¹H NMR (400 MHz, 298 K, CDCl₃): δ 1.24 (d, 12H, *J* = 6.50 Hz, CH(CH₃)₂), 1.37 (d, *J* = 6.38 Hz, 12H, CH(CH₃)₂), 2.73 (br s, 2H, NCH₂CH₂CH₂N), 2.97 (sept, *J* = 6.38 Hz, 4H, CH(CH₃)₂), 4.10 (br s, 4H, NCH₂CH₂CH₂N), 7.25 (d, *J* = 7.63 Hz, 4H, *ortho*-H of Dipp), 7.34 (t, *J* = 7.63 Hz, 2H, *meta*-H of B-Ph), 7.45 (t, *J* = 7.93 Hz, 2H, *para*-H of Dipp), 7.63 (br s, 1H, *para*-H of B-Ph), 7.84 (d, *J* = 7.13 Hz, 2H, *ortho*-H of B-Ph) ppm. ¹³C{¹H} NMR (101 MHz, 298 K, CDCl₃): δ 19.1, 24.6, 28.8, 48.5, 125.1, 131.3, 135.4, 145.3, 153.2 ppm. ¹¹B{¹H} NMR (128 MHz, 298 K, CDCl₃): δ 4.7 (s, 1B, BPhNO₃Cl) ppm. HRMS (CH₃CN): *m/z* calcd for C₃₄H₄₅BCIN₃O₃ [M + H]⁺, 589.3237; found, 589.3318.

Synthesis of 3. **1** (0.30 g, 0.53 mmol) and AgNO₃ (0.180 g, 1.06 mmol) were taken in a Schlenk flask in a 1:2 ratio and dissolved in 10 mL of dichloromethane. The reaction was stirred for 12 h at room temperature. The reaction mixture was dried completely, and 8 mL of toluene was added to the reaction mixture. After frit filtration, the filtrate was concentrated, and colorless crystals of **3** were isolated after storing the solution at room temperature for 4 days with a yield of 0.92 g (28%). mp 136 °C. ¹H NMR (400 MHz, 298 K, CDCl₃): δ 1.11 (d, 12H, *J* = 6.63 Hz, CH(CH₃)₂), 1.22 (d, *J* = 6.75 Hz, 12H, CH(CH₃)₂), 2.42 (q, *J* = 5.75 Hz, 2H, NCH₂CH₂CH₂N), 3.15 (sept, *J* = 6.75 Hz, 4H, CH(CH₃)₂), 3.74 (t, *J* = 5.88 Hz, 4H, NCH₂CH₂CH₂N), 6.26 (d, *J* = 8.13 Hz, 2H, *ortho*-H of B-Ph), 6.82 (t, *J* = 7.38 Hz, 2H, *meta*-H of B-Ph), 6.94 (t, *J* = 7.38, 1H, *para*-H of B-Ph), 7.21 (t, *J* = 7.75 Hz, 4H, *meta*-H of Dipp), 7.42 (t, *J* = 7.75 Hz, 2H, *para*-H of Dipp) ppm. ¹³C{¹H} NMR (101 MHz, 298 K, CDCl₃): δ 19.1, 24.6, 28.9, 48.4, 125.2, 127.9, 131.4, 132.7, 135.6, 145.5, 153.5 ppm. ¹¹B{¹H} NMR (128 MHz, 298 K): δ -1.4 (s, 1B, BPh(NO₃)₂) ppm.

Synthesis of 4. **1** (0.30 g, 0.53 mmol) and AlCl₃ (0.07 g, 0.53 mmol) were taken in a Schlenk flask, 10 mL of toluene was added to it at room temperature, and the reaction mixture was stirred for 4 h. The resulting solution was filtered through a canula. Concentrating and storing the reaction mixture at -4 °C afforded crystals of **4** with a yield of 0.24 g (65%). mp 196 °C. ¹H NMR (400 MHz, 298 K, CDCl₃): δ 1.24 (d, 12H, *J* = 5.88 Hz, CH(CH₃)₂), 1.39 (d, *J* = 5.24 Hz, 12H, CH(CH₃)₂), 2.80 (br s, 2H, NCH₂CH₂CH₂N), 3.05 (sept, *J* = 6.75 Hz, 4H, CH(CH₃)₂), 4.22 (br s, 4H, NCH₂CH₂CH₂N), 7.26 (d, *J* = 7.25 Hz, 4H, *ortho*-H of Dipp), 7.46 (t, *J* = 7.63 Hz, 2H, *para*-H of Dipp), 7.52 (t, *J* = 7.25 Hz, 2H, *meta*-H of B-Ph), 7.61 (t, *J* = 7.38, 1H, *para*-H of B-Ph), 8.25 (d, *J* = 6.75 Hz, 2H, *ortho*-H of B-Ph) ppm. ¹³C{¹H} NMR (101 MHz, 298 K, CDCl₃): δ 19.1, 21.4, 24.6, 29.0, 48.4, 125.2, 127.9, 131.4, 135.6, 145.5, 153.4 ppm. ¹¹B{¹H} NMR (128 MHz, 298 K, CDCl₃): δ 29.5 (s, 1B, BPhCl) ppm. HRMS (CH₃CN): *m/z* calcd for C₃₄H₄₅BCIN₂ [(M-AlCl₄)+Na]⁺, 550.3257; found, 550.4354.

Synthesis of 5. Compound **1** (0.09 g, 0.53 mmol) was dissolved in 10 mL of toluene in a Schlenk flask, and triflic acid (0.05 mL, 0.54 mmol) was added drop by drop to it at 0 °C. The reaction mixture was allowed to come to room temperature and stirred for another 2 h. After that, the solution was dried completely and washed with *n*-hexane to remove all the volatiles. Then, 8 mL of toluene was added, and the reaction mixture was filtered through a canula, concentrated, and kept at 4 °C, which yielded colorless crystals of **5** with a yield of 0.28 g (80%). Mp: 83 °C. ¹H NMR (400 MHz, 298 K, CDCl₃): δ 1.24 (d, 12H, *J* = 5.88 Hz, CH(CH₃)₂), 1.40 (d, *J* = 5.25 Hz, 12H, CH(CH₃)₂), 2.76 (br s, 2H, NCH₂CH₂CH₂N), 3.02 (sept, *J* = 6.88 Hz, 4H, CH(CH₃)₂), 4.11 (br s, 4H, NCH₂CH₂CH₂N), 7.29 (d, *J* = 7.25 Hz, 4H, *ortho*-H of Dipp), 7.47 (t, *J* = 7.63 Hz, 2H, *para*-H of Dipp), 7.52 (t, *J* = 7.50 Hz, 2H, *meta*-H of B-Ph), 7.61 (t, *J* = 7.38, 1H, *para*-H of B-Ph), 8.25 (d, *J* = 6.75 Hz, 2H, *ortho*-H of B-Ph) ppm. ¹³C{¹H} NMR (101 MHz, 298 K, CDCl₃): δ 19.0, 21.4, 24.7, 28.9, 48.4, 125.2, 127.5, 128.2, 129.0, 131.4, 134.1, 135.6, 145.6, 153.2 ppm. ¹¹B{¹H} NMR (128 MHz, 298 K, CDCl₃): δ 28.9 (s, 1B, BPhOH) ppm. ¹⁹F{¹H} NMR (377 MHz, 298 K, CDCl₃): δ -78.2 (s, 3F, OSO₂CF₃) ppm. HRMS (CH₃CN): *m/z* calcd. for C₃₄H₄₆BN₂O [(M-(M'-OTf)]⁺, 509.3698; found, 509.3700.

Synthesis of 6 and 7. 10 mL of toluene was added to a Schlenk flask containing **5** (0.30 g, 0.46 mmol) and 4-DMAP (0.112 g, 0.92 mmol), and the reaction mixture was stirred for 12 h at room temperature. The reaction mixture was filtered through a canula and stored at 4 °C to give a mixture of colorless crystals of compound **6** and **7**, which were separated by fractional crystallization.

6 and 7. ¹H NMR of **6** (400 MHz, 298 K, CDCl₃): δ 3.04 (s, 12H, CH₃NCH₃(DMAP)), 6.52–8.29 (m, 24H, H of B-Ph) ppm, ¹H NMR of **7** (400 MHz, 298 K, CDCl₃): δ 1.22 (d, 12H, *J* = 6.75 Hz, CH(CH₃)₂), 1.37 (d, *J* = 6.75 Hz, 12H, CH(CH₃)₂), 2.76 (q, *J* = 5.25 Hz, 2H, NCH₂CH₂CH₂N), 3.04 (sept, *J* = 6.88 Hz, 4H, CH(CH₃)₂), 4.26 (t, *J* = 5.63 Hz, 4H, NCH₂CH₂CH₂N), 7.24 (d, *J* = 7.75 Hz, 4H, *ortho*-H of Dipp), 7.44 (t, *J* = 7.75 Hz, 2H, *meta*-H of Dipp), 7.56 (*para*-H of dipp) ppm. ¹³C{¹H} NMR of **6** (101 MHz, 298 K, CDCl₃): δ 39.3, 106.5, 127.3, 129.1, 133.5, 145.9, 155.1 ppm. ¹³C{¹H} NMR of **7** (101 MHz, 298 K, CDCl₃): δ 19.1, 24.5, 28.6, 48.6, 124.9, 130.9, 135.3, 145.2, 152.7 ppm. ¹¹B{¹H} NMR of **6** (128 MHz, 298 K, CDCl₃): δ 20.5 (s, 1B, BOPh) ppm. ¹⁹F{¹H} NMR of **7** (377 MHz, 298 K, CDCl₃): δ -78.2 (s, 3F, OSO₂CF₃) ppm. HRMS (**6**) (CH₃CN): *m/z* calcd for C₃₂H₃₃B₃O₃N₄ [M + H]⁺, 556.2983; found, 556.2556. HRMS (**7**) (CH₃CN): *m/z* calcd for C₂₈H₄₁N₂ [M-OTf]⁺, 405.3264; found, 405.3256.

■ ASSOCIATED CONTENT

Supporting Information

The Supporting Information is available free of charge at <https://pubs.acs.org/doi/10.1021/acs.inorgchem.2c00611>.

Structural description of **1–7** and representative NMR spectra (PDF)

Accession Codes

CCDC 2102134, 2153460–2153461, and 2153463–2153465 contain the supplementary crystallographic data for this paper. These data can be obtained free of charge via www.ccdc.cam.ac.uk/data_request/cif, or by emailing data_request@ccdc.cam.ac.uk, or by contacting The Cambridge Crystallographic Data Centre, 12 Union Road, Cambridge CB2 1EZ, UK; fax: +44 1223 336033.

■ AUTHOR INFORMATION

Corresponding Author

Sakya S. Sen – Inorganic Chemistry and Catalysis Division, CSIR-National Chemical Laboratory, Pune 411008, India; Academy of Scientific and Innovative Research (AcSIR), Ghaziabad 201002, India; orcid.org/0000-0002-4955-5408; Email: ss.sen@ncl.res.in

Authors

Gargi Kundu – Inorganic Chemistry and Catalysis Division, CSIR-National Chemical Laboratory, Pune 411008, India; Academy of Scientific and Innovative Research (AcSIR), Ghaziabad 201002, India

Kajal Balayan – Inorganic Chemistry and Catalysis Division, CSIR-National Chemical Laboratory, Pune 411008, India; Academy of Scientific and Innovative Research (AcSIR), Ghaziabad 201002, India

Srinu Tothadi – Analytical and Environmental Sciences Division and Centralized Instrumentation Facility, CSIR-Central Salt and Marine Chemicals Research Institute, Bhavnagar 364002, India; Academy of Scientific and Innovative Research (AcSIR), Ghaziabad 201002, India; orcid.org/0000-0001-6840-6937

Complete contact information is available at:

<https://pubs.acs.org/10.1021/acs.inorgchem.2c00611>

Notes

The authors declare no competing financial interest.

ACKNOWLEDGMENTS

S.S.S. is thankful for SJF grant SB/SJF/2021-22/06, GOI, for financial assistance. G.K. and K.B. thank CSIR, India, for their research fellowships. S.T. is grateful to AESD&CIF, CSIR-CSMCRI, for instrumentation facilities and infrastructure. We are thankful to the reviewers for their critical feedbacks to improve the quality of the article.

REFERENCES

- (1) (a) Miyaura, N.; Suzuki, A. Stereoselective Synthesis of Arylated (E)-Alkenes by the Reaction of Alk-1-enylboranes with Aryl halides in the Presence of Palladium Catalyst. *J. Chem. Soc., Chem. Commun.* **1979**, *19*, 866–867. (b) Petasis, N. A.; Zavialov, I. A. A New and Practical Synthesis of α -Amino Acids from Alkenyl Boronic Acid. *J. Am. Chem. Soc.* **1997**, *119*, 445–446. (c) Sakai, M.; Ueda, H.; Miyaura, N. Rhodium-Catalyzed Addition of Organoboronic Acids to Aldehydes. *Angew. Chem., Int. Ed.* **1998**, *37*, 3279–3281.
- (2) Lee, D.; Taylor, M. S. Borinic Acid-Catalyzed Regioselective Acylation of Carbohydrate Derivatives. *J. Am. Chem. Soc.* **2011**, *133*, 3724–3727.
- (3) Wang, G.; Garrett, G. E.; Taylor, M. S. Borinic Acid-Catalyzed, Regioselective Ring Opening of 3,4-Epoxy Alcohols. *Org. Lett.* **2018**, *20*, 5375–5379.
- (4) Lee, D.; Williamson, C. L.; Chan, L.; Taylor, M. S. Regioselective, Borinic Acid-Catalyzed Monoacylation, Sulfonylation and Alkylation of Diols and Carbohydrates: Expansion of Substrate Scope and Mechanistic Studies. *J. Am. Chem. Soc.* **2012**, *134*, 8260–8267.
- (5) Michaelis, A. Untersuchungen über aromatische Borverbindungen. *Ber* **1894**, *27*, 244–262.
- (6) Weese, K. J.; Bartlett, R. A.; Murray, B. D.; Olmstead, M. M.; Power, P. R. Synthesis and Spectroscopic and Structural Characterization of Derivatives of the Quasi-Alkoxide Ligand [OBMe₂]₂ (Mes = 2,4,6-Me₃C₆H₂). *Inorg. Chem.* **1987**, *26*, 2409–2413.
- (7) Solovyev, A.; Geib, S. J.; Lacôte, E.; Curran, D. P. Reactions of Boron-Substituted N-Heterocyclic Carbene Boranes with Triflic Acid. Isolation of a New Dihydroxyborenium Cation. *Organometallics* **2012**, *31*, 54–56.
- (8) Kundu, G.; Ajithkumar, V. S.; Raj, K. V.; Vanka, K.; Tothadi, S.; Sen, S. S. Substitution at sp³ Boron of a Six-Membered NHC-BH₃: Convenient Access to a Dihydroxyborenium Cation. *Chem. Commun.* **2022**, *58*, 3783–3786.
- (9) Curran, D. P.; Solovyev, A.; Makhlof Brahmī, M.; Fensterbank, L.; Malacria, M.; Lacôte, E. Synthesis and Reactions of N-Heterocyclic Carbene Boranes. *Angew. Chem., Int. Ed.* **2011**, *50*, 10294–10317.
- (10) Ueng, S.-H.; Makhlof Brahmī, M.; Derat, É.; Fensterbank, L.; Lacôte, E.; Malacria, M.; Curran, D. P. Complexes of Borane and N-Heterocyclic Carbenes: A New Class of Radical Hydrogen Atom Donor. *J. Am. Chem. Soc.* **2008**, *130*, 10082–10083.
- (11) Ueng, S.-H.; Fensterbank, L.; Lacôte, E.; Malacria, M.; Curran, D. P. Radical Deoxygenation of Xanthates and Related Functional Groups with New Minimalist N-Heterocyclic Carbene Boranes. *Org. Lett.* **2010**, *12*, 3002–3005.
- (12) Brahmī, M. M.; Monot, J.; Desage-El Murr, M.; Curran, D. P.; Fensterbank, L.; Lacôte, E.; Malacria, M. Preparation of NHC Borane Complexes by Lewis Base Exchange with Amine- and Phosphine-Boranes. *J. Org. Chem.* **2010**, *75*, 6983–6985.
- (13) Solovyev, A.; Chu, Q.; Geib, S. J.; Fensterbank, L.; Malacria, M.; Lacôte, E.; Curran, D. P. Substitution Reactions at Tetracoordinate Boron: Synthesis of N-Heterocyclic Carbene Boranes with Boron-Heteroatom Bonds. *J. Am. Chem. Soc.* **2010**, *132*, 15072–15080.
- (14) Dai, W.; Geib, S. J.; Curran, D. P. Reactions of N-Heterocyclic Carbene Boranes with 5-Diazo-2,2-dimethyl-1,3-dioxane-4,6-dione: Synthesis of Mono- and Bis-hydrazone NHC-Boranes. *J. Org. Chem.* **2018**, *83*, 8775–8779.
- (15) Auerhammer, D.; Arrowsmith, M.; Braunschweig, H.; Dewhurst, R. D.; Jiménez-Halla, J. O. C.; Kupfer, T. Nucleophilic Addition and Substitution at Coordinatively Saturated Boron by Facile 1,2-Hydrogen Shuttling onto a Carbene Donor. *Chem. Sci.* **2017**, *8*, 7066–7071.
- (16) Kundu, G.; Pahar, S.; Tothadi, S.; Sen, S. S. Stepwise Nucleophilic Substitution to Access Saturated N-heterocyclic Carbene Haloboranes with Boron–Methyl Bonds. *Organometallics* **2020**, *39*, 4696–4703.
- (17) Bissinger, P.; Braunschweig, H.; Damme, A.; Hörl, C.; Krummenacher, I.; Kupfer, T. Boron as a Powerful Reductant: Synthesis of a Stable Boron-Centered Radical-Anion Radical-Cation Pair. *Angew. Chem., Int. Ed.* **2015**, *54*, 359–362.
- (18) Matsumoto, T.; Gabbai, F. P. A Borenium Cation Stabilized by an N-Heterocyclic Carbene Ligand. *Organometallics* **2009**, *28*, 4252–4253.
- (19) Valverde, M. F. S.; Schweyen, P.; Gisinger, D.; Bannenberg, T.; Freytag, M.; Kleeberg, C. N-Heterocyclic Carbene Stabilized Boryl Radicals. *Angew. Chem., Int. Ed.* **2017**, *56*, 1135–1140.
- (20) McArthur, D.; Butts, C. P.; Lindsay, D. M. A Dialkylborenium Ion via Reaction of N-Heterocyclic Carbene-Organoboranes with Brønsted Acids-Synthesis and DOSY NMR Studies. *Chem. Commun.* **2011**, *47*, 6650–6652.
- (21) Farrell, J. M.; Hatnean, J. A.; Stephan, D. W. Activation of Hydrogen and Hydrogenation Catalysis by a Borenium Cation. *J. Am. Chem. Soc.* **2012**, *134*, 15728–15731.
- (22) Weber, L.; Dobbert, E.; Stammer, H.-G.; Neumann, B.; Boese, R.; Bläser, D. Reaction of 1,3-Dialkyl-4,5-dimethylimidazol-2-ylidenes with 2-Bromo-2,3-dihydro-1H-1,3,2-diazaboroles (Alkyl = iPr and tBu). *Chem. Ber.* **1997**, *130*, 705–710.
- (23) Wang, Y.; Robinson, G. H. Carbene Stabilization of Highly Reactive Main-Group Molecules. *Inorg. Chem.* **2011**, *50*, 12326–12337.
- (24) Mansaray, H. B.; Rowe, A. D. L.; Phillips, N.; Niemeyer, J.; Kelly, M.; Addy, D. A.; Bates, J. I.; Aldridge, S. Modelling Fundamental Arene–Borane Contacts: Spontaneous Formation of a Dibromoborenium Cation Driven by Interaction between a Borane Lewis acid and an Arene π System. *Chem. Commun.* **2011**, *47*, 12295–12297.
- (25) Lawson, J. R.; Clark, E. R.; Cade, I. A.; Solomon, S. A.; Ingleson, M. J. Haloboration of Internal Alkynes with Borenium and Borenium Cations as a Route to Tetrasubstituted Alkenes. *Angew. Chem., Int. Ed.* **2013**, *52*, 7518–7522.
- (26) Koelle, P.; Noeth, H. The Chemistry of Borinium and Borenium Ions. *Chem. Rev.* **1985**, *85*, 399–418.
- (27) Piers, W. E.; Bourke, S. C.; Conroy, K. D. Borinium, Borenium, and Borenium Ions: Synthesis, Reactivity, and Applications. *Angew. Chem., Int. Ed.* **2005**, *44*, 5016–5036.
- (28) Cade, I. A.; Ingleson, M. J. syn-1,2-Carboration of Alkynes with Borenium Cations. *Chem.—Eur. J.* **2014**, *20*, 12874–12880.
- (29) Wu, X.; Liu, X.; Zhao, G. Catalyzed Asymmetric Aryl Transfer Reactions to Aldehydes with Boroxines as Aryl Source. *Tetrahedron: Asymmetry* **2005**, *16*, 2299–2305.
- (30) Stoy, A.; Härterich, M.; Dewhurst, R. D.; Jiménez-Halla, J. O. C.; Endres, P.; Eysel, M.; Kupfer, T.; Deissenberger, A.; Thiess, T.; Braunschweig, H. Evidence for Borylene Carbonyl (LHB=C=O) and Base-Stabilized (LHB=O) and Base-Free Oxoborane (RB≡O) Intermediates in the Reactions of Diborenes with CO₂. *J. Am. Chem. Soc.* **2022**, *144*, 3376–3380.
- (31) Inés, B.; Patil, M.; Carreras, J.; Goddard, R.; Thiel, W.; Alcarazo, M. Synthesis, Structure, and Reactivity of a Dihydrido Borenium Cation. *Angew. Chem., Int. Ed.* **2011**, *50*, 8400–8403.
- (32) Iglesias, M.; Beetstra, D. J.; Knight, J. C.; Ooi, L.-L.; Stasch, A.; Coles, S.; Male, L.; Hursthouse, M. B.; Cavell, K. J.; Dervisi, A.; Fallis, I. A. Novel Expanded Ring N-Heterocyclic Carbenes: Free Carbenes, Silver Complexes, and Structures. *Organometallics* **2008**, *27*, 3279–3289.

Article

Nucleophilic Substitution at a Coordinatively Saturated Five-Membered NHC·Haloborane Centre

Gargi Kundu^{1,2}, Srinu Tothadi³ and Sakya S. Sen^{1,2,*} 

¹ Inorganic Chemistry and Catalysis Division, CSIR-National Chemical Laboratory, Dr. Homi Bhabha Road, Pashan, Pune 411008, India; g.kundu@ncl.res.in

² Academy of Scientific and Innovative Research (AcSIR), Ghaziabad 201002, India

³ Analytical and Environmental Sciences Division and Centralized Instrumentation Facility, CSIR-Central Salt and Marine Chemicals Research Institute, Gijubhai Badheka Marg, Bhavnagar 364002, India; srinut@csmcri.res.in

* Correspondence: ss.sen@ncl.res.in

Abstract: In this paper, we have used a saturated five-membered N-Heterocyclic carbene (5SIDipp = 1,3-bis-(2,6-diisopropylphenyl)imidazolin-2-ylidene) for the synthesis of SNHC-haloboranes adducts and their further nucleophilic substitutions to put unusual functional groups at the central boron atom. The reaction of 5-SIDipp with RBCl_2 yields Lewis-base adducts, 5-SIDipp· RBCl_2 [R = H (1), Ph (2)]. The hydrolysis of 1 gives the NHC stabilized boric acid, 5-SIDipp· $\text{B}(\text{OH})_3$ (3), selectively. Replacement of chlorine atoms from 1 and 2 with one equivalent of AgOTf led to the formation of 5-SIDipp· $\text{HBCl}(\text{OTf})$ (4) and 5-SIDipp· $\text{PhBCl}(\text{OTf})$ (5a), where all the substituents on the boron atoms are different. The addition of two equivalents of AgNO_3 to 2 leads to the formation of rare *di*-nitro substituted 5-SIDipp· $\text{BPh}(\text{NO}_3)_2$ (6). Further, the reaction of 5-SIDipp with $\text{B}(\text{C}_6\text{F}_5)_3$ in tetrahydrofuran and diethyl ether shows a frustrated Lewis pair type small molecule activated products, 7 and 8.

Keywords: saturated NHC; NHC-haloboranes; nucleophilic substitution; tetra-coordinate boron



Citation: Kundu, G.; Tothadi, S.; Sen, S.S. Nucleophilic Substitution at a Coordinatively Saturated Five-Membered NHC·Haloborane Centre. *Inorganics* **2022**, *10*, 97. <https://doi.org/10.3390/inorganics10070097>

Academic Editor: Marina Yu. Stogniy

Received: 21 June 2022

Accepted: 4 July 2022

Published: 7 July 2022

Publisher's Note: MDPI stays neutral with regard to jurisdictional claims in published maps and institutional affiliations.



Copyright: © 2022 by the authors. Licensee MDPI, Basel, Switzerland. This article is an open access article distributed under the terms and conditions of the Creative Commons Attribution (CC BY) license (<https://creativecommons.org/licenses/by/4.0/>).

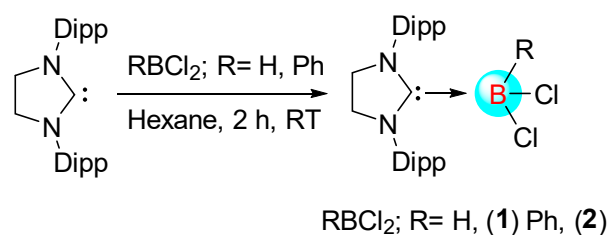
1. Introduction

While less than two decades ago, the N-heterocyclic carbene-borane adducts were conceived rare and exotic, they are now readily accessible owing to rapid synthetic development and constitute an important class of compounds because they display different chemistry from the most existing classes of boron compounds such as boranes or borates [1]. Since the unveiling of the concept that NHC·boranes undergo nucleophilic substitution at boron by the groups of Fensterbank, Lacôte, Malacria, and Curran, the chemistry of these systems has flourished [2–6]. However, these systems largely rely on imidazole-2-ylidene type carbenes. Braunschweig and coworkers recently broadened the range of Lewis base by demonstrating nucleophilic addition and substitution of cyclic alkyl amino carbene (*cAAC*) BH_3 adduct [7]. In our previous works, we have shown the nucleophilic substitution at 5-SIDipp· MeBCl_2 (5-SIDipp = 1,3-bis-(2,6-diisopropylphenyl)imidazolin-2-ylidene) [8]. Further, we have explored the substitution at 6-SIDipp· BH_3 (6-SIDipp = 1,3-di(2,6-diisopropylphenyl) tetrahydropyrimidine-2-ylidene) center and the introduction of rare functional groups such as $-\text{OTf}$, $-\text{NO}_3$ [9]. Although the saturated NHCs are more nucleophilic than its unsaturated analogue, the earlier work on the synthesis of more than two dozen of NHC·borane and haloborane complexes relied on the unsaturated five-membered NHC [1–6,10–16]. Clearly, the extension of unexplored carbenes in NHC·borane chemistry is desirable, as it may lead to the discovery of a range of interesting new applications. Due to our current interest in 5-SIDipp [17–19], we have prepared here haloboranes 5SIDipp· BHCl_2 , 1 and 5SIDipp· BPhCl_2 , 2 and studied their substitution reactions with AgOTf , AgNO_3 , and water. Furthermore, we have shown that

the combination 5-SIDipp and $B(C_6F_5)_3$ led to the activation of THF and diethyl ether via frustrated Lewis pair (FLP) way. Our results are reported herein.

2. Results and Discussion

In our previous work, we have reported the first carbene $MeBCl_2$ adduct via salt metathesis procedure [8]. In this work, we have prepared the 5SIDipp-haloborane adducts and shown their reactivities towards nucleophilic substitution. The addition of $BHCl_2$ -dioxane in the solution of 5SIDipp in *n*-hexane gives the white precipitation of 5-SIDipp· $BHCl_2$, **1** at room temperature (Scheme 1). The precipitate was further dissolved in toluene and dichloromethane to afford colorless crystals of **1** at -36 °C. The ^{11}B NMR spectrum of **1** displays a resonance at 6.9 ppm as a sharp singlet. The backbone four protons appeared at 4.08 ppm in the 1H NMR spectrum. **1** is characterized by single-crystal X-ray diffraction studies (Figure 1). **1** is crystallized in the monoclinic $P2_1/n$ space group. The B–C bond length in **1** [1.628(7) Å] is in good accordance with the previously reported 5-SIDipp· $MeBCl_2$ [1.6261(19) Å], but considerably longer compared to that in the 5-SIDipp· BH_3 [1.593(4) Å] [8]. The increase in the bond length can be ascribed to the enhancement of steric hindrance at the central boron atom. The average B–Cl distance is 1.86 Å, which matches with the previously reported carbene-haloborane adducts ($NHC\cdot BCl_3$, $NHC\cdot BRCl_2$, and $NHC\cdot BR_2Cl$).



Scheme 1. Synthesis of 5-SIDipp· $RBCl_2$ adducts **1** and **2**.

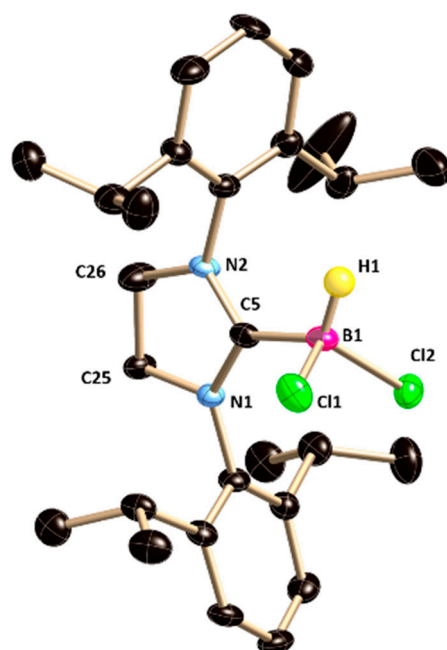


Figure 1. The molecular structure of **1** (hydrogen atoms except at the boron atom in **1** are omitted for clarity). Selected bond lengths [Å] or angles [deg]: C5–N1 1.337(5), C5–N2 1.329(6), C25–N1 1.491(6), C26–N2 1.477(6), C5–B1 1.628(7), B1–Cl1 1.865(5), B1–Cl2 1.869(5); N1–C5–N2 109.2(4), N1–C5–B1 128.9(4), N2–C5–B1 121.9(4), Cl1–B1–Cl2 110.1(3).

The reaction of 1.1 equivalent of PhBCl_2 with 5-SIDipp in *n*-hexane gives an immediate white precipitate formation of 5-SIDipp· PhBCl_2 (**2**) (Scheme 1). The ^{11}B NMR spectrum of **2** shows one resonance at 1.8 ppm. **2** crystallizes in the monoclinic $P2_1/n$ space group (Figure 2). The carbene carbon atom C5 is tri-coordinated and features a trigonal-planar geometry, and the boron atom connected with the C5 atom adopts a tetrahedral geometry. The B– C_{NHC} bond distance is 1.6661(10) Å, which is slightly longer in comparison to that in **1** due to the steric congestion of the phenyl group at the boron center. The B–Cl bonds are 1.8992(8) Å and 1.8698(8) Å, which match with the previously reported B–Cl bond distance [8].

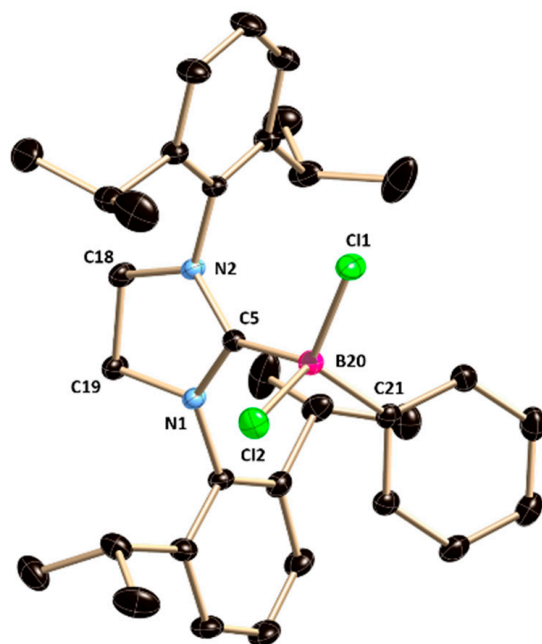


Figure 2. The molecular structure of **2**. Hydrogen atoms are omitted for clarity. Selected bond lengths [Å] or angles [deg]: C5–N1 1.3403(8), C5–N2 1.3443(8), C19–N1 1.4810(9), C18–N2 1.4756(9), C5–B20 1.6661(10), B20–C21 1.6204(10), B20–Cl1 1.8992(8), B20–Cl2 1.8698(8); N1–C5–N2 108.63(6), N1–C5–B20 127.41(6), N2–C5–B20 123.20(6), C5–B20–Cl1 100.88(4), C5–B20–C21 110.99(5), Cl1–B20–Cl2 106.42(4).

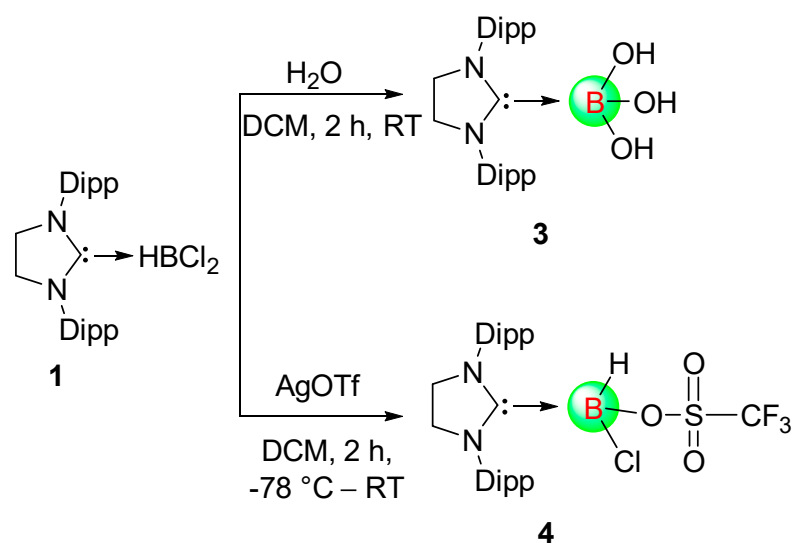
Treatment of 1.05 equivalents of water in a dichloromethane solution of **1** hydrolyzes all the B–H and B–Cl bonds and forms NHC-stabilized boric acid, 5-SIDipp· $\text{B}(\text{OH})_3$, **3** (Scheme 2) exclusively. In our earlier work, we have reported the isolation of 6-SIDipp· $\text{B}(\text{OH})_3$ as a minor product from the reaction of $\text{Br}_2/\text{H}_2\text{O}$ with 6-SIDipp· BH_3 [9]. Replacement of the chloride and the hydride groups by hydroxide moieties in **3** is accompanied by an upfield shift in the ^{11}B NMR spectrum (−1.6 ppm) from that of **1**. **3** crystallizes in the monoclinic $P2_1/c$ space group (Figure 3). The central boron-carbon distance is 1.650(5) Å, which is marginally shorter compared to that in 6-SIDipp· $\text{B}(\text{OH})_3$. The average B–(OH) bond distances are 1.38 Å.

Further, we added silver triflate to a dichloromethane solution of **1** at -78°C , which replaced one of the labile chlorine atoms by the triflate group (Scheme 2). In the ^{11}B NMR spectrum of **4**, the resonance for the central boron atom appears at −3.4 ppm. The resonance at −76.7 ppm in the ^{19}F NMR is characteristic of the triflate group attached to the central boron atom. Colorless crystals of **4** suitable for X-ray diffraction studies were grown from a saturated toluene solution at 4°C . The constitution of **4** was authenticated by a single-crystal X-ray study (Figure 4). **4** crystallizes in the monoclinic space group $P2_1/n$. The relevant bond length and angles are given in the legend of Figure 4. All the four substituents on the central boron atom are different in **4**. The central boron atom (B1) lies slightly below the plane of an imidazolium ring (torsion angles (deg): C(2)–N(1)–C(1)–B(1) = 174.4(2) and C(3)–N(2)–C(1)–B(1) = 166.5(2)) and the B–O bond is not orthogonal to

the plane of the imidazolinium ring with the torsion angles $N1-C1-B1-O1 = -41.6(2)^\circ$ and $N2-C1-B1-O1 = 148.4(2)^\circ$. The $B-O_{Tf}$ bond length is $1.515(2) \text{ \AA}$, which is in good agreement with the $B-O$ bond length in our previously reported $5\text{-SIDipp}\cdot\text{BMeOTfCl}$ ($B1-O3 1.503(3) \text{ \AA}$) [8].

Treatment of one and two equivalents of AgOTf and AgNO_3 with **2** in toluene afforded *mono*-triflate and *di*-nitro substituted 5-SIDipp -boranes, respectively. Substitution of one and two chlorine atoms from the tetra coordinated boron atom of **2** resulted in the formation of $5\text{-SIDipp}\cdot\text{BPhCl}(\text{OTf})$, **5a**, and $5\text{-SIDipp}\cdot\text{BPh}(\text{ONO}_2)_2$, **6** (Scheme 3). The functional groups such as nitrate and triflate are rarely found to bind with the boron atom [5,9,20–26]. **5a** crystallizes in the monoclinic $P2_1/n$ space group (Figure 5). The boron atom lies on a tetrahedral geometry, which can be confirmed from the bond angles around the boron atoms in **5a** ($C5-B2-C11 100.54(11)$, $C5-B2-O1 106.51(13)$, and $C5-B2-C7 118.55(14)$). The $B-C_{NHC}$ bond length in **5a** ($1.648(2) \text{ \AA}$) is in well agreement with that in **2**. The $B-O$ and $B-Cl$ bonds in **5a** is almost orthogonal to the plane (torsion angle: $N1-C5-B2-C11 76.96(17)^\circ$, $N2-C5-B2-C11 -89.6(2)^\circ$ and torsion angle: $N1-C5-B2-O1 -170.96(14)^\circ$, $N2-C5-B2-O1 22.5(2)^\circ$, respectively). However, the spectroscopic characterization of **5a** becomes complicated because of solvent-mediated slow hydrolysis. The only signal in the ^{11}B NMR spectra of the product, **5b** appears at 30.9 ppm as a singlet, which is indicative of a three-coordinated boron center, instead of a four-coordinated boron, as expected in **5a**. We regrow the crystals from the NMR tube and realized that there is hydrolysis taking place at the $B-Cl$ bond with adventitious water leading to 5-SIDipp stabilized borenium cation, with a triflate as a counter anion (**5b**). The constitution of **5b** rationalizes the resonance at 30.9 ppm in the ^{11}B NMR spectrum. Although the formation of the **5b** clearly can be seen from the molecular structure (Figure S2), but due to low-quality data we refrain from discussing its structural parameters. However, even after repeated attempts, we were unable to stop this hydrolysis and hence, could not characterize **5a** spectroscopically. The CF_3 group of the triflate moiety in **5b** resonates at -78.6 ppm in the ^{19}F NMR, which is slightly different from the resonances of triflates bound to the boron atom (-76.7 ppm in **4**) and is characteristic of the free triflate anion.

In the ^{11}B NMR, **6** shows resonance at 4.2 ppm , shifted slight low-field with respect to that in **2** (1.9 ppm), presumably due to electron-withdrawing nature of the ONO_2 moieties. The solid-state structure of **6** also was confirmed by X-ray crystal analysis. **6** crystallizes in the monoclinic $P2_1/c$ space group (Figure 6) and important structural parameters are given in the legend of Figure 6.



Scheme 2. Reactivity of **1** with H_2O and AgOTf .

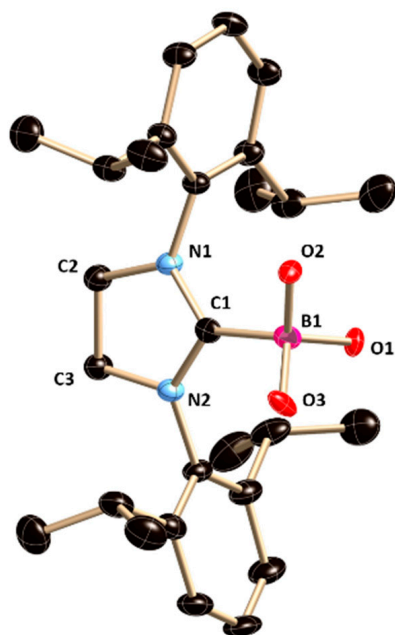


Figure 3. The molecular structure of **3**. Hydrogen atoms are omitted for clarity. Selected bond lengths [Å] or angles [deg]: N1–C1 1.316(4), N2–C1 1.337(4), C2–N1 1.471(4), C3–N2 1.478(4), C1–B1 1.650(5), B1–O1 1.375(4), B1–O2 1.386(4); N1–C1–N2 113.2(3), N1–C1–B1 125.4(3), N2–C1–B1 125.0(3), C1–B1–O1 110.4(3), C1–B1–O2 108.5(3), O1–B1–O2 111.1(3).

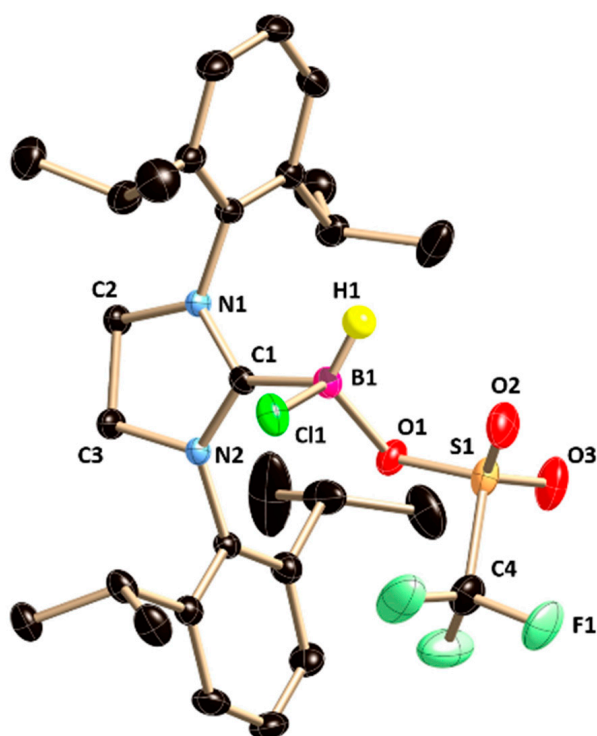
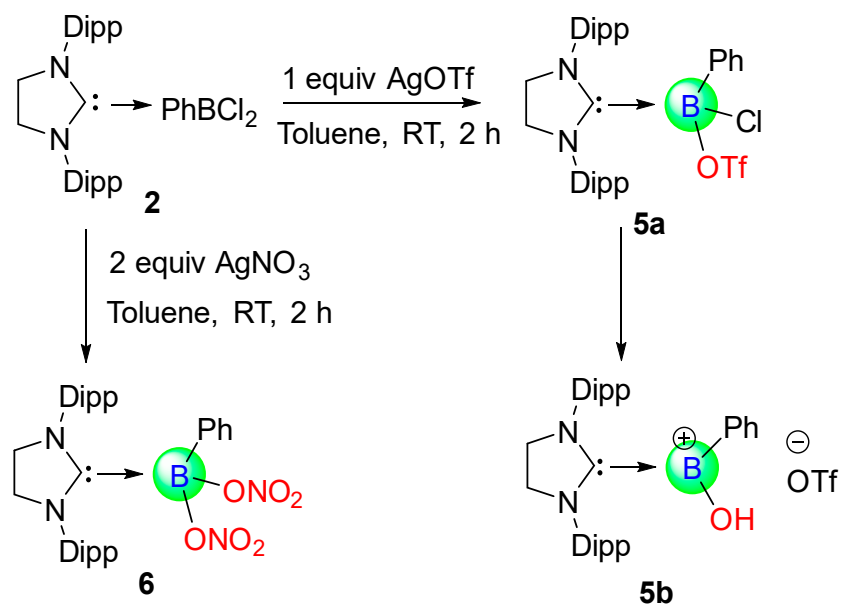


Figure 4. The molecular structure of **4**. Hydrogen atom except H1 in **4** are omitted for clarity. Selected bond lengths [Å] or angles [deg]: N1–C1 1.316(4), N2–C1 1.337(4), C2–N1 1.471(4), C3–N2 1.478(4), C1–B1 1.650(5), B1–O1 1.375(4); N1–C1–N2 113.2(3), N1–C1–B1 125.4(3), N2–C1–B1 125.0(3), C1–B1–O1 110.4(3).



Scheme 3. Nucleophilic substitution of **2** with AgOTf and AgNO₃.

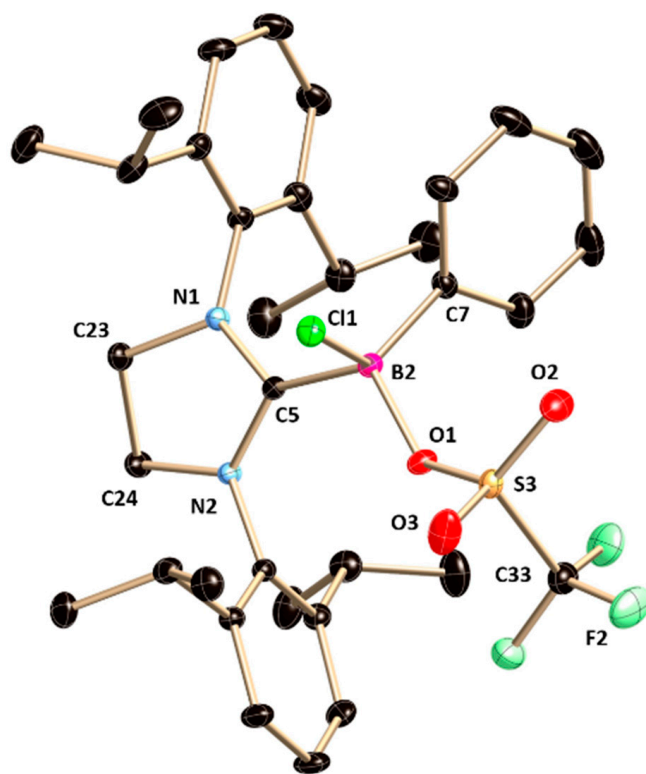


Figure 5. The molecular structure of **5a**. Hydrogen atoms are omitted for clarity. Selected bond lengths [Å] or angles [deg]: N1–C5 1.341(2), N2–C5 1.330(2), C23–N1 1.485(2), C24–N2 1.482(2), C5–B2 1.648(2), B2–Cl1 1.8948(19), B2–O1 1.532(2); N1–C5–N2 109.30(14), N1–C5–B2 123.00(14), N2–C5–B2 126.57(14), C5–B2–Cl1 100.54(11), C5–B2–O1 106.51(13), C5–B2–C7 118.55(14).

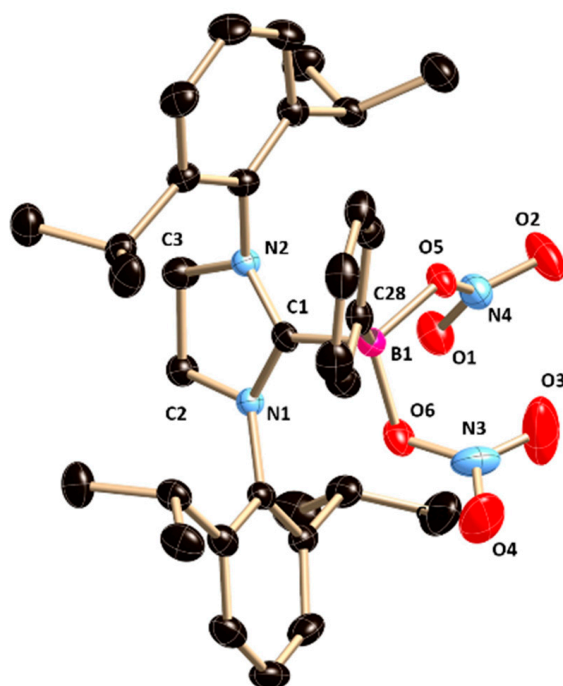
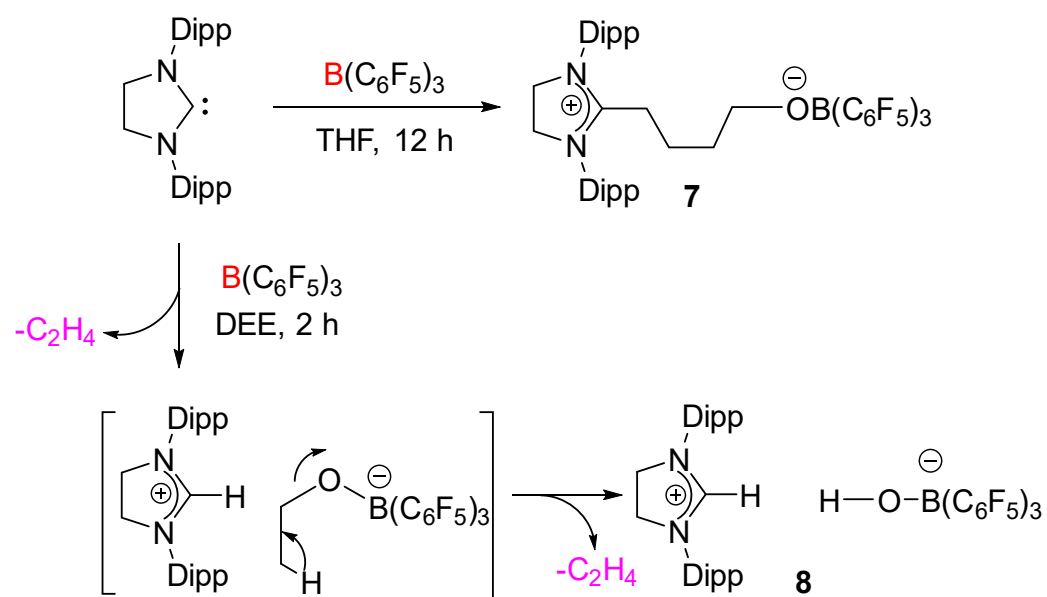


Figure 6. The molecular structure of **6**. Hydrogen atoms are omitted for clarity. Selected bond lengths [Å] or angles [deg]: N1–C1 1.337(3), C1–N2 1.340(3), N1–C2 1.480(3), N2–C3 1.484(3), C1–B1 1.662(4), B1–O5 1.535(4), B1–O6 1.522(3); N1–C1–N2 112.4(2), C1–N1–C2 112.4(2), C1–N2–C3 111.8(2), C1–B1–O5 101.59(19), C1–B1–O6 109.7(2), O5–B1–O6 111.3(2), C1–B1–C28 118.4(2).

The combination of N-heterocyclic carbene and $B(C_6F_5)_3$ has been exploited in FLP chemistry [27]. In our previous work, we have demonstrated the adduct formation between 5-SIDipp and $B(C_6F_5)_3$ [8]. We have prepared the adduct in toluene/*n*-hexane. When we performed the same reaction in THF or diethyl ether, it led to the activation of those ethereal solvents. The THF solution of the 5-SIDipp· $B(C_6F_5)_3$ was kept for 12 h at room temperature, which afforded the zwitterionic species **7** in quantitative yield as a white solid (Scheme 4). The molecular structure of **7** was additionally established by X-ray diffraction analysis (Figure 7). **7** crystallizes in the triclinic $P\bar{1}$ space group. One of the C–O bonds in the THF molecule is cleaved, and as a result, the THF ring becomes acyclic and inserts between the Lewis pairs. Similar to the case for 5-SIDipp· $B(C_6F_5)_3$, **7** is not stable in solution at room temperature, so we were unable to satisfactorily characterize it by NMR spectroscopy. The ^{11}B NMR resonance at -2.8 ppm is similar to those established for the tetra-coordinated boron compounds. The C5 atom adopts a trigonal planar geometry, which is confirmed by the sum of the bond angles [N1–C5–N2 $112.29(15)^\circ$, N1–C5–C6 $125.21(15)^\circ$, N2–C5–C6 $122.50(14)^\circ$]. The C5–C6 bond distance is marginally shorter compared to the adjacent C–C bond (C5–C6 $1.501(2)$ Å and C6–C7 $1.539(2)$ Å). The boron atom adopts a tetrahedral geometry. The C–O ($1.404(2)$ Å) and the B–O ($1.453(2)$ Å) bond distances are similar to the other previously reported structures [28]. This reactivity was extended to diethyl ether (DEE), which resulted in the isolation of imidazolium salt with a borate counter-anion (**8**). This compound presumably results from activation of the C–O bond of the diethyl ether with concomitant elimination of two ethylene molecules (Scheme 4). A signal at 8.9 ppm in the 1H NMR spectrum confirms the presence of an imidazolium cation. The ^{11}B NMR displays the characteristic resonance at -4.2 ppm, which can be assigned to a tetrahedral $[(HO)B(C_6F_5)_3]$ anion. X-ray crystallographic analysis later confirmed the structure of **8** (Figure 8).



Scheme 4. 5-SIDipp·B(C₆F₅)₃ Lewis pair mediated tetrahydrofuran and diethyl ether activation at room temperature.

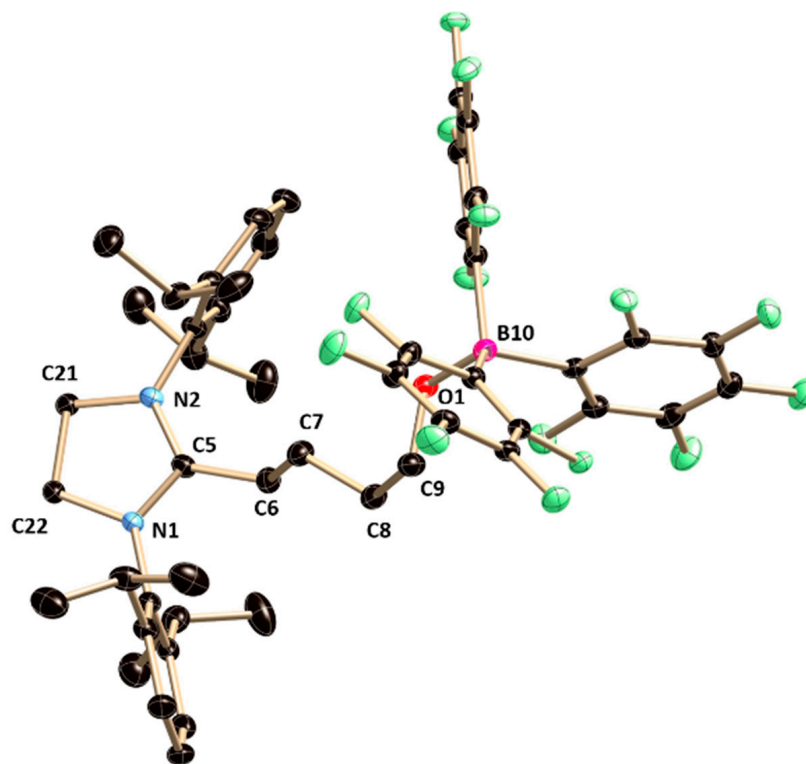


Figure 7. The molecular structure of **7**. Hydrogen atoms are omitted for clarity. Selected bond lengths [Å] or angles [deg]: N2–C5 1.322(2), N1–C5 1.327(2), N1–C22 1.479(2), N2–C21 1.484(2), C5–C6 1.501(2), C6–C7 1.539(2), C9–O1 1.404(2), O1–B10 1.453(2); N1–C5–N2 112.29(15), N1–C5–C6 125.21(15), N2–C5–C6 122.50(14), C9–O1–B10 117.96(13).

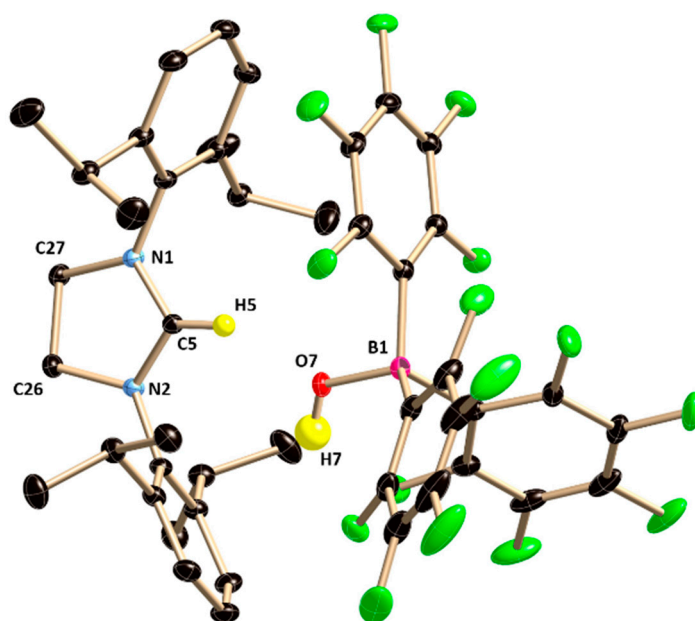


Figure 8. The molecular structure of **8**. Hydrogen atoms except the H5 and H7 are omitted for clarity. Selected bond lengths [Å] or angles [deg]: N1–C5 1.3156(11), N2–C5 1.3174(12), C5–H5 0.950, N1–C27 1.4810(13), N2–C26 1.4817(12), B1–O7 1.4696(12), O7–H1 0.83(2); N1–C5–N2 112.94(8), C27–N1–C5 110.17(8), C26–N2–C5 109.91(8), B1–O7–H7 114.3(15).

3. Conclusions

In summary, we have prepared 5-SIDipp·haloboranes adducts, 5-SIDipp·HBCl₂ (**1**), and 5-SIDipp·PhBCl₂ (**2**) and shown the selective nucleophilic substitution at the tetra-coordinated boron center to obtain several boranes with rare functional groups such as –ONO₂, –OTf, etc. The treatment of one equivalent of AgOTf with **1** and **2** led to the formation of haloboranes, 5-SIDipp·BHCl(OTf), **4** and 5-SIDipp·BPhCl(OTf), **5a**, respectively, where all three substituents of the boron atom are different. **5a** was found to be unstable and undergoes hydrolysis in the presence of adventitious water to give hydroxyborenum cation, **5b**. The treatment of two equivalents of AgNO₃ forms a rare di-nitrate substituted NHC-coordinated borane (**6**). The combination of 5-SIDipp and B(C₆F₅)₃ were shown to affect the C–O bond cleavage differently for THF and diethyl ether. As expected, the 5-SIDipp/B(C₆F₅)₃ combination in THF resulted in ring opening of the THF to produce borate **7**. In the case of diethyl ether, the rupture of the C–O bond takes place along with the elimination of two molecules of ethylene, leading to the formation of an imidazolium cation with tris (pentafluorophenyl) hydroxy borate as the counter anion (**8**).

4. General Procedures and Instrumentation

All manipulations were carried out in an inert atmosphere of argon using standard Schlenk techniques and in argon filled glove box. The solvents, especially toluene, tetrahydrofuran, dichloromethane, and *n*-hexane were purified by MBRAUN solvent purification system MB SPS-800. Other chemicals were purchased from Sigma Aldrich and TCI Chemicals and were used without further purification. The starting material, 5-SIDipp, was synthesized by using the literature procedure [29]. ¹H, ¹³C, ¹¹B NMR, and ¹⁹F spectra were recorded in CDCl₃, using Bruker Avance DPX 400, or a Bruker Avance DPX 500 spectrometer. CDCl₃ was dried by distillation over CaH₂. Chemical shifts (δ) are given in ppm. NMR spectra were referenced to external SiMe₄ (¹H and ¹³C), BF₃·OEt₂ (¹¹B), CFCl₃ (¹⁹F) respectively.

1: A slightly excess of BHCl₂·dioxane (0.20 mL, 0.58 mmol) was added to a 10 mL hexane solution of 5-SIDipp (0.20 g, 0.48 mmol) at room temperature in a Schlenk flask. Stirring the resulted mixture for 2 h at room temperature resulted in the generation of a

white precipitate. Colorless crystals of **1** were isolated after keeping the white powder in the mixture of 1 mL dichloromethane and 2 mL toluene solution at $-36\text{ }^{\circ}\text{C}$. Yield = 0.20 g (90%).

$^1\text{H NMR}$ (400 MHz, 298 K, CDCl_3): $\delta = 1.29$ (d, $J = 6.88$ Hz, 12 H, $\text{CH}(\text{CH}_3)_2$), 1.40 (d, $J = 6.63$ Hz, 12 H, $\text{CH}(\text{CH}_3)_2$), 3.17 (sept, $J = 6.75$ Hz, 4 H, $\text{CH}(\text{CH}_3)_2$), 4.08 (s, 4 H, $\text{NCH}_2\text{CH}_2\text{N}$), 7.23 (d, $J = 7.75$ Hz, 4 H, Ar-H), 7.40 (t, $J = 7.75$ Hz, 2 H, Ar-H) ppm (Figure S1).

$^{13}\text{C}\{^1\text{H}\}$ NMR (101 MHz, 298 K, CDCl_3): $\delta = 23.4, 26.0, 28.9, 53.1, 124.4, 129.8, 133.2, 146.1$ ppm (Figure S2).

$^{11}\text{B}\{^1\text{H}\}$ NMR (128 MHz, 298 K, CDCl_3): $\delta = 6.9$ (s, 1B, BHCl_2) ppm (Figure S3).

2: A slightly excess of $\text{BPhCl}_2 \cdot \text{dioxane}$ (0.090 g, 0.58 mmol) was added to a 10 mL hexane solution of 5-SIDipp (0.20 g, 0.48 mmol) at room temperature in a flask. Stirring the resulted mixture for further 2 h at room temperature accessed a white precipitate. Colorless crystals of **2** were isolated after keeping the white powder in the mixture of 1 mL dichloromethane and 2 mL toluene solution. Yield = 0.24 g (90%).

$^1\text{H NMR}$ (400 MHz, 298 K, CDCl_3): $\delta = 1.42$ (d, $J = 6.72$ Hz, 12 H, $\text{CH}(\text{CH}_3)_2$), 1.51 (d, $J = 6.65$ Hz, 12 H, $\text{CH}(\text{CH}_3)_2$), 3.39 (sept, $J = 6.75$ Hz, 4 H, $\text{CH}(\text{CH}_3)_2$), 4.22 (s, 4 H, $\text{NCH}_2\text{CH}_2\text{N}$), 6.95 (d, $J = 6.88$ Hz, 2 H, *ortho*-H of B-Ph), 7.25 (d, $J = 7.75$ Hz, 4 H, Ar-H), 7.26 (bs, 1 H, *para*-H of B-Ph), 7.44 (t, $J = 7.73$ Hz, 2 H, Ar-H), 7.49 (t, $J = 7.88$ Hz, *meta*-H of B-Ph) ppm (Figure S4).

$^{13}\text{C}\{^1\text{H}\}$ NMR (101 MHz, 298 K, CDCl_3): $\delta = 23.2, 26.2, 28.9, 53.9, 124.2, 129.6, 133.5, 135.2, 145.7$ ppm (Figure S5).

$^{11}\text{B}\{^1\text{H}\}$ NMR (128 MHz, 298 K, CDCl_3): $\delta = 1.8$ (s, 1 B, BPhCl_2) ppm (Figure S6).

3: 1.05 equivalent of water (0.01 g, 0.54 mmol) was added drop by drop to a 15 mL dichloromethane solution of **1** (0.20 g, 0.53 mmol) at room temperature in a flask. Stirring the resulted mixture for further 2 h at room temperature accessed a clear solution. The reaction mixture was concentrated to 5 mL and kept at $4\text{ }^{\circ}\text{C}$ to obtain the colorless crystals of **3**. Yield = 0.36 g (80%).

$^1\text{H NMR}$ (400 MHz, 298 K, CDCl_3): $\delta = 1.31$ (d, $J = 6.97$ Hz, 12 H, $\text{CH}(\text{CH}_3)_2$), 1.35 (d, $J = 6.85$ Hz, 12 H, $\text{CH}(\text{CH}_3)_2$), 3.07 (sept, $J = 6.85$ Hz, 4 H, $\text{CH}(\text{CH}_3)_2$), 4.06 (s, 4 H, $\text{NCH}_2\text{CH}_2\text{N}$), 7.23 (d, $J = 7.70$ Hz, 4 H, Ar-H), 7.39 (t, $J = 7.75$ Hz, 2 H, Ar-H) ppm (Figure S7).

$^{13}\text{C}\{^1\text{H}\}$ NMR (101 MHz, 298 K, CDCl_3): $\delta = 23.4, 25.4, 28.9, 53.3, 67.9, 124.2, 129.6, 133.1, 146.0$ ppm (Figure S8).

$^{11}\text{B}\{^1\text{H}\}$ NMR (128 MHz, 298 K, CDCl_3): $\delta = -1.6$ (s, 1 B, $\text{B}(\text{OH})_3$) ppm (Figure S9).

4: A DCM solution (20 mL) of **1** (0.47 g, 1 mmol) was added dropwise to a DCM solution (20 mL) of previously weighed AgOTf (0.25 g, 1 mmol) at $-78\text{ }^{\circ}\text{C}$ in the absence of light. A white precipitate of AgCl was formed immediately, and it was filtered through frit filtration after the reaction mixture was warmed to room temperature. The colorless toluene solution was concentrated (5 mL) and kept for crystallization at $4\text{ }^{\circ}\text{C}$, which afforded colorless crystals of **4** after 1–2 day(s). Yield = 0.48 g (82%).

$^1\text{H NMR}$ (400 MHz, 298 K, CDCl_3): $\delta = 1.31$ (d, $J = 6.88$ Hz, 12 H, $\text{CH}(\text{CH}_3)_2$), 1.40 (d, $J = 6.63$ Hz, 12 H, $\text{CH}(\text{CH}_3)_2$), 3.13 (sept, $J = 7.63$ Hz, 4 H, $\text{CH}(\text{CH}_3)_2$), 4.11 (s, 4 H, $\text{NCH}_2\text{CH}_2\text{N}$), 7.20 (d, $J = 7.38$ Hz, 4 H, Ar-H), 7.42 (t, $J = 7.63$ Hz, 2 H, Ar-H) ppm (Figure S10).

$^{13}\text{C}\{^1\text{H}\}$ NMR (101 MHz, 298 K, CDCl_3): $\delta = 21.4, 23.2, 25.9, 26.3, 28.9, 53.4, 124.7, 128.2, 130.2, 132.4, 137.8, 145.7, 145.9$ ppm (Figure S11).

$^{11}\text{B}\{^1\text{H}\}$ NMR (128 MHz, 298 K, CDCl_3): $\delta = 3.4$ (s, 1 B, $\text{BH}(\text{OTf})\text{Cl}$) ppm (Figure S12).

$^{19}\text{F}\{^1\text{H}\}$ NMR (377 MHz, 298 K, CDCl_3): $\delta = -76.7$ (s, 3 F, OSO_2CF_3) ppm (Figure S13).

5b: A toluene solution (20 mL) of **2** (0.55 g, 1 mmol) was added dropwise to a toluene solution (20 mL) of previously weighed AgOTf (0.25 g, 1 mmol) at $-30\text{ }^{\circ}\text{C}$ in the absence of light. A white precipitate of AgCl formed immediately, and it was filtered through frit filtration after the reaction mixture was warmed to room temperature. The colorless toluene solution was concentrated (5 mL) and was kept for crystallization at $4\text{ }^{\circ}\text{C}$, which afforded colorless crystals of **5b** after 1 day. Yield = 0.25 g (45%).

^1H NMR (400 MHz, 298 K, CDCl_3): δ = 1.24 (d, J = 6.88 Hz, 12 H, $\text{CH}(\text{CH}_3)_2$), 1.38 (d, J = 6.63 Hz, 12 H, $\text{CH}(\text{CH}_3)_2$), 2.99 (sept, J = 6.75 Hz, 4 H, $\text{CH}(\text{CH}_3)_2$), 4.59 (s, 4 H, $\text{NCH}_2\text{CH}_2\text{N}$), 7.29 (d, J = 7.75 Hz, 4 H, Ar-H), 7.48 (t, J = 7.75 Hz, 2 H, Ar-H), 7.52 (t, J = 7.50 Hz, 2 H, *meta*-H of B-Ph), 7.61 (t, J = 7.38 Hz, *para*-H of B-Ph), 8.25 (d, J = 6.75 Hz, 2 H, *ortho*-H of B-Ph) ppm (Figure S14).

$^{13}\text{C}\{^1\text{H}\}$ NMR (101 MHz, 298 K, CDCl_3): δ = 21.4, 23.8, 25.1, 29.2, 54.7, 125.0, 127.9, 129.0, 135.6, 137.8, 146.2 ppm (Figure S15).

$^{11}\text{B}\{^1\text{H}\}$ NMR (128 MHz, 298 K, CDCl_3): δ = 30.9 (s, 1 B, $\text{BPh}(\text{OH})$) ppm (Figure S16).

$^{19}\text{F}\{^1\text{H}\}$ NMR (377 MHz, 298 K, CDCl_3): δ = -78.6 (s, 3 F, OSO_2CF_3) ppm (Figure S17).

6: A toluene solution (20 mL) of **2** (0.55 g, 1 mmol) was added dropwise to a toluene solution (20 mL) of previously weighed AgNO_3 (0.34 g, 2 mmol) at -30 °C in the absence of light. A white precipitate of AgCl was formed slowly, and it was filtered via frit filtration after 6 h. The colorless toluene solution was concentrated (5 mL) and was kept for crystallization at 4 °C, which afforded colorless crystals of **6** after 2 days. Yield = 0.37 g (62%).

^1H NMR (400 MHz, 298 K, CDCl_3): δ = 1.12 (d, J = 6.75 Hz, 12 H, $\text{CH}(\text{CH}_3)_2$), 1.20 (d, J = 6.75 Hz, 12 H, $\text{CH}(\text{CH}_3)_2$), 3.13 (sept, J = 6.75 Hz, 4 H, $\text{CH}(\text{CH}_3)_2$), 4.15 (s, 4 H, $\text{NCH}_2\text{CH}_2\text{N}$), 6.50 (d, J = 6.88 Hz, 2 H, *ortho*-H of B-Ph), 6.89 (t, J = 7.38 Hz, 2 H, *meta*-H of B-Ph), 7.01 (t, J = 7.25 Hz, *para*-H of B-Ph), 7.24 (d, J = 7.88 Hz, 4 H, Ar-H), 7.46 (t, J = 7.75 Hz, 2 H, Ar-H), ppm (Figures S18 and S19).

$^{13}\text{C}\{^1\text{H}\}$ NMR (101 MHz, 298 K, CDCl_3): δ = 22.4, 26.8, 28.8, 53.8, 124.6, 127.1, 131.6, 134.5, 146.2 ppm (Figure S20).

$^{11}\text{B}\{^1\text{H}\}$ NMR (128 MHz, 298 K, CDCl_3): δ = 4.2 (s, 1 B, $\text{BPh}(\text{NO}_3)_2$) ppm (Figure S21).

7: A THF solution (5 mL) of 5-SIDipp (0.382 g, 1 mmol) was added dropwise to a THF solution (20 mL) of previously weighed $\text{B}(\text{C}_6\text{F}_5)_3$ (0.512 g, 1 mmol) at room temperature. The reaction mixture turned to a clear colorless solution immediately and run for 12 h. The solution was dried completely and 3 mL of toluene solution was added to dissolve the white solid product. Colorless crystals of **7** were afforded after keeping the toluene solution for crystallization at 4 °C after 2 days. Yield = 0.45 g (46%). The formation of **7** was accompanied by some other side products, which could not be identified. Hence, we did not have a spectroscopically pure product to record the ^1H and ^{13}C NMR.

$^{11}\text{B}\{^1\text{H}\}$ NMR (128 MHz, 298 K, CDCl_3): δ = -2.8 (s, 1 B, $\text{B}(\text{C}_6\text{F}_5)_3$) ppm (Figure S23).

8: A diethyl ether solution (5 mL) of 5-SIDipp (0.382 g, 1 mmol) was added dropwise to a diethyl ether solution (5 mL) of previously weighed $\text{B}(\text{C}_6\text{F}_5)_3$ (0.512 g, 1 mmol) at room temperature. The reaction mixture turned to a clear colorless solution immediately and run for 12 h. The solution was dried completely and 3 mL of toluene solution was added to dissolve the white solid product. Colorless crystals of **8** were afforded after keeping the toluene solution for crystallization at 4 °C after 1 day. Yield = 0.78 g (85%).

^1H NMR (400 MHz, 298 K, CDCl_3): δ = 1.20 (d, J = 6.88 Hz, 12 H, $\text{CH}(\text{CH}_3)_2$), 1.35 (d, J = 6.88 Hz, 12 H, $\text{CH}(\text{CH}_3)_2$), 2.87 (sept, J = 6.75 Hz, 4 H, $\text{CH}(\text{CH}_3)_2$), 4.39 (s, 4 H, $\text{NCH}_2\text{CH}_2\text{N}$), 7.29 (d, J = 7.75 Hz, 4 H, Ar-H), 7.54 (t, J = 7.88 Hz, 2 H, Ar-H), 8.90 (s, 1 H, N-CH-N) ppm (Figure S24).

$^{13}\text{C}\{^1\text{H}\}$ NMR (101 MHz, 298 K, CDCl_3): δ = 23.9, 24.4, 29.4, 53.6, 60.8, 125.2, 128.6, 131.9, 145.6, 160.3 ppm (Figure S25).

$^{11}\text{B}\{^1\text{H}\}$ NMR (128 MHz, 298 K, CDCl_3): δ = -4.2 (s, 1 B, $\text{HO-B}(\text{C}_6\text{F}_5)_3$) ppm (Figure S26).

$^{19}\text{F}\{^1\text{H}\}$ NMR (377 MHz, 298 K, CDCl_3): δ = -135.6, -162.4, -166.1 (15 F, $\text{B}(\text{C}_6\text{F}_5)_3$) ppm (Figure S27).

Supplementary Materials: The following supporting information can be downloaded at: <https://www.mdpi.com/article/10.3390/inorganics10070097/s1>. The Supplementary Materials contains structural description of **1–8** and representative NMR spectra. The callouts of each Figure given in the Supporting Information are provided in the main text. (accessed on 19 June). References [30–34] are cited in the Supplementary Materials.

Author Contributions: S.S.S. conceptualized the work, G.K. performed the experiments and characterizations. S.T. performed the single crystal X-ray analysis. S.S.S. and G.K. cowrote the paper. All authors have read and agreed to the published version of the manuscript.

Funding: The research was funded by CSIR, Young Scientist Contingency Grant (YSA000726).

Institutional Review Board Statement: Not applicable.

Informed Consent Statement: Not applicable.

Data Availability Statement: All the data reported in the study can be found in the supporting information and from the CCDC repository with accession numbers: 2180189-2180191, 2180197-2180200, 2180457.

Acknowledgments: GK thanks CSIR, India for senior research fellowship (SRF). ST is grateful to AESD&CIF, CSIR-CSMCRI for instrumentation facilities and infrastructure.

Conflicts of Interest: The authors declare no conflict of interests.

References

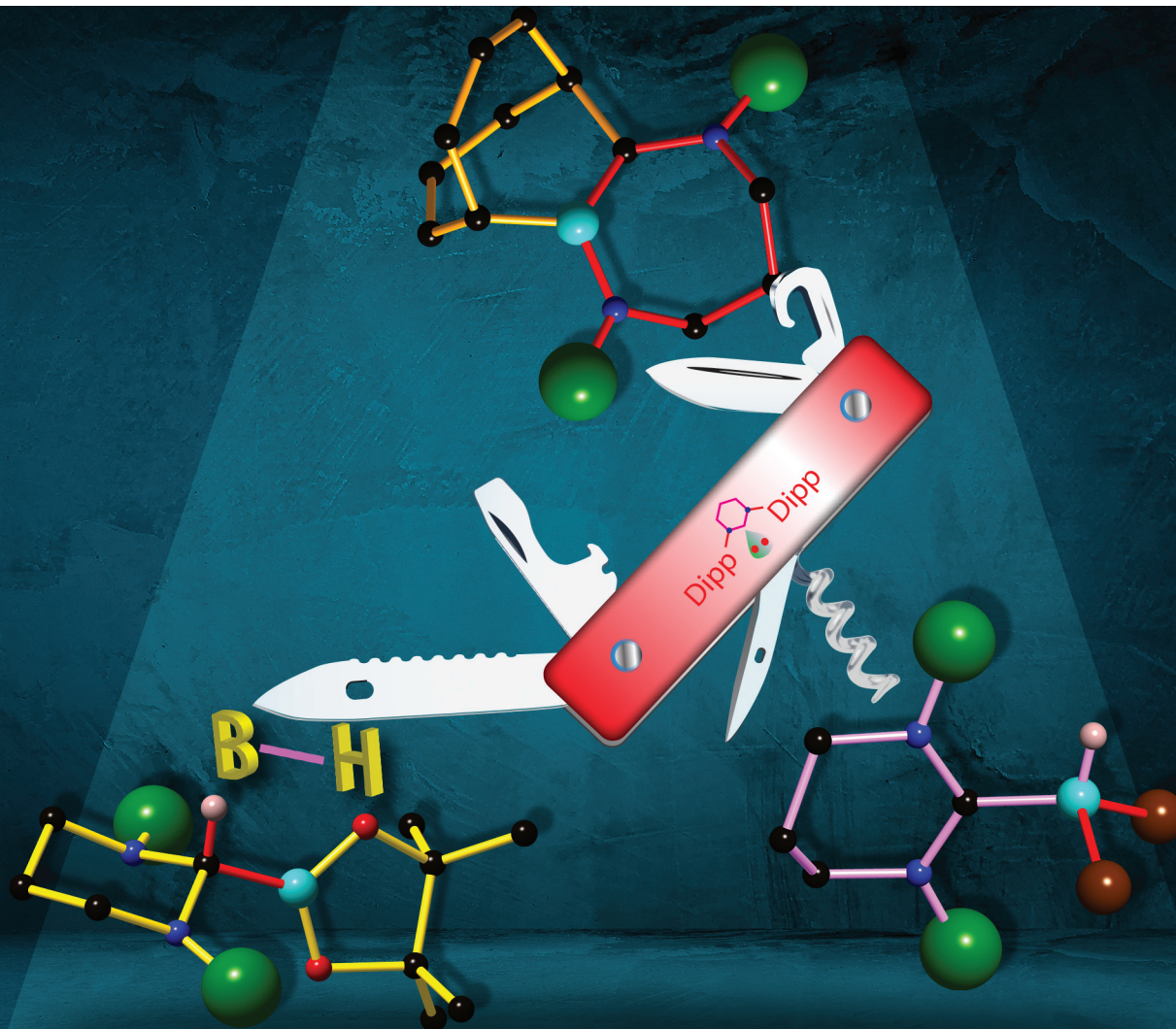
1. Curran, D.P.; Solovyev, A.; MakhlofBrahmi, M.; Fensterbank, L.; Malacria, M.; Lacôte, E. Synthesis and Reactions of N-Heterocyclic Carbene Boranes. *Angew. Chem. Int. Ed.* **2011**, *50*, 10294–10317. [[CrossRef](#)] [[PubMed](#)]
2. Ueng, S.-H.; MakhlofBrahmi, M.; Derat, É.; Fensterbank, L.; Lacôte, E.; Malacria, M.; Curran, D.P. Complexes of Borane and N-Heterocyclic Carbenes: A New Class of Radical Hydrogen Atom Donor. *J. Am. Chem. Soc.* **2008**, *130*, 10082–10083. [[CrossRef](#)] [[PubMed](#)]
3. Ueng, S.-H.; Fensterbank, L.; Lacôte, E.; Malacria, M.; Curran, D.P. Radical Deoxygenation of Xanthates and Related Functional Groups with New Minimalist N-Heterocyclic Carbene Boranes. *Org. Lett.* **2010**, *12*, 3002–3005. [[CrossRef](#)] [[PubMed](#)]
4. MakhlofBrahmi, M.; Monot, J.; Desage-El Murr, M.; Curran, D.P.; Fensterbank, L.; Lacote, E.; Malacria, M. Preparation of NHC Borane Complexes by Lewis Base Exchange with Amine- and Phosphine-Boranes. *J. Org. Chem.* **2010**, *75*, 6983–6985.
5. Solovyev, A.; Chu, Q.; Geib, S.J.; Fensterbank, L.; Malacria, M.; Lacôte, E.; Curran, D.P. Substitution Reactions at Tetracoordinate Boron: Synthesis of N-Heterocyclic Carbene Boranes with Boron-Heteroatom Bonds. *J. Am. Chem. Soc.* **2010**, *132*, 15072–15080. [[CrossRef](#)]
6. Dai, W.; Geib, S.J.; Curran, D.P. Reactions of N-Heterocyclic Carbene Boranes with 5-Diazo-2,2-dimethyl-1,3-dioxane-4,6-dione: Synthesis of Mono- and Bis-hydrazonyl NHC-Boranes. *J. Org. Chem.* **2018**, *83*, 8775–8779. [[CrossRef](#)]
7. Auerhammer, D.; Arrowsmith, M.; Braunschweig, H.; Dewhurst, R.D.; Jiménez-Halla, J.O.C.; Kupfer, T. Nucleophilic Addition and Substitution at Coordinatively Saturated Boron by Facile 1,2-Hydrogen Shuttling onto a Carbene Donor. *Chem. Sci.* **2017**, *8*, 7066–7071. [[CrossRef](#)]
8. Kundu, G.; Pahar, S.; Tothadi, S.; Sen, S.S. Stepwise Nucleophilic Substitution to Access Saturated N-heterocyclic Carbene Halo-boranes with Boron–Methyl Bonds. *Organometallics* **2020**, *39*, 4696–4703. [[CrossRef](#)]
9. Kundu, G.; Ajithkumar, V.S.; Raj, K.V.; Vanka, K.; Tothadi, S.; Sen, S.S. Substitution at sp^3 Boron of a Six-Membered NHC·BH₃: Convenient Access to a Dihydroxyborenum Cation. *Chem. Commun.* **2022**, *58*, 3783–3786. [[CrossRef](#)]
10. Bissinger, P.; Braunschweig, H.; Kraft, K.; Kupfer, T. Trapping the Elusive Parent Borylene. *Angew. Chem. Int. Ed.* **2011**, *50*, 4704–4707. [[CrossRef](#)]
11. Bissinger, P.; Braunschweig, H.; Damme, A.; Dewhurst, R.D.; Kraft, K.; Kramer, T.; Radacki, K. Base-stabilized boryl and cationic haloborylene complexes of iron. *Chem.-Eur. J.* **2013**, *19*, 13402–13407. [[CrossRef](#)] [[PubMed](#)]
12. Wang, Y.; Quillian, B.; Wei, P.; Wannere, C.S.; Xie, Y.; King, R.B.; Schaefer, H.F., III; Schleyer, P.V.R.; Robinson, G.H. A Stable Neutral Diborene Containing a B=B Double Bond. *J. Am. Chem. Soc.* **2007**, *129*, 12412–12413. [[CrossRef](#)] [[PubMed](#)]
13. Wang, Y.; Quillian, B.; Wei, P.; Xie, Y.; Wannere, C.S.; King, R.B.; Schaefer, H.F.; Schleyer, P.V.R.; Robinson, G.H. Planar, Twisted, and Trans-Bent: Conformational Flexibility of Neutral Diborenes. *J. Am. Chem. Soc.* **2008**, *130*, 3298–3299. [[CrossRef](#)] [[PubMed](#)]
14. Tamm, M.; Lügger, T.; Hahn, E.F. Isocyanide and Ylidene Complexes of Boron: Synthesis and Crystal Structures of (2-(Trimethylsiloxy)phenylisocyanide)–Triphenylborane and (1,2-Dihydrobenzoxazol-2-ylidene)–Triphenylborane. *Organometallics* **1996**, *15*, 1251–1256. [[CrossRef](#)]
15. Chase, P.A.; Stephan, D.W. Hydrogen and Amine Activation by a Frustrated Lewis Pair of a Bulky N-Heterocyclic Carbene and B(C₆F₅)₃. *Angew. Chem. Int. Ed.* **2008**, *47*, 7433–7437. [[CrossRef](#)]
16. Doddi, A.; Peters, M.; Tamm, M. N-Heterocyclic Carbene Adducts of Main Group Elements and Their Use as Ligands in Transition Metal Chemistry. *Chem. Rev.* **2019**, *119*, 6994–7112. [[CrossRef](#)] [[PubMed](#)]
17. Pait, M.; Kundu, G.; Tothadi, S.; Karak, S.; Jain, S.; Vanka, K.; Sen, S.S. C–F Bond Activation by a Saturated N-Heterocyclic Carbene: Mesoionic Compound Formation and Adduct Formation with B(C₆F₅)₃. *Angew. Chem. Int. Ed.* **2019**, *58*, 2804–2808. [[CrossRef](#)]
18. Kundu, G.; De, S.; Tothadi, S.; Das, A.; Koley, D.; Sen, S.S. Saturated N-Heterocyclic Carbene Based Thiele’s Hydrocarbon with a Tetrafluorophenylene Linker. *Chem. Eur. J.* **2019**, *25*, 16533–16537. [[CrossRef](#)]

19. Kundu, G.; Ajithkumar, V.S.; Bisai, M.K.; Tothadi, S.; Das, T.; Vanka, K.; Sen, S.S. Diverse reactivity of carbenes and silylenes towards fluoropyridines. *Chem. Commun.* **2021**, *57*, 4428–4431. [[CrossRef](#)]
20. Guibert, C.R.; Marshall, M.D. Synthesis of the Tetranitratoborate Anion. *J. Am. Chem. Soc.* **1966**, *88*, 189–190. [[CrossRef](#)]
21. Titova, K.V.; Rosolovskii, V.Y. Tetraalkylammonium Nitratoborates. *Bull. Acad. Sci. USSR Div. Chem. Sci.* **1970**, *19*, 2515–2519. [[CrossRef](#)]
22. Titova, K.V.; Rosolovskii, V.Y. Reaction of Nitrates of Monovalent Cations with BCl_3 . *Bull. Acad. Sci. USSR Div. Chem. Sci.* **1975**, *24*, 2246–2248. [[CrossRef](#)]
23. Becker, M.; Schulz, A.; Villinger, A.; Voss, K. Stable Sulfate and Nitrate Borane-Adduct Anions. *RSC Adv.* **2011**, *1*, 128–134. [[CrossRef](#)]
24. Zelenov, V.P.; Gorshkov, E.Y.; Zavaruev, M.V.; Dmitrienko, A.O.; Troyan, I.A.; Pivkina, A.N.; Khakimov, D.V.; Pavlikov, A.V. Synthesis and Mutual Transformations of Nitronium tetrakis(nitrooxy)- and tetrakis(2,2,2-trifluoroacetoxy)borates. *N. J. Chem.* **2020**, *44*, 13944–13951. [[CrossRef](#)]
25. Hawthorne, M.F.; Mavunkal, I.J.; Knobler, C.B. Electrophilic Reactions of Protonated Closo-B₁₀H₁₀I₂- with Arenes, Alkane Carbon-Hydrogen Bonds, and Triflate Ion Forming Aryl, Alkyl, and Triflate Nido-6-X-B₁₀H₁₃ Derivatives. *J. Am. Chem. Soc.* **1992**, *114*, 4427–4429. [[CrossRef](#)]
26. Berkeley, E.R.; Ewing, W.C.; Carroll, P.J.; Sneddon, L.G. Synthesis, Structural Characterization, and Reactivity Studies of 5-CF₃SO₃-B₁₀H₁₃. *Inorg. Chem.* **2014**, *53*, 5348–5358. [[CrossRef](#)]
27. Erker, G. Frustrated Lewis Pairs: Metal-free Hydrogen Activation and More. *Angew. Chem. Int. Ed.* **2010**, *49*, 46–76.
28. Kronig, S.; Theuergarten, E.; Holschumacher, D.; Bannenberg, T.; Daniliuc, C.G.; Jones, P.G.; Tamm, M. Dihydrogen Activation by Frustrated Carbene-Borane Lewis Pairs: An Experimental and Theoretical Study of Carbene Variation. *Inorg. Chem.* **2011**, *50*, 7344–7359. [[CrossRef](#)]
29. Filippou, A.C.; Chernov, O.; Schakenburg, G. Chromium Silicon Multiple Bonds: The Chemistry of Terminal N-Heterocyclic Carbene-Stabilized Halosilylidyne Ligands. *Chem.-Eur. J.* **2011**, *17*, 13574–13583. [[CrossRef](#)]
30. APEX3, SAINT-Plus and SADABS; Bruker AXS Inc.: Madison, WI, USA, 2006.
31. Apex CCD and SAINT v8.30C; Bruker AXS Inc.: Madison, WI, USA, 2013.
32. Sheldrick, G.M. A short history of SHELX. *Acta Crystallogr.* **2008**, *A64*, 112–122. [[CrossRef](#)]
33. Krause, L.; Herbst-Irmer, R.; Sheldrick, G.M.; Stalke, D. Comparison of silver and molybdenum microfocus X-ray sources for single-crystal structure determination. *J. Appl. Crystallogr.* **2015**, *48*, 3–10. [[CrossRef](#)] [[PubMed](#)]
34. Krause, L.; Herbst-Irmer, R.; Stalke, D. An empirical correction for the influence of low-energy contamination. *J. Appl. Crystallogr.* **2015**, *48*, 1907–1913. [[CrossRef](#)]

Dalton Transactions

An international journal of inorganic chemistry

rsc.li/dalton



ISSN 1477-9226

PAPER

Sakya S. Sen *et al.*

Versatile chemistry of six-membered NHC with boranes: bromination at sp^3 borane, activation of the B-H bond of HBpin, and ring expansion of NHC

Cite this: *Dalton Trans.*, 2022, **51**, 14452

Versatile chemistry of six-membered NHC with boranes: bromination at sp^3 borane, activation of the B–H bond of HBpin, and ring expansion of NHC \ddagger

Gargi Kundu,^{a,b} Ruchi Dixit,^{b,c} Srinu Tothadi,^d Kumar Vanka^{b,c} and Sanya S. Sen^{a,b}

The NHC-borane chemistry has been majorly restricted to imidazol-2-ylidene classes of carbenes. In our previous communication, we reported the synthesis of 6-SIDipp-BH₃ [6-SIDipp = 1,3-di(2,6-diisopropylphenyl) tetrahydropyrimidine-2-ylidene] and its electrophilic substitution reaction with iodine. Here, we have shown selective bromination of a 6-SIDipp stabilized sp^3 B–H bond. Treatment of 1.2 equivalents of *N*-bromosuccinamide with 6-SIDipp-BH₃ gives a mixture of mono- and disubstituted products 6-SIDipp-BH₂Br (**1**) and 6-SIDipp-BHBr₂ (**2**). However, the reactions with alkyl bromides or carbon tetrabromide resulted in 6-SIDipp-BH₂Br (**1**) selectively. Exploration of the chemistry of 6-SIDipp with BHCl₂ and 9-BBN (9-borabicyclo[3.3.1]nonane) led to mono-6-SIDipp adducts **3** and **6a**. Furthermore, **6a** undergoes ring expansion to afford a seven-membered product, **6b**, under mild conditions. Unlike BHCl₂ or 9-BBN, the B–H bond of HBpin undergoes oxidative addition upon reaction with 6-SIDipp, epitomizing the first example (**7**) of a B–H bond insertion at NHCs. The analogous reactivity with HBcat led to a tetrahydropyrimidinium salt with B(cat)₂ as a counteranion (**8**).

Received 1st June 2022,
Accepted 15th August 2022

DOI: 10.1039/d2dt01707e

rsc.li/dalton

Introduction

In contrast to five-membered Arduengo type *N*-heterocyclic carbenes (NHCs), the chemistry of six-membered NHCs has limited precedence in the literature, partly due to their less thermal stability and structural rigidity. Nonetheless, Aldridge and coworkers reported stable adduct formation of a saturated six-membered *N*-heterocyclic carbene (6-SIDipp) with AlH₃.¹ The same group also reported the synthesis of a 6-SIMES ligated dibromoborene cation (Br₂B⁺).² The groups of Jones and Stasch isolated monomeric complexes of 6-SIDipp and

group 15 element trichlorides.³ Besides, Tamm and coworkers used 6-SIDipp as a Lewis base component in an FLP for the activation of dihydrogen.⁴ Seminal work by both Curran and coworkers and Braunschweig and coworkers in carbene-borane chemistry involves either imidazole-2-ylidene or a cyclic alkyl amino carbene (CAAC).^{5–11} In the same line, Radius and coworkers established carbene-alane/gallane chemistry and its facile halogenation.^{12–14} Due to our current interest in boron chemistry,^{15–19} we proceeded to study the chemistry of 6-SIDipp with boranes. In our previous communication, we have shown that the reaction of a saturated six-membered *N*-heterocyclic carbene (6-SIDipp) with BH₃ led to the formation of an adduct, 6-SIDipp-BH₃.²⁰ The latter undergoes a facile electrophilic substitution reaction with I₂, leading to 6-SIDipp mono- and diboryl iodides, selectively.²⁰ However, the corresponding reaction with Br₂ was not selective, and resulted in a mixture of mono-, di-, and tribromide adducts, akin to what was noted by Curran and coworkers with 1,3-bis-(2,6-diisopropylphenyl)imidazole-2-ylidene (5-IDipp).⁷ In this paper, we have shown selective bromination at the sp^3 B–H bond. In addition, we have also performed the reaction of 6-SIDipp with other boranes such as BHCl₂, 9-BBN, and HBpin. While 6-SIDipp forms an adduct with BHCl₂, the carbene undergoes ring expansion with 9-BBN under mild conditions. The activation of the B–H bond of HBpin takes place

^aInorganic Chemistry and Catalysis Division, CSIR-National Chemical Laboratory, Dr. Homi Bhabha Road, Pashan, Pune 411008, India. E-mail: ss.sen@ncl.res.in

^bAcademy of Scientific and Innovative Research (AcSIR), Ghaziabad 201002, India

^cPhysical and Material Chemistry Division, CSIR-National Chemical Laboratory, Dr. Homi Bhabha Road, Pashan, Pune 411008, India

^dAnalytical and Environmental Sciences Division and Centralized Instrumentation Facility, CSIR-Central Salt and Marine Chemicals Research Institute, Gijubhai Badheka Marg, Bhavnagar 364002, India

†Dedicated to Professor Cameron Jones on the occasion of his 60th birthday.

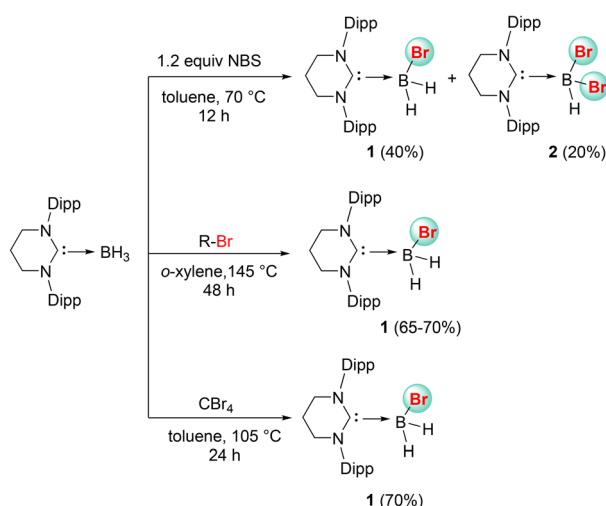
‡Electronic supplementary information (ESI) available: Synthesis and spectroscopic and structural data of **1**, **2**, **3**, **6a**, **6b**, **7** and **8**. CCDC 2123564 (**1**), 2176142 (**2**), 2102133 (**3**), 2102135 (**6a**), 2191019 (**6b**), 2102136 (**7**) and 2102137 (**8**). For ESI and crystallographic data in CIF or other electronic format see DOI: <https://doi.org/10.1039/d2dt01707e>

with the carbene, which is reminiscent of the oxidative addition of R_2BH on a transition metal fragment. It must be noted here that the analogous reaction with a five-membered saturated NHC (5-SIDipp) did not lead to 1,1-oxidative addition; instead, the rupture of the C–N bond took place leading to dimer formation.²¹

Results and discussion

In order to achieve selective bromination, we added 1.2 equivalents of NBS to the toluene solution of 6-SIDipp-BH₃ at a temperature of 70 °C, but a dibromo product **2** was obtained in 20% yield along with a monobromo product (**1**) in 40% yield (Scheme 1). The formation of both **1** and **2** was indicated by ¹¹B NMR spectroscopy, which shows the appearance of two new peaks at –20.1 ppm and –14.3 ppm, which are shifted downfield with respect to that in 6-SIDipp-BH₃ (–31.3 ppm).²⁰ We were unable to obtain the pure ¹H NMR spectrum of **2** due to the formation of a mixture of products. However, we were able to obtain the single crystals of **2** suitable for X-ray studies, which confirms its constitution (Fig. 1). Compound **2** was crystallized in the monoclinic $P2_1/n$ space group. The C5–B1 bond length in **2** is 1.639(4) Å, which is slightly longer than that in 6-SIDipp-BH₃ [1.602(3) Å].

To selectively prepare **1**, we reacted 6-SIDipp-BH₃ with *n*-octyl, *n*-decyl, and *n*-dodecyl bromides in *o*-xylene at 145 °C for a fixed time period of 48 h, which led to 65–70% conversion of borane to bromoborane **1**. Table S1† summarizes the results from this series of experiments (see the ESI†). A more facile route to obtain **1** involved heating of 6-SIDipp-BH₃ in CBr₄ in toluene at 105 °C for 24 h (entry 5, Table S1†). We obtained the single crystals of **1** from the latter methodology (Fig. 1). **1** crystallizes in monoclinic $P2_1/n$. The C5–B1 bond length in **1** [1.610(3) Å] is shorter compared to that in **2** [1.639(4) Å]. The molecular ion peaks for **1** and **2** were detected at *m/z* 497.2541 and 575.1605 in the HRMS spectrum.



Scheme 1 Synthesis of 6-SIDipp-BH₂Br (**1**) and 6-SIDipp-BHBr₂ (**2**).

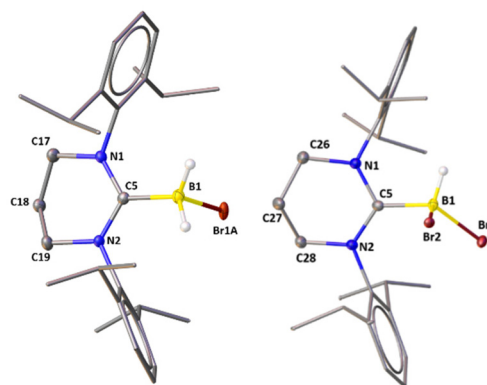
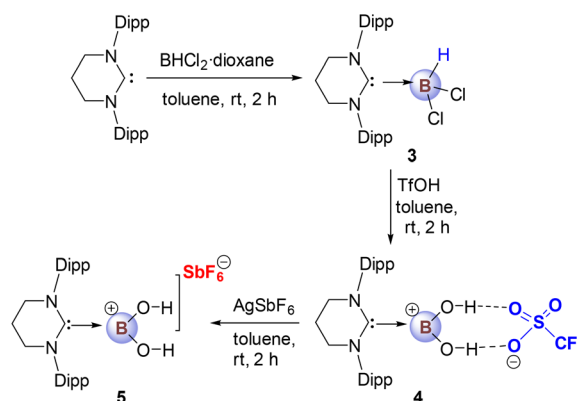


Fig. 1 The molecular structures of **1** and **2** (hydrogen atoms except on the boron atoms are omitted for the clarity of the picture). Selected bond lengths [Å], angles [deg] and torsion angles [deg]: **1**: C5–N1 1.344(2), N2–C5 1.341(2), B1–C5 1.610(3), B1–Br1A 2.0878(19); N1–C5–B1 120.92(15); N2–C5–B1 120.66(14), C5–B1–Br1A 103.85(11); C17–N1–C5–B1 174.61(14), C19–N2–C5–B1 173.25(15), N1–C5–B1–Br1A 85.44(15), N2–C5–B1–Br1A 85.44(15); **2**: C5–N1 1.356(3), N2–C5 1.348(3), B1–C5 1.639(4), B1–Br1 2.048(3), B1–Br2 2.018(3), B1–H1 1.000; N2–C5–N1 117.9(2), N1–C5–B1 116.1(2), N2–C5–B1 117.9(2), C5–B1–Br1 117.86(19), C5–B1–Br2 104.09(19), Br1–B1–Br2 115.36(16); N2–C5–B1–Br1 56.0(3), N1–C5–B1–Br1 133.9(2), N1–C5–B1–Br2 96.9(2), N2–C5–B1–Br2 73.2(3), C26–N1–C5–B1 158.8(3), C28–N2–C5–B1 172.7(2).

Following the isolation of 6-SIDipp-BH₃,²⁰ we were curious to study the reactions of 6-SIDipp with other boranes. The reaction of 6-SIDipp with one equivalent of BHCl₂ forms Lewis acid–base adducts (**3**) (Scheme 2), which show resonances at –7.4 ppm in the ¹¹B NMR spectrum. Inspection of the molecular structure of **3** reveals that the B–C bond length is 1.6414(8) Å, which is longer than that of 6-SIDipp-BH₃ [1.602(3) Å]. The lengthening is thought to be due to increased steric congestion at the boron center (Fig. 2). The other important bond lengths and angles are given in the legends of Fig. 2. In the HRMS spectrum, the molecular ion peaks were found at *m/z* 509.2636.

The facile synthesis of **3** prompted us to check whether it can be a suitable precursor for borenium cations.^{20,22–27}



Scheme 2 Preparation of **3–5**.

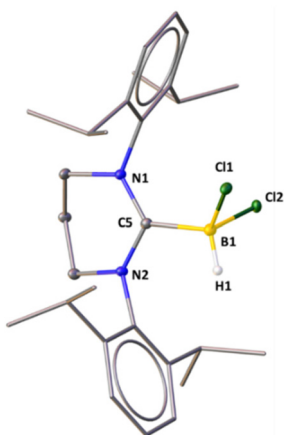
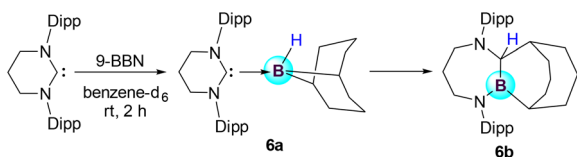


Fig. 2 The molecular structure of **3** (hydrogen atoms except the proton on the central boron atom for **3** are omitted for the clarity of the picture). Selected bond lengths [Å] and angles [deg]: C5–N1 1.3414(7), C5–N2 1.3468(7), C5–B1 1.6414(8), B1–Cl1 1.8814(7), B1–Cl2 1.8719(7), B1–H1 1.084(12); N1–C5–N2 118.34(5), N1–C5–B1 125.00(5), N2–C5–B1 116.09(5), Cl2–B1–Cl1 110.72(4).

Curran and coworkers recently showed the formation of a dihydroxyboreonium cation with the composition [5-IDippB(OH)₂]⁺OTf[−] from the reaction of 5-IDipp-BH₃ with TfOH; however, the reaction took 5 days to complete.²⁷ With **3** in hand, we attempted its reaction with two equivalents of TfOH, which smoothly afforded a stable dihydroxyboreonium cation with a triflate anion [6-SIDipp-B(OH)₂]⁺OTf[−], **4** (Scheme 2), within only 2 h. Compound **4** is air-stable but gradually decomposes in the presence of THF and Et₂O to [6-SIDipp-H]⁺OTf[−]. The ¹¹B NMR chemical shift for **4** was detected at 24.6 ppm, reflecting a tri-coordinate boron environment. The molecular ion peak for **4** was identified at *m/z* 599.3036 in the HRMS spectrum. An anion exchange reaction of **4** with AgSbF₆ in toluene at a low temperature led to the replacement of the OTf[−] anion with the SbF₆[−] moiety (**5**) (Scheme 2). As the molecular structures of **4**⁺ and **5**⁺ are identical to our previously reported dihydroxyboreonium cation generated from the reaction of 6-SIDipp-BH₃ with Br₂/H₂O,²⁰ we are not discussing their structural parameters here.

The reaction of 6-SIDipp with 9-BBN led to the formation of an adduct (**6a**), which is not very stable and undergoes ring expansion at room temperature to afford an unusual seven-membered BCNC₃N ring (**6b**) (Scheme 3). The conversion of **6a** to **6b** was monitored by ¹¹B NMR (see Fig. S23–S26[†]). After 30 minutes of the reaction, a doublet appears at −13.4 ppm



Scheme 3 Lewis acid–base adduct with 9-BBN and subsequent ring expansion.

($J_{B-H} = 63.81$ Hz) in the ¹¹B NMR spectrum, which is a characteristic of the tetra-coordinated boron center in **6a**. After 6 h of reaction, the latter resonance disappeared, and a new resonance was detected at 49.1 ppm, which is for the tri-coordinated boron atom of the ring expansion product, **6b**. It should be noted here that the group of Stephan demonstrated that a five-membered N-heterocyclic carbene with PR₂ (R = *t*Bu, *Ni*Pr₂) at the wingtip positions underwent ring expansion with 9-BBN,²⁸ while the typical 5-IDipp was shown to form a stable adduct with 9-BBN.²³ While the ring expansion of 5-NHCs in the presence of *s/p*-block hydrides is well established,^{29–33} there is only one literature precedence of the ring expansion of 6-SIMes to a seven-membered ring in the presence of PhSiH₃, which required 3 days and 110 °C.³⁴ Though we did not perform any theoretical studies, we can speculate from the literature that the mechanism proceeds *via* the initial coordination of the NHC to the boron center of 9-BBN (**6a**).²⁸ Afterwards, the hydrogen atom attached to the boron atom migrates to the electron-deficient carbene carbon atom. This hydride migration prompted the attack of one of the adjacent nitrogen atoms on the boron atom, thereby resulting in C–N bond cleavage and C–C bond formation.

Despite varying the reaction parameters, we were unsuccessful in obtaining **6a** and **6b** separately in preparative reasonable amounts that can permit their full characterization. However, we were able to grow the single crystals of **6a** and **6b** (Fig. 3). The B–C bond length in **6a** is 1.644(4) Å. After ring expansion, the same B–C bond length is slightly shortened to 1.612(3) Å.

The 1,1-addition of a B–H bond of HBpin to any NHC is not known. In 2010, Bertrand and coworkers studied the reaction of HBpin and 5-SIDipp and isolated an unexpected dimer *via* the ring cleavage of NHCs.²¹ On the other hand, a similar reaction with CAAC^{Me} or bicyclic (alkyl)(amino)carbene (BICAAC)

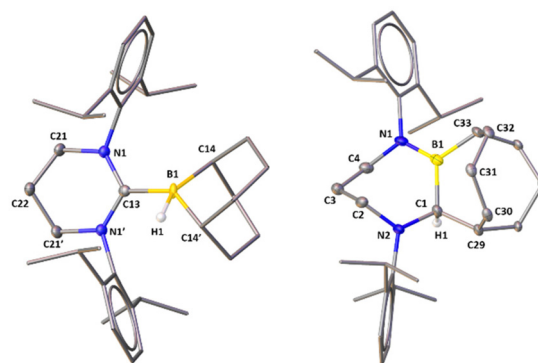
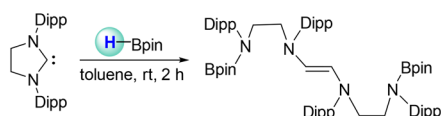


Fig. 3 The molecular structures of **6a** and **6b** (hydrogen atoms except on B1 in **6a** and C1 in **6b** are omitted for the clarity of the picture). Selected bond lengths [Å] and angles [deg]: **6a**: C13–N1 1.3530(19), B1–C13 1.644(4), B1–C14 1.529(4), N1–C21 1.477(2); N1–C13–N2 116.0(2), N1–C13–B1 122.00(10); **6b**: N1–B1 1.410(3), N1–C4 1.485(2), N2–C2 1.447(2), C2–C3 1.524(3), C3–C4 1.530(3), N2–C1 1.476(2), B1–C1 1.612(3), B1–C33 1.588(3), C1–C29 1.546(3); N1–B1–C1 118.91(16), N2–C1–B1 115.40(15), N2–C1–C29 110.40(15), N1–B1–C33 120.54(17), C2–C3–C4 113.19(15).

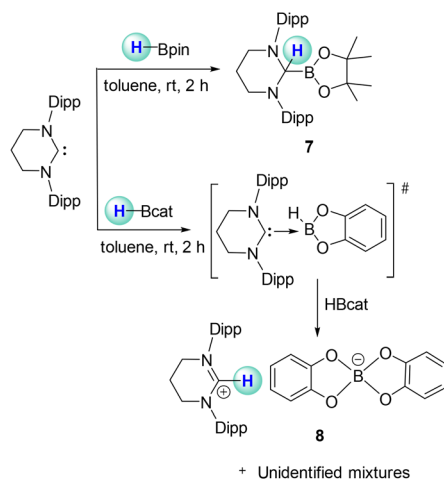
afforded a 1,1-activation product,^{21,35} which was rationalized by its increased nucleophilic characters over 5-SIDipp. As 6-SIDipp is more nucleophilic than 5-SIDipp,^{36,37} we studied its reaction with HBpin. Delightfully, the reaction led to the 1,1-addition of the B–H bond of HBpin at the carbene carbon (Scheme 4).

Storing the reaction mixture for 1 day at room temperature led to the formation of colorless crystals of **7**, which was analyzed by single crystal X-ray diffraction (Fig. 4, left). **7** crystallizes in the monoclinic space group, $P2_1/n$. The solid-state

C–N bond cleavage with 5-SIDipp (Bertrand and coworkers, 2010):



B–H bond activation with 6-SIDipp (This work):



Scheme 4 B–H activation of HBpin and HBcat with 6-SIDipp.

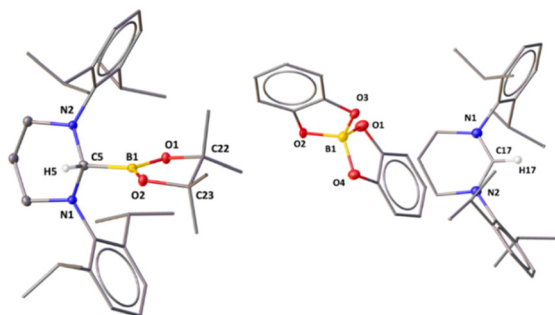


Fig. 4 The molecular structures of **7** and **8** (except hydrogen atoms attached to the C5 atom in **7** and the C17 atom in **8**, other hydrogen atoms are omitted for the clarity of the picture). Selected bond lengths [Å] and angles [deg]: **7**: B1–C5 1.590(2), B1–O1 1.3639(18), B1–O2 1.3693(18), C5–H5 0.980, C5–N1 1.4692(16), C5–N2 1.4704(16); N1–C5–N2 106.94(10), N2–C5–B1 112.81(11), N1–C5–B1 112.07(10), O1–B1–O2 114.06(12); **8**: N1–C17 1.308(2), C17–N2 1.3050(19), C17–H17 0.9500, B1–O1 1.474(2), B1–O2 1.472(2); N1–C17–N2 123.19(14), O1–B1–O2 111.47(15).

structure of **7** shows that the six-membered NHC ring adopts a perfect chair conformation. The distance between the B1 and C5 atoms is 1.590(2) Å, which is significantly longer than CAAC^{Me}-mediated B–H activated products (1.55 Å).²¹

The constitution of **7** was further confirmed by ¹¹B, ¹³C, and ¹H NMR spectroscopy, and mass spectrometry. The broad signal at 31.0 ppm in ¹¹B NMR spectra indicates the insertion of the carbene carbon atom into the B–H bond. The same carbon atom shows a broad resonance at 82.7 ppm in the ¹³C {¹H} NMR spectrum, which usually indicates sp³-hybridized carbon atoms. The hydrogen atom attached to the carbene carbon atom gives a peak at 4.88 ppm in the ¹H NMR spectra. The molecular ion peak was detected at m/z 533.4267 in the HRMS spectrum.

In order to understand the mechanism of oxidative addition of HBpin with the six-membered NHC (Fig. 5), we performed full quantum chemical calculations using the density functional theory (DFT). 6-SIDipp reacts with HBpin to give adduct **Int_1**, which is thermodynamically unstable by 0.2 kcal mol^{−1}, with a bond distance of 1.66 Å between NHC carbon and boron of HBpin. In the next step, **Int_1** was transformed into **7** via a three-membered transition state **TS_1** with an activation free energy barrier (ΔG^\ddagger) of 7.6 kcal mol^{−1} and a reaction free energy (ΔG) of −15.1 kcal mol^{−1}. The bond distance of 1.59 Å was found between NHC carbon and boron of HBpin in **7**. We have also studied why 5-SIDipp does not undergo 1,1-oxidative addition with HBpin. It was found that the oxidative addition with 6-SIDipp was favourable by ~15 kcal mol^{−1} than that with 5-SIDipp (see Fig. S37[†]).

The reaction of 6-SIDipp with HBcat yielded a tetrahydropyrimidinium salt with a [Bcat₂][−] counteranion (Scheme 4). From the appearance of a peak at 6.5 ppm in the ¹¹B NMR spectrum, it can be assumed that 6-SIDipp undergoes adduct formation immediately. The formation of such a [Bcat₂][−]

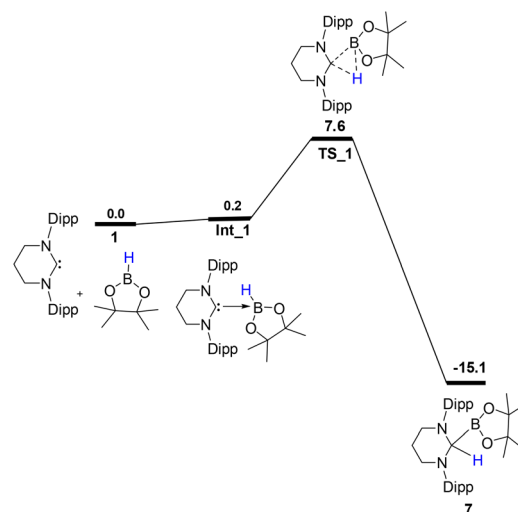


Fig. 5 The reaction energy profile diagram for the oxidative addition of HBpin with 6-SIDipp. The values (in kcal mol^{−1}) were calculated at the PBE/TZVP level of theory with DFT.

anion arises from the nucleophile-promoted degradation of HBcat, and subsequent substituent redistribution, which are documented in the literature.^{38–40} Colorless crystals of **8** were isolated after storing the solution for a day at room temperature. **8** crystallizes in the monoclinic $P2_1/c$ space group (Fig. 4, right). The ¹¹B NMR spectrum of **8** shows one signal at 14.3 ppm for the tetra-coordinated boron center. The proton attached to the tetrahydropyrimidinium salt gives a signal at 7.48 ppm in the ¹H NMR spectrum. The molecular ion peaks were detected at m/z 405.3260 and 226.9510 in the HRMS spectrum for the cation and anion, respectively.

Conclusions

We have demonstrated selective bromination at a sp^3 B–H bond supported by 6-SIDipp using alkyl halides or CBr₄. Subsequently, we have realized the stronger nucleophilic properties of a six-membered NHC (6-SIDipp) toward the 1,1-activation of the B–H bond of HBpin (**7**) at the carbene carbon. Although CAAC was shown to exhibit such reactivity, no NHC has been known to add the B–H bond of HBpin in this fashion. The same was observed with HBcat, but we speculated that a subsequent nucleophilic attack of another molecule of HBcat led to the tetrahydropyrimidinium salt with [Bcat₂][–] as the counteranion (**8**). Besides, we have also investigated the reactions of 6-SIDipp with BHCl₂ and 9-BBN, which resulted in monomeric adducts (**3** and **6a**). We have also shown the conversion of **6a** to a seven-membered ring expansion product, **6b**.

Author contributions

S.S.S. conceptualized the work. G.K. performed the experiments and characterization. S.T. performed the single crystal X-ray analysis. K.V. and R.D. performed the theoretical calculations. S.S.S. and G.K. co-wrote the paper. All authors have read and agreed to the published version of the manuscript.

Conflicts of interest

There are no conflicts to declare.

Acknowledgements

S. S. S. is thankful for SJF Grant SB/SJF/2021-22/06, GOI for financial assistance. G. K. and R. D. thank CSIR, India for their research fellowships. S. T. is grateful to AESD&CIF, CSIR-CSMCRI for instrumentation facilities and the infrastructure. The support and the resources provided by 'PARAM Brahma Facility' under the National Supercomputing Mission, Government of India at the IISER Pune are gratefully acknowledged. We are thankful to the reviewers for their critical comments to improve the manuscript.

References

- 1 J. A. B. Abdalla, I. M. Riddlestone, R. Tirfoin, N. Phillips, J. I. Bates and S. Aldridge, *Chem. Commun.*, 2013, **49**, 5547–5549.
- 2 H. B. Mansaray, A. D. L. Rowe, N. Phillips, J. Niemeyer, M. Kelly, D. A. Addy, J. I. Bates and S. Aldridge, *Chem. Commun.*, 2011, **47**, 12295–12297.
- 3 A. Sidiropoulos, B. Osborne, A. N. Simonov, D. Dange, A. M. Bond, A. Stasch and C. Jones, *Dalton Trans.*, 2014, **43**, 14858–14864.
- 4 S. Kronig, E. Theuergarten, D. Holschumacher, T. Bannenberg, C. G. Daniliuc, P. G. Jones and M. Tamm, *Inorg. Chem.*, 2011, **50**, 7344–7359.
- 5 D. P. Curran, A. Solovyev, M. M. Brahmi, L. Fensterbank, M. Malacria and E. Lacôte, *Angew. Chem., Int. Ed.*, 2011, **50**, 10294–10317.
- 6 S.-H. Ueng, M. M. Brahmi, É. Derat, L. Fensterbank, E. Lacôte, M. Malacria and D. P. Curran, *J. Am. Chem. Soc.*, 2008, **130**, 10082–10083.
- 7 A. Solovyev, Q. Chu, S. J. Geib, L. Fensterbank, M. Malacria, E. Lacôte and D. P. Curran, *J. Am. Chem. Soc.*, 2010, **132**, 15072–15080.
- 8 K. Nozaki, Y. Aramaki, M. Yamashita, S.-H. Ueng, M. Malacria, E. Lacôte and D. P. Curran, *J. Am. Chem. Soc.*, 2010, **132**, 11449–11451.
- 9 A. Solovyev, S.-H. Ueng, J. Monot, L. Fensterbank, M. Malacria, E. Lacôte and D. P. Curran, *Org. Lett.*, 2010, **12**, 2998–3001.
- 10 D. Auerhammer, M. Arrowsmith, H. Braunschweig, R. D. Dewhurst, J. O. C. Jiménez-Halla and T. Kupfer, *Chem. Sci.*, 2017, **8**, 7066–7071.
- 11 R. Bertermann, H. Braunschweig, C. K. L. Brown, A. Damme, R. D. Dewhurst, C. Hörl, T. Kramer, I. Krummenacher, B. Pfaffinger and K. Radacki, *Chem. Commun.*, 2014, **50**, 97–99.
- 12 H. Schneider, A. Hock, A. D. Jaeger, D. Lentz and U. Radius, *Eur. J. Inorg. Chem.*, 2018, 4031–4043.
- 13 A. Hock, L. Werner, C. Luz and U. Radius, *Dalton Trans.*, 2020, **49**, 11108–11119.
- 14 A. Hock, L. Werner, M. Riethmann and U. Radius, *Eur. J. Inorg. Chem.*, 2020, 4015–4023.
- 15 G. Kundu, S. Pahar, S. Tothadi and S. S. Sen, *Organometallics*, 2020, **39**, 4696–4703.
- 16 V. S. V. S. N. Swamy, K. V. Raj, K. Vanka, S. S. Sen and H. W. Roesky, *Chem. Commun.*, 2019, **55**, 3536–3539.
- 17 M. K. Bisai, V. S. V. S. N. Swamy, K. V. Raj, K. Vanka and S. S. Sen, *Inorg. Chem.*, 2021, **60**, 1654–1663.
- 18 M. K. Bisai, V. Sharma, R. G. Gonnade and S. S. Sen, *Organometallics*, 2021, **40**, 2133–2138.
- 19 G. Kundu, S. Tothadi and S. S. Sen, *Inorganics*, 2022, **10**, 97 (1–13).
- 20 G. Kundu, V. S. Ajithkumar, K. V. Raj, K. Vanka, S. Tothadi and S. S. Sen, *Chem. Commun.*, 2022, **58**, 3783–3786.
- 21 G. D. Frey, J. D. Masuda, B. Donnadieu and G. Bertrand, *Angew. Chem., Int. Ed.*, 2010, **49**, 9444–9447.

- 22 T. Matsumoto and F. P. Gabbaï, *Organometallics*, 2009, **28**, 4252–4253.
- 23 D. McArthur, C. P. Butts and D. M. Lindsay, *Chem. Commun.*, 2011, **47**, 6650–6652.
- 24 J. M. Farrell, J. A. Hatnean and D. W. Stephan, *J. Am. Chem. Soc.*, 2012, **134**, 15728–15731.
- 25 Y. Wang, M. Y. Abraham, R. J. Gilliard Jr., D. R. Sexton, P. Wei and G. H. Robinson, *Organometallics*, 2013, **32**, 6639–6642.
- 26 G. Kundu, K. Balayan, S. Tothadi and S. S. Sen, *Inorg. Chem.*, 2022, **61**, 12991–12997.
- 27 A. Solovyev, S. J. Geib, E. Lacôte and D. P. Curran, *Organometallics*, 2012, **31**, 54–56.
- 28 T. Wang and D. W. Stephan, *Chem. – Eur. J.*, 2014, **20**, 3036–3039.
- 29 M. Arrowsmith, M. S. Hill, G. Kociok-Köhn, D. J. MacDougall and M. F. Mahon, *Angew. Chem., Int. Ed.*, 2012, **51**, 2098–2100.
- 30 S. M. I. Al-Rafia, R. McDonald, M. J. Ferguson and E. Rivard, *Chem. – Eur. J.*, 2012, **18**, 13810–13820.
- 31 D. Schmidt, J. H. J. Berthel, S. Pietsch and U. Radius, *Angew. Chem., Int. Ed.*, 2012, **51**, 8881–8885.
- 32 S. K. Bose, K. Fucke, L. Liu, P. G. Steel and T. B. Marder, *Angew. Chem., Int. Ed.*, 2014, **53**, 1799–1803.
- 33 H. Schneider, A. Hock, R. Bertermann and U. Radius, *Chem. – Eur. J.*, 2017, **23**, 12387–12398.
- 34 L. García, K. H. M. Al Furaiji, D. J. D. Wilson, J. L. Dutton, M. S. Hill and M. F. Mahon, *Dalton Trans.*, 2017, **46**, 12015–12018.
- 35 N. Gautam, R. Logdi, P. Sreejyothi, N. M. Rajendran, A. K. Tiwari and S. K. Mandal, *Chem. Commun.*, 2022, **58**, 3047–3050.
- 36 D. Munz, *Organometallics*, 2018, **37**, 275–289.
- 37 T. Dröge and F. Glorius, *Angew. Chem., Int. Ed.*, 2010, **49**, 6940–6953.
- 38 S. Würtemberger-Pietsch, H. Schneider, T. B. Marder and U. Radius, *Chem. – Eur. J.*, 2016, **22**, 13032–13036.
- 39 S. A. Westcott, H. P. Blom, T. B. Marder, R. T. Baker and J. C. Calabrese, *Inorg. Chem.*, 1993, **32**, 2175–2182.
- 40 M. Eck, S. Würtemberger-Pietsch, A. Eichhorn, J. H. J. Berthel, R. Bertermann, U. S. D. Paul, H. Schneider, A. Friedrich, C. Kleeberg, U. Radius and T. B. Marder, *Dalton Trans.*, 2017, **46**, 3661–3680.